Topics in Organometallic Chemistry 44

Lukas J. Gooßen *Editor*

Inventing Reactions

Springer

44
Topics in Organometallic Chemistry

Topics in Organometallic Chemistry

Recently Published Volumes

Hydrofunctionalization
Volume Editors: Valentine P. Ananikov, Masato Tanaka
Vol. 43, 2013

Organometallics as Catalysts in the Fine Chemical Industry
Volume Editors: Matthias Beller, Hans-Ulrich Blaser
Vol. 42, 2012

Modern Organoaluminum Reagents: Preparation, Structure, Reactivity and Use
Volume Editors: Simon Woodward, Samuel Dagorne
Vol. 41, 2012

Organometallic Pincer Chemistry
Volume Editors: Gerard van Koten, David Milstein
Vol. 40, 2012

Organometallics and Renewables
Volume Editors: Michael A. R. Meier, Bert M. Weckhuysen, Pieter C. A. Bruijnincx
Vol. 39, 2012

Transition Metal Catalyzed Enantioselective Allylic Substitution in Organic Synthesis
Volume Editor: Uli Kazmaier
Vol. 38, 2011

Bifunctional Molecular Catalysis
Volume Editors: T. Ikariya, M. Shibasaki
Vol. 37, 2011

Asymmetric Catalysis from a Chinese Perspective
Volume Editor: Shengming Ma
Vol. 36, 2011

Higher Oxidation State Organopalladium and Platinum Chemistry
Volume Editor: A. J. Canty
Vol. 35, 2011

Iridium Catalysis
Volume Editor: P. G. Andersson
Vol. 34, 2011

Iron Catalysis – Fundamentals and Applications
Volume Editor: B. Plietker
Vol. 33, 2011

Medicinal Organometallic Chemistry
Volume Editors: G. Jaouen, N. Metzler-Nolte
Vol. 32, 2010

C-X Bond Formation
Volume Editor: A. Vigalok
Vol. 31, 2010

Transition Metal Complexes of Neutral η^1-Carbon Ligands
Volume Editors: R. Chauvin, Y. Canac
Vol. 30, 2010

Photophysics of Organometallics
Volume Editor: A. J. Lees
Vol. 29, 2010

Molecular Organometallic Materials for Optics
Volume Editors: H. Le Bozec, V. Guerchais
Vol. 28, 2010

Conducting and Magnetic Organometallic Molecular Materials
Volume Editors: M. Fourmigué, L. Ouahab
Vol. 27, 2009

Metal Catalysts in Olefin Polymerization
Volume Editor: Z. Guan
Vol. 26, 2009

Bio-inspired Catalysts
Volume Editor: T. R. Ward
Vol. 25, 2009

Directed Metallation
Volume Editor: N. Chatani
Vol. 24, 2007

Regulated Systems for Multiphase Catalysis
Volume Editors: W. Leitner, M. Hölscher
Vol. 23, 2008

Organometallic Oxidation Catalysis
Volume Editors: F. Meyer, C. Limberg
Vol. 22, 2007

Inventing Reactions

Volume Editor: Lukas J. Gooßen

With Contributions by

D.C. Behenna · G.L. Beutner · S.M. Bischof · J.W. Bode · B. Cardinal-David · N. Chatani · X. Cheng · I. Čorić · S.E. Denmark · K. Fagnou · K. Gooßen · L.J. Gooßen · B.G. Hashiguchi · A.S.K. Hashmi · T. Kawasaki · M.M. Konnick · B. List · S. Müller · R.A. Periana · K.A. Scheidt · K. Soai · B.M. Stoltz · D.R. Stuart · M. Tobisu · B.M. Trost · S. Vellalath · H. Yamamoto

Springer

Editor
Lukas J. Gooßen
TU Kaiserslautern
FB Chemie - Organische Chemie
Erwin-Schrödinger-Str. 54
67663 Kaiserslautern
Germany

ISSN 1436-6002 ISSN 1616-8534 (electronic)
ISBN 978-3-642-34285-1 ISBN 978-3-642-34286-8 (eBook)
DOI 10.1007/978-3-642-34286-8
Springer Heidelberg New York Dordrecht London

Library of Congress Control Number: 2012950322

Printed on acid-free paper

Springer is part of Springer Science+Business Media (www.springer.com)

Volume Editor

Lukas J. Gooßen

TU Kaiserslautern
FB Chemie - Organische Chemie
Erwin-Schrödinger-Str. 54
67663 Kaiserslautern
Germany
goossen@chemie.uni-kl.de

Editorial Board

Topics in Organometallic Chemistry Also Available Electronically

Topics in Organometallic Chemistry is included in Springer's eBook package *Chemistry and Materials Science*. If a library does not opt for the whole package the book series may be bought on a subscription basis. Also, all back volumes are available electronically.

For all customers who have a standing order to the print version of *Topics in Organometallic Chemistry*, we offer free access to the electronic volumes of the Series published in the current year via SpringerLink.

If you do not have access, you can still view the table of contents of each volume and the abstract of each article by going to the SpringerLink homepage, clicking on "Chemistry and Materials Science," under Subject Collection, then "Book Series," under Content Type and finally by selecting *Topics in Organometallic Chemistry*.

You will find information about the

- Editorial Board
- Aims and Scope
- Instructions for Authors
- Sample Contribution

at springer.com using the search function by typing in *Topics in Organometallic Chemistry*.
Color figures are published in full color in the electronic version on SpringerLink.

Aims and Scope

The series *Topics in Organometallic Chemistry* presents critical overviews of research results in organometallic chemistry. As our understanding of organometallic structures, properties and mechanisms grows, new paths are opened for the design of organometallic compounds and reactions tailored to the needs of such diverse areas as organic synthesis, medical research, biology and materials science. Thus the scope of coverage includes a broad range of topics of pure and applied organometallic chemistry, where new breakthroughs are being made that are of significance to a larger scientific audience.

The individual volumes of *Topics in Organometallic Chemistry* are thematic. Review articles are generally invited by the volume editors.

In references *Topics in Organometallic Chemistry* is abbreviated Top Organomet Chem and is cited as a journal. From volume 29 onwards this series is listed with ISI/Web of Knowledge and in coming years it will acquire an impact factor.

In memory of Professor Keith Fagnou,
inventor of great chemical reactions

Preface

In popular media, chemists are often portrayed as characters aimlessly throwing together concoctions of random ingredients in the hope of spectacular discoveries. As exaggerated as this may appear, the grain of truth behind this image is that some prominent chemical processes have indeed been found by serendipity rather than through rational thought processes. However, even in these cases, a substantial intellectual contribution was made by the discovering scientists, who grasped the significance of their experimental results and readjusted the focus of their research activity.

I am convinced that it has meanwhile become the rule rather than the exception for the discovery of a chemical reaction to result from an intentional invention process with a clearly defined target. A prominent advocate of this rational approach to innovation was Sir Derek Barton, Nobel laureate of 1969, who in his essays made strong arguments in favor of this approach [1].

It was Manfred Reetz who had the idea for a book spotlighting the creative process associated with recent inventions of chemical reactions, and I felt honored to be entrusted with this project. With such a book, which would include contributions by some of the most creative minds in chemistry telling the stories of great discoveries, we hoped to spark renewed enthusiasm for reaction development among students and colleagues.

Our strategy for recruiting competent contributors consisted of scanning the top journals in chemistry for new reactions that present creative solutions to long-standing problems in organic chemistry. This survey revealed that some author names appear time and again in the context of such discoveries. This alone is an argument that chance plays only a limited role in the development of new synthetic transformations. When contacting potential contributors, we received an overwhelmingly positive response and won over 12 outstanding scientists from a broad range of backgrounds and experience as coauthors.

In this volume, we aim to give insights into our creative process and reveal which combination of design and serendipity was involved in the discovery of some of our favorite reactions. Each chapter provides short overviews of the context and

subsequent developments of their respective transformations. I am deeply grateful to all authors for sharing such delicate information with the chemical community. This required their strong personal involvement, since unlike review-style book chapters, it is clear that such personal accounts cannot be delegated to coworkers.

When we initiated this book project at the OMCOS-15 meeting in Glasgow 2009, I approached Keith Fagnou with the intention of winning him over as a first author or, hopefully, even as a coeditor, and we had a long and fruitful discussion about this project. Sadly, his untimely passing away prevented his further involvement. In my opinion, the chemical community has lost one of its finest researchers. It means a lot to me to dedicate this volume to his memory.

Keith Fagnou was born on June 27, 1971, in Saskatoon, Saskachewan. He obtained a Bachelor of Education in his home town and briefly worked as a high school teacher. He then moved to the University of Toronto for his M.Sc. degree and joined the group of Mark Lautens for PhD research. In 2002, he started his independent academic career at the University of Ottawa. His inventive contributions to the rapidly emerging field of direct arylation reactions generated an enormous response, and he received numerous international awards. The University of Ottawa soon promoted him to become Research Chair in the Development of Novel Catalytic Transformations. I had the pleasure to attend several of his scientifically and didactically outstanding lectures, and shared stimulating discussions with him on arylation technology. Keith died on November 11, 2009, at the age of 38.

I am grateful to his former postdoctoral researcher, Dr. David Stuart, for accepting the task of writing Keith's chapter on the discovery and development of a palladium(II)-catalyzed oxidative cross-coupling of two unactivated arenes.

Keith's creative spirit and his pleasant character will forever remain engraved in our memory.

Lukas Gooßen

Reference

1. Barton DHR (1994) The invention of chemical reactions of relevance to the chemistry of natural products. Pure Appl Chem 66:1943–1954

Contents

Top Organomet Chem (2013) 44: 1–12
DOI: 10.1007/3418_2012_50

Published online: 17 August 2012

Catalysis: Unlimited Frontiers – Our Early Personal Journey into the World of Palladium

Barry M. Trost

Abstract Stimulated by our collaboration in the chemistry of insects, the absence of direct ways to replace allylic C–H bonds by C–C bonds led us to teach ourselves about the organic chemistry of palladium. This journey evolved beyond allylic alkylation and led to the semi-rational development of alkene–alkyne coupling and discovery of palladium complexes of trimethylenemethane as reactive intermediates for cycloadditions to five, seven, and nine membered carbo- and heterocycles. These new synthetic tools enabled facile strategies to complex structures possessing interesting properties, notably of biological relevance.

Keywords Allylation · Catalysis · Enantioselectivity · Palladium · Total synthesis

Contents

1 Introduction

Designing molecular structure for function is the grand challenge for chemists to improve the general well-being of society. Solving problems in diverse fields ranging from material science including nanotechnology to biology and everything

B.M. Trost (✉)
Department of Chemistry, Stanford University, Stanford, CA 94305-5080, USA
e-mail: bmtrost@stanford.edu

in between requires an understanding of the problem and how various chemical entities might impact that problem. While many scientists approaching such problems are limited to chemical entities that already exist, a chemist is not constrained by such limitations since the chemist can go into the laboratory and synthesize the structure thought to be desirable. Optimizing structure for function is limited by the need to be able to access the designed structure in a time-efficient manner.

We initiated a program to assist this process by increasing the toolbox of useful synthetic reactions. As we embarked upon our program to do so, our first efforts focused on more typical types of chemical reactions involving novel reagents employed stoichiometrically and largely focused on the organic chemistry of sulfur [1–14]. In this chapter, I describe how we became enchanted with transition metal-catalyzed processes all of which began with palladium.

2 Initiation: Allylic Alkylation

During those early years, I joined a collaboration to help identify the structure of the insect juvenile hormone, one of three such hormones thought to be the substances that controlled the maturation of insects from pupae to larvae and finally adults [15–18]. By understanding their chemistry, a safer approach for control of populations of harmful insects was envisioned. We determined the structure of juvenile hormone as **1**. In thinking about how such a compound might be derived biologically, we conjectured that maybe there existed an enzymatic process that transformed the common sesquiterpene

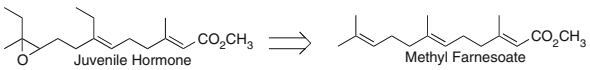

natural product methyl farnesoate **2** into juvenile hormone, a hypothesis that raised the question whether such a transformation could be achieved synthetically in the laboratory. Indeed, the oxygen analog

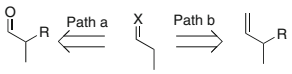

(1)

(Eq. 1, path a) constitutes one of the most fundamental transformations of organic chemistry – i.e., enol or enolate alkylation. Could there be such a process for the isoelectronic olefins (Eq. 1, path b)?

In thinking about such a possibility, we made our first foray into the field of transition metal chemistry [19–24]. Using the organic chemistry of homogenous palladium chemistry, we developed such a process as shown in Eq. 2 wherein a monoterpene, methyl geraniate, is homologated to a sesquiterpene, farnesol! Indeed, an allylic methylation procedure as required for juvenile hormone was also

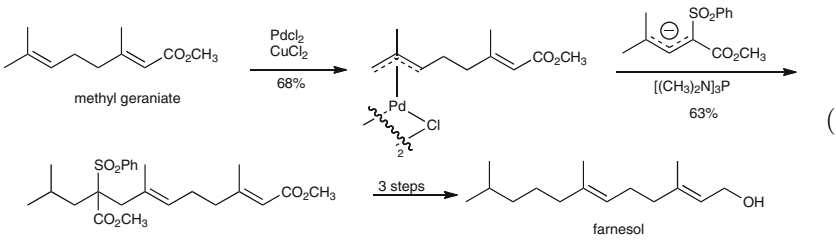

(2)

developed [24]. While the overall procedure is indeed an allylic alkylation, it differs fundamentally from enolate alkylation in that it is an "umpolung" process. Whereas "metalation" of carbonyl compounds generates nucleophiles, the "metalation" of the olefin generates electrophiles! We noted the requirement for phosphine ligands in order to accomplish the C–C bond forming event with substituted π-allylpalladium complexes [19, 21].

Subsequently, a catalytic process was developed in analogy to the conversion of the stoichiometric Heck reaction to a catalytic process – i.e., a leaving group was installed at the allylic position which could be readily accomplished by allylic oxidation protocols as shown in Scheme 1 [25–30]. The exquisite stereochemical

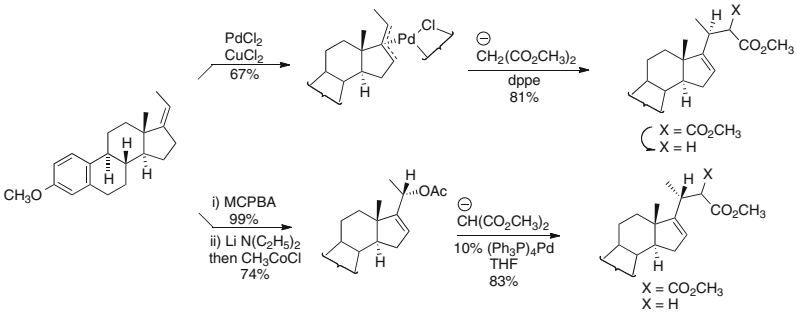

Scheme 1 Stoichiometric vs. catalytic allylic alkylation

control and the ability to transform the typical substitution process from one of inversion of configuration to one of retention by use of a transition metal combined with the opportunity also to control regioselectivity convinced us of the value of such metal-catalyzed processes compared to nonmetal-promoted reactions [31, 32].

The ultimate for control, of course, was enantioselectivity? The huge challenge of this objective became obvious upon understanding that both the bond breaking and making events in these palladium-based methodologies occur outside the coordination sphere of the metal [33]. Thus, the chiral ligands bound to palladium needed to control absolute stereochemistry that resides a great distance away from where they needed to exercise their influence. Ultimately, our design of "chiral space" to influence how substrates will fit in and move within that chiral space, in complete analogy to the active site of enzymes, became the key to success (see Fig. 1) [34–36].

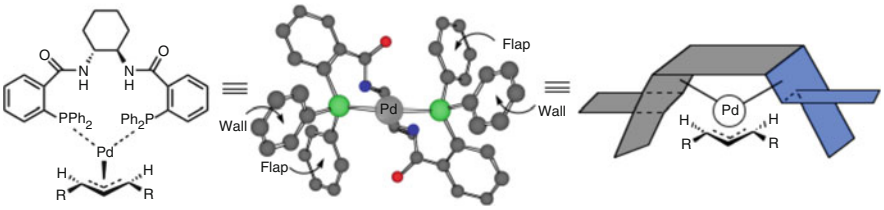

Fig. 1 Proposed chiral space of chiral ligands for asymmetric induction in Pd AAA

As a result, we have demonstrated the effectiveness of this design to the broadest scope of asymmetric induction as outlined in Scheme 2 [37–41]. The initial type of enantiodiscrimination involved desymmetrization of meso diester leaving groups wherein the ionization event induces the stereochemistry. The application of this method for the synthesis of nucleosides is illustrated in Scheme 2 as just one example of many [42–46]. Deracemization of 1,3-disubstituted substrates whose corresponding π-allylpalladium intermediate in the presence of achiral ligands is meso requires the catalyst to control the approach of the nucleophile to one of the two enantiotopic termini of the allyl unit [47–54]. Thus, an initial racemic starting material is deracemized. This process is illustrated for the case of the synthesis of an inositol phosphate [49]. A more complicated example involves a 1,3-unsymmetrically substituted allyl intermediate which requires a more complex method to effect deracemization and is illustrated in a synthesis of an aflatoxin [55–57]. Monosubstituted allyl intermediates have a dual problem wherein the ligand must control both the regioselectivity and enantioselectivity [58–65]. Nevertheless, this process has also been highly successful and is illustrated in a synthesis of vigabatrin among many others [59]. The most challenging is inducing stereochemistry at prochiral nucleophiles [66–80]. Nevertheless, this process has been quite successful as illustrated by the asymmetric enolate allylation which led to asymmetric total syntheses of both hamigeran B and allocyathin B_2 [70, 73, 74].

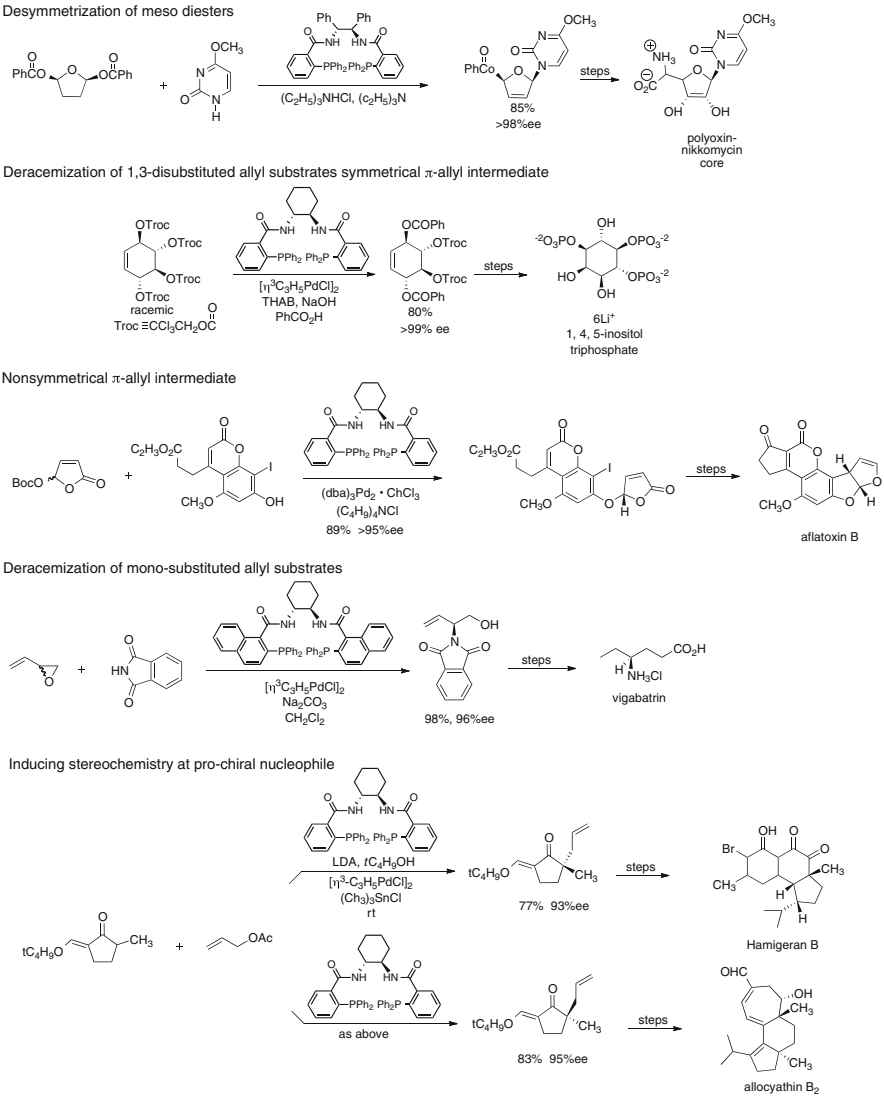

Scheme 2 Types of asymmetric induction in Pd AAA

3 Alkene–Alkyne Coupling

During the course of our studies on the Pd-catalyzed allylic alkylation in which we were examining tandem alkylation–cyclization, we examined the use of dimethyl propargylmalonate as the nucleophile with the intention to explore a subsequent thermal ene reaction to constitute an overall cyclopentane annulation as shown in Eq. 3 [81, 82]. While the alkylation proceeded well to give the cis product **1**,

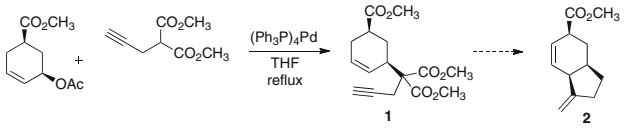

(3)

all attempts to effect the thermal cyclization led either to no reaction at temperature <650° or decomposition at temperatures >675°. During subsequent runs of the initial Pd-catalyzed alkylation that had proceeded for a more extensive period of time, we noted the formation of a new product whose ^{1}H NMR spectrum corresponded to the methylene cyclopentane **2**. Since we noted catalyst decomposition during this run, we considered the possibility of adventitious oxidation of Pd(0) to Pd(+2). Indeed, subjecting the single alkylation product **1** to palladium acetate even at room temperature in THF gave **2** in 60% yield. The optimum conditions proved to involve the use of $(Ph_3P)_2Pd(OAc)_2$ in benzene at 66° which gave an 85% yield of **2**. This reaction proved general. Furthermore, depending upon the nature of substituents, 1,3-dienes rather than 1,4-dienes could result as shown in Eq. 4 [83–86]. Thus, two mechanisms were considered for the alkene–alkyne coupling – a palladacycle mechanism (Eq. 5, path a) or a

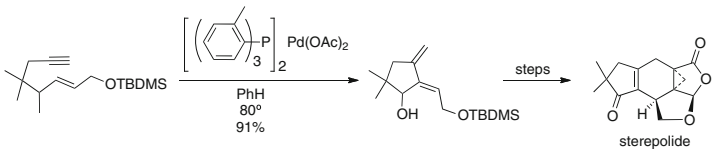

(4)

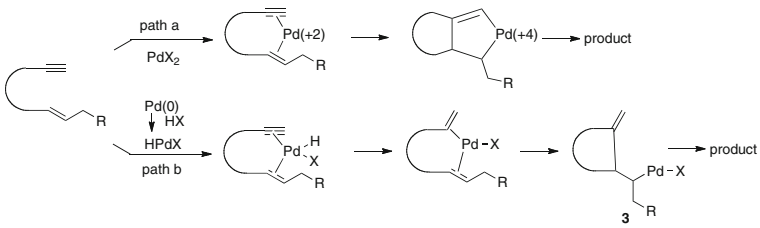

(5)

hydropalladation mechanism (Eq. 5, path b). Difficulty in the collapse of the palladacycle to form a 1,3-diene would seem to favor the latter pathway at least for such cases. Indeed, an alternative catalyst generated by treating Pd(0) with a carboxylic acid (acetic or formic acid) proved efficacious for these cycloisomerizations [87–90]. Indeed, treating $(dba)_3Pd_2{\bullet}CHCl_3$ with o-tolyphosphine and acetic acid led to a most effective catalyst, allowing the cycloisomerization to form 1,3-dienes to proceed at room temperature. Use of formic acid in lieu of acetic acid with no phosphine ligand gave further improvement and also formed 1,4-dienes if an allylic alcohol substituent was absent in the substrate (Eq. 6) as in a synthesis of cassiol (Eq. 6) [90].

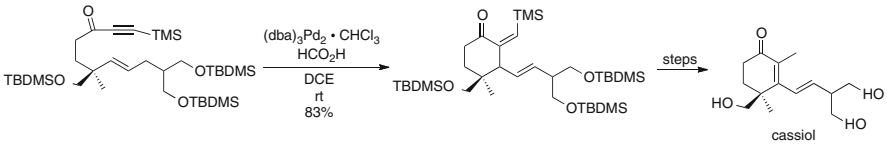

(6)

With the hypothesis that a σ-Pd(+2) intermediate **3** is involved in the catalytic cycle, we hypothesized that it may be intercepted by a silane to give the product of reductive enyne cyclization [91]. Equation 7 illustrates the implementation of this new concept in the context of a total synthesis of

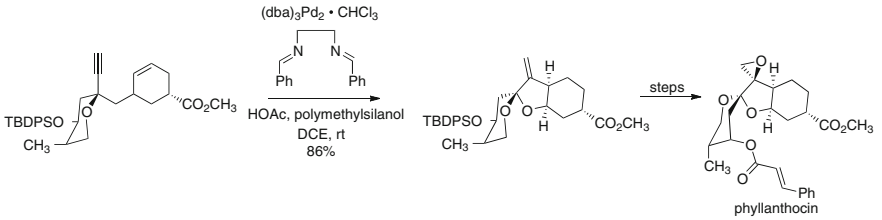

(7)

phyllanthocin [92, 93]. The uniqueness of this transformation should be noted given that chemoselective reduction of the 1,4-diene resulting from the cycloisomerization would not be possible in most cases. The ease of accessing the requisite substrates by metal-catalyzed allylic alkylations combined with the selective alkene–alkyne coupling constitutes a powerful method to 5- and 6-membered ring targets.

4 Trimethylenemethane Palladium Complex (TMM-PdL$_2$)

In considering the structure of π-allylpalladium cationic complexes, the nature of the charge distribution reveals that the terminal allyl carbons are somewhat negative, whereas the central carbon is somewhat positive. For example, the complex **4** (Fig. 2) has the indicated charges on the allyl fragment.

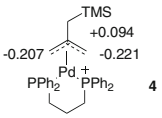

Fig. 2 Charge distribution of a π-allylpalladium cationic complex

Given the fact that silicon β to a carbocationic center easily cleaves to give an olefin, the fundamental basis of the Peterson olefination, we envisioned the reaction depicted in Eq. 8 [94–97]. In this scheme, the partial positive charge at C-2 of the

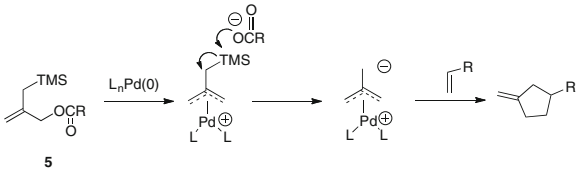

(8)

allyl is envisioned to labilize the silicon toward attack of an oxygen silylophile to form the Pd complex of trimethylenemethane. Trimethylenemethane itself has largely been studied as a novel reactive intermediate that did have the ability to effect cycloadditions with olefins. Unfortunately, the difficulty in generating such a reactive intermediate led to its not being used synthetically. If the process of Eq. 8 could lead to a similar type of cycloaddition, this process could have significant synthetic applications.

Treating **5** (R=CH_3) with a Pd(0) complex in the presence of an olefin bearing an electron – withdrawing group led to the methylenecyclopentane exactly as envisioned (Eq. 9) [94–97].

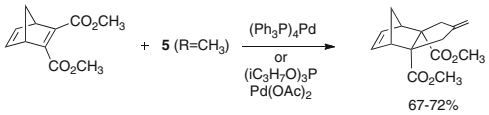

(9)

Use of preformed tetrakis (triphenylphosphine)(palladium) or an acetate with triisopropyl phosphite which serves as both the ligand and reducing agent gave exclusive attack on the alkene bearing an ester of the norbornadiene substrate, consistent with the dipolar nature predicted for the TMM-PdL_2 species.

The reaction shows characteristics of potentially being a concerted, albeit asynchronous, cycloaddition. Thus, comparing the **E** and **Z** enoates **6** and **7**

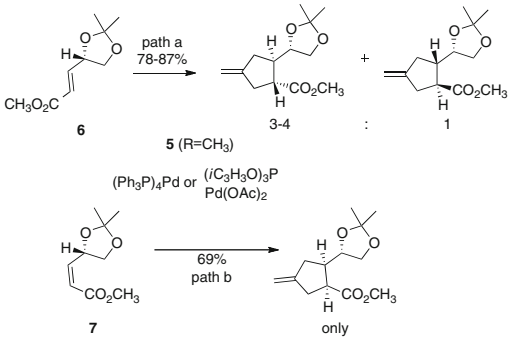

(10)

respectively led to the **E** and **Z** cycloadducts, respectively (Eq. 10), indicating faithful translation of olefin geometry into ring geometry [98]. This reaction was used in a synthesis of brefeldin A [99]. A study of heavy-atom isotope effects also supports a concerted process [100].

In addition to [3+2] cycloadditions, [3+4] [101] and [3+6] [102] cycloadditions have been observed (Eqs. 11 and 12, respectively). The [3+4] cycloaddition illustrates the complementarity of the new Pd-catalyzed reactions since the requisite TMM diene acceptors are readily accessed by the Pd-catalyzed alkene–alkyne coupling as shown in Eq. 11 [101]. One of the benefits of metal-catalyzed processes

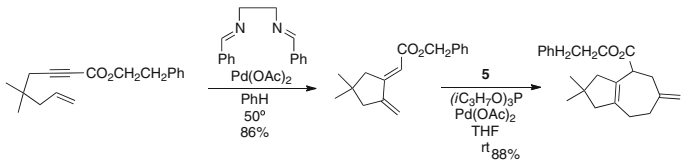

(11)

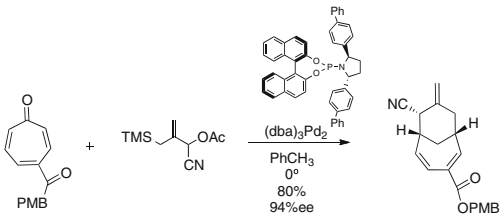

(12)

is the prospect for asymmetric catalysis. Indeed, these reactions can be performed with high enantioselectivity [103] as illustrated in the [3+6] cycloaddition (Eq. 12) [104]. This facile rapid construction of the bicyclo[4.3.1]decane ring system opens a facile strategy to indole alkaloids represented by the welwitindolinones.

5 Conclusions

In this personal account, I present the thinking that led us to involve ourselves in transition metal-mediated/catalyzed processes, notably in Pd chemistry, in spite of our not having any previous experiences in the field. I have included only the references to our work. The background references that helped guide our thinking can be found in the references cited in our papers. As shown, our program evolved via both designed concepts coming from basic mechanistic rationales as well as serendipity. From our evolution of the concept of metal-catalyzed allylic alkylations, the principles for the trimethylenemethane cycloadditions arose in a logical fashion. On the other hand, the metal-catalyzed alkene–alkyne coupling arose somewhat serendipitously. Our initial design was a simple two-stage ring-forming process – the first a Pd-catalyzed allylic alkylation and the second a thermal Alder-ene-type cyclization. During our failed efforts in building substrates to effect the thermal cyclization, we noticed that, in some of the runs in making the substrate in the Pd-catalyzed allylic alkylation, the cyclization proceeded as well! Indeed, this combination of rational design and serendipity has proven to be the key strategies that guided our entire catalysis program. While the organic chemistry of palladium was the start, our efforts have expanded well beyond palladium to embrace both main group and many other transition metal catalysts as well.

References

1. Trost BM, Lautens M (1967) J Am Chem Soc 89:138–142
2. Trost BM, Bogdanowicz MJ (1971) J Am Chem Soc 93:3773–3774
3. Trost BM, La Rochelle RS (1971) J Am Chem Soc 93:6077–6086
4. Trost BM, Salzmann TN (1973) J Am Chem Soc 95:6840–6842
5. Trost BM, Bridges AJ (1976) J Am Chem Soc 98:5017–5019
6. Trost BM, Reiffin M, Crimmin M (1979) J Am Chem Soc 103:257–259
7. Trost BM, Murayama E (1982) J Am Chem Soc 101:6529–6530
8. Trost BM, Shibata T (1981) J Am Chem Soc 104:3225–3228
9. Trost BM, Ghadiri MR (1984) J Am Chem Soc 106:7260–7261
10. Trost BM, Lautens M (1972) Top Curr Chem 41:1–29
11. Trost BM (1974) Acc Chem Res 7:85–92
12. Trost BM (1977) Acc Chem Res 11:453–461
13. Trost BM (1978) Chem Rev 78:363–382
14. Trost BM (1988) Bull Chem Soc Jpn 61:107–124
15. Röller H, Dahm KH, Sweely CC, Trost BM (1967) Angew Chem Int Ed 6:179–180
16. Dahm KH, Trost BM, Röller H (1967) J Am Chem Soc 89:6806
17. Dahm KH, Röller H, Trost BM (1968) Life Sci II 7:129
18. Trost BM (1970) Acc Chem Res 3:120–130
19. Trost BM, Fullerton TJ (1973) J Am Chem Soc 95:292–294
20. Trost BM, Fullerton TJ (1974) J Org Chem 39:737–738
21. Trost BM, Weber L (1975) J Am Chem Soc 97:1611–1612
22. Trost BM, Strege PE, Weber L, Fullerton TJ, Dietsche TJ (1978) J Am Chem Soc 100:3416–3426
23. Trost BM, Weber L (1975) J Org Chem 40:3617–3619
24. Trost BM, Weber L, Strege PE, Fullerton TJ, Dietsche TJ (1978) J Am Chem Soc 100:3426–3435
25. Trost BM, Verhoeven TR (1976) J Am Chem Soc 98:630–632
26. Trost BM, Verhoeven TR (1976) J Org Chem 41:3215–3216
27. Trost BM, Verhoeven TR (1978) J Am Chem Soc 100:3435–3443
28. Trost BM, Verhoeven TR (1979) J Am Chem Soc 101:1595–1597
29. Trost BM, Verhoeven TR (1980) J Am Chem Soc 102:4730–4743
30. Trost BM, Verhoeven TR (1980) J Am Chem Soc 102:4743–4763
31. Trost BM, Dietsche TJ (1973) J Am Chem Soc 95:8200–8201
32. Trost BM, Strege PE (1977) J Am Chem Soc 99:1649–1651
33. Trost BM, Murphy DJ (1985) Organometallics 4:1143–1145
34. Trost BM, Van Vranken DL (1992) Angew Chem Int Ed 31:228–230
35. Trost BM, Van Vranken DL, Bingel C (1992) J Am Chem Soc 114:9327–9343
36. Trost BM, Bunt RC (1996) Angew Chem Int Ed 35:99–102
37. Trost BM, Van Vranken DL (1996) Chem Rev 96:395–422
38. Trost BM (1996) Acc Chem Res 29:355–364
39. Trost BM, Crawley ML (2003) Chem Rev 103:2921–2944
40. Trost BM, Fandrick DR (2007) Aldrichimica Acta 40:59–72
41. Trost BM, Zhang T, Sieber JD (2010) Chem Sci 1:427–440
42. Trost BM, Li L, Guile SD (1992) J Am Chem Soc 114:8745–8747
43. Trost BM, Shi Z (1996) J Am Chem Soc 118:3037–3038
44. Trost BM, Madsen R, Guile SD, Elia AEH (1996) Angew Chem Int Ed 35:1569–1572
45. Trost BM, Madsen R, Guile SD, Brown BS (2000) J Am Chem Soc 122:5947–5956
46. Trost BM, Brown BS, McEachern EJ, Kuhn O (2003) Chem Eur J 9:4442–4451
47. Trost BM, Krueger AC, Bunt RC, Zambrano J (1996) J Am Chem Soc 118:6520–6521
48. Trost BM, Oslob JD (1999) J Am Chem Soc 121:3057–3064
49. Trost BM, Patterson DE, Hembre EJ (1999) J Am Chem Soc 121:10834–10835

50. Trost BM, Patterson DE, Hembre EJ (2001) Chem Eur J 7:3768–3775
51. Trost BM, Tang W (2002) Angew Chem Int Ed 41:2795–2797
52. Trost BM, Tang W (2002) J Am Chem Soc 124:14542–14543
53. Trost BM, Zhang T (2008) Angew Chem Int Ed 47:3759–3761
54. Trost BM, Tang W, Toste FD (2005) J Am Chem Soc 127:14785–14803
55. Trost BM, Toste FD (1999) J Am Chem Soc 121:3543–3544
56. Trost BM, Crawley ML (2002) J Am Chem Soc 124:9328–9329
57. Trost BM, Tang W, Toste FD (2003) J Am Chem Soc 125:3090–3100
58. Trost BM, Toste FD (1998) J Am Chem Soc 120:9074–9075
59. Trost BM, Bunt RC, Lemoine RC, Calkins TL (2000) J Am Chem Soc 122:5968–5976
60. Trost BM, Tang W, Schulte JC (2000) Org Lett 2:4013–4015
61. Trost BM, Thiel OR, Tsui H-C (2002) J Am Chem Soc 124:11616–11617
62. Trost BM, Thiel OR, Tsui H-C (2003) J Am Chem Soc 125:13155–13164
63. Trost BM, Fandrick DR (2003) J Am Chem Soc 125:11836–11837
64. Trost BM, Horne DB, Woltering MJ (2003) Angew Chem Int Ed 42:5987–5990
65. Trost BM, Aponick A, Stanzl B (2007) Chem Eur J 13:9547–9560
66. Trost BM, Radinov R, Grenzer EM (1997) J Am Chem Soc 119:7879–7880
67. Trost BM, Ariza X (1997) Angew Chem Int Ed 36:2635–2637
68. Trost BM, Ariza X (1999) J Am Chem Soc 121:10727–10737
69. Trost BM, Tang W (2003) J Am Chem Soc 125:8744–8745
70. Trost BM, Pissot-Soldermann C, Chen I, Schroeder GM (2004) J Am Chem Soc 126:4480–4481
71. Trost BM, Fredriksen MU (2005) Angew Chem Int Ed 44:308–310
72. Trost BM, Schroeder GM (2005) Chem Eur J 11:174–184
73. Trost BM, Dong L, Schroeder GM (2005) J Am Chem Soc 127:2844–2845
74. Trost BM, Dong L, Schroeder GM (2005) J Am Chem Soc 127:10259–10268
75. Trost BM, Xu J (2005) J Am Chem Soc 127:2846–2847
76. Trost BM, Quancard J (2006) J Am Chem Soc 128:6314–6315
77. Trost BM, Xu J, Reichle M (2007) J Am Chem Soc 129:282–283
78. Trost BM, Thaisrivongs DA (2009) J Am Chem Soc 131:12056–12057
79. Trost BM, Xu J, Schmidt T (2009) J Am Chem Soc 131:18343–18357
80. Trost BM, Malhotra S, Chan WH (2011) J Am Chem Soc 133:7328–7331
81. Trost BM, Lautens M (1985) J Am Chem Soc 107:1781–1783
82. Trost BM, Lautens M, Chan C, Jebaratnam DJ, Mueller T (1991) J Am Chem Soc 113:636–644
83. Trost BM, Chung JYL (1985) J Am Chem Soc 107:4586–4588
84. Trost BM, Hipskind PA, Chung JYL (1989) Angew Chem Int Ed 28:1502–1504
85. Trost BM, Hipskind PA (1992) Tetrahedron Lett 33:4541–4544
86. Trost BM, Tanoury GJ, Lautens M, Chan C, MacPherson DT (1994) J Am Chem Soc 116:4255–4267
87. Trost BM, Lee DC, Rise F (1989) Tetrahedron Lett 30:651–654
88. Trost BM, Lee DC, Rise F (1989) J Org Chem 54:2271–2274
89. Trost BM, Romero DL, Rise F (1994) J Am Chem Soc 116:4268–4278
90. Trost BM, Li Y (1996) J Am Chem Soc 118:6625–6633
91. Trost BM, Rise F (1987) J Am Chem Soc 109:3161–3163
92. Trost BM, Edstrom ED (1990) Angew Chem Int Ed 29:520–522
93. Trost BM, Kondo Y (1991) Tetrahedron Lett 32:1613–1616
94. Trost BM, Chan DMT (1979) J Am Chem Soc 101:6429–6432
95. Trost BM, Chan DMT (1983) J Am Chem Soc 105:2315–2325
96. Trost BM, Chan DMT (1983) J Am Chem Soc 105:2326–2335
97. Trost BM (1986) Angew Chem Int Ed 25:1
98. Trost BM, Mignani SM (1986) Tetrahedron Lett 27:4137–4140
99. Trost BM, Lynch J, Renault P, Steinman DJ (1986) J Am Chem Soc 108:284–291

100. Singleton DA, Schulmeier BE (1999) J Am Chem Soc 121:9313
101. Trost BM, MacPherson DT (1987) J Am Chem Soc 109:3483–3484
102. Trost BM, Seoane PR (1987) J Am Chem Soc 109:615–617
103. Trost BM, Stambuli JP, Silverman SM, Schwörer U (2007) J Am Chem Soc 129:12396–12397
104. Trost BM, McDougall PJ (2009) Org Lett 11:3782–3785

Top Organomet Chem (2013) 44: 13–34
DOI: 10.1007/3418_2012_41

Published online: 14 August 2012

Reinventing Amide Bond Formation

Jeffrey W. Bode

Abstract The chemical synthesis of peptides and proteins has long relied on innovative inventions of amide-forming reactions. Our group has discovered and developed an amide-forming ligation reaction by the coupling of α-ketoacids and hydroxylamine (KAHA ligation). This reaction does not require reagents or catalysts, proceeds in the presence of unprotected functional groups, and generates no nonvolatile by-products. This chapter recounts our discovery of this reaction, our development of novel methods for the preparation of α-ketoacids and hydroxylamines, and the application of these new methods to the synthesis of peptides and proteins.

Keywords Amide bonds · Mechanism · Peptides · Protein synthesis · Reaction development

Contents

J.W. Bode (✉)
Laboratorium für Organische Chemie, ETH-Zürich, Zürich 8093, Switzerland
e-mail: bode@org.chem.ethz.ch

Abbreviations

Ac	Acetyl
Acac	Acetylacetonate
Alk	Alkyl
Btw	By the way
Etc	Et cetera

1 Introduction

The majority of my research group currently works on some aspect of amide bond formation. This work now encompasses a broad range of applications, reaction types, and mechanistic paradigms. This focus—my graduate students might say obsession—began as a conversation over breakfast in Tokyo on 26 January 2003 with Prof. Naoki Umezawa, now at the School of Pharmaceutical Science at Nagoya City University. Naoki and I were discussing why it is so difficult to go directly from genetic information to a protein. Naoki, a bioorganic chemist, was asking me, a synthetic organic chemist, why organic chemists cannot readily synthesize the protein he wa s interested in studying? To make his proteins, he pointed out, he had to rely on bacteria.

After this conversation, I began to think and read more deeply about the problem. For the organic chemists of my generation, it was widely assumed that peptide and protein synthesis was largely a solved problem. I initially shared this naïve belief—and suffered later from reviewers who held similar views. I knew, of course, about the power of Merrifield's solid-phase peptide synthesis but soon learned from the literature that routinely making peptides longer than approximately 40 residues could be very difficult and was not routine [1, 2]. I was also not aware of the economical and environmental costs of solid-phase peptide synthesis and was surprised to learn that the cost of peptide synthesis can be roughly calculated as $300/residue/gram for natural peptides and as much as 10 times that for unnatural amino acids [3]. I also knew of the beautiful and impressive native chemical ligation of peptide thioesters and peptides and proteins containing N-terminal cysteines [4]. I was surprised to learn, however, that cysteine is one of the rarest amino acids and that they are not present in all proteins. The 864 amino acid *taq* DNA polymerase routinely used for PCR, for example, does not contain as single cysteine! I also learned that the biggest challenge to NCL, at least at that time, was the preparation of the peptide thioesters [5]. These had to be prepared by Boc chemistry, rather than the more user-friendly Fmoc chemistry, restricting their synthesis to hard-core peptide chemists and precluding many desirable peptides including glycopeptides.

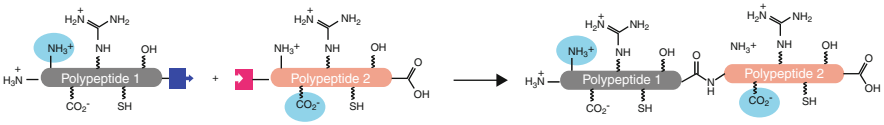

Scheme 1 Cartoon of a peptide ligation. The substrates combine chemoselectively to form a backbone amide bond in the presence of unprotected side chains, under water-compatible conditions, and without reagents or catalysts

2 Defining the Research Target

The almost magical chemistry of the native chemical ligation was an inspiration and set a very high bar for innovation. It made clear that any advance in synthetic protein chemistry would have to come in the form of a *peptide ligation reaction* that allowed two completely unprotected fragments to be selectively joined under water-compatible conditions. Furthermore, the reaction must work at low reactant concentrations and should not produce any toxic or reactive by-products. It would have to be a "general" reaction—not limited to sulfur-containing residues and ideally applicable to amide types other than α-peptides. Put another way, our task was to figure out what chemical functionalities the cartoon "puzzle pieces" in Scheme 1 could be.

This was obviously not a simple endeavor, and we were by no means the first to contemplate this problem. The goal of chemoselective peptide ligation had been outlined many years before us [6, 7]. The native chemical ligation had demonstrated that such peptide-forming ligations were indeed possible and had already begun to revolutionize the field of synthetic protein chemistry. A particularly clear and honest review by Kent published in 2000 outlined both the power and promise of native chemical ligation and highlighted the limitations [8]: the preparation of the fragments by solid-phase peptide synthesis and the requirement for a relatively rare and sometimes problematic cysteine residue at the ligation site.

When I began my first independent position in August 2003 at the University of California, Santa Barbara, we had two amide-forming projects in mind: (1) to devise an approach for catalytic, enantioselective peptide synthesis, which could potentially lower the cost and waste associated with classical solid-phase peptide synthesis, and (2) to develop a new peptide ligation that met or exceeded the specifications of the native chemical ligation. Both of these goals shared the same problem: the known mechanistic paradigms for amide formation were inadequate. Therefore, our first goal became the invention of mechanistically novel approaches to amide bond formation. This line of thinking led to two of the major lines of research in my group: (1) N-heterocyclic carbene-catalyzed generation of reactive intermediates (for an account of the new amide, ester, and C–C bond-forming reactions that this research program has led to, see [9]) and (2) the development of new amide-forming ligation reactions. This chapter will describe our discovery and development of the latter.

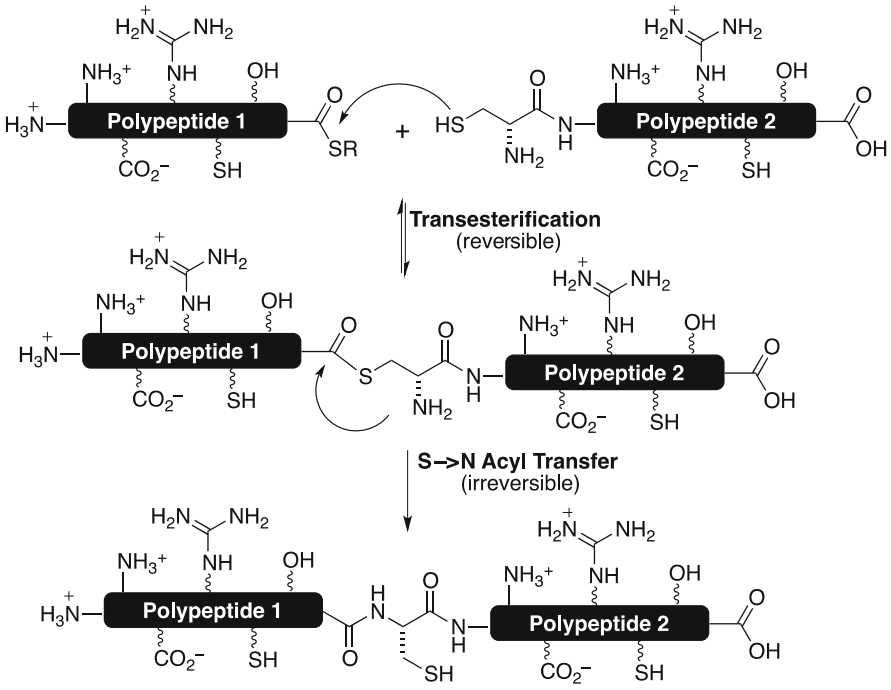

Scheme 2 The native chemical ligation (NCL) of C-terminal thioesters and peptides containing an N-terminal cysteine

3 The α-Ketoacid–Hydroxylamine (KAHA) Amide-Forming Ligation

The native chemical ligation, which is the chemical reaction that most closely meets the challenge set forth in Scheme 1, works because of the remarkably selective and reversible exchange of peptide thioesters under the reaction conditions (Scheme 2). When the thioester exchange occurs with the sulfur atom of an N-terminal cysteine residue, an irreversible migration can occur to give the amide bond. All of this occurs rapidly and in the presence of unprotected functional groups. The number of intermolecular organic reactions that proceed selectively, in water, and without reagents can be counted on one hand.

3.1 Invention of the KAHA Ligation

We began our efforts with one of these privileged reactions—oxime formation. It had long been recognized that the coupling of *O*-alkylhydroxylamines and aldehydes was rapid and selective, making it suitable for bioconjugation reactions (Scheme 3) [10]. Less well known is that *N*-alkylhydroxylamines also couple

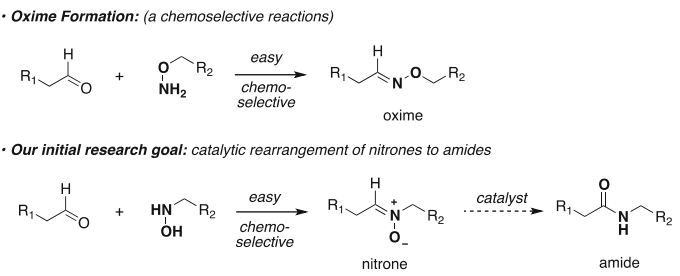

Scheme 3 The thinking behind our eventual development of the KAHA ligation. We recognized that nitrones, like oximes, are easily formed under aqueous, chemoselective conditions. We sought to selectively convert the unstable nitrone to the stable amide

rapidly with aldehydes to give nitrones. The reaction is reversible, but nitrone formation is often fast and selective [11]. This analysis led to our first idea: develop a catalyst for the rearrangement of nitrones to amides. This is a reaction that is known under photochemical conditions [12], but its low efficiency makes it unlikely to be useful for peptide ligation. We sought, instead, to find a catalyst or reagent to affect the conversion of the nitrone to the amide. The overall process is thermodynamically favored, and a number of reasonable mechanisms can be drawn. Despite our efforts, however, a suitable catalyst was never found—we still believe this would be a great transformation!

These investigations proved essential to our further thinking. In preparing various nitrones as substrates for catalytic rearrangement to amides, we learned a few important things about the chemistry of nitrones. First, we found that the formation of nitrones from *aldehydes* and *N*-alkylhydroxylamines is fast and selective. These two functional groups have a very high affinity for one another, and although the nitrone formation is reversible, the equilibrium lies completely on the side of nitrone (something that would come back to haunt us later). In contrast, the formation of nitrones from *ketones* had been reported to be slow, including one report that the equilibrium mixture favored the hemiaminal [13]. Second, we had used several oxidative nitrone formations including the work of Murahashi, who had reported the synthesis of nitrones by oxidative decarboxylation of amino acids [14] (Scheme 4).

These key precedents were combined, mentally at least, into an amide-forming reaction on a flight from Santa Barbara to Albuquerque, New Mexico, in November 2003. I hurried back a few days later to try out the reaction in the lab. Both α-ketoacids and hydroxylamines are commercially available, and it was simply a matter of mixing the two components together and looking for amide formation. We tried several solvents and on our first attempt found the desired amide product when CH_3CN was used (Scheme 5). The yield was not great, but it was undeniably a new reaction for amide formation. Most importantly, it did not require any reagents or catalysts, produced only water and CO_2 and by-products, and did not involve an activated carboxylic acid [15].

As anticipated from the chemistry of oxime and nitrone formation, we quickly found that the amide formation was remarkably chemoselective. Carboxylic acids,

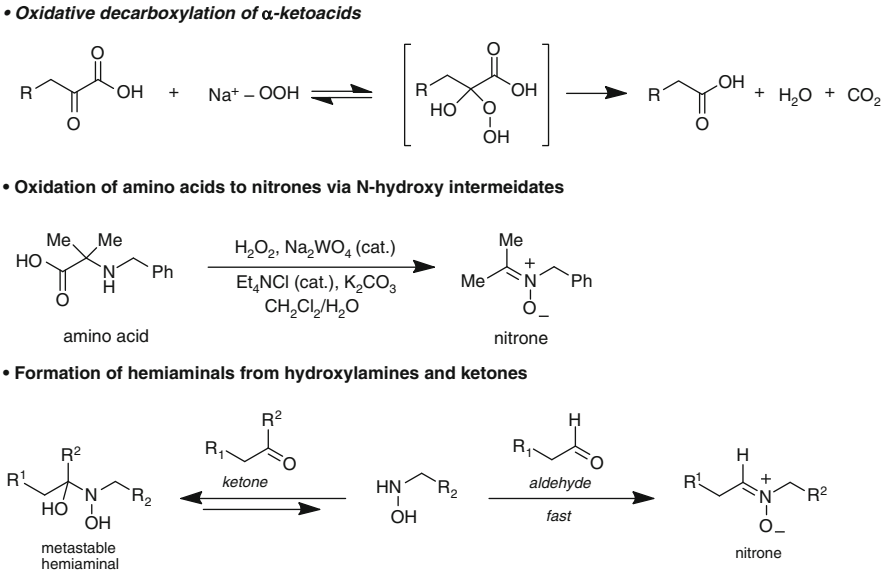

Scheme 4 Three key precedents for the design and invention of the KAHA ligation

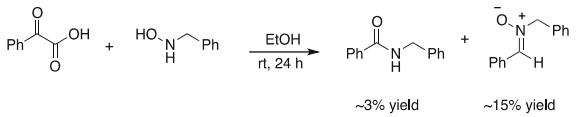

Scheme 5 Our first attempt at the KAHA ligation (December 2003)

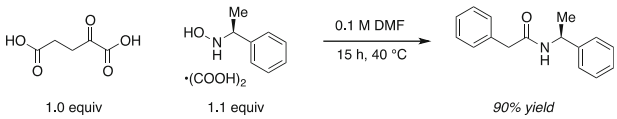

Scheme 6 Conditions for the formation of simple amides by KAHA ligation

amines, alcohols, and other functional groups did not disturb the amide formation. The amide formation proceeded best in polar, aprotic solvents such as DMF and DMSO, but nonpolar solvents suppressed the amide formation. Protic solvents such as MeOH and aqueous acids also worked well. The α-ketoacid and hydroxylamines could be used as their more easily handled salts, provided that the overall reaction was neutral or acidic. In all but a few cases, the amide ligations were remarkably clean. Years later, the "optimized" conditions for the formation of simple amides by KAHA ligation were published by Lei Ju in *Organic Synthesis* [16]. The experimental procedure is simply to combine an α-ketoacid and the salt of a hydroxylamine in DMF and warm to 40 °C (Scheme 6). After a few hours or overnight, removal of the solvent or extraction gives the amide products.

We were surprised—and perhaps a bit lucky—to discover that the KAHA amide formation was not a known reaction. Months of literature searching turned up only a single example of a something similar: the conversion of pyruvic acid to a hydroxyamic acid [17, 18]. Perhaps the unconventional reactivity of the reaction partners explains this. Formally, the highly electrophilic α-ketoacids acts as the "nucleophile" in the overall transformation. The nucleophilic hydroxylamine is the "electrophile" with the hydroxyl moiety as the leaving group. As we have learned over the years of studying this reaction and its starting materials, it is as if there is a parallel world of organic synthesis. For example, in many cases, we have found our chemistries work better in water, give higher yields in the presence of unprotected functional groups, and work most effectively on large molecules!

3.2 The KAHA Amide Formation as a General Peptide Ligation

At this point, we were faced with a strategic dilemma. The amide-forming reaction was interesting and novel, surely this merited publication in its own right. By the middle of 2004, we had done enough simple substrates and preliminary mechanistic investigations to prepare a communication. But we had not lost sight of our primary goal: a general peptide ligation that could be used to assemble proteins from constituent fragments. In our mind, establishing that the KAHA amide formation could be used for peptide ligation, at least in principle, was the necessary and appropriate step in its development. This was not only because of the importance of peptide ligation in general. We recognized that while the KAHA amide formation itself was simple, clean, and powerful, the starting materials were somewhat obscure; chemists were not going to synthesize α-ketoacids and hydroxylamines just to convert them into amides. In the context of peptide ligation, however, the syntheses of these functional groups might be justified or even transparently incorporated into the reagents or linkers used for solid-phase peptide synthesis. At this juncture we decided to put all of our efforts into applying the KAHA ligation to the chemoselective ligation of unprotected peptide fragments, and graduate student Ryan Fox joined the group to make this happen.

The strategy was now clear: we would demonstrate that the KAHA ligation could be used for the union of unprotected peptide fragments simply by mixing a peptide containing a C-terminal α-ketoacid with a peptide containing an N-terminal hydroxylamine amine. There was only one problem with this strategy: no one had ever made such compounds before! Furthermore, to be relevant to the field of peptide chemistry, we needed synthetic routes to these compounds that (1) could operate in the presence of all of the functional groups found in unprotected peptide side chains, (2) preserved the stereochemistry of the α-amino acid and did not epimerize, and (3) were compatible with Fmoc-based solid-phase peptide synthesis (Scheme 7). As we set out on this task, we did not fully appreciate what we were committing to.

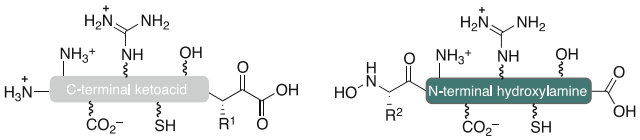

Scheme 7 Our new research goals: the synthesis of enantiopure, side-chain unprotected peptide α-ketoacids and hydroxylamines

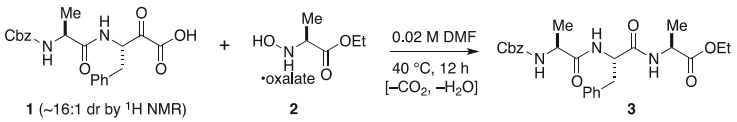

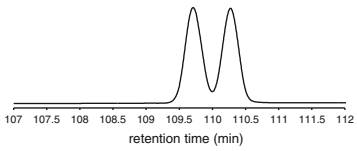

(b) HPLC chromatograph of *epi*-**3** prepared from Z-Ala-**D**/**L**-Phe-COCOOH.

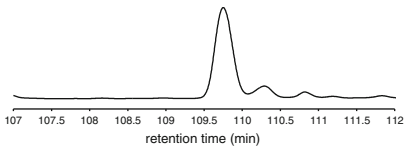

(b) HPLC chromatograph of **3** prepared by KAHA ligation with ketoacid **13** (Z-Ala-Phe-COCOOH, 16:1 dr).

Scheme 8 An early demonstration that enantiomerically enriched α-ketoacids do not epimerize under the conditions for the KAHA ligation. Actually synthesizing enantiopure peptide α-ketoacids is the real challenge

3.3 Chemoselective Synthesis of C-Terminal Peptide α-Ketoacids

The most important thing to recognize about α-ketoacids is that they are neither ketones nor carboxylic acids. Yes, they maintain some characteristics of these functional groups, but they have unique and often unpredictable chemistry of their own. For example, it is usually difficult to directly couple an α-ketoacid to an amine with standard coupling reagents.

An α-ketoacids does not always act like a ketone, but it still undeniably has ketone character. When complemented with an α-stereocenter, there is always the possibility of epimerization. Much of our early work on peptide ligation was spent establishing that the peptide α-ketoacids do not epimerize under the ligation conditions. Through laborious methods, we prepared a few model peptides to demonstrate that under the acidic conditions we preferred for the KAHA ligation, α-ketoacids were largely configurationally stable (Scheme 8). With a few exceptions, our years of experience with α-ketoacid confirm that they are configurationally and chemically stable when they are pure. Much to my surprise, my students found that the best way to do this is to first purify them by preparative HPLC. This is now common practice in our lab.

The actual synthesis of enantiopure α-ketoacids was the real challenge, and initially the best we could do was about 85% ee for protected dipeptides. There

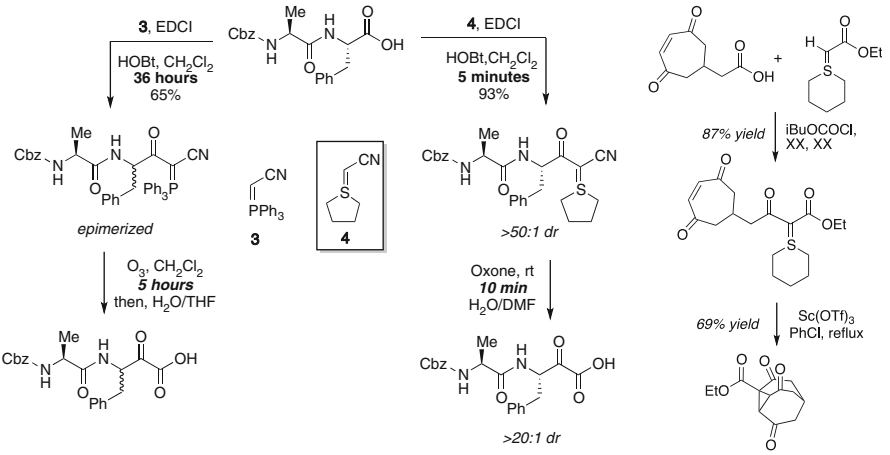

Scheme 9 Formation of alpha-ketoacids by oxidation of phosphorous and sulfur ylides. This work was inspired by sulfur ylide chemistry used in our synthesis of bullvalene

were almost no examples of peptide α-ketoacids and very few examples of enantioenriched α-ketoacids in general. The closest examples to our targets were the peptide α-ketoesters and α-ketoamides prepared by Wasserman using his elegant phosphonium ylide chemistry [19]. This chemistry initially looked very attractive for our purposes, especially as Rademann had reported a solid-supported variant that could be employed for solid-phase peptide synthesis [20]. This phosphorus chemistry was used for our first foray into ligations of α-peptides. But we quickly found serious problems.

First, with peptide monomers, the formation of the phosphonium ylides proceeded acceptably. But with larger peptides, the rate of coupling became intolerably slow, low yielding, and gave complete epimerization (Scheme 9a). We believed that this could be fixed by working on a solid support with routes that did not require transformation of the peptide C-terminus. Second, the larger problem was the conversion of the phosphorous ylide to the α-ketoacid. This required exhaustive ozonolysis, often requiring several hours of treatment with ozone at low temperatures followed by treatment with water. This difficult procedure could not be extended to larger peptides due to poor solubility and serious problems with epimerization.

A solution came from a completely different project in our group: the synthesis of shape-shifting, adaptive organic molecules [21, 22]. Alex Lippert, a graduate student, had devised as synthesis of oligosubstituted bullvalenes that featured and intramolecular cyclopropanation using a stabilized sulfur ylide (Scheme 9b). Unlike the phosphorous ylides, we had found the formation of the sulfur ylides to be fast and high yielding. We were pleased to find the same when we used peptide substrates and cyanosulfurylide **2**. Furthermore, Alex and another graduate student, Lei Ju, devised a procedure that used the easily handled sulfonium salt and standard peptide coupling conditions [23]. Most importantly, we found that the sulfur ylides

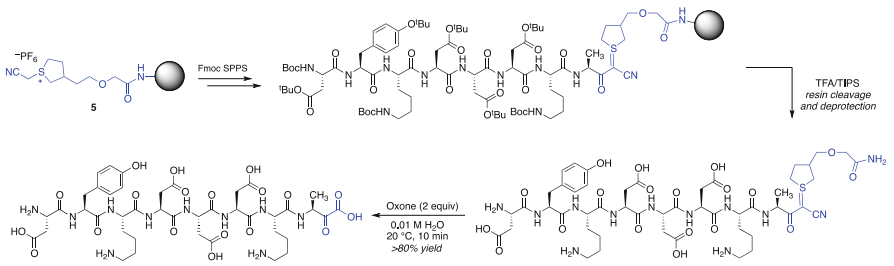

Scheme 10 Synthesis of C-terminal peptide α-ketoacids with solid-supported sulfur ylide linker **5**. This methodology has been routinely applied for the synthesis of unprotected α-ketoacids up to 35 residues long

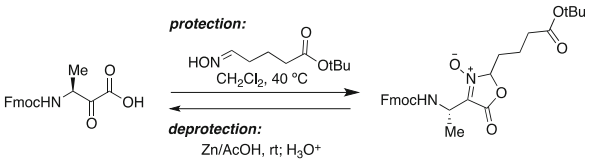

Scheme 11 Protection of α-ketoacids by direct annulations with oximes

were much more easily oxidized than their phosphorous counterparts. Exposure of fully unprotected C-terminal peptide sulfur ylides to aqueous Oxone in DMF gives the α-ketoacid within minutes. If there is a problem with this reaction, it is that it can be too fast and we often have to adjust the temperature and concentration to regulate the reaction times.

Lei went on to develop solid-supported sulfur ylide linker **5** that has become the standard practice in our group for preparing C-terminal peptide α-ketoacids (Scheme 10) [24]. Once the linker is loaded onto the resin, standard Fmoc-based solid-phase peptide synthesis can be used to grow peptide chains without difficulty. Deprotection and cleavage from the resin gives the fully unprotected peptide sulfur ylides that are easily handled and purified by standard methods. Exposure of these peptides to Oxone or DMDO gives the peptide α-ketoacids, which are usually isolated by preparative HPLC and lyophilized. Just one example out of many is shown in Scheme 10.

The oxidation of the sulfur ylides to the α-ketoacids is remarkable for its generality, functional group tolerance, and reliability. It is, however, an oxidative process and is not currently compatible with the sulfur-containing side chains cysteine and methionine. We have therefore devised other protecting groups for α-ketoacids such as cyclic nitrones (Scheme 11) [25]. Graduate student Melissa Flores found that α-ketoacids can be protected as cyclic nitrones by an unexpectedly facile cyclization with oximes. This and other strategies under development in our group can be used to prepare peptide α-ketoacids with methionine or cysteine residues. All of the enantiopure α-ketoacid starting materials, however, are prepared with sulfur ylide chemistry.

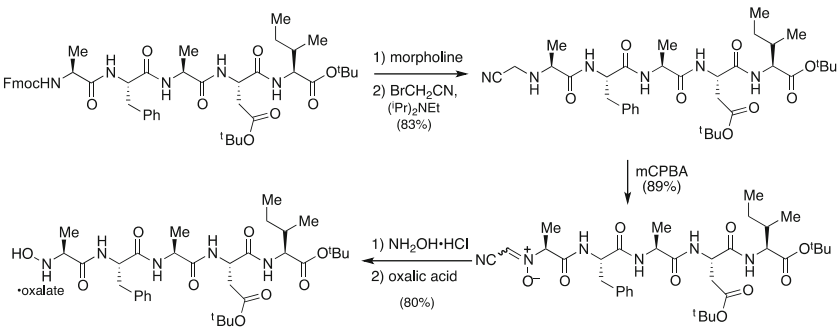

Scheme 12 Our original, inconvenient route to N-terminal peptide hydroxylamines by solution phase conversion of an N-terminal amine to the hydroxylamine

3.4 Synthesis of N-Terminal Peptide Hydroxylamines

When we first disclosed the KAHA ligation, the general sentiment was that making the α-ketoacids would be the major problem. In contrast, most chemists did not feel that the peptide hydroxylamines would present a serious obstacle. This intuition was supported by the literature. There were only a few scattered reports of peptide α-ketoacids but a respectable body of literature, including a *Chemical Reviews* article, on *N*-hydroxyamino acids and peptides [26].

We quickly found that the major problem was the identification of a suitable protecting group for the introduction of *N*-hydroxyamino acid monomers onto the end of a growing peptide chain. Like α-ketoacids, hydroxylamines are not simply the sum of their functional groups; they are not alcohols and are not amines. If anything they are the worst of both groups! They are susceptible both to oxidation and reduction, as well as elimination and epimerization. Standard amine protecting groups do not stay for long on the nitrogen atom, and if the nitrogen is suitably protected, the oxygen atom becomes difficult to mask.

In our early studies we avoided the issue by preparing short peptide fragments and converting the N-terminus to the hydroxylamine by a variation of Fukuyama's outstanding method (Scheme 12) [27, 28]. This was effective but not convenient. Following our first publication, we returned to the problem of peptide hydroxylamine synthesis.

The Fukuyama method was the most general and reliable approach to making peptide hydroxylamines. It suffered from two problems: (1) we had occasionally noted some epimerization during the three step process, and (2) it was rather long, synthetically involved, and not suitable for longer peptides. Diligent studies by Lei Ju and graduate student Irene Medina traced the epimerization to the "cyan-nitrone" intermediate. If this was hydrolyzed immediately, epimerization could be avoided. With some improvements, the Fukuyama method proved highly suited for the preparation of *N*-hydroxyamino acid monomers in enantiomerically pure form (Scheme 13). Introducing these monomers onto the end of a growing peptide,

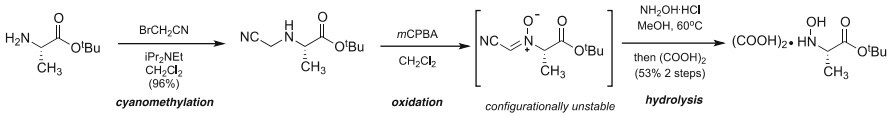

Scheme 13 Synthesis of enantiopure *N*-hydroxy α-amino acids with Fukuyama's method

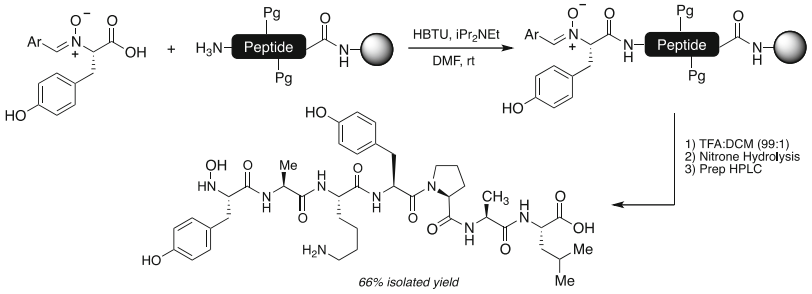

Scheme 14 Coupling of nitrone protected hydroxylamines to the N-terminus of a solid-supported peptide followed by resin cleavage and deprotection

however, initially proved to be problematic due to the failure of common protecting groups to mask the hydroxylamine.

An extensive survey of protection strategies suitable for protecting the hydroxylamine, coupling it to a solid-supported peptide under standard conditions, and cleavage after side-chain deprotection was undertaken. Most were unsuccessful but we eventually settled on the use of benzylidene nitrone protecting groups. This strategy had been reported by Bently and Brooks in 1976 but only with racemic hydroxylamines [29]. Based on our experience with the cyanonitrone intermediates in the Fukuyama protocol, we initially feared that these nitrones would not be configurationally stable. This fear proved unfounded and we were eventually able to prepare a number of benzylidene-protected peptide hydroxylamines and demonstrate their introduction into longer peptides. The nitrones had the advantage that they could be orthogonally deprotected in the presence of the side-chain protecting groups or left intact while acidic conditions removed the side-chain protecting groups without affecting the nitrone (Scheme 14). The nature and reactivity of the hydroxylamines made the formation and manipulation of these peptides the most challenging aspect of the ligation.

This protecting strategy led to another idea for hydroxylamine synthesis: a single reagent for the direct conversion of amines to hydroxylamines (Scheme 15). This fundamental transformation is essentially unknown, as most reagents lead to over oxidation of the initially formed hydroxylamine [30, 31]. A postdoctoral fellow, Dr. Takeo Fukuzumi, took on this challenge and designed bifunctional reagent 6 containing both an aldehyde and an oxaziridine [32]. An unprotected N-terminal amine can form an imine or hemiaminal with the aldehyde, which undergoes a subsequent intramolecular oxidation to give the hydroxylamine. This intermediate

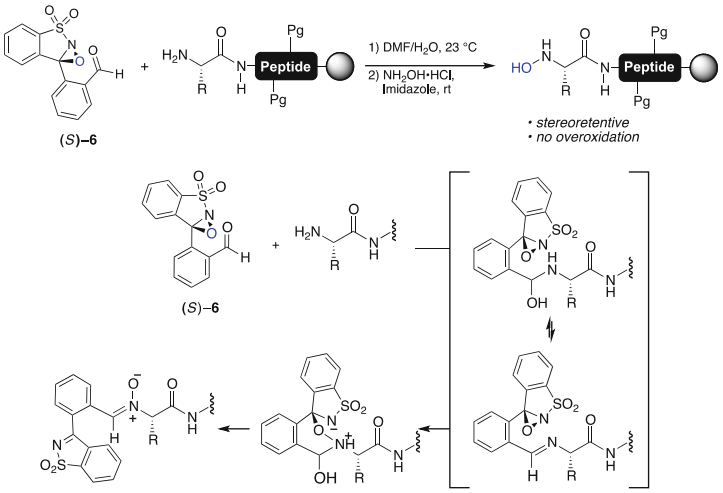

Scheme 15 An oxaziridine reagent for the oxidation of amines to hydroxylamines and a mechanistic proposal

forms the nitrone, protecting against further oxidation. A stereochemical mismatch between the racemic oxaziridine and the enantiopure peptides limits the synthetic utility of this reagent for peptides on larger scale, but the design principles are an excellent example of chemical problem solving and innovation.

3.5 KAHA Ligation for the Synthesis of Therapeutic Peptides: GLP-1

Shortly after our first publication on the KAHA ligation, we were approached by several companies interested in using this reaction for therapeutic peptide synthesis. This led to a collaboration with IPSEN/Biomeasure to test the KAHA ligation for the synthesis of human glucagon like peptide (GLP-1) and analogues, which were being developed as treatments for type II diabetes. IPSEN certainly had no trouble making the desired peptides, but as is often the case with therapeutic peptide synthesis, the purity of the final product was sometimes an issue and was not reproducible. We were asked if we could use our ligation to assemble two unprotected fragments to give the final product directly from the ligation.

At the time we took on this challenge, we had not yet developed our current methods for preparing the requisite N-terminal hydroxylamine or C-terminal α-ketoacids. If brought this problem today, it would take us no more than a few days to make the fragments and try the ligation. But in 2006 we had not yet even started doing solid-phase peptide synthesis in our laboratory!

Our first postdoc, Jian Wu, took on this project. Working in parallel on the GLP-1 fragments as well as and on general methods to prepare peptide hydroxylamines, Jian

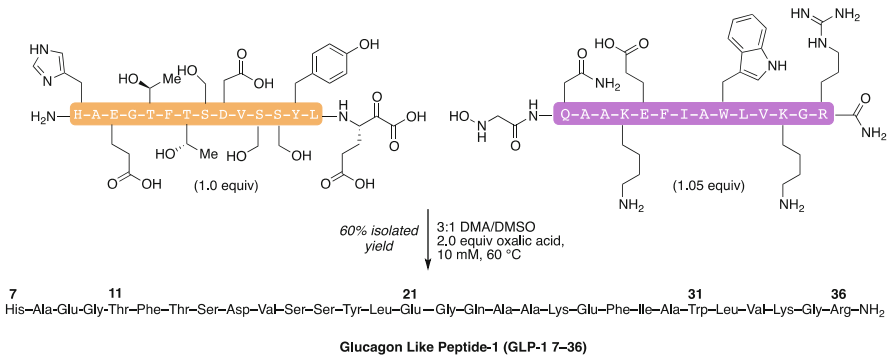

Scheme 16 Synthesis of human GLP-1 by KAHA ligation of two unprotected peptide fragments. This work demonstrated that the KAHA ligation has the potential to serve as a general peptide ligation strategy

used a side-chain glutamic acid to link a C-terminal sulfur ylide residue to the solid support and prepare the first fragment. The hydroxylamine fragment was prepared by displacement of a bromoacetyl peptide followed by deprotection and resin cleavage. At this point, another common problem in peptide chemistry arose: solubility. By careful experimentation, Jian was able to find a suitable solvent for both the ligation and the peptide and prepare GLP-1 from two completely unprotected fragments (Scheme 16) [33].

Jian's demonstration that larger, side-chain unprotected peptides that could be made by the KAHA ligation was a great encouragement. Several issues remained, but this was the first ligation of a fully unprotected peptide by a method other than native chemical ligation. A planned scale-up to gram quantities was unfortunately put on hold when the GLP-1 project was transferred from IPSEN to another company, but the support and patience of IPSEN was critical to advancing our experience and methodologies.

3.6 Cyclization of Unprotected Linear Peptides

The combination of our solid-phase methods for α-ketoacid and N-terminal hydroxylamine syntheses invited their application to the synthesis of macrocyclic peptides by the cyclization of side-chain unprotected linear peptides. Cyclic peptide is an important and rapidly growing area of new therapeutics, and novel methods for their facile preparation are in great demand. We reasoned that our methods could be used to prepare suitably functionalized linear peptides that should cyclize simply upon warming them in an appropriate solvent.

Takeo and Lei showed that it was indeed possible to use our methods for α-ketoacid and hydroxylamine synthesis to prepare several cyclic peptide natural products [34, 35]. No post-cyclization manipulations other than purification were required. The ability to perform the cyclization on unprotected side chains may

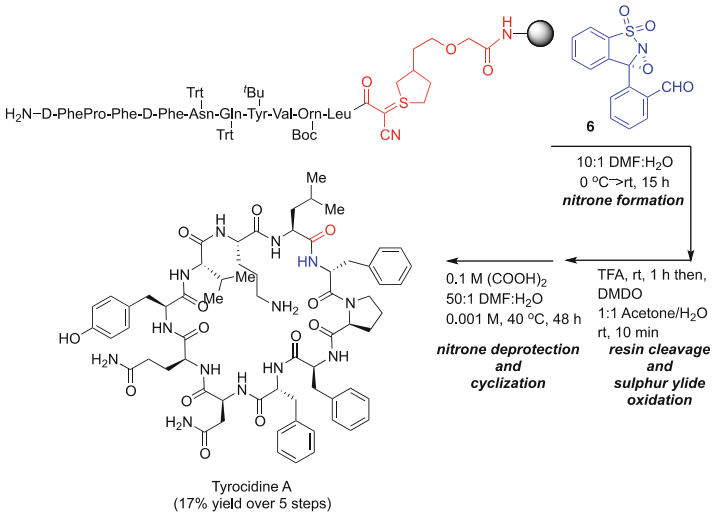

Scheme 17 Synthesis of peptide macrocycles by cyclization of unprotected linear peptides with the KAHA ligation

have advantages for difficult substrates where the protecting groups may interfere with the cyclization. It was even possible to use Takeo's hydroxylamine reagent to introduce the hydroxylamine (Scheme 17), suggesting that it is possible to prepare cyclic peptides simply by using the sulfur ylide linker and concluding the solid-phase synthesis with reagent **6**.

3.7 2010: A Critical Assessment of the KAHA Ligation

The end of 2009 brought the completion of our studies on the synthesis of α-ketoacids and N-terminal peptide hydroxylamines and our demonstration that the KAHA ligation could be applied to the synthesis of therapeutic peptides by the direct coupling of unprotected fragments as well as the macrocyclization of unprotected linear peptides. It also brought our second laboratory move in 3 years, this time from Philadelphia, USA, to Zürich, Switzerland. We left the USA having succeeded in our immediate goals: to develop Fmoc-compatible approaches to fully unprotected peptide fragments containing the requisite functional groups and their ligation to give medium-sized peptides.

Despite these successes, there were still problems. The preparation of the α-ketoacids was largely solved, although we have continued to work on specialized strategies for fragments containing sulfur atoms. The major problems resided with the hydroxylamines. The benzylidene nitrones were workable protecting groups but could be difficult to either remove or retain, depending on the peptide. Counterintuitively, smaller amino acid residues such as glycine and alanine were particularly challenging. Furthermore, these protecting groups were not kinetically stable and

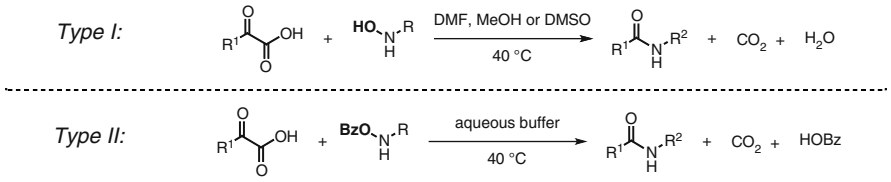

Scheme 18 The two prototypical types of the KAHA ligation. Type I ligations proceed with *O*-substituted hydroxylamines and prefer polar aprotic solvents. Type II ligations require *O*-substituted hydroxylamines and generally prefer water as the reaction solvent

could not be used for multiple segment condensations. Even in cases where we could not deprotect them, we found that they would undergo rapid exchange with other hydroxylamines. This prevented the sequential segment condensations that would be needed for synthesizing proteins. Even more problematic was the stability of the peptide hydroxylamines themselves. They were prone to oxidation, elimination, and disproportionation under the ligation conditions, and their purification could also be challenging. When the ligations failed, it was almost always due to the properties of the peptide hydroxylamine.

For reasons that we did not understand at the time, the ligation of α-ketoacids and *O*-unsubstituted hydroxylamines, which we now call type I ligations, occurred best in polar aprotic solvents such as DMSO or DMF (Scheme 18). Water was detrimental to the reaction rates and tended to accelerate the decomposition of the peptide hydroxylamine. In contrast, we had identified a number of other variants of the KAHA ligation with *O*-substituted hydroxylamines that occurred preferentially in water (type II ligations). Unfortunately, the most effective variants, *O*-Bz hydroxylamines, cannot be used for α-peptides due to facile elimination [36].

3.8 The Mechanism of the KAHA Ligation

The observation that different classes of hydroxylamines exhibited divergent behavior and reactivity coupled with the poor performance of the unsubstituted hydroxylamines in water prompted us to undertake a thorough investigation of the mechanism of the KAHA ligation. This work was started by one of our first new Ph.D. students at ETH-Zürich, Ivano Pusterla. Through a combination of kinetics, intermediate synthesis, and especially isotopic labeling studies, Ivano quickly realized that the KAHA ligation did not have a simple mechanism. Most surprisingly, KAHA ligations performed in ^{18}O–H_2O did not give any labeled amide products. After a laborious synthesis of ^{18}O-labeled hydroxylamine, Ivano found almost complete label transfer from the oxygen of the hydroxylamine into the oxygen of amide (Scheme 19)!

This unexpected result required a complete reevaluation of the mechanism. To make a long story short, we found that a key intermediate is an oxaziridine and

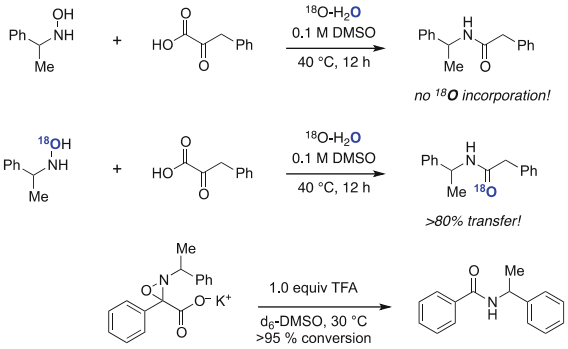

Scheme 19 Mechanistic investigations of the KAHA ligation ^{18}O-isotope labels and conversion of oxaziridine acids to amides

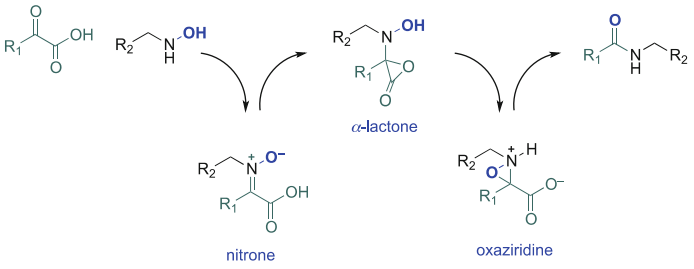

Scheme 20 The "three-ring circus" mechanism for the type I KAHA ligation. We were very surprised to find that the oxaziridine is involved in the amide formation

that it must arise by rearrangement of the nitrone. The full details of the mechanism were recently published. The overview of our "three-ring circus" mechanism for the type I KAHA ligations is shown in Scheme 20. The type II ligations proceed by a different mechanism, and efforts to elucidate this are currently underway.

Our mechanistic studies on the KAHA ligation taught us several important lessons. First, it showed us very clearly why water was detrimental for the type I ligations. The formation of the nitrone, which is slowed in the presence of water, is essential. We had long believed that the nitrone was an unproductive pathway that deterred amide formation. We had even thrown out ligation reactions when we observed the formation of the nitrone! Only with hindsight did we learn that leaving such reactions alone leads to good conversion to the amide. Second, this experience reinforced the idea that mechanistic studies are essential to progress in challenging areas. We have performed extensive mechanistic investigations on our NHC-catalyzed reactions [37]. With the KAHA ligation we had put our initial studies on simple asides aside in favor of learning how to build the complex, unprotected peptide fragments more relevant to the applications. In retrospect we should have worked on the mechanism earlier. The discovery of how the type I

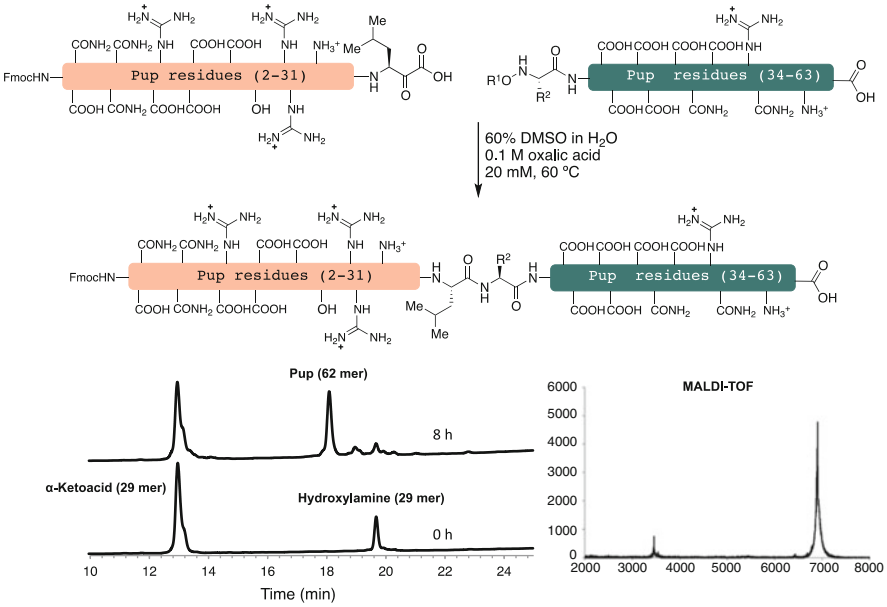

Scheme 21 Protein synthesis with the KAHA ligation

ligation works and the implicit limitations has already helped us advance the KAHA ligation much further.

3.9 The Next Steps . . . Protein Synthesis by KAHA Ligation

The realization that the use of *O*-unsubstituted hydroxylamines would preclude the aqueous conditions needed for most protein and large peptide synthesis set off a flurry of activity in our labs. Postdoc Vijay Pattabiraman and graduate student Ayo Ogunkoya began looking for a type II ligation of α-peptide substrates. The challenge here is that the obvious substrates, the *O*-acylated peptide hydroxylamines, are unstable toward elimination. The *O*-alkyl hydroxylamines generally require high reactant concentrations and long reaction times that are not suitable for peptide and protein synthesis. Just when it looked like we would never find a suitable approach, Ayo and Vijay came through with a fantastic solution. This will be published shortly, but as a preview, we can show the synthesis of Pup, a small ubiquitin-like protein, by direct ligation of two unprotected sequences (Scheme 21).

Based on this approach, Ayo and Vijay have already synthesized several other proteins. Finally, we are nearing our stated goal of protein synthesis by simply preparing modestly sized (approximately 30 residue) fragments with solid-phase peptide synthesis followed by complete deprotection and direct ligation. The next steps will be to apply this to much larger systems.

4 Outlook and Expectations

I sometimes tell my students that good science starts when no one knows how to do something. The project of "reinventing amide bond formation" has, by this measure, been a fantastic generator of good science. The first examples of the KAHA amide synthesis were achieved with nothing more than mixing commercially available chemicals together. Yet going forward and taking advantage of the real power of this reaction required the establishment of new synthetic and analytical techniques that have kept us busy for years. It has led to moments of great success, such as our first chemoselective peptide ligation and the generation of enantiopure α-ketoacids, but also enormous frustration. The perseverance and creativity of my students have finally allowed us to develop the KAHA ligation into a viable reaction for protein synthesis. The story of this reaction is just beginning.

Chemical protein synthesis has benefited from two revolutions in the last 50 years: solid-phase peptide synthesis and the native chemical ligation. Both of these advances have brought the field forward, but both have inherent limits. It seems unlikely that solid-phase peptide synthesis will ever allow the facile, routine preparation of peptides longer than 50 residues. Native chemical ligation is a fantastic tool for protein synthesis, but its strict requirements limit its application in many context. The field of synthetic peptide chemistry has progressed from the synthesis of a dipeptide by Fischer in 1902 [38] to the synthesis of the 200+-mer proteins by Kent and others in the 1990s. But put another way, the field has progress at the rate of about two amino residues/year. Without new reactions and concepts for chemical protein synthesis, it will still be many years before we can prepare proteins such as *taq* polymerase! The bacterial ribosome, on the other hand, can produce an 800-mer protein in less than 10 min! Clearly, the field of chemical protein synthesis and amide bond formation still has a long way to go [39]. We hope that the continued development of the KAHA ligation will be one way to overcome the asymptotic limits inherent to the current approach to peptide synthesis.

The KAHA ligation also has applications beyond the synthesis of peptide and proteins. It is a very rare example of a reaction that exhibits "absolute chemoselectivity" and does not require any reagents or catalysts. We are exploiting these unique properties for many different applications including small molecule and macrocycle synthesis, polymerization and oligomerization reactions, and site-specific labeling. In all of these endeavors, the major challenges remain the synthesis and incorporation of the key functional groups. Improvements in this demand continued innovation and creativity in the synthesis of organic molecules and the development of new reactions.

References

1. Merrifield RB (1963) Solid phase peptide synthesis. I. The synthesis of a tetrapeptide. J Am Chem Soc 85:2149–2154
2. Coin I, Beyermann M, Bienert M (2007) Solid-phase peptide synthesis: from standard procedures to the synthesis of difficult sequences. Nat Protocols 2:3247–3256

3. Latham P (1999) Therapeutic peptides revisited. Nat Biotechnol 17:755–757
4. Dawson PE, Muir TW, Clarklewis I, Kent SBH (1994) Synthesis of proteins by native chemical ligation. Science 266:776–779
5. Fields GB, Lauer-Fields JL, Liu R, Barany G (2002) In: Grant GA (ed) Synthetic peptides: a user's guide, 2nd edn. Oxford University Press, New York, pp 93–219
6. Kemp DS (1981) The amine capture strategy for peptide bond formation – an outline of progress. Biopolymers 20:1793–1804
7. Kemp DS, Carey RI (1993) Synthesis of a 39-peptide and a 25-peptide by thiol capture ligations: observation of a 40-fold rate acceleration of the intramolecular O,N-acyl-transfer reaction between peptide fragments bearing only cysteine protective group. J Org Chem 58:2216–2222
8. Dawson PE, Kent SBH (2000) Synthesis of native proteins by chemical ligation. Annu Rev Biochem 69:923–960
9. Chiang PC, Bode JW (2011) N-mesityl substituted chiral triazolium salts: opening a new world of N-heterocyclic carbene catalysis. TCI MAIL 149:2–17
10. Shao J, Tam JP (1995) Unprotected peptides as building blocks for the synthesis of peptide dendrimers with oxime, hydrazone, and thiazolidine linkages. J Am Chem Soc 117:3893–3899
11. Turega SM, Lorenz C, Sadownik JW, Philip D (2008) Target-driven selection in a dynamic nitrone library. Chem Commun 34:4076–4078
12. Splitter JS, Calvin M (1958) Preparation of oxaziranes by irradiation of nitrones. J Org Chem 23:651–651
13. Ishikawa T, Nagai K, Senzaki M, Tatsukawa A, Saito S (1998) Hemiaminai generated by hydration of ketone-based nitrone as an N,O-centered nucleophile in organic synthesis. Tetrahedron 54:2433–2448
14. Murahashi SI, Imada Y, Ohtake H (1994) Tungstate-catalyzed decarboxylative oxidation of N-alkyl-α-amino acids: an efficient method for regioselective synthesis of nitrones. J Org Chem 59:6170–6172
15. Bode JW, Fox RM, Baucom KD (2006) Chemoselective amide ligations by decarboxylative condensations of *N*-alkylhydroxylamines and *alpha*-ketoacids. Angew Chem Int Ed 45:1248–1252
16. Ju L, Bode JW (2010) Amide formation by decarboxylative condensation of hydroxylamines and alpha-ketoacids: synthesis of N-[(1S)-1-phenylethyl]-benzeneacetamide. Organic Synth 87:218–225
17. Tanasescu I, Ruse M (1959) Einwirkung von para-Nitroso-dimethylanilin auf Brenztraubensaure und ihre Derivate. Chem Ber 92:1265–1269
18. Corvett MD, Corbett BR (1980) Reaction of nitroso aromatics with glyoxylic acid. A new path to hydroxamic acids. J Org Chem 45:2834–2839
19. Wasserman HH, Ho WB (1994) (Cyanomethylene)phosphoranes as novel carbonyl 1,1-dipole synthons: an efficient synthesis of α-keto acids, esters, and amides. J Org Chem 59:4364–4366
20. Weik S, Rademann J (2003) A phosphorane as supported acylanion equivalent: linker reagents for smooth and Versatile C–C coupling reactions. Angew Chem Int Ed 42:2491–2494
21. Lippert AR, Kaeobamrung J, Bode JW (2006) Synthesis of oligosubstituted bullvalones: shapeshifting molecules under basic conditions. J Am Chem Soc 128:14738–14739
22. Lippert AR, Naganawa A, Keleshian V, Bode JW (2010) Synthesis of phototrappable shapeshifting molecules for adaptive guest binding. J Am Chem Soc 132:15790–15799
23. Ju L, Lippert AL, Bode JW (2008) Stereoretentive synthesis of C-terminal peptide α-ketoacids for chemoselective amide-forming ligation reactions. J Am Chem Soc 130:4253–4255
24. Ju L, Bode JW (2009) A general strategy for the preparation of C-terminal peptide alpha-ketoacids by solid phase peptide synthesis. Org Biomol Chem 7:2259–2264
25. Flores MA, Bode JW (2010) Chemoselective protection of alpha-ketoacids by direct annulations with oximes. Org Lett 12:1924–1927
26. Ottenheijm HCJ, Herscheid JDM (1986) N-hydroxy-α-amino acids in organic chemistry. Chem Rev 86:697–707

27. Tokuyama H, Kuboyama T, Amano A, Yamashita T, Fukuyama T (2000) A novel transformation of primary amines to *N*-monoalkylhydroxylamines. Synthesis 9:1299–1304
28. Tokuyama H, Kuboyama T, Fukuyama T (2003) Transformation of primary amines to *N*-monoalkylhydroxylamines: *N*-hydroxy-(S)-1-phenylethylamine oxalate. Org Synth 80:207–212
29. Bentley PH, Brooks G (1976) Semi-synthetic penicillins and cephalosporins incorporating a hydroxyamino group. Tetrahedron Lett 17:3735–3738
30. Field JD, Kropp PJ (2000) Surface-mediated reactions. 9. Selective oxidation of primary and secondary amines to hydroxylamine. J Org Chem 65:5937–5941
31. Wittman MD, Halcomb RL, Danishefsky SJ (1990) On the conversion of biologically interesting amines to hydroxylamines. J Org Chem 55:1981–1983
32. Fukuzumi T, Bode JW (2009) A reagent for the convenient, solid phase synthesis of N-terminal peptide hydroxylamines for chemoselective ligations. J Am Chem Soc 131:3864–3865
33. Wu J, Ruiz-Rodríguez J, Comstock JM, Dong JZ, Bode JW (2011) Synthesis of human GLP-1 (7–36) by chemoselective α-ketoacid- hydroxylamine peptide ligation of unprotected fragments. Chem Sci 2:1976–1979
34. Fukuzumi T, Ju L, Bode JW (2012) Chemoselective cyclization of unprotected linear peptides by alpha-ketoacid–hydroxylamine amide-ligation. Org Biomol Chem 10: 5837–5844
35. Huang YL, Frey R, Juarez-Garcia ME, Bode JW (2012) Synthesis of aza-surfactin and 3-epi-aza-surfactin. Heterocycles 84:1179–1191
36. Knowles DA, Mathews CH, Tomkinson NCO (2008) Oxidation of primary amines to ketones. Synlett 18:2769–2772
37. Mahatthananchai J, Zheng P, Bode JW (2011) Observation and mechanistic investigation of α,β-unsaturated acyl azoliums from N-heterocyclic carbene catalyzed reactions. Angew Chem Int Ed 50:1673–1677
38. Fischer E (1902) Chem. Z. 26:S.939f
39. Pattabiramin V, Bode JW (2011) Rethinking amide-bond formation. Nature 430:471–479

Top Organomet Chem (2013) 44: 35–54
DOI: 10.1007/3418_2012_42

Published online: 18 August 2012

Catalytic Transformations Involving the Activation of sp^2 Carbon–Oxygen Bonds

Mamoru Tobisu and Naoto Chatani

Abstract This review describes transition metal-catalyzed transformations of conventionally unemployed C(sp^2)–O bonds, specifically those of aryl and alkenyl ethers, carboxylates, and carbamates. Nickel-based catalysts are among the most intensively studied in this context, allowing for direct coupling using phenol- and enol-derived electrophiles. Reactions using other metals (Ru, Fe, and Rh) are also presented. The synthetic utility of these C–O bond activation reactions is illustrated in the synthesis of several elaborated molecules, especially through the orthogonal cross-couplings and oxygen-directed functionalization/C–O activation tandem.

Keywords Amination · Carbon–oxygen bond activation · Cross-coupling · Nickel · Reductive deoxygenation · Ruthenium

Contents

M. Tobisu (✉) and N. Chatani (✉)
Department of Applied Chemistry, Graduate School of Engineering, Osaka University, Suita Osaka 565-0871, Japan
e-mail: tobisu@chem.eng.osaka-u.ac.jp; chatani@chem.eng.osaka-u.ac.jp

1 Introduction

Chemical synthesis has been revolutionized by the invention of transition metal-catalyzed aromatic substitution reactions of aryl halides (Eq. (1), X = I, Br, Cl) [1]. Among the most powerful are the catalytic cross-couplings wherein organometallic reagents are used as a nucleophilic partner and have emerged as a reliable tool to introduce carbon-based fragments onto an aromatic ring [2, 3]. The importance of this class of catalytic transformations was recognized by the awarding of the 2010 Nobel Prize in chemistry to Akira Suzuki, Ei-ichi Negishi, and Richard Heck "for palladium-catalyzed cross-couplings in organic synthesis." The utility of the cross-coupling reactions has further been expanded by applying heteroatom-centered nucleophiles, such as amines and alcohols [4, 5].

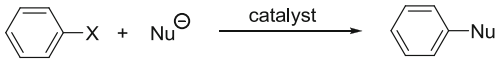

(1)

X = I, Br, Cl, OSO_2CF_3, OSO_2Me, OSO_2Ph, **OCOR'**, **OMe**, **OH**, etc.

nucleophile = RMgX, $RSnR'_3$, $RZnX$, $RB(OH)_2$, $RSiR'_3$, amine, alcohol, etc.

The catalytic aromatic substitution of aryl halides is enabled by the capability of transition metal complexes to activate C(aryl)–halogen bonds, which are classically considered unreactive, through oxidative addition. If phenol derivatives can be used as electrophilic components in place of aryl halides through the activation of C(aryl)–oxygen bonds, several advantages are expected. First, a diverse array of phenol derivatives are far more readily available compared to aryl halides, since many of them are naturally abundant [6, 7]. Second, replacing aryl halides with corresponding phenol derivatives avoids the potential toxicity associated with organic halides and thus leads to a more environmentally benign process. Despite these advantages, cross-coupling of phenol derivatives is not straightforward, unlike that of aryl halides, due to the reluctance of C(aryl)–OH bonds toward oxidative addition. Thus, conversion of a phenolic hydroxyl group into a better leaving group is normally required for the reactions to proceed. Triflates (OSO_2CF_3, OTf) are among the most widely used for this purpose [8]. However, the following drawbacks make triflates far from ideal coupling partners: (1) aryl triflates are prone to decomposition by moisture and heat, (2) the large mass of the leaving fragment (OTf = 149; Br = 80; Cl = 35.5) makes the cross-coupling less atom economical, and (3) costly and corrosive Tf_2O is required for their preparation. Although some improvements were accomplished by employing relatively robust sulfonates, such as tosylates (OSO_2(*p*-tolyl), OTs) and mesylates (OSO_2CH_3, OMs), or phosphates, recent efforts in this field have been directed toward the development of cross-couplings of more versatile phenol derivatives, such as aryl ethers, carboxylates, and carbamates [9–11]. Despite apparent advantages, the inertness of the C(aryl)–O bonds in these classes of compounds poses a formidable challenge when applied to catalytic transformation.

This chapter describes recent advances in transition metal-catalyzed cross-couplings involving the cleavage of C(sp^2)–O bonds in non-sulfonylated phenol and enol derivatives. The chapter is divided into three main sections: The first details the most intensively studied nickel-based catalyst system. The second deals with C–O bond transformations using metals other than nickel. Finally, the last section describes several examples that exemplify the potential utility of these classes of cross-coupling reactions.

2 Nickel-Catalyzed Carbon–Oxygen Bond Transformations

2.1 Cross-Coupling Reactions with Organometallic Reagents

In 1979 Wenkert reported the cross-coupling reaction of alkenyl methyl ethers with phenyl and methyl magnesium halides via the activation of C(sp^2)–OMe bonds by using $NiCl_2(PPh_3)_2$ as a catalyst precursor [Eq. (2)] [12, 13]. This alkenyl ether cross-coupling was further extended to silyl enol ethers [14] and cyclic ethers, such as dihydrofurans [15–23], which offer a unique method for the stereoselective construction of alkenes (see Sect. 4).

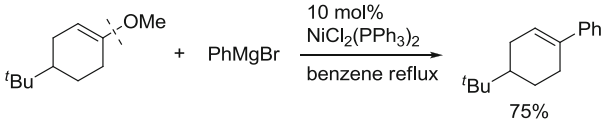

(2)

Although less successful, several aryl methyl ethers were also shown to be cross-coupled under these conditions [Eq. (3)] [12, 13]. However, at that time this intriguing finding at the dawn of the age of cross-coupling reactions did not attract significant attention from synthetic chemists, presumably because subsequently reported triflates proved to exhibit much higher reactivity and have since occupied a central position as phenolic coupling partners [8]. A special class of heteroaryl ethers was also reported to serve as non-sulfonylated phenolic electrophiles in nickel-catalyzed cross-coupling reactions [24, 25].

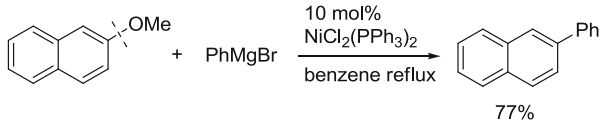

(3)

Guided by advances made in the late 1990s with respect to ligand design in cross-coupling reactions, in 2004 Dankwardt established a modified catalyst system for Wenkert's reaction [Eq. (4)] [26]. The scope of aryl ethers has significantly

expanded by the implementation of PCy_3 (PCy_3 is known as an effective ligand in palladium-catalyzed cross-couplings [27]) and $PPhCy_2$ ligands. A range of alkoxy groups, including trimethylsiloxy, can be substituted by an aryl group derived from Grignard reagents. Various anisole derivatives, as well as alkoxy-substituted heterocycles, efficiently afford the (hetero)biaryls. Later, Shi applied this catalyst system to the methylation of aromatic [28] and benzylic [29] ethers using MeMgX. Quite recently, Jarvo extended the methylation reaction to secondary benzylic ethers, wherein complete inversion of stereochemistry was observed [30].

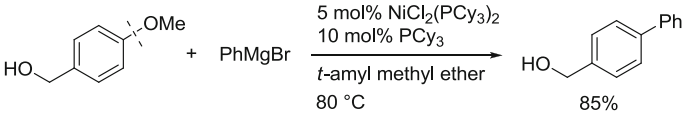

(4)

The report by Dankwardt clearly indicated that a low-valent nickel complex ligated by a bulky electron-rich phosphine can activate the inert C(aryl)–O bonds in aryl ethers probably through oxidative addition. Accordingly, it is expected that aromatic substitution by nucleophiles other than Grignard reagents could proceed via nickel-mediated C(aryl)–O bond activation. On the basis of this consideration, our group established the cross-coupling reaction of aryl methyl ethers with organoboron reagents under Ni(0)/PCy_3 catalysis [Eq. (5)] [31]. Protected boronic acids and a suitable base, such as CsF, were required for efficient coupling. In contrast to cross-coupling using Grignard reagents, ketones and esters survived under these conditions. The reactivity of Ar–OMe bonds in this Suzuki–Miyaura-type reaction was highly dependent on the structure of the Ar groups: fused aromatics (i.e., naphthalenes, phenanthrenes, etc.) produced biaryl products in good yields, while anisole derivatives delivered the corresponding product only when they contained electron-withdrawing groups. The reactivity difference between substrates allowed for selective activation of a C–OMe bond of naphthalene derivatives in the presence of an anisole moiety [see, the last example in Eq. (5)]. The catalyst system was successfully applied to alkenyl methyl ethers [32].

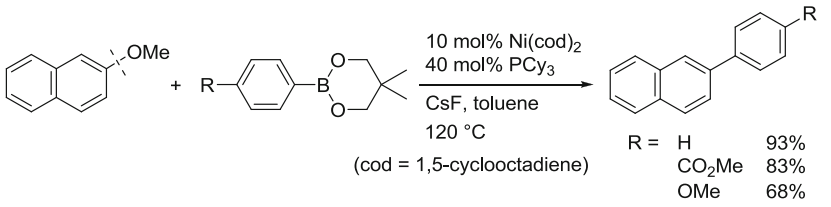

(5)

Following our report in 2008, a number of reports on nickel-catalyzed cross-couplings of non-sulfonylated phenolic electrophiles have appeared. They are summarized in Table 1.

Aryl carboxylates (or acylated phenol derivatives) represent another class of ideal coupling partners due to their accessibility. C(aryl)–O bonds of aryl

Table 1 Cross-coupling of aryl carboxylates and carbamates

Year	Author	Substrate	Nucleophile	Catalyst system	Reference
1992	Snieckus		RMgCl	$Ni(acac)_2$[a]	[44]
2008	Garg		$Ar'B(OH)_2$	$NiCl_2(PCy_3)_2$ K_3PO_4	[37]
2008	Shi	 (R = Me, ^{t}Bu, Ph)	$(Ar'BO)_3$ + $0.88H_2O$	$NiCl_2(PCy_3)_2$ K_3PO_4	[38]
2008	Shi		Ar′ZnCl	$NiCl_2(PCy_3)_2$	[41]
2009	Nakamura		Ar′MgX	$Ni(acac)_2$[a] hydroxyphosphine[b]	[45]
2009	Garg		$Ar'B(OH)_2$	$NiCl_2(PCy_3)_2$ K_3PO_4	[46]
2009	Snieckus		$Ar'B(OH)_2$ + $0.1(Ar'BO)_3$	$NiCl_2(PCy_3)_2$ $PCy_3{\cdot}HBF_4$ K_3PO_4	[47]
2009	Shi	 	R′MgCl	$FeCl_2$ SIMes·HCl[c]	[77]
2010	Shi		$(Ar'BO)_3$ + $1.0H_2O$	$NiCl_2(PCy_3)_2$ PCy_3 K_2CO_3	[48]
2010	Molander	 	$Ar'BF_3K$ + H_2O	$Ni(cod)_2$ $PCy_3{\cdot}HBF_4$ K_3PO_4	[50]

[a]Acetyl acetonate

[b] 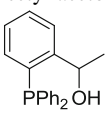

[c] 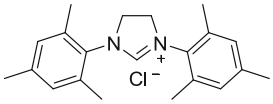

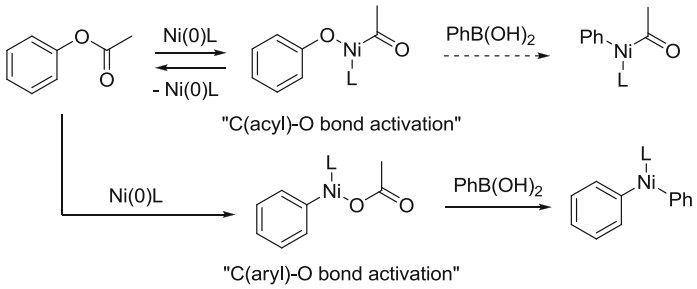

Scheme 1 Selectivity in C–O activation of aryl carboxylates

carboxylates are expected to be activated in a more facile manner than those of aryl methyl ethers since an electron-withdrawing acyl group renders an aromatic ring more electron deficient, which leads to a strengthening of the interaction with an electron-rich Ni(0)/L. However, when using aryl carboxylates, a selectivity issue arises. In addition to a C(aryl)–O bond, a C(acyl)–O bond could be activated by a nickel complex (Scheme 1). Comparison of the bond dissociation energies predicts that undesired C(acyl)–O bond cleavage would be more favorable (106 kcal/mol for C(aryl)–O bond fission vs. 80 kcal/mol for C(acyl)–O bond fission). Indeed, an early study by Yamamoto reported that the stoichiometric reactions of Ni(0)/phosphine with phenyl acetate implied that both modes of C–O activation could occur depending on the phosphine used [33] (our works on the catalytic activation of C(acyl)–O bonds [34–36]).

Garg and Shi simultaneously addressed the selectivity issue with nickel-catalyzed cross-coupling of aryl carboxylates using organoboron reagents. Garg's group identified boronic acids as suitable nucleophiles and pivalates as optimal substrates [37]. On the other hand, Shi's protocol used aryl boroxines and a 0.88 equivalent of water, which allowed for the cross-coupling of acetates, pivalates, and benzoates [38] (for the use of C–O bonds in *alkenyl* acetate, see [39]). In each method, a substantially wider scope of substrates was observed compared to aryl methyl ethers; phenyl and naphthyl carboxylates are both applicable. A computational study by Liu provides a rationale for the selectivity between C(aryl)–O and C(acyl)–O bond cleavage (Scheme 1) [40]. The C(acyl)–O bond undergoes oxidative addition in a relatively facile manner, and the process is reversible. However, the subsequent transmetalation between Ac–Ni–OAr and the organoboron reagent is energetically prohibited. In contrast, although oxidative addition of the C(aryl)–O bond is less favorable, the transmetalation of the resultant Ph–Ni–OAc is a feasible process, thus producing the desired product. Shi demonstrated that the same nickel catalyst also facilitates the cross-coupling of aryl and alkenyl pivalates with arylzinc halides [41].

The carboxylate cross-coupling was further extended to aryl carbamate substrates. Early examples of carbamates as electrophilic coupling partners were reported by Kocienski and Dixon (enol carbamates) [42, 43] and Snieckus (aryl carbamates) [44] around 1990 using Grignard reagents. In 2009 Nakamura developed a unique

hydroxyphosphine ligand that can affect a Kumada–Tamao–Corriu-type reaction of aryl carbamates through nickel/magnesium bimetallic C–O bond activation [45]. On the other hand, organoboron-based cross-coupling has been accomplished independently by Garg [46], Snieckus [47], and Shi [48]. Aryl carbonates were also shown to be effective electrophiles by Garg's group [46]. Controlling the amount of water present is supposedly crucial for an efficient catalysis [49]. Recently, Molander reported a nickel-catalyzed cross-coupling reaction of aryl pivalates and carbamates using aryltrifluoroborate salts as a nucleophile [50].

The use of carboxylates and carbamates as coupling partners allows for new strategies for regioselective synthesis of poly-substituted arenes on the basis of the ortho-directed ability of these functionalities (see Sect. 4).

As described thus far, recent studies established aryl ethers, carboxylates, and carbamates as readily available and cost-effective electrophiles in nickel-catalyzed cross-coupling reactions. However, the ideal partner along this line is phenol itself, although the large activation barrier for Ar–OH bonds makes such a process unlikely to occur. Nevertheless, Shi disclosed that naphthols were directly cross-coupled with Grignard reagents to furnish the biaryl products under nickel catalysis [Eq. (6)] [51]. The in situ-formed magnesium salt of naphthol, which is crystallographically characterized, was proposed to be essential for the key C–O bond activation. For comparison, the use of the corresponding lithium and potassium salts of naphthols significantly lowered the yield.

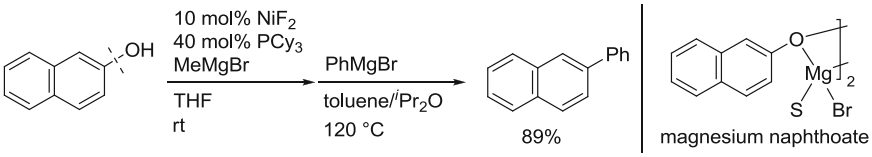

(6)

Organoboron reagents can also be used in the cross-coupling of naphthols in the presence of a stoichiometric amount of BEt_3 [Eq. (7)] [52]. Although these naphthol activation methods are currently inapplicable to phenols, these results promise future development of the direct cross-couplings of C(aryl)–OH bonds.

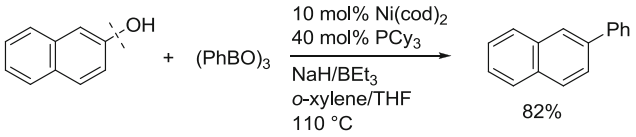

(7)

2.2 Other Reactions

Compared to the development of C–C bond formation reactions using organometallic reagents, other types of transformations through the C(sp^2)–O bond cleavage lag behind.

Our group reported a nickel-catalyzed C–N bond formation reaction of aryl methyl ethers using secondary amines [Eq. (8)] [53]. An *N*-heterocyclic carbene ligand was proven to be optimal for the amination reaction, although PCy_3 has been identified as a privileged ligand in nickel-mediated C(aryl)–O bond activation, as described in the previous section. Since the reaction did not proceed in the absence of the catalyst, a classical nucleophilic aromatic substitution mechanism is not operating in this reaction. Heteroaryl methyl ethers, such as methoxypyridines, also undergo these amination reactions efficiently to deliver a medicinally important aminated *N*-heteroarenes [54].

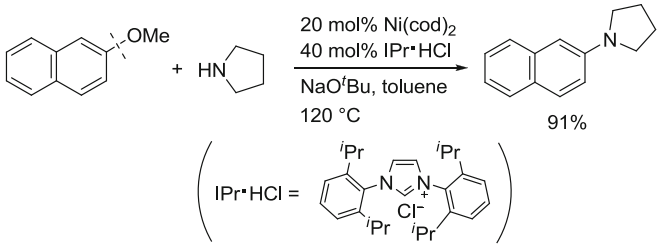

(8)

Aryl pivalates also serve as suitable substrates in this amination reaction [Eq. (9)] [55]. The effective shielding of the carbonyl group by a *tert*-butyl moiety completely suppressed the undesired aminative cleavage of C(acyl)–O bonds. A substantially wider range of substrates, when compared to the amination of aryl methyl ethers, were aminated under milder conditions. Aryl carbamates exhibit similar reactivity to the amination reaction under these nickel-catalyzed conditions [55, 56].

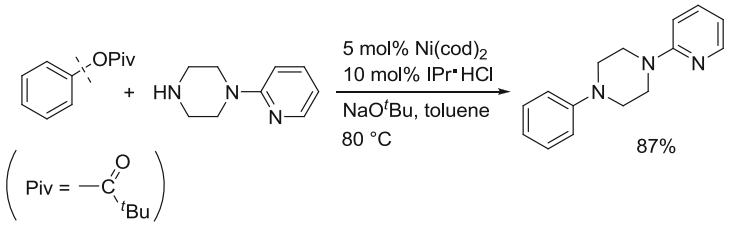

(9)

Reduction of inert C(sp^2)–O into C–H bonds represents a versatile transformation, which allows for the removal of oxygen functionalities catalytically. Such transformations can be accomplished when nickel-catalyzed C–O bond activation is conducted in the presence of suitable reducing agents. Isopropylmagnesium halides were reported to serve as an effective hydride donor in the reductive cleavage of cyclic alkenyl ethers (see Sect. 4) [57] and aryl carbamates [44]. Martin [58] and our group [59] independently reported a reductive cleavage reaction of Ar–OMe bonds using hydrosilane as a mild reducing agent [Eq. (10)]. Similar to other C(aryl)–OMe bond activation reactions so far described, fused aromatics exhibited superior reactivity to anisoles. The presence of *ortho*-directing groups, such as esters and *N*-heterocycles, significantly facilitates reductive deoxygenation.

It is also confirmed that incorporated hydride is derived from hydrosilane, rather than a methoxy group via β-hydrogen elimination (possible involvement of formal β-hydrogen elimination of nickel-methoxide species has been reported [60]).

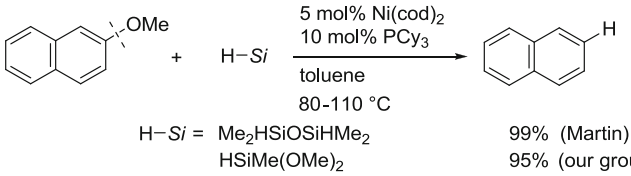

(10)

The catalytic protocol can also be applied to the reductive cleavage of pivaloxy groups on arenes, fused arenes, and heteroarenes [Eq. (11)] [59].

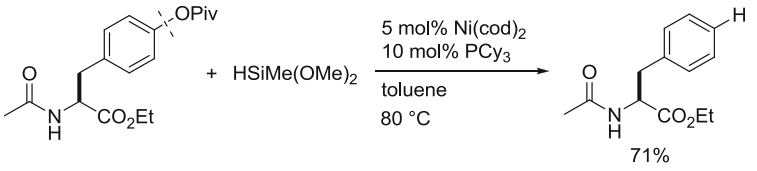

(11)

Hartwig and coworkers reported that 1 bar of hydrogen can also be used as a reducing agent for the nickel-catalyzed reductive cleavage of C–O bonds [Eq. (12)] [61]. Biaryl ethers are split into the corresponding arenes and phenols under these conditions.

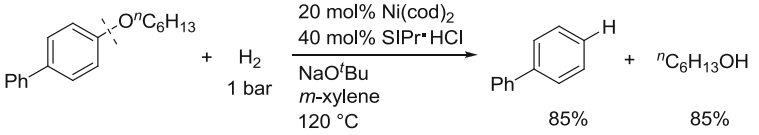

(12)

A catalytic borylation of aryl carbamates has been achieved by Shi's group [Eq. (13)] [62]. Aryl carboxylates also afforded the borylated products albeit with lower yields.

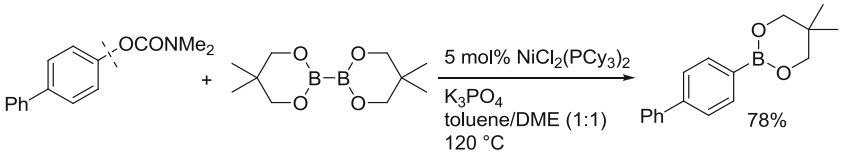

(13)

Itami's group developed a nickel-catalyzed cross-coupling of aryl pivalates, carbamates, and carbonates with azoles [Eq. (14)] [63]. The use of bidentate 1,2-bis(dicyclohexylphosphino)ethane is essential for the reaction to proceed.

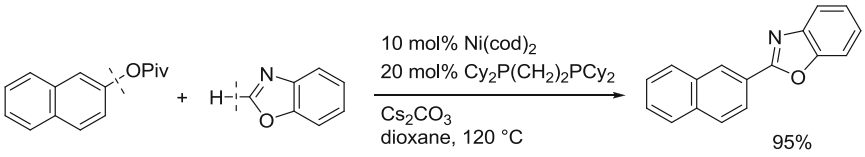

(14)

Mizoroki–Heck type reaction of aryl pivalates has been reported by Watson's group [Eq. (15)] [64]. A bidentate phosphine serves as an effective ligand in this reaction as well.

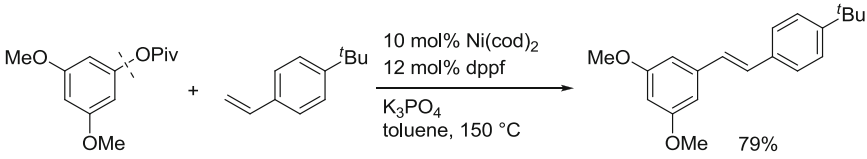

(15)

3 Carbon–Oxygen Bond Transformations Catalyzed by Other Metals

As described in the previous section, Ni(0)/PCy_3 is an effective catalyst system for cross-coupling using conventionally inert phenolic electrophiles, including aryl ethers, carboxylates, and carbamates. In this section, the C–O bond activation reactions catalyzed by other metals are described.

In 2004 Kakiuchi disclosed that alkoxyarenes bearing an ortho carbonyl group can be coupled with arylboronic esters in the presence of $RuH_2(CO)(PPh_3)_3$ [Eq. (16)] [65]. The reaction represents the first example of a Suzuki–Miyaura-type reaction of aryl ethers. Chelation assistance facilitates the oxidative addition of C–O bonds, which allows for a regioselective C–O bond cleavage of diaryl ethers.

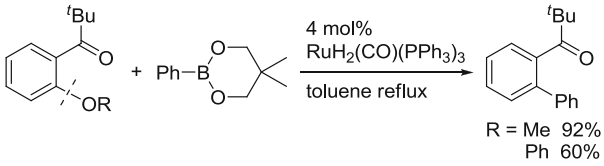

(16)

$RuH_2(CO)(PPh_3)_3$ is also known to be an effective catalyst for carbonyl-directed C–H bond activation [66]. Thus, both C–H and C–O bonds in the starting compound shown in Eq. (16) can be activated under the catalytic conditions. Kakiuchi established that the formation of a C–H bond-activated complex is kinetically favored, while C–O bond activation affords a more thermodynamically stable complex [67]. Sequential functionalization of C–H and C–O bonds can be

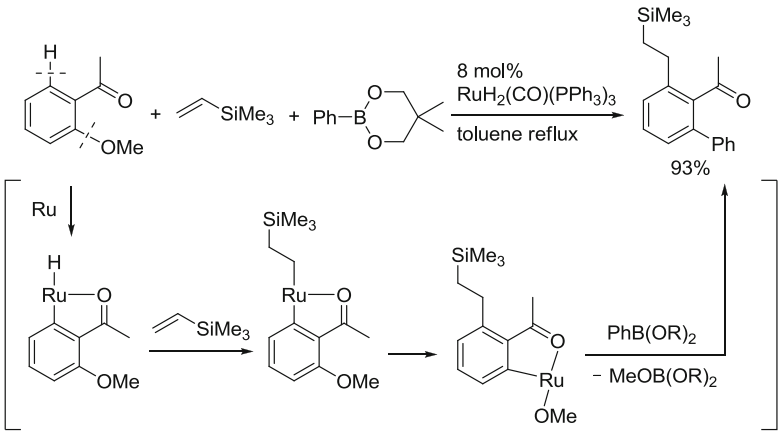

Scheme 2 Ru-catalyzed directed C-H/C-O bond transformation tandem

Table 2 Rh-catalyzed cross-coupling of vinyl acetate with arylboronic acid

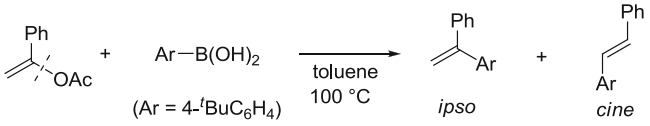

Reactions conditions	Yield (%)	*Ipso*:*cine*
2.5 mol% $[RhCl(cod)]_2$ 5.5 mol% $Ph_2P(CH_2)_4PPh_2$ K_3PO_4, *t*-amyl alcohol	61	100:0
1.5 mol% $[Rh(OAc)(cod)]_2$ 6.0 mol% cod K_3PO_4, *i*-Pr_2NH	67	17:83

accomplished in one pot by running the reaction in the presence of alkenes and boronic esters (Scheme 2). The catalyst was recently used in a C(sp^3)–OPh bond cleavage reaction by Bergman and Ellman [68].

Nickel complex is currently the only catalyst that can activate the C(aryl)–O bonds in aryl carboxylates. On the other hand, C–O bonds in *alkenyl* carboxylates can be activated by several other metal catalysts.

Kuwano [69] and Kwong [70] independently reported that a Suzuki–Miyaura-type cross-coupling of alkenyl acetates proceeds in the presence of a rhodium-based catalyst (*ipso* substitution in Table 2). Both groups identified chelating $Ph_2P(CH_2)_4PPh_2$ as the most suitable ligand in this process. Retention of the alkene configuration during the coupling event indicates that C–O bond activation occurred via oxidative addition to a rhodium center. Interestingly, Kuwano also reported that a *cine*-substitution dominated when the reaction was conducted in the presence of a diene-based ligand in place of phosphine (*cine*-substitution in Table 2) [71]. In the *cine*-substitution process, the activation mode is supposedly altered to

β-acetoxy elimination of an alkylrhodium intermediate, which is generated by the arylrhodation/isomerization sequence.

Iron is one of the catalysts for cross-couplings that was found in the earliest stage of their development [72]. Recent advances in iron catalysis have permitted a range of halides and sulfonates to be used in cross-coupling reactions [73–76]. In this context, Shi demonstrated the first iron-catalyzed cross-coupling of alkenyl *pivalates*. Several primary alkyl Grignard reagents can be used in the presence of $FeCl_2$/*N*-heterocyclic carbene catalyst (Eq. 17) [77]. Although the corresponding coupling using naphthyl pivalate resulted in a lower yield, naphthyl carbamate furnished the alkylated product in a good yield. A radical-based mechanism is supposedly involved based on the observations of complete reaction inhibition by TEMPO and loss of the alkene stereochemistry. An Fe-catalyzed reaction related to Eq. (17) has been reported [83].

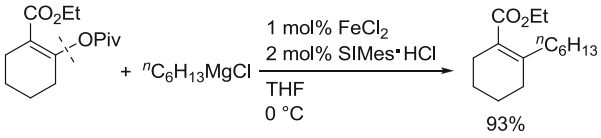

(17)

Kakiuchi reported that alkenyl acetates can function as alkenyl sources in the chelation-assisted C–H bond functionalization reaction, which is catalyzed by Ru(cod)(cot) [Eq. (18)] [78]. In this reaction, two normally unreactive bonds, i.e., C–H and C–OAc, are activated within the catalytic cycle. Oxazolines, tetrazoles, and thiazoles were also effective directing groups in this reaction.

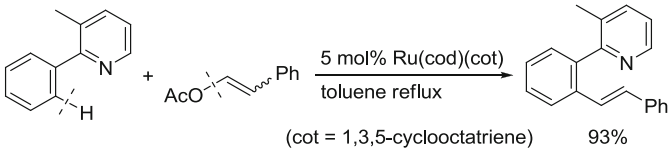

(18)

4 Synthetic Applications

The emergence of catalytic transformations of conventionally inert enolic and phenolic electrophiles has offered several advantages when applied to organic synthesis. First, derivatization of naturally occurring phenols can be accomplished by using readily accessible esters. In addition, the direct use of aryl methyl ethers, which are also prevalent substructures in nature, streamlines the synthesis of elaborate aromatic compounds. Second, the robustness of C–O bonds in ethers and esters under typical palladium-catalyzed cross-coupling conditions allows for the orthogonal transformation of C–O and C–halogen bonds. Third, a new synthetic strategy for regioselective arene functionalization is possible by combining the directing effects of oxygen functionalities and C–O bond transformations. In this section, several illustrative examples are provided.

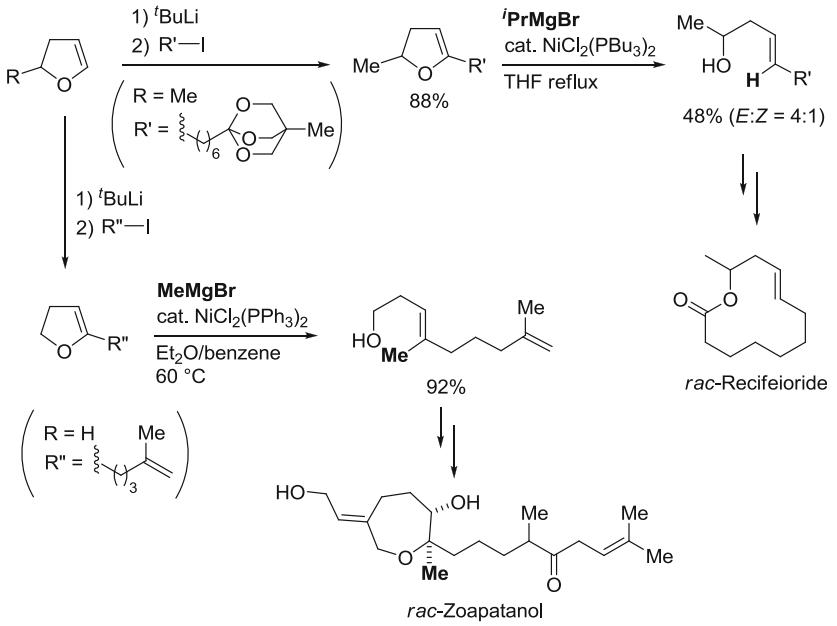

Scheme 3 Stereoselective synthesis of homoallyl alcohols via Ni-catalyzed C-O bond activation

Nickel-catalyzed Grignard cross-coupling enables readily accessible dihydrofurans to serve as versatile building blocks for the stereoselective synthesis of homoallylic alcohols (Scheme 3). Since the substitution at the vinylic carbon proceeds with retention of the alkene geometry, homoallylic alcohols bearing a hydroxyethyl group and the incorporated nucleophile in a syn fashion are formed. When isopropyl Grignard reagent was used, a $C(sp^2)$–O bond in dihydrofurans was cleaved by hydride, furnishing *trans* alkene, which was finally converted into the fungal metabolite recifeiolide [57]. Conversely, the use of MeMgBr resulted in the ring opening with the incorporation of a methyl group, furnishing tri-substituted homoallylic alcohol. This process was exploited in the key step of the total synthesis of the spasmogenic diterpenoid zoapatanol, wherein the suitably established alkene geometry was translated into the relative stereochemistry of the substituted oxepane ring [20, 79].

The nickel-catalyzed Suzuki–Miyaura-type C–O bond arylation has been successfully applied to steroidal architecture (Scheme 4). A hydroxyl moiety in estrone can readily be substituted by an array of aryl groups under nickel catalysis via conversion into pivalate instead of the typically used triflate [38]. The carbonyl moiety in estrone also serves as a suitable precursor for an alkenyl C–O electrophile. Treatment of estrone with 2-propenyl acetate affords the compounds bearing two acetate groups, both of which are potentially reactive toward nickel-catalyzed cross-coupling. However, selective arylation took place at the alkenyl position, and

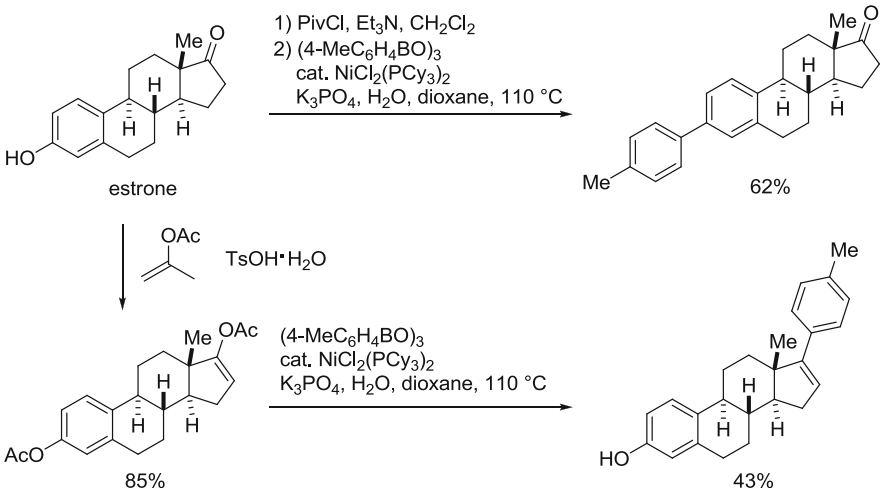

Scheme 4 Elaboration of estrone via Ni-catalyzed C-O bond activation

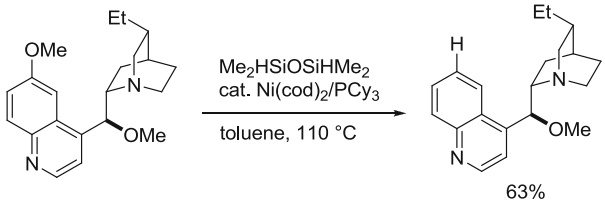

Scheme 5 Synthetic modification of alkaloids via Ni-catalyzed C-O bond activation

the remaining acetate on the aromatic ring was simply hydrolyzed under the catalytic conditions [39].

Direct transformation of C(aryl)–OMe groups affords numerous opportunities for elaborating the complex molecules. For example, 6-methoxyquinoline is a common motif in the cinchona alkaloid family and can serve as an electrophilic coupling partner in nickel catalysis. A deoxygenated analogue of quinine derivative was produced by a nickel-catalyzed reaction with hydrosilane (Scheme 5) [58]. Such structural modification of cinchona alkaloids through the direct transformation of a methoxy group is of great significance in view of their widespread utility as ligands for metal catalysts and also as nucleophilic organocatalysts.

Nickel-catalyzed methods have enabled methoxy and pivaloxy groups to serve as leaving groups in cross-coupling reactions. These transformations are valuable in terms of cost and atom efficiency, compared to the use of triflates. Furthermore, the utility of nickel-catalyzed C–O bond transformations is increased by combination with conventional halogen-based cross-coupling technology. As depicted in Scheme 6, a Suzuki–Miyaura reaction of 2-bromo-6-methoxynaphthalene under the standard palladium conditions furnished a biaryl compound bearing two methoxy groups. The more reactive methoxy group on the naphthalene ring can be arylated with boronic ester under nickel catalysis with the other methoxy group

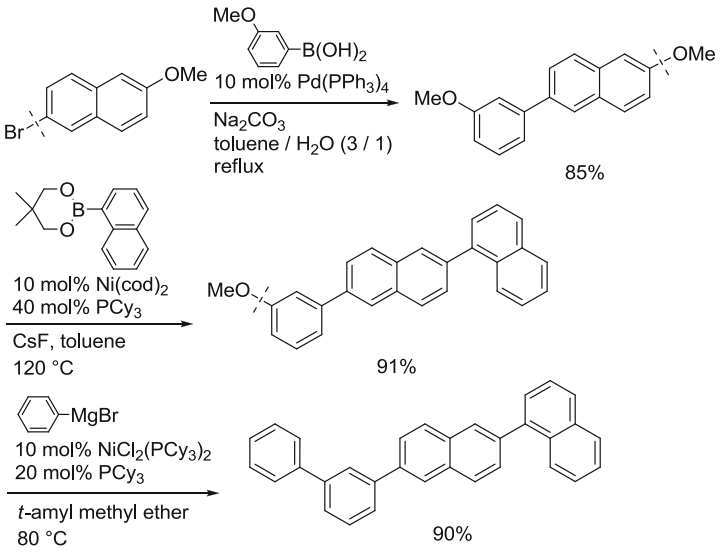

Scheme 6 Sequential cross-couplings of Ar-X and Ar-OMe

on benzene remaining intact. Finally, the least reactive methoxy group can be arylated using a more nucleophilic Grignard reagent. The orthogonal reactivity between halogen and two different methoxy groups allowed for the straightforward assembly of four arenes through three consecutive cross-couplings (Tobisu M, Shimasaki T, Konno Y, Chatani N, unpublished results). Tedious protection/deprotection or functional group manipulations would be required to synthesize this molecule using only halogen-based cross-coupling.

Oxygen functionalities on an aromatic ring are known to play a key role in controlling reactivity and regioselectivity in various arene functionalization reactions. However, the target compounds do not always contain oxygen functionalities, and thus, the removal or transformation of the oxygen functionalities after exploiting the desired reactivity and selectivity is frequently required in the synthesis of poly-substituted arenes. Traditionally such a C–O bond transformation must be conducted via the conversion into an activated form, such as C–OTf, which sacrifices multiple synthetic steps. Nickel catalysis can directly convert such oxygen functionalities into carbon- and nitrogen-based substituents as well as hydrogen, thereby eliminating the lengthy sequences for the functional group transformation.

Scheme 7 showcases the concept [59]. In the first step, a pivaloxy group activates the aromatic ring toward electrophilic bromination and simultaneously directs bromination at the *para* position. The robust nature of the pivaloxy group keeps it intact under Suzuki–Miyaura arylation at the bromide site. In the third step, the pivaloxy group functions as an *ortho* director in palladium-catalyzed C–H bond arylation reaction [80]. After playing several key roles, the pivaloxy group is finally removed by a nickel-catalyzed reaction with hydrosilane. Thus, a pivaloxy group serves as a *traceless* handle in the regioselective functionalization of arenes.

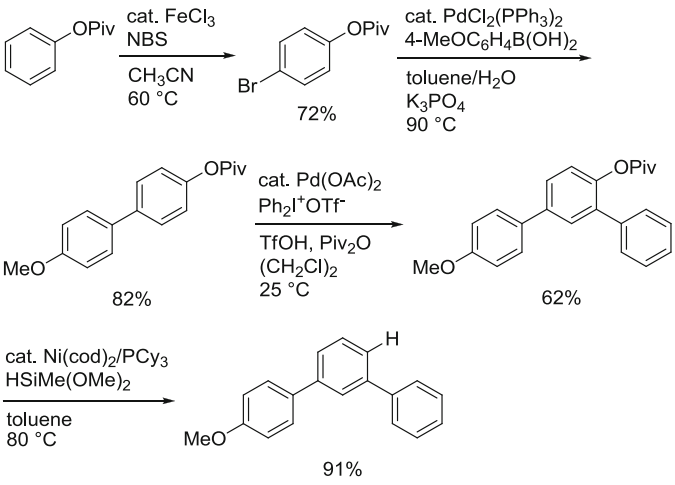

Scheme 7 A pivaloxy group as a removable director in aromatic transformations

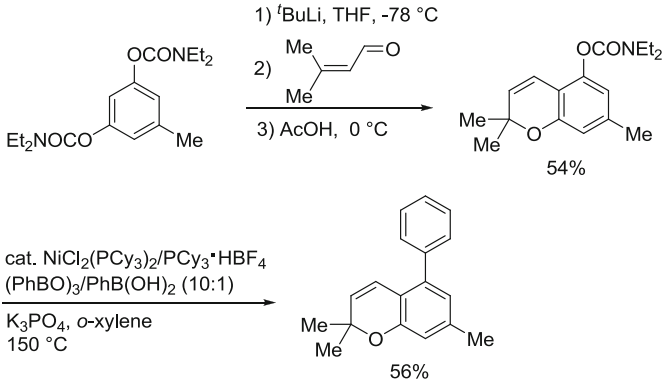

Scheme 8 A carbamate group as a convertible director in aromatic transformations

Directed *ortho*-metalation (D*o*M) chemistry [81] further reinforces the versatility of nickel-catalyzed C–O bond activation reactions. Based on the strong accelerating and *ortho*-directing effect of carbamate functionality in the base-induced deprotonation of arenes, an array of electrophiles can be introduced at the *ortho* position of aryl carbamates. For instance, D*o*M of dicarbamate, followed by 1,2-addition to α,β-unsaturated aldehyde and intramolecular cyclization, furnishes the 2*H*-chromene derivative (Scheme 8) [82]. The carbamate director can finally be arylated under a nickel-catalyzed Suzuki–Miyaura-type reaction [47].

5 Summary and Outlook

The transition metal-catalyzed transformations of phenol and enol derivatives through the activation of inert C(sp^2)–O bonds have been reviewed. More than 30 years after the seminal discovery by Wenkert, nickel catalysts have proven effective for several cross-couplings of aryl ethers, carboxylates, and carbamates. In addition, other metals, including ruthenium, iron, and rhodium, also have the potential to mediate the activation of a certain class of inert C–O bonds. These new transformations will find numerous opportunities for application to the synthesis of complex molecules by allowing several oxygen-based functionalities to be exploited as convertible directors. Despite these recent advances, the methodology is still immature in terms of scope and practicality when compared with halide-based cross-coupling technology. The sophistication of existing C–O bond transformations and the development of new modes of C–O bond activation reactions will continue to be an active area of research due to cost- and atom effectiveness as well as to the benign environmental impact of these reactions. Despite apparent similarities, the reaction design based on the simple extension of the chemistry of C–halogen bonds to that of C–O bonds often produces unsuccessful results. Thus, the elucidation of a precise mechanism for the C–O activation and the creation of more active catalyst systems will be required in future endeavors to invent novel and powerful C–O bond transformations.

References

1. Tsuji J (2004) Palladium reagents and catalysts. Wiley, Chichester
2. Miyaura N (ed) (2001) Top Curr Chem 219
3. de Meijere A, Diederich F (2004) Metal-catalyzed cross-coupling reactions, 2nd edn. Wiley, Weinheim
4. Surry DS, Buchwald SL (2008) Angew Chem Int Ed 120:6438
5. Hartwig JF (2008) Acc Chem Res 41:1534
6. Tyman JHP (1996) Synthetic and natural phenols. Elsevier, Amsterdam
7. Rappoport Z (ed) (2003) The chemistry of phenols. Wiley, Chichester
8. Ritter K (1993) Synthesis 735
9. Yu D-G, Li B-J, Shi Z-J (2010) Acc Chem Res 43:1486
10. Li B-J, Yu D-G, Sun C-L, Shi Z-J (2011) Chem Eur J 17:1728
11. Rosen BM, Quasdorf KW, Wilson DA, Zhang N, Resmerita A-M, Garg NK, Percec V (2011) Chem Rev 111:1346
12. Wenkert E, Michelotti EL, Swindell CS (1979) J Am Chem Soc 101:2246
13. Wenkert E, Michelotti EL, Swindell CS, Tingoli M (1984) J Org Chem 49:4894
14. Hayashi T, Katsuro Y, Kumada M (1980) Tetrahedron Lett 21:3915
15. Wenkert E, Ferreira VF, Michelotti EL, Tingoli M (1985) J Org Chem 50:719
16. Wadman S, Whitby R, Yeates C, Kocienski P, Cooper K (1987) J Chem Soc Chem Commun 241
17. Whitby R, Yeates C, Kocienski P, Costello G (1987) J Chem Soc Chem Commun 429
18. Kocienski P, Dixon NJ, Wadman S (1988) Tetrahedron Lett 29:2353
19. Kocienski P, Wadmana S, Cooper K (1988) Tetrahedron Lett 29:2357
20. Kocienski P, Love C, Whitby R, Roberts DA (1988) Tetrahedron Lett 29:2867

21. Ducoux J-P, Le Ménez P, Kunesch N, Kunesch G, Wenkert E (1990) Tetrahedron Lett 31:2595
22. Ducoux J-P, Le Ménez P, Kunesch N, Kunesch G, Wenkert E (1992) Tetrahedron 48:6403
23. Tingoli M, Panunzi B, Santacroce F (1999) Tetrahedron Lett 40:9329
24. Johnstone RAW, McLean WN (1988) Tetrahedron Lett 29:5553
25. Brigas AF, Johnstone RAW (2000) Perkin 1:1735
26. Dankwardt JW (2004) Angew Chem Int Ed 43:2428
27. Fu GC (2008) Acc Chem Res 41:1555
28. Guan B-T, Xiang S-K, Wu T, Sun Z-P, Wang B-Q, Zhao, K-Q, Shi Z-J (2008) Chem Commun 1437
29. Guan B-T, Xiang S-K, Wang B-Q, Sun Z-P, Wang Y, Zhao K-Q, Shi Z-J (2008) J Am Chem Soc 130:3268
30. Taylor BLH, Swift EC, Waetzig JD, Jarvo ER (2011) J Am Chem Soc 133:389
31. Tobisu M, Shimasaki T, Chatani N (2008) Angew Chem Int Ed 47:4866
32. Shimasaki T, Konno Y, Tobisu M, Chatani N (2009) Org Lett 11:4890
33. Ishizu J, Yamamoto T, Yamamoto A (1976) Chem Lett 1091
34. Chatani N, Tatamidani H, Ie Y, Kakiuchi F, Murai S (2001) J Am Chem Soc 123:4849
35. Tatamidani H, Kakiuchi F, Chatani N (2004) Org Lett 6:3597
36. Tatamidani H, Yokota K, Kakiuchi F, Chatani N (2004) J Org Chem 69:5615
37. Quasdorf KW, Tian X, Garg NK (2008) J Am Chem Soc 130:14422
38. Guan B-T, Wang Y, Li B-J, Yu D-G, Shi Z-J (2008) J Am Chem Soc 130:14468
39. Sun CL, Wang Y, Zhou X, Wu ZH, Li BJ, Guan BT, Shi ZJ (2010) Chem Eur J 16:5844
40. Li Z, Zhang S-L, Fu Y, Guo Q-X, Liu L (2009) J Am Chem Soc 131:8815
41. Li B-J, Li Y-Z, Lu X-Y, Liu J, Guan B-T, Shi Z-J (2008) Angew Chem Int Ed 47:10124
42. Kocienski P, Dixon N (1989) Synlett 52
43. Porée F-H, Clavel A, Betzer J-F, Pancrazi A, Ardisson J (2003) Tetrahedron Lett 44:7553
44. Sengupta S, Leite M, Raslan DS, Quesnelle C, Snieckus V (1992) J Org Chem 57:4066
45. Yoshikai N, Matsuda H, Nakamura E (2009) J Am Chem Soc 131:9590
46. Quasdorf KW, Riener M, Petrova KV, Garg NK (2009) J Am Chem Soc 131:17748
47. Antoft-Finch A, Blackburn T, Snieckus V (2009) J Am Chem Soc 131:17750
48. Xu L, Li B-J, Wu Z-H, Lu X-Y, Guan B-T, Wang B-Q, Zhao K-Q, Shi Z-J (2010) Org Lett 12:884
49. Quasdorf KW, Antoft-Finch A, Liu P, Silberstein AL, Komaromi A, Blackburn T, Ramgren SD, Houk KN, Snieckus V, Garg NK (2011) JACS 133:6352
50. Molander GA, Beaumard F (2010) Org Lett 12:4022
51. Yu D-G, Li B-J, Zheng S-F, Guan B-T, Wang B-Q, Shi Z-J (2010) Angew Chem Int Ed 49:4566
52. Yu D-G, Shi Z-J (2011) Angew Chem Int Ed 50:7097
53. Tobisu M, Shimasaki T, Chatani N (2009) Chem Lett 38:710
54. Tobisu M, Yasutome A, Yamakawa K, Shimasaki T, Chatani N (2012) Tetrahedron 68:5157
55. Shimasaki T, Tobisu M, Chatani N (2010) Angew Chem Int Ed 49:2929
56. Mesganaw T, Silberstein AL, Ramgren SD, Nathel NFF, Hong X, Liu P, Garg NK (2011) Chem Sci 2:1766
57. Ducoux J-P, Le Ménez P, Kunesch N, Wenkert E (1993) J Org Chem 58:1290
58. Álvarez-Bercedo P, Martin R (2010) J Am Chem Soc 132:17352
59. Tobisu M, Yamakawa K, Shimasaki T, Chatani N (2011) Chem Commun 47:2946
60. Kelley P, Lin S, Edouard G, Day MW, Agapie T (2012) J Am Chem Soc 134:5480
61. Sergeev AG, Hartwig JF (2011) Science 332:439
62. Huang K, Yu D-G, Zheng S-F, Wu Z-H, Shi Z-J (2011) Chem Eur J 17:786
63. Muto K, Yamaguchi J, Itami K (2012) J Am Chem Soc 134:169
64. Ehle AR, Watson MP (2012) Org Lett 14:1202
65. Kakiuchi F, Usui M, Ueno S, Chatani N, Murai S (2004) J Am Chem Soc 126:2706
66. Murai S, Kakiuchi F, Sekine S, Tanaka Y, Kamatani A, Sonoda M, Chatani N (1993) Nature 366:529

67. Ueno S, Mizushima E, Chatani N, Kakiuchi F (2006) J Am Chem Soc 128:16516
68. Nichols JM, Bishop LM, Bergman RG, Ellman JA (2010) J Am Chem Soc 132:12554
69. Yu J-Y, Kuwano R (2009) Angew Chem Int Ed 48:7217
70. Lee HW, Kwong FY (2009) Synlett 3151
71. Yu J-Y, Shimizu R, Kuwano R (2010) Angew Chem Int Ed 49:6396
72. Tamura M, Kochi JK (1971) J Am Chem Soc 93:1487
73. Bolm C, Legros J, Le Paih J, Zani L (2004) Chem Rev 104:6217
74. Sherry BD, Fürstner A (2008) Acc Chem Res 41:1500
75. Nakamura E, Yoshikai N (2010) J Org Chem 75:6061
76. Sun C-L, Li B-J, Shi Z-J (2010) Chem Rev 111:1293
77. Li B-J, Xu L, Wu Z-H, Guan B-T, Sun C-L, Wang B-Q, Shi Z-J (2009) J Am Chem Soc 131:14656
78. Matsuura Y, Tamura M, Kochi T, Sato M, Chatani N, Kakiuchi F (2007) J Am Chem Soc 129:9858
79. Kocieński PJ, Love CJ, Whitby RJ, Costello G, Roberts DA (1989) Tetrahedron 45:3839
80. Xiao B, Fu Y, Xu J, Gong T-J, Dai J-J, Yi J, Liu L (2010) J Am Chem Soc 132:468
81. Snieckus V (1990) Chem Rev 90:879
82. Chauder BA, Kalinin AV, Snieckus V (2001) Synlett 140
83. Silberstein AL, Ramgren SD, Garg NK (2012) Org Lett 14:3796

Top Organomet Chem (2013) 44: 55–90
DOI: 10.1007/3418_2012_43

Published online: 1 August 2012

The Interplay of Invention, Observation, and Discovery in the Development of Lewis Base Activation of Lewis Acids for Catalytic Enantioselective Synthesis

Gregory L. Beutner and Scott E. Denmark

Abstract This chapter chronicles the evolution of a paradigm shift in the conceptualization and development of chiral Lewis base catalysis of carbonyl addition reactions with organosilicon nucleophiles. Prior to 2000, these reactions were exclusively practiced through the agency of highly electrophilic silicon species such as allyltrichlorosilanes and enoxytrichlorosilanes derived from aldehydes, ketones, and esters. However, a serendipitous discovery made during the development of these processes led to a fundamentally new insight, namely, that silicon tetrachloride could be activated by chiral Lewis bases (primarily phosphoramides) and the resulting chiral silicenium ion could serve as a general and effective catalyst for the addition of many different enoxysilane nucleophiles derived from aldehydes, ketones, esters, nitriles, protected cyanohydrins, conjugated esters and amides, and isocyanides. In addition to providing high generality, high yield, and high stereoselectivity, the new family of Lewis base-catalyzed reactions could be investigated mechanistically, and the foundations of reactivity and selectivity could be revealed. An analysis of how this paradigm shift occurred and the circumstances that led to discovery are described.

Keywords Aldolization · Catalysis · Chiral phosphoramide · Lewis acid · Lewis base · Organosilicon

G.L. Beutner
Chemical Development, Bristol-Myers Squibb Company, 1 Squibb Drive, New Brunswick, New Jersey 08903, USA

S.E. Denmark (✉)
Department of Chemistry, University of Illinois, Urbana-Champaign,
245 Roger Adams Laboratory, 600 S. Mathews Avenue, Urbana, IL 61801, USA
e-mail: sdenmark@illinois.edu

Contents

1 Introduction

One can view science as proceeding in two distinct phases: normal science and revolutionary science. During periods of normal scientific progress, an established theory exists, which guides scientific research in a productive manner. By far, periods of normal science dominate the history of science and are only occasionally interrupted by moments better defined as revolutionary science. Periods of revolutionary science are often triggered by observations that cannot be easily rationalized within existing theory and shift the focus of research from applying an existing theory to discovering a new one. These events, termed scientific revolutions, lead to the establishment of new theoretical frameworks, or paradigms, that can rationalize all of the available data in a more comprehensive manner. The novel perspective provided by this change can also lead to dramatic innovations because questions and problems that before seemed irrelevant or intractable are now accessible. This view of science, first promulgated by Thomas Kuhn in his work "The Structure of Scientific Revolutions," has been used to understand massive shifts in scientific thought, such as the move from classical to quantum mechanics in physics [1]. However, such phenomena are not limited to such well-known historic moments in the progress of science. When research is considered in this light, scientific revolutions occur quite frequently, albeit on a far more modest or personal scale. New discoveries and innovations are frequently brought about by attempts to rationalize seemingly inconsistent results, unexpected failures, or random errors. Although these discovery processes are not often described in the literature, their existence is known to all practitioners of science.

In this chapter, we will chronicle one such modest scientific revolution and how it led to the development of a mechanistically novel and powerful family of Lewis base-catalyzed–Lewis acid-mediated reactions. Much like the more profound scientific revolutions with which we are all familiar, this discovery was presaged by two observations that appeared as inconvenient facts for the progress of our research program on Lewis base catalysis up until the end of the twentieth century. The attempt to understand these observations, leading to the initial disclosure of a Lewis base-catalyzed–Lewis acid-mediated allylation in 2001, established a mechanistic paradigm that has been applied to a wide variety of transformations and has

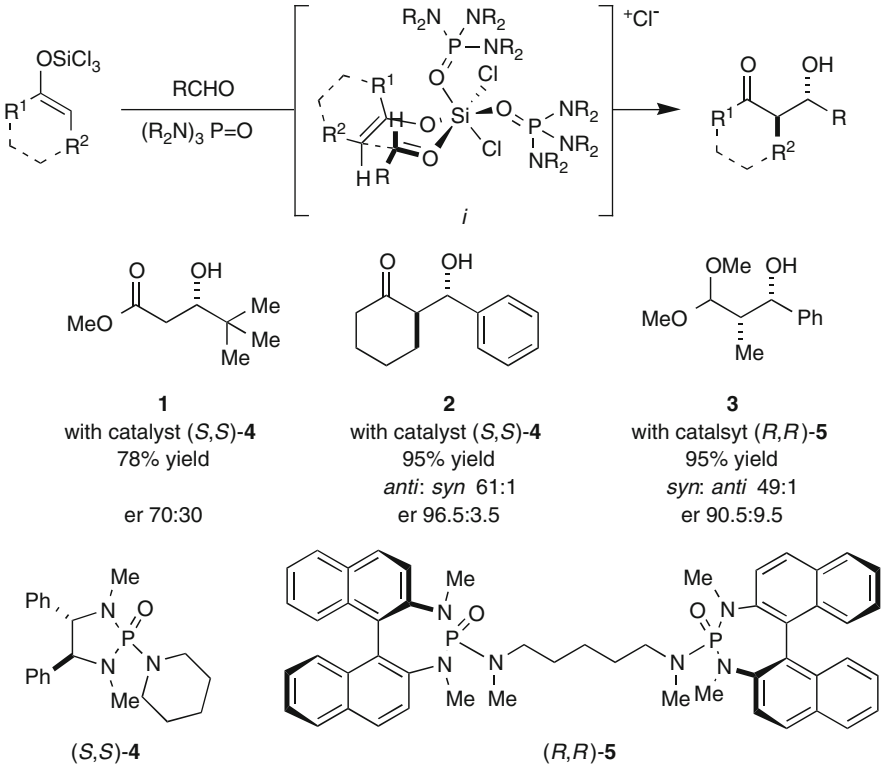

Fig. 1 Hypothetical transition structure assembly for phosphoramide-catalyzed additions of enoxytrichlorosilanes

provided solutions to difficult chemical transformations which remained elusive under the long-standing paradigm of Lewis acid catalysis [2, 3].

2 Lewis Base Catalysis Before 2000: The Established Paradigm

By 2000, the scope of the Lewis base-catalyzed reactions of organotrichlorosilanes had been well established [4, 5]. In these reactions, high reactivity and selectivity could be engendered for the carbonyl addition reactions of allyltrichlorosilanes [6–13] and enoxytrichlorosilanes (derived from esters [14–16], ketones [17–24], and aldehydes [25–27]) with aldehydes in the presence of sub-stoichiometric amounts of a chiral phosphoramide (Fig. 1). The high selectivity of these reactions could be rationalized through a closed transition state structure ***i*** organized around a highly electrophilic, cationic silicon atom [10, 28–30]. This structure provides a convincing explanation for the high reactivity observed in these systems. Binding of the strongly Lewis basic phosphoramide to the trichlorosilyl fragment of the enol

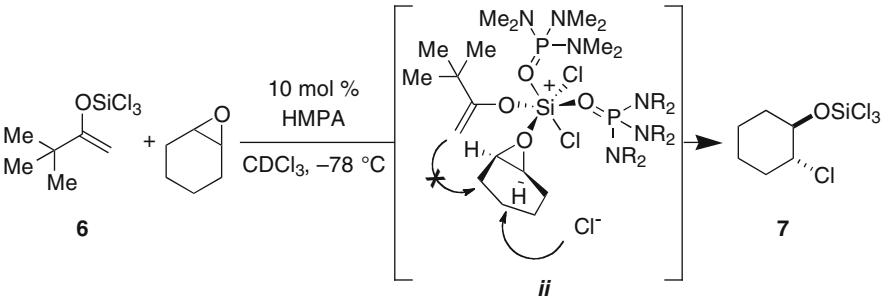

Scheme 1 Unexpected observation in the attempted opening of epoxides

ether leads to ionization of chloride and generation of cationic silicenium ion. Binding of the aldehyde to this intermediate provides electrophilic activation, but only in the chiral environment established by the phosphoramide. A second, less obvious form of nucleophilic activation occurs in the enol ether fragment of this complex. Rehybridization of the bonds around the silicon atom upon changing from the tetracoordinate ground state to a hexacoordinate transition state leads to a buildup of electron density in the peripheral ligands, most importantly the enol ether, further facilitating the carbon–carbon bond-forming event. This understanding, which is central to these Lewis base-catalyzed reactions, was summed up in the statement, "Lewis base catalysis involves simultaneous activation of the nucleophile and the electrophile *within the coordination sphere of the metal*" [4].

This concept of dual activation by a Lewis base provided an important guiding principle for further studies, enabling the understanding of reactivity and selectivity in more complex systems. However, at this point, two observations did not fit neatly into our unified mechanistic picture. The first was the reactivity of epoxides with trichlorosilanes, and the second was the dramatic difference in the reactivity of conjugated vs. aliphatic aldehydes. Our attempts to understand the importance of these aberrations proved crucial in making the conceptual leap to a novel form of catalysis.

3 Rationalizing the Aberrations: Toward a New Paradigm

As part of ongoing studies to expand the scope of Lewis base-catalyzed reactions, the reactivity of enoxytrichlorosilanes with epoxides was examined. Rather than seeing the expected carbon–carbon bond formation, exclusive formation of a vicinal chlorohydrin was observed (Scheme 1) [31]. When considering the guiding principle of dual activation of electrophile and nucleophile through a closed transition structure, it is not surprising that carbon–carbon bond formation was not observed. On the simple grounds of geometry, nucleophilic opening of the epoxide by the enol ether cannot occur in the coordination sphere of the metal, as is

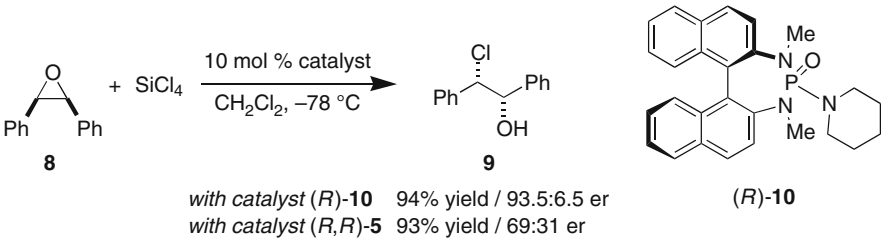

Scheme 2 Generalization of Lewis base-catalyzed opening of epoxides with $SiCl_4$

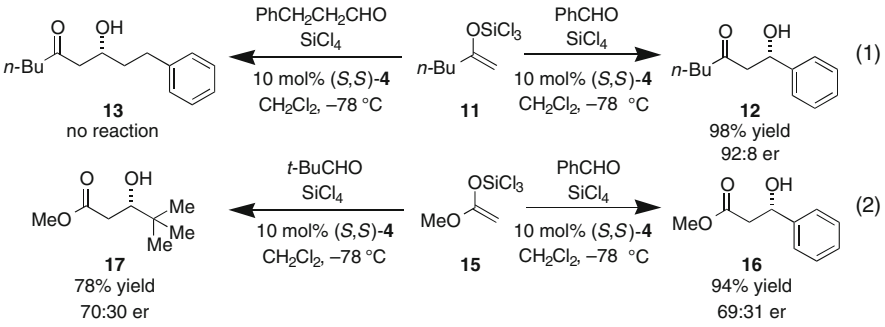

Scheme 3 Reactivity profile of enoxytrichlorosilanes derived from ketones and esters

the case in the carbonyl addition reactions described above. However, the fact that chloride could act as a nucleophile in an intermolecular fashion was remarkable.

On the basis of this result, the reactivity of the parent chlorosilane silicon tetrachloride, $SiCl_4$, was explored. In the presence of a chiral phosphoramide (*R*)-**10**, high reactivity and selectivity could be achieved in the enantioselective ring opening of *meso*-epoxides such as **8** (Scheme 2) [32, 33]. The major lesson learned from this work was that not all Lewis base-catalyzed reactions of trichlorosilanes have to occur within the confines of the coordination sphere of the central silicon atom.

A second and equally important lesson learned from the epoxide-opening process is that the ionized chloride ion, common to all of the Lewis base-catalyzed reactions of trichlorosilanes, is not innocuous. This fact is further highlighted by the divergent reactivity of conjugated and aliphatic aldehydes the aldol chemistry of enoxytrichlorosilanes. In the phosphoramide-catalyzed aldol reactions of these reagents, aromatic and other conjugated aldehydes are excellent substrates in terms of reactivity and selectivity [20, 23]. By contrast, simple aliphatic aldehydes are disappointingly unreactive [Scheme 3, Eq. (1)]. Only in the case of the highly reactive trichlorosilyl ketene acetals could any aldol addition be accomplished with aliphatic aldehydes [Eq. (2)] [16]. These results were initially interpreted as a problem with the reactivity of the nucleophile. In reality however, the electrophile is the source of this dramatic reactivity difference. When exposed to $SiCl_4$ and a phosphoramide, aliphatic aldehydes quickly and quantitatively form an unreactive

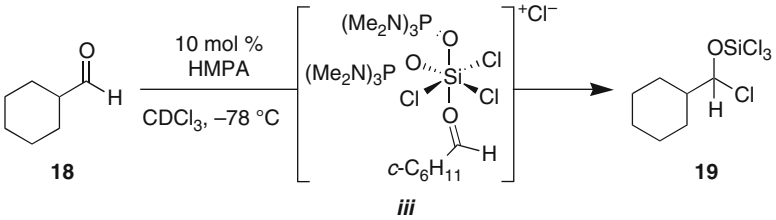

Scheme 4 Geminal trichlorosilyl chlorohydrin formation from aliphatic aldehydes

geminal chlorohydrin similar to **19** (Scheme 4). Not only could this species be observed spectroscopically, it could be isolated and characterized [25–27]. The difference between the reactivity of aliphatic and conjugated aldehydes towards chlorohydrin formation arises from the unfavorable loss of conjugation with unsaturated aldehydes, rendering the aliphatic aldehyde more reactive [34], as seen in this case.

Thus in the aldol addition, just as in the case of epoxide-opening reactions, the chloride ion, formed as a necessary consequence of the mechanism of Lewis base catalysis with chlorosilanes, is not innocuous. In fact, it is a competent nucleophile that can attack an aldehyde or an epoxide activated by the Lewis base-coordinated silicenium cation in an intermolecular fashion. The desire to understand these two seemingly inconsistent results obtained in our study of the Lewis base-catalyzed reactions of trichlorosilanes presented an opportunity for the development of novel catalytic processes. For example, if a chloride ion can capture these activated electrophiles, could other exogenous nucleophiles be employed to intercept these reactive intermediates? If so, a wide variety of bond-forming processes mediated by the phosphoramide-bound chiral Lewis acid $[LB{\cdot}SiCl_3]^+$ would be feasible. At this point it remained unclear if (1) an exogenous nucleophile could compete with the ion-paired chloride and (2) what kinds of nucleophiles could be compatible with the reaction conditions.

4 Lewis Base-Catalyzed–Lewis Acid-Mediated Reactions: The Paradigm Shift

Studies directed toward the selection and application of an exogenous nucleophile for use with this $SiCl_4$/phosphoramide system first focused on the use of allyltributylstannane **20** [35]. The stannane is a competent nucleophile in a wide variety of Lewis acid-promoted carbonyl addition reactions [13, 36–38], and in this system it would provide an effective trap for the ionized chloride through formation of tributyltin chloride. Initial experiments using the optimal phosphoramide catalyst (*R*)-**10** for the $SiCl_4$-mediated opening of *meso*-epoxides gave good yield and a moderate level of enantioselectivity in the addition of the allyl stannane to

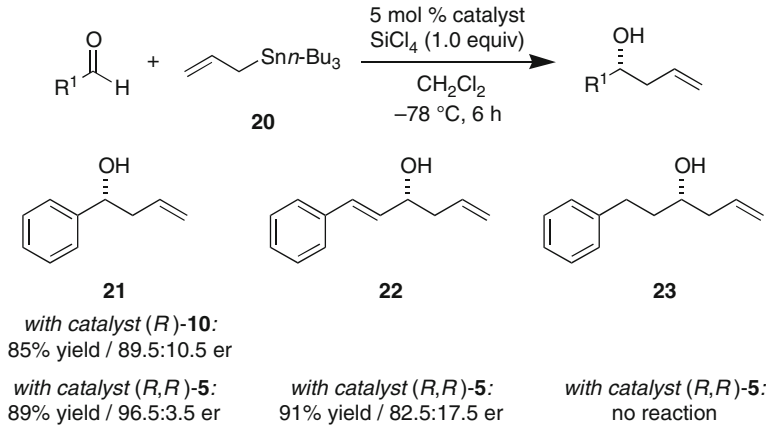

Scheme 5 Allylation of aldehydes with allyltributylstannane

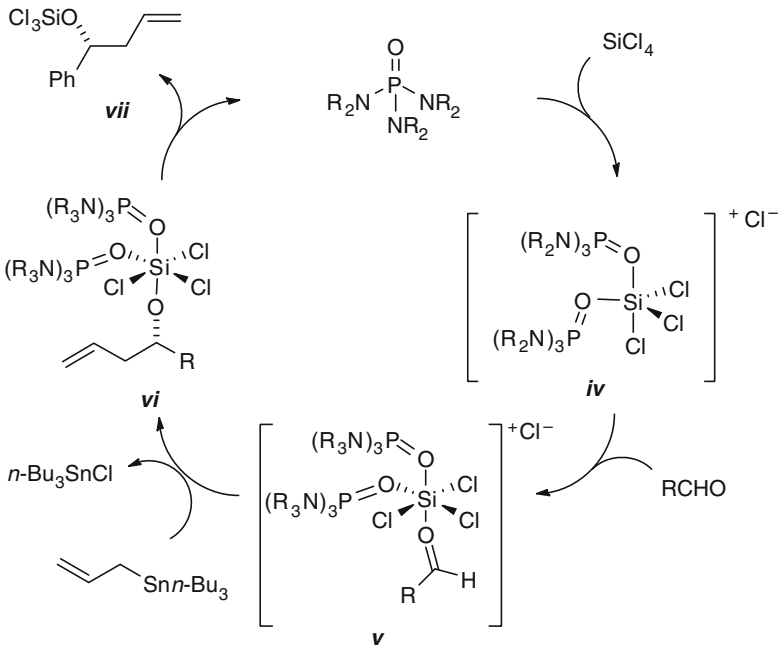

Fig. 2 Catalytic cycle for allylation under catalysis with $SiCl_4$/chiral phosphoramide

benzaldehyde, validating our hypothesis regarding an intermolecular pathway for nucleophile delivery (Scheme 5).

The initially formed product was determined to be the trichlorosilyl ether, rather than a stannyl ether, consistent with the proposed mechanism (Fig. 2). Binding of

the phosphoramide to the weakly Lewis acidic $SiCl_4$ leads to polarization of the silicon–chlorine bonds and eventual ionization of chloride to form the chiral silicenium ion ***iv***. Binding of the aldehyde to generate ***v***, followed by intermolecular attack of the stannane, leads to the catalyst-bound trichlorosilyl ether ***vi*** and tributyltin chloride. Dissociation of the catalyst then liberates the Lewis base to activate another molecule of $SiCl_4$, completing the catalytic cycle. This formulation of the catalytic cycle illustrates that although the active catalytic species in this reaction is a silicon-centered Lewis acid, only the Lewis basic phosphoramide is catalytic since each molecule of $SiCl_4$ is incorporated into the secondary alcohol product. Hence, we have termed these processes Lewis base-catalyzed–Lewis acid-mediated reactions.

With this promising result in hand, efforts to improve enantioselectivity through catalyst optimization identified the bisphosphoramide catalyst (*R*,*R*)-**5** that could provide the allylation product in high yield and good enantioselectivity. Thus, the addition is not only mechanistically intriguing but also a synthetically useful process. The use of such a bisphosphoramide was inspired by our hypothesis that two phosphoramides are bound to the silicon atom in the catalytically active species [28–30]. Under the optimized conditions, a wide variety of aldehydes give high yield and selectivity in the reactions with **20**, except for aliphatic aldehydes. Much to our disappointment, non-conjugated aldehydes as a class are completely unreactive in this reaction. The source of this reactivity problem was identified as chlorohydrin formation, similar to what had been observed in the earlier examples with organotrichlorosilanes.

Although the poor reactivity of aliphatic aldehydes proved to be an insurmountable obstacle in the case of the organotrichlorosilanes, the freedom to vary the nucleophilic component in this Lewis base-catalyzed–Lewis acid-mediated manifold provided a straightforward solution. Since the ionized chloride ion was clearly a competitive nucleophile when compared to allyltributylstannane, one potential solution to finding broader reactivity with respect to the aldehyde was to select a more reactive nucleophile. By considering the nucleophilicity scales for π-nucleophiles compiled by Mayr and coworkers [39–44], few options existed in the context of the allylation. However, the higher reactivity of silyl ketene acetals suggested that an aldol reaction with broad substrate scope might be possible. Initial experiments with the highly reactive acetate-derived silyl ketene acetal **24** and benzaldehyde or cinnamaldehyde gave good yield and excellent levels of enantioselectivity using the conditions developed for the allylation (Scheme 6) [45, 46]. Gratifyingly, the reaction also proceeded with hydrocinnamaldehyde, albeit with a slightly longer reaction time and lower level of enantioselectivity.

Given that the highly reactive acetate-derived silyl ketene acetal **24** displayed a broad substrate scope with respect to the aldehyde, we decided to explore other ester-derived silyl ketene acetals. Again, our hope was that these more reactive nucleophiles would maintain broad reactivity with respect to the aldehyde. The diastereoselectivity of this catalyst system could also be investigated, in this case by employing propanoate-derived silyl ketene acetals. The catalyst had already shown a high level of control over the facial approach of the nucleophile to the activated

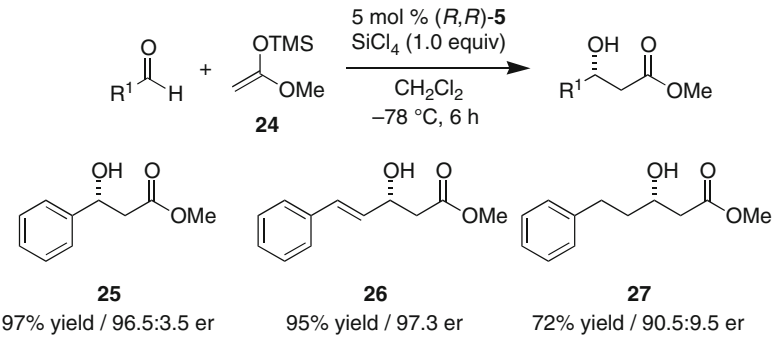

Scheme 6 Aldolization with an acetate-derived silyl ketene acetal

Table 1 Aldolization with propanoate-derived silyl ketene acetals

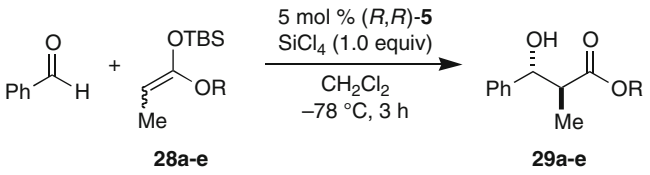

Entry	R	*E*:*Z*	Product	Yield (%)	er	dr
1	Me (**28a**)	82:18	**29a**	98	86:14	99:1
2	Et (**28b**)	95:5	**29b**	78	88:12	98:2
3	Ph (**28c**)	94:6	**29c**	98	94:6	94:6
4	*i*-Pr (**28d**)	71:29	**29d**	80	91.1:8.9	98:2
5	*t*-Bu (**28e**)	95:5	**29e**	93	>99:1	99:1
6	*t*-Bu (**28e**)	12:88	**29e**	73	>99:1	99:1

aldehyde. It remained to be seen if this level of selectivity could be translated to orientation of the approaching nucleophile. Initial experiments with the ethyl propanoate-derived silyl ketene acetal **28b** showed almost exclusive formation of the *anti*-diastereomer **29b** in good yield but with only modest enantioselectivity (Table 1, entry 2) [45, 46].

Fortunately, the enantioselectivity could be easily improved by employing larger ester groups (compare entries 1 and 5). In the case of the *tert*-butyl propanoate-derived silyl ketene acetal **28e**, near perfect enantio- and diastereoselectivity could be obtained. Furthermore, the reaction is diastereoconvergent; both the *E*- and *Z*-isomers lead to the *anti* product **29e** with similar levels of enantioselectivity (entries 5 and 6). This curious and somewhat unique result can be rationalized through consideration of the antiperiplanar open transition structures (Fig. 3). Minimization of steric interactions between the α-methyl substituent and the catalyst complex leads to a preference for the *E*-ap$_{anti}$ transition structure ***viii***, providing the observed anti-aldol product *anti*-**29e** [47]. Regardless of alkene configuration, if the avoidance of this steric interaction is dominant, the *anti* product will be favored.

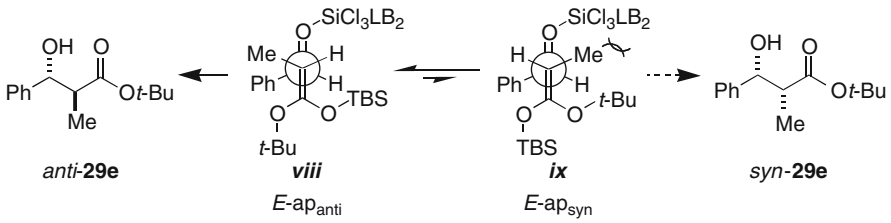

Fig. 3 Rationalization of *anti*-diastereoselectivity

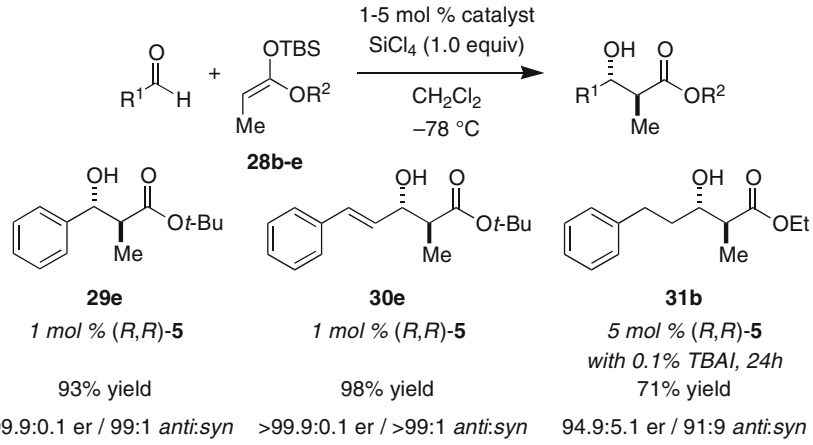

Scheme 7 Generality of *anti*-selective aldolization with propanoate silyl ketene acetal

Although increasing the steric bulk of the nucleophile is necessary to improve selectivity, it has detrimental consequences on reactivity with aliphatic aldehydes (Scheme 7). In reactions with the bulky silyl ketene acetal **28e**, aliphatic aldehydes are unreactive. Fortunately, reactivity can be recovered by decreasing the steric bulk of the ester group (from *tert*-butyl **28e** to ethyl **28b**) and by changing the reaction medium. The addition of tetrabutylammonium iodide, which presumably increases the ionic strength of the reaction medium, shifts the equilibrium between the activated aldehyde and the trichlorosilyl chlorohydrin and allows carbon–carbon bond formation to proceed even in the case of aliphatic aldehydes [48].

5 The Flowering of a New Paradigm: Building a Model

The reactions of allylic stannanes and silyl ketene acetals validated our hypothesis that an exogenous nucleophile could compete with a chloride ion and lead to carbon–carbon bond-forming processes. As to the question of what other kinds of nucleophiles could be employed, careful consideration of Mayr's *N* values began to

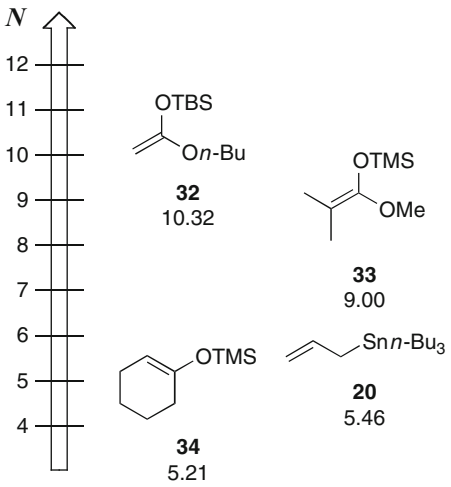

Fig. 4 Mayr's scale of nucleophilicities of various π-nucleophiles

form a predictive model. The dramatic nucleophilicity differences among the π-nucleophiles investigated thus far led us to hypothesize that nucleophiles with $N > 9$ would be competitive with ionized chloride and show broad substrate scope. Those with $N \sim 9$ would have somewhat lower reactivity, while those with $N < 9$ would be limited in scope to conjugated aldehydes (Fig. 4).

Therefore, as we looked to continue expanding the reaction scope of this catalyst system, the use of silyl enol ethers was an obvious extension but was predicted to have a limited scope based on the low N values for this class of compounds ($N \sim 5$). Silyl enol ethers are a particularly interesting class because a much more diverse structural array of ketone- and aldehyde-derived nucleophiles can be employed when compared to silyl ketene acetals. We found that silyl enol ether **35** and benzaldehyde react much more slowly than silyl ketene acetals, in accordance with the lower N value for this class of nucleophiles (Scheme 8) [49]. High conversion and enantioselectivity are maintained, but yields are moderate. The disconnection between high conversion and low yield could be solved by the use of additives such as tetrabutylammonium triflate and diisopropylethylamine (DIPEA). The addition of 10 mol% DIPEA is optimal. Presumably, this non-nucleophilic base serves a dual role as a proton scavenger and a salt additive, protecting the acid-sensitive enol ether from cleavage and accelerating the reaction rate upon formation of the ammonium chloride. Unfortunately, the lower reactivity of silyl enol ethers renders them unreactive with aliphatic aldehydes.

A similar pattern is observed in the reactions of silyl enol ethers derived from aldehydes. Aldehyde–aldehyde aldol reactions had already been reduced to practice in the context of the Lewis base-catalyzed aldol reaction of trichlorosilyl enol ethers, thanks to the stabilizing effect of the trichlorosilyl chlorohydrin (Scheme 9) [25–27]. Because the product of the aldehyde–aldehyde aldol reaction is an aliphatic aldehyde, it can be quickly transformed into an unreactive chlorohydrin such

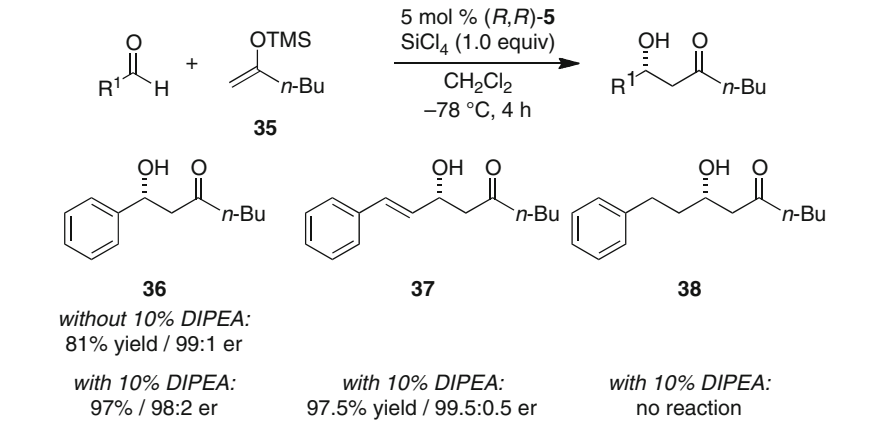

Scheme 8 Aldolization with methyl ketone-derived silyl enol ether

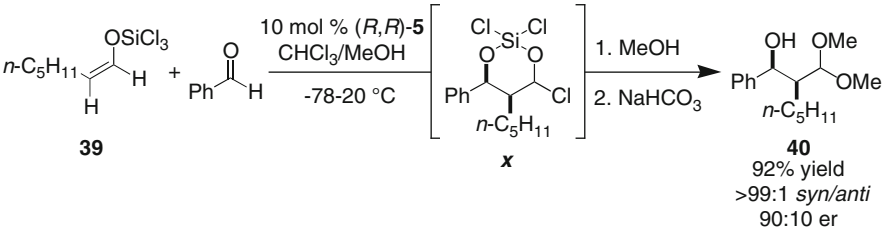

Scheme 9 Aldolization with an aldehyde-derived enoxytrichlorosilane

as ***x***, protecting it from the subsequent oligomerization or Tischenko processes which often render aldehyde–aldehyde aldol reactions unproductive.

In view of the active interest and synthetic challenge of aldehyde–aldehyde crossed aldol reactions, we were curious to apply our novel catalyst system to the reaction of aldehyde-derived silyl enol ethers. Although these species are relatively poor nucleophiles when compared to silyl ketene acetals, they still held some promise due to the success of the ketone-derived silyl enol ethers discussed above. The aldol addition of acetaldehyde TMS enol ethers **41a-d** with benzaldehyde using $SiCl_4$ and bisphosphoramide (*R*,*R*)-**5** gives good levels of enantioselectivity (Table 2) [50]. Similar to the trend observed in the reactions of propanoate-derived silyl ketene acetals, increasing the size of the silyl group leads to a dramatic decrease in reaction rate. Regardless, the addition of DIPEA improves not only the yield but also the enantioselectivity, suggesting competition from an achiral Brønsted acid pathway.

The scope of the aldehyde electrophile is limited to unsaturated aldehydes (Scheme 10). This fact is not surprising because of the low *N* value of these silyl enol ethers ($N \sim 4$ [43]). Yield and enantioselectivity are uniformly high with

Table 2 Aldolization of acetaldehyde-derived enol ethers

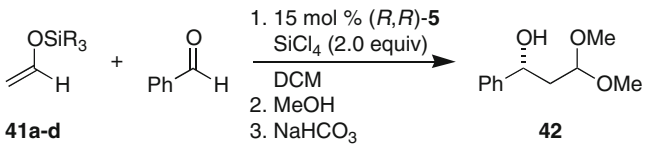

41a-d **42**

Entry	R_3Si	T (°C)	Additive	Yield (%)	er
1	Me_3Si (**41a**)	−78	–	77	92.7:7.3
2	Et_3Si (**41b**)	−78	–	15	ND
3	$PhMe_2Si$ (**41c**)	−78	–	5	ND
4	*t*-$BuMe_2Si$ (**41d**)	−78	–	5	ND
5	Me_3Si (**41a**)	−67	DIPEA (1.0)	84	97.1:2.9

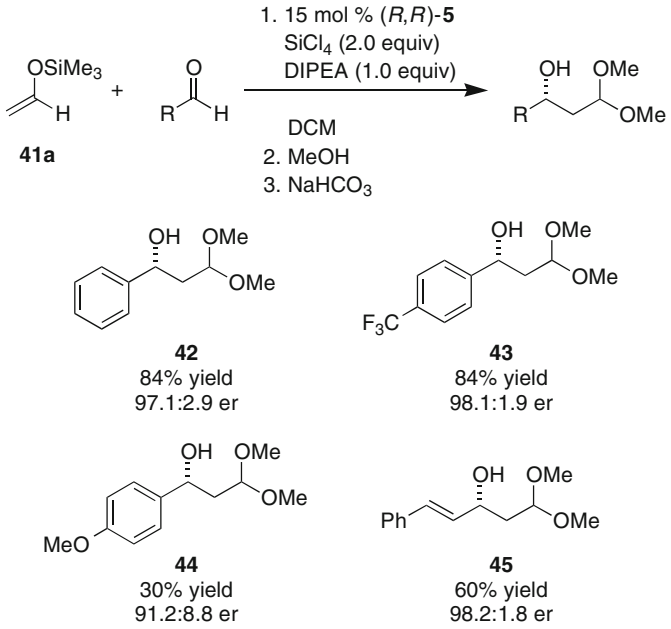

Scheme 10 Generalization of aldolization of ethenyloxytrimethylsilane

conjugated aldehydes, and only a slight loss in reactivity and selectivity is observed with electron-rich aldehydes.

The results of the aldol additions with silyl enol ethers further refined our new model of a Lewis base-catalyzed–Lewis acid-mediated pathway. Use of the *N* value was clearly predictive of substrate scope, validating our mechanistic scheme and the role of the ionized chloride in the complex. Gratifyingly, the sense of asymmetric induction in all these reactions is the same using the chiral bisphosphoramide (*R*,*R*)-**5**.

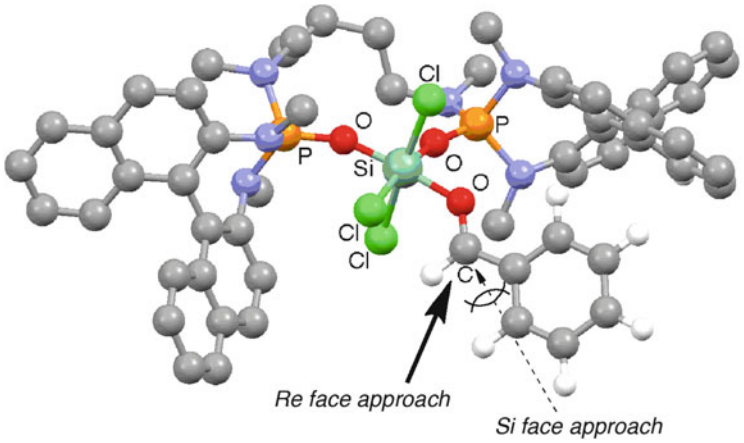

Fig. 5 Transition structure model for aldolization with catalyst (*R*,*R*)-**5**

The catalyst strongly favors the approach of the nucleophile to the *Re* face of the complexed aldehyde regardless of nucleophile structure, lending further support to the common intermediacy of the chiral silicenium complex (Fig. 5). The *N* value is not the only factor influencing the reactivity of the $SiCl_4$/bisphosphoramide (*R*,*R*)-**5** catalyst system. As was made clear in the optimization studies with the propanoate-derived silyl ketene acetals (Table 1) and silyl enol ethers (Table 2), steric effects must also be considered. The establishment of this new paradigm had brought us through a revolution in our thoughts about the scope of Lewis base catalysis. With this new paradigm firmly in hand, attention could now shift to elaborating more complex and innovative applications of this catalyst system and determining if the well-established trends of reactivity observed in Lewis acid-catalyzed reactions would hold or if new avenues would be open to exploration.

The chiral phosphoramide/$SiCl_4$ catalyst system demonstrated the ability to engender high levels of enantio- and diastereoselectivity with simple silyl enol ethers. We were curious to explore the influence of existing stereocenters in the nucleophile on the carbon–carbon bond formation (i.e., double diastereoselection) [51, 52]. Would the high level of facial selectivity exerted by catalyst (*R*,*R*)-**5** overwhelm the influence of existing stereocenters? These issues of double diastereoselectivity had already been explored for the aldol additions of enoxytrichlorosilanes and had predictable effects conforming with a reaction proceeding via a closed transition structure [53–56]. Because most of those enoxytrichlorosilanes are accessed by trans-silylation of the TMS enol ethers, these substrates were readily investigated in the current catalyst system and compared to the results from Lewis base-catalyzed aldol addition [57]. As in the case of the achiral silyl enol ethers shown above, only conjugated aldehydes participate in the aldolization, and the use of DIPEA or tetrabutylammonium iodide is required to obtain high yields. Regardless, high levels of catalyst control are observed in the aldol additions of the silyl enol ethers containing α- or β-stereocenters (Scheme 11). A slight influence of the existing stereocenter could be observed in the reaction of the

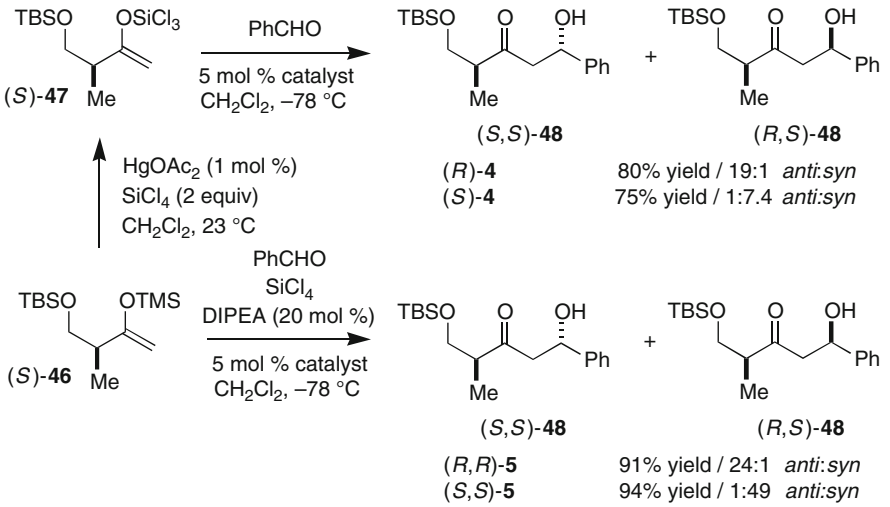

Scheme 11 Comparison of aldolization of chiral methyl ketones (*S*)-**46** and (*S*)-**47**

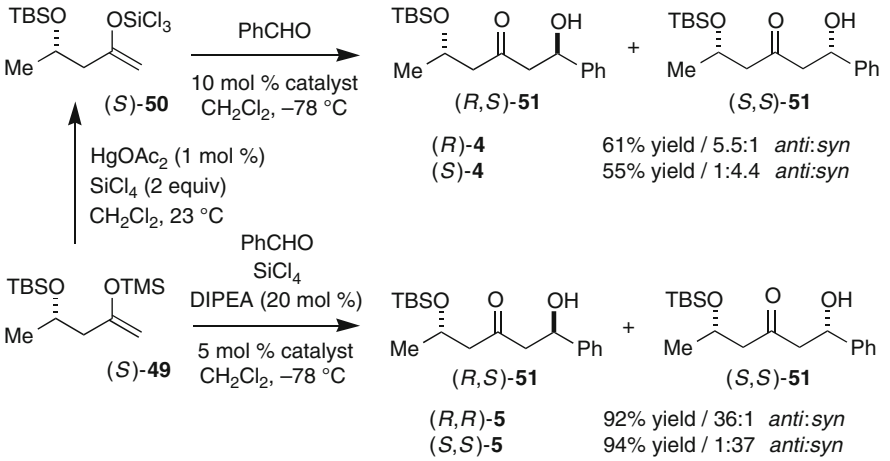

Scheme 12 Comparison of aldolization of chiral methyl ketones (*S*)-**49** and (*S*)-**50**

α-methyl silyl enol ether (*S*)-**46**, but its influence is more significant in the case of the enoxytrichlorosilanes, attesting to the stereocontrolling power of bisphosphoramide **5** when compared to the monophosphoramide **4**. For the addition of the β-TBS ether (*S*)-**49**, complete catalyst control is observed in the phosphoramide/$SiCl_4$ system (Scheme 12). An even more complex substrate in which both internal and relative diastereoselectivities are expressed again testifies to the overwhelming power of the bisphosphoramide/$SiCl_4$ catalyst system for controlling the disposition of the reactive components during the crucial bond-formation step, despite the fact that the reaction proceeds through an open transition structure (Scheme 13).

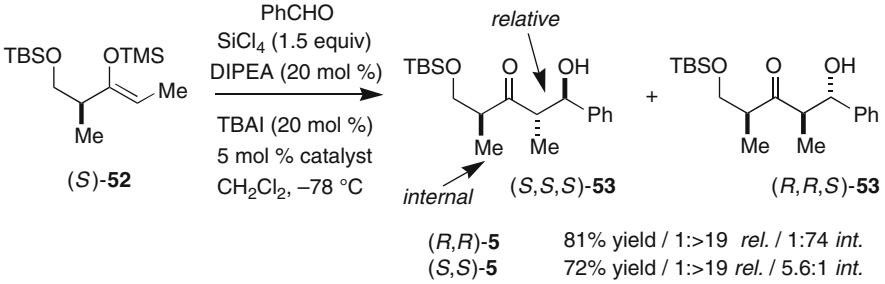

Scheme 13 Double diastereoselection with ethyl ketone (*S*)-**52**

Table 3 Aldolization with glycolate-derived silyl ketene acetals

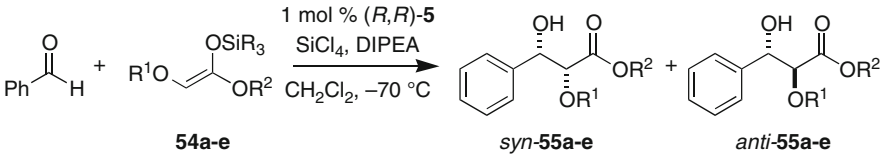

Entry	R^1	R^2	SiR_3	Yield (%)	*Syn*:*anti*	er (*syn*)	er (*anti*)
1	Me (**54a**)	Me	TMS	98 (**55a**)	57:43	74:26	82:19
2	*t*-Bu (**54b**)	Me	TMS	93 (**55b**)	99:1	93:7	ND
3	$PhMe_2C$ (**54c**)	Me	TMS	98 (**55c**)	99:1	96:4	ND
4	Me (**54d**)	*t*-Bu	TMS	93 (**55d**)	4:96	90:10	81:19
5	Me (**54e**)	*t*-Bu	TBS	92 (**55e**)	1:99	ND	92:8
6	Me (**54f**)	Et_2MeC	TBS	92 (**55f**)	1:99	ND	94:6

The complexity of the nucleophilic partner could also be expanded for the silyl ketene acetals. For example, replacement of an alkyl substituent with an alkoxy group on the double bond allows for the investigation of glycolate-derived silyl ketene acetals [58, 59]. These ketene acetals have three variable structural elements (R^1, R^2, and the silyl group, R), and the identity of the group on the α-oxygen (R^1) and the ester (R^2) was shown to be very important for all levels of stereoselectivity (Table 3). Silyl ketene acetals bearing small groups at R^2 afford high levels of *syn*-selectivity (entries 1–3)! In contrast, silyl ketene acetals bearing bulkier R^2 and silyl groups afford products that display the characteristically high levels of *anti*-diastereoselectivity observed earlier (entries 4–6).

The question now arose as to whether this change in substrate had revealed a fundamental change in mechanism or still fit within our proposed model. By analogy to the propanoate silyl ketene acetals, the *anti*-diastereoselectivity observed with the α-methoxy silyl ketene acetal **54f** can easily be rationalized by considering an antiperiplanar transition structure ***xi*** in which the methoxy group is placed away from the catalyst complex to minimize unfavorable steric interactions

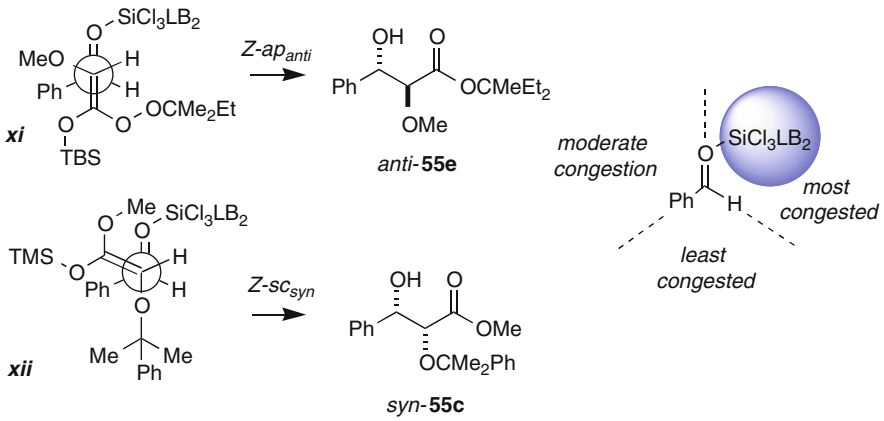

Fig. 6 Rationalization of *syn*- and *anti*-diastereoselectivity in glycolate aldolization

(Fig. 6). This analysis is supported by computational analysis of a simplified silyl ketene acetal structure. However, in the case of *syn*-selective reactions of **54c**, an antiperiplanar transition structure would require placing the bulky tertiary alkyl group R^1 between the bound catalyst complex and the aldehyde substituent, engendering an unfavorable steric interaction with the naphthyl rings of the catalyst. To avoid this unfavorable interaction, the silyl enol ether approach shifts to a +synclinal pathway as shown in ***xii***. Here, the bulky α-substituent can reside in the open lower sector, while the masked ester group, bearing less sterically demanding TMS- and methoxy-groups, can take up a position away from the bound catalyst complex. Even though this switch from an *anti*-diastereoselective process to a *syn*-diastereoselective process upon changing the glycolate structure appeared to challenge our unified model of the phosphoramide/$SiCl_4$ catalyst system, it is in fact consonant with that model. In the activated aldehyde complex, the upper right sector is the most congested, a fact that typically drives anti-diastereoselectivity, regardless of enoxysilane geometry. The upper left sector is the second most congested quadrant and can tolerate all but the largest substituents. The lower sector is the most sterically unencumbered in this chiral complex. Ordering of the groups around the active α-carbon within this scheme controls stereoselectivity in a predictive manner, as demonstrated by the exploration of these glycolate-derived silyl ketene acetals.

Glycolate silyl ketene acetals also highlight how nucleophilicity and steric effects govern the substrate scope of these reactions with respect to the aldehyde (Table 4). In the *syn*-selective glycolate aldol addition of **54c**, aliphatic aldehydes are completely unreactive, even under modified conditions (entry 1). Shifting the steric demand of the α-substituent away from the reactive center without decreasing the overall bulk of the nucleophile by using a *tert*-butyldimethylsilyl group did recover some reactivity (entry 2), but clearly the large steric demands of the α-substituent required to maintain the *syn*-selectivity overwhelm the inherent nucleophilicity of these ketene acetals.

Table 4 Aldolization of aliphatic aldehydes with glycolate-derived silyl ketene acetals

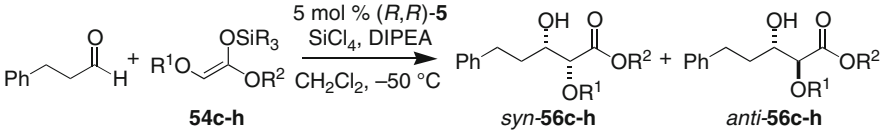

Entry	R^1	R^2	SiR_3	Yield (%)	*Syn*:*anti*	er (*syn*)	er (*anti*)
1	$PhMe_2C$ (**54c**)	Me	TMS	ND (**56c**)	ND	ND	ND
2	TBS (**54g**)	Me	TMS	49 (**56g**)	90:10	87:13	ND
3	Me (**54f**)	Et_2MeC	TBS	ND (**56f**)	ND	ND	ND
4	Me (**54h**)	*i*-Pr_2HC	TBS	88 (**56h**)	1:>99	ND	97:3

In contrast, α-methoxy glycolate silyl ketene acetal **54f** enjoys a wider substrate scope. Here, the steric bulk that biases selectivity resides farther from the reactive α-carbon. Despite an initial setback with **54f**, excellent results with aliphatic aldehydes could be secured by modulating the size of the ester substituent (entry 4). In fact, with silyl ketene acetal **54h**, a broad range of aliphatic aldehydes react with good yield and moderate to excellent selectivities.

The ability of the chiral phosphoramide catalyst to exert such uniform and predictable stereocontrol across a range of nucleophile–electrophile combinations encouraged us to challenge the system with another level of selectivity, namely, site selectivity. The vinylogous aldol addition is a well-known catalytic process in which site selectivity is dictated by a combination of frontier molecular orbital and steric approach control [60–62]. Whereas the reactions of metallodienolates give products of α-alkylation under a charge control model, the reactions of silyl dienol ethers give γ-selectivity in the presence of Lewis or Brønsted acid catalysts. The challenge for our system was to maintain the high level of enantio- and diastereoselectivity observed with silyl ketene acetals without compromising the scope of aldehyde partners. Because the steric contribution of the ester group in the silyl ketene acetal has a strong influence on enantioselectivity, it was unclear what effect moving that group farther from the reactive center would have. In practice, this class of nucleophiles shows good reactivity, excellent site-, and enantioselectivity with the full scope of aldehyde substrates, including aliphatic aldehydes, under the conditions employed for simple silyl ketene acetals (Scheme 14) [63]. High *anti*-diastereoselectivity is also observed here, but the increase in the steric demand of the substrate did lead to some loss in reaction rate and, hence, reactivity with aliphatic aldehydes.

A clear demonstration of the robust nature of this vinylogous aldol reaction can be seen in the total synthesis of RK-397 **65** (Scheme 15) [64]. The vinylogous aldol reaction of the α,β-unsaturated aldehyde **62** is an early key step and can be performed on multigram scale to provide the C19–C25 fragment.

In concert with the principle of vinylogy, the phosphoramide/$SiCl_4$ system could be applied to silyl dienol ethers derived from α,β-unsaturated esters, ketones [65],

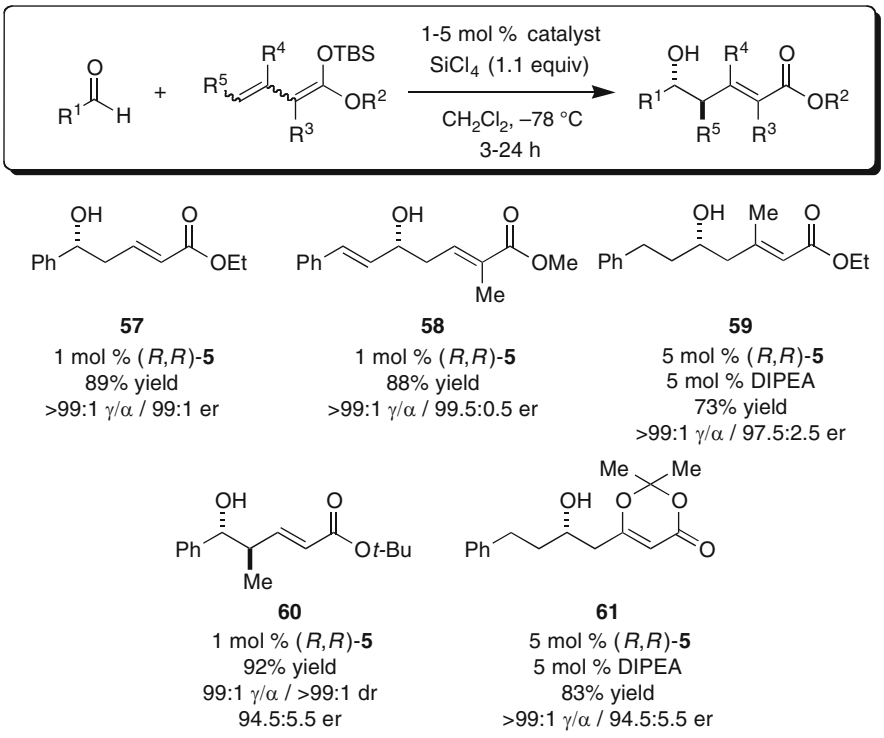

Scheme 14 Vinylogous aldolization with ester-derived silyl dienol ethers

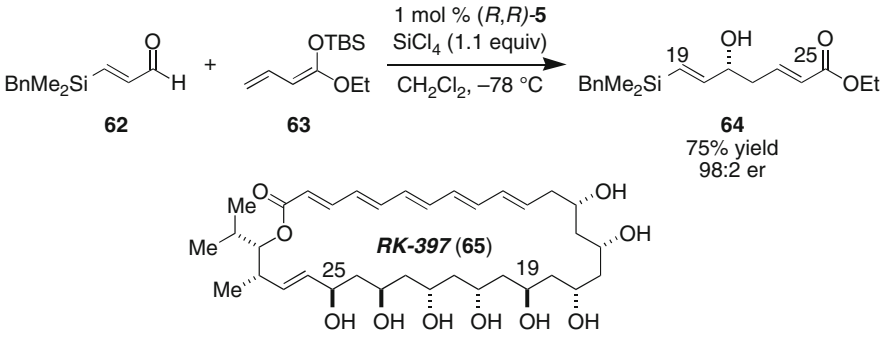

Scheme 15 Application of vinylogous aldolization in the total synthesis of RK-397

and even amides [66, 67]. The amide-derived silyl dienol ethers, by virtue of their enhanced nucleophilicity relative to the esters and ketones, provide the most attractive class of nucleophiles in view of their broad substrate scope with respect to the aldehyde (Scheme 16). Excellent yields and enantioselectivities are obtained using morpholine amide-derived silyl dienol ethers and a range of aliphatic

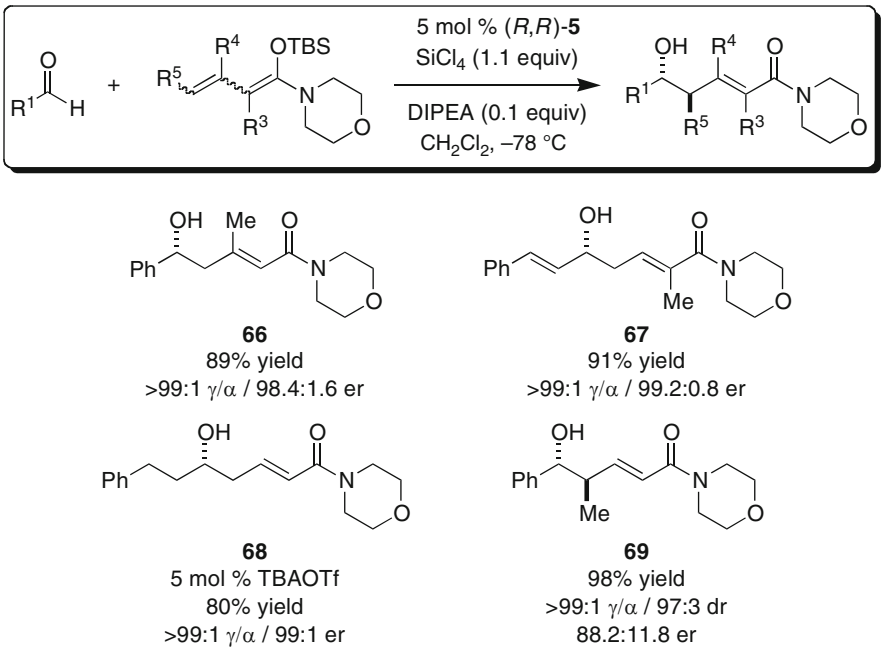

Scheme 16 Vinylogous aldolization with amide-derived silyl dienol ethers

aldehydes. Substitution on the dienol ether is accommodated and high *anti*-diastereoselectivity is also observed. The use of amide-derived silyl dienol ethers is particularly noteworthy from a synthetic perspective as the product amide can be transformed into a wide variety of functional groups, allowing access to vinylogous aldol products that might be inaccessible from the corresponding ester or ketone-derived silyl dienol ethers.

6 The Established Paradigm: Pushing into New Territory

The unique properties of this catalyst system, most significantly the activation of a weak Lewis acid by a strongly Lewis basic catalyst, bring with them some fundamental considerations, such as the often troublesome role played by the ionized chloride formed during the generation of the chiral silicenium ion. However, as seen in the case of the aldehyde–aldehyde aldol reaction discussed above, these traits can also provide tangible benefits. In the course of these investigations, the question of whether this catalyst system could go beyond the scope of normal Lewis acid-catalyzed processes was raised repeatedly and eventually found an answer in the development of two novel processes involving isocyanides and silyl ketene imines. Both reactions, but especially the Lewis base-catalyzed–Lewis acid-promoted Passerini reaction of isocyanides, capitalize on the unique features of this catalyst system (Scheme 17).

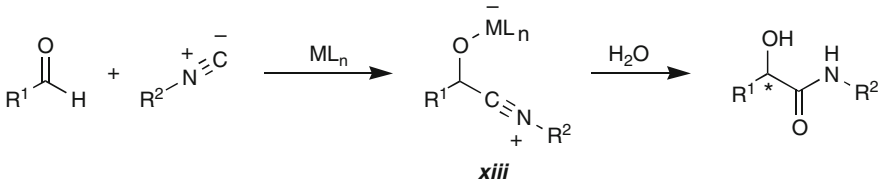

xiii

Scheme 17 The generalized Passerini reaction

The development of a catalytic, asymmetric Passerini reaction has long evaded chemists' efforts because of the basicity of isocyanides and the inherent reactivity of the initially formed isocyanide adduct ***xiii*** [68–73]. Competitive binding of the basic isocyanide to the Lewis acidic catalyst ML_n can lead to deactivation and low conversions. Addition of isocyanide to the initially formed nitrilium ion can also lead to low yields of the desired α-hydroxy amide after quenching. We felt that the phosphoramide/$SiCl_4$ system could address both these issues because (1) binding of the isocyanide to the weak Lewis acid $SiCl_4$ should be minimized and (2) the ionized chloride ion could serve as an internal trapping agent for the nitrilium ion intermediate ***xiii***. Indeed, the isocyanide itself could promote the Passerini reaction with $SiCl_4$, and good yields of the desired amide could be obtained after quenching (Table 5, entry 1) [74, 75]. The high-yield and low-impurity profile of the reaction validated our hypothesis about the positive role of the chloride ion in this process, although the complication of a competitive, achiral background reaction promoted by isocyanide suggested that binding of the isocyanide to $SiCl_4$ may still prove problematic. However, in the presence of a chiral phosphoramide, good yields and a promising level of enantioselectivity were observed for the formation of the α-hydroxy amide (entry 2). The background reaction promoted by the isocyanide could be minimized by slow addition of the isocyanide over 4 h, allowing for good yields and very high levels of enantioselectivity (entries 3–4). The fact that aliphatic aldehydes also react is surprising, considering the low nucleophilicity of *tert*-butyl isocyanide ($N = 5.47$ [42]), but it is not inconceivable, considering the compact nature of this reactive *sp*-hybridized nucleophile (entry 5).

One unique feature of this catalyst system is the observation that pyridine *n*-oxide also serves as an effective catalyst. Although chiral *n*-oxides are not effective asymmetric catalysts for this reaction, the discovery of another strong Lewis base aside from a phosphoramide serving as an effective promoter for a reaction mediated by $SiCl_4$ is gratifying [76–79].

Another question that intrigued us was whether the high-diastereoselectivity characteristic of this catalyst system could be harnessed for the construction of quaternary stereogenic centers. Because the formation of a single geometrical isomer of a α,α-disubstituted silyl enol ether or ketene acetal is often challenging, attainting high diastereoselectivity in the formation of quaternary centers via an aldol reaction is problematic, even if the transition structure is highly organized. We wondered if the diastereoconvergent nature of these Lewis base-catalyzed–Lewis acid-mediated aldol reactions could provide a solution. Unfortunately, α,α-disubstituted nucleophiles are

Table 5 Catalytic, enantioselective Passerini-type reactions

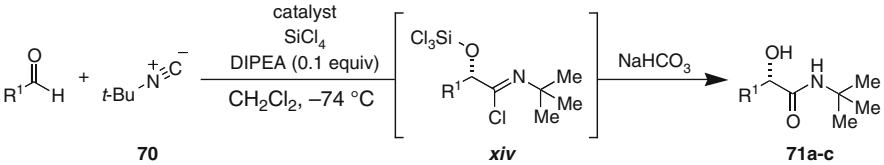

Entry	R	Catalyst	Addition	Yield (%)	er
1	Ph	–	–	79 (**71a**)	–
2	Ph	5 mol% (*R*,*R*)-**5**	–	83 (**71a**)	90.2:9.8
3	Ph	5 mol% (*R*,*R*)-**5**	4h	96 (**71a**)	>99:1
4	PhCH=CH	5 mol% (*R*,*R*)-**5**	4h	81 (**71b**)	97.8:2.2
5	$PhCH_2CH_2$	5 mol% (*R*,*R*)-**5**	4h	92 (**71c**)	81.9:18.1

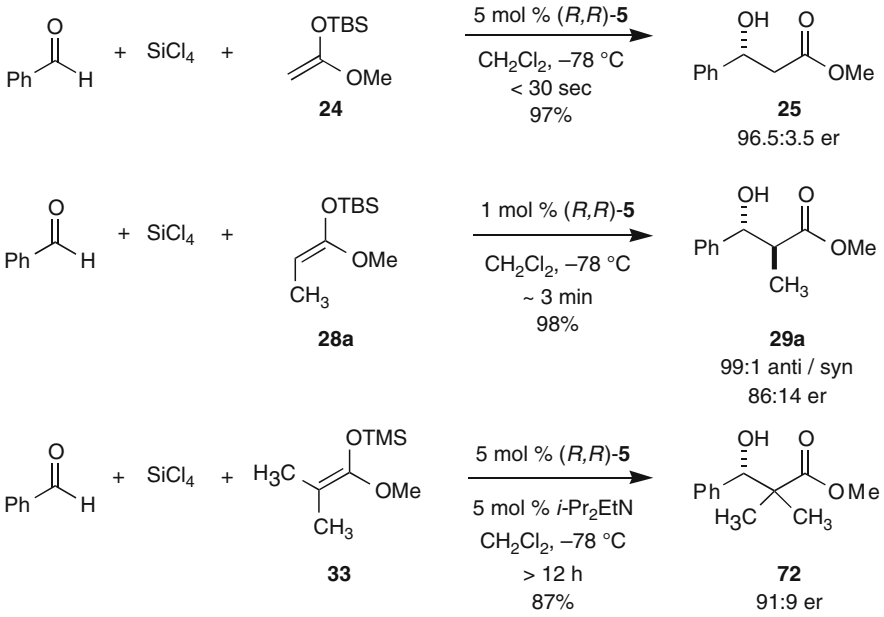

Scheme 18 Comparison of reactivity of various silyl ketene acetals

too sterically encumbered to react with the full scope of aldehydes under catalysis by the phosphoramide/$SiCl_4$ system. For example, comparison of the reactions of acetate-, propanoate-, and isobutyrate-derived silyl ketene acetals with benzaldehyde clearly shows this trend in reactivity (Scheme 18). Aliphatic aldehydes proved completely unreactive with the isobutyrate silyl ketene acetal **33**. Unsymmetrically α,α-disubstituted silyl ketene acetals led to similarly disappointing results.

Table 6 Catalytic, enantioselective additions of silyl ketene imines to 2-naphthaldehyde

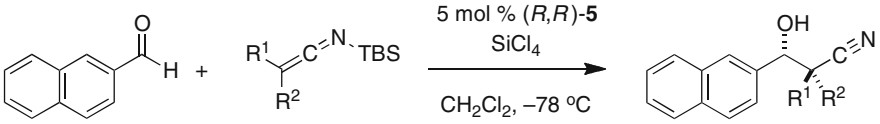

73a-f **74a-f**

Entry	R^1	R^2	Yield (%)	dr	er
1	Ph (**73a**)	Me	87 (**74a**)	95:5	98.5:1.5
2	Ph (**73b**)	Et	78 (**74b**)	97:3	92.7:7.3
3	Ph (**73c**)	*i*-Bu	90 (**74c**)	99:1	99.6:0.4
4	Ph (**73d**)	*i*-Pr	73 (**74d**)	61:39	78.9:21.1
5	*i*-Pr (**73e**)	Me	92 (**74e**)	60:40	92.1:7.9
6	$-(CH_2)_5-$ (**73f**)		85 (**74f**)	NA	91.2:8.8

To address this problem, we became interested in an under-explored class of silyl π-nucleophiles, namely, silyl ketene imines. Silyl ketene imines have a number of important structural differences compared to silyl ketene acetals. Most notable are the orthogonality of terminal substituents and the degree of steric hindrance on the distal end of the nucleophile. In silyl ketene acetals, the bulk of the two substituents flanking the sp^2-hybridized carbon atom has a significant effect on selectivity (see Table 1). More importantly, they have an equally significant impact on reaction rate. This trend is also clearly illustrated in the reactivity of aldehyde-derived silyl enol ethers (Table 2). In contrast, the sp-hybridized atom of the silyl ketene imine bears only a single nitrogen substituent. By virtue of this decrease in the steric demands of silyl ketene imines compared to silyl ketene acetals, we hypothesized that the silyl ketene imine should be more reactive, even with unsymmetrically α,α-disubstituted substrates. In that case, it might be possible to extend the high levels of enantio- and diastereocontrol exerted by this catalyst system to the formation of quaternary stereogenic centers.

Much to our delight, the silyl ketene imines gave high levels of enantio- and diastereoselectivity under the standard reaction conditions (Table 6) [80]. Similarly, the *anti*-diastereoselectivity observed with α-substituted nucleophiles is retained such that the relative disposition of the alcohol and the larger substituent R^1 in the β-hydroxy nitrile product is anti, consistent with our model for selectivity. Diastereo- and enantioselectivity are generally high for silyl ketene imines bearing a one aliphatic and one aromatic substituent. Only in the case of bulky isopropyl-substituted silyl ketene imines is any significant erosion in *anti*-diastereoselectivity observed (entries 4 and 5), consistent with earlier observations that branching in an aliphatic substituent proximal to either reactive center has an unexpectedly negative impact on selectivity. Moreover, reaction times are surprisingly short, in accordance with our assumptions about the relief of steric interactions between the nucleophile and activated aldehyde catalyst complex.

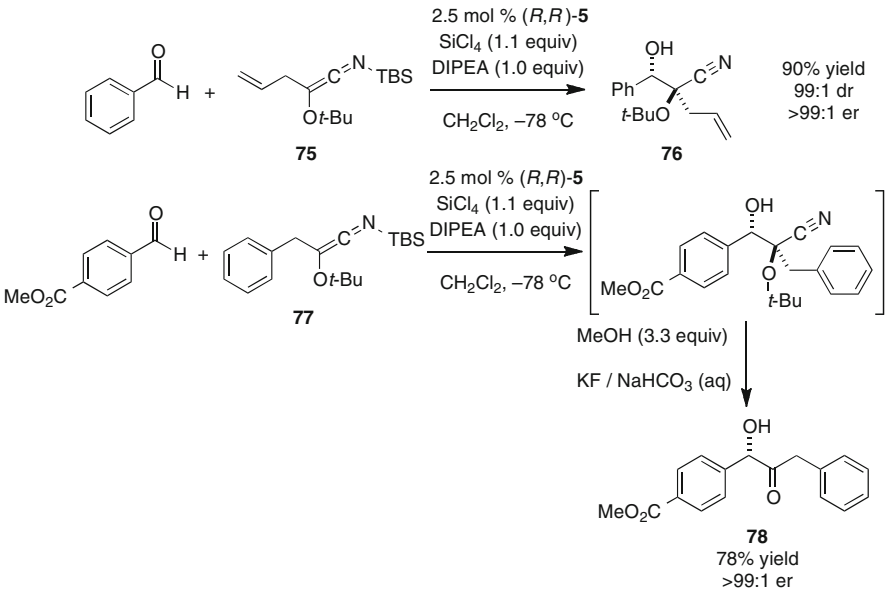

Scheme 19 Catalytic, enantioselective additions of *N*-silyl oxyketene imines

An interesting extension of this method involves the reaction of *N*-silyl oxyketene imines derived from cyanohydrins (Scheme 19) [81]. By judicious selection of the protecting group on the oxygen, highly functionalized β-hydroxy cyanohydrins can be accessed with high levels of enantio- and diastereoselectivity. These products can then be transformed into a diversity of structural motifs (amines, aldehydes, imines, ketones) important for the synthesis of polyketide and other classes of natural products. In addition, the ethers can be easily converted to enantiomerically enriched unsymmetrical benzoins, thus revealing the synthetic equivalency of *N*-silyl oxyketene imines as acyl anions (Scheme 19).

The high reactivity of α,α-disubstituted silyl ketene imines relative to α,α-disubstituted silyl ketene acetals led us to believe that they would show broad substrate scope with respect to aldehydes. However, in numerous tests, even under the modified conditions that had allowed for a recovery of reactivity with other classes of nucleophiles, no reaction was found with aliphatic aldehydes. This result attests to the subtle interplay of nucleophilicity and steric effects which impacts all aspects of this catalyst system.[1] This new paradigm and the underlying model based on *N* values remain a potent guiding principle for reaction design with the $SiCl_4$/phosphoramide catalyst system, but as always, unexpected results can challenge our assumptions and suggest the need for a deeper understanding.

[1] This hypothesis is further supported by the observation that conjugated silyl ketene imines (derived from unsaturated nitriles) react efficiently and selectively with aliphatic aldehydes at the less hindered γ-carbon. Wilson TW unpublished results from these laboratories.

7 A Fuller Mechanistic Understanding Emerges

The mechanistic picture that guided the majority of this work was one based on knowledge gained by the careful study of the Lewis base-catalyzed reactions of organotrichlorosilanes [28–30]. The broad applicability and unique selectivity of the $SiCl_4$/bisphosphoramide catalyst system prompted us to gain a more secure understanding of the proposed mechanism of these Lewis base-catalyzed–Lewis acid-mediated reactions. Before refining the mechanism, it is helpful to again review the salient features of this reaction mechanism which are believed to be common to all the chemistry described thus far (Fig. 7). Beginning with the binding of two equivalents of phosphoramide to the weakly Lewis acidic $SiCl_4$, polarization of the silicon–chlorine bonds and ionization of chloride generate the chiral silicenium ion catalyst ***iv***. Binding of the aldehyde followed by reaction of the π-nucleophile with the *Re* face [assuming the use of the (*R*,*R* catalyst)] of the activated aldehyde complex ***v*** leads to the catalyst-bound trichlorosilyl ether ***xv***. Dissociation of catalyst then frees the Lewis base to activate another molecule of $SiCl_4$. As is clear in this description, each turnover of the Lewis basic catalyst consumes a single molecule of $SiCl_4$. Although the active species is a Lewis acid derived from the stoichiometric reagent $SiCl_4$, it is only the action of the Lewis basic catalyst that renders it sufficiently Lewis acidic to promote a bond-forming event.

Earlier kinetic studies on the simpler, but closely related, $SiCl_4$-mediated ring opening of *meso*-epoxides in the presence of hexamethylphosphoric triamide (HMPA) led to the realization that the reaction was second order in the monomeric phosphoramide (*R*)-**10** catalyst and zero order in $SiCl_4$ [32]. Second-order kinetic dependence on a monomeric phosphoramide had already been documented in the reactions of enoxytrichlorosilanes and is not surprising. The zero-order dependence on $SiCl_4$ means that the phosphoramide is saturated with $SiCl_4$ in a preequilibrium under the reaction conditions, and thus, additional $SiCl_4$ does not increase the rate. Thus, a silicenium ion complex related to ***iv*** is the likely resting state of the phosphoramide catalyst. Indeed, low-temperature ^{29}Si NMR experiments reveal the presence of a hypervalent silicon-containing species which displays strong ^{31}P coupling to two phosphorus atoms, thereby providing support for the kinetic data and the existence of the intermediate **80** (Scheme 20). These observations are qualitatively consistent with our proposed mechanism and added further support for the unique features of the proposed mechanism, namely, the idea of a chiral silicenium ion as the catalyst resting state.

The high rate of the epoxide-opening reaction made a thorough kinetic analysis challenging. Reexamination of the kinetic profile of a phosphoramide/$SiCl_4$-catalyzed reaction with an aldehyde electrophile proved more feasible because the broad substrate scope of these reactions allowed for the selection of reaction partners that give reasonable reaction rates and a more detailed analysis to be obtained without moving away from synthetically relevant reaction conditions.

Using a home-built rapid injection NMR system (RINMR), our plan was to determine the order in each of the reactive components. RINMR is uniquely suited

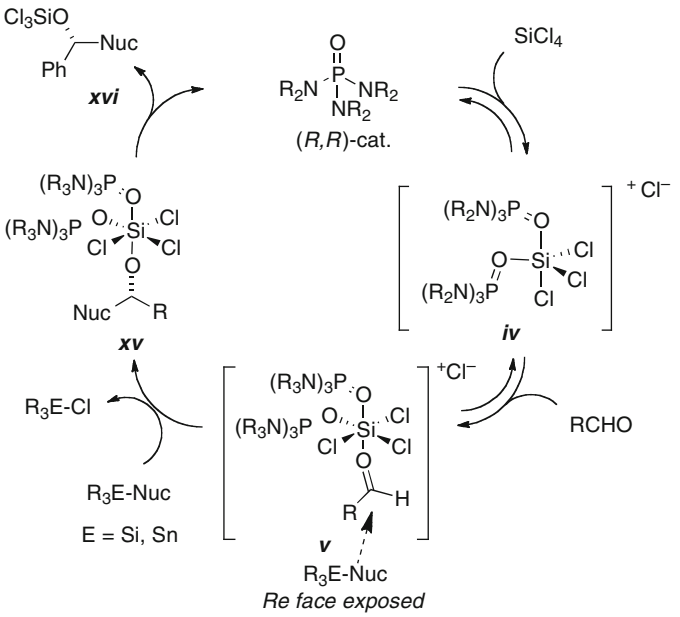

Fig. 7 Generalized catalytic cycle for Lewis base-catalyzed–Lewis acid-promoted aldolization

Scheme 20 Mechanistic details of HMPA catalyzed opening of *cis*-stilbene oxide with $SiCl_4$

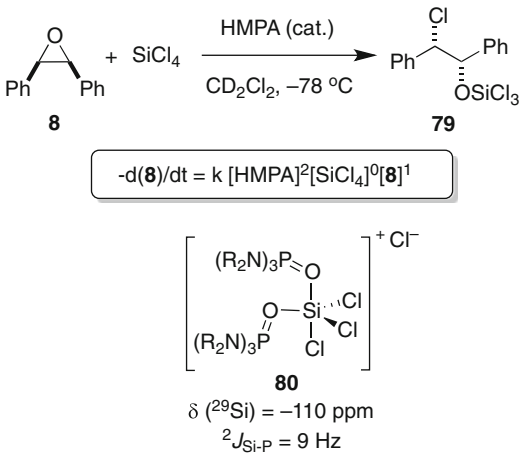

to address the challenges posed by studying this reaction [82]. The ability to obtain highly accurate data in a noninvasive manner made this technique far superior to the use of in situ IR or traditional time point monitoring with either HPLC or GC. The RINMR analysis showed that the reaction between 1-naphthaldehyde and the propanoate-derived silyl ketene acetal **28e** is first order in both the aldehyde and silyl ketene acetal (Scheme 21) [83]. The reaction was zero order in DIPEA as well as in $SiCl_4$. A slight inverse order of −0.2 was observed when tetrabutylammonium

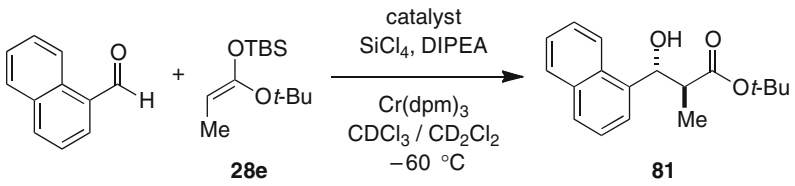

Scheme 21 Aldolization of propanoate-derived silyl ketene acetal used for RINMR studies

Table 7 Summary of fractional order in catalyst from aldolization by RINMR

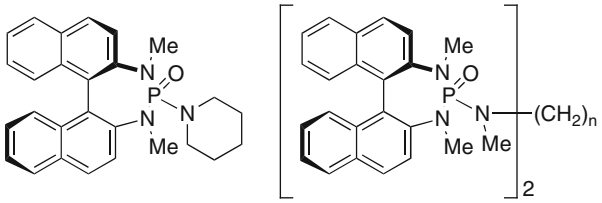

(*R*)-**10** (*R*,*R*)-**5**,**82**-**84**

Entry	Catalyst	Order
1	HMPA	0.64
2	(*R*)-**10**	1
3	(*R*,*R*)-**82** ($n = 3$)	0.95
4	(*R*,*R*)-**83** ($n = 4$)	0.95
5	(*R*,*R*)-**5** ($n = 5$)	0.5
6	(*R*,*R*)-**84** ($n = 6$)	0.48

chloride was examined as an additive, in accordance with a common ion effect expected for formation of the silicenium ion. Thus far, the kinetic analysis agreed with the lessons learned from studying the epoxide-opening reaction, but the similarity ends there. Surprisingly, the order in the bisphosphoramide catalyst (*R*,*R*)-**5** is 0.5! This fractional order with respect to catalyst at first seems to controvert the proposed mechanism that hinges on the intermediacy of the discrete silicenium ion bound by a chelating bisphosphoramide. Examination of several other phosphoramide catalysts revealed a more complex picture where the dependence on catalyst loading proved highly sensitive to changes in the structure of the phosphoramide (Table 7). Fractional orders obtained upon examination of some monomeric phosphoramides further challenged our apparently oversimplified reaction mechanism.

The fractional order revealed with the optimal bisphosphoramide catalysts could be readily explained when taken together with data from ^{29}Si NMR and X-ray crystallographic studies of a variety of $SiCl_4$/phosphoramide mixtures [84]. ^{29}Si NMR investigations of mixture of the bisphosphoramide (*R*,*R*)-**5** and $SiCl_4$ reveal presence of three species in addition to free $SiCl_4$. One signal assigned to **85** ($\delta = -118.4$ ppm, t, $J = 14$ Hz) appears in the region characteristic of five

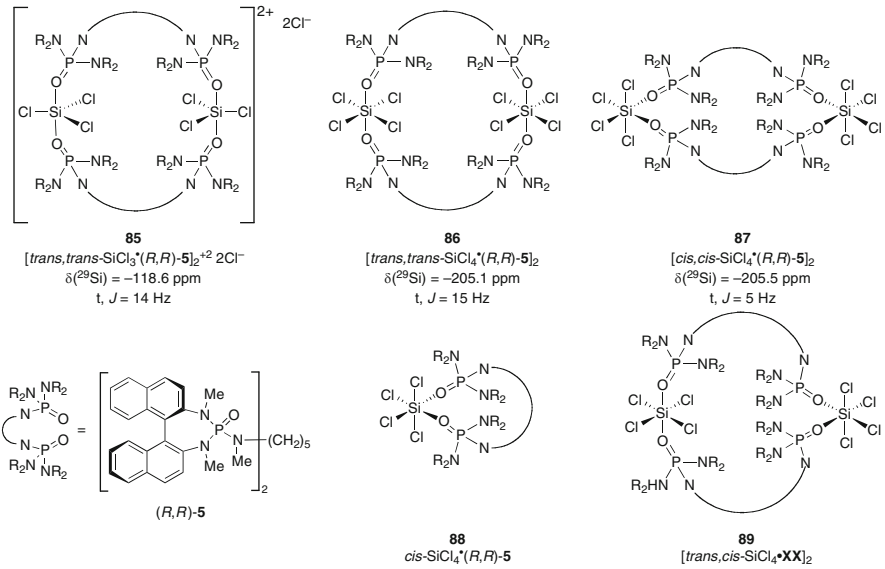

Fig. 8 Phosphoramide·$SiCl_4$ complexes detected by solution NMR

coordinate silicon species [85–88] and is clearly bound by two phosphoramides due to the ^{31}P coupling. The remaining two species **86** and **87** also appear to be bound by two phosphoramides but reside in a chemical-shift regime indicative of a six coordinate silicon species (ca. 205 ppm). In analogy with the ^{29}Si NMR and X-ray crystallographic data obtained using HMPA, the signals could be assigned, as shown in Fig. 8. Therefore, to rationalize the 0.5 order in catalyst, a mechanism can be proposed where the catalytically inactive dimeric resting state must dissociate to the catalytically active monomeric complex prior to binding aldehyde. Additional support for this conclusion is garnered from the lack of observation of any nonlinear effect when catalyst of varying levels of enantiopurity was employed.

On the basis of these results and the zero-order dependence on $SiCl_4$, the bisphosphoramide catalyst must be saturated with $SiCl_4$; however, it does not yield a single, well-defined species, but rather a mixture of inactive equilibrating complexes. The exact position and identity of the species in this equilibrium are highly sensitive to catalyst structure. However, in each case, the fractional order in catalyst makes clear that dissociation of a chelated bisphosphoramide complex is involved in the productive reaction pathway. Changes in the nature of this equilibrium mixture dependent on catalyst structure help rationalize the various but consistently fractional catalyst order observed in these processes.

With this information, a unified reaction mechanism and kinetic equation can be proposed for the highly selective carbonyl addition reactions promoted by the bisphosphoramide (*R*,*R*)-**5** and $SiCl_4$ (Fig. 9). Initial binding of the phosphoramide to $SiCl_4$ is rapid and quantitative, as expected for zero-order behavior in $SiCl_4$. This leads to a catalytically inactive mixture of $SiCl_4$-phosphoramides species, including

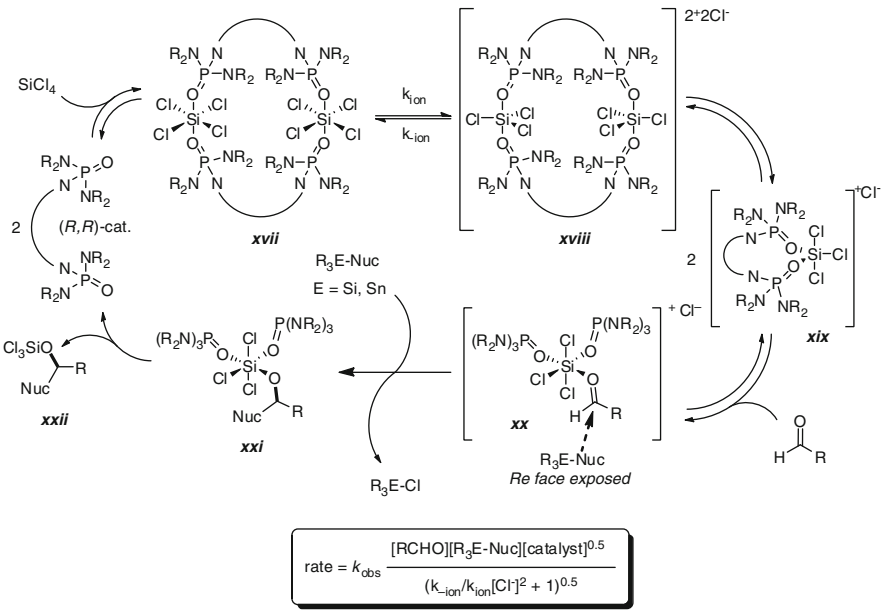

Fig. 9 Catalytic cycle of aldolization derived from kinetic and spectroscopic analysis

both neutral and cationic 5- and 6-coordinate complexes. The position of the ionization preequilibrium (k_{ion}/k_{-ion}) dictates the chloride ion dependence. Dissociation of a dimeric complex such as **85** then leads to formation of the catalytically active silicenium ion similar to ***iv***, in accordance with a half-order dependence on catalyst. The binding of the aldehyde to the silicenium ion is reversible and substoichiometric as seen in the first-order dependence on aldehyde. The rate- and stereochemistry-determining step is the attack of the π-nucleophile (first-order dependence on silyl ketene acetal) on the activated aldehyde complex which leads to the catalyst-bound trichlorosilyl ether. Dissociation of the catalyst from the trichlorosilyl ether then frees the Lewis base to activate another molecule of $SiCl_4$, completing the catalytic cycle. This process clearly defines these reactions as Lewis base catalyzed and Lewis acid mediated. $SiCl_4$ by itself is too weakly Lewis acidic to activate the aldehyde. Only upon the action of the Lewis base can a competent Lewis acid be generated to facilitate the desired carbon–carbon bond-forming event.

8 Conclusions and Outlook

The formulation of a unified mechanistic scheme for Lewis base-catalyzed–Lewis acid-mediated reactions brings our journey full circle, a journey that began with attempts to understand aberrations in our study of the Lewis base-catalyzed

reactions of organotrichlorosilanes. A new and well-supported paradigm has now been established that provides a predictive model based on a consideration of steric effects and well-known principles of π-nucleophilicity. This catalytic system has been adopted by others, and its scope expanded to more complex substrates and novel reactions [89].

Most importantly, the paradigm of Lewis base activation of Lewis acids has deepened our understanding of Lewis base catalysis as a novel alternative to the traditional mode of Lewis acid activation of organic reactions [90] and has inspired the investigations of Lewis base-catalyzed reactions beyond silicon. Indeed, the concept of Lewis base activation of Lewis acids is not limited to the chemistry of $SiCl_4$; it should be generally applicable to the chemistry of all main group and many transition metal compounds. Specifically, those electrophilic reagents in groups 13 and 15–17 should be susceptible to activation by Lewis basic donors in unprecedented ways. Indeed, the ability to catalyze electrophilic chalcogenation and halogenation has been demonstrated and is now being developed in novel asymmetric transformations [91–98]. Furthermore, these investigations have provided practical benefits to synthetic organic chemists by describing a useful and highly reliable method amenable to the synthesis of complex molecule targets [99–101].

It is our hope that this account serves as a reminder to scientists to not ignore or dismiss data that does not fit into even the most well-defined or well-established mechanistic scheme. When inconsistent results transition from the realm of the irreproducible to that of the reproducible but irreconcilable, they can be as valuable as any high-yielding or highly selective transformation. As Kuhn pointed out, it is often the momentary disruptions and confusion caused by these inconsistencies that are the gateway to new discoveries.

Acknowledgments We are grateful to the National Institutes of Health (R01 GM08525) and the National Science Foundation (NSF CHE 0414440, 0717989 and 1012663) for continuing support of this project.

References

1. Kuhn TS (1962) The structure of scientific revolutions. University of Chicago Press, Chicago
2. Santelli M, Pons J-M (1996) Lewis acids and selectivity in organic synthesis. CRC Press, Boca Raton
3. Yamamoto H (2001) Lewis acids in organic synthesis. Wiley-VCH, Weinheim
4. Denmark SE, Stavenger RA (2000) Asymmetric catalysis of aldol reactions with chiral lewis bases. Acc Chem Res 33:432–440
5. Denmark SE, Fujimori S (2004) Catalytic, enantioselective aldol reactions with chiral lewis bases. In: Mahrwald R (ed) Modern aldol reactions. Wiley-VCH, Weinheim
6. Denmark SE, Coe DM, Pratt NE, Griedel BD (1994) Asymmetric allylation of aldehydes with chiral lewis bases. J Org Chem 59:6161–6163
7. Denmark SE, Fu J (2000) On the mechanism of catalytic, enantioselective allylation of aldehydes with chlorosilanes and chiral lewis bases. J Am Chem Soc 122:12021–12022

8. Denmark SE, Fu J (2001) Catalytic, enantioselective addition of substituted allylic thrichlorosilanes using a rationally-designed 2,2′-bispyrrolidine-based bisphosphoramide. J Am Chem Soc 123:9488–9489
9. Denmark SE, Fu J (2002) Asymmetric construction of quaternary centers by enantioselective allylation: application to the synthesis of the serotonin antagonist LY426965. Org Lett 4:1951–1953
10. Denmark SE, Fu J, Coe DM, Su X, Pratt NE, Griedel BD (2006) Chiral phosphoramide-catalyzed enantioselective addition of allylic trichlorosilanes to aldehydes. preparative and mechanistic studies with monodentate phosphorus-based amides. J Org Chem 71:1513–1522
11. Denmark SE, Fu J, Lawler MJ (2006) Chiral phosphoramide-catalyzed enantioselective addition of allylic trichlorosilanes to aldehydes. Preparative studies with bidentate phosphorus-based amides. J Org Chem 71:1523–1536
12. Denmark SE, Fu J (2003) Catalytic enantioselective allylation with chiral lewis bases. Chem Commun 167–170
13. Denmark SE, Fu J (2003) Catalytic enantioselective addition of allylic organometallic reagents to aldehydes and ketones. Chem Rev 103:2763–2793
14. Denmark SE, Fan Y, Eastgate MD (2005) Lewis base catalyzed, enantioselective aldol addition of methyl trichlorosilyl ketene acetal to ketones. J Org Chem 70:5235–5248
15. Denmark SE, Fan Y (2002) Catalytic, enantioselective aldol additions to ketones. J Am Chem Soc 124:4233–4235
16. Denmark SE, Winter SBD, Su X, Wong K-T (1996) The chemistry of trichlorosilyl enolates. 1. New reagents for catalytic asymmetric aldol additions. J Am Chem Soc 118:7404–7405
17. Denmark SE, Fujimori S, Pham SM (2005) Base catalyzed aldol additions of chiral trichlorosilyl enolates and silyl enol ethers. J Org Chem 70:10823–10840
18. Denmark SE, Pham SM (2003) Stereoselective aldol additions of achiral ethyl ketone-derived trichlorosilyl enolates. J Org Chem 68:5045–5055
19. Denmark SE, Stavenger RA, Wong K-T, Su X (1999) Chiral phosphoramide-catalyzed aldol additions of ketone enolates. Preparative aspects. J Am Chem Soc 121:4982–4991
20. Denmark SE, Stavenger RA (2000) The chemistry of trichlorosilyl enolates. Aldol addition reactions of methyl ketones. J Am Chem Soc 122:8837–8847
21. Denmark SE, Stavenger RA, Wong K-T (1998) Asymmetric aldol additions catalyzed by chiral phosphoramides: electronic effects of the aldehyde component. Tetrahedron 54:10389–10402
22. Denmark SE, Su X, Nishigaichi Y (1998) The chemistry of trichlorosilyl enolates. 6. Mechanistic duality in the lewis base-catalyzed aldol addition reaction. J Am Chem Soc 120:12990–12991
23. Denmark SE, Stavenger RA, Wong K-T (1998) Lewis base-catalyzed, asymmetric aldol additions of methyl ketone enolates. J Org Chem 63:918–919
24. Denmark SE, Wong K-T, Stavenger RA (1997) The chemistry of trichlorosilyl enolates. 2. Highly-selective asymmetric aldol additions of ketone enolates. J Am Chem Soc 119:2333–2334
25. Denmark SE, Ghosh SK (2007) Unexpected ambidoselectivity in crossed-aldol reaction of α-oxy aldehyde trichlorosilyl enolates. Tetrahedron 63:8636–8644
26. Denmark SE, Bui T (2004) Chiral phosphoramide-catalyzed, enantioselective, directed cross-aldol reactions of aldehydes. Proc Natl Acad Sci USA 101:5439–5444
27. Denmark SE, Ghosh SK (2001) The first catalytic, diastereoselective, and enantioselective crossed-aldol reactions of aldehydes. Angew Chem Int Ed 40:4759–4762
28. Denmark SE, Pham SM, Stavenger RA, Su X, Wong K-T, Nishigaichi Y (2006) Chiral phosphoramide-catalyzed aldol additions of ketone trichlorosilyl enolates. Mechanistic aspects. J Org Chem 71:3904–3922
29. Denmark SE, Pham SM (2000) Kinetic analysis of the divergence of reaction pathways in the chiral lewis base promoted aldol addition of trichlorosilyl enolates: a rapid injection NMR study. Helv Chim Acta 83:1846–1853

30. Denmark SE, Su X (1999) Solid state and solution structural studies of chiral phosphoramide-tin complexes relevant to lewis base catalyzed aldol addition reactions. Tetrahedron 55:8727–8738
31. Wong K-T (1998) Post-doctoral report. University of Illinois, Urbana-Champaign
32. Denmark SE, Barsanti PA, Beutner GL, Wilson TW (2007) Enantioselective ring opening of epoxides with silicon tetrachloride in the presence of a chiral lewis base. Mechanism studies. Adv Synth Catal 349:567–582
33. Denmark SE, Barsanti PA, Wong K-T, Stavenger RA (1998) Enantioselective ring opening of epoxides with chlorosilanes in the presence of Lewis-bases. J Org Chem 63:2428–2429
34. Guthrie JP (1978) Equilibrium constants for a series of simple aldol condensations, and linear free energy relations with other carbonyl addition reactions. Can J Chem 56:962–973
35. Denmark SE, Wynn T (2001) Lewis base activation of lewis acids: catalytic enantioselective allylation and propargylation of aldehydes. J Am Chem Soc 123:6199–6200
36. Denmark SE, Almstead NG (2000) Allylation of carbonyls: methodology and sterechemistry. In: Otera J (ed) Modern carbonyl chemistry. Wiley-VCH, Weinheim
37. Chemler SR, Roush WR (2000) Recent applications of the allylation reaction in the total synthesis of natural products. In: Otera J (ed) Modern carbonyl chemistry. Wiley-VCH, Weinheim
38. Yanagisawa A (1999) Allylation of carbonyl groups. In: Jacobsen EN, Pfaltz A, Yamamoto H (eds) Comprehensive asymmetric catalysis, vol II. Springer, Heidelberg
39. Mayr H, Kempf B, Ofial AR (2003) π-Nucleophilicity in carbon-carbon bond-forming reactions. Acc Chem Res 36:66–77
40. Mayr H (2011) Database of nucleophilicities and electrophilicities. Ludwig Maximilians-Universität München, Munich. http://www.cup.uni-muenchen.de/oc/mayr/DBintro.html. Accessed 9 Aug 2011
41. Tumanov VV, Tishkov AA, Mayr H (2007) Nucleophilicity parameters for alkyl and aryl isocyanides. Angew Chem Int Ed 19:3563–3566
42. Tokuyasu T, Mayr H (2004) Nucleophilic reactivities of ketene acetals. Eur J Org Chem 13:2791–2796
43. Mayr H, Bug T, Gotta MF, Hering N, Irrgang B, Janker B, Kempf B, Loos R, Ofial AR, Remennikov G, Schimmel H (2001) Reference scales for the characterization of cationic electrophiles and neutral nucleophiles. J Am Chem Soc 123:9500–9512
44. Burfeindt J, Patz M, Mueller M, Mayr H (1998) Determination of the nucleophilicities of silyl and alkyl enol ethers. J Am Chem Soc 120:3629–3634
45. Denmark SE, Beutner GL, Wynn T, Eastgate MD (2005) Lewis base activation of lewis acids: catalytic, enantioselective addition of silyl ketene acetals to aldehydes. J Am Chem Soc 127:3774–3789
46. Denmark SE, Wynn T, Beutner GL (2002) Lewis base activation of lewis acids. Addition of silyl ketene acetals to aldehydes. J Am Chem Soc 124:13405–13407
47. Heathcock CH, Davidsen SK, Hug KT, Flippin LA (1986) Acyclic stereoselection. 36. Simple diastereoselection in the Lewis acid mediated reactions of enol silanes with aldehydes. J Org Chem 51:3027–3037
48. Short JD, Attenoux S, Berrisford DJ (1997) Additive effects on ligand activated allylation of aldehydes by allyltrichlorosilane. Tetrahedron Lett 38:2351–2354
49. Denmark SE, Heemstra JR (2003) Lewis base activation of lewis acids. Catalytic enantioselective addition of silyl enol ethers of achiral methyl ketones to aldehydes. Org Lett 5:2303–2306
50. Denmark SE, Bui T (2005) Lewis base-catalyzed enantioselective aldol addition of acetaldehyde-derived silyl enol ether to aldehydes. J Org Chem 70:10190–10193
51. Masamune S, Choy W, Petersen JS, Sita LR (1985) Double asymmetric synthesis and a new strategy for stereochemical control in organic synthesis. Angew Chem Int Ed 24:1–30
52. Kolodiazhnyi OI (2003) Multiple stereoselectivity and its application in organic synthesis. Tetrahedron 59:5953–6018

53. Denmark SE, Fujimori S (2002) Diastereoselective aldol additions of chiral beta-hydroxy ethyl ketone enolates catalyzed by Lewis bases. Org Lett 4:3473–3476
54. Denmark SE, Fujimori S (2002) The effects of a remote stereogenic center in the lewis base catalyzed aldol additions of chiral trichlorosilyl enolates. Org Lett 4:3477–3480
55. Denmark SE, Pham SM (2001) Highly diastereoselective aldol additions of a chiral ethyl ketone enolate under lewis base catalysis. Org Lett 3:2201–2204
56. Denmark SE, Fujimori S (2000) Diastereoselective aldol addition reactions of a chiral methyl ketone trichlorosilyl enolate under lewis base catalysis. Synlett 1024–1029
57. Denmark SE, Fujimori S, Pham SM (2005) Base catalyzed aldol additions of chiral trichlorosilyl enolates and silyl enol ethers. J Org Chem 70:10823–10840
58. Denmark SE, Chung W-J (2008) Lewis base activation of lewis acids: catalytic, enantioselective addition of glycolate-derived silyl ketene acetals to aldehydes. J Org Chem 73:4582–4595
59. Denmark SE, Chung W-J (2008) Lewis base activation of lewis acids: catalytic enantioselective glycolate aldol reactions. Angew Chem Int Ed 47:1890–1892
60. Casiraghi G, Battistini L, Curti C, Rassu G, Zanardi F (2011) The vinylogous aldol and related addition reactions: ten years of progress. Chem Rev 111:3076–3154
61. Denmark SE, Heemstra JR, Beutner GL (2005) Catalytic, enantioselective, vinylogous aldol reactions. Angew Chem Int Ed 44:4682–4698
62. Casiraghi G, Zanardi F, Appendino G, Rassu G (2000) The vinylogous aldol reaction: a valuable, Yet understated carbon-carbon bond-forming maneuver. Chem Rev 100:1929–1972
63. Denmark SE, Beutner GL (2003) Lewis base activation of lewis acids. Vinylogous aldol reactions. J Am Chem Soc 125:7800–7801
64. Denmark SE, Fujimori S (2005) Total synthesis of RK-397. J Am Chem Soc 127:8971–8973
65. Denmark SE, Heemstra JR Jr (2004) Lewis base activation of lewis acids: vinylogous aldol additions of dienol ethers to aldehydes. Synlett 2411–2416
66. Denmark SE, Heemstra JR (2007) Lewis based activation of lewis acids: catalytic, enantioselective vinylogous aldol addition reactions. J Org Chem 72:5668–5688
67. Denmark SE, Heemstra JR (2006) Lewis base activation of Lewis acids. Vinylogous aldol addition reactions of conjugated N,O-silyl ketene acetals to aldehydes. J Am Chem Soc 128:1038–1039
68. Banfi L, Riva R (2005) The Passerini reaction. Org React 65:1–140
69. Zhu J (2003) Recent developments in the isonitrile-based multicomponent synthesis of heterocycles. Eur J Org Chem 1133–1144
70. Hulme C, Gore V (2003) Multi-component reactions: emerging chemistry in drug discovery from xylocain to crixivan. Curr Med Chem 10:51–80
71. Dömling A (2002) Recent advances in isocyanide-based multicomponent chemistry. Curr Opin Chem Biol 6:306
72. Dömling A, Ugi I (2000) Multicomponent reactions with isocyanides. Angew Chem Int Ed 39:3168–3210
73. Armstrong RW, Combs AP, Tempest PA, Brown SD, Keating TA (1996) Multiple-component condensation strategies for combinatorial library synthesis. Acc Chem Res 29:123–131
74. Denmark SE, Fan Y (2005) Catalytic, enantioselective alpha-additions of isocyanides: lewis-base-catalyzed Passerini-type reactions. J Org Chem 70:9667–9676
75. Denmark SE, Fan Y (2003) The first catalytic, asymmetric alpha-additions of isocyanides. Lewis-base-catalyzed, enantioselective Passerini-type reactions. J Am Chem Soc 125:7825–7827
76. Nakajima M, Yokota T, Saito M, Hashimoto S (2004) Enantioselective aldol reactions of trichlorosilyl enol ethers catalyzed by chiral *N*,*N*-dioxides and monodentate *N*-oxides. Tetrahedron Lett 45:61–64

77. Shimida T, Kina A, Hayashi T (2003) A new synthetic route to enantiomerically pure axially chiral 2,2′-bipyridine N,N′-dioxides. Highly efficient catalysts for asymmetric allylation of aldehydes with allyl(trichloro)silanes. J Org Chem 68:6329–6337
78. Nakajima M, Saito M, Uemura M, Hashimoto S (2002) Enantioselective ring opening of meso-epoxides with tetrachlorosilane catalyzed by chiral bipyridine N,N′-dioxide derivatives. Tetrahedron Lett 43:8827–8829
79. Tao B, Lo MM-C, Fu GC (2001) Planar-chiral pyridine *N*-oxides, a new family of asymmetric catalysts: exploiting an η^5-C_5Ar_5 ligand to achieve high enantioselectivity. J Am Chem Soc 123:353–354
80. Denmark SE, Wilson TW, Burk MT, Heemstra JR (2007) Enantioselective construction of quaternary stereogenic caarbons by the lewis base catalyzed additions of silyl ketene imines to aldehydes. J Am Chem Soc 127:14864–14865
81. Denmark SE, Wilson TW (2010) *N*-silyl oxyketene imines are underused yet highly versatile reagents for catalytic asymmetric synthesis. Nat Chem 2:937–943
82. Denmark SE, Williams BJ, Eklov BM, Pham SM, Beutner GL (2010) Design, validation, and implementation of a rapid-injection NMR system. J Am Chem Soc 75:5558–5572
83. Denmark SE, Eklov BM, Yao PJ, Eastgate MD (2009) On the mechanism of lewis base catalyzed aldol addition reactions: kinetic and spectroscopic investigations using rapid-injection NMR. J Am Chem Soc 131:11770–11787
84. Denmark SE, Eklov BM (2008) Neutral and cationic phophoramide adducts of silicon tetrachloride: synthesis and characterization of their solution and solid-state structures. Chem Eur J 14:234–239
85. Kennedy JD, McFarlane W (1987) Silicon, germanium, tin, and lead. In: Mason J (ed) Multinuclear NMR. Plenum, New York
86. Kobayashi S, Nishio K (1993) Facile and highly stereoselective allylation of aldehydes using allyltrichlorosilanes in DMF. Tetrahedron Lett 34:3453–3456
87. Olsson L, Ottosson CH, Cremer D (1995) Properties of R3SiX compounds and R3Si+ ions: Do silylium ions exist in solution? J Am Chem Soc 117:7460–7479
88. Arshadi M, Johnels D, Edlund U, Ottosson C-H, Cremer D (1996) Solvated silylium cations: structure determination by NMR spectroscopy and the NMR/Ab initio/IGLO method. J Am Chem Soc 118:5120–5131
89. Nakanishi K, Kotani S, Sugiura M, Nakajima M (2008) First asymmetric Abramov-type phosphonylation of aldehydes with trialkyl phosphites catalyzed by chiral lewis bases. Tetrahedron 64:6415–6419
90. Denmark SE, Beutner GL (2008) Lewis base catalysis in organic synthesis. Angew Chem Int Ed 47:1560–1638
91. Denmark SE, Burk MT (2010) Lewis base catalysis of bromo- and iodolactonization, and cycloetherification. Proc Natl Acad Sci USA 107:20655–20660
92. Denmark SE, Kalyani D, Collins WR (2010) Preparative and mechanistic studies toward the rational development of catalytic, enantioselective selenoetherification reactions. J Am Chem Soc 132:15752–15765
93. Denmark SE, Burk MT, Hoover AJ (2010) On the absolute configurational stability of bromonium and chloronium ions. J Am Chem Soc 132:1232–1233
94. Denmark SE, Vogler T (2009) Synthesis and reactivity of enantiomerically enriched thiiranium ions. Chem Eur J 15:11737–11745
95. Denmark SE, Kornfilt DJP, Vogler T (2011) Observation of direct sulfenium and selenenium group transfer from thiiranium and seleniranium ions to alkenes. J Am Chem Soc 132:15308–15311
96. Denmark SE, Collins WR, Cullen MD (2009) Observation of direct sulfenium and selenenium group transfer from thiiranium and seleniranium ions to alkenes. J Am Chem Soc 131:3490–3492
97. Denmark SE, Collins WR (2007) Lewis base activation of Lewis acids: development of a Lewis base catalyzed selenolactonization. Org Lett 9:3801–3804

98. Denmark SE, Edwards MG (2006) On the mechanism of the selenolactonization reaction with selenenyl halides. J Org Chem 71:7293–7306
99. Curti C, Ranieri B, Battistini L, Rassu G, Zambrano V, Pelosi G, Casiraghi G, Zanardi F (2010) Catalytic, asymmetric vinylogous mukaiyama aldol reactions of pyrrole- and furan-based dienoxy silanes: how the diene heteroatom impacts stereocontrol. Adv Synth Catal 352:2011–2022
100. Fang L, Xue H, Yang J (2008) Synthesis of the C1-C12 fragment of iriomoteolide 1a by sequential catalytic asymmetric vinylogous aldol reactions. Org Lett 10:4645–4648
101. Kujat C, Bock M, Kirschning A (2006) Synthesis of the C1-C5 and C6-C24 fragments of the RNA polymerase inhibitors ripostatin A and B. Synlett 419–422

Top Organomet Chem (2013) 44: 91–120
DOI: 10.1007/3418_2012_52

Published online: 11 August 2012

The Discovery and Development of a Palladium(II)-Catalyzed Oxidative Cross-Coupling of Two Unactivated Arenes

David R. Stuart and Keith Fagnou

Abstract The process of discovery and development of a palladium(II)-catalyzed oxidative cross-coupling of *N*-acetyl and *N*-pivaloylindoles with simple aromatic compounds is described. Within this process our inspiration was primarily derived from the organometallic literature and in particular the recent emergence of new and novel mechanisms for C–H bond cleavage by Pd(II)-complexes. During these studies it was realized that high levels of regio-control for C–H bond cleavage at indole could be obtained and a subsequent investigation has led to the proposal of a C3,C2-palladium migration for the C2-arylation of *N*-pivaloylindole. The current state of the art in transition-metal catalyzed oxidative cross-coupling is also presented.

Keywords C–H functionalization · Indole · Oxidative cross-coupling · Palladium

Contents

D.R. Stuart (✉) and K. Fagnou
Department of Chemistry, Centre for Catalysis Research and Innovation, University of Ottawa, 10 Marie Curie, Ottawa, Canada K1N 6N5
e-mail: dstuart@pdx.edu

Abbreviations

[O]	Oxidant
Ac	Acetyl
acac	Acetylacetonate
AcO^-	Acetate
BQ	Benzoquinone
CMD	Concerted metalation–deprotonation
DFT	Density functional theory
DMA	*N*,*N*-dimethylacetamide
DMF	*N*,*N*-dimethylformamide
DMSO	Dimethylsulfoxide
M	Metal pre-activating group (BR_2, SnR_3, etc.)
Me	Methyl
Ph	Phenyl
Piv	Pivaloyl
$PivO^-$	Pivalate
Py	Pyridine
R	Carbon-containing organic functional group
t-Am	*tert*-Amyl
TBAB	Tetrbutylammonium bromide
t-Bu	*tert*-Butyl
TFA	Trifluoroacetate

1 Introduction

Chemists are continually inspired by Nature's efficiency when exploring and developing new chemical reactivity and in the design of synthetic pathways to complex targets. The coupling of two simple aromatic compounds to form a biaryl unit, with concomitant loss of two protons and two electrons, is certainly a desirable transformation and one that Nature carries out with exquisite control and efficacy. Enzymatic machinery accomplishes this coupling via a series of single electron/proton transfer steps to form the desired biaryl C–C bond by reaction of a carbon-centered radical and an electron-rich arene (Scheme 1a) [1]. As a consequence of this mechanism of action, naturally occurring biaryls are typically found with significant oxygenation in polyphenolic environments, for example vancomycin, dioncophylline B and knipholone (Scheme 1b) [1]. In this vein, a significant amount of work has been directed towards the preparation of binaphthols and related compounds in a bio-inspired manner but the substrate scope is limited as a corollary of the mechanism [2]. The substitution pattern around biaryls found in leading pharmaceuticals and functional organic materials is in stark contrast to those typically found in Nature and, as a result, the synthetic approach to these compounds is necessarily distinct (Scheme 1c, d). Traditionally, these motifs are

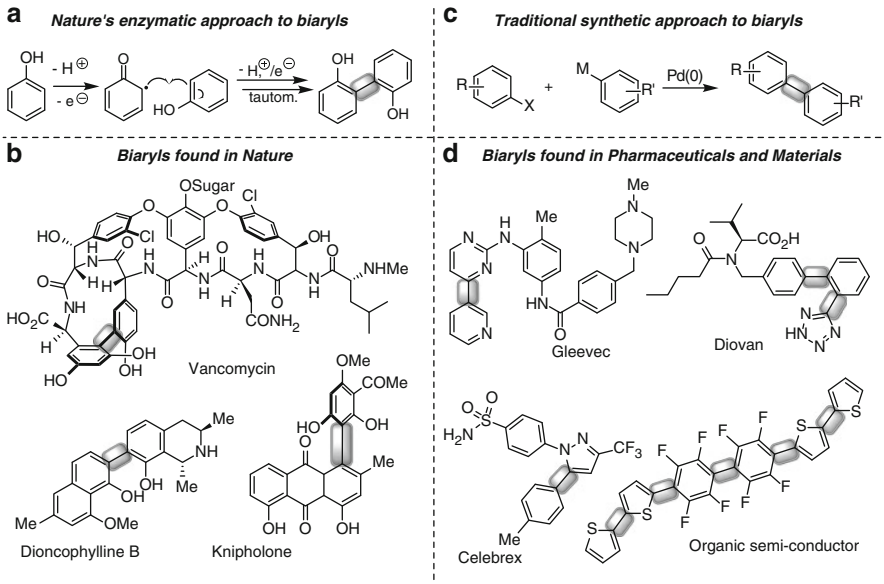

Scheme 1 Nature's and traditional synthetic approach to biaryls

formed by the coupling of two pre-activated aromatic compounds, an aryl (pseudo) halide and an aryl organometallic, catalyzed by a transition metal such as palladium; this chemistry has been extensively reviewed and will only be discussed here in brief [3, 4]. While biaryls formed in Nature are done so with enviable efficiency, the substrate scope accessible by traditional cross-coupling methods is unparalleled by other means.

We have, in our group, a long-standing interest in the development of transition-metal-catalyzed reactions which take place at (hetero)aromatic C–H bonds, primarily focusing on direct arylation (vide infra). Given the level of sophistication that direct arylation has reached and the knowledge of the mechanism of C–H bond cleavage obtained in recent years, we were intrigued to explore the possibility that these principles could be extended to an oxidative cross-coupling of two simple arenes with the ultimate goal of bridging the gap between the efficiency of Nature and the substrate compatibility of modern cross-coupling. To this end, this chapter will focus on the process of developing a palladium(II)-catalyzed oxidative cross-coupling of two simple arenes, indole and benzene, carried out in the Fagnou research group with an emphasis on the prior art and mechanistic insights from palladium-catalyzed direct arylation that stimulated these investigations. A survey of the recent literature to highlight the current state of the art in the oxidative cross-coupling of simple arenes and an outlook on the continuing challenges facing chemists in elevating this transformation to a general and synthetically useful reaction will also be presented.

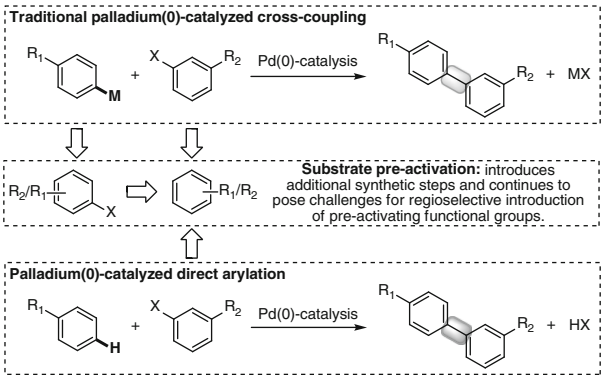

Scheme 2 Traditional palladium-catalysis and direct arylation as approaches to biaryls

2 Mechanistic Inspiration and Prior Art

The vast impact of modern palladium-catalyzed cross-couplings, such as the Suzuki, Negishi, and Heck reactions, on chemical synthesis has garnered the inventors of these reactions the highest scientific honour [5, 6]. As outlined above, these reactions proceed by the coupling of an aryl (pseudo)halide with an aryl organometallic reagent, under palladium(0)-catalysis, to produce the desired C–C bond (Scheme 2). Notwithstanding the immense utility of these reactions, chemists have continued to explore the limits of reaction efficiency and, as a result, direct arylation has emerged as a synthetically valuable transformation. The intensity of research directed in this area has resulted in a number of excellent reviews and the reader is directed to these for a more in-depth analysis [7–10]. In these reactions, one of the two pre-activated coupling partners (typically the aryl organometallic) is replaced by a simple arene therefore increasing the overall efficiency and reducing the overall *cost and waste* of these processes (Scheme 2). The variety of simple arenes that has been employed in these transformations continues to expand and includes electron-rich (hetero)arenes, those with Lewis basic directing groups, simple arenes such as benzene, and electron-deficient (hetero)arenes [5].

Direct arylation represents a significant advance in the efficiency of biaryl formation. However, these reactions continue to employ an aryl halide which must be prepared in a regioselective manner from a simple arene, and therefore the coupling of two distinct simple arenes via their C–H bonds represents the most direct means to unsymmetrical biaryl molecules [11]. This approach, in the context of transition metal catalysis, introduces an additional level of complexity compared to those encountered in direct arylation. With two unactivated arenes present in the reaction medium, the catalyst must display orthogonal selectivity with each of these arenes at distinct steps within the catalytic cycle in order to achieve successful cross-coupling and avoid undesired homo-coupling (Scheme 3). In actuality, the challenges associated with a successful cross-coupling of two unactivated arenes

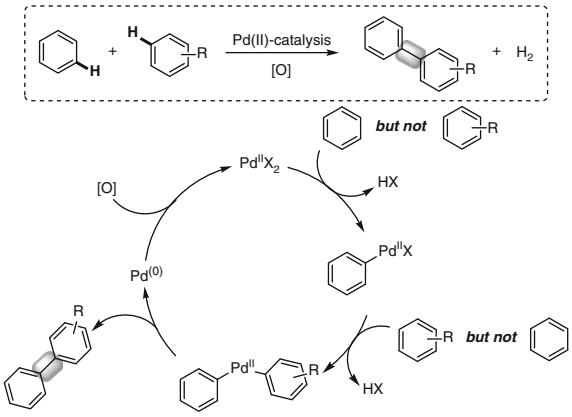

Scheme 3 Proposed catalytic cycle of an oxidative cross-coupling

are threefold: *reactivity*, *regioselectivity*, *and chemoselectivity*. First, the catalyst must successfully react with the C–H bond of a simple unactivated arene (reactivity), which is not a trivial process, despite increasing advances in the field. Second, in this event the catalyst must selectively react with one of the multiple potentially reactive aromatic C–H bonds (regioselectivity). Third, the catalyst must selectively react with only one of the two arenes at distinct steps of the catalytic cycle (chemoselectivity) delivering a successfully cross-coupled product (Scheme 3).

Despite the impressive efficiency of Nature, we have primarily focused on the organometallic literature for inspiration and answers to the three challenges posed by a transition-metal-catalyzed oxidative cross-coupling. Traditional organometallic chemistry and the emerging field of direct arylation have provided ample support for the feasibility of the former two challenges with respect to both the reactivity of a variety of simple arenes (with a number of transition metals) and the regioselectivity of C–H bond cleavage (by those metals). The pioneering work of Ryabov and others established Lewis base-directed cyclometallation as a reliable method for the regioselective metallation of aromatic rings (Scheme 4) [12, 13]. The ability of Lewis basic functional groups embedded in a molecule to bring the metal into close proximity with one specific aryl C–H bond biases the reaction and results in exclusive site-selectivity. Direct arylation has utilized this strategy heavily to obtain synthetically useful selectivities [5] (Scheme 4), and this tactic has also been exploited in oxidative cross-coupling reactions (vide infra).

An alternative strategy to obtain both reactivity and regioselectivity in reactions of transition metals with arenes is to exploit the inherent electronic nature of the aromatic π-system. The direct arylation of π-rich heterocycles has a substantial history and has received considerable attention from the synthetic community since its origins (Fig. 1) [5]. This is perhaps a consequence of the typically good regioselectivity observed for these compounds in direct arylation reactions, which was originally proposed to be a result of the inherent nucleophilicity of specific carbon atoms within the individual heterocycles (vide infra). A significant number of

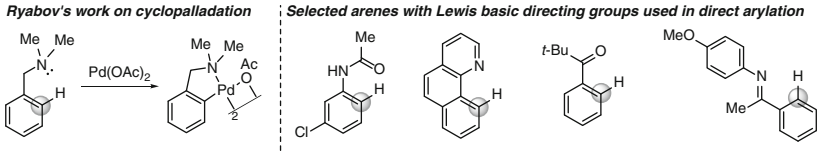

Scheme 4 Directing group approach to regioselectivity

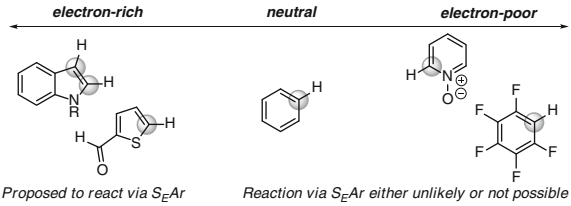

Fig. 1 Electronic nature of arenes used in direct arylation

heterocycles have been found to undergo efficient direct arylation and these include: indoles and indolazines, pyrroles, oxazoles and benzoxazoles, imidazoles and benzimidazoles, thiazoles and benzothiazoles, thiophenes and benzothiophenes, and furans and benzofurans [5]. More recently, the breadth of compatible substrates in direct arylation reactions has come to include electron-neutral benzene [14] and electron-deficient pyridine *N*-oxide [15–18] and pentafluorobenzene with both palladium [19, 20] and copper [21] as catalyst (Fig. 1). These arenes do not contain Lewis basic directing groups or nucleophilic centers to facilitate high regioselectivity and therefore their ability to participate in site-selective direct arylation reactions counters the conventional view of the transition-metal-catalyzed aryl C–H bond cleavage mechanism.

The latter challenge, the necessary chemoselectivity of the metal for each of the two arenes at distinct steps of the reaction was, at the time of our investigation, unprecedented under catalytic conditions and represented the largest hurdle. The differential selectivity of the catalyst with each of the arenes has yet to be fully understood though a number of research groups are making significant advances toward a more complete picture (vide infra). During our initial discussions, in the spring of 2006, on how to approach the issue of chemoselectivity, we hypothesized that the orthogonal selectivity must be rooted in the mechanism by which the catalyst cleaves the aromatic C–H bonds. The emergence of a number of arenes that did not "fit the mould" of π-nucleophiles or those containing Lewis basic directing groups has led to the evolution of an alternative mechanism for aryl C–H bond cleavage in direct arylation (Scheme 5) [12, 13, 17, 22–24]. The concerted metalation–deprotonation (CMD) mechanism has become uniquely tied to this reaction class though it has a rich history in stoichiometric organometallic chemistry [25]. We, therefore, initially reasoned that by judicious choice of arene substrates with different reactivity profiles toward the metal catalyst a successful cross-coupling could be achieved. In this case Pd(II)X_2 would preferentially react

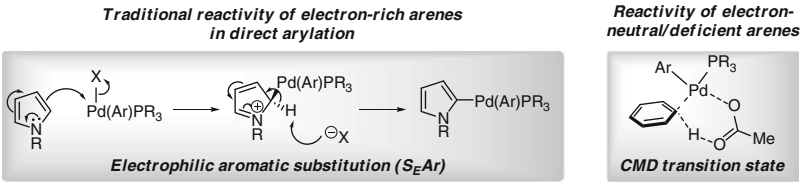

Scheme 5 Proposed mechanisms of C–H bond cleavage for electronically dissimilar arenes

with one arene (via a given mechanism) at the outset of the reaction and the subsequent ArPd(II)X would react with the other arene (via an alternative mechanism) (Schemes 3 and 5).

3 Reaction Development

3.1 Substrate Selection

Indole has featured prominently in both direct arylation reactions and other transition metal mediated/catalyzed oxidative transformations which significantly guided our substrate selection and a number of leading references are provided for the interested reader [26–31]. Namely, the palladium(II)-mediated oxidative cyclization of *N*-benzoylindoles to form tetracyclic products reported by Itahara and coworkers in 1979 [Eq. (1)] [26]. This report was followed in 1981 by the palladium (II)-mediated intermolecular coupling of *N*-acetylindole with benzene under acidic conditions [Eq. (2)] [32, 33]. These two reports provided early evidence for the key reactivity and the possibility of selective cross-coupling of two simple arenes and further encouraged our investigation of a catalytic reaction. Additionally, insights reported by Stoltz on palladium-catalyzed intramolecular aerobic annulation of indole via an oxidative Heck reaction were also instructive in the development of this chemistry. Stoltz and Ferreira found that the nature of the substituent on the pyridine ligand, specifically the use of ethyl nicotinate, modulated the reactivity of the known $Pd(OAc)_2$/pyridine system sufficiently to facilitate cyclization of **1** [Eq. (3)] [28].

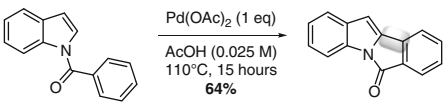

(1)

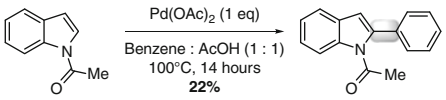

(2)

Table 1 Selected data for optimization of the cyclization of *N*-benzoylindole

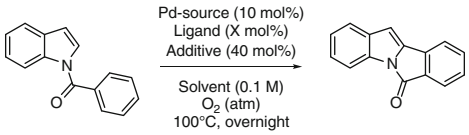

Entry	Pd-source	Ligand (mol%)	Additive	Solvent	Conversion (%)[a]
1	$Pd(OAc)_2$	3-CNpy (20)	NaOAc	*t*-AmOH:AcOH (4:1)	47
2	$Pd(TFA)_2$	3-CNpy (20)	NaOAc	*t*-AmOH:AcOH (4:1)	61
3	$Pd(TFA)_2$	3-CNpy (10)	NaOAc	*t*-AmOH:AcOH (4:1)	71
4	$Pd(TFA)_2$	3-CNpy (10)	KOPiv	*t*-AmOH:PivOH (4:1)	78
5	$Pd(TFA)_2$	4-CNpy (10)	KOPiv	*t*-AmOH:PivOH (4:1)	64
6	$Pd(TFA)_2$	3-CO_2Mepy (10)	KOPiv	*t*-AmOH:PivOH (4:1)	71
7	$Pd(TFA)_2$	3-NO_2py (10)	KOPiv	*t*-AmOH:PivOH (4:1)	87
8	$Pd(TFA)_2$	–	KOPiv	*t*-AmOH:PivOH (4:1)	44
9	$Pd(TFA)_2$	3-NO_2py (10)	CsOPiv	*t*-AmOH:PivOH (4:1)	99 (74)

[a]GC/MS conversion, isolated yield in parentheses

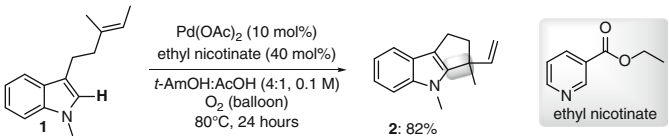

(3)

3.2 Intramolecular Reactivity

In the summer of 2006, after a couple of months of unsuccessful attempts at the "homerun" intermolecular reaction, we initiated work on rendering Itahara's palladium-mediated cyclization of *N*-benzoylindole catalytic in palladium. Selected data from the optimization of this reaction are presented in Table 1. As described earlier, we were largely inspired in our early work by Stoltz's report that pyridine ligands were beneficial for indole annulations and modification of the conditions reported therein resulted in 47% GC/MS conversion (Table 1, entry 1) [28]. It was found, during optimization, that when a more electrophilic palladium source, $Pd(TFA)_2$, was employed the conversion could be amplified to 61% (entry 2). Additionally, fine-tuning of the ligand to metal stoichiometry (2:1–1:1) and the identity of the acid/base additives ($AcOH/AcO^-$ to $PivOH/PivO^-$) proved beneficial, further augmenting the conversion to 78% (entries 3 and 4). A series of other pyridine derivatives were also evaluated as potential ligands and it was observed that 3-nitropyridine was most effective, resulting in a GC/MS conversion of 87% (entries 4–7). It should also be noted that only modest conversion (44%) was observed in the absence of ligand (entry 8). Complete conversion was finally obtained by use of CsOPiv as the additive (entry 9), possibly due to the greater solubility of this base in *t*-AmOH. Under these conditions 74% isolated yield of the desired cyclization product was obtained.

Table 2 Selected data for optimization of an intermolecular oxidative cross-coupling

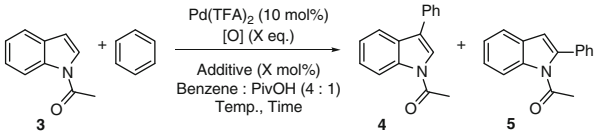

Entry	[O] (equiv.)	Additives (mol%)	Temperature (°C)	Time (h)	Ratio (**4**:**5**)[a]	Conversion[a]
1	O_2	3-NO_2pyridine (10) CsOPiv (40)	110	24	1:2.3	22
2	BQ (2)	3-NO_2pyridine (10) CsOPiv (40)	110	24	–	–
3[b]	$Cu(OAc)_2$ (3)	3-NO_2pyridine (5) CsOPiv (40)	110	21	11:1	42
4	$Cu(OAc)_2$ (3)	3-NO_2pyridine (10) CsOPiv (40)	110	48	16:1	89
5	$Cu(OAc)_2$ (3)	None	110	48	33:1	70
6	$Cu(OAc)_2$ (3)	3-NO_2pyridine (10) CsOPiv (40)	140[c]	5	8.9:1	>99(87)

[a]Determined by GC/MS, isolated yield in parentheses
[b]5 mol% $Pd(TFA)_2$
[c]Under microwave heating

3.3 *Intermolecular Reactivity*

Itahara also pioneered the intermolecular oxidative cross-coupling of two unactivated arenes mediated by stoichiometric amounts of palladium salts [30, 31]. In his report, the reaction of *N*-acetylindole, **3**, and benzene resulted in an isolated yield of 22% for the C2-phenylated indole, **5**, though no discussion of the possible regioisomeric product distribution was presented [30]. Given our success in the intramolecular variant of this reaction, we set out to explore the possibility of a catalytic direct intermolecular cross-coupling of indole and benzene. Under slightly modified conditions (replacement of the solvent *t*-AmOH with benzene), we found that modest conversion and regioselectivity were obtained, with the C2-phenylated isomer, **5**, constituting the major product of the reaction (Table 2, entry 1). Other oxidants, including benzoquinone and inexpensive transition metal oxidants, were surveyed. It was found that while benzoquinone was not a competent oxidant under the given conditions, $Cu(OAc)_2$ was, providing 42% GC/MS conversion and *an inversion of regioselectivity* to provide the C3-phenylated indole, **4**, as the major regioisomer (entries 2 and 3). Under thermal heating, it was found that long reaction times (48 h) and increased catalyst loadings (10 mol%) were necessary for high conversion of starting material to product (entry 4). Removal of the pyridine additive and sub-stoichiometric base resulted in decreased conversion (entry 5). However, heating the reaction under microwave irradiation proved to be efficient in this process providing the C3-phenylated indole in 87% isolated yield (entry 6).

Following our initial report in the winter of 2007 [34], detailing our discovery and optimization of the C3-oxidative cross-coupling of *N*-acetylindole and benzene, we undertook a secondary investigation into the various reaction parameters with a focus on two particular aspects of reactivity. First, we were interested in a departure from microwave heating and a return to more mild thermal reaction conditions. Second, during our initial optimization we made some interesting observations regarding subtle changes in C2/C3-regioselectivity with changes in oxidant and we were intrigued by the ability to control this parameter of the reactivity profile. More specifically, could we control and obtain high regioselectivity by selection of the appropriate oxidant/additive? Table 3 highlights the most relevant results in our efforts towards these two objectives.

We chose to set the catalyst loading at 5 mol% and screened a wider variety of palladium catalyst precursors. The best result was attained with $Pd(acac)_2$ as the palladium source providing a GC/MS yield of the C3-phenylated product of 62%, a 20% increase in yield compared to the use of $Pd(TFA)_2$ (Table 3, entries 1 and 2). It was found that when using $Pd(acac)_2$, the 3-nitropyridine ligand and the sub-stoichiometric base were not necessary. Their removal resulted in a 95% conversion and 84% isolated yield of the desired product (entry 3). Entries 3–6 demonstrate the important influence that the stoichiometry of pivalic acid had on the reaction. As the pivalic acid loading is decreased so is the GC/MS conversion and when omitted from the reaction altogether the conversion is reduced to 26%. A small number of indoles and arenes were selected to validate these second-generation conditions and good isolated yields could be obtained for the C3-arylated *N*-acetylindole products (Table 4).

In our early studies, we identified that under an O_2 atmosphere (as the terminal oxidant) the major product, albeit in low regioselectivity, was the C2-phenylated indole (Table 3, entry 7). After recognizing that the use of $Cu(OAc)_2$ resulted in an inversion of regioselectivity, and optimizing for the C3-phenylated product, we returned to take a closer look at the effect of the oxidant on the C2/C3-selectivity. Silver(I) acetate stood out in our oxidant screen as it effected an inversion in selectivity back to the C2-regioisomer (entry 8) with a slight increase in conversion. Upon investigation of the nature of the indole nitrogen protecting group, a further increase in the C2 selectivity of the reaction was observed when a pivaloyl group was used in place of an acetyl group (entries 8 and 9). Analogous to our second-generation conditions for the C3-oxidative cross-coupling, a removal of both ligand (3-nitropyridine) and sub-stoichiometric base (CsOPiv) resulted in a beneficial effect on both the conversion and the regioselectivity (entries 10–14). Furthermore, this catalyst system proved to be much more reactive; the reaction was complete within 3 h (entry 10) and 2 mol% Pd was sufficient to obtain 87% GC/MS yield (entry 11). Small amounts of both indole and benzene homo-coupled products were observed with the increase in reactivity. However, indole homo-coupling could be avoided at higher dilution (0.15 M), though biphenyl was still produced. Monitoring the reaction course by GC/MS revealed that biphenyl began to appear only after $>$ 90% conversion of indole,

Table 3 Selected data for optimization of a C3 or C2 oxidative cross-coupling of indole

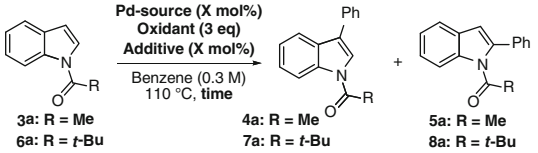

Entry	R-group (concentration)	Pd (mol%)	Oxidant (equiv.)	Additive (mol%)	Time (h)	Ratio[a]	Yield[a]
1	Me (0.3 M)	$Pd(TFA)_2$ (5)	$Cu(OAc)_2$ (3)	3-NO_2py (5) CsOPiv (40) PivOH (600)	21	11:1	42%
2	Me (0.3 M)	$Pd(acac)_2$ (5)	$Cu(OAc)_2$ (3)	3-NO_2py (5) CsOPiv (40) PivOH (600)	21	10:1	62%
3	Me (0.3 M)	$Pd(acac)_2$ (5)	$Cu(OAc)_2$ (3)	PivOH (600)	21	20:1	95% (84%)
4	Me (0.3 M)	$Pd(acac)_2$ (5)	$Cu(OAc)_2$ (3)	PivOH (300)	21	15:1	91%
5	Me (0.3 M)	$Pd(acac)_2$ (5)	$Cu(OAc)_2$ (3)	PivOH (100)	21	14:1	88%
6	Me (0.3 M)	$Pd(acac)_2$ (5)	$Cu(OAc)_2$ (3)	PivOH (0)	21	–	26%
7	Me (0.3 M)	$Pd(TFA)_2$ (10)	O_2 (atm)	3-NO_2py (10) CsOPiv (40) PivOH (600)	24	1:2.3	22%
8	Me (0.3 M)	$Pd(TFA)_2$ (10)	AgOAc (2.2)	3-NO_2py (10) CsOPiv (40) PivOH (600)	24	1:4	32%
9	*t*-Bu (0.3 M)	$Pd(TFA)_2$ (10)	AgOAc (2.2)	3-NO_2py (40) CsOPiv (40) PivOH (600)	24	1:9	78%
10	*t*-Bu (0.15 M)	$Pd(TFA)_2$ (5)	AgOAc (3)	PivOH (600)	3	1:25	99% (84%)
11	*t*-Bu (0.15 M)	$Pd(TFA)_2$ (2)	AgOAc (3)	PivOH (600)	15	1:14	87%
12	*neo*-Pentyl (0.15 M)	$Pd(TFA)_2$ (5)	AgOAc (3)	PivOH (600)	5	1:5	49%
13	*i*-Pr (0.15 M)	$Pd(TFA)_2$ (5)	AgOAc (3)	PivOH (600)	5	1:3	50%
14	Cyclopropyl (0.15 M)	$Pd(TFA)_2$ (5)	AgOAc (3)	PivOH (600)	5	–	0%

[a]Determined by GC/MS, isolated yield in parentheses

thus confirming a selective cross-coupling process. A number of other nitrogen protecting groups were tested under the reaction conditions, and, while those that did provide product did so with bias for the C2-isomer none was more effective that the pivaloyl group (entries 10 and 12–14).

Under our optimized conditions (Table 2, entry 6; Table 3, entries 3 and 10), the generality of the reaction was investigated with respect to both the indole and the arene coupling partner. Substitution at both C5 and C6 was tolerated in the form of electron-donating groups (methoxy), halides (Cl), alkyl groups (methyl),

Table 4 Scope of the C3 and C2 oxidative cross-coupling of indole with simple arenes

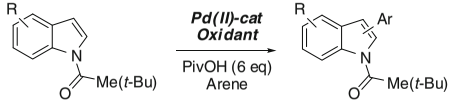

C3-Oxidative Arylation

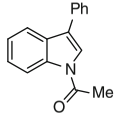

87% (9:1)[a]
84% (20:1)[c]

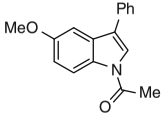

84% (11:1)[a]
76%[c]

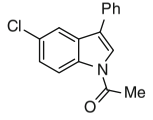

63% (7:1)[a,b]
85%[c]

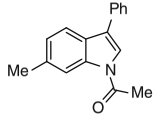

81% (10:1)[a]
95%[c]

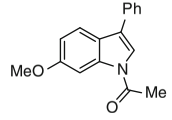

74% (11:1)[a]

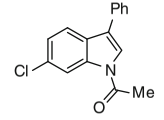

61% (6:1)[a,b]

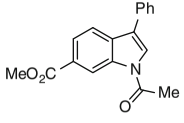

54% (3:1)[a,d]

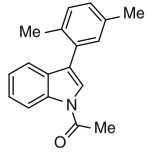

45% (10:1)[a,d]

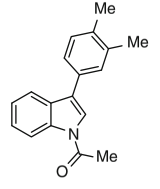

61% (19:2:1)[c,e]

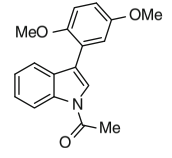

52% (7:1)[a,d]

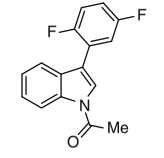

42% (10:1)[a,d]

C2-Oxidative Arylation

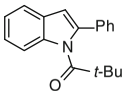

84% (25:1)[f]

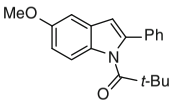

90% (46:1)[f]

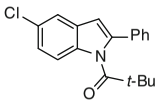

86% (31:1)[f]

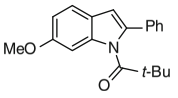

76% (26:1)[f]

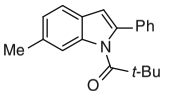

88% (31:1)[f]

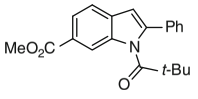

86% (31:1)[f]

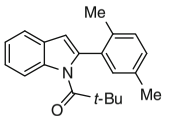

58% (31:1)[f,g]

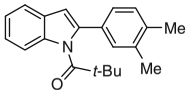

75% (30:1:trace)[f,g]

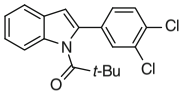

55% (17:2:1)[f,g]

[a]Indole (1 equiv.; 0.3 M), $Pd(TFA)_2$ (10 mol%), 3-nitropyridine (10 mol%), CsOPiv (40 mol%), $Cu(OAc)_2$ (3 equiv.), PivOH (6 equiv.), in benzene, 140 °C (MW), 5 h

[b]Heated thermally (110 °C) in a Schlenk tube

[c]Indole (1 equiv.; 0.3 M), $Pd(acac)_2$ (5 mol%), $Cu(OAc)_2$ (3 equiv.), PivOH (6 equiv.), in benzene, 110 °C (oil bath), 24 h

[d]20 mol% $Pd(TFA)_2$

[e]10 mol% $Pd(acac)_2$

[f]Indole (1 equiv.; 0.15 M), $Pd(TFA)_2$ (5 mol%), AgOAc (3 equiv.), PivOH (6 equiv.), in benzene, 110 °C (oil bath), 3–5 h

[g]10 mol% $Pd(TFA)_2$

and electron-withdrawing groups (CO_2Me) providing the C3-phenylated indole in moderate (54%) to good (84%) isolated yield. C3:C2 regioselectivity ranged from 3:1 (6-CO_2Me) to 11:1 (5-OMe) under the first-generation microwave conditions. It should also be noted that halide functional groups were not compatible with the microwave conditions due to a competing hydro-dehalogenation process. Therefore, these substrates were submitted to thermal heating in Schlenk tubes. Under the thermal second-generation conditions, comparable yields were obtained and the C3/C2-regioselectivity (where shown) displays a marked increase. Substitution at the C2-position was not compatible in this chemistry and is consistent with the low levels of diarylation observed on indole. The breadth of compatible arenes remains limited. Simple arenes of varying electronic dispositions and substitution patterns were subjected to the reaction conditions; however, controlling regioselectivity and separating the mixture of regioisomers was a significant challenge and not possible in the vast majority of cases. A few representative substrates that are symmetrical, therefore removing issues of regioselectivity, or for steric reasons provided products with good regioselectivity are shown in Table 4. Again, moderate-to-good regioselectivities were obtained and moderate yields of the C3-arylated products were achieved for electron-rich (R = OMe), neutral (R = Me), and electron-deficient (R = F) arenes. *ortho*-Xylene provided the sole example of good regioselectivity for a simple arene with multiple reactive sites [35].

The reaction displayed uniformly good yields (76–90%) and high C2 selectivity (>25:1) for a similar range of substituted indoles when AgOAc was used as the terminal oxidant. Arenes other than benzene were also evaluated as potential coupling partners in this chemistry. 1,2-Dichlorobenzene, like *ortho*-xylene, reacted with good regioselectivity at the more sterically accessible C–H bond. The oxidative cross-coupling of pyrrole substrates with benzene and *ortho*-xylene was developed by my lab-mate, Elisia Villemure, to expand the substrate scope of compatible heteroarenes [36].

3.4 Mechanistic Investigation

Amid the myriad of mechanistic complexities associated with a successful oxidative cross-coupling reaction, we were particularly intrigued with our ability to manipulate the C–H bond cleavage at indole. The capacity to obtain *and control* high levels of site-selectivity is rare in transition-metal-catalyzed reactions at aromatic C–H bonds and we chose to focus our mechanistic investigation primarily on this aspect of the chemistry. The following section outlines our thought process as we encountered a number of interesting, though at times puzzling, results and our final mechanistic proposal to account for these observations.

A scenario that we first considered was the involvement of copper-indoyl and silver-indoyl species that could participate in a transmetallation with Pd(II) and afford orthogonal placement of the metal on indole. However, if present, the

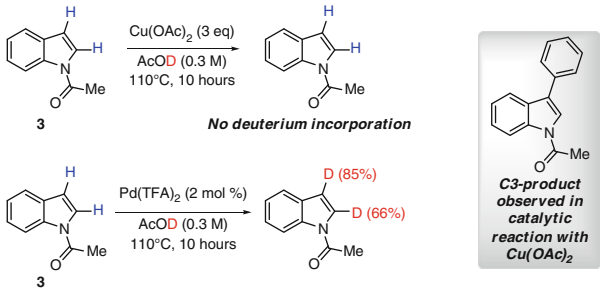

Scheme 6 Deuterium incorporation experiments with *N*-acetylindole

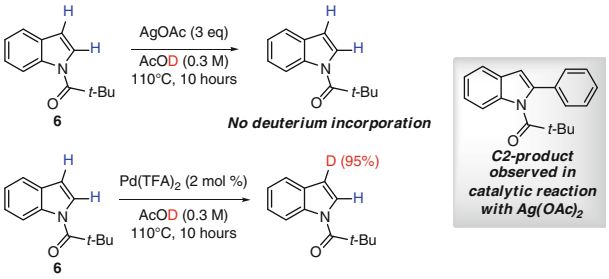

Scheme 7 Deuterium incorporation experiments with *N*-pivaloylindole

putative transient species would be highly reactive and very difficult to isolate or characterize spectroscopically. Therefore, to investigate their short-lived existence, deuterium was used as an isotopic probe. It was presumed that a highly reactive organometallic species would deutero-demetalate in the presence of acetic acid-*OD*, leading to deuterium incorporation at the position of metallation (Schemes 6 and 7). The results of these experiments provide two interesting and important pieces of information. The first being that no deuterium is incorporated on indole in the presence of either only $Cu(OAc)_2$ or AgOAc and therefore precludes the initial formation of a C3-copper-indoyl or C2-silver-indoyl species. The second relates to the levels of deuterium incorporation at the C2 and C3 positions for the *N*-acetylindole and *N*-pivaloylindole in the presence of Pd(II). Under modified reaction conditions (2 mol% palladium, no oxidant and replacement of benzene with acetic acid-*OD*) **3** undergoes deuterium incorporation at both C2 (66%) and C3 (85%). This result is consistent with a poorly selective reaction in the absence of an external oxidant (vide supra). We were particularly struck by the level of deuterium incorporation into **6** under analogous conditions (Scheme 7). Deuterium is exclusively, and near quantitatively, incorporated into the C3 position (95%), despite a non-selective reaction in the absence of external oxidant and highly C2-selective reaction under catalytic conditions with 3 equiv. of AgOAc present (vide supra). These results are consistent with reversible palladation at both the C3 and C2-positions for *N*-acetylindole and *only at the C3-position* for *N*-pivaloylindole [33].

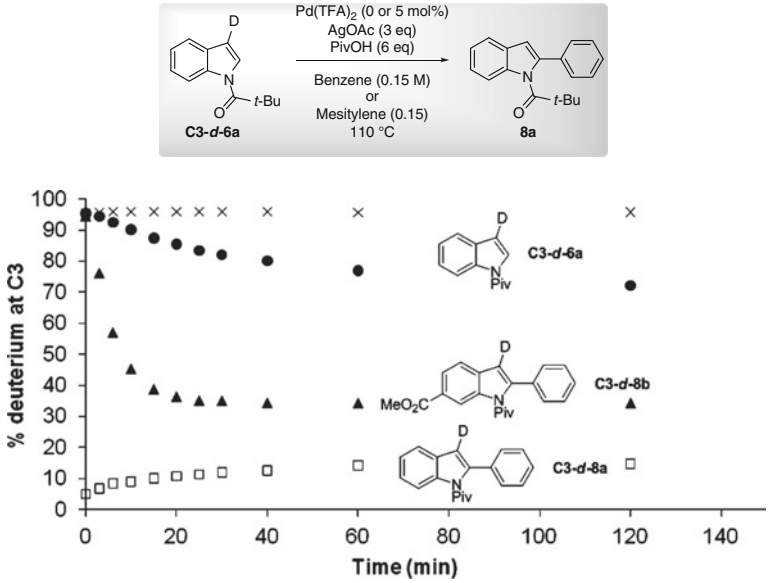

Fig. 2 Measuring deuterium loss over the course of the reaction with GC/MS

In order to monitor the events taking place at the C3-position of *N*-pivaloylindole more closely, we prepared the C3-*d*-analogue as a more sensitive isotopic label and subjected it to a number of different reaction conditions. Aliquots were taken at specific time intervals and analyzed by GC/MS. The intensity of the mass peaks (*M* and *M*+1) corresponding to the non-deuterated and deuterated starting material (and product) were compared to provide a relative percentage of deuterium at the C3 position and this was plotted against time (Fig. 2). Three different experiments were run in order to reveal different aspects of the reaction. First, in the absence of $Pd(TFA)_2$ no loss of deuterium from the starting material was observed (Fig. 2, ×), therefore dismissing an operative background loss of deuterium. However, under the standard reaction conditions (5 mol% $Pd(TFA)_2$, 3 equiv. of AgOAc, 6 equiv. of PivOH in benzene), the level of deuterium in the starting material disappeared (Fig. 2, •) over the course of the reaction, providing evidence for palladation (and protodemetallation with PivOH) at the C3-position of the *N*-pivaloylindole. Furthermore, when C2-*d*-*N*-pivaloylindole was subjected to the standard reaction conditions there was no loss of deuterium from the starting material over the course of the reaction suggesting that palladation at this position is irreversible and only leads to the desired C2-phenylated product (not shown in Fig. 2). Most informative from these experiments was the percent deuterium in the product under the standard reaction conditions (Fig. 2, □). Even at very low conversion (~10% yield of **8a**, ~2 min), deuterium is near quantitatively absent in the product (~5% deuterium) and only leaches slightly back into the product (~14% deuterium) over time, perhaps due to competing mechanisms or the presence of PivOD later in the reaction. A control

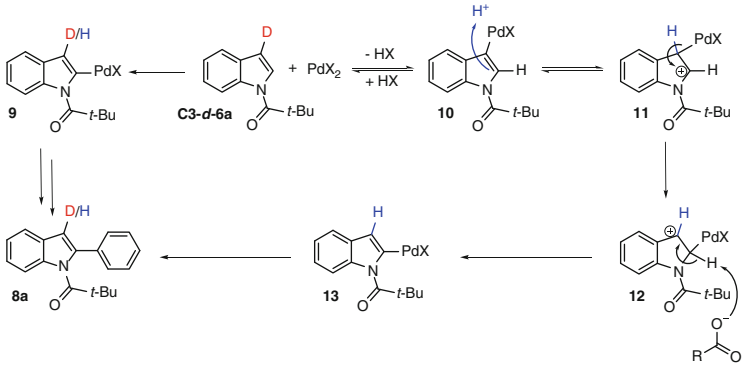

Scheme 8 Proposed mechanism to account for deuterium loss experiments

experiment was performed to ensure that the immediate loss in deuterium in the product is a direct result of the mechanism of the reaction and not simply very fast deuterium loss from the product. Product **C3-*d*-8b** (95% initial deuterium incorporation; Fig. 2, ▲) was added at the beginning of a typical reaction between **C3-*d*-6a** and benzene and the loss of deuterium followed. Particularly revealing is that early in the control reaction (~2 min, ~10% conversion of **6a** to **8a**) the added product, **C3-*d*-8b**, exhibits ~75% deuterium incorporation compared to ~5% deuterium in the newly formed **8a**. Thus, these results exclude the possibility of deuterium loss in the product as an artifact of the reaction conditions and point toward a mechanism for C2-palladation which involves an initial and reversible C3-palladation [33].

Sames and Gaunt have both observed that the C2/C3 selectivity for related transition metal catalyzed reactions of indole may be influenced by reaction conditions and the steric/electronic nature of the nitrogen protecting group [29, 37, 38]. Proposals from both of these groups for the observed variation in C2/C3 regioselectivity have involved an initial C3-metallation followed by a subsequent C3,C2-metal migration, and thus we considered this scenario as well as direct C2-palladation (outlined in Scheme 8). In the former pathway (C3,C3-palladium migration) **C3-*d*-6a** could undergo a reversible palladation at C3 accounting for the observed loss in deuterium at this position of the starting material. En route to reverting back to protio-**6a**, protonation of compound **10** would form the Wheland-intermediate **11**. C3,C2-palladium migration in compound **11** could then take place to afford compound **12**, containing a C3-carbocation. Irreversible, deprotonation at the C2-position would then re-aromatize **12** to form **13**, and subsequent reaction with benzene yields product **8a**. This scenario is consistent with the very low percentage of deuterium at the C3-position in the product very early in the reaction time course. When Wheland-intermediate **11** is formed the C3 position is exclusively protonated (not deuterated), and thus after migration to form **12**, the high level of protium (low level of deuterium) is reflected in the product, **8a** [33]. In the later pathway, starting material **C3-*d*-6a**

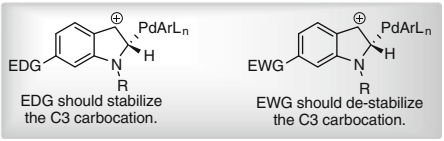

Fig. 3 Effect of C6-group on a C3,C2-palladium migration

could undergo direct palladation at C2 to form **9** followed by reaction with benzene and formation of **8a**. However, this pathway is inconsistent with the quantitative loss of deuterium in the product early in the reaction. If this were the case, it would be expected that **C3-*d*-6a** and **8a** would have similar levels of deuterium at the C3 position at any time during the reaction.

A Hammett correlation was carried out to assess the hypothesis of a C3,C2-palladium migration and to probe the existence of a C3-carbocation, **12**. As presented in Fig. 3, an electron-donating group should promote the C3,C2-palladium migration by stabilizing the putative C3-carbocation, whereas an electron-withdrawing group should destabilize the C3-carbocation intermediate. Competition experiments between C6-substituted *N*-pivaloylindoles and unsubstituted *N*-pivaloylindole were used to observe the possibility of an electronic influence at this position during the reaction. The Hammett correlation provided a ρ-value of -0.8 which indicates a small amount of increasing positive charge adjacent to the aromatic ring (Figs. 3 and 4). This value is similar to the ρ-value obtained by Sames (-0.71) for the direct arylation of *N*-methylindole under palladium-catalysis in which a similar C3,C2-palladium migration was proposed [27]. The Hammett correlation, together with our deuterium erosion experiments are consistent with an initial and reversible C3-palladation and subsequent C3,C2-palladium migration resulting in high levels of C2-arylation in the oxidative cross-coupling of *N*-pivaloylindole [33].

While these results are intriguing, they fail to explain the vastly different regioselectivity obtained for oxidative arylation of *N*-acetylindole and *N*-pivaloylindole in the presence of a copper acetate and silver acetate oxidant, respectively. To gain further insight, a number of experiments were conducted with a focus on the regioselectivity of the reactions. Both oxidants and additives that simulate the basic anion of the oxidant were employed to this effect (Table 5). In the presence of stoichiometric palladium, both *N*-acetyl and *N*-pivaloylindole have a propensity to undergo arylation at C3 with similar levels of selectivity (Table 5, entries 1 and 4). Under catalytic conditions, in the presence of $Cu(OAc)_2$ as oxidant, C3 arylation is favoured for both reactions (entries 2 and 6), with *N*-acetylindole being more C3 selective (16:1 vs. 5:1). Most instructive in this set of experiments is the variation in C3/C2-selectivity with the variation in $Pd(TFA)_2$ loading for *N*-pivaloylindole. Super-stoichiometric quantities of $Pd(TFA)_2$ provide almost exclusively C3-product in the absence of any oxidant (entry 3). The level of C3-arylation product is reduced upon lowering the $Pd(TFA)_2$ loading to 100 mol% and 20 mol% (entries 4 and 5). Under catalytic conditions (5 mol% Pd), the introduction of

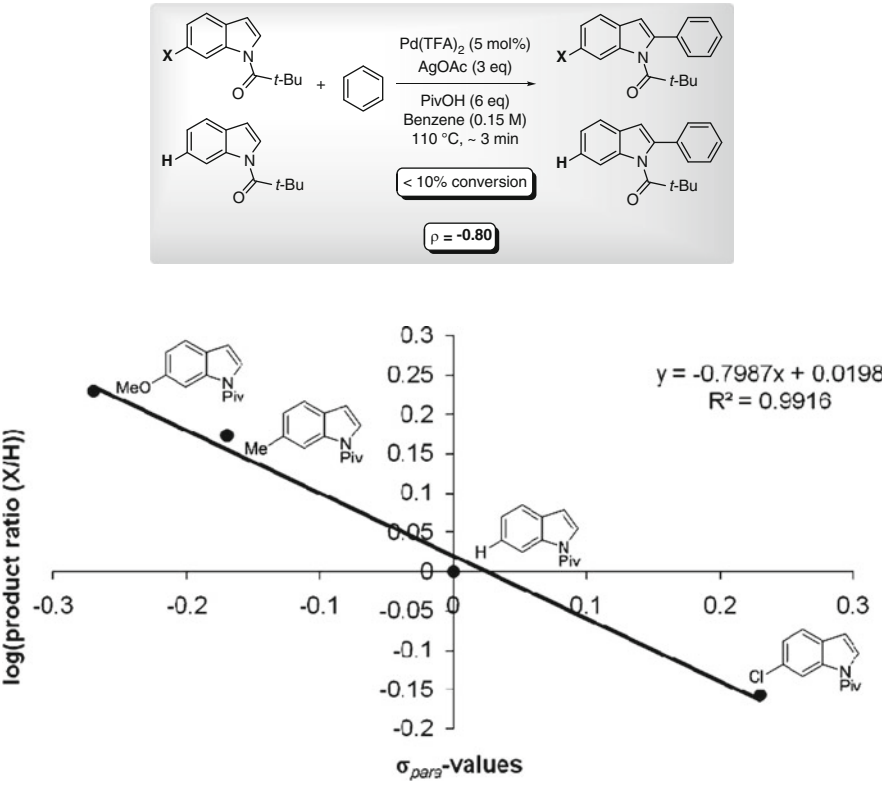

Fig. 4 Hammett correlation for C6-substituents on the C2-oxidative cross-coupling

AgOAc as oxidant induces a drastic inversion in selectivity to 1:25 for C3:C2 (entry 7). Interestingly, for *N*-pivaloylindole under 20 mol% $Pd(TFA)_2$, in the absence of a silver oxidant, the introduction of CsOAc further increases the C2-selectivity to 1:99 for C3:C2 (entry 8). Thus, we favour an explanation for these results which does not include the redox active component (Cu^{II} or Ag^{I}) of the oxidant but more importantly the nature of the added acetate. Perhaps the source (different cation; Cu vs. Ag and Cs) of added acetate modulates the relative basicity of the reaction medium, therefore, affecting the protonation/deprotonation events necessary for a C3,C2-palladium migration and the resulting C3/C2-selectivity. Additionally, and consistent with the variation in Pd concentration (entries 3–5), added acetate (in its various forms) may influence the aggregation state of Pd(II) resulting in different regioselective outcomes for different Pd(II)-aggregation states [36]. A further factor that must also be considered in the context of differing C3/C2-selectivity for *N*-acetyl and *N*-pivaloylindole is the nature of steric requirement of the indole nitrogen protecting group and the related amide conformations that may result. Entries 2 and 6 illustrate that under analogous conditions (Pd-catalyst loading and nature of added acetate) the size (CH_3 vs. $C(CH_3)_3$) of the amide R-group has an

Table 5 Additive effects on the C3/C2 selectivity

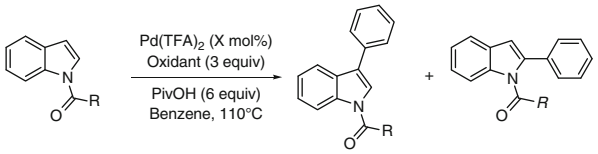

Entry	R-group	mol% Pd	Oxidant (equiv.)	Additive (equiv.)	Ratio C3:C2
1	Me	100	–	–	4.4:1
2[a]	Me	10	$Cu(OAc)_2$ (3)	–	16:1
3	*t*-Bu	300	–	–	99:1
4	*t*-Bu	100	–	–	3.7:1
5	*t*-Bu	20	–	–	1.1:1
6[a]	*t*-Bu	10	$Cu(OAc)_2$ (3)	–	5:1
7	*t*-Bu	5	AgOAc (3)	–	1:25
8	*t*-Bu	20	–	CsOAc (2)	1:99

[a]In the presence of 3-nitropyridine (10 mol%) and CsOPiv (40 mol%)

influence on the C3/C2-regioselective outcome of the reaction. Therefore, the ability of different amide conformers to participate in a C3/C2-palladium migration should also be considered in the development of future regioselective C–H functionalization reactions at indole.

4 State of the Art in Oxidative Cross-Coupling

In addition to our group, in 2007, the DeBoef and Sanford research groups simultaneously disclosed the first examples of a high yielding and highly selective oxidative cross-coupling of two unactivated arenes. The subsequent four years have witnessed extensive growth in the discovery of compatible reaction partners for oxidative cross-coupling reactions by a number of additional research groups. Importantly, late in 2010 and early in 2011 a push toward a more complete understanding of the mechanistic complexities associated with this reaction was reported by the DeBoef and Sanford groups, respectively. This section will highlight the accomplishments of the previous four years in oxidative cross-coupling and briefly describe the level of mechanistic knowledge gained thus far.

DeBoef and co-workers used a strategy similar to ours in the cross-coupling of an electron-rich arene, benzofuran, with benzene [Eq. (5)]. In the initial report, both electron-rich indoles and benzofurans were regioselectively cross-coupled with benzene, or its derivatives. In this case C2-selectivity on the heterocyclic arene was observed [39]. In a subsequent report, an observation correlating C3/C2-regioselectivity with the choice of oxidant ($Cu(OAc)_2$ or AgOAc) was made [40] and was consistent with the observations previously reported by our group [36] and presented herein (vide supra).

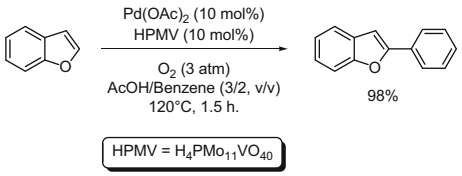

(5)

Sanford's seminal report involved the regioselective coupling of benzo[*h*]quinoline to benzene, and its derivatives, catalyzed by $Pd(OAc)_2$ (10 mol%) with Ag_2CO_3 (2 equiv.) as the oxidant in the presence of benzoquinone (0.5 equiv.), and DMSO (4 equiv.) [Eq. (6)] [41]. A significant body of work from the direct arylation literature had established that the site of reactivity of the benzo[*h*]quinoline was governed by the directing ability of the Lewis basic nitrogen and was exclusive to this position. However, the C–H bond cleavage event at the other arene coupling partner was much less regioselective and much less predictable. Through careful optimization, specifically the steric properties of the benzoquinone ligand, an increase in *meta*-selectivity was observed when mono-substituted arenes, such as anisole, were employed. An in-depth mechanistic analysis was carried out on this reaction and recently reported in the literature [42]. The mode of C–H bond cleavage at the benzo[*h*]quinoline was not investigated, though the mechanism of related cyclometallations with palladium has been previously reported to proceed via a CMD transition state. The C–H bond cleavage at the other arene coupling partner was the subject of their investigation. All mechanistic data pointed toward the involvement of a σ-bond metathesis pathway which is characterized by a concerted C–H bond cleavage and C–Pd bond formation. An S_EAr mechanism was ruled out based on their observation of *meta* selectivity in reactions of anisole.

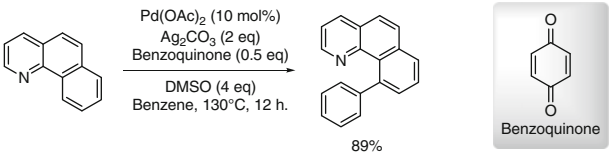

(6)

In 2008, two other oxidative cross-coupling reactions employing arenes with Lewis basic directing groups appeared in the literature, as well as, the first report of the use of an electron-deficient arene, pyridine *N*-oxide, participating in an oxidative cross-coupling with benzene and its derivatives. Shi and Buchwald have both used amides as directing groups in this class of chemistry. Shi reported the oxidative cross-coupling of acetanilides with benzene and its derivatives catalyzed by Pd(II) with a $Cu(OTf)_2$ (cat.)/O_2 oxidant system [43]. These reactions proceed in moderate-to-excellent yield and were applied to the synthesis of 4-deoxycarbazomycin B, a degradation product of the natural product carbazomycin B [Eq. (7)]. In Buchwald's work, the first example of the direct oxidation of Pd(0) by molecular oxygen in an oxidative arene cross-coupling was reported and this metal free oxidation system represents a significant advantage over the previously described systems [44]. This chemistry also utilized *N*-acetanilides and benzene or

its derivatives [Eq. (8)]. In these two reports, the reactions involving benzene derivatives were regioselective for reaction at the more sterically accessible C–H bonds, though only moderate selectivity was observed. Chang has reported the first example of an oxidative cross-coupling of an electron-deficient arene, pyridine *N*-oxide, with a simple arene, benzene [Eq. (9)] [45]. These reactions are highly regioselective for the 2-position of pyridine *N*-oxide and moderately selective for the most sterically accessible C–H bond of the other arene coupling partner. The mono-arylation product was also accompanied by the product of diarylation (when possible). Chang and co-workers suggest that the *N*-oxide moiety facilitates regioselective C–H bond cleavage by acting as a Lewis base. This report represents a significant advance as it expands the list of compatible substrates which couple with benzene to include electron-deficient arenes.

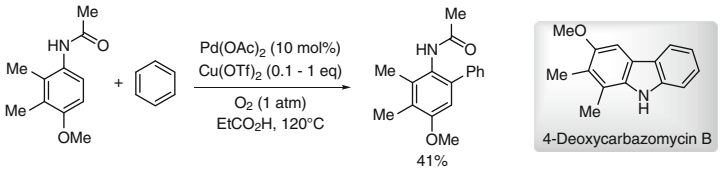

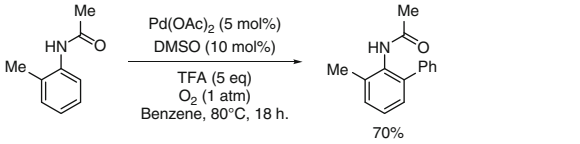

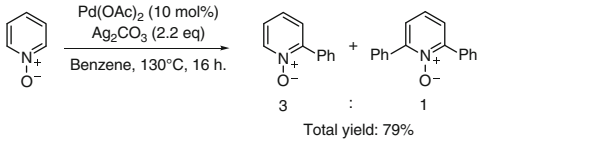

While the only report of intermolecular catalytic oxidative cross-coupling in 2009 was Sanford's impressive mechanistic work [41], 2010 was an exciting year with respect to new advances in compatible reaction partners. Dong contributed to the scope of substrates with Lewis basic directing groups by employing versatile *O*-phenylcarbamates in these transformations [Eq. (10)] [46]. These reactions demonstrate good substrate scope and exclusive regioselectivity with respect to the *O*-phenylcarbamate coupling partner. The regioselectivity for substituted benzenes is primarily at the least sterically encumbered C–H bond, which is consistent with results previously reported in the field. The authors also carried out preliminary mechanistic studies and favoured an electrophilic aromatic substitution-type (S_EAr) pathway for the palladation of the non-directing arene, though other mechanisms could not be ruled out at the time. This conclusion was in contrast to that of Sanford and co-workers, whose work pointed toward a σ-bond metathesis pathway for palladation of the simple arene in their system (vide supra) [41].

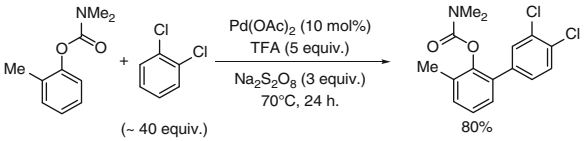

(10)

All previous reports in the oxidative cross-coupling literature relied on an electron-rich arene or an arene possessing a Lewis basic directing group to couple with an excess of benzene or a simple derivative thereof. The year 2010 saw not only the introduction of new substrate classes that were compatible in these reactions but also the use of new and unprecedented combinations of substrates. Zhang described the effective Pd(II)-catalyzed cross-coupling of electron-rich heteroaromatics with pentafluorobenzene and related analogues [Eq. (11)] [47]. One of the most significant advances in this chemistry is the push toward equal stoichiometry of the two coupling partners. In these cases, only 3 equiv. (relative to the heteroaromatic) of the fluorinated arene are employed compared to 30 equiv. of benzene for related transformations (vide supra) [32, 34, 38, 39]. Su showed, later the same year, that fluorinated arenes were compatible coupling partners with simple arenes, such as benzene [Eq. (12)] [48]. This demonstrated for the first time that benzene can oxidatively couple with an arene that is not electron-rich and possesses no Lewis basic directing group. Good yields were obtained for substituted and heteroaromatic fluorinated arenes. In addition, mono-substituted benzenes could be employed though low levels of regioselectivity (~3:1) were obtained for the *meta*- over the *para*-position. The authors also identified palladation of the non-fluorinated arene as the rate determining step. Finally, late in 2010 You developed the oxidative cross-coupling of two electron-rich heteroaromatics [Eq. (13)] [49]. Biologically relevant xanthines were coupled to a range of furans or thiophenes with only a threefold excess of the latter necessary for selective cross-coupling. This is a particularly impressive discovery as for the first time the catalyst displays the necessary chemoselectivity at each step of the catalytic cycle with two electronically (rich) similar arenes. Density functional theory (DFT) calculations shed some light on the energetics of the reaction and the cause of the impressive chemoselectivity. The calculations dictate that the catalyst reacts first with thiophene and that the subsequent reaction with xanthine, characterizing a cross-coupling, is a lower energy pathway than a reaction with a second molecule of thiophene, characterizing homo-coupling. The authors also demonstrate that by judicious choice of arene substrates excellent yields may be obtained at relatively low catalyst loadings (2.5 mol% Pd) as evidenced by the results for thiophenes and furans substituted with electron-withdrawing groups in comparison to those substituted with electron-donating groups.

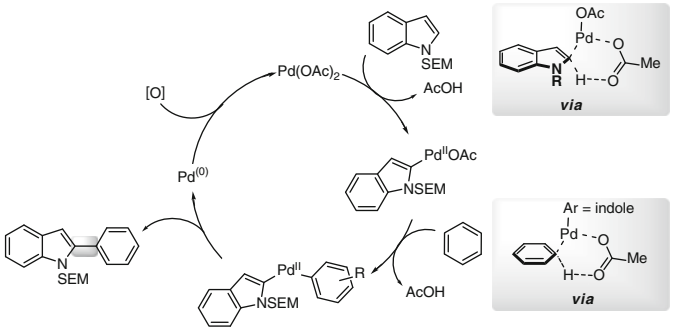

Scheme 9 DeBoef and Gorelsky's proposed mechanism

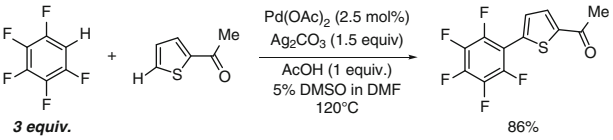

(11)

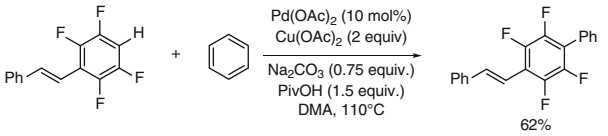

(12)

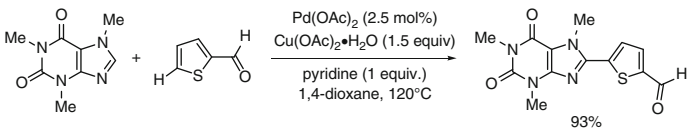

(13)

Also in 2010, DeBoef and Gorelsky reported a combination of experimental and computational work to elucidate the mechanism of C2-oxidative cross-coupling of indoles with benzene previously reported by DeBoef in 2008 [50]. The results of their work led to the conclusion that both C–H bond cleavage events proceeded via a single unifying mechanism—a concerted metallation–deprotonation process (Scheme 9). Furthermore, their experiments lead them to the conclusion that the palladation at indole takes place directly at the C2-position without C3-palladation and subsequent C3/C2-palladium migration as previously reported [27, 35] and described herein (vide supra).

Early 2011 has produced additional advances in both scope and mechanistic understanding of oxidative cross-coupling reactions, as well as, an application of this chemistry to the synthesis of a pharmacologically relevant compound. With respect to advancing the scope of compatible reaction partners in oxidative cross-coupling reactions, Beifuss communicated the direct coupling of xanthines with simple benzene and its derivatives in which the regioselectivity for the simple arene

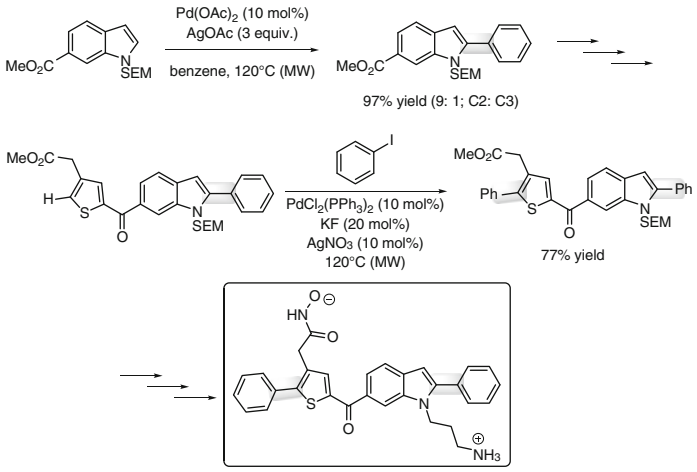

Scheme 10 DeBoef's route to a botulinum neurotoxin inhibitor employing an oxidative cross-coupling

was consistently at the more sterically accessible C–H bond [Eq. (14)] [51]. Zhang and Li, shortly thereafter, reported the direct coupling of azine *N*-oxides with indoles (and other azoles) in a 4:1 stoichiometry [52]. The reaction displays excellent regioselectivity for both the azine *N*-oxide at the C2-position and the indole at the C3-position and displays broad substrate scope with respect to both coupling partners [Eq. (15)].

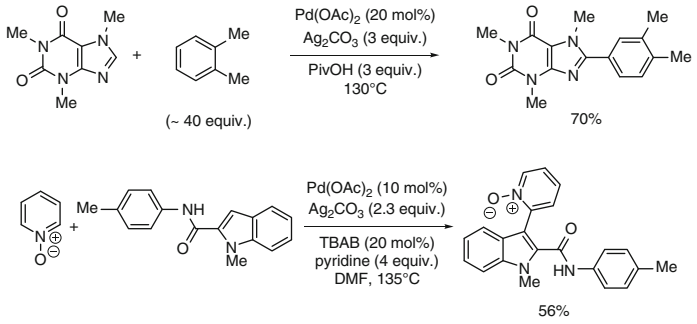

DeBoef demonstrated the utility of the C2-selective oxidative cross-coupling of indole and benzene previously reported by his group in the expedient synthesis of a botulinum neurotoxin inhibitor (Scheme 10) [53]. The streamlined synthesis featured an oxidative cross-coupling of methyl-*N*-SEM-indole-6-carboxylate with benzene, and after further elaboration, a direct arylation of a thiophene moiety that had been incorporated into the molecule. This formal synthesis highlights the efficiency of transition metal catalyzed reactions at C–H bonds in the planning of synthetic routes.

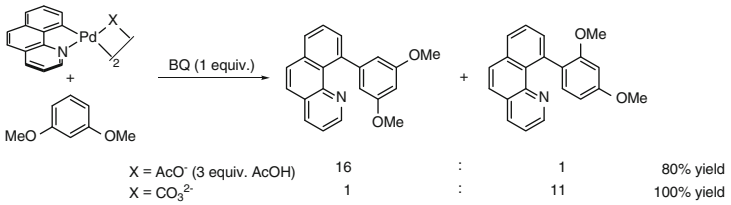

Scheme 11 Sanford's control of regioselectivity

Sanford and co-workers followed up on their 2009 mechanistic work with an extensive investigation of the parameters that contribute to site-selectivity in the direct coupling of 1,3- and 1,2,3-substituted simple arenes with cyclometallated arenes (Scheme 11) [54]. These studies lead to the development of two sets of reaction conditions that provide orthogonal regioselectivity for 1,3- and 1,2,3-substituted arenes. The authors found that by careful selection of the X^- ligand on palladium (Scheme 11) and the addition or deletion of acid additives, the reaction could be tuned to provide high levels of site-selectivity, leading to one of two regioisomers. These experiments also helped to rule out certain mechanisms based on the observed selectivity. The origin of selectivity in these reactions and the extension to a catalytic system is an area of continued investigation in the Sanford group.

5 Outlook and Perspectives

The work described above represents an account of our discovery and development of an oxidative direct coupling of indole and benzene. A number of groups have made significant strides towards understanding the factors that control both chemoselectivity and regioselectivity in these direct coupling reactions. DeBoef and Gorelsky have provided evidence for a unifying CMD mechanism being operative in both C–H bond cleavage steps in their system. Thus, this poses the question: What is the basis for chemoselectivity in the face of a single C–H bond cleaving mechanism [55]? Other groups have proposed an S_EAr-type mechanism for C–H bond cleavage and other mechanistic investigations have resulted in equally deserving questions regarding issues of regioselectivity in the C–H bond cleavage of simple arenes. Despite these arising questions, the chemical community has demonstrated impressive breadth of scope for oxidative cross-coupling reactions in just a few short years, thus inching our way closer to the efficiency of Nature and the substrate compatibility of traditional cross-coupling methods. The largest challenges that continue to face synthetic chemists in the expansion of oxidative cross-coupling reactions to more practical applications are chemoselectivity and regioselectivity. The determination of the factors that control chemoselectivity across a broad range of arenes and the ability to maintain high levels of chemoselectivity at equimolar ratios of coupling partners is a challenge of

paramount importance. Equal to this is the need to gain an understanding of the factors that control regioselectivity in the oxidative coupling of mono- and poly-substituted benzene derivatives that lack directing groups.

For my part, (DRS) as a graduate student involved in the inventive processes of developing a new reaction, the guidance, patience and constant encouragement of my supervisor, Professor Keith Fagnou, made this one of the most intellectually stimulating and gratifying periods of my life. Keith was a very special person and will be missed by many as a mentor and friend. The spirit he instilled of always asking interesting and unanswered questions and his creative and enthusiastic approach toward solving them will surely live on in those he taught and worked alongside.

Note Added in Proof: After the submission of this manuscript, the field of oxidative cross-coupling continued to advance and a number of elegant examples have appeared in the literature later in 2011 and early in 2012. Noteworthy among these is a report by the Yu group as it begins to address one of the most daunting challenges in this field: the general ability to control the regioselectivity of simple mono-substituted arenes that do not contain Lewis-basic directing groups. They propose that a high-valent Pd(IV)-intermediate is an integral species for electrophilic attack on the mono-substituted arene and results in high *and reliable para*-selectivity as this coupling partner [56].

Acknowledgements I (DRS) will forever be indebted to Professor Keith Fagnou. His guidance, both scientifically and personally, was a constant source of inspiration during my graduate studies in his group. The entire Fagnou group is acknowledged for their support, in particular those that contributed to this chemistry: Elisia Villemure, Ivan Petrov, and Ho-Yan Sun. Sophie Rousseaux and Catherine Stuart are thanked for critical reading of this chapter at its various stages; and Prof. Gooβen is thanked for the opportunity to contribute to this anthology

References

1. Bringmann G, Günther C, Ochse O, Schupp O, Tasler S (2001) Progress in the chemistry of organic natural products. Springer, Wien/New York
2. Lessene G, Feldman KS (2002) Oxidative aryl-coupling reactions in synthesis. In: Astruc D (ed) Modern arene chemistry. Wiley-VCH, Weinheim
3. Hassan J, Svignon M, Gozzi C, Schultz E, Lemaire M (2002) Aryl-aryl bond formation one century after the discovery of the Ullman reaction. Chem Rev 102:1359–1469
4. Diederich F, Stang PJ (eds) (2004) Metal-catalyzed cross-coupling reactions. Wiley-VCH, New York
5. Suzuki A (2011) Cross-coupling reactions of organoboranes: an easy way to construct C-C bonds (Nobel lecture). Angew Chem Int Ed 50:6722–6737
6. Negishi E (2011) Magical power of transition metal: past, present, and future (Nobel lecture). Angew Chem Int Ed 50:6738–6764
7. Alberico D, Scott ME, Lautens M (2007) Aryl-aryl bond formation by transition-metal-catalyzed direct arylation. Chem Rev 107:174–238
8. Campeau L-C, Stuart DR, Fagnou K (2007) Recent advances in intermolecular direct arylation reactions. Aldrichmica Acta 40:35–41
9. Seregin IV, Gevorgyan V (2007) Direct transition-metal-catalyzed functionalization of heteroaromatic compounds. Chem Soc Rev 36:1173–1193

10. Colby DA, Bergman RG, Ellman JA (2009) Rhodium-catalyzed C-C bond formation via heteroatom-directed C-H bond activation. Chem Rev 110:624–655
11. Liu C, Zhang H, Shi W, Lei A (2011) Bond formations between two nucleophiles: transition metal catalyzed oxidative cross-coupling reactions. Chem Rev 111:1780–1824
12. Ryabov AD, Sakodinskaya IK, Yatsimirsky AK (1985) Kinetics and mechanism of ortho-palladation of ring-substituted *N*,*N*-dimethylbenzylamines. J Chem Soc Dalton Trans 2629
13. Ryabov AD (1990) Mechanisms of intramolecular activation of carbon-hydrogen bonds in transition-metal complexes. Chem Rev 90:403–424
14. Lafrance M, Fagnou K (2006) Palladium-catalyzed benzene arylation: incorporation of catalytic pivalic acid as a proton shuttle and a key element in catalyst design. J Am Chem Soc 128:16496–16497
15. Campeau L-C, Rousseaux S, Fagnou K (2005) A solution to the 2-pyridyl organometallic cross-coupling problem: regioselective catalytic direct arylation of pyridine *N*-oxides. J Am Chem Soc 127:18020–18021
16. Leclerc J-P, Fagnou K (2006) Palladium-catalyzed cross-coupling reactions of diazine *N*-oxides with aryl chlorides, bromides and iodides. Angew Chem Int Ed 45:7781–7786
17. Campeau L-C, Stuart DR, Leclerc JP, Bertrand-Laperle M, Villemure E, Sun H-Y, Lasserre S, Guimond N, Lecavallier M, Fagnou K (2009) Palladium-catalyzed direct arylation of azine and azole *N*-oxides: reaction development, scope and applications in synthesis. J Am Chem Soc 131:3291–3306
18. Sun H-Y, Gorelsky SI, Stuart DR, Campeau L-C, Fagnou K (2010) Mechanistic analysis of azine *N*-oxide direct arylation: evidence for a critical role of acetate in the $Pd(OAc)_2$ precatalyst. J Org Chem 75:8180–8189
19. Lafrance M, Rowley CN, Woo TK, Fagnou K (2006) Catalytic intermolecular direct arylation of perfluorobenzenes. J Am Chem Soc 128:8754–8756
20. Lafrance M, Shore D, Fagnou K (2006) Mild and general conditions for the cross-coupling of aryl halides with pentafluorobenzene and other perfluoroaromatics. Org Lett 8:5097–5100
21. Do H-Q, Daugulis O (2008) Copper-catalyzed arylation and alkenylation of polyfluoroarene C-H bonds. J Am Chem Soc 130:1128–1129
22. Gorelsky SI, Lapointe D, Fagnou K (2008) Analysis of the concerted metallation-deprotonation mechanism in palladium-catalyzed direct arylation across a broad range of aromatic substrates. J Am Chem Soc 130:10848–10849
23. Özdemir I, Demir S, ζetinkaya B, Gourlaouen C, Maseras F, Bruneau C, Dixneuf PH (2008) Direct arylation of arene C-H bonds by cooperative action of NHCarbene-ruthenium(II) catalyst and carbonate via proton abstraction mechanism. J Am Chem Soc 130:1156–1157
24. Mota AJ, Dedieu A, Bour C, Suffert J (2005) Cyclocarbopalladation involving an unusual 1,5-palladium vinyl to aryl shift as termination step: theoretical study of the mechanism. J Am Chem Soc 127:7171–7182
25. Lapointe D, Fagnou K (2010) Overview of the mechanistic work on the concerted metallation-deprotonation pathway. Chem Lett 39:1118–1126
26. Huestis MP, Fagnou K (2009) Site-selective azaindole arylation at the azine and azole rings via *N*-oxide activation. Org Lett 11:1357–1360
27. Labrasseur N, Larrosa I (2008) Room temperature and phosphine free palladium catalyzed direct C-2 arylation of indoles. J Am Chem Soc 130:2926–2927
28. Deprez NR, Kalyani D, Krause A, Sanford MS (2006) Room temperature palladium-catalyzed 2-arylation of indoles. J Am Chem Soc 128:4972–4973
29. Lane BS, Brown MA, Sames D (2005) Direct palladium-catalyzed C-2 and C-3 arylation of indoles: a mechanistic rationale for regioselectivity. J Am Chem Soc 127:8050–8057
30. Ferreira EM, Stoltz BM (2003) Catalytic C-H bond functionalization with palladium(II): aerobic oxidative annulation of indoles. J Am Chem Soc 125:9578–9579
31. Itahara T (1979) Intramolecular ring closure of 1-aroylindoles by palladium acetate. Synthesis 2:151–152
32. Itahara T (1981) Arylation of *N*-acyl-pyrroles and -indoles with arenes and palladium acetate. J Chem Soc Chem Commun 254–255

33. Itahara T (1985) Arylation of aromatic heterocycles with arenes and palladium(II) acetate. J Org Chem 50:5272–5275
34. Stuart DR, Fagnou K (2007) The catalytic cross-coupling of unactivated arenes. Science 316:1172–1175
35. Stuart DR (2010) Transition-metal-catalyzed oxidative functionalization and preparation of nitrogen containing heterocycles. Ph.D. Thesis, University of Ottawa, Ottawa
36. Stuart DR, Villemure E, Fagnou K (2007) Elements of regiocontrol in palladium-catalyzed oxidative arene cross-coupling. J Am Chem Soc 129:12072–12073
37. Grimster NP, Gauntlett C, Godfrey CRA, Gaunt MJ (2005) Palladium-catalyzed intermolecular alkenylation of indoles by solvent-controlled regioselective C-H functionalization. Angew Chem Int Ed 44:3125–3129
38. Beck EM, Grimster NP, Hatley R, Gaunt MJ (2006) Mild aerobic oxidative palladium(II) catalyzed C-H bond functionalization: regioselective and switchable C-H alkenylation and annulation of pyrroles. J Am Chem Soc 128:2528–2529
39. Dwight TA, Rue NR, Charyk D, Josselyn R, DeBoef B (2007) C-C bond formation via double C-H functionalization: aerobic oxidative coupling as a method for synthesizing heterocoupled biaryls. Org Lett 9:3137–3139
40. Potavathri S, Dumas AS, Dwight TA, Naumiec GR, Hammann JM, DeBoef B (2008) Tetrahedron Lett 49:4050–4053
41. Hull K, Sanford MS (2007) Catalytic and highly regioselective cross-coupling of aromatic C-H substrates. J Am Chem Soc 129:11904–11905
42. Hull KL, Sanford MS (2009) Mechanism of benzoquinone-promoted palladium-catalyzed oxidative cross-coupling reactions. J Am Chem Soc 131:9651–9653
43. Li B-J, Tian S-L, Fang Z, Shi Z-J (2008) Multiple C-H activations to construct biologically active molecules in a process completely free of organohalogen and organometallic components. Angew Chem Int Ed 47:1115–1118
44. Brasche G, Garcia-Fortanet J, Buchwald SL (2008) Twofold C-H functionalization: palladium-catalyzed ortho arylation of anilides. Org Lett 10:2207–2210
45. Cho SH, Hwang SJ, Chang S (2008) Palladium-catalyzed C-H functionalization of pyridine *N*-oxides: highly selective alkenylation and direct arylation with unactivated arenes. J Am Chem Soc 130:9254–9256
46. Zhao X, Yeung CS, Dong VM (2010) Palladium-catalyzed ortho-arylation of *O*-phenylcarbamates with simple arenes and sodium persulfate. J Am Chem Soc 132:5837–5844
47. He C-Y, Fan S, Zhang X (2010) Pd-catalyzed oxidative cross-coupling of perfluoroarenes with aromatic heterocycles. J Am Chem Soc 132:12850–12852
48. Wei Y, Su W (2010) $Pd(OAc)_2$-catalyzed oxidative C-H/C-H cross-coupling of electron-deficient polyfluoroarenes with simple arenes. J Am Chem Soc 132:16377–16379
49. Xi P, Yang F, Qin S, Zhao D, Lan J, Gao G, Hu C, You J (2010) Palladium(II)-catalyzed oxidative C-H/C-H cross-coupling of heteroatoms. J Am Chem Soc 132:1822–1824
50. Potavathri S, Pereira KC, Gorelsky SI, Pike A, LeBris AP, DeBoef B (2010) Regioselective oxidative arylation of indoles bearing *N*-alkyl protecting groups: dual C-H functionalization via a concerted metallation-deprotonation mechanism. J Am Chem Soc 132:14676–14681
51. Malakar CC, Schmidt D, Conrad J, Beifuss U (2011) Double C-H activation: the palladium-catalyzed direct C-arylation of xanthines with arenes. Org Lett 13:1378–1381
52. Gong X, Song G, Zhang H, Li X (2011) Palladium-catalyzed oxidative cross-coupling between pyridine and *N*-oxides and indoles. Org Lett 13:1766–1769
53. Potavathri S, Kantak A, DeBoef B (2011) Increasing synthetic efficiency via direct C-H functionalization: formal synthesis of an inhibitor of botulinum neurotoxin. Chem Commun. doi:10.1039/c1cc10755k
54. Lyons TW, Hull KL, Sanford MS (2011) Controlling site selectivity in Pd-catalyzed oxidative cross-coupling reactions. J Am Chem Soc 133:4455–4464
55. Meir R, Kozuch S, Uhe A, Shaik S (2011) How can theory predict the selectivity of palladium-catalyzed cross-coupling of pristine aromatic molecules? Chem Eur J 17:7623–7631
56. Wang X, Leow D, Yu J-Q (2011) Pd(II)-catalyzed *para*-selective C-H arylation of monosubstituted arenes. J Am Chem Soc 133:13864–13867

Top Organomet Chem (2013) 44: 121–142
DOI: 10.1007/3418_2012_44

Published online: 28 August 2012

Decarboxylative Coupling Reactions

Lukas J. Gooßen and Käthe Gooßen

Abstract Transition metal-catalyzed decarboxylative couplings have recently emerged as a promising concept for C–C and C–heteroatom bond formation. Our contribution to this rapidly evolving field was the development of redox-neutral decarboxylative cross-couplings. In these catalytic transformations, carboxylic acids extrude CO_2 to give organometallic intermediates, which react with aryl electrophiles under regioselective formation of a new C–C bond. This reaction concept compares favorably to traditional cross-couplings involving preformed organometallic reagents, as it draws on stable and broadly available carboxylic acids as the source of carbon nucleophiles. In this chapter, we describe the invention process that resulted in the discovery of the first active catalyst systems and in the stepwise extension of this concept to a broadly applicable synthetic concept. A short overview on recent developments in this field is also provided.

Keywords Aryl halides · Carboxylic acids · Copper · Cross-coupling · Decarboxylation · Palladium

Contents

L.J. Gooßen (✉) and K. Gooßen
FB Chemie – Organische Chemie, TU Kaiserslautern, Erwin-Schrödinger-Str. Geb. 54, 67663 Kaiserslautern, Germany
e-mail: goossen@chemie.uni-kl.de

Abbreviations

[M]	Metal in ligand environment
Ac	Acetyl
acac	Acetyl acetonate
Ar	Aryl
dCypp	1,3-Bis(dicyclohexylphosphino)propane
DFT	Density functional theory
DMF	*N*,*N*-dimethylformamide
DMSO	Dimethylsulfoxide
dppf	1,1′-Bis(diphenylphosphino)ferrocene
dppp	1,3-Bis(diphenylphosphino)propane
Het	Heteroatom-containing group, e.g., OR, SR, NRR′
L	Ligand
Me-2,2′-bipy	4,4′-Dimethyl-2,2′-bipyridine
MS	Molecular sieves
NMP	*N*-methylpyrrolidone
phen	1,10-Phenanthroline
rac-BINAP	Racemic 2,2′-bis(diphenylphosphino)-1,1′-binaphthyl
RT	Room temperature
^{t}BuXPhos	2-(Di-*tert*-butylphosphino)-2′,4′,6′-triisopropyl-1,1′-biphenyl
Tf	Triflate
TFA	Trifluoroacetate
Tol-BINAP	2,2′-Bis(di-*p*-tolylphosphino)-1,1′-binaphthyl
tpa	Tons per annum
X	Leaving group (e.g., halide, triflate, tosylate, etc.)
Y	Spacer group, e.g., CH_2, NH, O
μW	Microwave

1 Introduction

Catalytic decarboxylative cross-couplings have emerged within recent years as a powerful strategy to form carbon–carbon or carbon–heteroatom bonds starting from carboxylic acids. The impressive progress achieved in this field has been recently reviewed [1–4]. The carboxylate function is used as a leaving group to direct the coupling to an electrophilic center, with concurrent loss of carbon dioxide. This strategy allows for the regioselective coupling of specific types of carboxylic acids

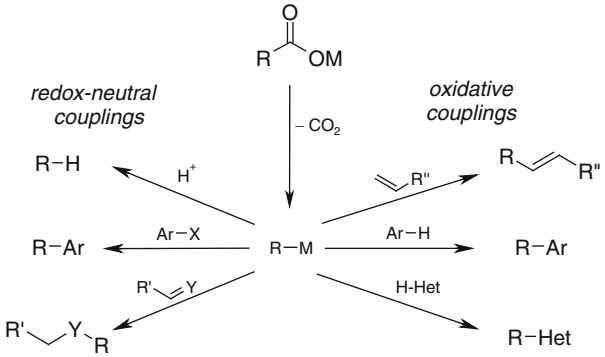

Scheme 1 Examples of decarboxylative coupling reactions

with aryl halides, Michael acceptors, nitriles, and other electrophiles to a range of valuable building blocks (Scheme 1). Under oxidative conditions, carboxylic acids can also decarboxylatively couple with nucleophiles. The basis for this rapidly developing field of research (170 publications since 2006) [5] was laid with the discovery of catalysts that effectively mediate the extrusion of carbon dioxide from aromatic carboxylic acids with formation of aryl-metal species and their incorporation into coupling reactions [6–10].

2 Defining the Research Target

The invention process of redox-neutral decarboxylative cross-couplings mediated by bimetallic catalysts began in 2003. While I was assistant professor (Habilitand) at the Max Planck Institute for Coal Research in Mülheim, my group had developed several sustainable metal-catalyzed synthetic methods based on carboxylic acid derivatives [11]. In April 2003, I gave a colloquium at Bayer AG on this topic. An animated discussion ensued with experienced industrial chemists, centered on synthetic problems that are regularly troublesome in industrial practice, but paradoxically viewed as "solved" by academic scientists. Examples of this were metal-catalyzed carbon–carbon bond formations, such as the Suzuki–Miyaura reaction. What particularly struck me that day was the difficulty of synthesizing boronic acids on industrial scales, as opposed to the ease of coupling them. In a subsequent conversation, Dr. Hugl (at that time head of Organic Synthesis Research at Bayer Chemicals) encouraged me to search for alternative strategies for carbon–carbon bond formation and promised generous funding for any convincing concept I would present for the regioselective synthesis of biaryls, however far-fetched it may be.

In the ensuing months, I drew up diverse approaches to novel biaryl syntheses on the blackboard and refined them in intense discussions with coworkers and colleagues in Mülheim. Most of the ideas had to be dismissed because we found

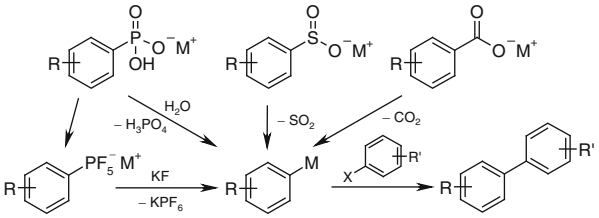

Scheme 2 Alternative sources of carbon nucleophiles in Suzuki-type arylations

no satisfactory catalyst cycle based only on thermodynamically feasible individual steps. The first concept to withstand these discussions consisted of using either arylphosphonic rather than arylboronic acids or aryl hexafluorophosphate rather than aryl trifluoroborate salts as the source of aryl nucleophiles in Suzuki-type coupling reactions. An analogous use of arylsulfinic acid derivatives also appeared to be feasible (Scheme 2). An even more speculative idea was to convert benzoate salts into aryl nucleophiles by extrusion of carbon dioxide.

We used DFT calculations to clarify whether these substrate classes were at least theoretically suited as carbon nucleophiles. My Ph.D. student Debasis Koley investigated the polarity of the carbon–phosphorus and carbon–sulfur bonds and came to the conclusion that both reagents can be derivatized in a way that the adjacent carbon atoms would indeed become negatively charged. The decarboxylation of metal benzoates was predicted to be exergonic, but with a large activation barrier. A literature search revealed that Nilsson had shown already in 1968 that copper arenecarboxylates extrude carbon dioxide at high temperatures with formation of transient aryl-copper species. These are believed to act as intermediates in Cu-mediated protodecarboxylations [12–16]. All these pieces of evidence convinced us that at least one of these approaches had a chance of succeeding.

3 Designing a Catalytic Process

Following intensive evaluation of the literature and of potential reaction mechanisms, we drafted a research plan that we presented to specialists at Bayer in October 2003. In it, we elaborated on the use of arylphosphonic, arylsulfinic, and arylcarboxylic acids as alternatives to arylboronic acids in cross-coupling reactions. The decarboxylative version was placed third because at the time, we viewed this approach as the least promising, fearing that the temperatures required for it to work would be prohibitively high for industrial applications. For each reaction, the proposal included draft catalytic cycles composed for the most part of elementary steps known from other metal-catalyzed reactions or from stoichiometric conversions of organometallic compounds [17, 18]. The inventive effort lies mostly in designing these novel combinations of elementary steps. We took our chances

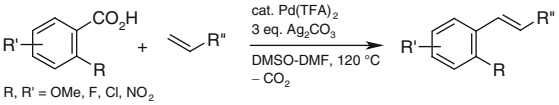

Scheme 3 Oxidative decarboxylative Heck reaction

with this proposal, lacking the financial means and personnel to support our plans with experimental studies.

Dr. Hugl and his colleagues at Bayer carefully examined our research plan and ultimately offered to finance the project for two years. They did not request any experimental support for the validity of the postulated reaction mechanisms, but based their decision solely on the theoretical calculations, mechanistic considerations, and our previous track record of successfully developing new catalytic transformations [19–25]. While they rated the probability for this project to succeed as very low, they viewed the potential gain for Bayer as so high that they were prepared to take their chances.

This industrial support was critical for the success of this high-risk project considering it took us almost one year to furnish the proof of concept, which then allowed us to submit an experimentally validated proposal to public funding agencies. Method developers regularly face the challenge of demonstrating preliminary work to support their proposals because it may take years to reach proof-of-concept stage for one of the many reactions they investigate. Once there, the newly discovered reaction can often be led to preparative utility within weeks.

In Dr. Guojun Deng, I found an excellent coworker, as is indispensible for such a challenging project, and we began our experimental work in early 2004. The first months were taken up by intensive investigations of the arylphosphonate cross-coupling. Whereas we had some encouraging results, we had to admit that the corrosiveness of the required reaction conditions was likely to impede any industrial implementation of this approach. For the sulfinic acid derivatives, we suspected similar issues, so that we moved straight on to the decarboxylative reactions.

Our original mechanism for decarboxylative reactions included a monometallic palladium catalyst related to that postulated in 2002 by Myers for his oxidative decarboxylative Heck reactions (Scheme 3) [6].

In this process, carboxylic acids and olefins are converted to vinylarenes in the presence of palladium in catalytic amounts and silver in overstoichiometric amounts (Scheme 4). It is initiated by formation of a silver arenecarboxylate salt, which then reacts with a palladium(II) halide complex (**a**) to give the silver halide and palladium carboxylate **b**. The extrusion of carbon dioxide, and thus the conversion of the carboxylate to the organometallic species **c**, occurs within the ligand sphere of palladium. The subsequent steps, i.e., insertion of the olefin into the palladium–carbon bond, internal rotation, and β-hydride elimination, correspond to the classical Heck reaction [26]. An additional oxidation step converts the palladium(0) species **f** back to palladium(II). It is this oxidation by silver that

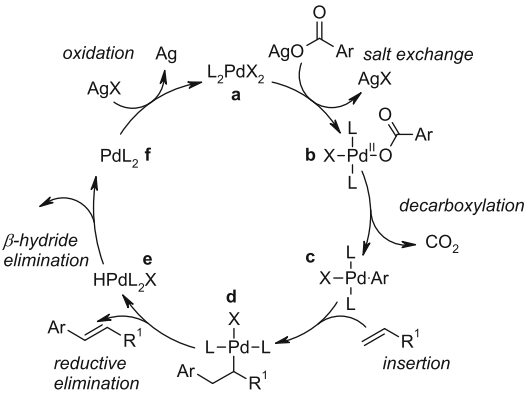

Scheme 4 Proposed mechanism for Myers' decarboxylative Heck reaction

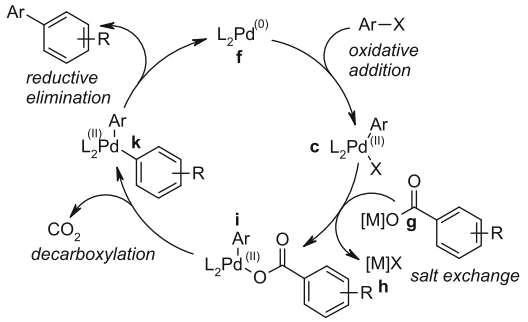

Scheme 5 First design of a catalytic decarboxylative cross-coupling

causes the arylpalladium species **c** generated via the extrusion of CO_2 from a carboxylate ion to react as an aryl electrophile rather than aryl nucleophile.

We reasoned that such a decarboxylation step could also be employed in a redox-neutral cross-coupling reaction with carbon electrophiles. On this basis, we drew up a catalytic cycle that starts with an oxidative addition of aryl halides or pseudohalides to a coordinatively unsaturated palladium(0) species **f** (Scheme 5). The more weakly coordinating the leaving group X, the easier should be its subsequent replacement by a carboxylate. At least for X = OTf, the palladium(II) carboxylate **h** should form quantitatively, whereas for X = halide, it should be possible to enforce this step by employing silver or thallium salts as species **g**. The ensuing thermal decarboxylation of the palladium(II) intermediate **i** represents the most critical step. Myers' results indicated that certain palladium(II) carboxylates liberate carbon dioxide on heating. However, it remained unclear whether arylpalladium (II) carboxylate complexes such as **i** would display a similar reactivity. If this were to be the case, they would form Ar–Pd–Ar′ intermediates **k**, which in turn are

known to eliminate the desired biaryls. This would close the catalytic cycle with regeneration of palladium in the original zero oxidation state (**f**).

This first plan for a decarboxylative cross-coupling carried with it certain weaknesses for potential industrial applications. It was to be expected that the salt metathesis between alkali metal carboxylates and late transition metal halides would be thermodynamically disfavored. We expected the formation of a palladium benzoate complex **i** from palladium bromide complexes **c** and potassium benzoate (**g**) to proceed well only in the presence of a stoichiometric quantity of silver to capture bromide ions [27]. However, we did not like the idea of using stoichiometric quantities of silver salts or of expensive aryl triflates in the place of aryl halides. Finally, the published substrate scope of the oxidative Heck reaction led to concerns that palladium catalysts mediate the decarboxylation only of a narrow range of carboxylates, precluding use of this reaction as a general synthetic strategy.

These concerns were supported by the first test reactions in which we tried to couple benzoic acid with 4-bromoanisole in the presence of palladium complexes. We encountered great difficulties with generating the palladium benzoate from palladium bromide complexes in the absence of silver salts. Phosphine-stabilized palladium benzoates, especially arylpalladium(II) benzoates similar to **i**, did not extrude CO_2 even at high temperatures. Only a small spectrum of palladium arenecarboxylates and phenylacetates was identified that lost CO_2 upon heating. This is in agreement with a study of the protodecarboxylation activity of palladium published subsequently by Kozlowski [28].

In none of our extensive test reactions of aryl halides with benzoic acids carried out in the presence of diverse palladium catalysts, we were able to detect even traces of the unsymmetrical biaryl. Instead, we observed mostly homocoupling and dehalogenation products in some cases along with phenol esters. The conversion of aryl triflates with potassium benzoates did not lead to the desired biaryls, either, but to the phenol esters instead.

4 Designing a Bimetallic Catalyst System

In view of this lengthy period of discouraging results, we returned to the drawing board to look for alternative reaction mechanisms. At the time, it appeared that palladium-based protocols would at best allow us to convert a limited range of benzoates with a few particularly robust aryl triflates. We therefore decided to alter our concept by introducing a cocatalyst designed to effectively mediate specifically the decarboxylation step and then transfer the aryl residue to the palladium cross-coupling catalyst.

Nilsson et al. had previously demonstrated that arylcopper species intermediately form in copper-mediated protodecarboxylation reactions [12–16]. Moreover, they isolated 2-nitrobiphenyl along with nitrobenzene and several by-products in the pyrolysis of copper 2-nitrobenzenecarboxylate at 250°C in the presences of excess iodobenzene. Due to the limitations of known copper-mediated Ullmann-

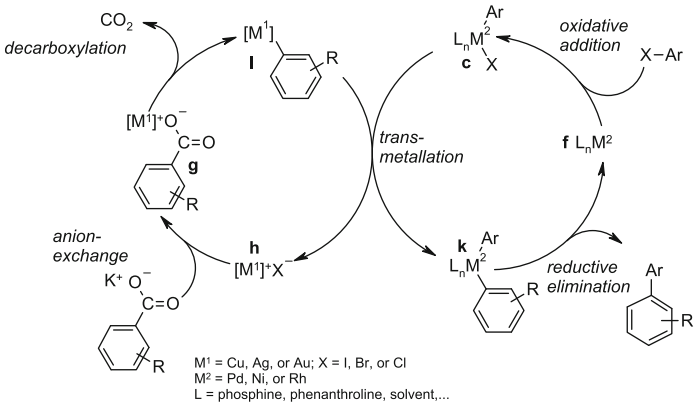

Scheme 6 Pathway for a decarboxylative coupling cooperatively catalyzed by two metals

type couplings [29], namely, the low selectivity for the heterocoupling and stoichiometric use of copper, we were very skeptical that this trapping experiment could be turned into a preparatively useful biaryl synthesis. We thus sketched a mechanism in which two different metal complexes cooperatively catalyze the decarboxylative cross-coupling. The first complex, a copper, silver, or gold catalyst, would mediate the extrusion of carbon dioxide from arenecarboxylates. The second, a two-electron catalyst such as palladium, nickel, or rhodium, would be responsible for the cross-coupling with an aryl halide (Scheme 6).

In the new catalytic cycle, the carboxylic acid is deprotonated with a mild base, and the carboxylate group is transferred onto a copper- or silver-based decarboxylation catalyst **h** via salt exchange with formation of the corresponding carboxylate complex **g**. The metal would then have to insert into the C–C(O) bond under extrusion of CO_2 to form a stable arylcopper or arylsilver intermediate **l**. For these polarizable late transition metals, the metal–carbon bond should be particularly stable in comparison to the metal–oxygen bond, thus providing a driving force for this step in addition to the entropically favored loss of gaseous CO_2. The carbon residue is then transferred onto an arylpalladium species **c**, generated in the reaction of the aryl electrophile with the second catalyst component, a low-valent palladium (0) species **f**. Finally, the carbon–carbon bond is formed in a reductive elimination from **k**, regenerating the original palladium species **f**. For further turnover of the decarboxylation catalyst to occur, the copper salt **h** formed in the transmetallation step would have to undergo a salt metathesis with the next carboxylate molecule. However, in the initial test reactions, we used stoichiometric amounts of copper or silver salts, so that this step was not yet required.

In these test reactions, we preformed copper(II) benzoate by treating benzoic acid with basic copper(II) carbonate, dried the resulting salt, and heated it to 150°C with 4-bromoanisole in the presence of various palladium complexes. This led to several products (Scheme 7). The formation of benzene indicated that the decarboxylation step worked, but that the intermediate arylcopper species

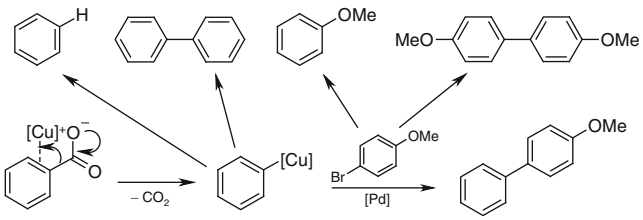

Scheme 7 Products observed in the attempted decarboxylative couplings

was protonated before transfer of the aryl group to the palladium could occur. Radical processes could account for the formation of biphenyl. Debromination of 4-bromoanisole and its homocoupling to 4,4′-dimethoxybiphenyl gave evidence for a successful oxidative addition step, which, however, was not in balance with the remainder of the complex catalytic cycle. The desired cross-coupling product 4-methoxybiphenyl was detected first only in traces, and after optimizing temperature and reaction time, we were able to isolate an isomerically pure product in up to 10% yield.

I was now fully convinced that this project would succeed. I wrote a proposal for a Heisenberg research fellowship in which I drafted a research plan for the upcoming years and enthusiastically explained the opportunities of decarboxylative cross-couplings. When I showed it to my wife, who is also a chemist, she said, "But you don't really think that this is actually going to work, do you?" Dr. Deng still set up an average of 20 carefully planned reactions per day, but I realized that he, too, was losing hope, and I was not surprised when he informed me that he had started writing job applications.

5 The Right Test Substrate

In a series of protodecarboxylation experiments with several benzoic acids, Dr. Deng confirmed our suspicion that our model compound, benzoic acid, was particularly unreactive, but found that 2-nitrobenzoic acid seemed to decarboxylate much more easily. At that time, the fungicide boscalid was starting its success story [30], and I encouraged him to switch to the reaction of 4-bromochlorobenzene with 2-nitrobenzoic acid as the test system. This renewed our motivation, as a successful coupling of these substrates would be of immediate interest as an alternative entry to the biaryl building block of boscalid (meanwhile produced on 1,500 tpa scale). Scheme 8 illustrates how a decarboxylative coupling could save two steps in the overall synthesis.

This new test reaction was the strike of fortune that led to the breakthrough in the catalyst development. Using preformed copper(II) 2-nitrobenzoate, we started to obtain reproducible yields of around 30%, which finally permitted us to systematically study the influence of catalyst components, solvents, and additives. Based on

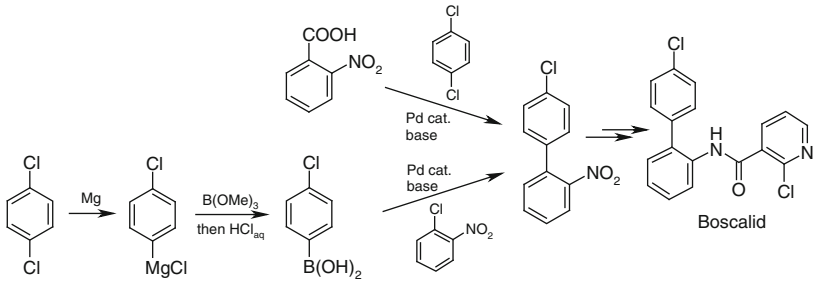

Scheme 8 Boscalid synthesis via decarboxylative coupling and Suzuki reaction

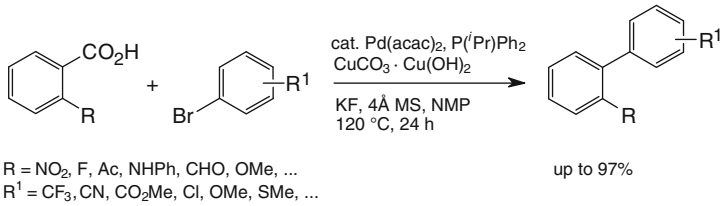

Scheme 9 The first high-yielding decarboxylative cross-coupling protocol

these findings, we optimized the catalyst system and steadily improved the yields. Interestingly, the yields seemed to hit a ceiling at 50% – we had to be missing something important. We found a potential explanation for this in a study by Kaeding et al., who reported that in the pyrolysis of Cu(II) benzoate, phenyl benzoate is formed as a by-product [31]. Maybe, only one of the two carboxyl groups coordinated to the copper was extruding CO_2, precluding the reaction to proceed to completion. We thus added stoichiometric amounts of various potassium salts to the copper 2-nitrobenzoate reaction mixtures to facilitate the formation of copper complexes with a single coordinated carboxylate.

On carnival 2005, I went to our laboratory at the RWTH Aachen to pick up Dr. Deng and take him to the traditional Rosenmontag parade. However, when I opened the door, I immediately realized that something had happened. Dr. Deng was smiling broadly, and he appeared to be in the middle of a chromatographic purification. Next to him was a beautifully clean gas chromatogram which showed the desired product in near-quantitative yield along with the internal standard only. Needless to say, we spend this carnival in the lab optimizing the first protocol of a decarboxylative cross-coupling. The reaction that had given such clean conversion contained KF as the additive (Scheme 9), and we saw the sharply increased yield as evidence for the intermediate formation of ArC(O)OCuF, which seemed to have a much lower decarboxylation barrier that the homoleptic copper(II) carboxylate.

Within a few days, we found a reliable reaction protocol in which a combination of the benzoic acid and aryl bromide in NMP is stirred for several hours at 120°C in the presence of stoichiometric amounts of basic copper carbonate and potassium fluoride, molecular sieves, and 2 mol% of a $Pd(acac)_2$/P(*i*-Pr)Ph_2 catalyst [36, 37]. The addition of molecular sieves, which effectively trapped the reaction water, allowed to deprotonate the benzoic acid in situ with carbonate bases. It was thus no longer necessary to use preformed and carefully dried copper benzoates. Beside copper, silver carbonate was also found to be effective, but due to the higher cost of this metal, we initially did not follow up on this.

6 The Transition to a Doubly Catalytic Protocol

Our first reaction protocol proved to be broadly applicable with regard to aryl bromides, but only in combination with 2-nitrobenzoic acid and a few other highly activated carboxylic acids (Scheme 9). It was a decisive first step, but failed to fulfill my high expectations. I will never forget the face of Dr. Deng when I told him that I did not yet want to publish the results of his meanwhile more than 1,200 reactions. I did not want to draw the attention of big research groups to this concept until our two-man team had achieved the next critical step and made the reaction catalytic also with regard to the decarboxylation catalyst. Fortunately, we did not know that despite all our mechanistic considerations, this would require another 800 experiments.

Whenever we tried to reduce the amount of basic $CuCO_3$ to 30 mol% and supplement the rest of it with K_2CO_3, the yields dropped to below the amount of copper employed. According to our proposed mechanism (Scheme 6), the copper salt should be regenerated after each transmetallation step, so that a catalytic amount should theoretically suffice. However, it was the anion exchange step from **h** to **g** that proved to be difficult. Raising the temperature above 120°C or prolonging the reaction time did not help. In either case we observed a color shift from green to brown, which we attributed to a partial reduction of Cu(II) to Cu(I).

We were reluctant to switch from copper(II) to copper(I) complexes as decarboxylation catalysts, having observed that copper(I) carboxylates lose CO_2 only above 160°C. In a systematic study we found that chelating bipyridine ligands, and 1,10-phenanthroline in particular, dramatically enhance the decarboxylation activity of copper(I) salts. After many experiments, we achieved more than one turnover of the copper using phenanthroline as the ligand for both copper and palladium at a temperature of 160°C. A rigorous exclusion of water was crucial to avoid protodecarboxylation becoming the main reaction pathway. At this stage, the exact reaction conditions, including heating rates and the purity of reagents and solvents, often influenced the reaction outcome more than the composition of the catalyst. In a situation like this, it is crucial to reproduce systematic studies several times before reaching any conclusions. If one reaction works better than the other, the reason may not be that one of the phosphines tested is more effective than others, but

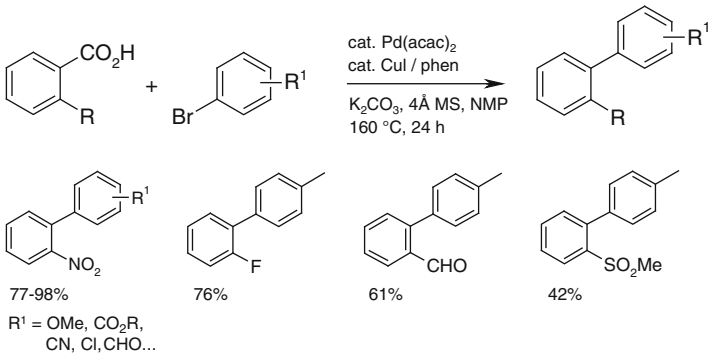

Scheme 10 The first decarboxylative cross-coupling catalytic in two transition metals

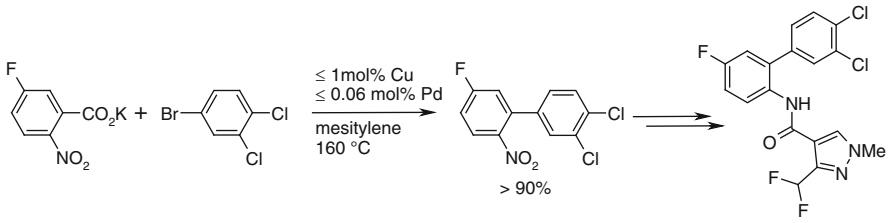

Scheme 11 Pilot plant synthesis of a bixafen intermediate on 50-kg scale

simply that of one of the phosphines is more pure. If the trend observed in a systematic study is hard to rationalize, our experience is that the experiments differ in more than just the intended way.

It took us some time to discover that the optimal way to trap the reaction water during the in situ deprotonation of 2-nitrobenzoate by potassium carbonate was to continuously distill off part of the reaction solvent. However, this strategy could not be used in screening experiments, and we thus added an excess of rigorously dried, finely powdered molecular sieves. This way, the model reaction gave almost quantitative yields using only 1% CuI, 0.5% $Pd(acac)_2$ and 3% phenanthroline in NMP at 160°C (Scheme 10).

Once we had found this protocol and acquired sufficient practice with the model reaction to reliably reproduce our own results, we went on to explore the generality of this protocol. We were delighted to find that it allowed coupling various aryl bromides and even some chlorides with 2-nitrobenzoic acid.

However, the extension to other carboxylic acids proved to be troublesome. Continuous fine-tuning of the copper–phenanthroline catalysts was required to extend the protocol catalytic in both metals first to carboxylic acids with other strongly coordinating groups in *ortho* position that significantly increase the copper-ligating quality of the carboxylate substrate (2-acyl, 2-formyl), then to carboxylic acids with weakly coordinating *ortho* substituents (2-fluoro, 2-cyanobenzoic acid), and finally to vinylic or heterocyclic derivatives (cinnamic, thiophenecarboxylic acid). Initially, we reoptimized the conditions for almost every carboxylic acid, until we eventually found more generally applicable catalyst systems [35, 37].

Our partners at Bayer, by now Lanxess, realized already at this early state of development that the new decarboxylative biaryl synthesis would open up opportunities for the industrial synthesis of high-value pharmaceutical intermediates and were pleased to find that it worked also on kilogram scales [32–34] (Scheme 11).

In October 2005, after Dr. Deng had already left my group and I had moved to the TU Kaiserslautern, we finally submitted our results for publication. However, the referees were skeptical, viewing our reaction as an extension of existing cross-coupling technology. In contrast, my wife was now so convinced of the wide-ranging opportunities of decarboxylative cross-couplings that she would not allow us to give up now rather than addressing each individual referee's comment. It took more than a year and as many as three resubmissions to see the manuscript accepted [35]. One argument that was repeatedly held up against this reaction was that it releases a stoichiometric amount of CO_2 and thus contributes to global warming. Another was that the reaction scope was still very limited and that it might well be intrinsically limited to *ortho*-substituted carboxylic acids [36, 37]. The latter was indeed a critical issue, and we addressed it with highest priority.

7 Overcoming Substrate Limitations

In order to evaluate what caused the limitation to *ortho*-substituted carboxylic acids, we investigated the decarboxylation step separately from the cross-coupling step. In the presence of only the copper(I) phenanthroline/quinoline decarboxylation catalyst (15 mol%), a wide range of aromatic, heteroaromatic, and vinylic carboxylates protodecarboxylated to the corresponding hydrocarbons on heating to 160°C (Scheme 12). However, added halide ions, as would inevitably be released in a decarboxylative cross-coupling (Scheme 6), prevented the decarboxylation for all non-*ortho*-substituted or not otherwise activated aromatic carboxylic acids.

The results suggested that the halides competed with the carboxylates for coordination sites at the copper. Therefore, a general process catalytic in both metals should be possible as soon as decarboxylation catalysts with a stronger preference for carboxylate over halide ions could be found. An alternative strategy to achieve coupling the full range of aromatic carboxylates was to avoid the formation of halide salts altogether, by employing electrophiles with non-coordinating leaving groups such as aryl triflates. Unfortunately, known palladium catalysts for the cross-couplings of aryl triflates require special catalyst systems that stabilize cationic palladium intermediates with chelating phosphines and/or added halides. As both these additives had previously found to impede the copper-mediated decarboxylation step, it was a real challenge to find a suitable catalyst system for the desired reaction.

Dr. Nuria Rodríguez, who joined my group as postdoc in 2006, led this project to success. She carefully investigated how the individual components of the decarboxylation and cross-coupling catalysts interact with each other and found that the clue to success lies in the choice of the phosphine ligand. A catalyst system

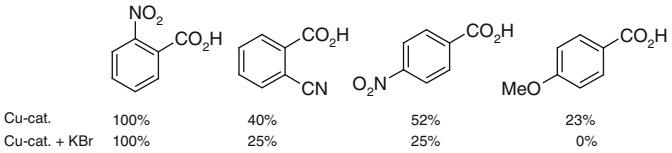

Scheme 12 Effect of halides on copper-catalyzed protodecarboxylations

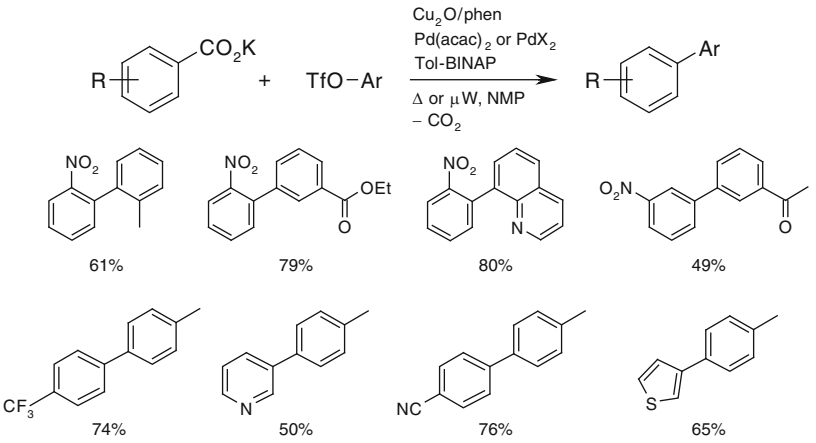

Scheme 13 Decarboxylative coupling of benzoate salts with aryl triflates

consisting of copper(I) oxide, 1,10-phenanthroline, and palladium(II) iodide along with the sterically demanding, moderately electron-rich chelating phosphine Tol-BINAP ideally strikes the delicate balance of stabilizing the palladium on one hand and maintaining the decarboxylation activity of the copper at the highest possible level on the other. As anticipated, the triflate ions released in the process were unable to block the carboxylates out of the coordination sphere of the decarboxylation catalyst, so that this protocol allowed the conversion of a much broader range of carboxylate substrates, now also including *meta*- and *para*-substituted benzoates (Scheme 13) [38, 39]. This gave the experimental proof that decarboxylative cross-couplings are not intrinsically limited to a narrow range of substrates, but indeed held the potential to become a generally applicable technology for regioselective C–C and C–heteroatom bond formation.

8 State of the Art in Decarboxylative Couplings

Since 2006, the efficiency of decarboxylative couplings has steadily been improved, and they are on the way to becoming standard tools for organic synthesis [1–4]. A growing number of researchers have developed a wealth of catalytic transformations starting from carboxylic acids with release of CO_2, providing

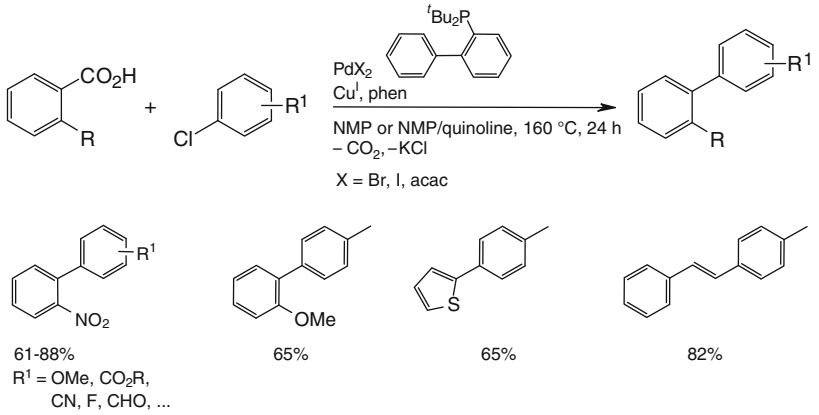

Scheme 14 Decarboxylative couplings of aryl chlorides

new synthetic entries to various valuable product classes. Some of the new decarboxylative couplings seem to have been inspired mainly by the work of Saegusa [8] and Tsuji [9] on decarboxylative allylations [11, 40–45], others by Myers' oxidative Heck reaction [6], and yet others by the redox-neutral cross-coupling processes discussed above. Only a few of them can be introduced here.

The applicability of the decarboxylative biaryl synthesis was rapidly extended to a broad range of aryl electrophiles with the help of new catalyst generations, including not only aryl iodides, bromides, and triflates but also the inexpensive but unreactive aryl chlorides and tosylates [46, 47]. Its preparative utility was demonstrated, e.g., in the synthesis of telmisartan and valsartan [48, 49]. The key factor in these advances was the identification of ligands that strongly activate the palladium catalysts toward oxidative addition steps while not interfering with the decarboxylation activity of the copper cocatalysts (Scheme 14).

Besides bimetallic palladium/copper systems, palladium/silver catalysts have been employed. The silver catalysts allow for lower reaction temperatures than the copper catalysts, but can be used in substoichiometric amounts only in couplings of aryl triflates in combination with certain *ortho*-substituted benzoic acids [50, 51]. The design of low-temperature decarboxylation catalysts was guided by DFT calculations, in which the influence of the central metal and ligand environment on activation energies was systematically studied [52–54]. Calculations revealed that 2-fluorobenzoates of silver or gold should decarboxylate much more easily than the corresponding copper complexes. These findings, which were confirmed in experimental studies, led to the development of a palladium/silver-catalyzed decarboxylative coupling that proceeds already at moderate temperatures (Scheme 15) [55]. This is a good example of how DFT calculations can support rational catalyst development and help to reduce the number of screening experiments needed. In this and several other decarboxylative couplings, microwave heating was demonstrated to have a beneficial effect [76]. Flow reactors have also been shown to be advantageous, as they mimize the exposure of the products to thermal stress [77].

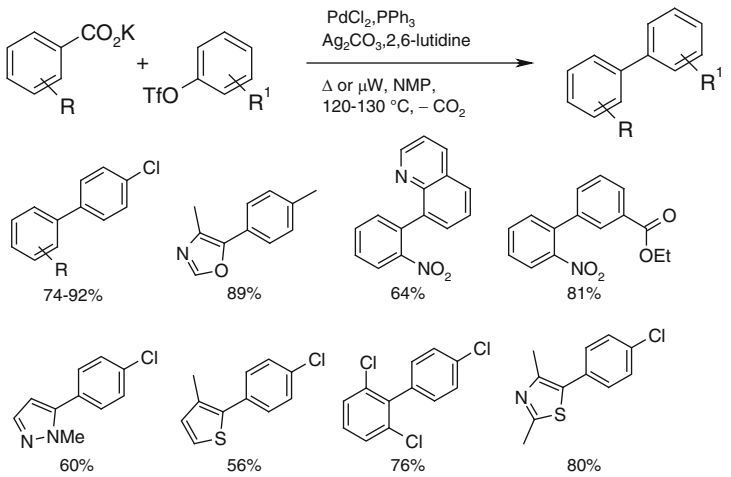

Scheme 15 Ag-/Pd-catalyzed low-temperature decarboxylative biaryl synthesis

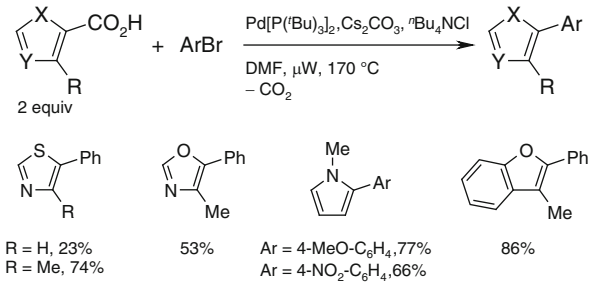

Scheme 16 Arylation of heteroarenecarboxylates catalyzed by monometallic Pd systems

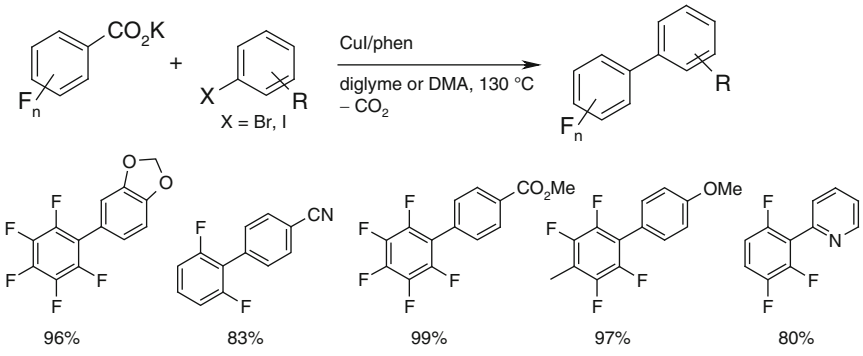

Scheme 17 Decarboxylative cross-couplings mediated by monometallic copper systems

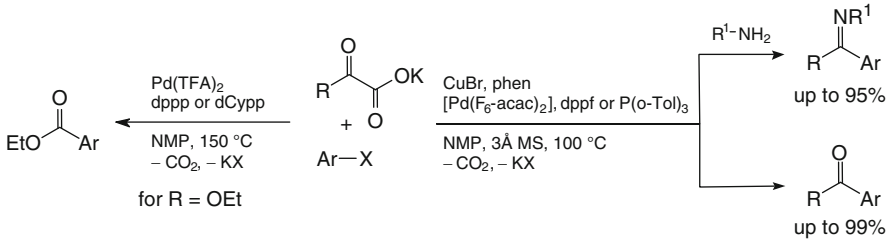

Scheme 18 Decarboxylative couplings of α-oxocarboxylic acid derivatives

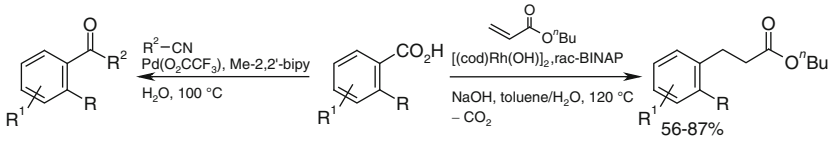

Scheme 19 Decarboxylative conjugate addition reactions

The ability of palladium to mediate decarboxylations of certain heteroaromatic carboxylates was demonstrated by Steglich et al. for intramolecular couplings, as well as by Forgione and Bilodeau for intermolecular couplings (Scheme 16) [56–58]. However, the scope of this reaction indeed seems to be more limited than its bimetallic counterpart. It so far includes mainly five-ring heteroarenes with carboxylate groups in the 2-position. Alkynylcarboxylic acids have also been decarboxylatively coupled with palladium alone [59].

Monometallic copper complexes were also found to mediate decarboxylative couplings, but these reactions have a rather limited scope as well [60]. They are advantageous particularly for the coupling of polyfluorinated benzoic acids with aryl halides (Scheme 17).

The application range of decarboxylative couplings has continuously been extended from aromatic carboxylic acids and β-oxocarboxylic acids to propiolic, phenylacetic, α-oxocarboxylic acids and oxalic acid monoesters [1–4]. The use of α-carbonyl carboxylic acids is particularly surprising as it is counterintuitive that unprotected acyl anion equivalents can be generated by decarboxylation. This allows a polarity reversal of the bond formation of traditional ketone syntheses (Scheme 18, right side, bottom) [61]. In the presence of amines, the corresponding azomethines are formed (Scheme 18, right side, top) [62, 63]. The analogous coupling of oxalic acid monoesters allows the convenient one-step synthesis of benzoate esters from aryl halides (Scheme 18, left side) [64].

The in situ generation of carbon nucleophiles via extrusion of CO_2 from benzoates cannot only be combined with cross-coupling processes but also with 1,2- and 1,4-addition reactions. An example is the rhodium-catalyzed decarboxylative conjugate addition of activated benzoic acids to acrylic esters or amides developed by Zhao et al. (Scheme 19, right side) [65]. A nice application is the decarboxylative addition of aromatic carboxylic acids to nitriles in the presence of

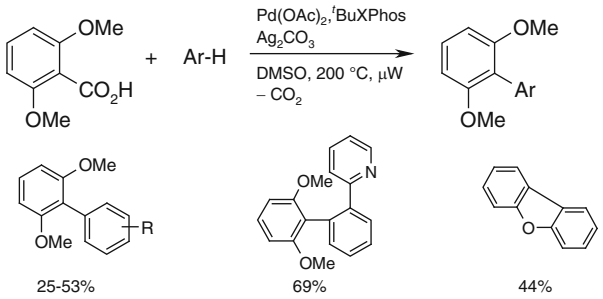

Scheme 20 Decarboxylative coupling with C–H activation

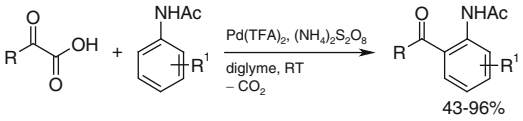

Scheme 21 Decarboxylative *ortho* arylation of acetanilides

a rhodium catalyst by Larhed et al., which proceeds under neutral conditions and allows a novel, waste-minimized synthesis of aryl ketones (Scheme 19, left side) [66].

Myers' oxidative decarboxylative Heck reaction became the prototype for a whole series of regiospecific oxidative couplings in which carboxylic acids adopt the reactivity of aryl electrophiles in the corresponding redox-neutral processes [67–72]. Crabtree et al. developed a process in which arenes react with aromatic carboxylates under C–H activation in the presence of a palladium catalyst and excess silver carbonate to yield biaryls. This reaction is useful especially for intramolecular couplings (Scheme 20) [73, 74]. Recently, a palladium-free, silver-catalyzed radical variant has been disclosed [78].

Under oxidative conditions, α-oxocarboxylic acids seem to decarboxylate at particularly low temperatures. This reactivity was utilized by Fang et al. in palladium-catalyzed decarboxylative α-acylations of acetanilides, which proceed already at room temperature (Scheme 21) [75]. This last example illustrates once again that decarboxylative couplings do not inherently require high temperatures, which nurtures the hope that someday, such low temperatures can be reached also for redox-neutral decarboxylative couplings. Other examples of oxidative decarboxylative couplings are biaryl syntheses starting from boronic esters and carboxylic acids [79], and homo- and heterocouplings of arenecarboxylic acids [80, 81].

Beyond C–C bond forming reactions, decarboxylative couplings have recently found application in regiospecific formations of carbon-halogen [82, 83], carbon-sulfur [84, 85], carbon-phosphorus [86, 87], carbon-nitrogen [88], and carbon-oxygen bonds [89].

9 Conclusion and Outlook

The invention of decarboxylative cross-couplings was driven by a combination of rational catalyst and process design. In addition, it required large numbers of individually planned serial experiments. These reiterative series of parallel reactions were indispensable to generate data points laying the basis for our understanding of how each single component influenced the complex catalyst system. Based on these systematic studies, increasingly effective protocols could be devised. One of the indispensable strikes of luck was a talk on boscalid at a critical moment in time that inspired us to change our model system to a substrate combination, that turned out to be ideal.

The selected examples demonstrate that only few decarboxylative couplings are close to synthetic maturity. Many inventive steps are still required to overcome remaining limitations and to unleash the full potential of this new reaction concept. New decarboxylation catalysts have to be designed that operate at low temperatures and tolerate a broad variety of carboxylic acids. For several decarboxylative reactions, the proof of concept has been achieved only for a very limited scope of substrates. Extending these processes to the full range of carboxylic acids remains a challenging task.

Most importantly, many decarboxylative reactions are still to be invented as a replacement of traditional coupling reactions based on preformed organometallic reagents.

References

1. Rodríguez N, Goossen LJ (2011) Chem Soc Rev 40:5030–5048
2. Gooßen LJ, Collet F, Gooßen K (2010) Isr J Chem 50:617–629
3. Gooßen LJ, Rodríguez N, Gooßen K (2008) Angew Chem Int Ed 47:3100–3120
4. Weaver JD, Recio A III, Grenning AJ, Tunge JA (2011) Chem Rev 111:1846–1913
5. SciFinder search 27 January 2012, catalytic decarboxylative coupling, publication years 2006–2012, duplicates and enzymatic reactions removed
6. Myers AG, Tanaka D, Mannion MR (2002) J Am Chem Soc 124:11250–11251
7. Shimizu I, Yamada T, Tsuji J (1980) Tetrahedron Lett 21:3199–3202
8. Tsuda T, Chujo Y, Nishi S-I, Tawara K, Saegusa T (1980) J Am Chem Soc 102:6381–6384
9. Tsuji J, Yamada T, Minami I, Yuhara M, Nisar M, Shimizu I (1987) J Org Chem 52:2988–2995
10. Nilsson M (1966) Acta Chem Scand 20:423–426
11. Gooßen LJ, Gooßen K, Rodríguez N, Blanchot M, Linder C, Zimmermann B (2008) Pure Appl Chem 80:1725–1731
12. Nilsson M, Ullenius C (1968) Acta Chem Scand 22:1998–2002
13. Shepard AF, Winslow NR, Johnson JR (1930) J Am Chem Soc 52:2083–2090
14. Cairncross A, Roland JR, Henderson RM, Sheppard WF (1970) J Am Chem Soc 92:3187–3189
15. Cohen T, Schambach RA (1970) J Am Chem Soc 92:3189–3190
16. Cohen T, Berninger RW, Wood JT (1978) J Org Chem 43:837–848
17. Appel R, Ruppert I, Knoll F (1972) Chem Ber 105:2492–2507

18. Inoue A, Shinokubo H, Oshima K (2003) J Am Chem Soc 125:1484–1485
19. Gooßen LJ (2001) Chem Commun 7:669–670
20. Gooßen LJ, Ghosh K (2001) Chem Commun 20:2084–2085
21. Gooßen LJ, Paetzold J (2002) Angew Chem 114:1285–1289
22. Gooßen LJ, Paetzold J, Winkel L (2002) Synlett 10:1721–1723
23. Gooßen LJ, Paetzold J (2004) Angew Chem 116:1115–1118
24. Gooßen LJ, Döhring A (2003) Adv Synth Catal 345:943–947
25. Gooßen LJ, Ghosh K (2002) Eur J Org Chem 19:3254–3256
26. Beletskaya IP, Cheprakov AV (2000) Chem Rev 100:3009–3066
27. Grushin VV, Alper H (1995) J Am Chem Soc 117:4305–4315
28. Dickstein JS, Mulrooney CA, O'Brien EM, Morgan BJ, Kozlowski MC (2007) Org Lett 9:2441–2444
29. Hassan J, Sevignon M, Gozzi Cl, Schulz E, Lemaire M (2002) Chem Rev 102:1359–1469
30. BASF SE (2005): Boscalid - a modern fungicide for specialty crops. http://www.basf.com/group/corporate/en/innovations/publications/innovation-award/2005/boscalid. Last accessed on July 11, 2012
31. Kaeding WW, Kerlinger HO, Collins JR (1965) J Org Chem 30:3754–3759
32. Gooßen LJ, Deng G (2006) US Patent application WO002006136135
33. Cotté A, Mueller N, Rodefeld L, Gooßen LJ, Linder C (2008) US Patent application WO002008122555A1
34. Cotté A, Gotta M, Gooßen LJ, Rudolphi F, Oppel C, Rodríguez N (2009) US Patent application EP000002069101
35. Gooßen LJ, Deng G, Levy LM (2006) Science 313:662–664
36. Gooßen LJ, Rodríguez N, Melzer B, Linder C, Deng G, Levy LM (2007) J Am Chem Soc 129:4824–4833
37. Gooßen LJ, Thiel WR, Rodríguez N, Linder C, Melzer B (2007) Adv Synth Catal 349:2241–2246
38. Gooßen LJ, Rodríguez N, Linder C (2008) J Am Chem Soc 130:15248–15249
39. Gooßen LJ, Linder C, Rodríguez N, Lange PP (2009) Chem Eur J 15:9336–9349
40. Tsuda T, Chujo Y, Nishi SI, Tawara K, Saegusa T (2007) J Am Chem Soc 102:6381–6384
41. Mohr JT, Behenna DC, Harned AW, Stoltz BM (2005) Angew Chem Int Ed 44:6924–6927
42. Enquist JA Jr, Stoltz BM (2008) Nature 453:1228–1231
43. Burger EC, Tunge JA (2004) Org Lett 6:4113–4115
44. Burger EC, Tunge JA (2006) J Am Chem Soc 128:10002–10003
45. Waetzig SR, Tunge JA (2007) J Am Chem Soc 129:14860–14861
46. Gooßen LJ, Zimmermann B, Knauber T (2008) Angew Chem Int Ed 47:7103–7106
47. Gooßen LJ, Rodríguez N, Lange PP, Linder C (2010) Angew Chem Int Ed 49:1111–1114
48. Goossen LJ, Knauber T (2008) J Org Chem 73:8631–8634
49. Gooßen LJ, Melzer B (2007) J Org Chem 72:7473–7476
50. Becht J-M, Catala C, Le Drian C, Wagner A (2007) Org Lett 9:1781–1783
51. Becht J-M, Le Drian C (2008) Org Lett 10:3161–3164
52. Gooßen LJ, Linder C, Rodríguez N, Lange PP, Fromm A (2009) Chem Commun 7173–7175
53. Gooßen LJ, Rodríguez N, Linder C, Lange PP, Fromm A (2010) ChemCatChem 2:430–442
54. Sun ZM, Zhang J, Zhao PJ (2010) Org Lett 12:992–995
55. Gooßen LJ, Lange PP, Rodríguez N, Linder C (2010) Chem Eur J 16:3906–3909
56. Peschko C, Winklhofer C, Steglich W (2000) Chem Eur J 6:1147–1152
57. Forgione P, Brochu MC, St-Onge M, Thesen KH, Bailey MD, Bilodeau F (2006) J Am Chem Soc 128:11350–11351
58. Bilodeau F, Brochu MC, Guimond N, Thesen KH, Forgione P (2010) J Org Chem 75:1550–1560
59. Moon J, Jeong M, Nam H, Ju J, Moon JH, Jung HM, Lee S (2008) Org Lett 10:945–948
60. Shang R, Fu Y, Wang Y, Xu Q, Yu HZ, Liu L (2009) Angew Chem Int Ed 48:9350–9354
61. Gooßen LJ, Rudolphi F, Oppel C, Rodríguez N (2008) Angew Chem Int Ed 47:3043–3045

62. Rudolphi F, Song B, Goossen LJ (2011) Adv Synth Catal 353:337–342
63. Collet F, Song B, Rudolphi F, Gooßen LJ (2011) Eur J Org Chem 2011:6486–6501
64. Shang R, Fu Y, Li JB, Zhang SL, Guo QX, Liu L (2009) J Am Chem Soc 131:5738–5739
65. Sun ZM, Zhao PJ (2009) Angew Chem Int Ed 48:6726–6730
66. Lindh J, Sjöberg PJR, Larhed M (2010) Angew Chem Int Ed 49:7733–7737
67. Tanaka D, Meyers AG (2004) Org Lett 6:433–436
68. Tanaka D, Romeril SP, Meyers AG (2005) J Am Chem Soc 127:10323–10333
69. Zhang SL, Fu Y, Shang R, Guo QX, Liu L (2010) J Am Chem Soc 132:638–646
70. Hu P, Kann J, Su W, Hong M (2009) Org Lett 11:2341–2344
71. Fu Z, Huang S, Su W, Hong M (2010) Org Lett 12:4992–4995
72. Gooßen LJ, Zimmermann B, Knauber T (2010) Beilstein J Org Chem 6. doi:10.3762/bjoc.6.43
73. Voutchkova A, Coplin A, Leadbeater NE, Crabtree RH (2008) Chem Commun 6312–6314
74. Wang CY, Piel I, Glorius F (2009) J Am Chem Soc 131:4194–4195
75. Fang P, Li M, Ge H (2010) J Am Chem Soc 132:11898–11899
76. Gooβen LJ, Zimmermann B, Linder C, Rodríguez N, Lange PP, Hartung J (2009) Adv Synth Catal 351:2667–2674
77. Lange PP, Gooβen LJ, Podmore P, Underwood T, Sciammetta N (2011) ChemComm 47:3628–3630
78. Seo S, Slater M, Greaney MF (2012) Org Lett 14:2650–2653
79. Dai JJ, Liu JH, Luo DF, Liu L (2011) ChemComm 47:677–679
80. Cornella J, Lahlai H, Larrosa I (2010) Chem Commun 46:8276–8278
81. Xie K, Wang S, Yang Z, Liu J, Wang A, Li X, Tan Z, Guo CC, Dong W (2011) Eur J Org Chem 2011:5787–5790
82. Kulbitski K, Nisnevich G, Gandelman M (2011) Adv Synth Catal 353:1438–1442
83. Luo Y, Pan X, Wu J (2010) Tetrahedron Lett 51:6646–6648
84. Duan Z, Ranjit S, Zhang P, Liu X (2009) Chem Eur J 15:3666–3669
85. Becht JM, Le Drian C (2011) J Org Chem 76:6327–6330
86. Hu J, Zhao N, Yang B, Wang G, Guo LN, Liang YM, Yang SD (2011) Chem Eur J 17:5516–5521
87. Yang D, Zhao D, Mao L, Wang L, Wang R (2011) J Org Chem 76:6426–6431
88. Jia W, Jiao N, (2010) Org Lett 12:2000–2003
89. Bhadra S, Dzik WI, Gooβen LJ (2012) 134:9938–9941

Top Organomet Chem (2013) 44: 143–164
DOI: 10.1007/3418_2012_45

Published online: 1 August 2012

Gold-Catalyzed Organic Reactions

A. Stephen K. Hashmi

Abstract Although homogeneous gold catalysis was known previously, an exponential growth was only induced 12 years ago. The key findings which induce that rise of the field are discussed. This includes early reactions of allenes and furanynes and intermediates of these conversions as well as hydroarylation reactions. Other substrate types addressed are alkynyl epoxides and *N*-propargyl carboxamides. Important vinylgold intermediates, the transmetalation from gold to other transition metals, the development of new ligands for gold catalysis, and significant contributions from computational chemistry are other crucial points for the field highlighted here.

Keywords Catalysis · Cycloisomerization · Gold · Heterocycles · Intermediates · Ligands · Proton transfer · Transmetalation · Vinylidene

Contents

A.S.K. Hashmi (✉)
Organisch-Chemisches Institut, Ruprecht-Karls Universität Heidelberg, Im Neuenheimer Feld 270, 69120 Heidelberg, Germany
e-mail: hashmi@hashmi.de

Abbreviations

ICP	Inductively coupled plasma
IPr	*N*,*N*′-Bis-[2,6-(di-isopropyl)phenyl]imidazol-2-ylidene
KITPHOS	11-Dicyclohexylphosphino-12-phenyl-9,10-ethenoanthracene
LUMO	Lowest unoccupied molecular orbital
Me	Methyl
Mes	Mesityl
NAC	Nitrogen-acyclic carbene
NHC	Nitrogen-heterocyclic carbene
NHOC	Nitrogen-heterocyclic oxo-carbenes
Ph	Phenyl
RT	Room temperature
$S_{E'}$	Electrophilic substitution with rearrangement
Tf	Trifluoromethylsulfonyl
THT	Tetrahydrothiophene

1 Introduction

Prior to the year 2000, homogeneous gold catalysis was not considered to be a versatile tool for organic synthesis. Although there existed scattered and singular reports on catalytic activity [1–4], only two reactions had been explored with regard to their potential for synthesis. The first reaction is the Ito–Sawamura–Hayashi asymmetric aldol reaction [5, 6], which, although being the first catalytic asymmetric aldol reaction, was mainly investigated by the groups of Yoshihiko Ito and Antonio Togni in a series of about 35 publications between 1986 and 1998 [7]. The second reaction is the addition of amines, alcohols, or water to alkynes [8]; this was explored in overall only four publications and one patent by K. Utimoto and H. Teles between 1989 and 1998 [8–13].

The reactivity patterns of these two reaction types, the formation of C–C and/or of C–heteroatom bonds and the activation of C–C multiple bonds or C–heteroatom multiple bonds, are central to the field. But subsequently, more unique reactivity patterns have been added to the arsenal of homogeneous gold catalysis.

After the last report in 1998, the activity in this field had ceased, and the subject was endangered to fall into oblivion.

2 Entry to Gold Catalysis and Demonstrating the Potential for Complex Organic Transformations

The initiation of the current "gold rush" in homogeneous catalysis in fact began in 1997, when I was working as a habilitand (assistant professor) at the Johann Wolfgang Goethe Universität in Frankfurt. My group (two coworkers and myself) was working on the chemistry of chiral organopalladium compounds [14–17] as well as catalytic transformations of allenes by palladium and other transition metals [18–22]. In the context of this research project, different selectivities were observed with Ag(I) catalysts (d^{10} configuration) and Pd(II) catalysts (d^8 configuration). Thus, I wanted to investigate the selectivity with a catalyst combining both properties, like silver being an element of the group 11 and like palladium(II) possessing a d^8 configuration. Since the stability of the higher oxidation state of a transition metal increases when going to the heavier transition metals, I considered gold(III) to be the ideal candidate. In the catalogues of the fine chemical suppliers, I discovered that gold(III) chloride was commercially available. I ordered it, tested it, and observed an entirely different selectivity, which was highly interesting. As during my study of chemistry, I had never heard about gold-catalyzed reactions, and after these initial experiments, I immediately looked up what was known in the literature about gold catalysis, just finding the references discussed above in the Introduction.

These first experiments were performed at a time when my habilitation was coming to an end, which would automatically terminate my DFG fellowship for the habilitation. One of the few opportunities to obtain further funding was the Heisenberg fellowship. Thus, I wrote my Heisenberg proposal on homogeneous gold catalysis (basing on the little literature evidence and our few preliminary results). Obviously, the referees considered this proposal innovative, and I obtained the funding (our first child was born during that time, which automatically makes you less ready to take any risks – I still remember very well how at the age of 35 I opened the letter from the DFG with trembling hands . . .).

After that, one of my two coworkers and I worked on the results for the first two publications. During that time, a crucial emphasis was on control experiments. Was it really the gold? Was there something else initiating the same conversion? We spent a lot of time with uncounted control experiments with other transition metals, other Lewis or Bronsted acids or bases, photochemical activation, thermal activation, high-pressure experiments, electrochemical experiments, and electron transfer reagents as well as combinations of these methods. At the end, it was clear that the gold was responsible for the catalysis, and in 2000, our first two publications on two different substrate types and two different reactions appeared [23, 24].

Even from today's perspective, it is interesting to see how many different reaction types of homogeneous gold catalysis, which still are a topic in latest investigations, are already described in these two publications. In addition, the reactions readily proceeded at room temperature, and neither water nor oxygen had to be excluded – two more principles reported for most of the reactions that followed. The first

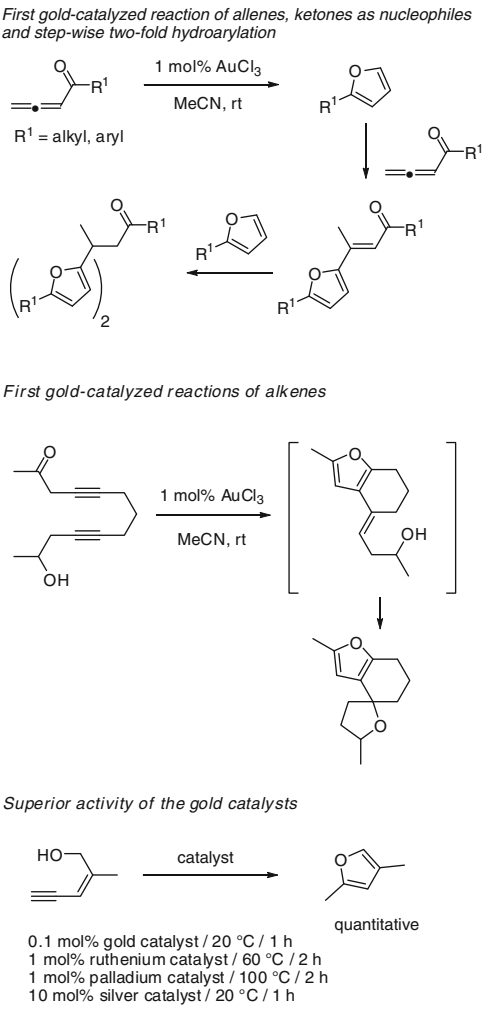

Scheme 1 New observations reported in our first communication

communication [23] now has been cited more than 425 times, a number which is remarkable for one reason: One must keep in mind that for the first 4–5 years there was only a very limited number of people working in the field, and thus the number of publications potentially citing this paper was small. High citation numbers were observed from 2006 onward. This first communication (Scheme 1) covers the first report on the use of allenes in homogeneous gold catalysis. A cycloisomerization using a ketone as a weak nucleophile as well as a subsequent single and a twofold hydroarylation of allenyl ketones was published; the chemo-selectivity differs from the related palladium-catalyzed conversions. Furthermore, that publication includes the observation of a gold-catalyzed nucleophilic addition to an alkene intermediate. Previously, only strongly activated alkenes, namely, enol ethers, were known to react with such nucleophiles in the presence of gold catalysts. And the superiority to other catalysts used at that time was demonstrated too.

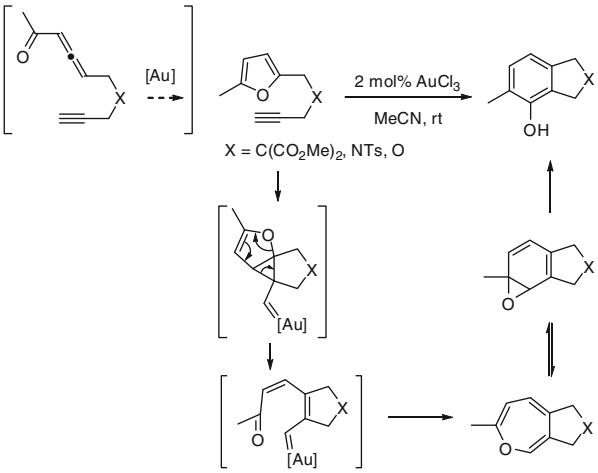

Scheme 2 New reactivity patterns in our second communication

The second communication of that year [24] is now cited more than 225 times, which also represents a remarkable number. This communication also comprised new reactivity patterns (Scheme 2). Based on the results from the first communication discussed above, a furan ring is formed from an allenyl ketone. Then the furanyne intermediate underwent a previously unknown transformation to an annelated phenol. Since they are easily accessible, furanynes can also be used directly.

When we published that paper, we had no direct evidence on the mechanism and thus suggested a simple mechanism which was based on classical reactivity and would explain the product formation and at the same time not upset the referees. Still, the initial referee reports on that manuscript all were very negative (e.g., "... scope of the reaction is very narrow ..."), and I had to appeal against the initial rejection in order to finally get the manuscript into the journal. Nowadays, most of my manuscripts are directly rejected by the editors of that journal. Amazingly, the quality of my science seems to have eroded so much that I have not been able to place a single publication in that journal for more than 11 years since the submission of the manuscript discussed here.

In the following year Antonio Echavarren reported side products for the analogue platinum-catalyzed reaction and, supported by results from computational chemistry, suggested cyclopropyl carbenoid and vinylcarbenoid intermediates [25, 26]. Later we succeeded in isolating similar side products from gold-catalyzed reactions too [27]. The next intermediates of the catalytic cycle are oxepines and arene oxides, as we could show by in situ spectroscopy and trapping reactions [28, 29]; for a summary of the mechanism, see [30]. The further development of this interesting reaction included the use in a small total synthesis [31], the use of very bulky substrates [32], efforts for an intermolecular version [33], domino reactions [34, 35], stereoselective reactions [36, 37], and even the application of heterogeneous catalysts [38]. The overall very intense and detailed study of this transformation, which is a special variation of the enyne cycloisomerization, has resulted in this reaction now being called "Hashmi phenol synthesis" [39–41].

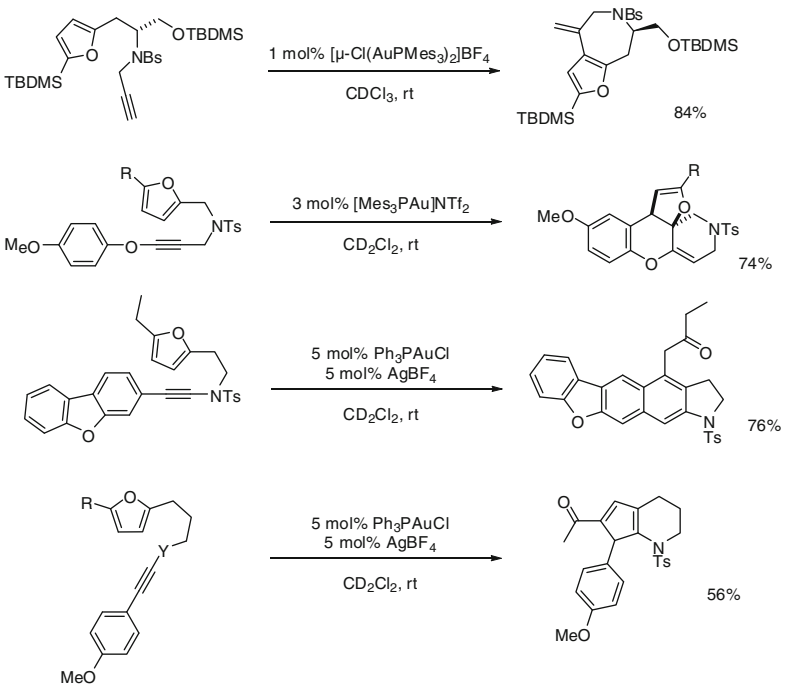

Scheme 3 Modifications in the substrates open new reaction pathways

As we now had a detailed picture of the mechanism, it was possible to design a number of new reaction pathways for furanyne substrates, which in a predictable way led to other products. Each of the examples in Scheme 3 represents a whole family of transformations.

In some of these new reactions, a significant increase of molecular complexity could be observed; the furanynes delivered polycyclic anellated heterocyclic product [42, 43]. The educts for these reactions are easily accessible, and the products would be difficult to synthesize by traditional heterocycle synthesis basing on classical condensation chemistry. In every case, it is possible to rationalize how the addition of functional groups in the substrate induces a switch in the reaction pathway [44].

A recent finding in the field of furanyne cycloisomerization was the synthesis of benzofurans with aryl substituents on 7-position (Scheme 4). These are difficult to access by other methods, but again are conveniently available from simple starting materials by gold catalysis [45]. The most interesting feature of this conversion is the migration of the tether, placing the aryl group in 7- rather than in 4-position.

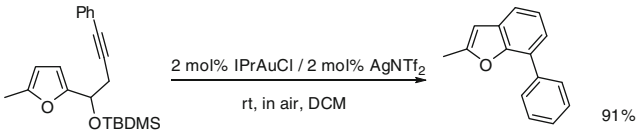

Scheme 4 An easy entry to 7-arylbenzofuran

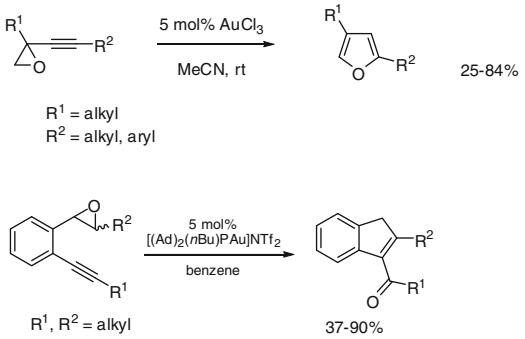

Scheme 5 Ring expansion and anellation chemistry by gold-catalyzed conversions of epoxides

3 The Next Steps

In 2000, only two other publications concerning homogeneous gold catalysis appeared (one entry in a table in [46, 47]), one of them with gold in a single entry in one table (one entry in a table in [46]). But it did not take long until the first competitors entered the field. They mainly focused on the gold-catalyzed enyne cycloisomerization [48–50]. Since they had been working on the enyne cycloisomerization with other transition metals for years and a broad range of substrates waiting in their freezers, we did not even try to compete in this field.

Instead, after an intermezzo on hydroarylation chemistry [51, 52] which at the same time was intensively investigated by a number of other groups [50, 53], we turned to strained substrates, alkynyl epoxides (Scheme 5) [54]. In this case the epoxide oxygen atom serves as an intramolecular nucleophile ring opening, and elimination then delivers furans. Another type of epoxides, the *o*-alkynylphenyl epoxides, yields acylindenes [55]. Again, gold carbenoids are involved, as was proven by parallel work of Rai-Shung Liu [56].

4 Reactions of Amides

In addition to the enyne cycloisomerization, the reactivity patterns of propargylic esters were investigated intensively [57], which were based on early work of Uemura for other metals [58, 59]. Thus, we chose propargylic amides as substrates,

Scheme 6 Synthesis of *N*,*O*-heterocycles from amides

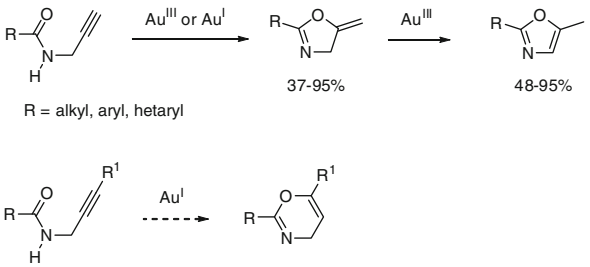

which as expected entered an entirely different reaction pathway (Scheme 6). As with the esters, a 5-*exo-dig* cyclization is observed in the initial step. But then, different from the situation in propargylic esters, the proton on nitrogen can be eliminated. The five-membered alkylideneoxazoline ring remains intact; in the case of gold(I), indeed, the elusive alkylideneoxazolines could be isolated in excellent yields [60, 61]. On the other hand, with gold(III) catalysts, the reactions proceed to the thermodynamic stabilomer, the aromatic oxazole ring [62].

By isotopic labeling studies, we could show that the initial step is an *anti*-oxyauration, followed by a stereoselective protodeauration.

This principle was very important for the synthesis of a diverse range of heterocycles and has been used by other groups too. Placing the alkyne at a different distance is also possible [63]. With a substituent on nitrogen, the elimination of the proton is not possible; in this case, water is not innocent anymore. A hydrolysis of the intermediate iminium salt delivers allylic amines with acyloxy groups on the central position of the allyl substituent [64].

Internal propargylic amides show a different regioselectivity, and a 6-*endo-dig* cyclization leading to oxazines is observed, too [65]. A completely selective conversion to the oxazines can be achieved when allenes instead of alkynes are used as substrates [66]. In this reaction it could be shown that σ-allylgold(I) intermediates are involved, and the π-allyl species is a transition state of the 1,3-metallotropic shift. Isotope-labeling studies indicated that the protodeauration proceeds by an $S_{E'}$ pathway with rearrangement of the allylic system from the more stable σ-allylgold(I) species with gold on the exocyclic position to the oxazine with the deuterium label on the endocyclic position of the allyl moiety.

5 Isolation of Vinylgold Intermediates

The use of internal propargylamides also allowed the first isolation of stable vinylgold intermediates derived from alkynes [67]. The simple trick of capturing the proton, which would decompose the vinylgold species by protodeauration, by a simple base as triethylamine, worked beautifully (Scheme 7). This principle could be extended to other reaction types as hydroalkoxylation and hydroaminations [68].

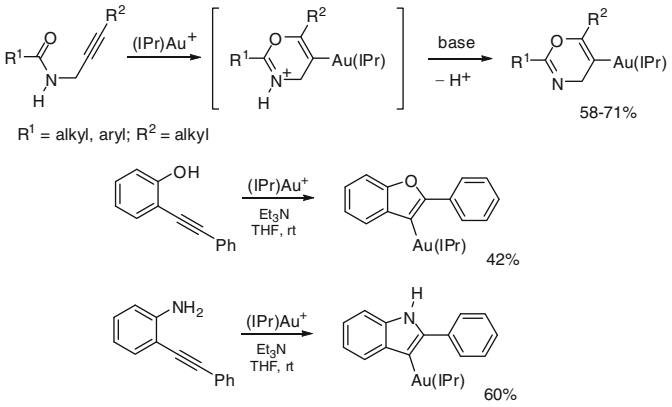

Scheme 7 NHC complexes of vinylgold(I) compound

With a gold(I) hydroxy complex, a species recently introduced by Nolan et al., we could achieve a regioselectivity switch once more [69]. The hydroxide immediately deprotonates the amide, then the corresponding anion undergoes the cyclization, which changes the interactions in the transition state, and the 5-*exo-dig* mode dominates again.

6 C–C Bond Formation Induced by Sources of Electrophilic Fluorine

When studying gold-catalyzed cyclizations of allenyl ketones, we observed C–C bond formation initiated by Au(III). This C–C bond formation was detected as a side product only, and the amount matched and increased with the amount of gold(III) used as the catalyst, indicating a process that is stoichiometric in gold, reducing gold(III) to gold(I) (Scheme 8). The latter then still is a cycloisomerization catalyst, but fails to induce C–C bond formation [70].

Then, we studied the reactivity of different organogold complexes with electrophiles. While with H^+ (D^+), I^+, Br^+, and Cl^+ donors always a formation of a bond between carbon and these electrophiles was observed, with F^+ donors, always a C–C bond formation was induced, in this case a homodimerization (Scheme 9) [71]; for a detailed full paper on this chemistry, see [72].

Soon after our publication on this new reactivity pattern, beautiful work of Liming Zhang et al. extended the scope to catalytic heterocouplings by using an unsaturated substrate for gold-catalyzed cycloisomerization, one equivalent of a boronic acid as the coupling partner and Selectfluor as the F^+-donor [73]. As immediately many people joined that area [74], we did not proceed here but decided to explore the use of other electrophiles like palladium(II) that would potentially also allow C–C bond formation but not require stoichiometric amounts of F^+ donors.

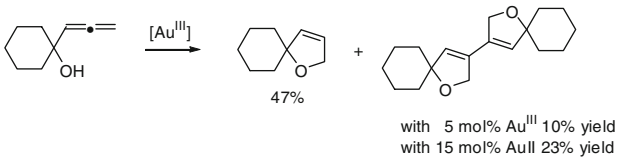

Scheme 8 C–C bond formation in an oxidative dimerization induced by gold(III)

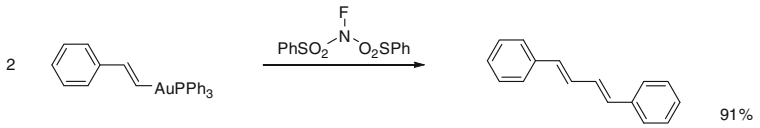

Scheme 9 A new reactivity pattern – F^+-induced C–C bond formation in stoichiometric reactions of organogold(I) compounds

7 Gold-Catalyzed Cross Coupling?

One vision to achieve a C–C bond formation by cross coupling involving gold was the option to use organopalladium(II) species as electrophiles (Scheme 10). The latter, like in any palladium-catalyzed cross coupling, would originate from oxidative addition to palladium(0). The organogold species could be the intermediate of a gold-catalyzed reaction. Thus, the precious (functionalized) organogold intermediate would be used for the formation of a new C–C bond rather than being wasted to a simple proton for the formation of a C–H bond. Initial efforts to achieve this with catalytic amounts of both metals failed. Since we knew that each individual catalytic cycle involving the two metals works perfectly, we assumed that the new step, the transmetalation from gold to palladium, represented the problem. In order to investigate this new step in more detail, we conducted these palladium-catalyzed cross couplings with stoichiometric amounts of various organogold compounds [75, 76]. This worked perfectly; vinyl, aryl, hetaryl and alkynyl gold(I) compounds and aryl iodides, activated aryl bromides, and acid chlorides gave the corresponding cross coupling products.

The problem was the halide anion resulting from the aryl halide partner – it blocked the gold(I) center by coordination; no further gold-catalysis was possible. One way to avoid this is the use of reagents for the oxidative addition not based on halogens as leaving group.

Aryl triflates failed in our hands, but there is a report on the coupling of aryl triflate which we cannot confirm to proceed without deactivation of the gold catalyst [77]. Suzanne Blum et al. published a wonderful reaction using gold and palladium complexes in catalytic amounts and allylic esters as nucleophilic groups – at a time when we were investigating exactly these substrates too. This was painful for us. But in addition, we did not share their point of view; carefully designed control experiments revealed that in these reactions, only the unsubstituted allyl group indeed needed both gold and palladium for the couplings (Scheme 11) [78].

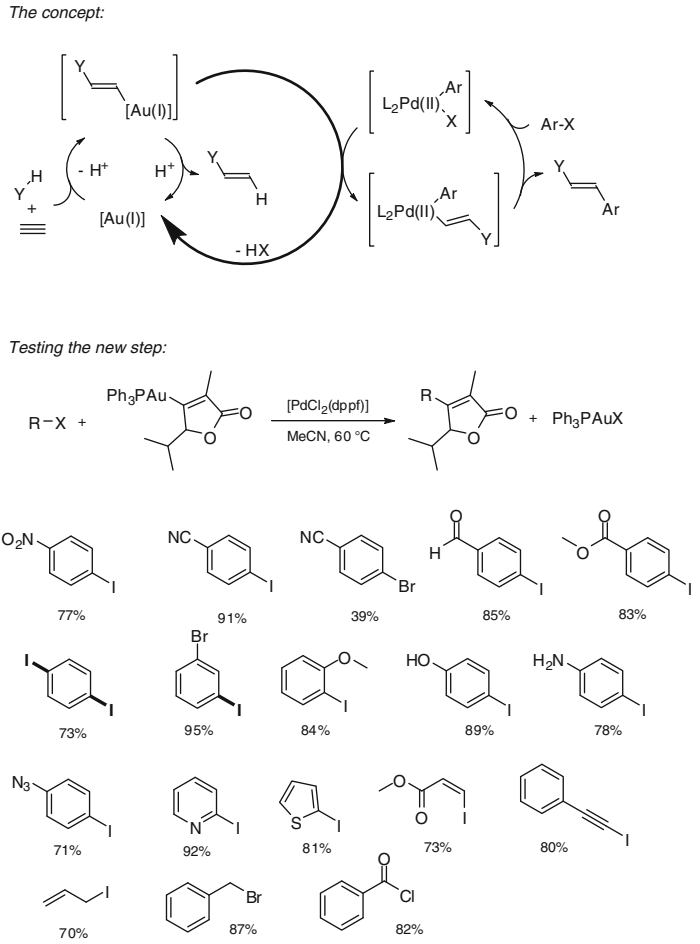

Scheme 10 A new step had to be explored: palladium-catalyzed cross coupling of organogold(I) complexes

With the electron-poor allenic esters, palladium(0) is able to catalyze the reaction without gold. The reaction then is initiated at the other end, after oxidative addition of the aryl halide to the electrophilic palladium(II) species cycloisomerizes the allenic ester and then forms the product by reductive elimination. With *o*-alkynylbenzoates, the intermediate vinylgold species contains an enol ether substructure and is able to directly intercept the activated allyl donors, even in the absence of palladium. In both cases, by careful trace analysis (ICP), the presence of the other metal was excluded [78].

With this investigation, we could also contribute to the discussion whether gold complexes are able to catalyze cross coupling like the Suzuki or the Sonogashira coupling. Initial work of Corma et al. [79–81] on this subject could not be

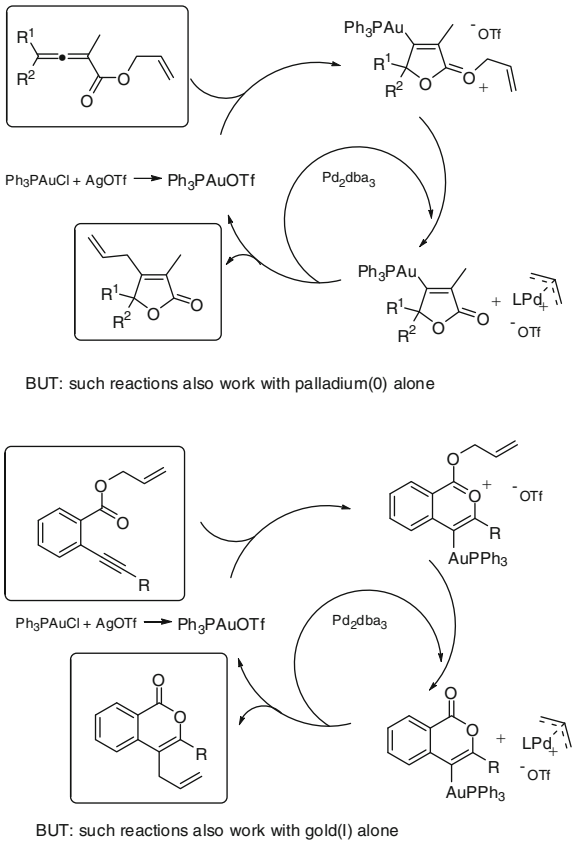

Scheme 11 Investigations on gold/palladium bimetallic catalysis

confirmed by Echavarren et al. [82] in a detailed subsequent investigation. For the subsequent proof that heterogeneous gold catalysts are responsible for the cross coupling, see [83]. While control experiments from our work from Scheme 10 [75, 76] in principle already excluded a direct cross coupling by gold only, in our investigation, we prepared specific substrates like the vinylgold(I) complex shown in Scheme 12. The latter carries both a two-coordinated d^{10} organogold(I) center and an aryl iodide in a distance which conveniently would allow an oxidative addition to gold, but this is not observed, and the compound is stable. This nicely documents the *orthogonality* of gold and palladium complexes, which with regard to organometallic catalysis tolerate different functional groups.

Since iron-catalyzed cross coupling also is a hot topic, we investigated the transmetalation from gold(I) to iron or ruthenium, which proceeded readily (Scheme 13) [84].

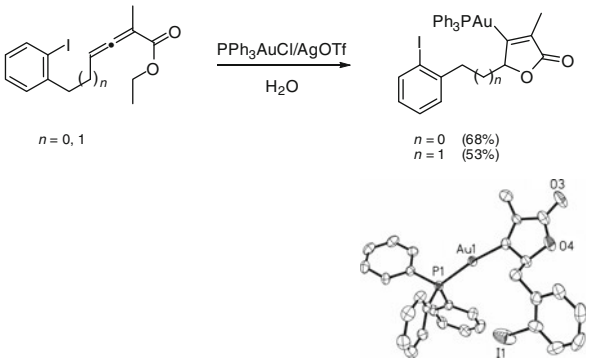

Scheme 12 Not even an intramolecular oxidative addition of an aryl iodide to gold(I) is observed

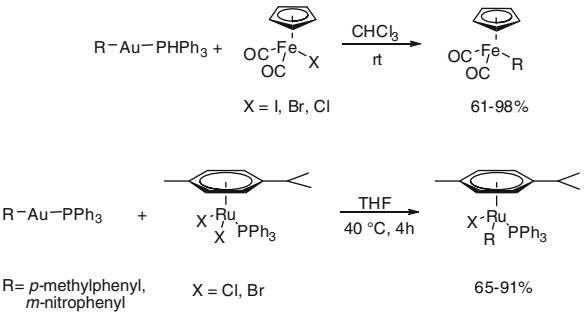

Scheme 13 Even the transmetalation from gold to iron or ruthenium is possible

8 Ligand Design

With regard to the turnover numbers, in our initial publications, we had started from 5 to 2 mol% of catalyst, which corresponded to 20–50 turnovers. For the gold-catalyzed phenol synthesis, we then could reach up to 1,180 turnovers (0.07 mol% of catalyst) with pyridine complexes of gold(III) (one of these complexes recently even became commercially available, Scheme 14) [85]. Later, we could also use pyridine–gold(III) complexes as catalyst in homogeneous gold-catalyzed oxidative esterification reactions [86]. A next step forward was the use of the KITPHOS ligand family [87–89], which previously had been used in palladium catalysis. The use of phosphane and NHC ligands with ancillary pyridyl groups on gold(I) gave no superior results [90, 91]. The same is true for some water-soluble complexes prepared [92]. Finally, one of the most successful ligand systems for gold(I) catalysts was obtained by a very simple one-step route to carbene complexes. Mixing (tht)AuCl, an isonitrile and a primary or secondary amine, directly gave the gold(I) nitrogen-acyclic carbene (NAC) complexes, which in the gold-catalyzed phenol synthesis allowed a turnover number of 3,050 [93]. This method of catalyst

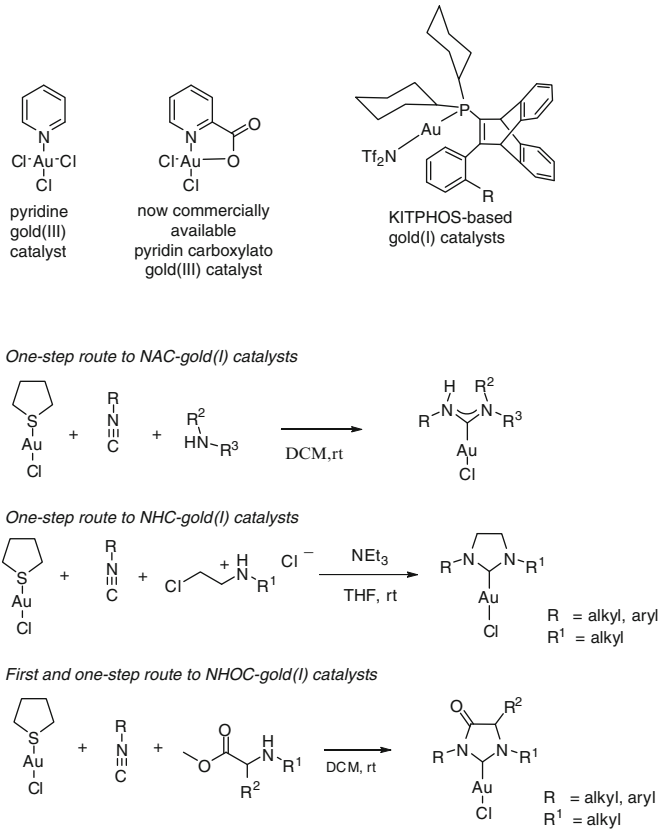

Scheme 14 Successful ligands developed for gold catalysis

preparation could even be extended to nitrogen-heterocyclic carbene (NHC) complexes by using amines with leaving groups in β-position [94] or the previously unknown nitrogen-heterocyclic oxo-carbenes (NHOC) complexes of gold by using α-amino acid esters [95]. The synthetic potential of the latter is currently explored.

9 Input from Theory

Some central questions of the field could only be answered by computational chemistry. Often, the superior reactivity of gold was globally explained by "relativistic effects," which per se is not a good argument. Platinum has 80% of the relativistic effects of gold, and thus it should show 80% of the catalytic activity. But the observed rate differences can be 1,000 and more as described in Fig. 5 of

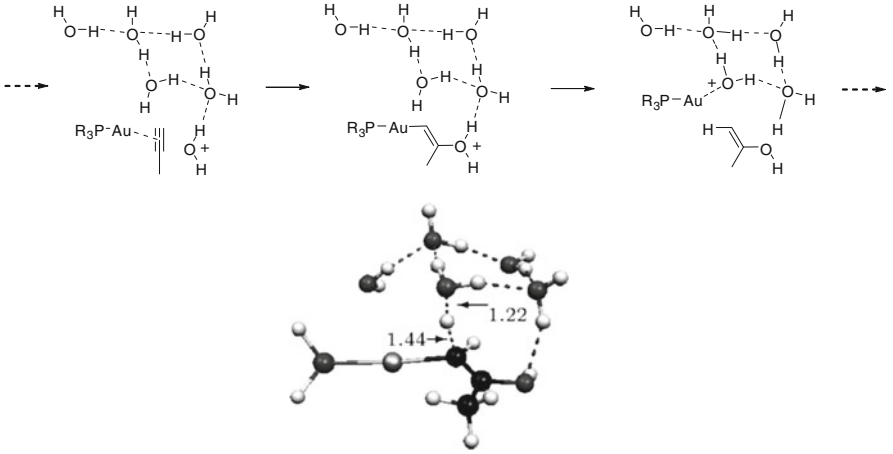

Scheme 15 Water as efficient proton shuttle in the protodeauration step

[85] and early test described in Hashmi [96]. A close (fully relativistic) analysis of the frontier orbitals of platinum and gold complexes of propyne revealed significant differences in the LUMO energies, the orbitals which are crucial for the reaction with nucleophiles, and thus explain the rate differences [97, 98]. Another critical point was the protodeauration, the final step in most gold-catalyzed conversions. Whenever there is a larger geometrical distance between the initial position of the proton (usually on the incoming nucleophile) and the gold–carbon bond, a proton shuttle is needed. By reinvestigating the gold-catalyzed addition of water and methanol to propyne, we could show that the initial assumption of a *syn*-oxyauration was an artifact of a gas phase calculation, and the *anti*-oxyauration has the lower barrier of activation when the role of the solvent is included. In addition, small water clusters play a crucial role as proton shuttles and lowering the barrier of activation enormously (Scheme 15) [99].

10 A New Horizon: Gold Vinylidenes

While preparing this chapter, an important new reactivity pattern in gold catalysis was discovered. In the reaction of arene-1,2-diynes in addition to the expected product, an α-phenylnaphthalene, the completely unexpected β-phenylnaphthalene was observed too (Scheme 16).

An in-depth mechanistic study of the reason for this divergent conversion revealed three important facts: (1) While the expected product was formed by a kind of "classical" activation of the alkyne by the gold catalyst, the unexpected product originated from a *dual activation*, that is, the initial formation of a gold acetylide and a subsequent activation of the other alkynyl group by a gold catalyst. (2) The best

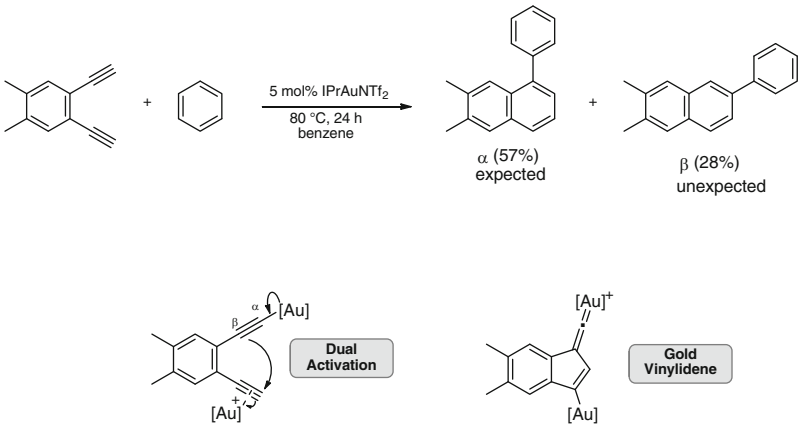

Scheme 16 An unexpected product as the key for a new reactivity pattern and new intermediates

explanation for the switch in selectivity was a change of the regioselectivity of the initial cyclization, a change which was based on a change in polarization by formation of the gold acetylide. This will deliver a *gold vinylidene* intermediate. (3) For an efficient catalytic cycle, the *catalyst transfer* is crucial, and the arylgold species formed at the end of the reaction must directly react with the terminal alkyne in the substrate to deliver the product and the gold acetylide.

We submitted these findings to an important journal, but once more it was rejected without refereeing. We then submitted to Organometallics, and the referees asked for some changes and a revision.

In the meantime, we had found two additional reactions which more directly indicated the involvement of gold vinylidene species, the formation of benzofulvenes by activation of an alkyl C–H bond by this new intermediate (Scheme 17) and the formation of dibenzopentalenes by electrophilic attack at an aryl group (Scheme 18). In both cases, the aurated and the *gem*-diaurated organometallic species could be isolated and characterized by X-ray crystal structure analyses. And it could be shown that the *gem*-diaurate species are ideal *"instant dual activation precatalysts"* for this new type of reaction, immediately providing an ideal 1:1 ratio of both the cationic LAu^+ species and the species for the catalyst transfer to the gold acetylide, two species needed for the dual activation process (Scheme 17).

In December 2011, while we were finalizing the revision of the Organometallics manuscript and at the same time were writing up the other two manuscripts, I was in Australia in the context of a DAAD project with the University of Queensland in Brisbane. In the middle of the night in my hotel room, I received an e-mail of my coworker Ingo Braun, alerting me about a beautiful paper by the group of Liming Zhang on exactly the benzofulvene synthesis we were writing up. On that day, that competing paper [100] had appeared in the "just accepted" section of the journal which had rejected our paper without refereeing. Stimulated by that shock, we immediately submitted our revision of the Organometallics manuscript, and we

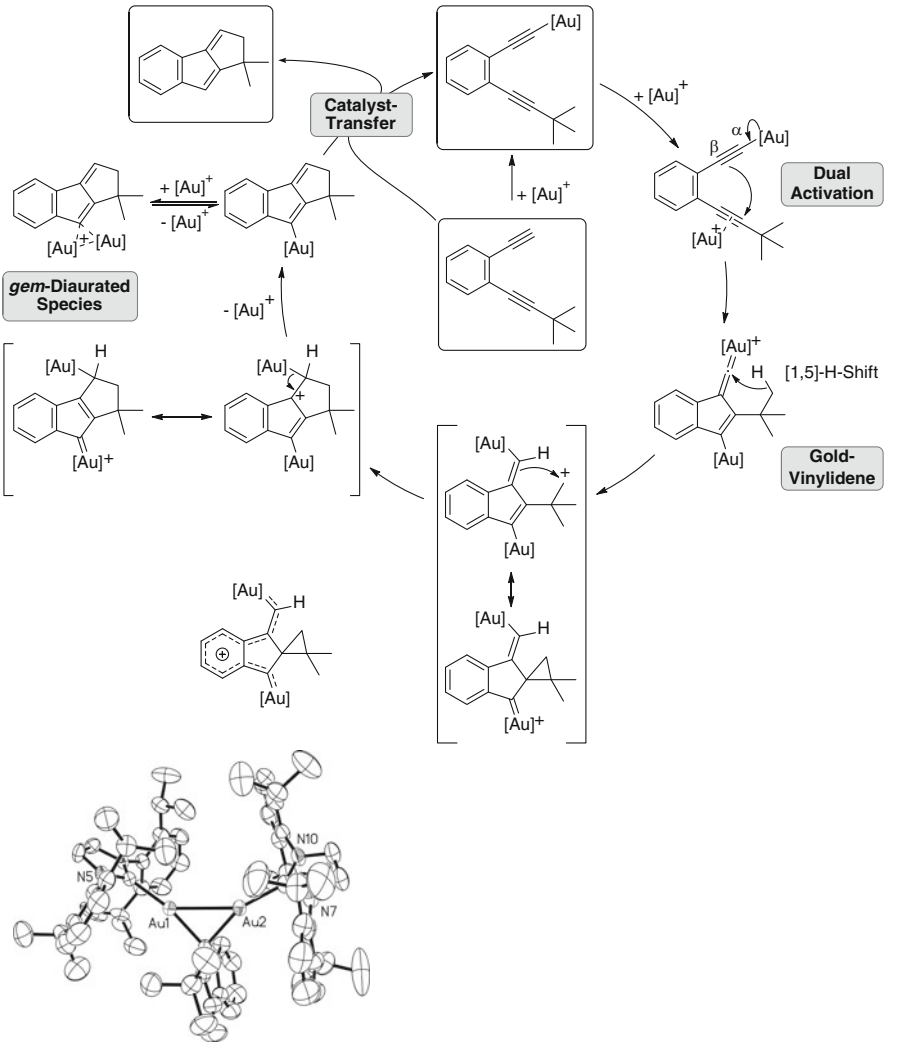

Scheme 17 The benzofulvene products more directly reflect the gold vinylidene intermediate. The *gem*-diaurated species as an "*instant dual activation precatalyst*" shows three times the activity of other gold catalysts

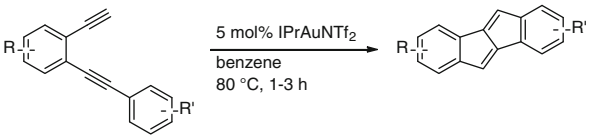

Scheme 18 The dibenzopentalene products also are good indicators for a gold vinylidene intermediate

were delighted that it was accepted the next day [101]. Then, we submitted our two other manuscripts; the benzofulvene synthesis was accepted in Angewandte Chemie [102] and the dibenzopentalene synthesis in Advanced Synthesis and Catalysis [103].

As the highly interesting intramolecular C–H activation of an alkyl C–H bond already indicated, the gold vinylidene intermediates show interesting new reactivity patterns, and certainly in the close future this will emerge as an entirely new and highly innovative sector of homogeneous gold catalysis.

11 Critical Comments

Looking back at the literature published in the last 11 years, there are numerous reactions which without any doubt work with gold catalysts – but are not dependent on gold catalysts. Other Lewis or Bronsted acids might catalyze these reactions too, maybe even with similar reaction rates and selectivities. Under the impression of a specific type of reaction being published as gold catalyzed, we finally published our own findings and control experiments [104]. As the control experiments clearly had shown that the reaction is catalyzed by protons, we previously had never intended to publish these results (which we had in our drawer for about 5 years).

One should never forget that the LAu^+ group is isolobal to a proton [105]. Once more, I would like to remind the people in the field that control experiments with Bronsted acids and hard and soft Lewis acids are compulsory. Not including them might lead to unpleasant surprises later . . .

12 Conclusion and Outlook

The exponential growth of homogeneous gold catalysis is based on two publications from 2000 which really provided momentum for the field. It is a pleasure for me to witness that 11 years later in almost every issue of every journal covering homogeneous catalysis, one can find at least one publication on homogeneous gold catalysis. For 2011, overall, we will probably see more than two publications in average for every working day of the year. Even more fascinating is the creativity of all the people working in the field; not only more publications are produced, but continuously new and previously unknown reactivity patterns are observed and used in synthesis. In 2000, homogeneous gold catalysis was the little brother of heterogeneous gold catalysis, but this also has changed, and now with regard to the number of yearly publications and citations, they have become equally strong.

I want to mention that gold catalysis also has experienced criticism, for example, in the years after I started, statements like *". . . I find it surprising and depressing that so few of them pursue lines of research which could eventually be useful to*

mankind. For instance, gold has recently become a fashionable element for catalyst researchers. Catalysis using gold has hitherto been neglected, so it is not difficult to make new discoveries here. But the chances of gold catalysts being as successful as, for example, the Wilkinson catalysts, are remote. . . .” [106] (there is a whole series of interesting comments to gold catalysis by this editor, with fascinating titles like *“Affordability Matters Too”*, [107] *“Let Them Eat Cake”*, [108] and *“This Precious Bane”* [109]), and “. . . he expressed the opinion that it (gold) was just platinum chemistry in disguise. Then he surprised me by saying *‘But we need gold chemistry, because we’re going to run out of platinum in a few years time”*, [110]. But in spite of these comments, the field is prospering.

So far, the focus has been on academic research, and there in addition to the vast work on methodology in the past years, an increasing number of applications in total synthesis were reported. The next important step will be the implementation of an industrial application, either in bulk or fine chemical production. From the increasing number of invitations from pharmaceutical companies in the last 2 years and very specific questions during these visits, I can only guess that at least for fine chemicals these applications are at the gates or already exist.

References

1. Schwemberger W, Gordon W (1935) Chem Zentralbl 106:514
2. Gassman PG, Meyer GR, Williams FJ (1972) J Am Chem Soc 94:7741–7748
3. Meyer LU, de Meijere A (1976) Tetrahedron Lett 497–500
4. Gasparrini F, Giovannoli M, Misiti D, Natile G, Palmieri G (1983) Tetrahedron 39:3181–3184
5. Ito Y, Sawamura M, Hayashi T (1986) J Am Chem Soc 108:6405–6406
6. Togni A, Pastor SD (1990) J Org Chem 55:1649–1664
7. Sawamura M, Ito Y (2000) In: Ojima I (ed) Catalytic asymmetric synthesis. Wiley-VCH, Weinheim, pp 493–512
8. Fukuda Y, Utimoto K, Nozaki H (1987) Heterocycles 25:297–300
9. Fukuda Y, Utimoto K (1991) Synthesis 975–978
10. Fukuda Y, Utimoto K (1991) J Org Chem 56:3729–3731
11. Fukuda Y, Utimoto K (1991) Bull Chem Soc Jpn 64:2013–2015
12. Teles JH, Schulz M (1997) (BASF AG), WO-A1 9721648 [Chem. Abstr. 127 (1997) 121499]
13. Teles JH, Brode S, Chabanas M (1998) Angew Chem 110:1475–1478; Angew Chem Int Ed 37:1415–1418
14. Hashmi ASK, Naumann F, Probst R, Bats JW (1997) Angew Chem 109:127–130; Angew Chem Int Ed Engl 36:104–106
15. Hashmi ASK, Schwarz L (1997) Chem Ber/Recueil 130:1449–1456
16. Hashmi ASK, Naumann F, Bolte M (1998) Organometallics 17:2385–2387
17. Hashmi ASK, Rivas Nass A, Bats JW, Bolte M (1999) Angew Chem 111:3565–3567; Angew Chem Int Ed Engl 38:3370–3373
18. Hashmi ASK (1995) Angew Chem 107:1749–1751; Angew Chem Int Ed Engl 34:1581–1583
19. Hashmi ASK, Ruppert TL, Knöfel T, Bats JW (1997) J Org Chem 62:7295–7304
20. Hashmi ASK, Schwarz L, Bolte M (1998) Tetrahedron Lett 39:8969–8972
21. Hashmi ASK, Choi J-H, Bats JW (1999) J Prakt Chem 341:342–357
22. Hashmi ASK, Schwarz L, Bats JW (2000) J Prakt Chem 342:40–51

23. Hashmi ASK, Schwarz L, Choi J-H, Frost TM (2000) Angew Chem 112:2382–2385; Angew Chem Int Ed 39:2285–2288
24. Hashmi ASK, Frost TM, Bats JW (2000) J Am Chem Soc 122:11553–11554
25. Martín-Matute B, Cardenas CDJ, Echavarren AM (2001) Angew Chem 113:4890–4893; Angew Chem Int Ed 40:4754–4757
26. Martin-Matute B, Nevado C, Cardenas DJ, Echavarren AM (2001) J Am Chem Soc 125:5757–5766
27. Hashmi ASK, Wölfle M, Ata F, Hamzic M, Salathé R, Frey W (2006) Adv Synth Catal 348:2501–2508
28. Hashmi ASK, Rudolph M, Weyrauch JP, Wölfle M, Frey W, Bats JW (2005) Angew Chem 117:2858–2861; Angew Chem Int Ed 44:2798–2801
29. Hashmi ASK, Kurpejovic E, Wölfle M, Frey W, Bats JW (2007) Adv Synth Catal 349:1743–1750
30. Hashmi ASK, Rudolph M, Siehl H-U, Tanaka M, Bats JW, Frey W (2008) Chem Eur J 14:3703–3708
31. Hashmi ASK, Ding L, Bats JW, Fischer P, Frey W (2003) Chem Eur J 9:4339–4345
32. Hashmi ASK, Salathé R, Frey W (2006) Chem Eur J 12:6991–6996
33. Hashmi ASK, Blanco MC, Kurpejovic E, Frey W, Bats JW (2006) Adv Synth Catal 348:709–713
34. Hashmi ASK, Grundl L (2005) Tetrahedron 61:6231–6236
35. Hashmi ASK, Häffner T, Rudolph M, Rominger F (2011) Chem Eur J 17:8195–8201
36. Hashmi ASK, Hamzic M, Rominger F, Bats JW (2009) Chem Eur J 15:13318–13322
37. Hashmi ASK, Hamzic M, Rudolph M, Ackermann M, Rominger F (2009) Adv Synth Catal 351:2469–2481
38. Carrettin S, Blanco MC, Corma A, Hashmi ASK (2006) Adv Synth Catal 348:1283–1288
39. Hutchings GJ (2007) Catalysis Today 122:196–200
40. Toste FD, Gorin DJ, Sherry BD, Toste FD (2008) Chem Rev 108:3351–3378
41. Chen Y, Yan W, Akhmedov NG, Shi X (2010) Org Lett 12:344–347
42. Hashmi ASK, Rudolph M, Huck J, Frey W, Bats JW, Hamzic M (2009) Angew Chem 121:5962–5966; Angew Chem Int Ed 48:5848–5852
43. Hashmi ASK, Pankajakshan S, Rudolph M, Enns E, Bander T, Rominger F, Frey W (2009) Adv Synth Catal 351:2855–2875
44. Hashmi ASK (2010) Pure Appl Chem 82:1517–1528
45. Hashmi ASK, Yang W, Rominger F (2011) Angew Chem 123:5882–5885; Angew Chem Int Ed 49:5762–5765
46. Arcadi A, Cerichelli G, Chiarini M, Di Giuseppe S, Marinelli F (2000) Tetrahedron Lett 41:9195–9198
47. Ito H, Yajima T, Tateiwa J-i, Hosomi A (2000) Chem Commun 981–982
48. Echavarren AM, Nevado C (2004) Chem Soc Rev 33:431–436
49. Bruneau C (2005) Angew Chem 117:2380–2386; Angew Chem Int Ed 44:2328–2334
50. Ma S, Yu S, Gu Z (2006) Angew Chem 118:206–209; Angew Chem Int Ed 45:200–203
51. Dyker G, Muth E, Hashmi ASK, Ding L (2003) Adv Synth Catal 345:1247–1252
52. Hashmi ASK, Blanco MC (2006) Eur J Org Chem 4340–4342
53. Zhang L, Sun J, Kozmin SA (2006) Issue 348:2271–2296
54. Hashmi ASK, Sinha P (2004) Adv Synth Catal 346:432–438
55. Hashmi ASK, Bührle M, Salathé R, Bats JW (2008) Adv Synth Catal 350:2059–2064
56. Lin G-Y, C-w L, Hung S-H, Liu R-S (2008) Org Lett 10:5059–5062
57. Nevado C (2010) Chimia 64:247–251
58. Miki K, Ohe K, Uemura S (2003) Tetrahedron Lett 44:2019–2022
59. Miki K, Ohe K, Uemura S (2003) J Org Chem 68:8505–8513
60. Hashmi ASK, Rudolph M, Schymura S, Visus J, Frey W (2006) Eur J Org Chem 4905–4909
61. Weyrauch JP, Hashmi ASK, Schuster A, Hengst T, Schetter S, Littmann A, Rudolph M, Hamzic M, Visus J, Rominger F, Frey W, Bats JW (2010) Chem Eur J 16:956–963

62. Hashmi ASK, Weyrauch JP, Frey W, Bats JW (2004) Org Lett 6:4391–4394
63. Hashmi ASK, Salathé R, Frey W (2007) Synlett 1763–1766
64. Hashmi ASK, Moliari L, Rominger F, Oeser T (2011) Eur J Org Chem 2256–2264
65. Hashmi ASK, Schuster AM, Schmuck M, Rominger F (2011) Eur J Org Chem 4595–4602
66. Hashmi ASK, Schuster AM, Litters S, Rominger F, Pernpointner M (2011) Chem Eur J 17:5661–5667
67. Hashmi ASK, Schuster A, Rominger F (2009) Angew Chem 121:8396–8398; Angew Chem Int Ed 48:8247–8249
68. Hashmi ASK, Ramamurthi TD, Rominger F (2010) Adv Synth Catal 352:971–975
69. Hashmi ASK, Schuster AM, Gaillard S, Cavallo L, Poater A, Nolan SP (2011) Organometallics 30:6328–6337
70. Hashmi ASK, Blanco MC, Fischer D, Bats JW (2006) Eur J Org Chem 1387–1389
71. Hashmi ASK, Ramamurthi TD, Rominger F (2009) J Organomet Chem 694:592–597
72. Hashmi ASK, Ramamurthi TD, Todd MH, Tsang AS-K, Graf K (2010) Aust J Chem 63:1619–1626
73. Zhang G, Peng Y, Cui L, Zhang L (2009) Angew Chem 121:3158–3161; Angew Chem Int Ed 48:3112–3115
74. Hopkinson MN, Gee AD, Gouverneur V (2010) Isr J Chem 50:675–690
75. Hashmi ASK, Lothschütz C, Döpp R, Rudolph M, Ramamurthi TD, Rominger F (2009) Angew Chem 121:8392–8395; Angew Chem Int Ed 48:8243–8246
76. Hashmi ASK, Döpp R, Lothschütz C, Rudolph M, Riedel D, Rominger F (2010) Adv Synth Catal 352:1307–1314
77. Peña-López M, Ayán-Varela M, Sarandeses LA, Pérez Sestelo J (2010) Chem Eur J 16:9905–9909
78. Hashmi ASK, Lothschütz C, Döpp R, Ackermann M, De Buck J, Rudolph M, Scholz C, Rominger F (2012) Adv Synth Catal 354:133–147
79. González-Arellano C, Abad A, Corma A, García H, Iglesias M, Sánchez F (2007) Angew Chem 119:1558–1560; Angew Chem Int Ed 46:1536–1538
80. Li P, Wang L, Wang M, You F (2008) Eur J Org Chem 5946–5951
81. Corma A, Gutiérrez-Puebla E, Iglesias M, Monge A, Pérez-Ferreras S, Sánchez F (2006) Adv Synth Catal 348:1899–1907
82. Lauterbach T, Livendahl M, Rosellón A, Espinet P, Echavarren AM (2010) Org Lett 13:3006–3009
83. Corma A, Juárez R, Boronat M, Sánchez F, Iglesias M, García H (2011) Chem Commun 47:1446–1448
84. Hashmi ASK, Molinari L (2011) Organometallics 30:3457–3460
85. Hashmi ASK, Weyrauch JP, Rudolph M, Kurpejovic E (2004) Angew Chem 116:6707–6709; Angew Chem Int Ed 43:6545–6547
86. Hashmi ASK, Lothschuetz C, Ackermann M, Doepp R, Anantharaman S, Marchetti B, Bertagnolli H, Rominger F (2010) Chem Eur J 16:8012–8019
87. Hashmi ASK, Loos A, Littmann A, Braun I, Knight J, Doherty S, Rominger F (2009) Adv Synth Catal 351:576–582
88. Doherty S, Knight JG, Hashmi ASK, Smyth CH, Ward NAB, Robson KJ, Tweedley S, Harrington RW, Clegg W (2010) Organometallics 29:4139–4147
89. Hashmi ASK, Loos A, Doherty S, Knight JG, Robson KJ, Rominger F (2011) Adv Synth Catal 353:749–759
90. Khin C, Hashmi ASK, Rominger F (2010) Eur J Inorg Chem 1063–1069
91. Pažický M, Loos A, Ferreira MJ, Rominger F, Jäkel C, Hashmi ASK, Limbach M (2010) Organometallics 29:4448–4458
92. Schäfer S, Frey W, Hashmi ASK, Cmrecki V, Luquin A, Laguna M (2010) Polyhedron 29:1925–1932
93. Hashmi ASK, Hengst T, Lothschütz C, Rominger F (2010) Adv Synth Catal 352:1315–1337

94. Hashmi ASK, Lothschütz C, Böhling C, Hengst T, Hubbert C, Rominger F (2010) Adv Synth Catal 352:3001–3012
95. Hashmi ASK, Lothschütz C, Graf K, Häffner T, Schuster A, Rominger F (2011) Adv Synth Catal 354:1407–1412
96. Hashmi ASK, Frost TM, Bats JW (2001) Org Lett 3:3769–3771
97. Pernpointner M, Hashmi ASK (2009) J Chem Theory Comput 5:2717–2725
98. Lein M, Rudolph M, Hashmi ASK, Schwerdtfeger P (2010) Organometallics 29:2206–2210
99. Krauter CM, Hashmi ASK, Pernpointner M (2010) ChemCatChem 2:1226–1230
100. Ye L, Wang Y, Aue DH, Zhang L (2012) J Am Chem Soc 134:31–34
101. Hashmi ASK, Braun I, Rudolph M, Rominger F (2012) Organometallics 31:644–661
102. Hashmi ASK, Braun I, Nösel P, Schädlich J, Wieteck M, Rudolph M, Rominger F (2012) Angew Chem 124:4532–4536; Angew Chem Int Ed 51:4456–4460
103. Hashmi ASK, Wieteck M, Braun I, Nösel P, Jongbloed L, Rudolph M, RomingerR (2012) Adv Synth Catal 354:555–562
104. Hashmi ASK, Schwarz L, Rubenbauer P, Blanco MC (2006) Adv Synth Catal 348:705–708
105. Hoffmann R (1982) Angew Chem 94:725–739; Angew Chem Int Ed Engl 12:711–724
106. Comyns AE (2001) Focus on Catalysts. Elsevier Advanced Technology
107. Comyns AE (2001) Focus on Catalysts, August 2001, Page 1
108. Comyns AE (2002) Focus on Catalysts 3: March 2002, Page 1–2. http://www.sciencedirect.com/science/journal/13514180/2002/3
109. Comyns AE (2004) Focus on Catalysts 6: June 2004, Page 1. http://www.sciencedirect.com/science/journal/13514180/2004/6
110. Andrew Mitchinson (Associate Editor, Nature). http://blogs.nature.com/thescepticalchymist/2007/04/endangered_elements_1.html

Top Organomet Chem (2013) 44: 165–194
DOI: 10.1007/3418_2012_53

Published online: 28 August 2012

Developing Catalytic Asymmetric Acetalizations

Ilija Čorić, Sreekumar Vellalath, Steffen Müller, Xu Cheng, and Benjamin List

Abstract Acetals are among the most common stereocenters in Nature. They form glycosidic bonds that link together essential molecules of life, carbohydrates, including starch and cellulose, the most abundant organic material on Earth. Stereogenic acetals are also common motifs in other natural products, from small insect pheromones to highly complex spiroacetal polyketides. Although far less common than *O,O*-acetals, chiral *N,N*-, *N,O*-, and *N,S*-acetals are structural motifs also found in a number of natural products and pharmaceuticals. Here, recent progress towards chiral acetals using asymmetric Brønsted acid catalysis is summarized, with particular emphasis on *O,O*-acetalizations. In this context the development of novel catalyst classes, namely spirocyclic phosphoric acids and confined Brønsted acids, proved crucial and is also presented.

Keywords Acetals · Acetalizations · Spiroacetals · Asymmetric catalysis · Brønsted Acid catalysis · Confined acids

Contents

I. Čorić, S. Vellalath, S. Müller, X. Cheng and B. List (✉)
Max-Planck-Institut für Kohlenforschung, Kaiser-Wilhelm-Platz 1, 45470 Mülheim an der Ruhr, Germany
e-mail: list@kofo.mpg.de

1 Introduction

How do chemists invent new reactions? There are different answers to this as there are various approaches. Sometimes, a reaction is designed to solve a specific problem, let us say the efficient coupling of two aryls. In other cases, a reaction is discovered by serendipity and then advances into a useful and general transformation, consider for example olefin metathesis. There are also approaches that are driven by plain curiosity.

We are particularly attracted to hypothetical reactions that may be conceivable but, for one or the other reason, have not been invented yet. Such reactions certainly do not need to be useful at all on the first sight. This is a privilege of basic research and the true usefulness of a reaction is often revealed only much later (consider again olefin metathesis). This type of research is primarily a highly rewarding intellectual enterprise. Can we conceive a reaction that has not been conceived yet? We often try to answer this question in our laboratory by designing asymmetric catalytic versions of well-established classic organic reactions. Examples include the reactions named after Mannich [1], Pictet-Spengler [2], Knoevenagel [3], or the Fischer indolization [4]. The latter reaction invention has been particularly interesting as it was initially completely unclear (a) how and if we would be able to convert a reaction that delivers a planar aromatic molecule into an asymmetric version, and (b) whether or not such a process would eventually be useful for anything at all.

The concept of developing catalytic asymmetric acetalization reactions originates from the very early days of our laboratory and may, at least in retrospect, be even more obscure. How could such processes be designed considering their inherent reversibility, and why would anybody need chiral acetals in the first place? Fortunately, such questions are mostly irrelevant to us. We feel indeed privileged to be able to conduct long-term research that lacks success guarantee or immediate societal relevance, and that does not need to be frequently

justified. Our curiosity-driven asymmetric acetalization enterprise ultimately delivered solutions to actual problems and thereby became a highly rewarding success story, revealed here.

2 Chiral Acetals in Nature and Synthesis

Acetals are among the most common stereocenters in Nature. They form glycosidic bonds that link together essential molecules of life, carbohydrates, including starch and cellulose, the most abundant organic material on Earth [5]. Stereogenic acetals are also common motifs in other natural products, from small insect pheromones to highly complex spiroacetal polyketides (Scheme 1) [6–8]. Controlling the relative and absolute configuration of the acetal stereocenter is extremely important. For example, starch and cellulose only vary in the configuration at their anomeric acetal stereocenter, yet they perform very different biological roles. Chiral acetals are also important motifs in pharmaceuticals and various bioactive compounds. Nevertheless, methods for the enantioselective synthesis of stereogenic acetals are very limited and usually based on chiral starting materials or reagents. Although far less common than *O*,*O*-acetals, chiral *N*,*N*-, *N*,*O*-, and *N*,*S*-acetals are structural motifs also found in a number of natural products and pharmaceuticals.

3 On Route to Acetals: Oxocarbenium and Iminium Ions

We have a long-standing interest in developing catalytic asymmetric reactions that form various acetals, including *O*,*O*-, *N*,*N*-, and *N*,*O*-acetals (Scheme 2).

Making acetals that contain *N*-atoms has been a fairly straightforward effort, following the advent of asymmetric phosphoric acid catalysis [9, 10]. Since the reports of Akiyama and Terada, asymmetric additions of nucleophiles to imines became a well-developed area of asymmetric Brønsted acid catalysis [11, 12]. Consequently, heteroatom nucleophiles were shown to be viable nucleophiles and various *N*,*N*-, *N*,*O*-, and *N*,*S*-acetals could be prepared for the first time in a catalytic asymmetric fashion. These reactions are briefly summarized in the next section.

However, *O*,*O*-acetals present a particular challenge, as their synthesis does not involve an iminium ion. Controlling the enantioselective addition to an oxocarbenium ion, the commonly invoked intermediate in the synthesis of acetals, is an important issue in asymmetric Brønsted acid catalysis (Scheme 3). In contrast to the reactions involving the related iminium ion that features a strong hydrogen bond with its chiral counteranion, there are only scarce examples of asymmetric additions of nucleophiles to oxocarbenium ions [13–15].

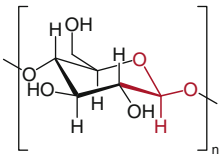

Cellulose:

- basic structural component of plant cell walls
- about 33% of all vegetable matter (90% of cotton and 50% of wood)
- **the most abundant organic material on Earth**

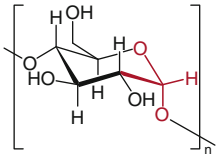

Starch:

- manufactured in the green leaves of plants from excess glucose
- serves the plant as a reserve food supply
- food for humans and animals

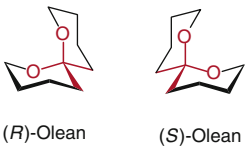

(*R*)-Olean (*S*)-Olean

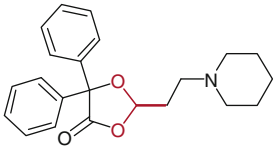

Pipoxolan

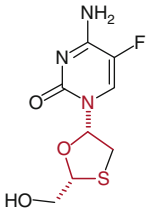

Emtricitabine

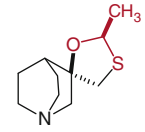

Cevimeline

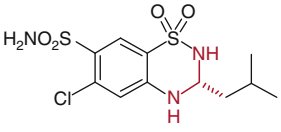

(*R*)-Thiabutazide

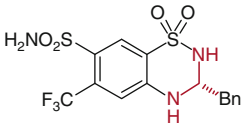

(*R*)-Bendroflumethiazide

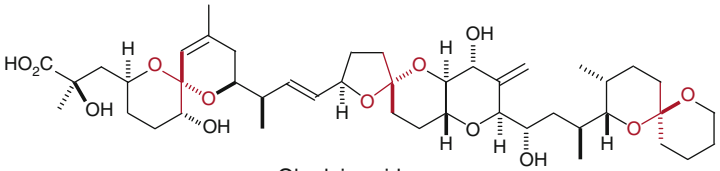

Okadaic acid

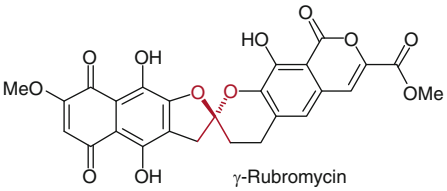

γ-Rubromycin

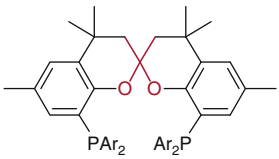

chiral ligand

Scheme 1 Stereogenic acetals

Scheme 2 Towards direct catalytic asymmetric acetalizations

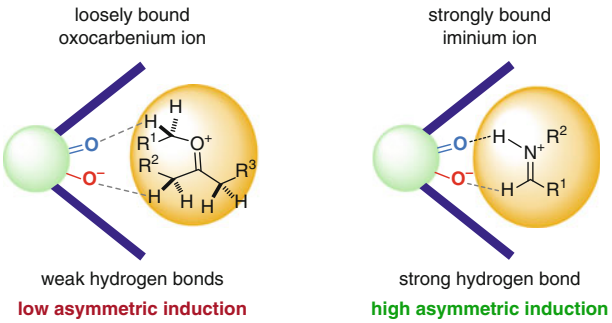

Scheme 3 Oxocarbenium and iminium ions bound to chiral phosphate anions

4 Asymmetric Additions to Imines: A Straightforward Route to *N,X*-Acetals (X = N, O, S, Se)

4.1 Acyclic N,X-Acetals

Despite the massive advancements in asymmetric catalysis over the last several decades, the catalytic enantioselective generation of *N,N*-, *N,O*-, *N,S*-, and *N,Se*-acetals only recently became a possibility with the advent of asymmetric Brønsted acid catalysis [16–22]. Asymmetric syntheses of acyclic *N,N*-, *N,O*-, *N,S*-, and *N,Se*-acetals catalyzed by chiral phosphoric acids were developed in the Antilla group utilizing the addition of heteroatom nucleophiles to *N*-protected imines (Scheme 4) [16–18, 22].

4.2 Direct N,N- and N,O-Acetalizations of Aldehydes

Our group developed direct asymmetric *N,N*- and *N,O*-acetalizations of aldehydes to access cyclic *N,N*- and *N,O*-acetals, which are found in several pharmaceuticals [19, 20]. In a condensation reaction of *o*-aminobenzamides and aliphatic aldehydes, phosphoric acid catalysts **4** delivered chiral *N,N*-acetals in high yield and with high enantioselectivity (Scheme 5). The methodology has been applied to the first asymmetric synthesis of several aminal drugs including (*R*)-thiabutazide. A variant of the direct asymmetric *N,N*-acetalization of aldehydes employing aromatic aldehydes was subsequently published by Rueping et al. [21]

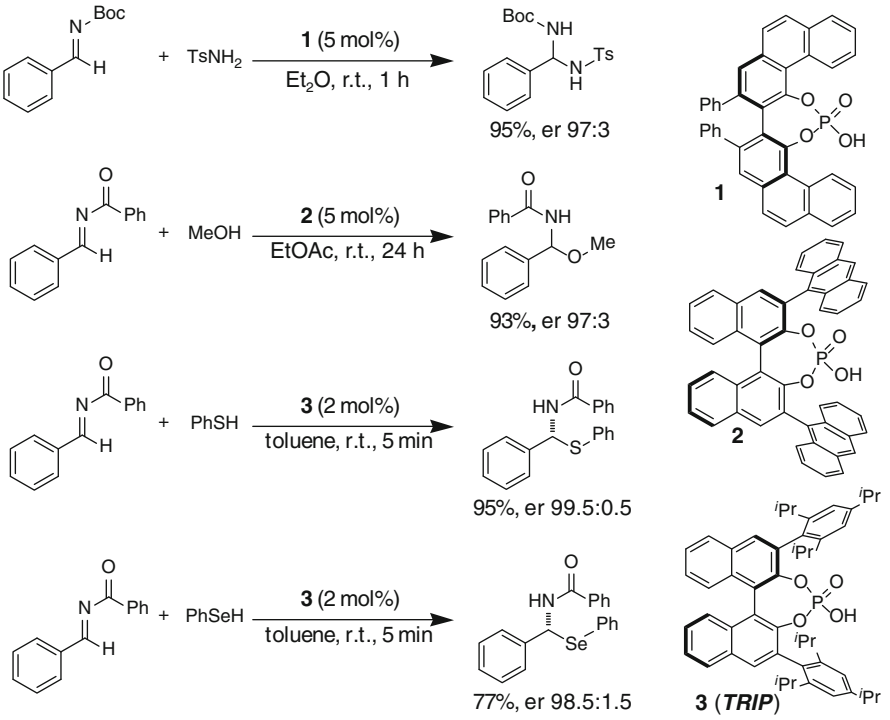

Scheme 4 Asymmetric *N*,*X*-acetalizations reported by the Antilla group

A structurally related condensation reaction of *o*-hydroxybenzamides and aliphatic aldehydes to benzoxazinones was found to be very challenging utilizing a variety of established chiral catalysts. Therefore, chiral *N*-phosphinyl phosphoramide has been designed as a new motif for asymmetric Brønsted acid catalysis. Readily accessible catalyst **5** proved to be highly efficient and enantioselective in catalyzing the first direct asymmetric *N*,*O*-acetalization of aldehydes (Scheme 6). The synthetic utility of this methodology was demonstrated with the first catalytic asymmetric synthesis of the analgesic pharmaceutical (*R*)-chlorothenoxazine.

All of the above mentioned *N*,*X*-acetalizations are based on the well-established ability of phosphoric acids and their derivatives to catalyze asymmetric additions of nucleophiles to imines. Imines are readily activated by Brønsted acids due to their relatively high basicity, and the intermediate iminium ion possesses strong hydrogen bonding to the chiral anion (Scheme 7). This makes the ion pair reasonably well organized enabling an efficient enantiocontrol. The crucial step in the direct *N*,*N*- and *N*,*O*-acetalizations of aldehydes is the intramolecular asymmetric addition to an iminium ion intermediate, which is formed after the condensation of the amide or amine moiety with the aldehyde (Scheme 7).

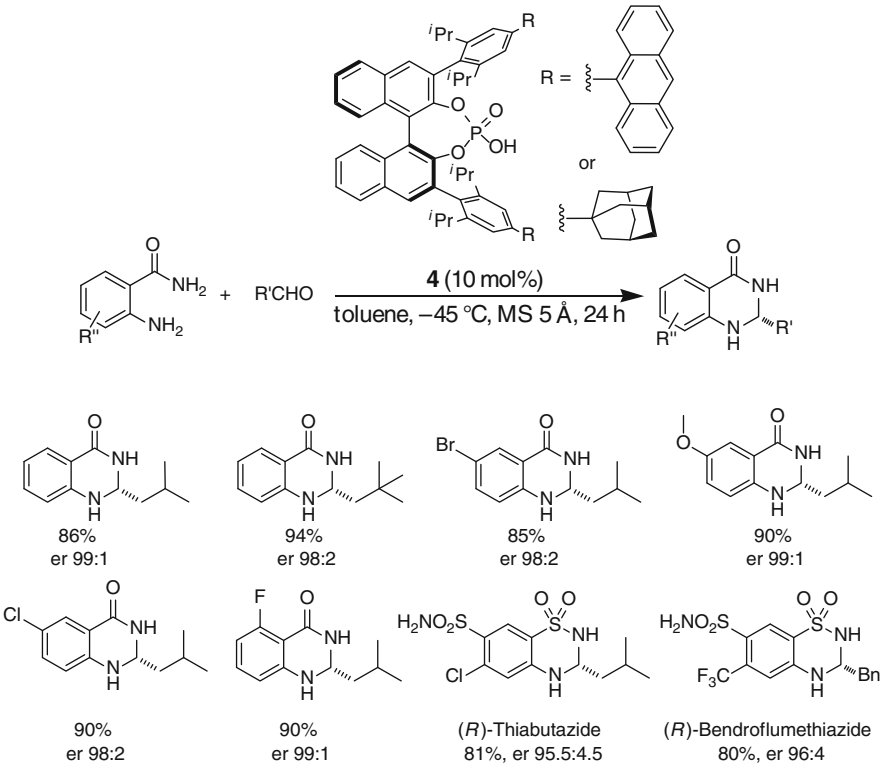

Scheme 5 Direct *N*,*N*-acetalization of aldehydes

5 Making *O*,*O*-Acetals

5.1 The Challenging Oxocarbenium Ion Intermediate

O,*O*-acetals present a challenge for asymmetric Brønsted acid catalysis. Before our studies commenced, Brønsted acid-catalyzed reactions for the asymmetric construction of *O*,*O*-acetals were entirely unknown, despite the fact that they represent a much more common motif in natural products and organic synthesis than the analogous *N*,*N*-, *N*,*O*-, or *N*,*S*-acetals. The critical oxocarbenium ion intermediate possesses only weakly acidic C–H groups to bind a chiral anion of the catalyst (Scheme 8). Furthermore, the oxocarbenium ion possesses a number of such C–H bonds giving multiple possibilities for anion binding. Such weak and geometrically unrestricted interaction with the chiral anion results in the presence of numerous transition state geometries for the nucleophilic attack leading to low enantioselectivity. Unlike oxocarbenium ions, iminium ions possess a strong N^+–H···$^-$X* hydrogen bond, which fixes the position of the chiral anion, a scenario that rationalizes the success of numerous enantioselective additions of nucleophiles to imines.

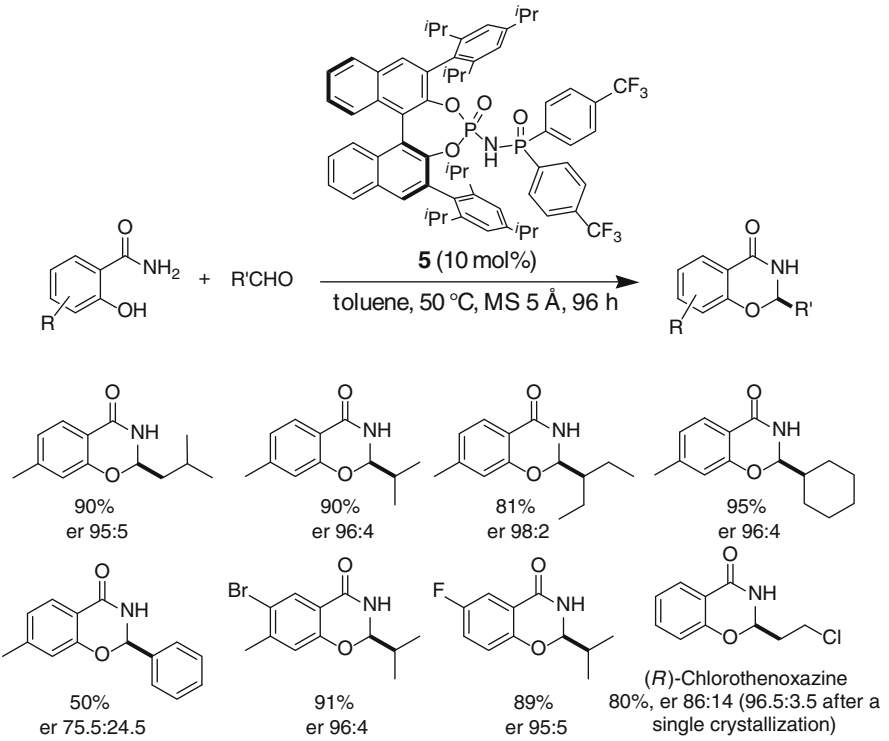

Scheme 6 Direct *N*,*O*-acetalization of aldehydes

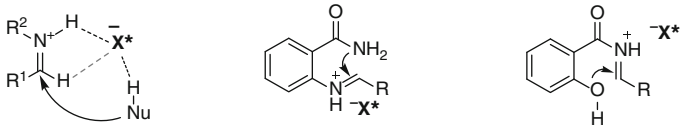

Scheme 7 Enantioselective steps in the reported *N*,*X*-acetalizations

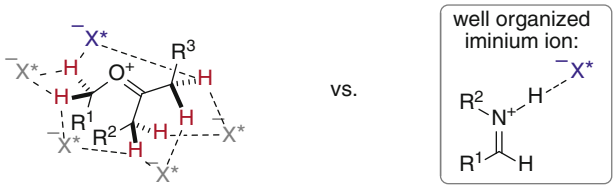

Scheme 8 Suggested indiscriminate binding of an oxocarbenium ion with its chiral counteranion as compared to a well-defined iminium cation–anion pair

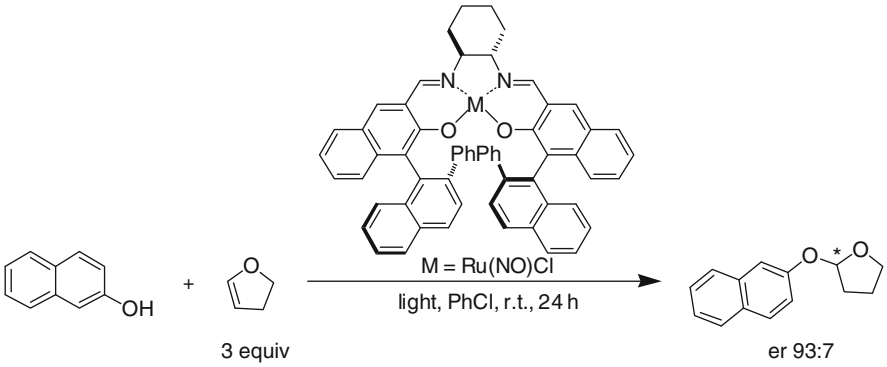

Scheme 9 First catalytic asymmetric acetal formation

5.2 *Metal-Catalyzed Asymmetric Acetalization by Nagano and Katsuki*

A single example of a catalytic asymmetric formation of chiral acetals was previously described by Nagano and Katsuki, based on a metal-catalyzed hydroetherification of enol ethers (Scheme 9) [23]. Enantiomeric ratios up to 93:7 could be achieved with a ruthenium catalyst, although the exact mechanism of this transformation is unknown. This reaction is to the best of our knowledge the first catalytic asymmetric acetalization reaction.

5.3 *Attempts Toward Direct O,O-Acetalization of Aldehydes*

Encouraged by the results with our direct *N*,*N*- and *N*,*O*- acetalizations of aldehydes, we attempted to perform the direct *O*,*O*-acetalization in a similar manner. However, only low enantioselectivity was achieved using the chiral phosphoric acid ***TRIP*** and various other catalysts failed to provide improvement (Scheme 10).

As we were unable to effect a highly enantioselective acetalization reaction in this manner, we turned our attention to the development of other asymmetric reactions that form chiral acetals.

6 Catalytic Asymmetric Transacetalization

We have developed a catalytic enantioselective synthesis of *O*,*O*-acetals via a transacetalization reaction [24]. Transacetalization reactions usually require relatively strong Brønsted acid catalysts and proceed via oxocarbenium ion intermediates (Scheme 11a). An obvious issue related to the transacetalization reaction is the functional similarity of the starting material and the product.

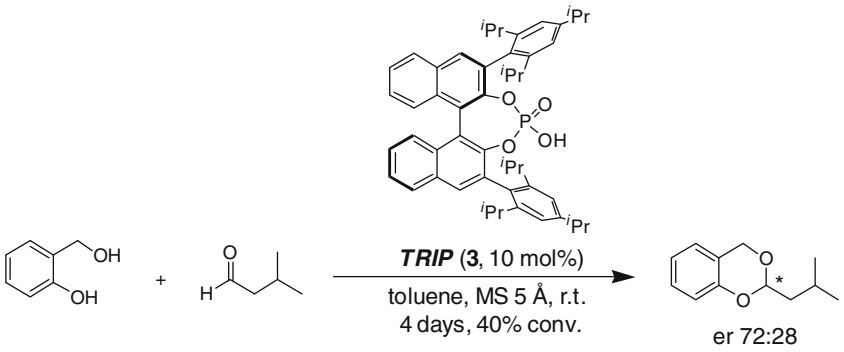

Scheme 10 Attempted direct *O*,*O*-acetalization of aldehydes

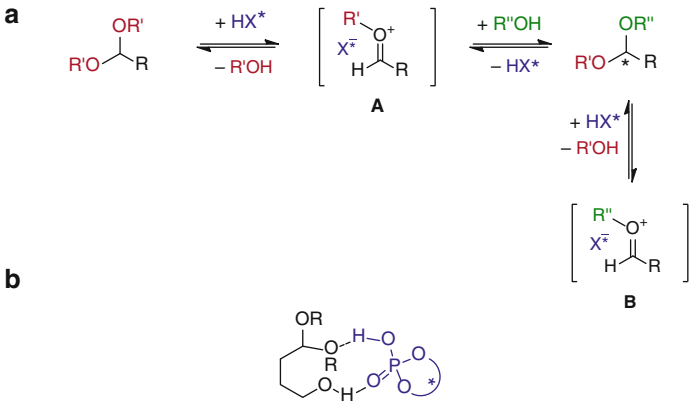

Scheme 11 (**a**) Intermolecular transacetalization reaction; (**b**) proposed bifunctional activation of the substrate in the intramolecular version

Both are acetals, and the product could be activated by the catalysts as well, reversibly forming oxocarbenium ions **A** and **B** (Scheme 11a), leading to racemization of the product.

However, it was reasoned that an intramolecular variant of the transacetalization reaction might be amenable to mild asymmetric Brønsted acid catalysis. A hydrogen-bonded complex of the substrate and chiral acid was proposed, selectively activating the hydroxyl acetal over the product, which does not possess an OH-moiety (Scheme 11b). The hydroxyl group of the substrate might serve as a catalyst-directing group and also increase the acidity of the phosphoric acid through hydrogen bonding. We envisioned that this design could potentially address problems resulting from the reversibility of the reaction and product racemization.

The chiral phosphoric acid ***TRIP*** (**3**) was found to be an efficient and highly enantioselective catalyst of the intramolecular transacetalization reaction of hydroxyacetals enabling the asymmetric synthesis of acetals with the acetal carbon

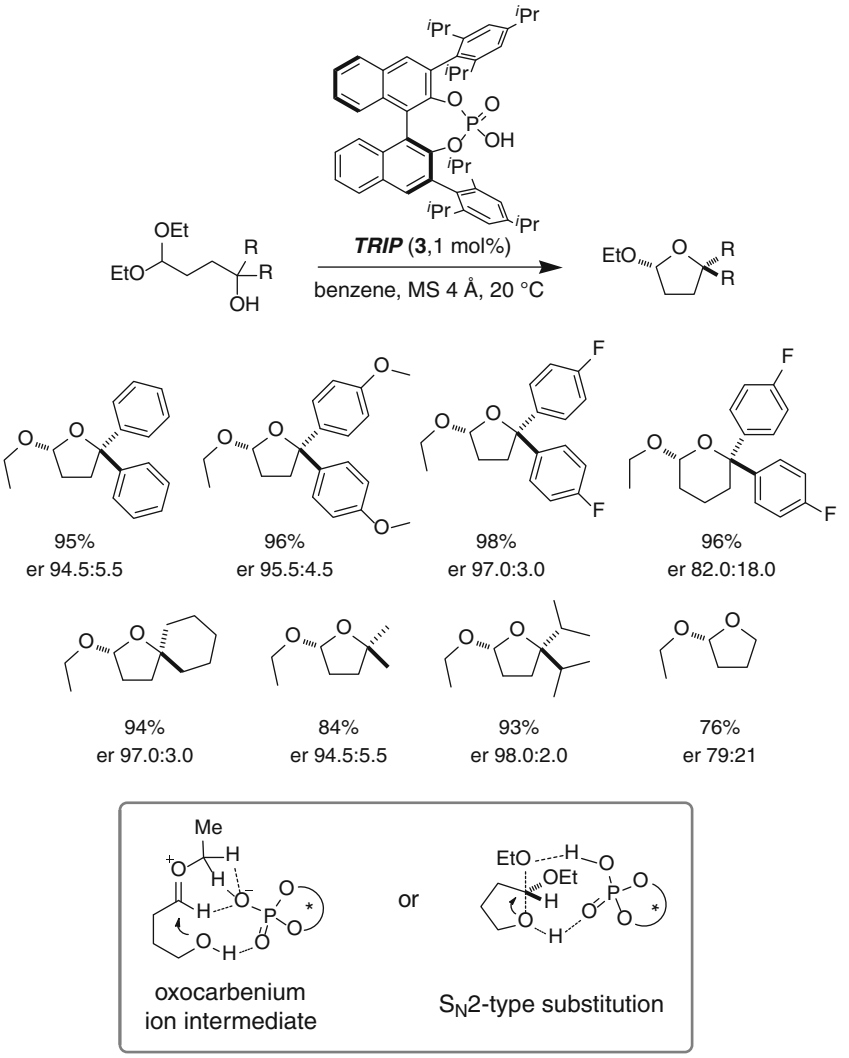

Scheme 12 Catalytic asymmetric transacetalization

as the only stereogenic center (Scheme 12) [24]. Enantiomeric ratios of up to 98:2 could be achieved with tertiary alcohols, although a small unsubstituted primary alcohol substrate underwent the reaction with lower enantioselectivity. Simple *O*, *O*-acetals usually require stronger Brønsted acid catalyst to be activated, and this reaction represented the first example of a phosphoric acid-catalyzed enantioselective addition of nucleophiles to simple *O*,*O*-acetals. However, it is currently still uncertain whether this reaction proceeds through an oxocarbenium ion or through an S_N2-type mechanism (Scheme 12).

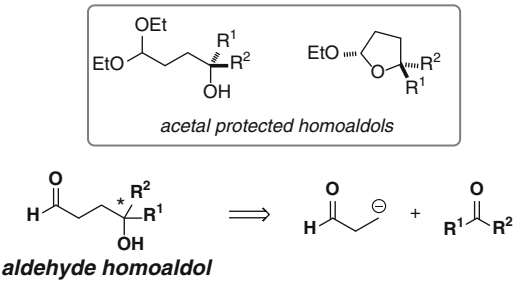

Scheme 13 Problematic homoaldol retrosynthetic disconnection

6.1 Kinetic Resolution of Alcohols Via Acetal Formation

Although initially developed as a rather exotic reaction, the intramolecular transacetalization reaction can also be a very useful tool in asymmetric synthesis of important chiral compounds and natural products. Both, starting materials and products of the intramolecular transacetalization reaction are protected γ-hydroxycarbonyl compounds, or homoaldols (Scheme 13). Homoaldols are versatile motifs in organic synthesis that can be easily transformed into a vast array of important chiral compounds. However, due to the problematic homoaldol disconnection, these compounds are not readily available in a catalytic asymmetric fashion.

A highly enantioselective kinetic resolution of protected homoaldols via a catalytic asymmetric transacetalization reaction could be achieved with a novel phosphoric acid ***STRIP*** (**6**) (Table 1) [25]. A catalyst loading of 1 mol% could be routinely used at 20°C, and even 0.1 mol% of the catalyst can give very similar enantiomeric ratios. The method is applicable to the resolution of a wide range of secondary and, most remarkably, of tertiary homoaldols. In most cases, both acyclic homoaldols **7** and cyclic homoaldols **8** could be obtained in enantiomeric ratios exceeding 95:5. Although chemical kinetic resolutions of secondary alcohols by other methods are well developed [26], these are not readily applicable to kinetic resolutions of tertiary alcohols [27–34].

The reaction of a linear aliphatic-substituted homoaldol illustrates an interesting feature of this kinetic resolution (Scheme 14). As an additional acetal stereocenter is created in the transacetalization reaction, the high catalyst control of its formation results in a highly diastereoselective reaction [26, 35, 36]. Thus, even in cases where the enantiodifferentiation of the starting material is not very pronounced, the less reactive enantiomer is converted into the minor *trans*-diastereomer (Scheme 14).

Such kinetic resolutions via intramolecular transacetalization reaction represent an atom economic method that does not require any stoichiometric reagents and forms ethanol as the only by-product. This reaction also is the first example of a kinetic resolution of alcohols via acetal formation and the first example of a chiral Brønsted acid-catalyzed kinetic resolution of alcohols. The utility of the reaction

Table 1 Kinetic resolution of homoaldols via catalytic asymmetric transacetalization

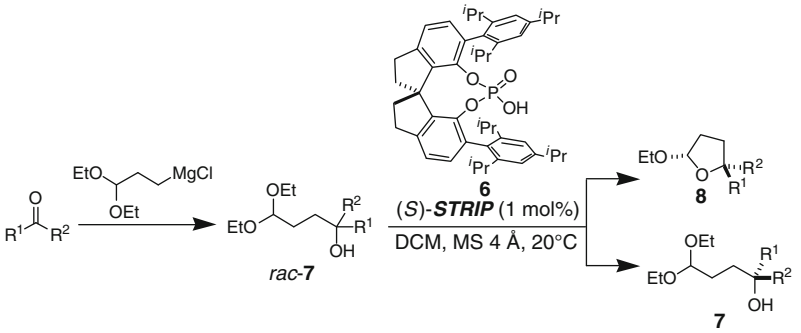

Entry	Conversion (time)	**8**	er **8**	dr **8**	er **7**
1	55% (18 h)	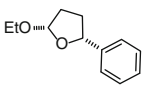	97:3	13:1	98.5:1.5
2	55% (16 h)	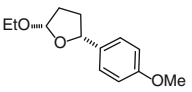	97:3	12:1	98:2
3	54% (14 h)	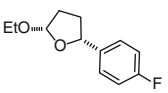	96.5:3.5	13:1	97.5:2.5
4	53% (14 h)	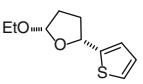	97.5:2.5	19:1	98.5:1.5
5	56% (14 h)	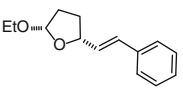	98:2	8:1	98:2
6	55% (4 h)	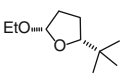	93.5:6.5	19:1	98:2
7	55% (12 h)	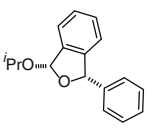	89.5:10.5	44:1	96.5:3.5

(continued)

Table 1 (continued)

Entry	Conversion (time)	**8**	er **8**	dr **8**	er **7**
8	55% (12 h)	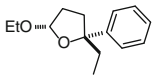	98.5:1.5	9:1	98.5:1.5
9	55% (28 h)	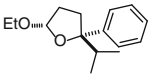	97.5:2.5	7:1	92:8
10	54% (40 h)	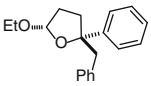	99:1	11:1	97.5:2.5
11	51% (3 h)	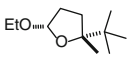	99:1	18:1	96.5:3.5

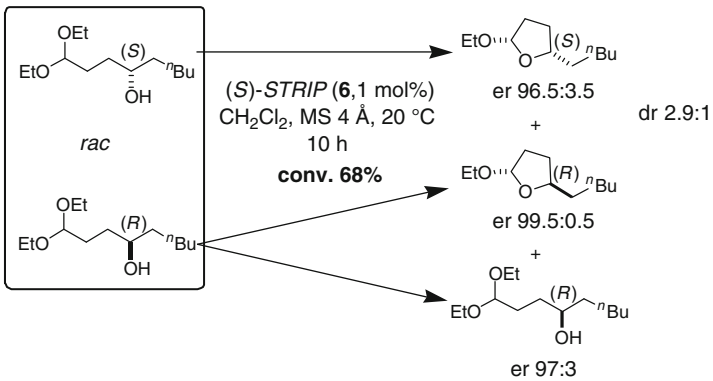

Scheme 14 Role of the created acetal stereocenter

was exemplified by a short asymmetric total synthesis of the natural product boivinianin A (Scheme 15).

6.2 ***STRIP*** Catalyst

Since the initial reports of Akiyama and Terada [9–12], BINOL-derived phosphoric acids became very general and popular catalysts. The design of new chiral phosphoric acids has been usually directed to variations of the 3,3′-substituents on the BINOL backbone [16, 37]. We were particularly interested in exploring

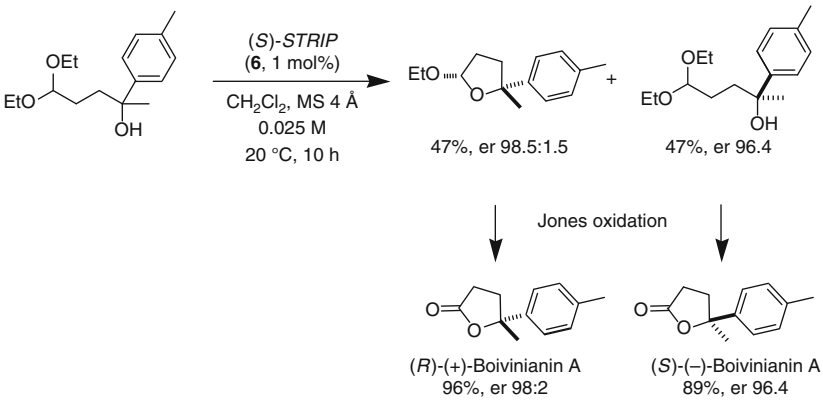

Scheme 15 Application in natural product synthesis

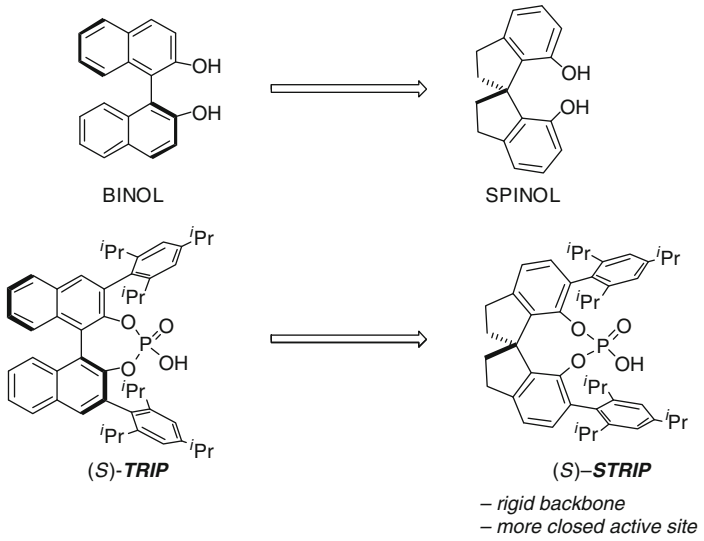

Scheme 16 Design of ***STRIP*** catalyst

1,1′-spirobiindane as a backbone for new phosphoric acid catalysts [38]. Although this backbone is well appreciated in metal catalysis [39–41], the corresponding phosphoric acids have never been used as catalysts. We expected these phosphoric acids to provide a geometrically different and more rigid chiral pocket than their BINOL-derived counterparts, offering potentially complementary tools for asymmetric Brønsted acid catalysis. We were particularly interested in the ***STRIP*** (spiro-***TRIP***) derivative corresponding to one of the more useful and general phosphoric acid catalysts ***TRIP*** with bulky 2,4,6-$^{i}Pr_3C_6H_2$ substituents on the backbone [42, 43] (Scheme 16).

Table 2 Comparison of phosphoric acids based on different backbones

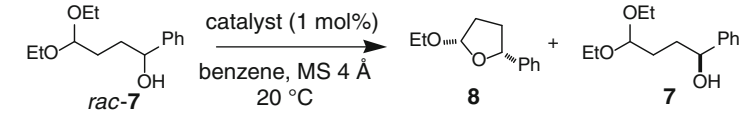

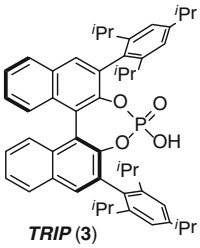

***TRIP* (3)**

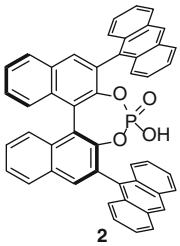

2

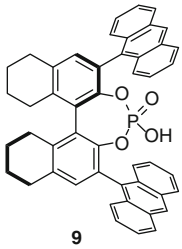

9

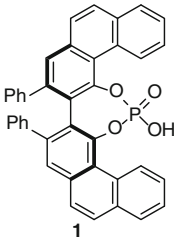

1

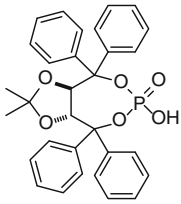

10

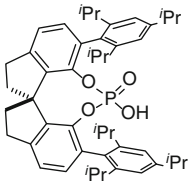

***STRIP* (6)**

Entry	Cat.	Conversion (%)	er **8**	dr	er **7**
1	**3**	41	25:75	14:1	36:64
2	**2**	47	39:61	17:1	42:58
3	**9**	38	61.5:38.5	17:1	55.5:44.5
4	**1**	41	62.5:37.5	7:1	57:43
5	**10**	26	45:55	7:1	49:51
6	**6**	51	95:5	21:1	92:8
7[a]	**6**	55	96.5:3.5	12:1	99:1

[a]In CH_2Cl_2

Spirocyclic phosphoric acid catalyst ***STRIP*** (**6**) turned out to be crucial in the development of the kinetic resolution of homoaldols. The SPINOL backbone outperformed a variety of other previously described phosphoric acids based on BINOL (**3** and **2**), H8-BINOL (**9**), VAPOL (**1**), and TADDOL (**10**) backbones (Table 2).

The synthesis of ***STRIP*** was achieved according to the route shown in Scheme 17. In a simultaneous report, Ling, Wang, and coworkers showed that the corresponding naphthyl-substituted SPINOL-derived phosphoric acid is a competent catalyst for the venerable asymmetric Friedel–Crafts reaction of indoles with imines [44], giving comparable results to BINOL-derived phosphoric acids. Subsequently, several groups have utilized SPINOL-based phosphoric acids as Brønsted

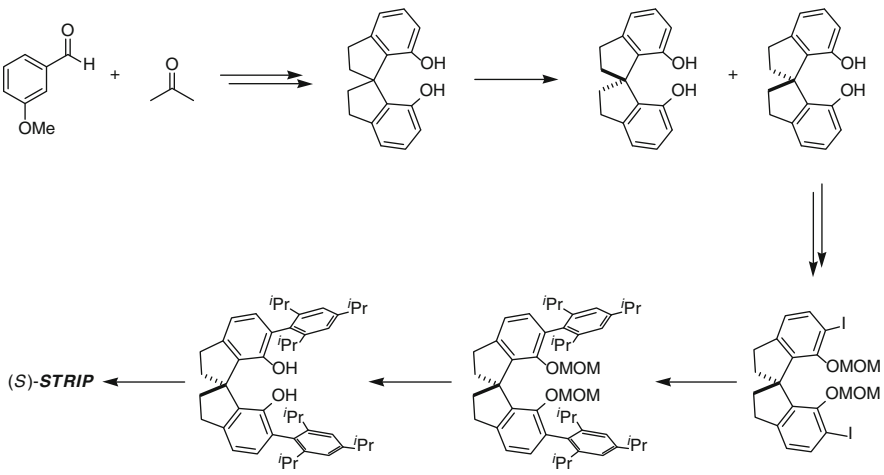

Scheme 17 Synthesis of ***STRIP***

acid catalysts, in some cases demonstrating distinct advantages over BINOL counterparts. However, for their broader application, the currently long and demanding synthesis, which includes more than ten steps, including a resolution, should be replaced with a more efficient route.

7 Catalytic Asymmetric Spiroacetalization

A structurally particularly recognizable subgroup of acetals are spiroacetals. These fascinating small spirocycles are a core motif of a variety of natural products [6–8]. To mention a few, protein phosphatase inhibitor okadaic acid is a toxin associated with diarrhetic seafood poisoning [45]; spongistatins are structurally complex tubulin polymerization-inhibiting macrolides that display extraordinary antitumor activities [6]; integramycin is an HIV-1 protease inhibitor [46]; and the ionophore monensin A is an antibiotic widely used in animal feeds [47]. The spiroacetal subunit was demonstrated to be a privileged pharmacophore, essential for the biological activity of natural products [48–51].

Interestingly, even natural products that contain a spiroacetal as the only stereogenic element are known [52]. The parent 6,6-spiroacetal is also a natural product, olean, the major female-produced sex pheromone of the olive fruit fly (Scheme 18) [53]. Although it has been isolated from natural sources as a racemic mixture, it was found that its two mirror enantiomers display a remarkable sex-specific property. The (*R*)-enantiomer is active on males and the (*S*)-enantiomer on females of the olive fruit fly [54].

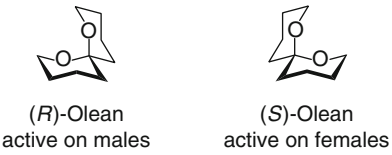

Scheme 18 Two enantiomers of olean from olive fruit fly

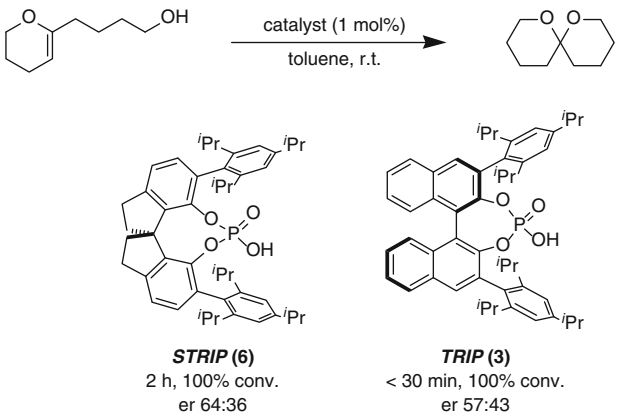

Scheme 19 Attempted 6,6-spiroacetalization

7.1 Problems with Small Substrates

We were particularly fascinated by the small and simple compound olean and attempted its asymmetric synthesis via a Brønsted acid-catalyzed cyclization of the corresponding hydroxyenolether substrate [57]. However, only low enantioselectivity could be obtained (Scheme 19). We faced a similar failure with the construction of the even smaller 5,5-spiroacetal (Scheme 20). Silver salts were also tested as catalysts; however, this only resulted in a reduced reaction rate. It is likely that the corresponding acid, which can be formed via an H^+/Ag^+ exchange with the substrate or water, is the actual catalyst. Although the acid-catalyzed spiroacetalization reactions were very facile at room temperature, lowering the temperature did not result in an improvement of enantioselectivity.

In the failure of the phosphoric acid catalysts, we recognized a much more general issue in current Brønsted acid catalysis, that is, small aliphatic substrates and loosely bound intermediates such as oxocarbenium ions represent essentially unsolved problems in the area. Instead of focusing on the decoration of the spiroacetalization substrates with bulky or aromatic groups, we turned to the development of a catalyst class that could solve these general problems in asymmetric Brønsted acid catalysis [57].

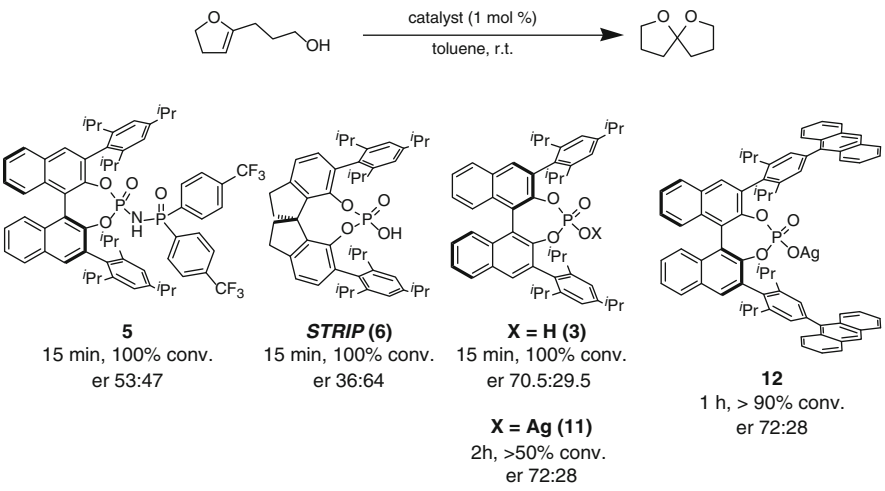

Scheme 20 Attempted 5,5-spiroacetalization

7.2 Confined Chiral Brønsted Acid Catalysts

Brønsted acid catalysis, especially with chiral phosphoric acid type catalysts, has become one of the most successful subfields of organocatalysis [9, 10]. However, numerous reactions are still elusive, and the smallest substrates frequently give the poorest selectivity. A probable cause could be traced to a limited interaction of the small substrate with the catalysts structure when approaching its open active site (Scheme 21). With large substrates, the steric interaction is more pronounced, resulting in higher selectivity.

Additionally, successful asymmetric reactions with transition states that are not well organized with covalent or hydrogen bonding interactions between the catalyst and the substrates are also very rare. Such a situation is encountered with the oxocarbenium ion, a common intermediate in the synthesis of acetals. As opposed to the reactions involving related iminium ion featuring a strong hydrogen bond, there are only scarce examples of the addition of nucleophiles to oxocarbenium ions (Scheme 3) [13–15].

The inability of the existing catalysts to impart efficient steric control for the small oxocarbenium ion intermediate was deemed responsible for the lack of selectivity in the asymmetric spiroacetalization reaction (Scheme 22a). While large active sites are able to accommodate a certain transition state diversity, a confined space was proposed to limit this freedom and thereby increase selectivity (Scheme 22b) [57].

Our design of a new and extremely sterically demanding Brønsted acid was based on the analysis of highly successful chiral phosphoric acids [9–12], *N*-triflyl phosphoramides introduced by Yamamoto [55] and *N*-phosphinyl phosphoramides

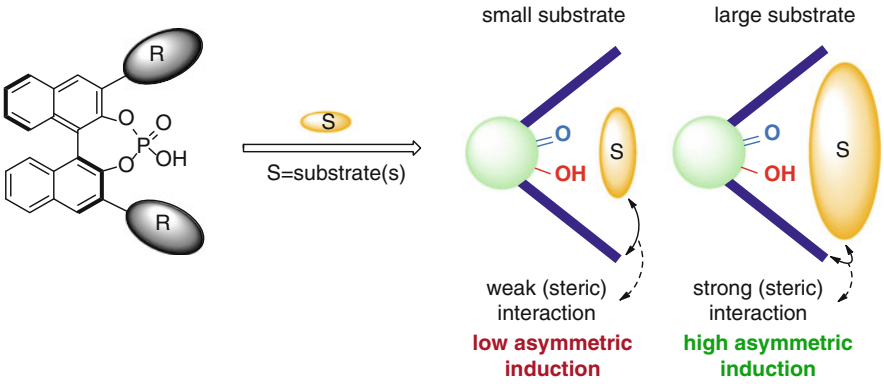

Scheme 21 Limitations of phosphoric acid type catalysts with small molecules

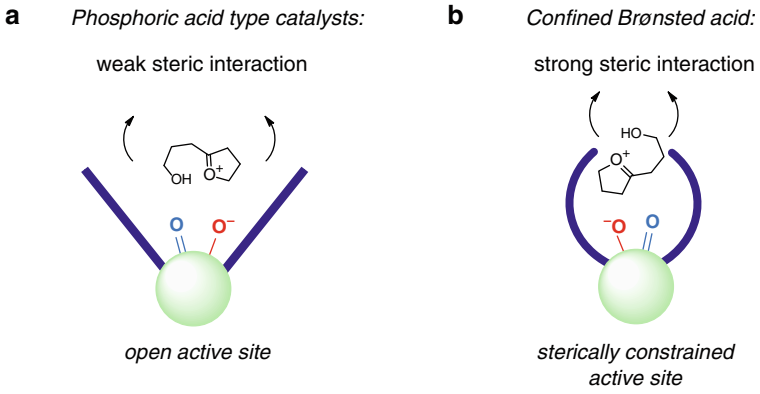

Scheme 22 Catalyst design

(anions shown in Scheme 24) [20]. The remarkable success of phosphoric acids in asymmetric catalysis is widely attributed to a bifunctional activation, in which one Brønsted acidic (–OH) and one Brønsted basic site (=O) are involved in the stabilization of a transition state (Scheme 23) [9, 10].

Although phosphates **A** and **B** have found wide application in asymmetric catalysis, it is challenging to further modify their steric environment because 3,3′-substituents on BINOL and SPINOL backbones radiate away from the active site (Scheme 24). C_1-symmetric anions **C** and particularly **D** provide a simple alternative way of introducing additional steric demand close to the active site via the additional *N*-substituent (Scheme 24). However, both of these possess several different Brønsted basic sites which can interact differently with the cationic intermediate resulting in low selectivity. Similarly, in the corresponding acid, an ensemble of catalytically active bifunctional species could be formed stabilizing

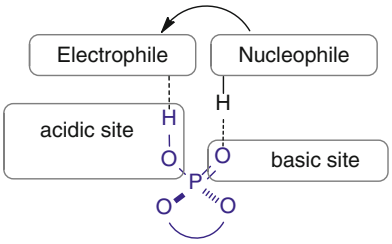

Scheme 23 Bifunctional activation of reactants with Brønsted acid/base pair in phosphoric acid catalysis

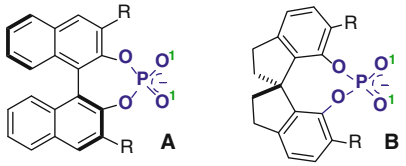

Feature: single Brønsted acid/base pair (C_2 symmetry)
Issue: 3,3'-substituents on BINOL radiate away from the active site

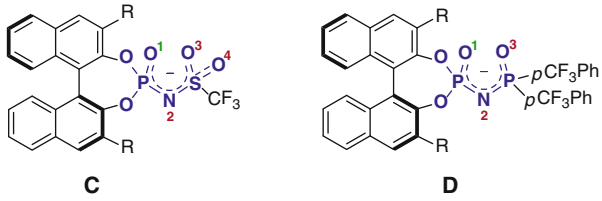

Feature: a simple way of introducing additional steric demand close to the active site
Issue: several different Brønsted basic sites, ensemble of catalytically active species

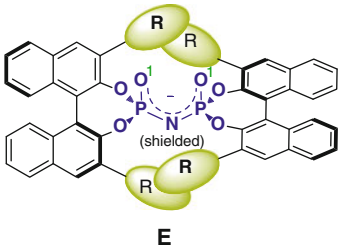

Feature: a simple way of introducing additional steric demand close to the active site
Feature: single Brønsted acid/base pair (C_2 symmetry)

Scheme 24 Development of conformationally locked C_2-symmetric imidodiphosphates

Table 3 Anion analysis

	A/B	C	D	E
Symmetry	C_2	C_1	C_1	C_2
Distinct Brønsted basic sites	**1**	**4**	**3**	**1**
Possible bifunctional sites in acid	**1**	**12**	**6**	**1**
Relative position of acidic/basic sites	Fixed	P–N, N–S rotation	P–N rotation	Fixed
Maximum steric demand	High	Variable[a]	Variable[a]	Very high

[a]Depending on the catalytic acid/base sites involved

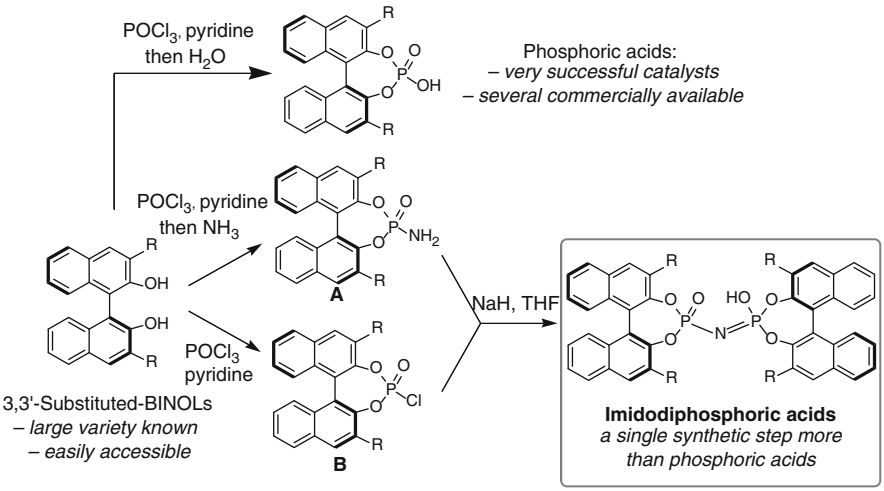

Scheme 25 Synthetic strategy for C_2-symmetric imidodiphosphoric acids

different transition states resulting in low selectivity. Structural analysis of anions **A**–**D** is given in Table 3.

A novel class of chiral anions **E** based on a C_2-symmetric imidodiphosphate anion was consequently designed featuring a single type of Brønsted basic site as found in C_2-symmetric phosphates **A** and **B** and increased steric bulk introduced via *N*-substitution like in anions **C** and **D** (Scheme 24). The catalyst architecture restricts the imidodiphosphate moiety to a single *O*,*O*-*syn* conformation between two identical interlocking BINOL subunits with bulky 3,3′-substituents. In this way, rotation around *P*–*N* bonds is prevented giving geometrically fixed acid/base pair. Additionally, the access to the undesirable alternative Brønsted basic *N*-site is blocked.

The "dimeric" structure of C_2-symmetric imidodiphosphoric acids enables a highly convergent synthetic approach. The synthesis requires only a single additional synthetic step compared to the synthesis of the corresponding phosphoric acids (Scheme 25) [57].

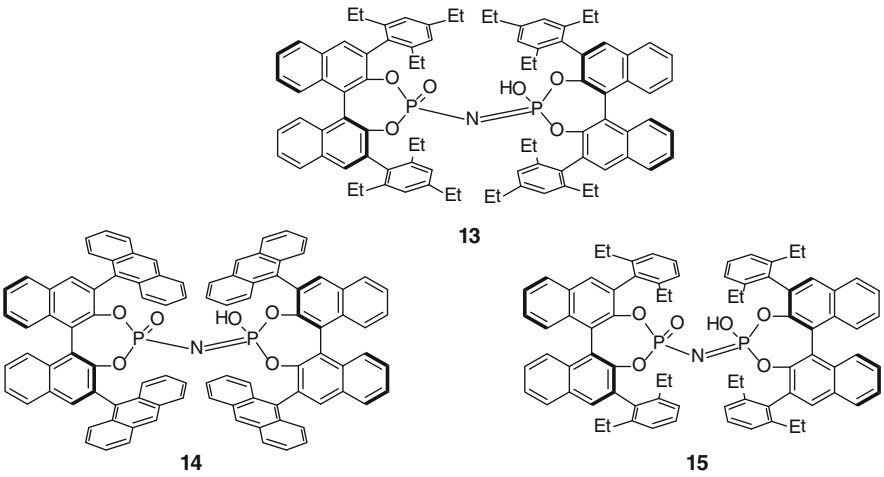

Scheme 26 Chiral C_2-symmetric imidodiphosphoric acids

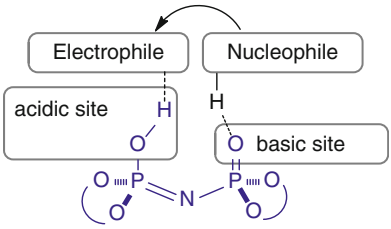

Scheme 27 Bifunctional activation of reactants with Brønsted acid/base pair in imidodiphosphoric acid catalysis

Based on this synthetic strategy, three imidodiphosphoric acids **13–15** with bulky substituents on the 3,3′-positions of the two BINOL backbones were reported (Scheme 26) [57].

Confined imidodiphosphoric acids provide completely different active moiety and significant increase in the steric demand of the chiral environment, while keeping crucial features of the phosphoric acids: C_2-symmetry of the anion and a single type of bifunctional active site. Compared to phosphoric acid catalysts, additional two atoms *P═N* are introduced between the Brønsted acidic and Brønsted basic sites (Scheme 27).

The crystal structure of imidodiphosphoric acid **13** revealed a confined active site placed within a extremely sterically demanding chiral environment (Fig. 1). Top view at the catalytic moiety shows how the two BINOL substituents surround the active site (Fig. 1b). From the bottom half, two remaining BINOL subunits completely block access to the imidodiphosphate (Fig. 1c) [57].

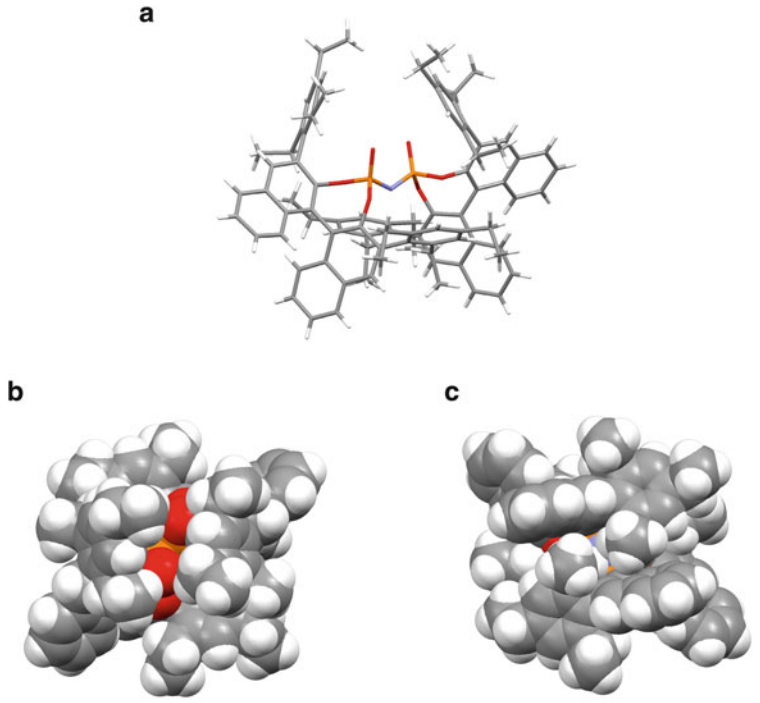

Fig. 1 Crystal structure of confined acid **13**: (**a**) *side view*; (**b**) *top view*; (**c**) *bottom view*

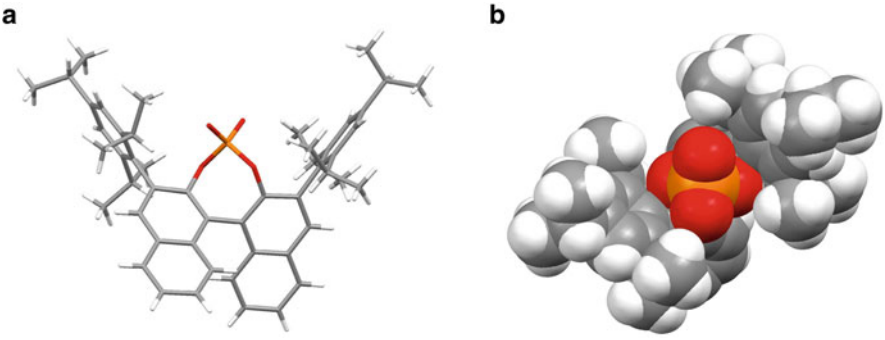

Fig. 2 (**a**) Crystal structure of ***TRIP*** anion; (**b**) view at the active site

For comparison, the crystal structure of one of the most popular and sterically demanding phosphoric acids, TRIP (**3**), is given in Fig. 2 [56]. The active site of TRIP is very open and accessible, while confined acid **13** possesses a cavity similar to those in enzymes.

7.3 Spiroacetalization

Extremely sterically demanding Brønsted acid catalyst **13** indeed efficiently catalyzed the asymmetric conversion of small and further unfunctionalized hydroxy enol ether substrates. Various spiroacetals were obtained with high enantioselectivity independent of the ring size of the enol ether by the formation of either 6- or 5-membered rings (Table 4) [57]. Catalyst **13** also enabled the first catalytic asymmetric synthesis of the natural product olean (entry 2). All these small spiroacetals in Table 4 are core structures of many natural products [6–8].

The formation of nonthermodynamic spiroacetals, featuring the less stable configuration of the spiroacetal stereocenter, presents a substantial challenge for organic synthesis. Confined Brønsted acid catalyst **13** enabled catalyst controlled access to both nonthermodynamic and thermodynamic spiroacetals in mild kinetic conditions [57]. Independent of the stereochemistry of the starting material, the formation of the spiroacetal stereocenter was controlled by the catalyst to give preferably the (*S*)-configuration. Nonthermodynamic spiroacetals were obtained with diastereomeric ratios from 5:1 to 23:1, although under thermodynamic conditions (aq. 3N HCl), the thermodynamic diastereomers were preferred with a dr of up to 1:124 (Scheme 28). Under kinetic conditions with achiral diphenylphosphoric acid, a 1:1–1:3 mixture of nonthermodynamic to thermodynamic spiroacetal is obtained.

Although the thermodynamic spiroacetal can be easily obtained in strongly acidic conditions that epimerize the acetal stereocenter, catalyst **13** is capable of providing the thermodynamic spiroacetal under kinetic conditions. Thermodynamic spiroacetals can be obtained with excellent diastereoselectivities that can even exceed thermodynamic ratios (Scheme 28) [57]. Such mild conditions for the spiroacetalization reaction might be essential in syntheses when other acid sensitive groups are present in the molecule, for example, other acetals and spiroacetals.

The spiroacetalization reaction might prove useful in the synthesis of natural products and biologically active molecules for which the desired spiroacetal stereocenter configuration cannot be accessed under thermodynamic conditions. Additionally, the method could also be applicable to obtaining either spiroacetal epimer in reactions that give similar mixtures of spiroacetal isomers under thermodynamic and kinetic conditions.

8 Conclusion

Although *O*,*O*-acetals are among the most common stereocenters in organic molecules, their catalytic asymmetric syntheses have only been achieved recently. Due to problems associated with asymmetric additions to oxocarbenium ions using chiral Brønsted acid catalysts, intermediates in the synthesis of acetals, design of a suitable reaction was necessary. We have presented the invention of a catalytic asymmetric intramolecular transacetalization reaction for the synthesis of acetals

Table 4 Catalytic asymmetric spiroacetalization

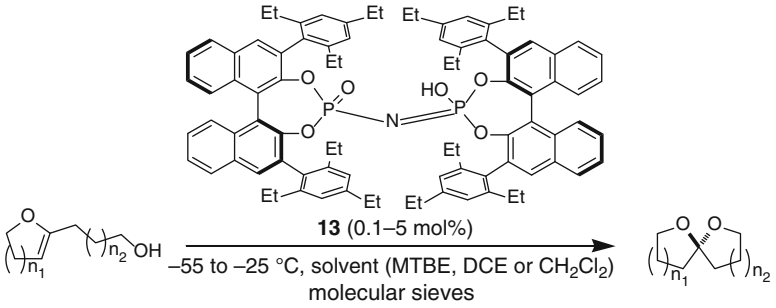

Entry	Substrate	Product	Yield (%)	er
1	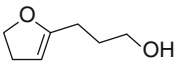		62	96:4
2	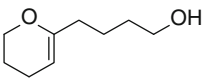	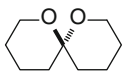	77	98:2
3	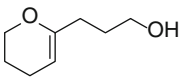	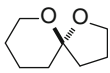	81	95.5:4.5
4	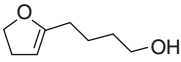	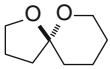	69	96:4
5	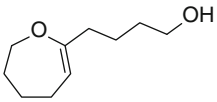	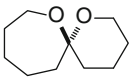	78	96:4
6	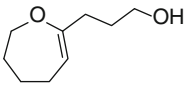	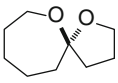	88	98.5:1.5

with the acetal carbon as the only stereogenic element. This somewhat unusual reaction later proved synthetically very useful for the kinetic resolution of homoaldols, highly valuable chiral building blocks. Kinetic resolutions of alcohols via acetal formation have not been known before.

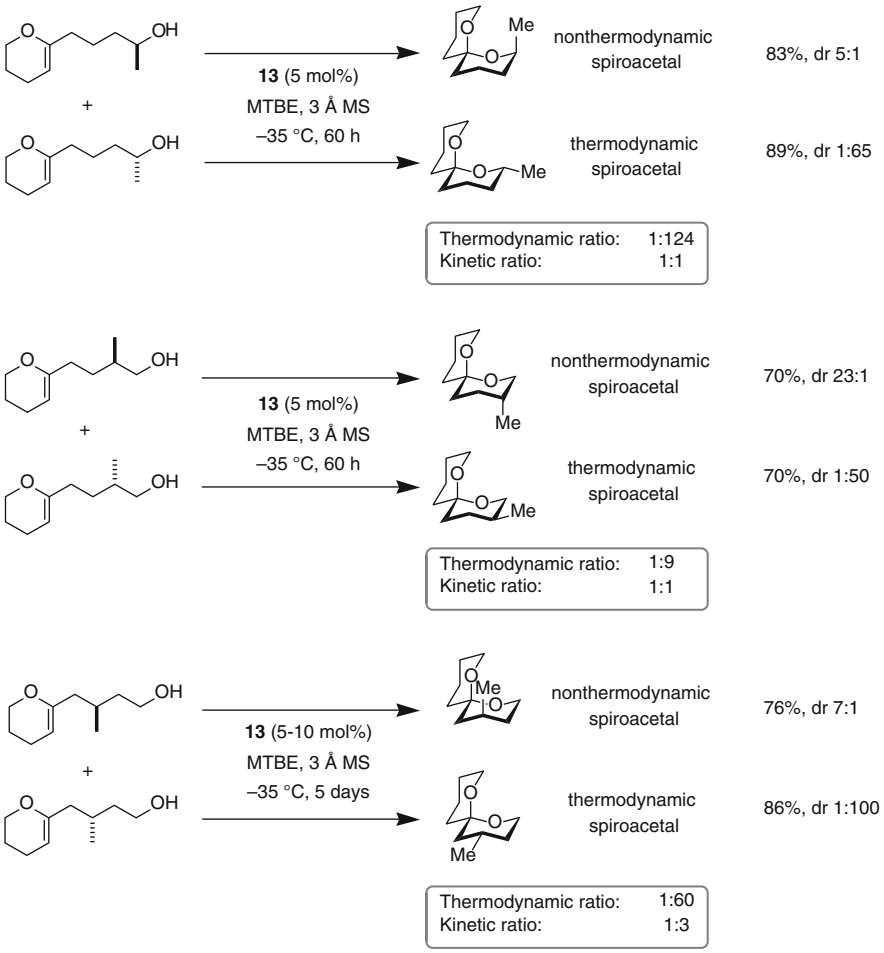

Scheme 28 Nonthermodynamic and thermodynamic spiroacetals

Fascinated by spiroacetals, a very distinctive subgroup of *O*,*O*-acetal, we next pursued their asymmetric synthesis. To achieve this goal we have rationally designed confined chiral Brønsted acid catalysts featuring extremely tight chiral pockets, reminiscent of those of enzymes. These catalysts enabled the development of the first asymmetric spiroacetalization reaction to access the natural product olean and other small unfunctionalized spiroacetals. In addition, the confined acid was able to control the formation of thermodynamic and nonthermodynamic spiroacetals, a long-standing issue in the synthesis of spiroacetal natural products.

We believe the concept of confined acids to be very general, even beyond Brønsted acid catalysis, and these and similar catalysts to be of use in tackling current challenges with reactions that include small volume and/or loosely organized transition states [58].

References

1. List B (2000) The direct catalytic asymmetric three-component Mannich reaction. J Am Chem Soc 122:9336–9337
2. Seayad J, Seayad AM, List B (2006) Catalytic asymmetric Pictet-Spengler reaction. J Am Chem Soc 128:1086–1087
3. Lee A, Michrowska A, Sulzer-Mosse A, List B (2011) The catalytic asymmetric Knoevenagel condensation. Angew Chem Int Ed 50:1707–1710
4. Müller S, Webber MJ, List B (2011) The catalytic asymmetric Fischer indolization. J Am Chem Soc 133:18534–18537
5. Carey FA (2006) Organic chemistry, 6th edn. McGraw-Hill, New York
6 Aho JE, Pihko PM, Rissa TK (2005) Chem Rev 105:4406
7 Perron F, Albizati KF (1989) Chem Rev 89:1617
8 Francke W, Kitching W (2001) Curr Org Chem 5:233
9 Akiyama T (2007) Chem Rev 107:5744
10 Terada M (2010) Synthesis 1929
11 Akiyama T, Itoh J, Yokota K, Fuchibe K (2004) Angew Chem Int Ed 43:1566
12 Uraguchi D, Terada M (2004) J Am Chem Soc 126:5356
13 Reisman SE, Doyle AG, Jacobsen EN (2008) J Am Chem Soc 130:7198
14 Terada M, Tanaka H, Sorimachi K (2009) J Am Chem Soc 131:3430
15 Zhang Q-W, Fan C-A, Zhang H-J, Tu Y-Q, Zhao Y-M, Gu P, Chen Z-M (2009) Angew Chem Int Ed 48:8572
16 Rowland GB, Zhang H, Rowland EB, Chennamadhavuni S, Wang Y, Antilla JC (2005) J Am Chem Soc 127:15696
17 Liang Y, Rowland EB, Rowland GB, Perman JA, Antilla JC (2007) Chem Commun 4477
18 Li G, Fronczek FR, Antilla JC (2008) J Am Chem Soc 130:12216
19 Cheng X, Vellalath S, Goddard R, List B (2008) J Am Chem Soc 130:15786
20 Vellalath S, Čorić I, List B (2010) Angew Chem Int Ed 49:9749
21 Rueping M, Antonchick AP, Sugiono E, Grenader K (2009) Angew Chem Int Ed 48:908
22 Ingle GK, Mormino MG, Wojtas L, Antilla JC (2011) Org Lett 13:4822
23 Nagano H, Katsuki T (2002) Chem Lett 31:782
24 Čorić I, Vellalath S, List B (2010) J Am Chem Soc 132:8536
25 Čorić I, Müller S, List B (2010) J Am Chem Soc 132:17370
26 Vedejs E, Jure M (2005) Angew Chem Int Ed 44:3974
27 Kourist R, Domínguez de María P, Bornscheuer UT (2008) Chembiochem 9:491
28 List B, Shabat D, Zhong G, Turner JM, Li A, Bui T, Anderson J, Lerner RA, Barbas CF III (1999) J Am Chem Soc 121:7283
29 S-y Tosaki, Hara K, Gnanadesikan V, Morimoto H, Harada S, Sugita M, Yamagiwa N, Matsunaga S, Shibasaki M (2006) J Am Chem Soc 128:11776
30 Hara K, Tosaki S-y, Gnanadesikan V, Morimoto H, Harada S, Sugita M, Yamagiwa N, Matsunaga S, Shibasaki M (2009) Tetrahedron 65:5030
31 Shintani R, Takatsu K, Hayashi T (2008) Org Lett 10:1191
32 Jarvo ER, Evans CA, Copeland GT, Miller SJ (2001) J Org Chem 66:5522
33 Angione MC, Miller SJ (2006) Tetrahedron 62:5254
34 Zhao Y, Mitra AW, Hoveyda AH, Snapper ML (2007) Angew Chem Int Ed 46:8471
35 Vedejs E, Chen X (1997) J Am Chem Soc 119:2584
36 Dehli JR, Gotor V (2002) Chem Soc Rev 31:365
37 Akiyama T, Saitoh Y, Morita H, Fuchibe K (2005) Adv Synth Catal 347:1523
38 Birman VB, Rheingold AL, Lam K-C (1999) Tetrahedron Asymmetry 10:125
39 Xie J-H, Zhou Q-L (2008) Acc Chem Res 41:581
40 Chung YK, Fu GC (2009) Angew Chem Int Ed 48:2225
41 Jiang M, Zhu S-F, Yang Y, Gong L-Z, Zhou X-G, Zhou Q-L (2006) Tetrahedron Asymmetry 17:384

42 Hoffmann S, Seayad AM, List B (2005) Angew Chem Int Ed 44:7424
43 Adair G, Mukherjee S, List B (2008) Aldrichimica Acta 41:31
44 Xu F, Huang D, Han C, Shen W, Lin X, Wang Y (2010) J Org Chem 75:8677
45 Cohen P, Holmes CFB, Tsukitani Y (1990) Trends Biochem Sci 15:98
46 Singh SB, Zink DL, Heimbach B, Genilloud O, Teran A, Silverman KC, Lingham RB, Felock P, Hazuda DJ (2002) Org Lett 4:1123
47 Agtarap A, Chamberlin JW, Pinkerton M, Steinrauf LK (1967) J Am Chem Soc 89:5737
48 Ueno T, Takahashi H, Oda M, Mizunuma M, Yokoyama A, Goto Y, Mizushina Y, Sakaguchi K, Hayashi H (2000) Biochemistry 39:5995
49 Uckun FM, Mao C, Vassilev AO, Huang H, Jan S-T (2000) Bioorg Med Chem Lett 10:541
50 Barun O, Kumar K, Sommer S, Langerak A, Mayer TU, Müller O, Waldmann H (2005) Eur J Org Chem 4773
51 Zinzalla G, Milroy L-G, Ley SV (2006) Org Biomol Chem 4:1977
52 Brasholz M, Sörgel S, Azap C, Reißig H-U (2007) Eur J Org Chem 3801
53 Baker R, Herbert R, Howse PE, Jones OT, Francke W, Reith W (1980) J Chem Soc Chem Commun 52
54 Haniotakis G, Francke W, Mori K, Redlich H, Schurig V (1986) J Chem Ecol 12:1559
55 Nakashima D, Yamamoto H (2006) J Am Chem Soc 128:9626
56 Klussmann M, Ratjen L, Hoffmann S, Wakchaure V, Goddard R, List B (2010) Synlett 2189
57 Čorić I, List B (2012) Nature 483:315
58 I. Čorić (2012) Asymmetric Brønsted Acid Catalysis: Acetals & Confined Catalysts, Köln University.

Top Organomet Chem (2013) 44: 195–232
DOI: 10.1007/3418_2012_46

Published online: 1 August 2012

Designing Molecular Catalysts for Selective CH Functionalization

Steven M. Bischof, Brian G. Hashiguchi, Michael M. Konnick, and Roy A. Periana

Abstract The design of molecular catalysts for the selective hydroxylation of hydrocarbons is an important challenge. Designing systems that couple the CH activation reaction with oxy-functionalization of the resulting M–R intermediates has emerged as a promising strategy to meeting this goal. A large number of well-defined CH activation systems have been reported, but relatively few have been utilized as efficient hydroxylation catalysts. The primary reason for this observation is that most efficient CH activation catalysts are incompatible with the conditions required for oxy-functionalization of M–R. Significantly, the reported systems for CH hydroxylation suffer from a combination of challenges related to product protection, poor reaction selectivity, low catalytic activity, stability, and/or expensive product separation which have prevented further development. The design of next generation systems that are more active for both the CH activation and M–R functionalization steps will be directly dependent on improving reaction selectivity and stability of the catalyst systems. Herein, we outline the requirements for meeting these goals in regard to developing new oxy-functionalization catalysts and describe our efforts in this area.

Keywords CH activation · CH functionalization · Functionalization · Hydrocarbons · Hydroxylation · Oxidation

Contents

S.M. Bischof, B.G. Hashiguchi, M.M. Konnick, and R.A. Periana (✉)
Department of Chemistry, The Scripps Energy & Materials Center, The Scripps Research Institute, Jupiter, FL 33458, USA
e-mail: rperiana@scripps.edu

Abbreviations

[M]	Ligated metal complex
BAM	Base- or acid-modulated catalysis
Bpy	2,2′-Bipyridine
Bpym	2,2′-Bipyrmidine
BV	Baeyer–Villiger
Cp^*	Pentamethylcyclopentadienyl
DFT	Density functional theory
EDG	Electron-donating group
EWG	Electron-withdrawing group
HL	Protic ligand
HOMO	Highest unoccupied molecular orbital
IPI	2,6-Diimidizoylpyridine
L	Ligand
LUMO	Lowest unoccupied molecular orbital
M	Metal
MTO	Methyltrioxorhenium
Ox	2-Electron acceptor oxidant
P	Protecting group
R	Hydrocarbon
RT	Room temperature
TOF	Turnover frequency
TON	Turnover number
TRF	Transalkyl reductive functionalization
TS	Transition state
X	Leaving group (e.g., halide, triflate, sulfate)
YO	O-atom transfer oxidant

1 Introduction

The selective oxidative functionalization of alkanes can play an important role in more efficiently utilizing the world's carbon feedstocks. Such technology can help to reduce emissions, reduce costs, and provide a transition to a nonfossil fuel-based economy. The current technologies utilized by the petrochemical industry typically involve high temperature methods for transforming alkanes into more useful

functionalized products; examples include catalytic cracking, steam reforming, and the Fischer–Tropsch process [Eqs. (1)–(3)] [1–7]. Unfortunately, these processes are both energy and capital intensive and do not operate at optimal atom or energy efficiencies. A much more attractive method would involve a lower temperature and selective process that converts alkanes directly to primary oxidation products such as olefins, alcohols, and long-chain hydrocarbons.

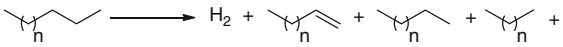

(1)

$$CH_4 + H_2O \rightarrow CO + 3H_2 \tag{2}$$

$$(2n+1)H_2 + nCO \rightarrow C_nH_{(2n+2)} + nH_2O \tag{3}$$

Direct, selective CH functionalization of alkanes at lower temperatures, particularly of methane, is a difficult challenge due to several factors, including the large C–H homolytic bond strengths (104.9 kcal/mol) [8, 9], high ionization potentials (12.5 eV) [10, 11], low solubility (~1 mM) [12–15], low electron affinity (1.2 eV) [16], low acidity ($pK_a = 48$), and proton affinity (~127 kcal/mol) [17]. The most desirable products from alkane feedstocks are the primary oxidation products (i.e., olefins and alcohols). However, commercially available oxidation catalysts are not sufficiently selective for the generation of these compounds from the parent alkanes in the high yields required for large-fuel or commodity-scale processes. Likely, this is because the mechanisms for the current catalysts involve free radicals or reactions that proceed with radical character. This would result in faster rates of reactions of the primary oxidation products (e.g., methanol where the CH bond strength is ~96 kcal/mol) relative to the parent alkanes (~105 kcal/mol for CH_4). Consistent with that, there are only a few cases in which, the homolytic CH bond strengths of the product are uniquely higher than the starting alkane (e.g., in butane to maleic anhydride or propane to acrylic acid), where the product CH bonds are all vinylic (CH = ~110 kcal/mol) [18–20]. These considerations suggest that the development of low temperature, direct, and selective processes for the conversion of alkanes to primary oxidation products such as alcohols will require new classes of catalysts that operate without the generation of free radicals or by CH cleavage transition states with significant radical character.

1.1 The Early Focus: CH Activation

From my early days in chemistry, my interests have been focused on reactivity and reaction mechanisms rather than the synthesis of materials such as polymers or organic molecules. I did not realize it then, but now, I see that it was the idea of controlling and understanding the imaginary transition state that fascinated me. Given this interest, much of my career has focused on the design of catalysts for the selective,

low temperature conversion of small molecules such as methane. I considered methane to be an ideal target for two primary reasons: (a) the enormous value of the solution and resulting strong interest from industry and scientific community would allow for sustained efforts and support and (b) methane contains only one type of bond, that in contrast to more complex molecules with many types of bonds, could yield to "rational" (or so-called enlightened empiricism) catalyst design.

My first significant encounter with the chemistry of poorly reactive CH bonds was during a lecture by Prof. George Olah (1994 Nobel Prize in Chemistry) at UC Berkeley where he described the fascinating reaction of "magic acid" with alkanes. The idea that a simple proton reacts so readily with "inert" CH bonds made a lasting impression. It was an exciting time for CH bond chemistry, as the Bergman group had just reported the first well-defined example of CH activation of an alkane with a transition metal complex [21]. My goal was to understand the mechanism of this amazing reaction. I recall considering that there had to be a connection between the cleavage of CH bonds with transition metal complexes and those with more classical species such as protons, carbocations, carbenes, and carbanions. The analogies made by Hoffmann [22–24] between CH cleavage with a singlet carbene and the Bergman [25] $CpIr(PMe_3)$ system solidified this view. A defining consideration from my early graduate work was providing strong evidence that the CH activation reactions with alkanes involved the so-called alkane complex that was analogous to an olefin complex. This made it clear to me that one can consider the CH activation reaction to involve separate CH coordination and CH cleavage steps. These considerations set the stage for my later discoveries at Catalyica on the reactions of electrophilic metals in sulfuric acid solvent.

A particularly attractive method for functionalizing hydrocarbons would be to utilize the CH activation reaction with homogenous transition metal complexes to generate M–R intermediates, followed by oxy-functionalization of this intermediate to generate the product, RX, and regenerate the catalyst, MX (Scheme 1) [26–31]. We define the CH activation reaction as a formal heterolytic cleavage reaction between a metal complex and a hydrocarbon CH bond to generate an M–R intermediate without the involvement of free radicals or transition states with radical character. Many systems that carry out the CH activation reaction have been reported, and much is now known about the reaction mechanism and subsequent chemistry [25, 26, 29]. Several characteristics of the CH activation reaction led us to believe that it would be an ideal starting platform for the development of new C–H functionalization methodologies, including (a) many of the reactions proceed by concerted, two-electron (heterolytic) atom transfers rather than by homolytic cleavages; (b) reactions proceed in the first coordination sphere of the metal and can be controlled for both CH bond coordination and CH cleavage; (c) the high energy costs of breaking the strong CH bond can be reduced by the concerted formation of a M–C bond; (d) transition metals allow access to multiple geometries and oxidation states; (e) the catalyst properties can be tuned through the use of spectator ligands; and (f) the steric and electronic properties differ from that of classical strong acid/base or radical chemistry with different reaction selectivity. These considerations led us and many others to believe that when properly tuned, CH activation-based catalysts may facilitate the

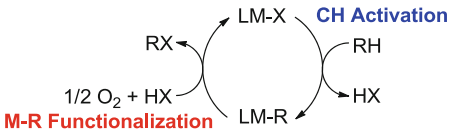

Scheme 1 General catalytic cycle for the CH activation/M–R functionalization of a hydrocarbon (RH)

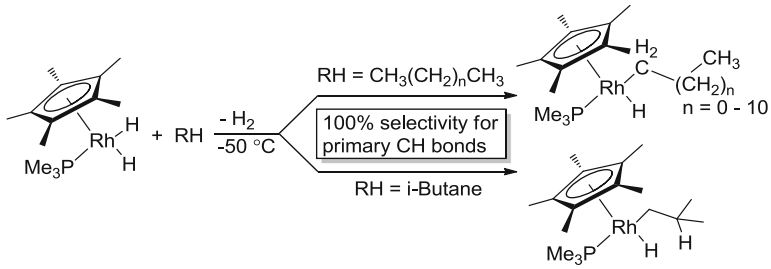

Scheme 2 Bergman $Cp^*Rh(PMe_3)H_2$ system

partial oxidation of hydrocarbons at far lower temperatures and with higher selectivity than is currently possible.

Indeed, the selective characteristics of the CH activation reaction can be exemplified by the reactions of the $[Cp^*Rh(PMe_3)]$ motif developed in the Bergman group, and that was the basis for my thesis [32–34]. As shown in Scheme 2, this metal complex reacts at −50°C and with almost 100% regioselectivity with primary over secondary or tertiary alkane CH bonds. Consistent with the reaction proceeding via a concerted, heterolytic, two-electron atom-transfer reaction mechanism (rather than by the more typical hydrogen atom or hydride abstraction), this selectivity is different from those exhibited in reactions with free radicals (or via transition states with significant radical character) or carbocations. Typically, the relative rates of radical reactions strongly correlate with the relative homolytic bond strength of the CH bond. However, it is generally observed that in systems that operate by the CH activation reaction, sp^2 CH bonds with higher homolytic bond strengths (~112.8 kcal/mol for $H–C_6H_5$) react faster than sp^3 CH bonds with lower homolytic bond strengths (~104.9 kcal/mol for $H–CH_3$). This is in part due to the driving force for the formation of the M–C bond, which, in the case of sp^2 carbons, is strengthened by both σ and π bonding contributions [35, 36]. Furthermore, the significant difference in selectivity is also shown in the reactivity of aliphatic alcohols relative to the parent alcohols. The homolytic bond strengths of sp^3 CH bonds alpha to the hydroxyl group (e.g., ~96.0 kcal/mol for $H–CH_2OH$) are lower than the CH bonds in the parent hydrocarbon (e.g., ~105 for $H–CH_3$), and, as expected, alcohols are much more reactive in radical reactions. In contrast, it has been shown that while the CH activation reaction does not show higher reactivity for the parent hydrocarbon relative to the alcohol, these substrates show relatively similar reactivity [37].

While the selective characteristics of the CH activation reaction may lead to substantial benefits over the previously described industrial hydrocarbon oxidation catalysts, the advantages of the CH activation reaction to generate M–R

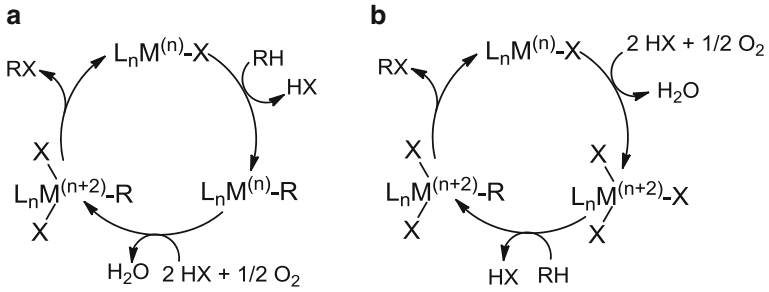

Scheme 3 Catalytic cycles for CH activation/M–R reductive functionalization of RH to RX, where (**a**) CH activation occurs when M is in the n oxidation state and (**b**) M is in the $n + 2$ oxidation state

intermediates from hydrocarbons are moderated by an inherent key challenge, the requirement for a subsequent M–R functionalization reaction to be carried out that *must* be compatible with the CH activation reaction. As shown in Scheme 1, the coupling of these two steps is the minimum requirement for efficient catalysis. In addition, it is also ideal for the functionalization reaction to proceed within the coordination sphere of the metal in order to maximize selectivity, reaction control, and avoid free radicals. These requirements are likely why only a few systems for the functionalization of hydrocarbons have been developed that operate by the CH activation reaction.

Following the pioneering work by Shilov [38] with Pt^{II} in aqueous HCl, the first report of efficient catalysts for the selective functionalization of hydrocarbons was based on the use of electrophilic metals in acidic media and operated by a general CH activation/M–R functionalization sequence (Scheme 3). Several systems have been developed based on soft, late, transition metals such as Pt^{II} [26, 39], Hg^{II} [40, 41], Pd^{II} [42, 43], and $Au^{I/III}$ [44, 45] in strong acid solvents. Studies have shown that these catalysts operate via facile CH activation to generate discrete M–R intermediates and a subsequent M–R functionalization to generate oxygenated products. Many of these systems showed extraordinarily high rates of CH activation and moderate yields of oxy-functionalized hydrocarbons.

As shown in Scheme 3, electrophilic CH activation-based catalysts can undergo CH activation in either the lower (LM^nX) or higher oxidation ($LM^{(n+2)}X_3$) states of the catalyst. Thus, in systems such as Hg^{II} and Pd^{II}/Pd^0, it is believed that the CH activation is much faster and proceeds in the higher oxidations states. In the case of the Pt^{II}/Pt^{IV} systems, calculations and experiment have shown that the CH activation is carried out with the lower oxidation state. Interestingly, in the case of the Au^I/Au^{III} system, both oxidation states are active for CH activation. These differences can be attributed to the requirement that the metal center must be both labile and highly electrophilic. Lability is important since the CH bond, a very weak nucleophile, must enter the first coordination sphere of the metal for the CH cleavage to take place. Indeed, in all of these systems, the energetics for this coordination step substantially contributes to the overall activation barrier.

These considerations demonstrate that strongly acidic media are essential in electrophilic systems. The acid solvent plays an important role as a weakly coordinating media that is resistant to oxidation and facilitates in alkane coordination by anion protonation increasing metal lability. The acid also plays an important role in the M–R functionalization step. In all of these systems, M–R functionalization proceeds by reductive functionalization where the metal center is reduced by two oxidation states from M^{n+2} to M^n [Eq. (4)]. Consequently, as with the CH cleavage, it can be expected that this step would be facilitated by increased electrophilicity at the metal center as this favors reductive functionalizations.

$$L_nM^{n+2}(R)X_2 \rightarrow L_nM^nX + RX \tag{4}$$

Unfortunately, the very strong electrophilic properties that lead to the efficiency of the reported systems also led to strong inhibition of the CH activation reaction as the oxidation reactions progressed. This inhibition results from competitive coordination of the water and methanol to the active metal center, given the much stronger nucleophilicity of these species relative to hydrocarbon CH bonds. This competitive inhibition limits the concentration of methanol and water that can be produced during the course of the reaction. At higher concentrations, the reaction rates are impractically slow for commercialization. As a result of the high affinity between the strong acid solvent and products, studies show that the cost of separation of the products makes a process based on Scheme 3 uneconomical [26].

To alleviate these challenges, we [46–49] and others [50–52] have moved to utilize lower oxidation state (I, II, or III) cations of the less electronegative transition metals to the left of Pt and Pd in the periodic table such as Ir, Rh, Os, Ru, and Re. Electronegative metals further to the left (such as W, Mo, Ta, etc.) were considered to be too oxophilic and likely generate insoluble oxides under the oxidative conditions necessary for the conversion of methane to methanol [53–55]. A second, related strategy is to utilize the same electronegative metals (Pt, Pd, etc.) by moderating the electrophilicity of the metal cations with strong donor ligands. The expectation is that with these less or non-electrophilic metal cations, competitive inhibition of the CH activation reaction by coordination of either methanol or water may be minimized. Importantly, if facile CH activation reactions in less or nonacidic solvents were developed, more coordinating species such as methanol or water would have a lower binding affinity, and economical product separations might be possible.

Indeed, most of the early reported CH activation reactions are based on these less electronegative metals, and in many cases, the reactions are extraordinarily facile and selective [25–31]. However, the general observation is (unlike the more electrophilic metals utilized in current working systems) that these reactions have not led to catalytic systems that convert hydrocarbons to oxy-functionalized products. A primary reason for this is that the oxy-functionalization reaction of M–R required does not operate by the mechanism shown in Scheme 3. The fundamental basis for this is the cations of the less electronegative metals such as

Ir^{III} and Ru^{III} that are much less oxidizing and electrophilic than metal cations such as Pd^{II} or Pt^{IV}. As a result, the M–R intermediates resulting from metals such as Ir and Ru are much less positively charged and electrophilic at the R group. Therefore, they cannot undergo facile attack by weak nucleophiles to generate functionalized products by a two-electron reduction metal center [56, 57]. However, by making these same metals more electron-rich by utilizing the lower oxidation state cations (e.g., Ir^{I} and Ru^{II} vs Ir^{III} and Ru^{III}) of the less electrophilic transition metals to the left of Pt in the periodic table might provide a strategy to overcome the product inhibition issues.

The issues encountered in the early developmental stages of the electrophilic systems will require new advances on understanding CH activation and M–R functionalization pathways. Product separation, product protection, catalyst stability, catalytic rates, and selectivity will need to be addressed, emphasized, and balanced to develop a viable process in next generation systems. Herein, we discuss our perspective on the development of the first generation systems which have led us to design second generation, less electrophilic catalysts in an effort to address the challenges encountered in developing hydrocarbon functionalization catalysts which utilize the extraordinary characteristics of the CH activation reaction.

2 Discussion

We have identified four general challenges that have prevented or would prevent the use of most of the known poorly or non-electrophilic CH activation systems for the design of new hydroxylation catalysts based on a CH activation/M–R functionalization catalytic sequence: (a) systems are unstable, (b) the CH activation is inhibited by conditions required for M–R functionalization, (c) there is no facile pathway for the M–R functionalization reaction, and (d) there is no way to limit reaction of the product from over oxidation. In addition to these challenges, it is critical to consider that useful catalysts must *simultaneously* meet three minimum target requirements of high selectivity, fast rates, and long life. As noted elsewhere [28, 31], strategies to meet these target requirements must be considered simultaneously in any de novo catalyst design. This can be *extraordinarily challenging* since all three requirements depend on both catalyst composition and structure as well as reaction conditions. At the fundamental level, the enormity of the challenge becomes apparent since meeting these requirements is dependent on simultaneously controlling the relative energies of several transition states (TS) (Scheme 4). Specifically, the rates of both CH activation and functionalization must be enhanced (k_1 and k_2 must be fast, Scheme 4) in order to achieve the target rates for product synthesis. Simultaneously, the transition states for catalyst decomposition and product over oxidation must be raised to provide high selectivity (k_3, k_4, and k_5 must be slow, Scheme 4). This suggests the optimal conditions for product generation occur when k_1 and k_2 are maximized while k_3, k_4, and k_5 are minimized. Given these challenges, it would be

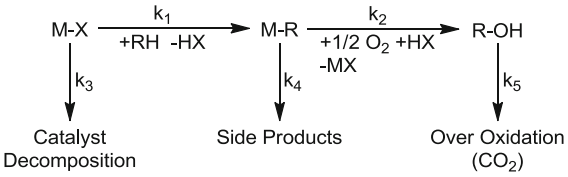

Scheme 4 Controlling transition states to maximize product generation, product selectivity, and avoid catalyst decomposition

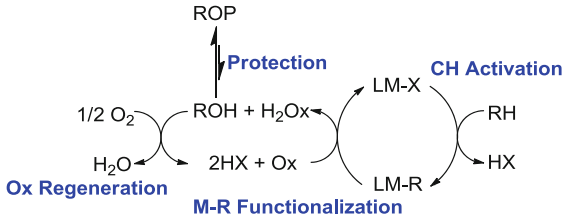

Scheme 5 General strategy for catalyst design based on coupling CH activation with M–R functionalization using an O-atom donor or electron-acceptor, Ox, that is regenerated by air in a separate step

ideal to identify one of the three requirements to provide a focal point in the design of new systems.

The general approach we are following in designing such catalysts is shown in Scheme 5. In this scheme, hydrocarbons react with an LM–X species to give LM–R via CH activation. In the functionalization step, an O-atom donor or electron-acceptor, Ox, is utilized to generate the product, and the reduced species, H_2Ox, is regenerated in a separate step by reaction with molecular oxygen. This approach of using an air-recyclable oxidant is fundamentally different from approaches requiring the direct use of O_2 or non-air-recyclable oxidants. The merits of this approach have been discussed elsewhere [58]. One key component of this method is that during the course of the reaction, the product is rapidly converted to a protected species to overcome issues with over oxidation (k_4 and k_5 in Scheme 4). We have identified that the concept of product protection is a main guiding factor in the design of new oxy-functionalization catalyst systems.

2.1 The De Novo Approach

The most important component to any new system is high selectivity. As previously discussed, the bonds strengths between H–CH_3 (104.9 kcal/mol) and H–CH_2OH (96.0 kcal/mol) present a challenge that heterogeneous catalysts have yet to overcome. Furthermore, the volatility of the products versus rate of reaction is of further consideration when discussing highly selective catalysts. This presents a key challenge to developing practical processes where products are of comparable reactivity to the substrate. In the case when the product is much less volatile with

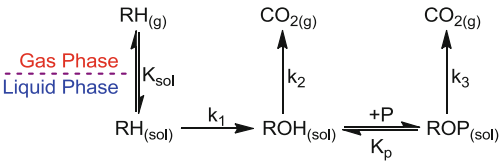

Scheme 6 The overall kinetic requirement for high yields and selectivity by product protection (*g* gas phase, *sol* solution phase). Poor selectivity is observed when $K_p < 1$ and $k_2 > k_1$. High selectivity is observed when $K_{sol} \gg 1$, $K_p \gg 1$ and $k_3 \ll k_2 \ll k_1$

comparable reactivity toward the catalyst, poor selectivity will be observed at high conversion since the concentration of starting hydrocarbon exposed to the catalyst will be much lower than that of the product. In that case, where the product is of comparable or higher volatility, the selectivity at high conversion will be higher, but kinetic analysis would show that even in this case, the requirements for high conversion at high selectivity cannot be met.

Due to the similar reactivity of possible oxidation products relative to the parent alkane, we have identified that product protection will likely be an underlying factor in any successful oxy-functionalization catalyst. Therefore, we must understand why product protection will be essential to any catalytic system. The overall general kinetic basis and requirements for one form of protection are shown in Scheme 6. In this strategy, the desired product (an alcohol) is converted to a protected form with a protecting group (P) to give ROP. A key requirement for this strategy is that the protected form of the product must be considerably less reactive than both the desired product and the starting hydrocarbon. The protection reaction must also be both rapid and essentially convert the desired product to the protected form (when $K_p \gg 1$). This ensures that the concentration of the desired, unprotected product is significantly lower than that of the hydrocarbon substrate. Poor reaction selectivity would be observed if the concentrations of the product and substrate were of similar reactivity (k_2 and k_3 are large). This is particularly challenging in cases where the substrate is more volatile than the product, as this leads to very low concentrations of substrate and high concentrations of product in the catalyst phase under practical reaction conditions. Methane exemplifies the situation where light hydrocarbons are more volatile than their respective oxygenated products. Practical considerations would mandate that the protecting group be present in large excess (to ensure high TON and high concentrations of the protected product), inexpensive, and the reaction be readily reversible in a separate step after completion of the reaction. Ideally, large concentrations of product could be built up when $K_{sol} \gg 1$, $K_p \gg 1$ and $k_2 \ll k_3 \ll k_1$; thereby, maximization of protected product (ROP) would be realized.

We believe that it will be important to implement a general protection strategy for all systems because it is unlikely that any catalyst, including those based on the CH activation reaction, could be designed that would be substantially more reactive with the parent hydrocarbon than the product without some form of product modification. Therefore, we must decide on what is the most ideal product for the

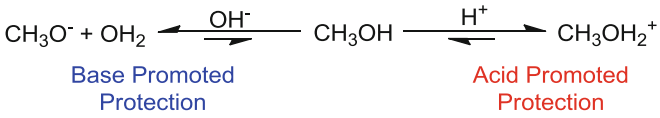

Scheme 7 Product protection strategies for CH_3OH in the overall oxidation of methane

oxidation transformation. One stipulation of choosing an intended route is to decide on a way to protect the product from further reaction as highlighted in Scheme 6, where poor product selectivity may arise due to lack of product protection. Due to the comparable reactivity between C–X bonds and C–H bonds, we must utilize methods of conversion and protection that do not rely on radical processes as whatever C–X product was formed would readily react further and overall reaction selectivity would be reduced. Consequently, our catalyst design must be based on a protection strategy that can meet the kinetic requirements discussed above. Importantly, a review of the outlined requirements for any protection strategy suggests the following: (a) the protected product must be less reactive than either the substrate or product, (b) essentially completely convert the product to the protected form, (c) be present in large excess, (d) be inexpensive, and (e) be capable of being easily and inexpensively removed and recycled in a separate reaction step. Typical organic protection strategies will likely not be practical since these reagents are expensive, react too slowly, decompose or react during the course of the reaction, or inhibit catalysis.

Knowing that any reaction for a commercial process would be executed on very large scale suggests that whatever mechanism is used to "protect" the product must be fast, selective, reversible, and low cost. The other requirement for any protection methodology is that it should be readily reversible as reactions must build up >1 M product to be viable. One possible approach would be the use of acids or bases. Acid or base reactions are typically diffusion controlled, instantaneous, and are easily reversible. Therefore, protonation or deprotonation of a substrate may be an ideal electronic protection methodology to avoid over oxidation of our C–X species. An effort to reduce the number of electron or oxidation state changes is also ideal, and given that acid/base reactions are a possible protection strategy, we identify that methanol may be an optimal target. CH_3OH is the first oxidation state change of CH_4, and the reactive alcohol group would readily be available for base or acid electronic modification (Scheme 7). This allows the use of a simple acid protonation or base deprotonation to give a strongly withdrawing or donating protecting group; therefore, further reaction with the catalyst due to the fast, simple, and easy electronic protection would be prevented.

The use of an electronic protection strategy may seem like an odd approach; however, there is precedent for such a methodology. For example, the nitration of benzene by an electrophilic Friedel–Crafts reaction generates the primary functionalized product, mono-nitrobenzene, at high conversion of benzene with high selectivity. The mono-nitrobenzene is protected relative to benzene because the nitro group is electron-withdrawing, and the mechanism of reaction generates positive charge in the TS during the rate limiting step. Similarly, protonation of the

lone pair on the oxygen of the –OH group of MeOH to generate $[CH_3OH_2]^+$ could lead to a similar electronic protection of methanol. Since the $–OH_2^+$ group is strongly electron-withdrawing relative to –OH group, the protonated methanol is protected because if CH activation proceeds through an electrophilic mechanism, positive charge would be built up during the cleavage TS leading to selectivity for CH_4 over MeOH. This is not unexpected since a protonation would be expected to substantially change the electronic properties of a substrate.

In a similar, but complimentary, manner to the use of a strongly acidic solvent to protect by protonation, it seems plausible that strongly basic solvents could also be used to deprotonate MeOH. The deprotonation of methanol to CH_3O^-, as shown in Scheme 7, would also be viewed as an analogous electronic protection strategy. The electronic properties of the methoxide methyl group are substantially different from that in methanol, and the protection is based on proton transfer reactions that can readily be reversed in a separate reaction by addition of water. However, due to the strong nucleophilic character of methoxide, the use of an electrophilic mechanism would likely not lead to success. The generation of positive charge buildup in an electrophilic-type mechanism would readily react with CH_3O^-. Therefore, the use of nucleophilic mechanisms, where negative charge is built up during the TS, would likely be required for an approach based on this strategy.

In considering the basis for protection and effectiveness of which strategy was best, it was apparent to us that the strategy of proton transfer between the solvent and the product could be particularly effective and potentially quite unique given the characteristics discussed above. It would likely only be successful with a product such as methanol with nonbonding lone pairs on the oxygen that can be reversibly protonated or a mildly acidic hydroxyl group that can be deprotonated. This led us to believe that alcohols (MeOH specifically for CH_4) are the best targets for oxy-functionalized products of hydrocarbons. It is unlikely this strategy would operate with hydrocarbon products such as olefins (it is likely that addition of the acid to the olefin would not be sufficiently fast or generate a "protected" product) and almost certainly not with saturated products such as higher alkanes (that are effectively inert to acids). This could suggest that two potentially practical schemes for protection of methanol exist based on either protonation or deprotonation of the substrate.

Importantly, the keys to utilizing such a protection scheme are identifying catalysts that can operate in strongly acidic or basic media. For systems that operate in acidic media, the following conditions must be met: (a) facile CH activation by mechanisms with positive charge buildup in the TS; (b) CH activation that does not react with protonated, protected MeOH; (c) compatible M–R functionalization reactions; and (d) acid soluble and stable catalysts. Conversely, systems that operate in basic media would need to have the following criteria met: (a) facile CH activation reactions that operate by mechanisms that will ensure protection of the methoxide from by retarding further functionalization of the CH bonds of methoxide, (b) facile M–R functionalization steps that are compatible with the CH activation steps and the reaction media, and (c) systems that are soluble and stable to strongly alkaline media. Additionally, this protection strategy will be coupled to an oxidant regeneration strategy (Scheme 5). These considerations provided a framework for our design of catalysts that operate via the CH activation

reaction to convert hydrocarbons to oxy-functionalized products, specifically methane to methanol.

2.2 Two Classes of Catalysts

The identification of MeOH protection strategies has highlighted that two distinct sets of conditions exist that lead to protection. Recalling Scheme 7, we have highlighted that either strong acids or bases efficiently protect MeOH using low-cost, easily reversible, proton transfer reactions to chemically protect the product. We further identified that to avoid reactions with the chemically protected product, that reactions must proceed by either electrophilic (protonation-based protection of MeOH to $MeOH_2^+$) or nucleophilic (deprotonation-based protection of MeOH to MeO^-) mechanisms. To garner a better understanding of what the ideal catalytic motif may look like, we considered a product to reactant analysis of our general catalytic cycle (Scheme 5). This allows for consideration of the LM–R functionalization step, which we have identified in our work as the least developed and likely most important step in an overall catalytic cycle, without considering the CH activation step. This thinking is crucial because while many systems are known to do CH activation, very few have led to oxy-functionalized products in one step. A product to reactant analysis leads to general considerations of the properties, reaction conditions, and mechanism for the facile functionalization of an LM–R complex. Organic chemistry provides an excellent starting point, as this field can be seen as the largest body of systematized, concerted, selective, atom-transfer reactions with carbon. A simple, but powerful, concept in organic chemistry is that reactions can occur by three possible electronic reaction mechanisms: electrophilic, ambiphilic, or nucleophilic. Therefore, we can reason that the best way to induce efficient functionalization is to increase either the electrophilicity or nucleophilicity of the hydrocarbyl fragment. We considered that extending the concepts of nucleophilic and electrophilic C–O bond-forming reactions in organic chemistry to the field of organometallic chemistry would lead to new reactions for the conversion of LM–R to oxy-functionalized products.

As it might be expected, reaction with negatively or positively charged carbon groups to generate C–O bonds is mechanistically different. As shown in Fig. 1, there are two well-established groups of C–O bond-forming reactions in organic chemistry that proceed without the involvement of free radicals. In one class, the carbon groups are electrophilic as a result of attachment to electron-withdrawing groups (EWG), e.g., $Cl–CH_3^{\delta+}$ and $CF_3OS(O)O–CH_3^{\delta+}$, and react by facile concerted, non-free radical, heterolytic displacement reactions with O-nucleophiles, such as HO^- or H_2O, to generate a C–O bond [59]. In contrast, formation of C–O bonds from carbon groups that are nucleophilic, as a result of attachment of the carbon group to electron-donating groups (EDG), proceeds by fundamentally different mechanisms. Thus, as shown in Fig. 1b, C–O bond formation in these cases proceeds by intramolecular attack of the nucleophilic carbon on O-electrophiles. One of the most facile examples of this type of C–O bond formation by a facile, concerted, non-free radical, heterolytic reaction is the

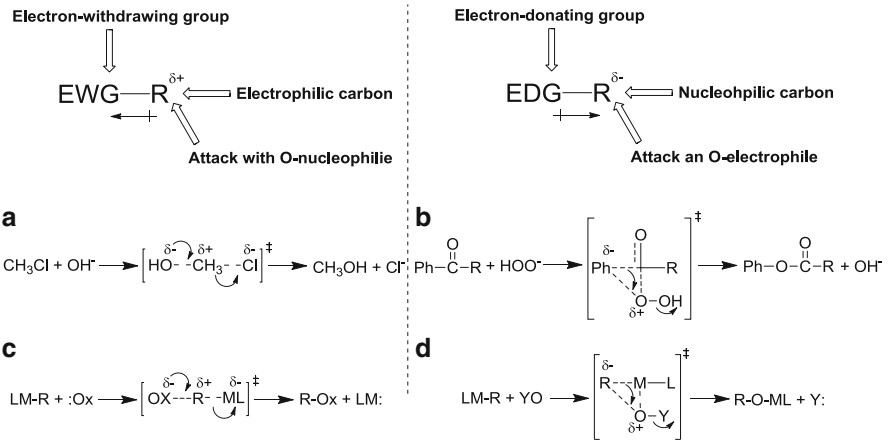

Fig. 1 Comparisons showing the similarities between C–O bond-forming reactions in organic and organometallic chemistry

Baeyer–Villiger or Dakin reaction for the conversion of phenyl ketones to phenyl esters [60, 61]. The concerted atom migration reaction in Fig. 1b proceeds by a fundamentally different mechanism than the displacement reaction shown in Fig. 1a. In this case, the C–O bond formation proceeds by attack of the nucleophilic carbon of $[(HOO)(R')C(O)–R^{\delta-}]^-$ on an electrophilic O-atom of HOO^- that is generated by loss of OH^-. Here, the EDG group on the nucleophilic carbon is the negatively charged $[(HOO)(R)C(O)]]^-$ fragment.

The generation of R–O bonds in organic chemistry based on whether the R is electrophilic (Fig. 1a) or nucleophilic (Fig.1b) has proven an effective tool. Extension of this strategy can be used to predict two strategies for oxy-functionalization of LM–R intermediates based on whether the R group is electrophilic and attacked by an O-nucleophile (Fig. 1c) or nucleophilic and functionalized by reaction with an incipient O-electrophile (Fig. 1d). Significantly, as in organic chemistry, the predicted character of the LM motifs and reaction conditions to generate either intermediates as well as the mechanisms of reaction would be expected to be very different. It would be anticipated that the generation of $LM–R^{\delta+}$ intermediates would require LM motifs that are strongly electron-withdrawing along with compatible reaction conditions that favor the displacement reaction. In contrast, the generation of $LM–R^{\delta-}$ intermediates would require LM motifs that are strongly electron-donating and conditions that support the associated character. In addition to facile reactions to generate C-O products, an important requirement is for the functionalization reaction to generate an LM–**X** intermediate that can facilitate the CH activation reaction. Another requirement is the M–C to C–O transformation must proceed by concerted atom-transfer reactions that ideally occur within the coordination sphere of M in order to avoid the generation of highly reactive species such as free radicals and to maximize selectivity by using the LM motif to impart steric and electronic control on the reaction products.

We reasoned that extension of reaction mechanisms to organometallic chemistry would also lead to facile C–O bond-forming reactions.

In addition to the phenomenological differences between displacements and insertion reactions, the electronic characteristics of these functionalization reaction mechanisms are fundamentally different with respect to the changes at the LM fragment during the functionalization reaction. As can be seen in Fig. 1c, the key difference is that when electrophilic LM–$R^{\delta+}$ species react with O-nucleophiles, the LM is the "leaving group" and is formally reduced as it leaves with two additional electrons (at least by formal oxidation state assignment) relative to the LM fragment in LM–R. In contrast, in the reaction of nucleophilic LM–$R^{\delta-}$ species with O-electrophiles, there is no formal change in oxidation state at the metal center. This organometallic equivalent to the organic BV reaction would be considered the formal O-atom insertion into an M–R fragment, as shown in Fig. 1d, where M is any transition metal and YO is an O-atom donor. Analogous to the organic reaction, migration of the negatively charged carbon fragment to the electrophilic O where Y is a good leaving group allows for the generation of C–O bonds.

While formal oxidation states are not always an accurate description, differences in electronic change during a reaction can provide a basis for generalized classification and prediction of new reactions. Significantly, it is anticipated that the composition of the LM motif along with the reaction conditions for these two types of functionalization reactions is very different. These considerations along with the observation that the LM motifs must either be strongly electrophilic (electron-withdrawing) or strongly nucleophilic (electron-donating) to induce the positive or negative charges on R, respectively, can serve to specify the character of L, M, the reaction solvent, and other considerations for the development of new catalyst systems.

We have now clearly identified two classes of catalysts for the functionalization of a charged M–R intermediate. The next step is to consider whether CH activation reactions that are *compatible* with the reaction conditions and LM motifs capable of M–R functionalization can be developed. The requirement for compatibility is *essential* for an active catalytic system because these reactions occur consecutively in the same pot. This key consideration would point to the requirement for general types of CH activation reactions for the greatest possible compatibility. One type would operate with strongly electrophilic LM motifs and the corresponding reactions conditions. The other type of CH activation would operate with strongly nucleophilic LM motifs and corresponding reactions conditions. This requirement for similarity in electronic character (and of course reaction conditions) is essential because drastic electronic changes between CH activation and functionalization reactions are likely not feasible in a one-pot reaction. Importantly, we must consider that oxidation state and minor electronic changes likely occur between the two reactions and the use of reaction conditions that stabilize/facilitate such changes is crucial. In an ideal system, both CH activation and LM–R functionalization should benefit from an LM fragment with similar electronic character and by the same reaction conditions.

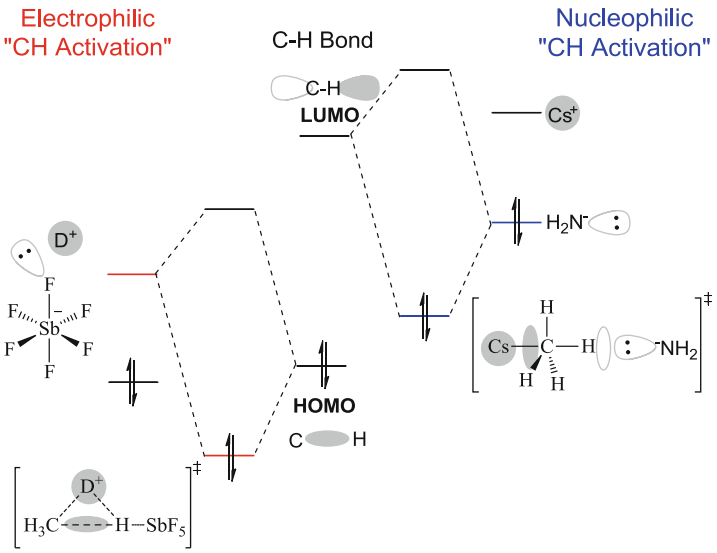

Fig. 2 Organic examples of electrophilic and nucleophilic "CH activation" showing the frontier molecular orbital HOMO/LUMO interactions

Fortunately, organic chemistry can once again provide us with general models for concerted CH cleavage reactions that provide a conceptual framework for CH activation reactions with both nucleophilic and electrophilic mechanisms. Electrophilic and nucleophilic "CH activation" analogs in organic chemistry are reactions of CH bonds with strong acids or strong bases. The H/D exchange reaction between the superacid, $D^+SbF_6^-$, and CH_4 proceeds rapidly at room temperature [Eq. (5)] [62–64]. This reaction is an example of an electrophilic substitution reaction and proceeds via protonation of the CH bond through the coordination of the CH bond to the H^+ followed by concerted CH cleavage involving transfer of the proton to the solvent. The D^+ in a superacid media is essentially a poorly coordinated electrophile characterized by a low-lying LUMO of appropriate symmetry to interact with the low-lying HOMO of the CH bond (Fig. 2). In this type of system, the interaction of the acid HOMO (the lone pairs on fluoride of SbF_6^-) with the LUMO of the CH bond is not involved in the reaction to any significant degree early in the reaction, and the net result is that electrons are net transferred from the CH bond to the D^+, and substantial positive charge builds up on the carbon in the transitions state for CH cleavage.

$$D^+SbF_6^- + CH_4 \xrightarrow[RT]{} H^+SbF_6^- + CD_nH_{4-n} \tag{5}$$

The nucleophilic analogue in organic chemistry is the deprotonation of CH bonds with strong bases that were widely utilized in the early 1960s by Andy Streitweiser to determine the pK_as of alkanes [Eq. (6)] [65–67]. As shown in Fig. 2, the deprotonation of a CH bond with a strong base, e.g. KNH_2, can be conceptually

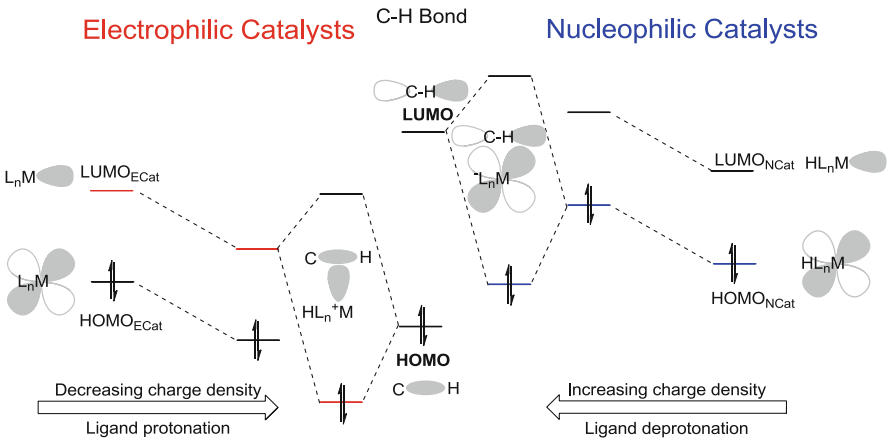

Fig. 3 Conceptual frontier molecular orbital diagram for interaction of electrophilic and nucleophilic catalysts with the CH bond and contribution of ligand protonation or deprotonation to facilitate correct orbital overlap

viewed as an example of nucleophilic substitution "CH activation" where the H_2N^- group can be generally viewed as a nucleophile that attacks the H and displaces CH_3^-. In this nucleophilic reaction, the H_2N^- is a nucleophile with a high-lying HOMO with the appropriate symmetry to attack the high-lying CH LUMO of $H–CH_3$ [68]. In contrast to the reactions of CH bonds with electrophiles, the interaction with the HOMO of the CH bond with the LUMO of the $CsNH_2$ (which would be localized on the Cs^+) is likely not significant in the early stages of the CH cleavage, and substantial negative charge builds up on the carbon during cleavage.

$$Cs^+NH_2^- + RH \xrightarrow[\text{Cyclohexylamine}]{} NH_3 + Cs^+R^- \tag{6}$$

Extending this general framework of concerted atom-transfer CH cleavage reactions in organic chemistry to transition metal chemistry predicts that two types of CH activation reactions should be conceivable (Fig. 3). A key advantage of transition metal LM motifs over main group atoms utilized in classical organic chemistry is that the frontier orbital interactions with the CH bond can be more favorable as a result of the greater polarizability, symmetry, and size of the orbitals of transition metals. In electrophilic CH activation reactions, the LM motifs should be electron-deficient, and reaction conditions should facilitate generation of a low-energy and polarizable LUMO with σ-symmetry on the metal center that can favor interactions with the low-lying, poorly polarizable HOMO of the CH bond. Sigma bonding would be the dominant mode of charge transfer since the interactions between the $HOMO_{LMX}$ and $LUMO_{CH}$ would be expected to be unimportant early in the CH cleavage. Consequently, in these systems, substantial charge should develop on the carbon during cleavage, and the alkyl group of the resulting

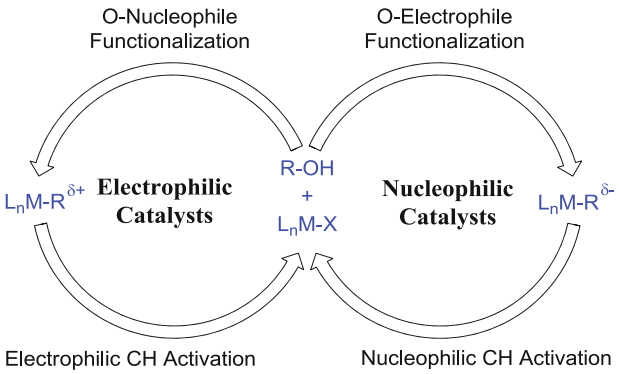

Scheme 8 Products to reactants analysis predict two classes of electrophilic and nucleophilic catalysts could exist for the oxy-functionalization of hydrocarbons that operate via fundamentally different types of CH activation and LM–R functionalizations reactions

LM–$R^{\delta+}$ product should be highly electrophilic as desired for electrophilic functionalization reactions with O-nucleophiles.

Continuing with the extension from simple organic CH cleavage reactions in nucleophilic CH activation, the LM motif should be an electron-rich metal center with a high-energy, polarizable, metal-centered HOMO. The HOMO should have π-symmetry that can interact with the LUMO of the CH bond. In contrast to the electrophilic CH activation systems, the dominant charge transfer in nucleophilic CH activation occurs from the LM motif into a π antibonding orbital leading to CH bond cleavage. The charge transfer from the $HOMO_{CH}$ to the $LUMO_{LM}$ is not significant early in the cleavage reaction due to the high electron density of the metal. This should lead to negative charge buildup on the carbon during cleavage and generation of LM–$R^{\delta-}$ intermediates that could be highly nucleophilic as desired for functionalization reactions with O-electrophiles.

The scope of nucleophilic and electrophilic CH activation may be further expanded through use of non-innocent spectator ligands [69–76]. The concept behind non-innocent spectator ligands is to allow not only the metal to participate in the reaction but the ligand as well. For example, pincer-ligated complexes have been used for shuffling protons and hydrides [77, 78]. Another approach is to allow the ligand to pick up and distribute charges or electrons to allow greater oxidation state flexibility at the metal center [79]. Alternatively, the spectator ligands could be designed to interact with the solvent or substrates by ligand protonation or deprotonation to modulate the electronic character at the metal center. This could be accomplished by the use of acidic or basic solvents, respectively.

The use of acidic or basic solvents can also be used to enhance electrophilic and nucleophilic CH activation reactions. The basis for this is shown conceptually in Fig. 3. In the case of acidic solvents, protonation of ligands will remove electron density, leading to lower energy LUMO orbitals on the metal center, thereby increasing the electrophilicity and interaction with the $HOMO_{CH}$. In the case of basic solvents, deprotonation of protic ligands on electron-rich metal centers could

analogously increase the nucleophilicity of the metal center by generating a higher energy HOMO and favoring interaction with the $LUMO_{CH}$.

Significantly, these broad considerations allow us to consider a product to reactants analysis (Scheme 8) for catalysts that operate by the generalized mechanism shown in Scheme 5 that predicts two fundamentally different types of catalyst systems, electrophilic and nucleophilic based on our protection strategy (Scheme 7). Electrophilic catalysts would be expected to be based on strongly electrophilic LM motifs, supported by strongly acidic reaction conditions, and would operate by an electrophilic CH activation to generate $LM–R^{\delta+}$ intermediates followed by a functionalization reaction with O-nucleophiles. In contrast, nucleophilic catalysts would be predicted to be based on strongly nucleophilic LM motifs, supported by basic solvents, and would operate by a nucleophilic CH activation reaction to generate $LM–R^{\delta-}$ intermediates that could be functionalized by reaction with O-electrophiles. We will now consider the implications of such an approach to develop CH bond oxy-functionalization catalysts.

3 Electrophilic Hydrocarbon Hydroxylation Catalysts

We anticipated that strong, oxidizing electrophilies such as Tl^{III} may undergo stoichiometric reactions via a CH activation mechanism to generate methanol. Strong acid solvents such as H_2SO_4, oleum (H_2SO_4/SO_3 mixtures), or H_3PO_4/P_2O_5 mixtures were emphasized in order to increase the electrophilicity of the metal cations. Even though likely to be an impractical acid, CF_3SO_3H was also utilized in initial screening studies as this was a very strong acid comparable to concentrated H_2SO_4 in which it was expected that CH_4 may be more soluble.

The first reaction examined was a 0.1 M solution of $Tl(CF_3SO_3)_3$ prepared in situ by addition of black/brown Tl_2O_3 to neat CF_3SO_3H and gentle heating. This led to rapid dissolution of the black oxide and generation of a clear solution presumed to be $Tl(CF_3SO_3)_3$ which upon cooling to RT led to the formation of clear, well-formed crystals of $Tl(CF_3SO_3)_3$. This solution was then placed in a glass vial, inserted into a high pressure metal reactor, pressurized with 500 psi of methane, and heated to 180°C for 2 h. The reactor was examined upon completion of the reaction, and it was immediately clear that no crystalline $Tl(CF_3SO_3)_3$ remained. With great anticipation and trepidation, given the lack of success in the program to date, the reaction mixture was analyzed. I still recall the excitement when the strip-chart recorder pen started to move up at the retention time for methanol. Since the analytical methods were tuned to detect very low levels of product, it was with great excitement to see the pen rapidly jump off the scale, with the characteristic grinding sound of the pen being stopped by the limiter in the chart recorder. Subsequent analysis confirmed that the yield of methyl triflate was almost quantitative based on Eq. (7).

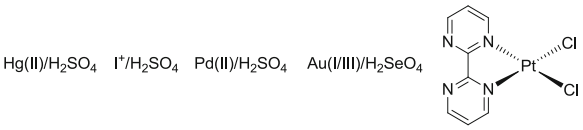

Fig. 4 Reported electrophilic catalysts that convert CH_4 to CH_3OH in >1 M yield at high selectivity

$$TI(CF_3SO_3)_3 + CH_4 \xrightarrow[\substack{\text{Triflic Acid}\\ 180^\circ C,\ 2\,h}]{} CH_3OSO_2CF_3 + TI(CF_3SO_3) + CF_3SO_3H \tag{7}$$

Interestingly, all of the reported catalysts to date for methane hydroxylation fall into the electrophilic class of catalysts. Thus, studies of the known systems based on Pt^{II} [2, 26, 39], Hg^{II} [40, 41], Pd^{II} [42, 43] and $Au^{I/III}$ [44, 45] in acidic solvent all operate via electrophilic CH activation followed by O-nucleophile functionalization. A key basis for the efficiency of these systems is the electrophilicity of the LM motif through the use of metal ions with high electron affinity and acidic solvents. The increase in electrophilicity improves the efficiency of both the CH activation and functionalization steps. This begins to highlight the requirement for one-pot compatibility between the CH activation and functionalization steps. Importantly, in systems described below, the key points are that both steps are enhanced or not inhibited by strong acid solvents and strong electrophilic metal character and allow for implementing the outlined protection strategy (vide supra). Initial work involving the CH activation and oxy-functionalization reactions of CH_4 began with the use of simple metal salts in strong mineral acids. Examples of catalysts that generate >1 M of functionalized product are shown in Fig. 4. These catalysts have been found to operate by the general CH activation-based pathways discussed previously. Importantly, the key to these electrophilic systems efficiency is the use of strong acids that activate the catalyst for both the electrophilic CH activation and functionalization steps. An in-depth discussion of these systems has been reported, and we will not belabor the point here. The take-home message is that (a) the use of strong acidic solvents allowed for the various soft, polarizable cations to generate >1 M CH_3OH before inhibition occurred; (b) all reactions proceeded through CH activation pathways; (c) the acid acted as both solvent and oxidant; and (d) all the systems showed high selectivity (>90%) and efficient CH_4 conversion (>20%).

One of the most efficient systems for the selective, low temperature oxidation of methane to methanol is the (bpym)$PtCl_2$/H_2SO_4 or "Periana" system (where bpym = 2,2′-bipyrimidine) [39]. The proposed reaction mechanism for the so-called Periana system is shown in Scheme 9 and has been substantiated by several studies [80–86]. The LM–R functionalization step that generates the product, CH_3OSO_3H, belongs to the electrophilic class of catalysts. The reaction proceeds by O-nucleophilic attack on the methyl group of LPt^{IV}–CH_3 to generate the oxy-functionalized product by displacement of $LPt^{II}X$, the leaving group. In spite of the obvious changes in coordination number changes at the Pt center, this reaction is fundamentally similar to

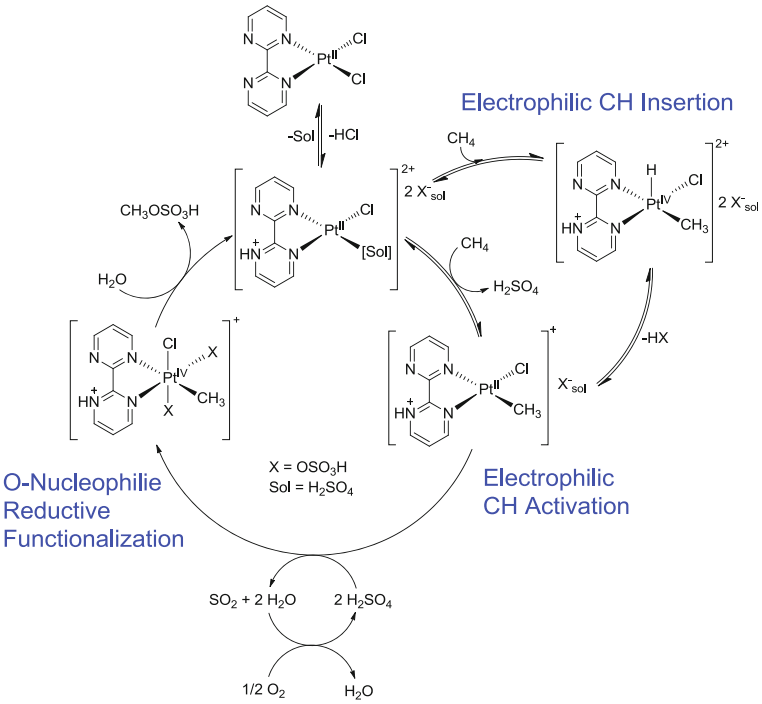

Scheme 9 Proposed mechanism for the "Catalytica" system electrophilic-type mechanism for CH hydroxylation of CH_4 catalyzed by the (bpym)$PtCl_2$/H_2SO_4

the reaction of CH_3Cl with HO^-, as shown in Fig. 1a, where OH^- is the nucleophile and Cl^- is the leaving group. This is consistent with the expectation that parallels between organic reactions for C–O bond formation and those in organometallic chemistry exist. Similarly, the electrophilic carbons in $CF_3OS(O)O–CH_3^{\delta+}$ (organic) and $LM–R^{\delta+}$ (organometallic) undergo nucleophilic attack by O-nucleophilies to give C–O bond formation. In the case of the organic group, this electrophilicity is induced by the EWG groups such as Cl^- or $CF_3S(O)O^-$. Interestingly, in spite of the electronic similarities of these reactions, as a result of formalism adopted in the two fields, the organic reaction is described as a nucleophilic displacement with O-nucleophiles, while the organometallic reaction is a nucleophilic reduction (otherwise known as reductive functionalization). The LM motif in this case must be both strongly electrophilic to facilitate attack on the methyl group of $LPt^{IV}–CH_3$ by the very weak O-nucleophile, solvated $[OSO_3H]^-$, and the leaving group, LPt^{II}, must be relatively stable. These requirements are likely the reason that the oxy-functionalization proceeds from $LPt^{IV}–CH_3$ rather than from $LPt^{II}–CH_3$.

In addition to these considerations, protection by protonation was effective because: (a) the CH_3OH is in equilibrium with the protected form since protons transfers between oxygen atoms are fast, (b) the use of a strong acid as the solvent leads to essentially complete conversion of the methanol product to the protected

form, and the concentration of free methanol at equilibrium is lower than the dissolved methane, and (c) the solvent is used in large excess relative to the catalyst allowing generation of high TONs of protected product. This system was potentially practical since the strong acid solvent utilized was inexpensive, stable, and the protected form of CH_3OH ($CH_3OH_2^+$) was easily deprotected by the addition of water.

The LM–R functionalization step strongly depends on the electronics of the LM motif; analysis of this system suggests that CH activation may be facilitated by increased electrophilic properties given the high efficiency of this system. Studies show (Scheme 8) that the CH activation proceeds by an electrophilic substitution of a three-coordinate $[LPt^{II}Cl]^+$ solvento species to generate the $[LPt(CH_3)(H)]^+$ intermediate. This is followed by oxidation of the Pt^{II} center by H_2SO_4 to give the $[LPt^{IV}(CH_3)X_3]^+$ species, which then undergoes a formal reductive functionalization to give methyl bisulfate and regenerate the active Pt^{II} species.

Consequently, the reaction of the three-coordinate $[LPt^{II}]^+$ motif with the CH bond is fundamentally related to the reaction of H^+ with a CH bond, as shown in Fig. 1. The reaction is net electrophilic in character and only phenomenologically different because of the ability of Pt^{II} to expand its coordination number and formal oxidation state. While, it may be considered that this reaction is facile because of the possibility for Pt^{II} to both accept and donate electrons. It should be noted that reactions with Hg^{II} in sulfuric acid are actually more facile than reactions of $[LPt^{II}]$ in spite of the lack of the donation of electrons from Hg^{II} [40].

The description of the CH activation reaction as an electrophilic reaction resulting from a strongly electrophilic $[LPt^{II}]^+$ motif is consistent with the observed >90% reaction selectivity even after 1 M of products are generated. Studies show [86] that the high selectivity of the reaction is a direct result of product protection in the form of $CH_3OH_2^+$ or CH_3OSO_3H. The protection is induced by the electron-withdrawing characteristics of the OH_2^+ and OSO_3H groups that minimize electrophilic reaction of the CH bond in these products with the highly electrophilic $[LPt^{II}]^+$ motif. The reactivity of $CH_3OH_2^+$ or CH_3OSO_3H is on the order of 100 times less reactive than CH_4 with the Pt catalyst. Thereby, we can deduce that protection plays an important role in allowing compatibility between the CH activation and functionalization steps to avoid product destruction. These studies point to other important reasons for the high efficiency of the Periana system which occurs because of the compatibility between CH activation and functionalization steps facilitated by the use of strongly acidic solvent.

The use of strongly acidic solvents allowed the $Pt(bpym)Cl_2$ to have sufficient electrophilicity to have proper orbital overlap for reaction with the CH bond of methane. The Periana system operates in neat CF_3SO_3H ($H_o = 13.7$) [87, 88] or H_2SO_4 ($H_o = 11.10$ at 100%) [89, 90], but no reaction is observed in <70% H_2SO_4 ($H_o = <5.80, <11.48$ M) [89, 90] or neat CF_3CO_2H ($H_o = 2.7$) [87]. These studies show that in addition to providing a medium that is stable to reaction conditions by ensuring favorable thermodynamics for the overall catalytic conversion, the strongly acidic solvent increases reaction rate by increasing the electrophilicity of the LM motif by proton transfer from the solvent to the ligands of the catalyst in

both the CH activation and functionalization steps. Thus, in the O-nucleophilic functionalization step, protonation of the anions coordinated to six-coordinate $LPt^{IV}–CH_3$, followed by generation of a 5-coordinate cationic species, increases the electrophilicity of the methyl group of $LPt^{IV}–CH_3$. In a similar manner, solvent protonation of the $LPt^{II}–X$ ligands also increases electrophilicity and ligand lability that is required for methane coordination and electrophilic CH cleavage. Other essential roles of protonation are only possible when concentrated sulfuric acid (or other strong acid) is used as the solvent to maintain a low activity of free water and methanol and to protect the product. Since water and MeOH are much stronger O-nucleophiles than those of H_2SO_4 solvent ($[OSO_3H]^-$), they can severely inhibit the strongly electrophilic LM motif. Furthermore, protection of the product as $CH_3OH_2^+$ is important because the CH bonds of $CH_3OH_2^+$ are 100 times less reactive than CH_4 and >1,000 times less reactive than those of free CH_3OH. Practical considerations require high catalyst turnover before product separation, and systems operating by an electrophilic mechanism will be required to operate in the presence of at least 1 M product concentrations [31]. Therefore, efficient and complete product protection as CH_3OSO_3H or $CH_3OH_2^+$ of methanol will be needed to avoid catalyst inhibition or decomposition, which suggests that H_2SO_4 is an ideal solvent for electrophilic catalysts such as the Periana system.

Unfortunately, the Periana system has never been commercialized, and this is due to several important considerations. Although product yields were greater than 1 M, the process economics of the system require that product yields must be greater than 5 M [28]. The reaction of the strongly electrophilic catalyst is plagued by severe water/product inhibition at concentrations required for commercialization leading to costly separation techniques [26]. The requirement for several equivalents of water to be added to convert the methyl bisulfate ester to methanol before being removed from the reaction required the solvent to be concentrated in a separate step to >90% H_2SO_4 before being returned to the process. This would have then required an additional SO_2 to SO_3 plant to be constructed in the development of a commercial process, thus leading to the requirement of 5 M CH_3OH before product separation to be economically viable with current market rates of CH_3OH. Therefore, new designs of catalysts will be required to prevent these inhibition problems that have plagued all systems highly electrophilic in nature to date.

3.1 More Efficient Electrophilic Catalysts

Significantly, in spite of the efficiency of the Periana and other electrophilic systems that require strong acidic media, to our knowledge, none are under commercial development. This is primarily because product separation becomes more expensive as the acid strength increases due to the affinity of the catalyst to bind water and CH_3OH. Unfortunately, electrophilic systems are the most efficient at high acid and low product concentrations due to the increased product protection. Another key disadvantage of the requirement for strongly acidic media is that the oxy-functionalized products of higher hydrocarbons are either more challenging to

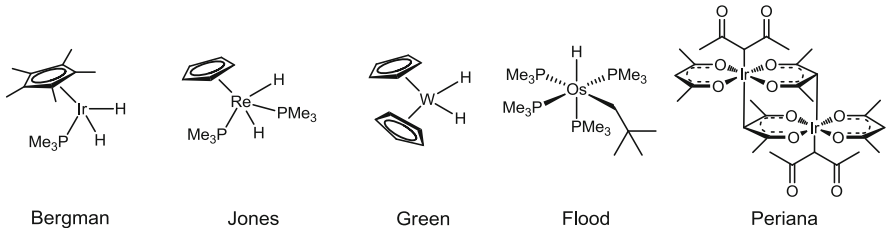

Fig. 5 Catalytic systems based on Ir^{III} (Bergman [21] and Periana [91, 92]), Re^{III} (Jones) [93], W^{IV} (Green) [94], and Os^{II} (Flood) [95] that undergo CH activation with hydrocarbons but do not give oxy-functionalized products

isolate, unstable to the reaction conditions, or lack product selectivity. One strategy to address these challenges involves designing catalysts that are less electrophilic and could operate without inhibition in weaker acids or in the presence of large amounts of product.

Interestingly, early work on CH activation showed that many capable systems based on less electronegative metals such as Ir, Rh, Ru, and Re catalyze CH activation (Fig. 5) [46, 48, 50, 52, 96–102]. Several observations show that these systems are not as electrophilic as those based on Pt^{II}, Pd^{II}, or Hg^{II}. In general, there is no requirement for strongly acidic media, and the systems operate efficiently in water, organic solvents, or weak acids. Density functional theory (DFT) calculations show that many of these systems, such as Bergman's $[Cp^{*}Ir^{III}(PMe_3)CH_3]^{+}$, are electrophilic in character as characterized by positive charge buildup on the carbon during CH activation, but not as strongly as in the Periana (bpym)$PtCl_2$/H_2SO_4 system [103, 104]. Unfortunately, none of these less electrophilic systems that operate outside the regime of strong acids have led to very efficient hydrocarbon partial oxidation. The most likely reason for their shortcomings was the lack of available and compatible facile LM–R functionalization reactions. The electrophilicity of the LM–$R^{\delta+}$ fragment is not sufficiently high to facilitate reactions with weak O-nucleophiles, and the metal center is not sufficiently oxidizing to facilitate a reductive functionalization [21, 31, 93–95, 105–116]. The lack of facile C–O bond-forming reactions of weakly electrophilic LM–R complexes may be attributed to the lack of significant positive charge buildup on the R group as a result of the reduced electrophilicity of the LM motifs. Indeed, recent theoretical calculations show that many of the CH activation systems based on these metals are deemed ambiphilic in nature [21, 93–95, 105–116].

The development of less electrophilic CH oxy-functionalization systems that operate via CH activation so far has been met with limited success. A few examples have been reported, including the pioneering work of Shilov, in which a Pt catalyst was used along with stoichiometric amounts of Pt^{IV} as oxidant that operated in water; however, the amount of product generated was extraordinarily small, and rates were very slow to those systems employing more electrophilic conditions. It would also be expected that minimal protection could be afforded by the solvent alone in reactions taking place in water, weak acids, or organic solvents. The use of such solvents would necessitate the use of a different protection strategy that on

commodity scale may prove too costly. Therefore, we realized, given our products to reactants approach, that the only appropriate place to provide high rates of product formation and high levels of product protection is either the acidic or basic regimes, where solvent can be used to enhance the properties of the catalytic system and provide efficient protection by either protonation or deprotonation to generate $CH_3OH_2^+$ or CH_3O^-, respectively. Thus, it was clear that exploration of a new regime for the oxy-functionalization of hydrocarbons would be a necessity. The goal is to address whether basic media would facilitate a program to develop working hydrocarbon, oxy-functionalization catalysts.

4 Nucleophilic Hydrocarbon Hydroxylation Catalysts

We previously predicted two classes of catalysts based on strongly electrophilic and strongly nucleophilic LM motifs. Given the issues with systems based on strongly electrophilic systems supported by strong acid solvents, we have begun a focused effort to designing CH hydroxylation systems based on strongly nucleophilic LM motifs. As noted above, such systems should generate LM–$R^{\delta-}$ intermediates that readily react with O-electrophiles and operate by nucleophilic CH activation reactions to ensure compatibility. However, to our knowledge, no LM–X systems with these characteristics have been reported.

To begin the de novo design of nucleophilic catalysts for CH bond hydroxylation, some general considerations that guide the work are essential. The LM motifs will be based on less electrophilic metals such as Os, Ru, Re, Ir, etc., as these metals are known, especially in the lower oxidations states to bind to weak π-donors such as N_2 and may be ideal for interacting with the high-lying LUMO of the CH bond and generating nucleophilic LM–$R^{\delta-}$ intermediates that react with O-electrophilies (Fig. 3). Basic solvents may also play a similar role to acidic solvents for electrophilic systems by supporting the generation of nucleophilic metal centers through deprotonation of protic non-innocent ligands or addition of HO^- to the metal center. Furthermore, solvents that deprotonate methanol ($pK_a = 15.5$) to generate methoxide allow the use of the previously outlined protection strategy. Plausible solvents that may meet these requirements include very concentrated NaOH, eutectics of anhydrous KOH/NaOH (that melt below 250°C), or mixtures of Na_2O in NaOH. Therefore, to begin addressing reactions of the nucleophilic regime, we began our program on the examination of oxy-functionalization reactions of M–$R^{\delta-}$ complexes with the intent on eventually coupling them to the CH activation reaction based on our product to reactants analysis of hydrocarbon functionalization (Scheme 8).

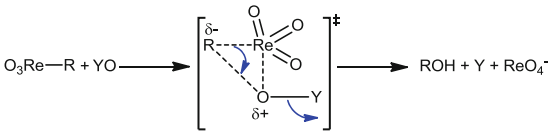

Scheme 10 BV-type oxidation of R–ReO_3 with YO to generate ROH

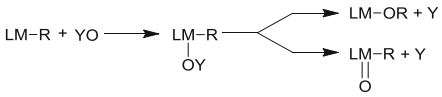

Scheme 11 Possible complications to a BV-type mechanism involving O-atom transfer to the metal center

4.1 Oxy-Functionalization Reactions of LM–$R^{\delta-}$ Intermediates

The known, facile functionalization of nucleophilic hydrocarbyl groups in organic chemistry by mechanisms such as the BV reaction offers a starting point for design of facile oxy-functionalization reactions of LM–$R^{\delta-}$ intermediates (Fig. 1c, d). We focused our initial studies on the reaction of known, stable, metal alkyls of Re, Ru, and Ir as reactions of these metal-hydrocarbyls were not well known. This was crucial with a product-to-reactant-type approach because as previously shown, several systems (Fig. 5) based on the less electronegative metals have been developed for CH activation but do not show oxy-functionalization. It was therefore essential to understand the possible properties of LM–R motifs and the corresponding reaction conditions that lead to facile functionalization.

Espenson had originally reported an undesirable side reaction of methyltrioxorhenium (MTO) catalysts to generate CH_3OH in a series of studies [117]. Further examination of this side reaction has shown, despite the high oxidation state of MTO (Re^{VII}), that dissolution in acidic or basic water does not generate CH_3OH and a Re^{V} species. This is interesting given that although Re is in its highest oxidation state (+7), the complex does not readily undergo oxy-functionalization where the Re^{VII} center is reduced as was previously observed (e.g., the LPt^{IV}–CH_3 systems). Instead, the reaction requires the addition of an O-atom donor, YO, such as H_2O_2, $NaIO_4$, or PhIO, to generate CH_3OH (>80% yield) and the ReO_4^- anion where the Re remains in the +7 oxidation state. Conley et al. showed that reactions of MTO with various YOs generated CH_3OH and proposed a BV-like pathway (Scheme 10), which was further substantiated by computational examination of the reaction mechanism [56, 118]. Labeling studies show that the oxygen in the product is not derived from the oxo of rhenium or solvent but rather from labeled $Y^{18}O$. This was consistent with DFT analysis of the system via the proposed BV-type mechanism. These reactions can proceed in the presence of added base and involve the formal attack of a nucleophilic CH_3 group on an electrophilic oxygen. This is accompanied by displacement of the leaving group such as OH^-, Py, etc., depending on the YO. These results suggest that the reaction could be viable with LM motifs that are

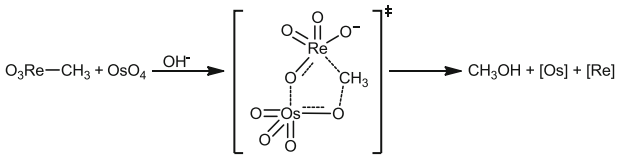

Scheme 12 Route for oxy-functionalizing of negatively polarized metal-alkyl complexes via a [2+3] type mechanism to generate an alcohol

nucleophilic. It has also been found that the Baeyer–Villiger-type reaction also proceeds when R = aryl to cleanly generate phenols [119]. It should be noted that one possible complication with the use of a BV-type mechanism for the functionalization of a nucleophilic LM–R motif, that can be formally oxidized, is a side reaction involving O-atom transfer to the metal center rather than the R group, as shown in Scheme 11. This is of course not possible in the case of MTO and therefore may pose problems in using BV-type functionalization when M is not in the highest oxidation state or coordinately saturated.

To expand on nucleophilic oxy-functionalization reactions, we examined the reaction of MTO with a more complex O-atom donor, OsO_4. To our delight, treatment of MTO with OsO_4 generated CH_3OH in very high yields (>95%) (Scheme 12) [57]. Significantly, this reaction only proceeds upon the addition of excess base to water mixtures of MTO and OsO_4. The reaction is nearly quantitative upon mixing at RT. An unexpected result highlighted by a DFT study showed added OH^- does not activate the OsO_4 toward reaction, but instead activates the MTO by generation of a $[O_3ReMe(OH)]^-$ species. The OH^- reorganization leads to an increased negative charge on the $Re–Me^{\delta-}$ leading to facile reaction. This is surprising given that in the ground state, OH^- readily binds to OsO_4 to form the OH^--ligated $O_4Os–OH$ species. The lowest energy transition state shows reaction between $[O_3ReMe(OH)]^-$ and OsO_4. This electronic organization facilitates the reaction by generating a negatively polarized methyl group and an electrophilic oxygen in OsO_4. This highlights a reaction involving oxo transfer that should be well suited for the oxy-functionalization of nucleophilic $LM–R^{\delta-}$-type intermediates and could also benefit from the use of basic media.

To begin to address the possible complication where O-atom transfer to the metal center versus the R group is possible because the metal is not in the highest oxidation state and could be potentially oxidized (Scheme 11), we moved to examine the oxy-functionalization of LM–R model complexes, where M was *not* in the highest oxidation state. It was found that the readily synthesized $Re(CO)_5R$ [120] undergoes efficient alkyl transfer reactions to electrophiles such as SeO_2 (which exists as H_2SeO_3 in water) [121] to generate $MeSeO_2H$. Industrially, SeO_2 is a well-known cocatalyst for carrying out hydrocarbon oxidation reactions [122–128]. It was previously reported that $R–Se^{IV}(O)OH$ under oxidizing conditions can readily generate alkanols and H_2SeO_3 by proceeding through $R–Se^{VI}(O)_2OH$ [129]. It was found that reactions of $Re(CO)_5R$ in the presence of catalytic amounts of SeO_2 (10 mol%) in H_2O:CH_3CN mixtures with excess oxidant readily gave >80% yields of CH_3OH when R = Me, as shown in Scheme 13 [130].

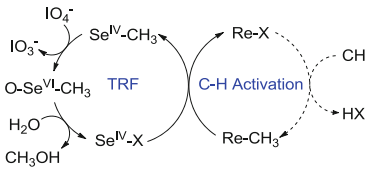

Scheme 13 Plausible route to alcohols, ROH, using M as a C–H activation catalyst via O-atom insertion by a transalkyl reductive functionalization (TRF) cycle where to yield ROH

The reaction was shown to proceed by the following sequence: (1) insertion of SeO_2 into the Re–CH_3 bond, (2) oxidation of Se^{IV} to Se^{VI}, and (3) outersphere backside attack by water on the Se^{VI}, leading to the corresponding alcohol via a process we refer to as transalkyl reductive functionalization (TRF).

Interestingly, the reaction proceeded by undergoing alkyl transfer and avoided other possible scenarios. One possibility is that the Re^{I} center could have been oxidized by the relatively strong oxidant IO_4^- to generate a less reactive, oxidized Re^{II}–CH_3 (or Re^{III}–CH_3) species. These observations suggest that reactions at the R group could be made more facile than reactions at the metal center and that the oxy-functionalization of LM–$R^{\delta-}$ systems, where the metal can be formally oxidized, would be possible. In addition, due to the reduced oxidation/reduction potentials of earlier transition metals, it may prove useful to develop cocatalytic systems with one catalyst responsible for CH activation and another redox active catalyst capable of oxy-functionalization. This would allow each catalyst to be tailored directly toward the specific task (one for CH activation and one for functionalization) where ligands and metals can be chosen appropriately for the chemistry required. However, a cocatalyst strategy may prove difficult due to the requirement that two active catalysts need to be coupled in a single, one-pot reaction.

The utilization of the more electron-rich $(CO)_3(bpy)Re^{I}$–Me species results in significant improvements in alkyl transfer to Se. Removal of two electron-withdrawing CO ligands and replacement by the stronger σ-donating bipyridine ligand increased the electron density on the methyl group allowing for more facile reaction with electrophiles. This is consistent with reactions using SeO_2 proceeding at RT upon mixing, whereas, $Re(CO)_5Me$ required heating (50°C for 2 h) to induce quantitative alkyl transfer. Additionally, the rate of protonolysis also dramatically increases upon addition of the bipyridine ligand. The correlation of reaction rate increasing with electron density at the metal center shows that these systems are good models of functionalization of nucleophilic LM–$R^{\delta-}$-type intermediates. This is similar to previous results with MTO that show functionalization in the presence of OH^-, an σ-donor, leads to increased rates of CH_3OH formation [57]. Furthermore, Espenson found that treatment of MTO leads to increased rates of protonolysis of MTO likely explained by coordination of OH^- to increase the nucleophilicity of the methyl groups toward H^+ [120].

An important observation in this study is that reaction of $Re(CO)_5R$ where R is *n*-propyl underwent reactions in the presence of SeO_2 to regioselectively generate the corresponding *n*-propanol. This shows that oxy-functionalization reactions of

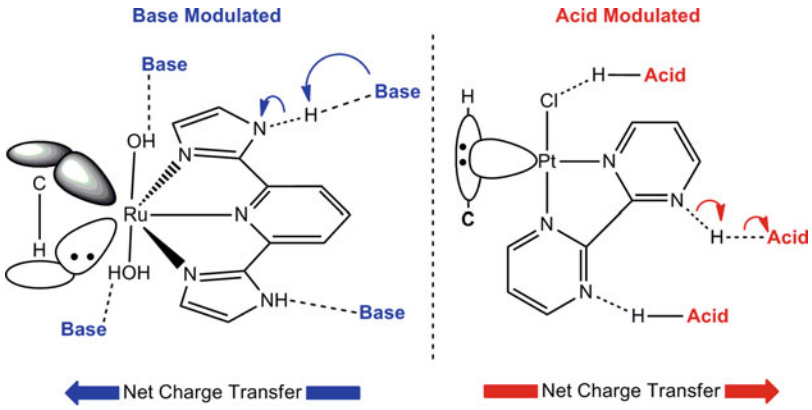

Fig. 6 Base- or acid-modulated (BAM) catalysts

nucleophilic LM–R species could precede regioselectively and with the observed preference for primary CH activation may generate primary alcohols (if the selectivity is carried through the functionalization step). In the case of methane, the observation for preserved regioselectivity is unimportant; however, the conversion of longer chain hydrocarbons to oxy-functionalized products (e.g., ethylene glycol, 1,6-hexanediol) may benefit from such mechanisms. This allows the regioselectivity to be set during the CH activation step, which preferentially activates the primary position [32–34].

Unfortunately, the development of oxy-functionalization reactions of LM–$R^{\delta-}$ motifs to alcohols is only one step of the overall process required for the development of nucleophilic CH bond functionalization catalysts. None of the motifs shown above have proven useful for CH activation of unactivated substrates such as benzene or methane. Therefore, continued study of both LM–R motifs for oxy-functionalization coupled with development of new nucleophilic CH activation catalysts will be required for the future. This is critical as both steps of the catalytic cycle must be well understood and eventually coupled to complete the overall cycle.

4.2 CH Activation with Nucleophilic Catalysts

Our work on electrophilic CH activation systems clearly demonstrated that acidic media played several essential roles in the catalyst systems. As shown in Fig. 6, one of these roles was the activation of the electrophilic catalyst by protonation of ligands from the acidic solvent that effectively removed electron density and enhanced the electrophilicity of the metal center. Applying the conjugate acid/base mechanism [131, 132] suggested that under basic conditions that metal complexes containing deprotonatable ligands such as HL–M–OH_2 might benefit from the use of basic solvent by a generalized concept we refer to as base- or acid-modulated (BAM) catalysis (Fig. 6). As was observed in the electrophilic systems

in acid, an important basis for trying to develop reactions in basic media was the additional roles that the solvent could play in enhancing the functionalization and product protection steps when using solvent-activated catalysts.

A key requirement for designing BAM catalysts that operate under basic conditions is that the basic solvent cannot bind tighter than the conjugate acid of the solvent as this would lead to severe inhibition via a ground-state stabilization effect. For example, if the ground state of the catalyst is M–OH_2, then coordination of OH^- cannot be thermodynamically downhill in energy [Eq. (8)]. This requirement cannot be met for catalysts based on metals such as Pt^{II}, $Au^{I/III}$, Hg^{II}, Pd^{II}, and even Ir^{III} (without strongly donating ligands) due to their electrophilic nature. Water or hydroxide readily coordinates to the electrophilic metals and leads to severe inhibition by formation of metal hydroxides or bridging species [100, 133–139]. However, it seemed plausible that an electropositive metal, with strong π-donor ligands, would not suffer from inhibition by strong σ-donors such as OH^- since such systems could be strong bases, as shown in Eq. (8).

$$\mathrm{M-OH_2 + OH^- \longrightarrow [M-OH]^- + H_2O} \quad \text{where } \Delta G \geq 0\,\text{kcal/mol} \tag{8}$$

Given the concept outlined above, we reasoned that metal hydroxide complexes based on metals such as $Re^{I/III}$, Os^{II}, Ru^{II}, or Ir^{I} may not be inhibited by strong σ-donors. This led us to recently report the first example of an aqueous base soluble Ru^{III} pre-catalyst capable of base accelerated CH activation upon reduction to Ru^{II}. We found that (IPI)$Ru^{III}Cl_3$ pre-catalyst (where IPI = 2,6-diimidizoylpyridine) was capable of activating both sp^2 and sp^3 CH bonds in a variety of activated or unactivated substrates [140]. The imidazole ligands contain a mildly acidic N–H group which, upon deprotonation, enhances the π-nucleophilic character of the Ru due to the increased electron density at the metal center. Furthermore, upon solvation in basic media, the chloride ligands are readily substituted for water or hydroxide ligands to give a $Ru^{III}(OH)_y(OH_2)_n$ species. Deprotonation of an aquo complex (e.g., $M(OH_2)_3$) in strongly basic solvents could generate more labile and reactive metal hydroxo (e.g., $M(OH)(H_2O)_2$) ground states. The effect is related to known observations by Basolo and Jackson that ligand substitution in systems with protic spectator ligands can be accelerated by the "conjugate base mechanism" [131, 132].

To garner a better understanding of the catalytic system, the reactivity of the Ru^{II} catalyst was monitored by H/D exchange reactions between deuterated KOD/D_2O solutions and water-soluble arenes possessing either sp^2 or sp^3 CH bonds. The rate of H/D exchange was monitored from 2 to 8 M [KOH]; however, beyond 8 M, most substrates became insoluble. The study found that increasing hydroxide concentration led to rapid acceleration in the rate of catalytic CH activation characterized by increased deuterium incorporation into the arene substrates (Fig. 7). The correlation between hydroxide concentration and increase in rate would suggest that hydroxide is directly involved in the rate-determining step(s) for CH activation. Hydroxide may be participating to promote either CH bond coordination or cleavage in several ways: (a) deprotonation of an imidazole N–H proton, (b) deprotonation of a coordinated

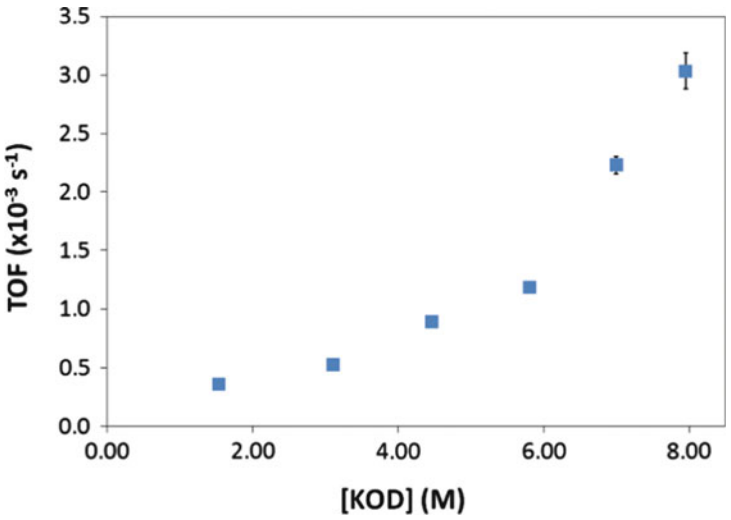

Fig. 7 Base-accelerated CH activation of *meta* position of isopthalic acid in KOD at 50°C using the (IPI)$Ru^{III}Cl_3$ pre-catalyst [140]

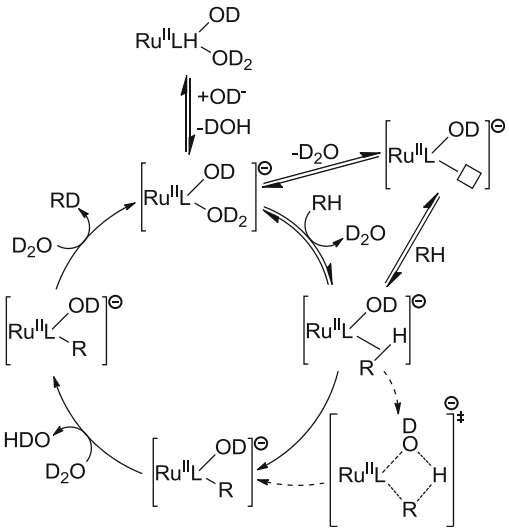

Scheme 14 Proposed mechanism for CH activation of (IPI)Ru^{II} showing H/D exchange between a hydrocarbon and aqueous base

water or hydroxide, or (c) an outer sphere hydroxide assisting in the CH cleavage step. A proposed mechanism for CH activation based on the observed rate acceleration with increasing base concentration is shown in Scheme 14. Importantly, the CH activation occurs via a heterolytic deprotonation of the incoming hydrocarbon.

These conclusions suggest the reactivity of base-activated catalysts could be further enhanced by higher base concentrations as the activity of OH^- is known to increase exponentially at high concentrations [141]. This is parallel to the reactivity seen in strongly acidic solvents such as H_2SO_4 using Hg and Pt catalysts, where the activity increases exponentially at higher concentrations of H^+ [39, 40, 42]. Another possibility for the observed rate acceleration is the generation of new, higher energy, and more reactive ground states. This may provide access to previously inaccessible low-energy pathways for CH bond cleavage through complete deprotonation of protic ligands which leads to an increase in $LUMO_{NCat}$ energy levels (Fig. 6), which will lead to enhanced π-nucleophilic character of the catalyst. Both CH activation and C–O bond formation, using metals that generate nucleophilic $M–R^{\delta-}$ fragments, have been demonstrated. Ideally, the two steps will be coupled using a single system that facilitates the overall transformation of RH to ROH while employing nucleophilic catalysts, catalysts enhanced or not inhibited by basic media, and product protection imparted on the alcohol by the basic media to give the alkoxide.

5 Conclusion

The future goal will be to understand how base-accelerated CH activation can be coupled to our previously examined functionalization pathways. Recent discoveries in nucleophilic $LM–R^{\delta-}$ functionalization suggest that connection to catalytic CH activation systems will be plausible. However, the key to connecting M–R functionalization and CH activation will be finding conditions in which both reaction steps are compatible. This requires that both steps operate using the same metal and ligand sets with minimal oxidation state changes. Coupling of nucleophilic M–R functionalization with catalysts that operate by the CH activation reaction may lead to a new route for the development of hydrocarbon functionalization catalysts.

Importantly, with two plausible pathways identified (Scheme 15), it will be crucial to clearly outline the requirements for enabling either route. Requirements that need to be met for electrophilic CH functionalization and in many cases have been address include: (a) facile CH activation facilitated by an electrophilic catalyst, (b) oxy-functionalization by an O-nucleophile, (c) reoxidation of the system using molecular oxygen as terminal oxidant, and (d) product protection using a low-cost, fast, and reversible method (e.g., protonation by strong acids). On the other front involving nucleophilic CH functionalization, several of the requirements have not been met, but are currently being addressed in our laboratories including: (a) facile CH activation facilitated by a nucleophilic catalyst, (b) oxy-functionalization by an O-electrophile, (c) reoxidation of the system using molecular oxygen as terminal oxidant, and (d) product protection using a low-cost, fast, and reversible method (e.g., deprotonation using strong bases). Therefore, it will be ideal to have a series of catalysts, compatible oxidants capable of facilitating the

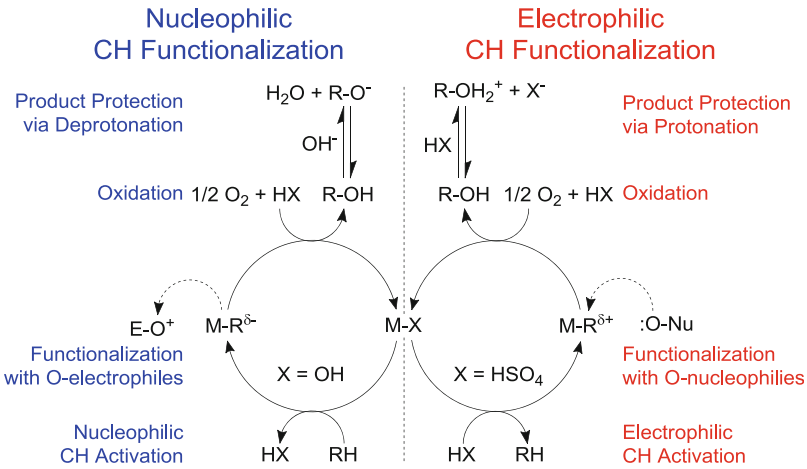

Scheme 15 Two plausible strategies for the oxy-functionalization of hydrocarbons using nucleophilic or electrophilic CH activation

oxy-functionalization reaction in either strong acid or base mediums. With conditions, mechanisms, and types of catalysts identified, the future will involve coupling the CH activation and functionalization steps into a complete catalytic cycle with a thrust toward commercialization.

The goal of understanding how to couple base-accelerated CH activation with base-induced functionalization of the M–R intermediates, in an effort to design new hydrocarbon functionalization systems, is currently ongoing. The application of a product to reactants analysis for the CH activation problem has allowed us to identify and develop several strategies for the functionalization of metal alkyls, where the alkyl group is positively or negatively charged. The key to any future catalytic systems for the activation and functionalization of hydrocarbons will require the consideration that both the CH activation and M–R functionalization steps are compatible and can appropriately be connected. Coupling this concept to the use of BAM catalyst ligand design for use in strongly basic or acidic solvents could be extended to activate other weak π-acceptors (e.g., N_2, CO_3^{2-}), and these studies are currently underway in our laboratories.

Acknowledgements We gratefully acknowledge financial support of our research by the Chevron Corporation for R.A.P. and The Center for Catalytic Hydrocarbon Functionalization, a DOE Energy Frontier Research Center (DOE DE-SC000-1298) for S.M.B., B.G.H., and M.M.K.

References

1. Olah GA, Molnar A (2003) Hydrocarbon chemistry, 2nd edn. Wiley Interscience
2. Olah GA, Goeppert A, Prakash GKS (2006) Beyond oil and gas: the methanol economy. Wiley-VCH, Weinhem

3. Wolf EE (ed) (1992) Methane conversion by oxidative processes. Van Nostrand Reinhold, New York
4. Periana RA (2001) C E News 79:287
5. Curry-Hyde HE, Howe RF Howe (eds) (1994) Natural gas conversion, 2nd edn. Elsevier, New York
6. Derouane EG, Haber J, Lemos F, Ribeiro FR, Guisnet M (eds) (1997) Catalytic activation and functionalization of light alkanes. In: Advances and challenges. Nato ASI Series, Kluwer Academic, Dordrecht
7. Brooks BT, Dunstan AE (eds) (1953) The science of petroleum: synthetic products of petroleum. Oxford University Press, London
8. Voge HH (1948) J Chem Phys 16:984
9. Blanksby SJ, Ellison GB (2003) Acc Chem Res 36:255
10. Glockler G (1926) J Am Chem Soc 48:2021
11. Lide D (ed) (2008) CRC handbook, 88th edn. Taylor and Francis Group, New York
12. Reamer HH, Sage BH, Lacey WN (1952) Ind Eng Chem 44:609
13. Dhima A, de Hemptinne J-C, Jose J (1999) Ind Eng Chem Res 38:3144
14. Dhima A, de Hemptinne J-C, Moracchini G (1998) Fluid Phase Equilib 145:129
15. Clever HL (1987) Solubility Data Series 27:56
16. Lide, DR (ed) (2007–2008) CRC Handbook of Chemistry and Physics 88th edn. CRC Press Taylor & Francis, Boca Raton
17. Bordwell FG (1988) Acc Chem Res 21:456
18. Naito S (2000) Catal Surv Japan 4:3
19. Lunsford JH (1995) Angew Chem Int Ed 34:970
20. Mleczko L, Baerns M (1995) Fuel Process Technol 42:217
21. Janowicz AH, Bergman RG (1982) J Am Chem Soc 104:352
22. Goddard RJ, Hoffmann R, Jemmis ED (1980) J Am Chem Soc 102:7667
23. Saillard J-Y, Hoffmann R (1984) J Am Chem Soc 106:2006
24. Rabaii H, Saillard J-Y, Hoffmann R (1986) J Am Chem Soc 108:4327
25. Arndtsen BA, Bergman RG, Mobley TA, Peterson TH (1995) Acc Chem Res 28:154
26. Hashiguchi BG, Bischof SM, Konnick MM, Periana RA (2012) Acc Chem Res 45:885
27. Shilov AE, Shul'pin GB (1997) Chem Rev 97:2879
28. Periana RA, Bhalla G, Tenn WJ III, Young KJH, Liu XY, Mironov O, Jones CJ, Ziatdinov VR (2004) J Mol Catal A Chem 220:7
29. Crabtree RH (2004) J Org Chem 689:4083
30. Lersch M, Tilset M (2005) Chem Rev 105:2471
31. Conley BL, Tenn WJ III, Young KJH, Ganesh SK, Meier SK, Ziatdinov VR, Mironov O, Oxgaard J, Gonzales J, Goddard WA III, Periana RA (2006) J Mol Catal A Chem 251:8
32. Periana RA, Bergman RG (1986) J Am Chem Soc 108:7332
33. Periana RA, Bergman RG (1986) J Am Chem Soc 108:7346
34. Periana RA, Bergman RG (1984) J Am Chem Soc 106:7272
35. Schaller CP, Cummins CC, Wolczanski PT (1996) J Am Chem Soc 118:591
36. Bennett JL, Wolczanski PT (1997) J Am Chem Soc 119:10696
37. Lin M, Shen C, Garcia-Zayas EA, Sen A (2001) J Am Chem Soc 123:1000
38. Gol'dschleger NF, Es'kova VV, Shilov AE, Shteinman AA (1972) Russ J Phys Chem 46:785
39. Periana RA, Taube DJ, Gamble S, Taube H, Satoh T, Fujii H (1998) Science 280:560
40. Periana RA, Taube DJ, Evitt ER, Löffler DG, Wentrcek PR, Voss G, Masuda T (1993) Science 259:340
41. Gang X, Birch H, Zhu Y, Hjuler HA, Bjerrum NJ (2000) J Catal 196:287
42. Periana RA, Mironov O, Taube D, Bhalla G, Jones CJ (2003) Science 301:814
43. Zerella M, Mukhopadhyay S, Bell AT (2004) Chem Commun 1948
44. Jones CJ, Taube D, Ziatdinov VR, Periana RA, Nielsen RJ, Oxgaard J, Goddard WA III (2004) Angew Chem Int Ed 43:4626
45. De Vos DE, Sels BF (2005) Angew Chem Int Ed 44:30
46. Tenn WJ III, Young KJH, Bhalla G, Oxgaard J, Goddard WA III, Periana RA (2005) J Am Chem Soc 127:14172

47. Tenn WJ III, Young KJH, Oxgaard J, Nielsen RJ, Goddard WA III, Periana RA (2006) Organometallics 25:5173
48. Young KJH, Mironov OA, Periana RA (2007) Organometallics 26:2137
49. Bischof SM, Ess DH, Meier SK, Oxgaard J, Bhalla G, Nielson RJ, Goddard WA III, Periana RA (2010) Organometallics 29:742
50. Klei SR, Golden JT, Tilley D, Bergman RG (2002) J Am Chem Soc 124:2092
51. Feng Y, Lail M, Barakat KA, Cundari TR, Gunnoe TB, Petersen JL (2002) J Am Chem Soc 127:14174
52. Kloek SM, Heinekey DM, Goldberg KI (2007) Angew Chem Int Ed 46:4736
53. Cotton FA, Wilkinsin G (1988) Advanced inorganic chemistry, 5th edn. Wiley, New York
54. Wheatly AEH (2001) Chem Soc Rev 30:265
55. Carpentier J-F (2010) Dalton Trans 39:37
56. Conley BL, Ganesh SK, Gonzales JM, Tenn WJ III, Young KJH, Oxgaard J, Goddard WA III, Periana RA (2006) J Am Chem Soc 128:9018
57. Conley BL, Ganesh SK, Gonzales JM, Ess DH, Nielsen RJ, Ziatdinov VR, Oxgaard J, Goddard WA III, Periana RA (2008) Angew Chem Int Ed 41:7849
58. Hashiguchi BG, Hövelmann CH, Bischof SM, Lokare KS, Leung CH, Periana RA (2010) In: Crabtree RH (ed) Energy production and storage. Wiley, New York, p 101
59. Smith MB, March (2007) March's advanced organic chemistry, 6th edn. Wiley-Interscience, Hoboken, p 519
60. Baeyer A, Villiger A (1899) Chem Ber 32:3625
61. Baeyer A, Villiger V (1900) Chem Ber 33:858
62. Olah GS, Schlosberg RH (1968) J Am Chem Soc 90:2726
63. Olah GA (2005) J Org Chem 70:2413
64. Olah GA, Prakash GKS (1985) Superacids. Wiley, New York
65. Streitwieser A Jr, Taylor DR (1970) J Chem Soc Chem Commun 1248
66. Streitwieser A Jr, Boerth DW (1978) J Am Chem Soc 100:755
67. Streitwieser A Jr, Scannon PJ, Niemeyer HM (1972) J Am Chem Soc 94:7936
68. Handa H, Baba T, Ono Y (1998) J Chem Soc Faraday Trans 94:451
69. Crabtree RH (2010) Science 330:455
70. Crabtree RH (2011) New J Chem 35:18
71. Das S, Incarvito CD, Crabtree RH, Brudvig GW (2006) Science 312:1941
72. Lee DH, Kwon HJ, Patel PP, Liable-Sands LM, Rheingold AL, Crabtree RH (1999) Organometallics 18:1615
73. Billig E, Williams R, Bernal I, Waters JH, Gray HB (1964) Inorg Chem 3:663
74. Ward MD, McCleverty JA (2002) J Chem Soc Dalton Trans 275
75. Ringenberg MR, Kokatam SL, Heiden ZM, Rauchfuss TB (2008) J Am Chem Soc 130:788
76. Miller AJM, Labinger JA, Bercaw JE (2010) J Am Chem Soc 132:3301
77. Balaraman E, Gunanathan C, Zhang J, Shimon LJW, Milstein D (2011) Nat Chem 3:609
78. Kohl SW, Weiner L, Schwartsburd L, Konstantinovoski L, Shimon LJW, Ben-David Y, Iron MA, Milstein D (2009) Science 324:74
79. Bart SC, Chlopek K, Bill E, Bouwkamp MW, Lobkovsky E, Neese F, Wieghardt K, Chirik PJ (2006) J Am Chem Soc 128:13901
80. Gilbert TM, Hristov I, Ziegler T (2001) Organometallics 20:1183
81. Hristov IH, Ziegler T (2003) Organometallics 22:1668
82. Kua J, Xu X, Periana RA, Goddard WA III (2002) Organometallics 21:511
83. Paul A, Musgrave CB (2007) Organometallics 26:793
84. Xu X, Kua J, Periana RA, Goddard WA III (2003) Organometallics 22:2057
85. Ahlquist M, Periana RA, Goddard WA III (2009) Chem Commun 2373
86. Ahlquist M, Nielsen RJ, Periana RA, Goddard WA III (2009) J Am Chem Soc 131:17110
87. Saito S, Saito S, Ohwada T, Shudo K (1991) Chem Pharm Bull 39:2718
88. Atkins PJ, Palling DJ, Poon NL, Hall CD (1982) J Chem Soc Perkin Trans II 1107
89. Paul MA, Long FA (1957) Chem Rev 57:1
90. O'Connor CJ (1969) J Chem Ed 46:686
91. Matsumoto T, Taube DJ, Periana RA, Taube H, Yoshida H (2000) J Am Chem Soc 122:7414

92. Bhalla G, Liu XY, Oxgaard J, Goddard WA III, Periana RA (2005) J Am Chem Soc 127:11372
93. Jones WD, Maguire JA (1986) Organometallics 5:590
94. Giannotti C, Green MLH (1972) J Chem Soc Chem Commun 1115
95. Harper TGP, Shinomoto RS, Deming MA, Flood TC (1988) J Am Chem Soc 110:7915
96. Klei SR, Tilley D, Bergman RG (2002) Organometallics 21:4905
97. Feng Y, Lail M, Barakat K, Cundari T, Gunnoe TB, Peterson JL (2005) J Am Chem Soc 127:14174
98. Leung CW, Zheng W, Wang D, Ng SM, Yeung CH, Zhou Z, Lin Z, Lau CP (2007) Organometallics 26:1924
99. Tenn WJ III, Young KJH, Oxgaard J, Nielsen RJ, Goddard WA III, Periana RA (2006) Organometallics 25:173
100. Meier SK, Young KJH, Ess DH, Tenn WJ III, Oxgaard J, Goddard WA III, Periana RA (2009) Organometallics 28:5293
101. Prechtl MHG, Hoelscher M, Ben-David Y, Theyssen N, Loshcen R, Milstein D, Leitner W (2007) Angew Chem Int Ed 46:2269
102. Gutierrez-Puebla E, Monge A, Paneque M, Poveda ML, Taboada S, Trujillo M, Carmona E (1999) J Am Chem Soc 121:346
103. Ess DH, Goddard WA III, Periana RA (2010) Organometallics 29:6459
104. Ess DH, Nielsen RJ, Goddard WA III, Periana RA (2009) J Am Chem Soc 131:11686
105. Wax MJ, Stryker JM, Buchanan JM, Kovac CA, Bergman RG (1984) J Am Chem Soc 106:1121
106. Mobley TA, Schade C, Bergman RG (1998) Organometallics 17:3574
107. Hoyano JK, Graham WAG (1982) J Am Chem Soc 104:3723
108. Hoyano JK, McMaster AD, Graham WAG (1983) J Am Chem Soc 105:7190
109. Wenzel TT, Bergman RG (1986) J Am Chem Soc 108:4856
110. Leung DH, Bergman RG, Raymond KN (2006) J Am Chem Soc 128:9781
111. Young GB, Whitesides GM (1978) J Am Chem Soc 100:5808
112. Desrosiers PJ, Shinomoto RS, Flood TC (1986) J Am Chem Soc 108:7964
113. Jensen MP, Wick DD, Reinartz S, White PS, Templeton JL, Goldberg KI (2003) J Am Chem Soc 125:8614
114. Ng SM, Lam WH, Mak CC, Tsang CW, Jia G, Lin Z, Lau CP (2003) Organometallics 22:641
115. Holtcamp MW, Labinger JA, Bercaw JE (1997) J Am Chem Soc 119:848
116. Luinstra GA, Wang L, Stahl SS, Labinger JA, Bercaw JE (1995) J Organomet Chem 504:75
117. Abu-Omar MM, Hansen PJ, Espenson JH (1996) J Am Chem Soc 118:4966
118. Gonzales JM, Distaiso R Jr, Periana RA, Goddard WA III, Oxgaard J (2007) J Am Chem Soc 129:15794
119. Bischof SM, Cheng M-J, Nielsen RJ, Gunnoe TB, Goddard WA III, Periana RA (2011) Organometallics 3:2079
120. Schmidt SP, Trogler WC, Basolo F (2007) Inorg Synth 28:160
121. Waitkins GR, Clark CW (1945) Chem Rev 36:235
122. Sharpless KB, Gordon KM (1976) J Am Chem Soc 98:300
123. Corey EJ, Schaefer JP (1960) J Am Chem Soc 82:918
124. Nicolaou KC, Petasis NA (1984) Selenium in natural products synthesis. CIS, Philadelphia
125. Sharpless KB, Lauer RF (1972) J Am Chem Soc 94:7154
126. Umbreit MA, Sharpless KB (1977) J Am Chem Soc 99:5526
127. Patel BM, Price GL (1990) Ind Eng Chem Res 29:730
128. Mann RS, Lao KC (1967) Ind Eng Chem Res 6:263
129. Bird L, Challenger F (1942) J Chem Soc 570
130. Tenn WJ III, Conley BL, Hövelmann CH, Ahlquist M, Nielsen RJ, Ess DH, Oxgaard J, Bischof SM, Goddard WA III, Periana RA (2009) J Am Chem Soc 131:2466
131. Basolo F (1968) Pure Appl Chem 17:37
132. Jackson WG (2002) Inorg React Mech 4:1

133. Bianchini C, Meli A, Vizza F (2004) J Organomet Chem 689:4277
134. Longato B, Pilloni G, Valle G, Corain B (1988) Inorg Chem 27:956
135. Kiyooka S, Matsumoto S, Kojima M, Sakonaka K, Maeda H (2008) Tetrahedron Lett 49:1589
136. Tsukada N, Murata K, Inoue Y (2005) Tetrahedron Lett 46:7515
137. Bercaw JE, Hazari N, Labinger JA, Oblad PF (2008) Angew Chem Int Ed 47:9941
138. Williams TJ, Caffyn AJM, Hizari N, Oblad PF, Labinger JA, Bercaw JE (2008) J Am Chem Soc 130:2418
139. Kuiper JL, Shapley PA (2007) J Organomet Chem 692:1653
140. Hashiguchi BG, Young KJH, Yousufuddin M, Goddard WA III, Periana RA (2010) J Am Chem Soc 132:12542
141. Rochester CH (1966) Q Rev Chem Soc 20:511

Top Organomet Chem (2013) 44: 233–260
DOI: 10.1007/3418_2012_47

Published online: 18 August 2012

Carbene Catalysis: Beyond the Benzoin and Stetter Reactions

Benoit Cardinal-David and Karl A. Scheidt

Abstract The discovery and development of new *N*-heterocyclic carbene-catalyzed reaction is described. Based on inspiration from nature, we have taken thiazolium-based approaches to umpolung reactivity and invented a suite of related reactions involving acyl anions, homoenolate, and enolate nucleophiles all generated under catalytic conditions.

Keywords Asymmetric methodology · Biomimetic · Catalysis · Lewis base · Umpolung

Contents

B. Cardinal-David and K.A. Scheidt (✉)
Department of Chemistry, Center for Molecular Innovation and Drug Discovery, Chemistry of Life Processes Institute, Northwestern University, Evanston, IL 60208, USA
e-mail: scheidt@northwestern.edu

Abbreviations

Ar	Aryl
Bn	Benzyl
Cy	Cyclohexyl
DABCO	1,4-Diazabicyclo[2,2,2]octane
DBU	1,8-Diazabicyclo[5.4.0]undec-7-ene
DCM	Dichloromethane
DMAP	*N*,*N*-4-dimethylaminopyridine
E^+	Electrophile
Ee	Enantiomeric excess
Et	Ethyl
H	Hour
HOMO	Highest occupied molecular orbital
i-Pr	*iso*-Propyl
L.A.	Lewis acid
Me	Methyl
Mes	Mesityl
NHC	*N*-heterocyclic carbene
NMR	Nuclear magnetic resonance
Np	Naphthyl
Nu^-	Nucleophile
p	Para
Ph	Phenyl
Pr	Propyl
TADDOL	2,2-Dimethyl-α,α,α′,α′-tetraphenyl-1,3-dioxolane-4,5-dimethanol
TBD	1,5,7-Triazabicyclo[4.4.0]dec-5-ene
TBDPS	*tert*-Butyldiphenylsilyl
t-Bu	*tert*-Butyl
Tf	Trifluoromethanesulfonyl
THF	Tetrahydrofuran
Tol	Tolyl
Ts	*p*-Toluenesulfonyl
X^-	Counterion

1 Introduction

The development of new efficient catalytic reactions lies at the heart of the synthesis of enantioenriched biologically active molecules. Until recently, the use of transition metal complexes and enzymes were the main channels to achieve this goal (see [1] and references therein). While early reports hinted at the possibilities of future, the first report of a highly enantioselective reaction catalyzed by proline in 1971 helped focus attention on the great potential of

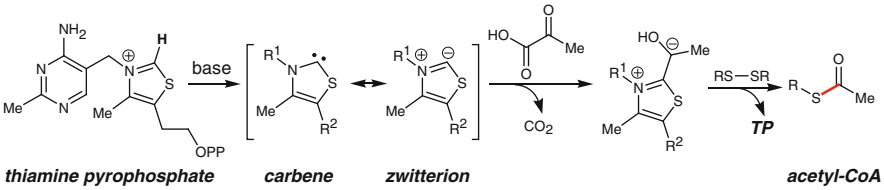

Scheme 1 Production of acetyl CoA by vitamin B_1

small organic molecules as efficient catalysts [2]. Since then, an explosion of powerful organocatalyzed reactions have been developed and contributed to the development of an established and recognized way to synthesize enantioenriched molecules that complements transition metal catalysis [3–9]. In general, these reactions can be categorized as Brønsted acid catalysis [10–15], Brønsted base catalysis [16], phase-transfer catalysis (for an excellent review, see [17]), and nucleophilic or Lewis-basic catalysis [4, 18–24]. Interestingly, for each of these categories of reactions, the catalytic activity is based on fundamental interactions found in enzymatic catalysis [25]. Inspiration by nature has always played a major role in the evolution of this field, and the invention of new organic catalysts that can reproduce the remarkable levels of reactivity and selectivity of enzymes is an ongoing objective with great potential impact on society. While almost all of the examples of reactions catalyzed by enzymes involve molecules reacting in their normal polarity mode, an interesting enzyme, pyruvate dehydrogenase, is an exception to this rule and attracted our interest when we established the laboratory at Northwestern. This enzyme takes advantage of vitamin B_1, or thiamine, an unusual cofactor acting as a Lewis base catalyst that converts pyruvic acid into an acyl anion equivalent to produce acetyl CoA (Scheme 1). The structure of vitamin B_1 was elucidated by Robert R. Williams in 1936 [26], and the active form of thiamine was initially proposed in the early 1950s to be a "pseudo base" with a hydroxyl moiety added at C2 of the thiazolium core [27]. Today, this type of catalyst is known as an *N*-heterocyclic carbene and can be also viewed as its tautomer, a zwitterion [28–35]. Since the discovery of thiamine, considerable work has been focused at the isolation of NHCs ([36–41, 42] and references therein).

Although the concept of *umpolung* [43–46] was formalized in the late 1970s [47, 48], the first reaction involving an acyl anion equivalent, namely, the benzoin reaction, was reported in 1832 by Wöhler and Liebig (Scheme 2) [49]. Lapworth helped formulate the basic aspects of affinity patterns that we employ today and proposed the formation of an acyl anion equivalent in 1903 [50]. In 1943, Ugai and collaborators reported the first thiazolium-catalyzed benzoin reaction which obviated the use of cyanide for this process [51]. The discovery of this reaction, along with the pyruvate dehydrogenase-catalyzed formation of acetyl CoA, triggered many questions regarding the mechanism of these closely

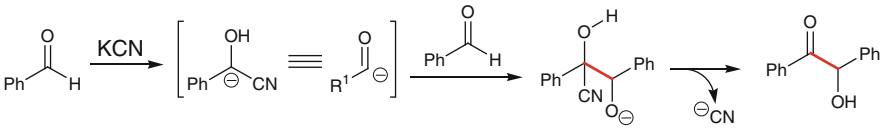

Scheme 2 Benzoin reaction

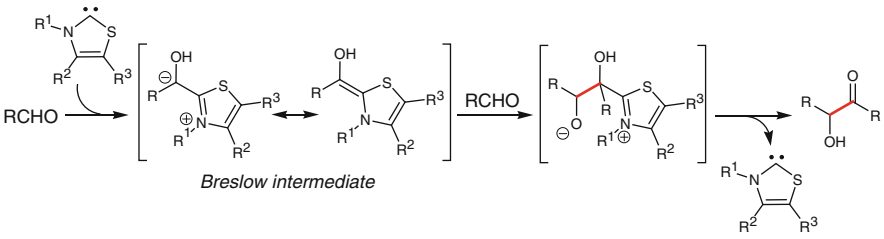

Scheme 3 NHC-catalyzed Benzoin reaction

related processes. Breslow ingeniously proposed in 1958 that the nucleophilic attack of the active *N*-heterocyclic carbene catalyst onto an aldehyde generates an acyl anion equivalent in the form of an unusual tetrasubstituted olefin, today referred to as the "Breslow intermediate" (Scheme 3) [52]. Since this seminal proposal, substantial studies have supported this mechanism [53], including a highly detailed recent investigation by Leeper and coworkers [54]. Overall, the nucleophilic carbene relocates the electron density on the carbon atom that originally belonged to the carbonyl of the aldehyde. This fascinating and distinct ability of nucleophilic carbenes to generate a secondary nucleophile in the flask led to the development of unique reactivity patterns in the past decade. In this chapter, our contributions to this exciting field of research are described (see also [55]).

2 Modern Acyl Anion Reactions

2.1 Benzoin Reaction

In 1966, Sheehan reported a remarkable asymmetric benzoin reaction catalyzed by chiral thiazolium salts with moderate levels of enantioselectivity [56–59]. In 2002, Enders and coworkers made an important breakthrough when they reported the first highly enantioselective intermolecular benzoin reaction catalyzed by a triazolium salt derived from *tert*-leucine [Eq. (1)] [60]. Since then, catalyst development for NHC catalysis has seen exponential growth for new triazolium salts derived from chiral amino acids and amino alcohols.

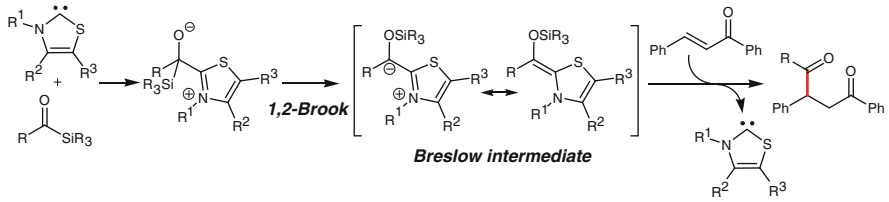

Scheme 4 The Sila–Stetter reaction

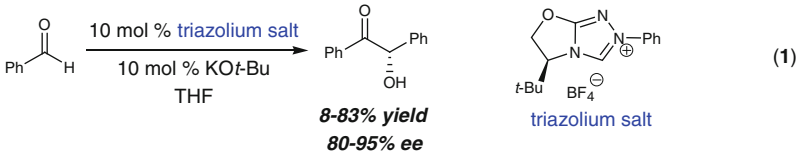

(**1**)

2.2 Stetter Reaction: Defining the Research Problem

In 1976, Stetter reported the NHC-catalyzed conjugate addition of acyl anion equivalents to Michael acceptors [61]. Following this initial report, researchers capitalized upon this reaction to synthesize 1,4-dicarbonyl compounds, precursors of important building blocks for natural product synthesis [62, 63]. More recently, Enders [64] and Rovis [65–68] have demonstrated that high levels of enantioselectivity can be obtained with chiral triazolium salts. Although good success has been achieved in the development of the intramolecular Stetter reaction, its *intermolecular* version circa late 2011 has proven to be much more challenging [69–73]. A major issue is that the acyl anion precursor (i.e., aldehyde) is a more active electrophile than a typical conjugate acceptor molecule.

At the inception of our laboratory in 2002, we were drawn to finding a solution to this perplexing drawback and initiated a research program aimed at the invention of new Lewis base-catalyzed reactions. We hypothesized that the use of an acylsilane [74–76] as the acyl anion precursor might prevent nucleophilic addition of the Breslow intermediate to the carbonyl through increased steric hindrance (Scheme 4). Following the nucleophilic addition of the NHC to the acylsilane, the tetrahedral intermediate would undergo a 1,2-Brook rearrangement [77] and collapse to the more stable Breslow intermediate. Although Heathcock [78] and Degl'Innocenti [79] had previously demonstrated that such a sequence of event can be triggered by small nucleophiles like fluoride or cyanide, it was unclear if the acylsilane would undergo the initial addition of the relatively large NHC. A second important question was whether the NHC possessed a similar nucleophilicity/basicity balance as cyanide to promote this type of transformation. Our idea for inventing a new NHC reaction in 2002 was to explore new opportunities in the area of catalytic umpolung chemistry and use Lewis bases as potential catalysts.

Table 1 Optimization of the Sila–Stetter reaction

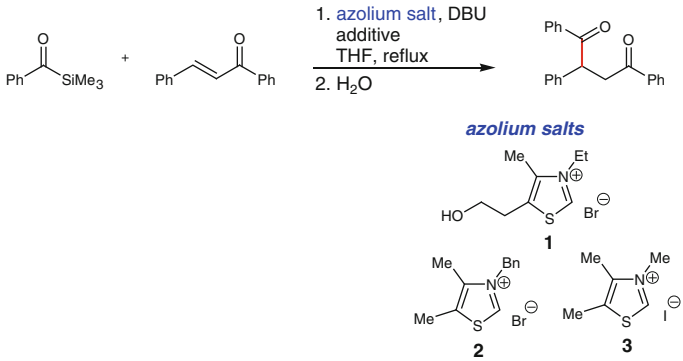

Entry	Azolium salt (equiv.)	Additive	%Yield
1	**1** (1.0)	None	71
2	**2** (1.0)	None	0
3	**1** (3.0)	None	43
4	**1** (3.0)	*i*-PrOH	77
5	**3** (3.0)	*i*-PrOH	77

After an initial examination of conjugate acceptors, we discovered that chalcone was a suitable electrophile to survey conditions to promote acylsilane additions (Table 1) [80, 81]. Our investigations began by testing the reaction with a stoichiometric amount of the thiazolium salt **1** in presence of DBU. Employing these conditions, the 1,4-diketone could be isolated in 71% yield (Table 1, entry 1). Surprisingly, the reaction afforded only small amounts of the product when precatalyst **2** was used (entry 2). A comparison of both catalyst structures led to the hypothesis that the primary alcohol in **1** was responsible for this striking difference in reactivity. In a serendipitous turn for our nascent NHC program in 2003, only the thiazolium salt with the pendent alcohol was commercially available at the time since it was derived presumably from thiamine. We decided to explore this variable by dropping the catalyst loading to 30 mol% of azolium salt **1**, which afforded only 43% yield of the diketone (entry 3). While keeping the amount of azolium salt constant, the yield could be improved to 77% by simple addition of *iso*propanol to the reaction mixture (entry 4). Finally, when this key additive was used with thiazolium salt **3**, the diketone could be obtained in the same yield, confirming our initial assumption.

As shown in Scheme 5, the scope of the reaction with respect to the chalcone component is broad. Electron-withdrawing and electron-donating substituents are well tolerated and afford the 1,4-diketone in good yields. Interestingly, methyl vinyl ketone and ethyl acrylate are suitable partners in the acyl silane addition reaction,

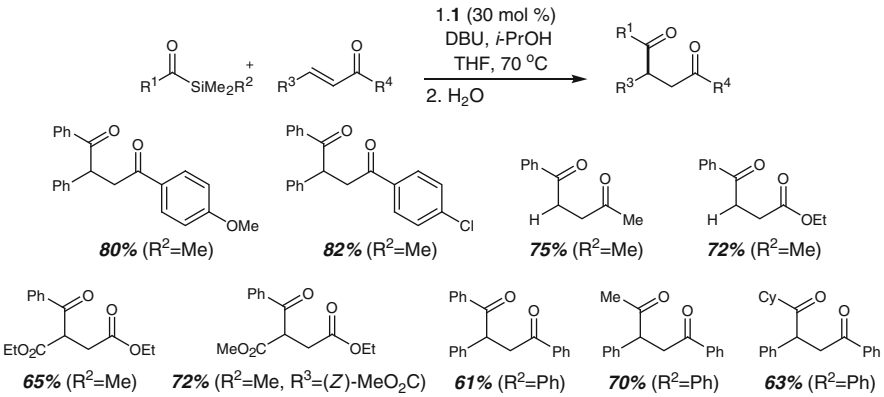

Scheme 5 Scope of the Sila–Stetter reaction

as well as diethyl fumarate and dimethyl maleate. The compatibility of these highly reactive electrophiles is remarkable when considering their exposure to many other nucleophiles in solution. The substitution on the acylsilane was also investigated. It was found that many aromatic acylsilanes can undergo addition to chalcone [80], but most notably, enolizable acylsilanes can react cleanly without any contamination by Michael or aldol products.

The efficiency of the Sila–Stetter reaction for the synthesis of 1,4-dicarbonyl compounds prompted us to extend this methodology to a single-flask protocol for the Paal–Knorr synthesis of furans and pyrroles [82, 83]. Finally, we also took advantage of acylsilanes to develop the 1,2-addition of carbanion equivalents to activated imines for the synthesis of α-amino ketones [84].

Conscious of the many advantages of employing acylsilanes to access the Breslow intermediate without the use of an aldehyde, we decided to investigate other ways to capture the acyl anion reactivity in the Stetter reaction while avoiding the benzoin reaction. Inspired by thiamine-dependent pathways, we hypothesized that α-keto acids would constitute excellent candidates for the generation of acyl anion equivalents in aqueous media. Such a biomimetic approach would provide 1,4-diketones in an environmentally benign reaction medium. At the onset of these investigations, only one publication by Stetter and Lorenz described the use of alpha keto acids as acyl anion precursors in nonenzymatic reactions [85]. The authors employed catalytic amounts of a triazolium salt with excess triethylamine (2.0 equiv.) at 80°C, limiting the use of substrates bearing base-sensitive groups. The substrate scope is also limited to vinyl ketones having no substituent at the β-position. The harsh reaction conditions and the narrow substrate scope provided an impetus to solve these problems and attempt to implement aqueous reaction conditions.

We employed our previous conditions using 20 mol% of a thiazolium salt with DBU in THF as a platform to identify suitable acceptors with pyruvic acid as the acyl anion precursor. After a brief survey, 2-acyl *N*-methyl imidazole [86, 87] was

Table 2 Optimization and scope of the biomimetic Stetter reaction

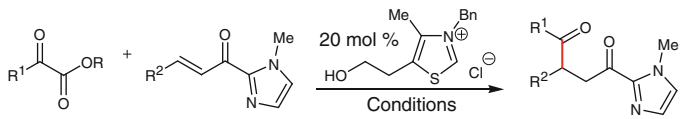

Entry	R	R^1	R^2	Solvent	Base	%Yield
1	H	Me	Ph	THF	DBU	85
2	NA	Me	Ph	MeOH/buffer[a]	pH 7.2	92
3	NA	Me	4-MeOPh	MeOH/buffer[a]	pH 7.2	87
4	NA	Me	4-ClPh	MeOH/buffer[a]	pH 7.2	87
5	NA	Me	2-Furyl	MeOH/buffer[a]	pH 7.2	80
6	NA	Me	2-Thiophene	MeOH/buffer[a]	pH 7.2	90
7	NA	Pr	Ph	MeOH/buffer[a]	pH 7.2	92
8	NA	Ph	Ph	MeOH	DBU	90
9	NA	2-Thiophene	Ph	MeOH/buffer[a]	pH 7.2	76

[a]1.3:1, v:v (MeOH:100 mM phosphate-based buffer)

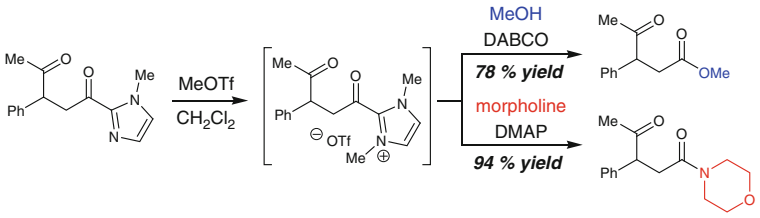

Scheme 6 Functionalization of 2-acyl imidazoles

found to engage as a conjugate acceptor to afford the desired compound in high yield (Table 2, entry 1). Although this result was encouraging, excess DBU was still needed. Employing the sodium salt of pyruvic acid not only alleviated the use of an external base but also provided the opportunity to perform the reaction in a methanol/buffer mixture at a neutral pH, affording the 1,4-diketone in 92% yield (entry 2) [88].

The optimized reaction conditions accommodated a wide range of substrates, both on the unsaturated ketones and the keto acid salts. Electron-donating and electron-withdrawing aryl substituents on the α,β-unsaturated 2-acyl *N*-methyl imidazole performed equally well, and heteroaromatic substituents were also suitable. Alkyl, aryl, and heteroaryl-substituted keto acid salts underwent the conjugate addition very cleanly. The reaction conditions needed to be altered with regard to the solvent system in isolated cases, the solubility of the substrates and product being at the origin of this modification. Finally, the activation of the 2-acyl imidazole with methyl triflate allows for an easy conversion to the methyl ester [86] or the morpholine amide [89] (Scheme 6). These mild reaction conditions offer great potential for applications in synthesis, and current investigations are being focused at the development of an enantioselective variant of this decarboxylative Stetter reaction.

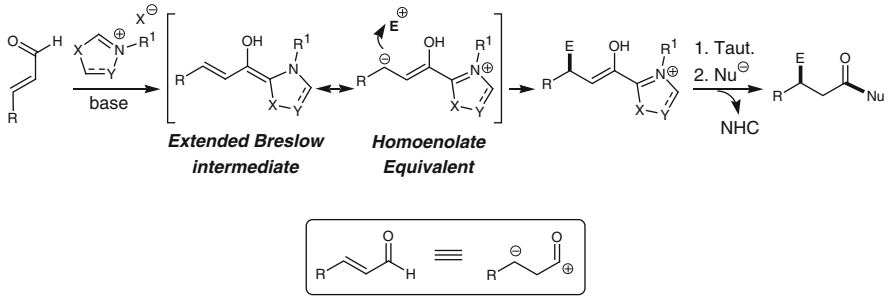

Scheme 7 New concept: NHC-catalyzed generation of homoenolate equivalents

3 Homoenolate Chemistry: Designing a Catalytic Approach

Our early success with the conjugate addition of acylsilanes to conjugate acceptors certainly expanded the breadth of the Stetter reaction. While this original process allows for the direct addition of acyl anion equivalents at the beta position, we also felt that conjugate additions were limited in terms of the possible nucleophiles [90, 91]. Expanding the spectrum of the possible substituents that can be incorporated at this position would be highly beneficial. We thought that we could achieve this objective by inventing reactions based on the inversion of the normal polarity mode of a conjugated acceptor (Scheme 7). Inspired by our initial success, we were intrigued by the possibility of accessing a Breslow intermediate bearing an additional unsaturation unit. On paper, the idea that the addition of a carbene to an enal would generate an extended enamine where the electron density is relocated at C3 of the unsaturated aldehyde was very exciting. We intended to capitalize on this original way of accessing homoenolate equivalents [92, 93] and provide new opportunities for valuable applications with *N*-heterocyclic carbenes (for an excellent review on NHC-catalyzed homoenolate generation, see [94]). We disclosed our independent early findings combining thiazolium salts and α,β-unsaturated aldehydes at the 2004 Natural Products Gordon Conference with the publication of this work appearing 6 months later in early 2005 [95, 96]. The reaction was by no means perfect, and our initial activities were focused too heavily on thiazolium-derived NHCs. During our forays into extending our Sila–Stetter work toward homoenolates, two seminal papers appeared in late 2004 from the Glorius and Bode laboratories detailing the NHC-catalyzed combination of unsaturated aldehydes and aromatic aldehydes to produce γ-lactones [97, 98]. The independent Glorius and Bode publications nicely indicated the superiority of IMes (imidazolium NHCs) and put the community on notice of NHC-homoenolate potential. Clearly, the idea to extend carbene catalysis from benzoin type reaction to related reactivity modes with unsaturated aldehydes had been ongoing in multiple laboratories, seemingly simultaneously with very interesting new directions and applications.

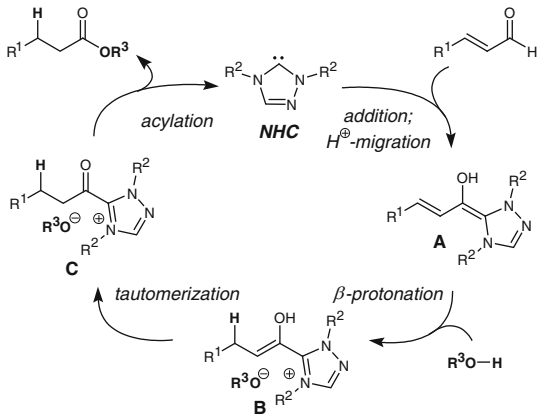

Scheme 8 Proposed mechanism for β-protonation

3.1 β-Protonation

We started our investigations of this NHC-homoenolate reactivity in July of 2004 with the simplest electrophile, a proton [95, 96]. The reaction of an enal with a suitable alcohol should provide the corresponding saturated ester as illustrated in the pathway of Scheme 8. Following the addition of the NHC to the aldehyde, a 1,2-proton migration ensures the formation of the extended Breslow intermediate **A**. The electron density is thus relocated at the β position of the conjugated aldehyde, allowing for protonation to generate the enol **B**. Tautomerization provides an activated ester in the form of acyl azolium **C**, which is poised to undergo addition of a nucleophile with concomitant regeneration of the catalyst.

We selected phenol as the proton source to probe conditions with cinnamaldehyde, 30 mol% **4** and DBU in toluene. This combination of reagents led to a moderate 55% yield of the saturated ester (result not shown). Unexpectedly, performing the reaction in undistilled dry chloroform (filtered over Al_2O_3) afforded a substantial amount of the saturated ethyl ester. The latter compound clearly arises from residual amounts of ethanol used to stabilize chloroform. This important result provided us with the information that the reactivity of the proton donor and the nucleophile can be dissociated. Taking simultaneous advantage of the more acidic phenol for the β-protonation and a more nucleophilic alcohol to improve the rate of acylation/catalyst turnover was the key to achieve high yields in this reaction. As shown in Scheme 9, a variety of primary and secondary alcohols can be employed with low catalyst loading. Both electron-donating and electron-withdrawing aryl substituents can be employed on the starting enal. Saturated (hexenal) and unsaturated (*trans*, *trans*-2,4-hexadienal) alkyl chains provided the saturated esters in 90% and 70% yield, respectively. We also found that β,β-disubstituted enals are competent in this reaction, provided that at least one of the substituents is an aryl group.

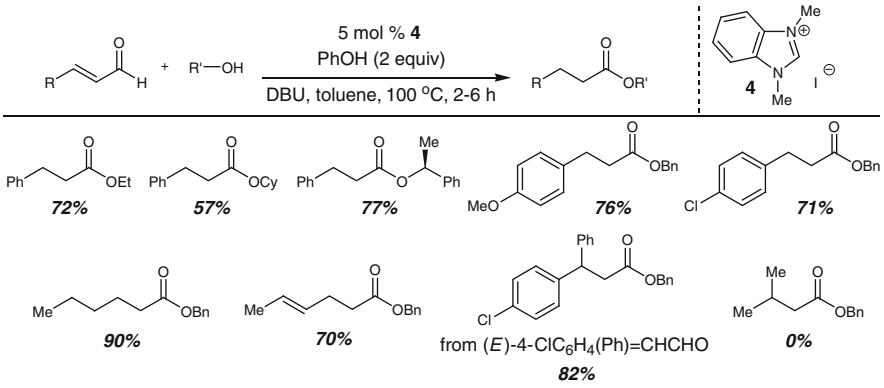

Scheme 9 Scope of the homoenolate β-protonation reaction

Our initial studies uncovered a novel class of unconventional homoenolate nucleophiles accessible from the addition of an NHC to an unsaturated aldehyde. The *umpolung* addition of an alcohol across an enal to generate saturated esters has opened new possibilities for the development of useful acylation and oxidation reactions [99–106].

3.2 Formal [3+2] and [3+3] Cycloadditions

We were fascinated by the possibility of employing different electrophiles for the creation of carbon–carbon and carbon–heteroatom bonds. Ideally, a suitable secondary electrophile should also incorporate a latent nucleophile, which upon homoenolate addition, is able to trigger the final acylation to ensure efficient catalyst turnover. For example, we envisioned that ylides would represent suitable dipolarophiles for formal cycloaddition reactions with homoenolates [107–110], as they possess both electrophilic and nucleophilic functionalities (Scheme 10, pathway a). Although the development of such a strategy might lead to the formation of unique molecular scaffolds, it is also fundamentally hampered by an important side reaction, the dimerization of the starting enal. This competing pathway is the "vinylogous" benzoin problem that we used acylsilanes to solve earlier. A common and undesired formal [3+2] cycloaddition reaction is the carbon–carbon bond formation arising from the addition of the homoenolate onto another equivalent of enal (Scheme 10, pathway b) [95, 96]. The electrophilicity of the secondary electrophile can be increased to some extent, but an excessive change in that direction can cause irreversible addition of the NHC and inhibit the reaction. This delicate balance illustrates how subtle changes in the structure of the secondary electrophile and the catalyst, as well as in the reaction conditions, can have significant impact on the outcome of the reaction.

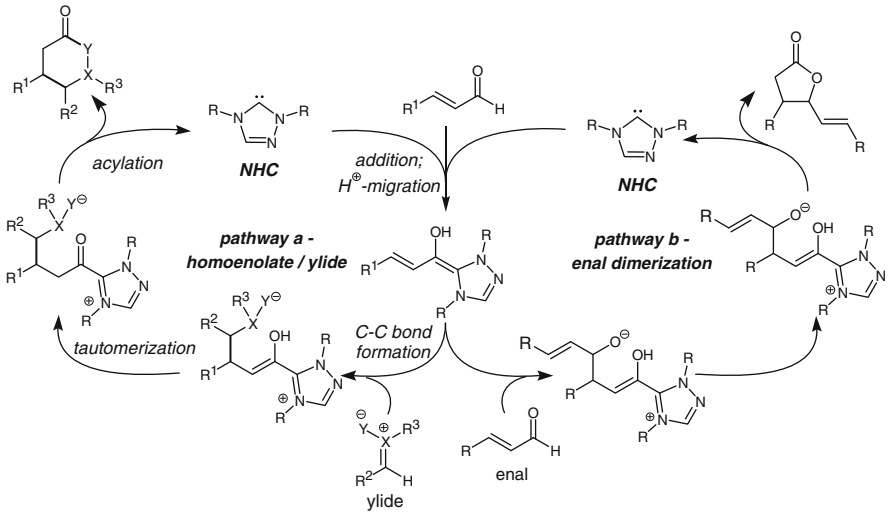

Scheme 10 Competing pathways in formal cycloaddition reactions of enals to ylides

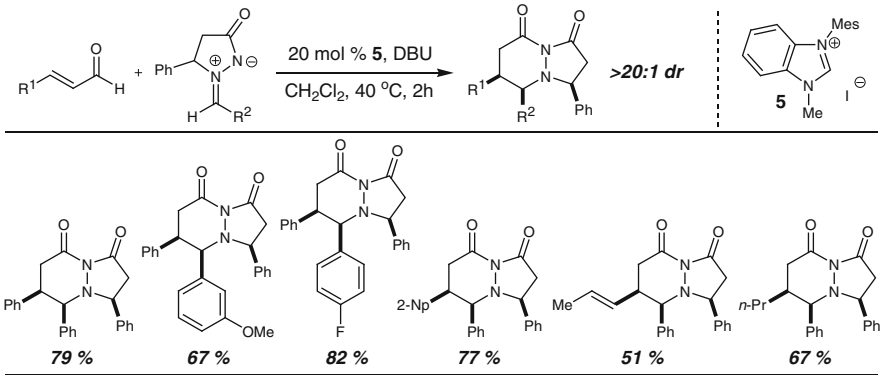

Scheme 11 Formal [3+3] cycloadditions of homoenolates with azomethine ylides

3.2.1 Carbon–Carbon Bond Formation

We decided to evaluate our new strategy with azomethine imines [111–116] as a possible reacting partner with homoenolates [117]. Contrary to our findings with the β-protonation of homoenolates, the *N*,*N*-dimethyl substituted benzimidazole **4** was observed by NMR spectroscopy to interact irreversibly with the secondary electrophile, the starting azomethine imine [118]. The more bulky *N*-mesityl-*N*-methylbenzimidazolium salt **5** was employed in order to sequester this nonproductive pathway (Scheme 11). The use of 20 mol% of this precatalyst in combination with DBU at 40°C catalyzed the reaction between enals and azomethine imines to afford tetrahydropyridazinones as a single diastereoisomer (all *cis*). A variety of substituents are tolerated on the azomethine imine. It was found that phenyl

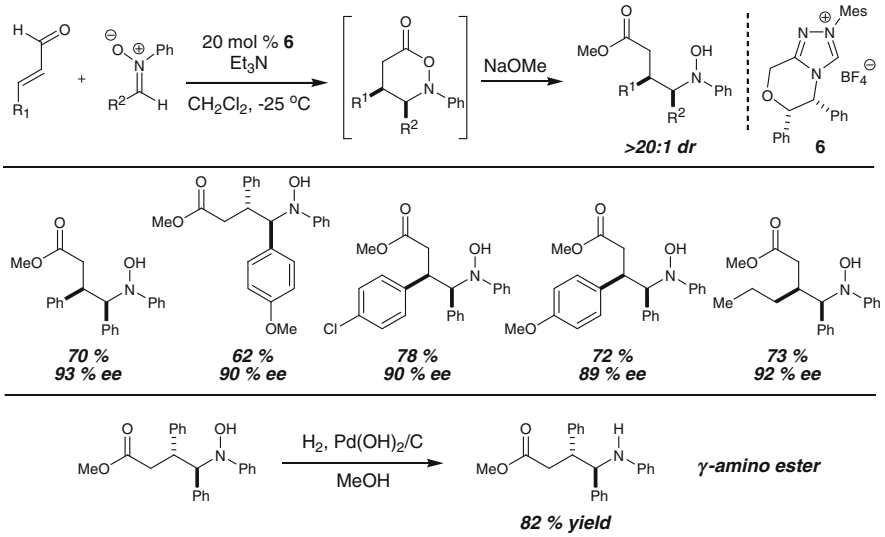

Scheme 12 Formal [3+3] cycloadditions of homoenolates with nitrones

substitution at the position 5 of the azomethine imine is necessary to improve its solubility in CH_2Cl_2. Unfortunately, azomethine imines originating from enolizable aldehydes are not suitable substrates for the process. The reaction was also investigated with respect to the starting aldehyde. α,β-Unsaturated aldehydes bearing electron-donating aryl rings are well tolerated. However electron-withdrawing groups led to very low yields. Finally, it is interesting to note that the diastereoselectivity level is excellent for every case reported. We postulate that hydrogen bonding between the Breslow intermediate and the azomethine imine leads to a highly organized transition state [118]. While the true nature of hydrogen bonding in this reaction is difficult to analyze since it only proceeds in dichloromethane, the idea that an organizational element (in this case, a proton) could facilitate a highly diastereoselective reaction inspired us to investigate Lewis acids as a replacement for this proton (vide infra).

Our initial success with azomethine imines prompted us to explore the breadth of formal cycloaddition reactions by incorporating nitrones [119–123] as a reacting dipole (Scheme 12). Careful catalyst screening led to the identification of chiral amino alcohol-derived azolium **6** as the most efficient to promote the reaction with high stereocontrol [124]. In the course of our investigations, it was found that the six-membered cycloadduct is unstable to flash chromatography and undergoes extensive decomposition. This problem was resolved by treatment with MeONa, which gives access to γ-amino-esters, an important class of compounds for the treatment of neurodegenerative diseases [125–127]. The variety of substrates that can undergo this transformation makes this reaction very useful. Surprisingly, even alkyl substituents are tolerated at the γ-position of the homoenolate, as demonstrated by the reaction with *n*-hexenal (73% yield, 92% ee). Finally, removal

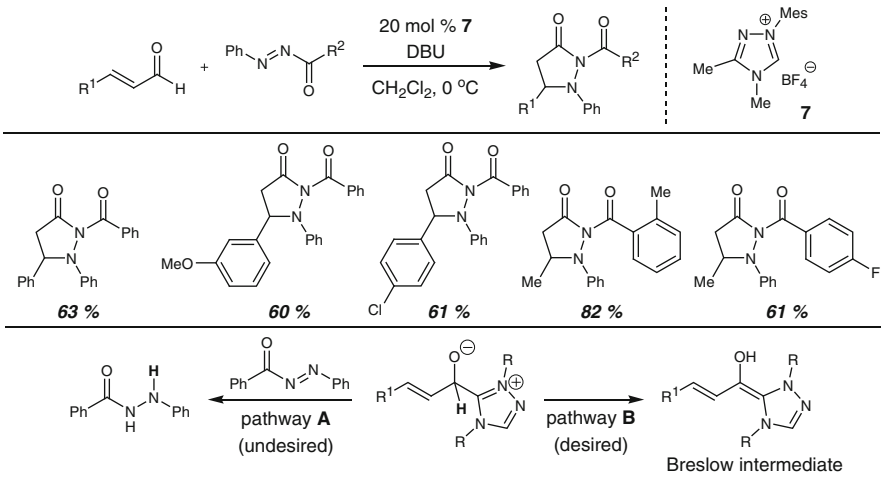

Scheme 13 Formal [3+2] cycloadditions with diazenes: NHC-catalyzed amination

of the *N*-hydroxyl group was accomplished with $Pd(OH)_2/C$ and H_2 to enable further transformations.

3.2.2 Carbon–Nitrogen Bond Formation

The successful implementation of formal cycloaddition reactions with azomethine imines and nitrones prompted us to expand the possibilities of homoenolate chemistry for the creation of carbon–nitrogen bonds. We envisioned that an umpolung amination strategy, employing an electrophilic nitrogen reagent, would complement the existing conventional nucleophilic amination strategies [128–131]. After an initial screen of potential electrophilic amination reagents, diazenes were found to be superior and selected for further optimization (Scheme 13). The development of efficient reaction conditions proved to be challenging. Substantial reduction of the diazene could be observed in a Cannizzaro-type reaction from the tetrahedral intermediate (pathway **A**, Scheme 8), a pathway that we have previously explored and taken advantage of in the development of an NHC-catalyzed hydroacylation reaction [132]. Modification of the precatalyst structure and lowering the temperature favored the selection of the desired pathway. Finally, benzoyl removal followed by SmI_2-promoted N–N bond cleavage afforded the corresponding β-amino amide [128].

3.3 Enolate Chemistry

Our proposed mechanistic model for homoenolate addition suggests the existence of a transient enolate after the nucleophilic addition at the gamma position (Scheme 14). We decided to explore the possibility of intercepting the enol and utilize a second electrophile to functionalize the homoenolate at α-position and

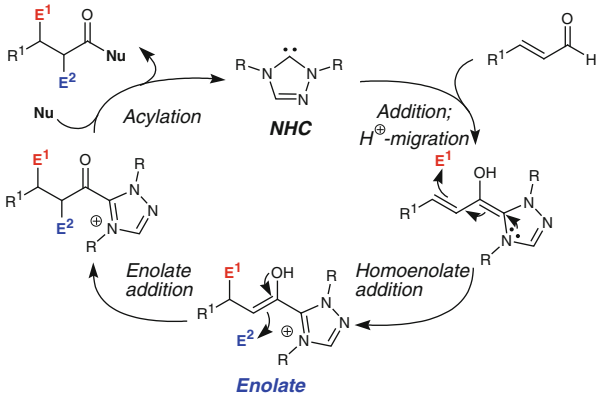

Scheme 14 Proposed pathway for poly-functionalization of homoenolates

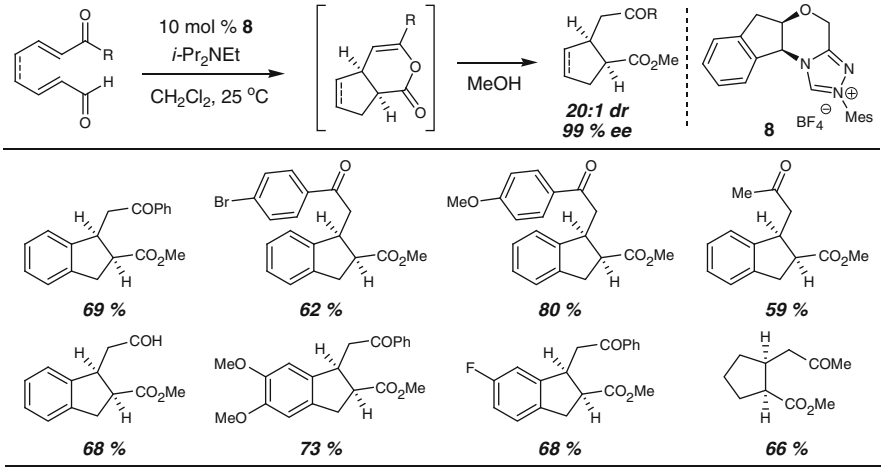

Scheme 15 Proposed NHC-catalyzed intramolecular Michael reactions

expand the breadth of NHC-catalyzed homoenolate reactions. Such a transformation, after catalyst turnover, would result in a tandem three-point functionalization of the starting α,β-unsaturated aldehyde.

3.3.1 Intramolecular Michael Additions

To test our hypothesis, we selected substrates where the enol could react intramolecularly with a tethered functionality while offering the potential for the synthesis of complex frameworks (Scheme 15). We envisaged that β-protonation of the homoenolate would lead to the formation of the enol and trigger a Michael addition

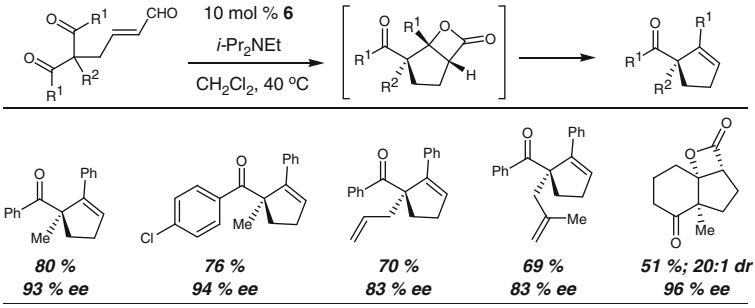

Scheme 16 NHC-catalyzed desymmetrization of 1,3-diketones

as the C–C bond forming step [133, 134]. It was found that *i*-Pr_2NEt is the most efficient base to promote the β-protonation. With the use of 10 mol% **8**, this complex reaction cascade affords a variety of disubstituted indanes with good yields and excellent enantioselectivity levels [135]. We were pleased to find that the substrate scope of this reaction displays great generality with regard to the substrate. Electron-donating and withdrawing substituents are well tolerated on the aryl ring. It was also demonstrated that the Michael acceptor can be an enolizable ketone or an aldehyde. Finally, the reaction can be performed with substrates lacking the aryl ring, which served as a rigid backbone to facilitate the Michael addition.

3.3.2 Desymmetrization of 1,3-Diketones

Our initial success with the intramolecular Michael addition stimulated the development of new NHC reactions involving the trapping of the short-lived enol. We hypothesized that 1,3-diketones could potentially undergo a desymmetrization in which the stereodetermining step is an intramolecular aldol reaction (Scheme 16) [136, 137]. This unusual reaction gives access to cyclopentenes bearing a stereogenic quaternary center with excellent enantioselectivity level. Following β-protonation, the enol undergoes an aldol reaction followed by an acylation, providing a β-lactone. The latter intermediate usually decarboxylates rapidly to give the cyclopentene. In rare cases, mostly when R_1 is an alkyl, the β-lactone is more stable and can be isolated. It is then possible to induce the decarboxylation process by stirring in benzene with SiO_2 at 80°C. Following these initial studies, we demonstrated the utility of this reaction for the synthesis of the bakkenolide natural products [138].

3.4 Rebound Catalysis

The generation of transient enolate species from α,β-unsaturated aldehydes led to the development of new chemical reactions for the construction of complex molecular frameworks. Following these exciting developments, we decided to focus our

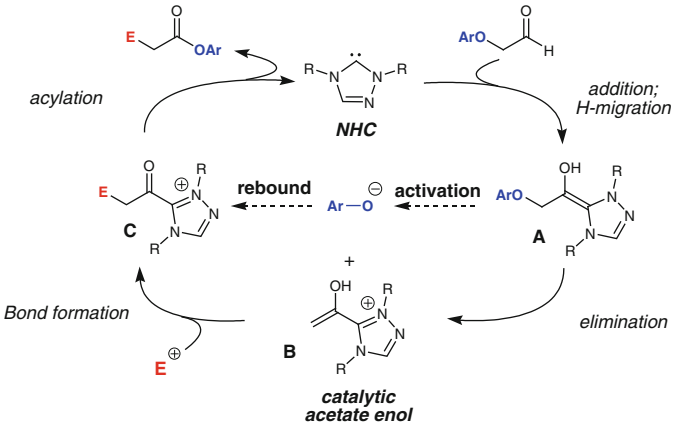

Scheme 17 Proposed pathway for Rebound catalysis

efforts at expanding the variety of enolate nucleophiles that can be accessed with NHC catalysis. We envisioned that acetate enols, an important class of nucleophiles (for recent reviews, see [139, 140]), could be formed catalytically from α-aryloxy-acetaldehydes. Upon formation of the Breslow intermediate **A**, elimination of the aryloxy would provide enol **B**, which could potentially react with a variety of electrophiles (Scheme 17). The aryloxy group (ArO^-) would then participate in the final acylation/catalyst regeneration. The development of such an approach was challenging and needed the following requirements to be met in order to be successful: (1) the aryloxy needs to fulfill the dual ability of being a good leaving group for enol formation and an efficient nucleophile for catalyst turnover, (2) addition of the enol to the electrophile E^+ must be faster than the corresponding homo-aldol reaction (addition of the catalytic enol on the starting aldehyde), and (3) addition of the enol to the electrophile E^+ must be faster than tautomerization/acylation with the aryloxy group.

3.4.1 3,4-Dihydrocoumarins Synthesis

We decided to evaluate our hypothesis with readily available substrates having a tethered enone to the starting aldehyde in order to maximize the chances of bond formation (Scheme 18) [141]. After screening for reaction conditions, we found that the use of 10 mol% of azolium salt **7** in the presence of DBU was the most efficient combination to promote the reaction and afford 3,4-dihydrocoumarins structures in high yield. The reaction was performed in acetonitrile at low concentration to prevent homo-aldol coupling. In this process, acylation of the alkoxide followed by intramolecular Michael addition was a plausible pathway, but it was ruled out after subjecting the acylated substrate to the reaction conditions, which was found to be unreactive.

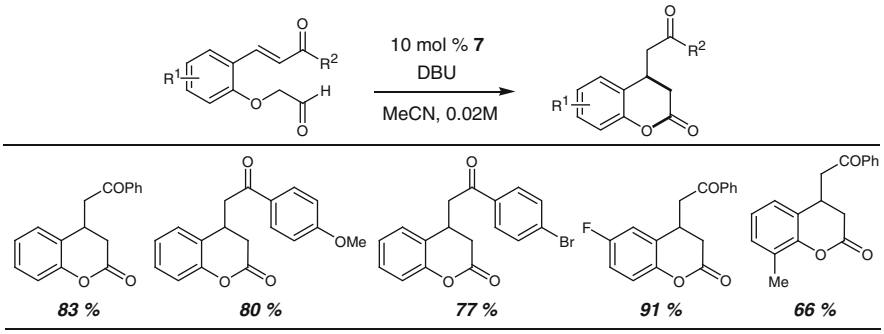

Scheme 18 NHC-catalyzed synthesis of 3,4-dihydrocoumarins

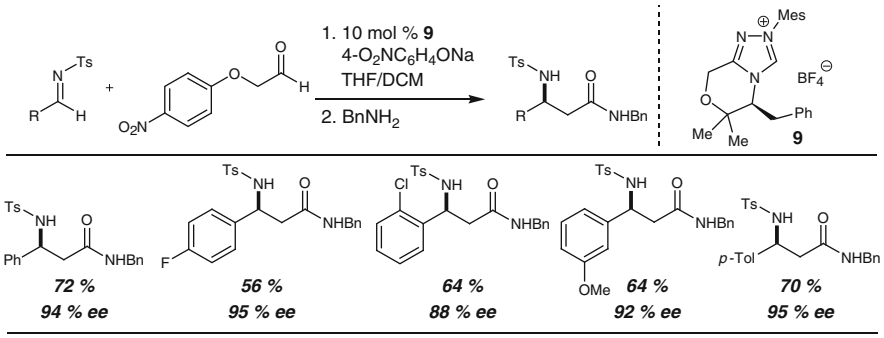

Scheme 19 NHC-catalyzed enantioselective Mannich reactions

3.4.2 NHC-Catalyzed Reactions of α-Aryloxyaldehydes

The successful implementation of NHC-catalyzed enol reactivity for the synthesis of 3,4-dihydrocoumarins prompted us to extend this concept to an intermolecular Mannich process (Scheme 19). Our objective was to develop a suitable acetate enol precursor incorporating a leaving group capable of performing the final acylation step to regenerate the NHC [142]. The search for a substituent that can fulfill this delicate balance with respect to leaving group ability and nucleophilicity revealed that 4-nitrophenoxide is the most efficient. An interesting aspect of this reaction is the selection of the base. Unlike the previously developed NHC reactions that typically required an amine, sodium 4-nitrophenoxide was found to be the best in this case, presumably assisting in the catalyst regeneration. The direct product of this reaction, the 4-nitrophenoxide ester, was found to be unstable toward flash chromatography. It was thus converted to the corresponding β-amino amide, which could be isolated with good yields and excellent stereoinduction levels.

The formation of an activated ester as the product allowed simple in situ functionalization with a variety of nucleophiles, providing direct access to products having a different oxidation state, as depicted in Scheme 20.

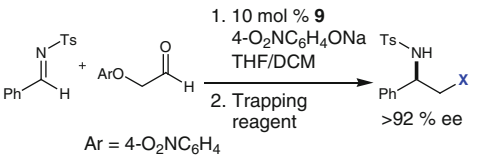

Trapping reagent	X	% Yield
MeOH/aq. NaOH	COOH	71
$LiBH_4$	CH_2OH	70
MeONa	CO_2Me	61
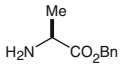	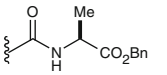	51

Scheme 20 Enantioselective Mannich/functionalization

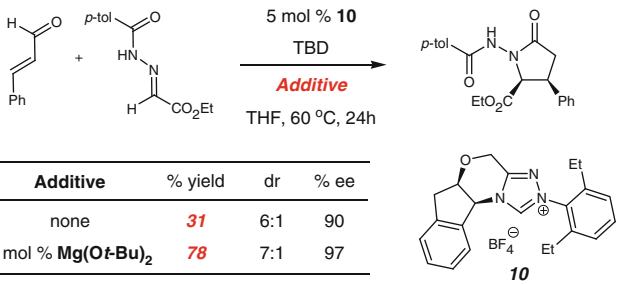

Additive	% yield	dr	% ee
none	*31*	6:1	90
5 mol % **Mg(O*t*-Bu)$_2$**	*78*	7:1	97

Scheme 21 Impact of a Lewis acid in the [3+2] formal cycloaddition to γ-lactams

3.5 NHC-Catalyzed Reactions with Lewis Acids

3.5.1 Cooperative NHC/Lewis Acid Catalysis for the Synthesis of γ-Lactams

In the course of our work, we became interested in the development of an NHC-catalyzed synthesis of γ-lactams from a formal [3+2] cycloaddition reaction between enals and imines. While this reaction had been first reported by Bode [143], its enantioselective version remained elusive at the onset of our studies. We identified aminoindanol-derived azolium salt **10** as an efficient precatalyst to afford γ-lactams with excellent enantioselectivity level when cinnamaldehyde reacts with *N*-acyl hydrazones derived from ethyl glyoxylate (Scheme 21) [144]. Unfortunately, this reaction proved to be sluggish, affording a low yield of the target product after 24 h of reaction time.

To resolve this reactivity problem, we explored the possibility of employing a Lewis acid to activate the *N*-acyl hydrazone by lowering its LUMO energy (Scheme 22) [145–147]. If successful, such an achievement would expand the possibilities for the development of new NHC reactions. The most important challenge to this idea is the known ability of carbenes to act as ligands and form stable complexes, particularly with late transition metals such as palladium and copper [148–151]. We hypothesized that early metals would react reversibly with NHCs, allowing for the development of a cooperative catalytic system. After

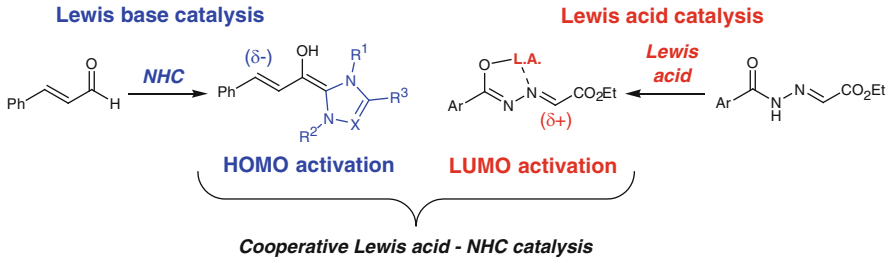

Scheme 22 Cooperative catalysis with NHCs

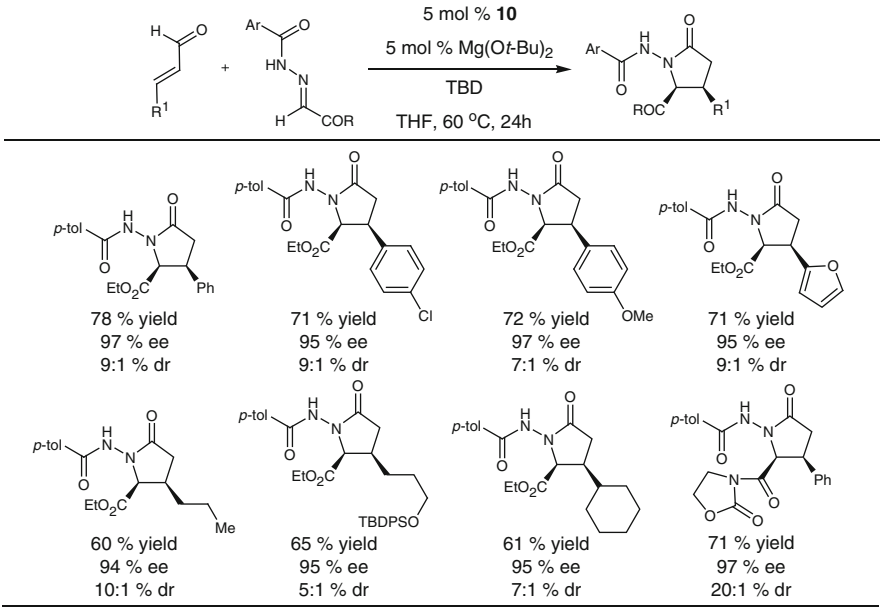

Scheme 23 Cooperative NHC/Lewis acid catalysis for the synthesis of γ-lactams

extensive investigation, we found that the addition of 5 mol% of $Mg(O\textit{t}\text{-}Bu)_2$ increased the reactivity and the yield of the reaction dramatically (Scheme 21).

The substrate scope of this reaction extends to a wide variety of substrates (Scheme 23). Enals bearing electron-withdrawing, electron-donating aryl groups, and heterocycles are well tolerated and react with the hydrazone to afford the lactams in good yields and excellent enantioselectivity levels. Additionally, enals bearing primary and secondary alkyl groups can participate in this reaction. Finally, it was shown that the diastereoselectivity could be improved by using an oxazolidinone amide on the hydrazone, affording the *cis* lactam in 71% yield as a single diastereoisomer and 97% ee.

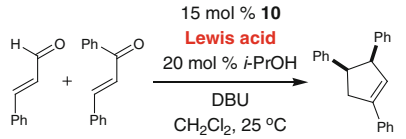

L. A. (equiv)	% yield	*cis*:*trans*	% ee *cis*
none	84	1:5	99
$Ti(O\textit{i}\text{-}Pr)_4$ (0.2)	74	>20:1	99

Scheme 24 Cooperative NHC/Lewis acid catalysis with $Ti(O\textit{i}\text{-}Pr)_4$

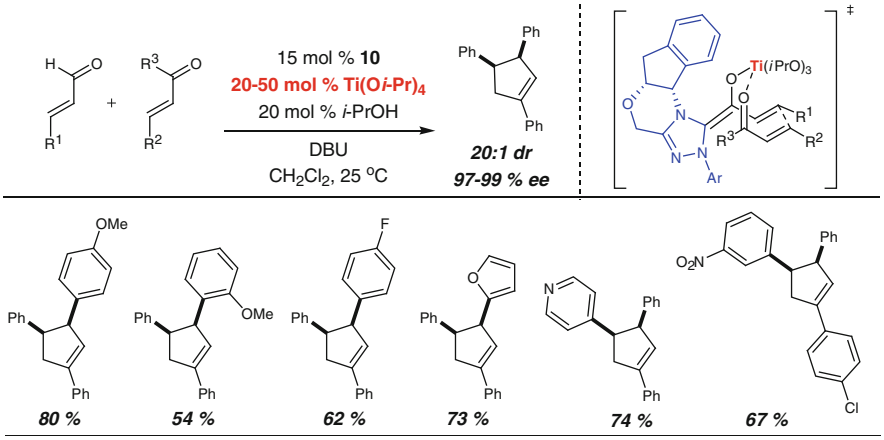

Scheme 25 Substrate scope for the synthesis of *cis*-cyclopentenes

3.5.2 Cooperative NHC/Lewis Acid Catalysis for the Synthesis of Cyclopentenes

Prompted by the new possibility of employing Lewis acids for substrate activation in NHC reactions, we decided to take advantage of the ability of Lewis acids to influence substrate pre-organization and impact the selectivity level. We hypothesized that a known reaction, the NHC-catalyzed synthesis of cyclopentenes [152, 153], could benefit of the presence of a Lewis acid to facilitate the access to the *cis* cycloadducts. We began our investigation by reacting cinnamaldehyde with chalcone in the presence of azolium salt **10**. After screening a number of Lewis acids, we found that the use of a catalytic amount of $Ti(O\textit{i}\text{-}Pr)_4$ caused a remarkable reversal in the diastereoselectivity from *trans* to *cis* (Scheme 24) [154]. The presence of *i*-PrOH as an additive was found to have a positive effect on the rate of the reaction (data not shown), presumably by assisting in the decomplexation and regeneration of the Lewis acid in the catalytic cycle.

The cooperative catalytic cyclopentene formation works very well for a variety of aromatic substituents on the unsaturated aldehyde and either one of the positions of the chalcone. Electron-withdrawing and electron-donating groups, as well as heterocycles, are well tolerated and afford the target cyclopentene as a single diastereoisomer (Scheme 25). Our model for the observed *cis*-selectivity involves a boat-type transition state in which the chalcone reacts in its most stable s-*cis* conformation [155]. Most importantly, the titanium Lewis acid organizes the substrates through coordination to the oxygen atoms.

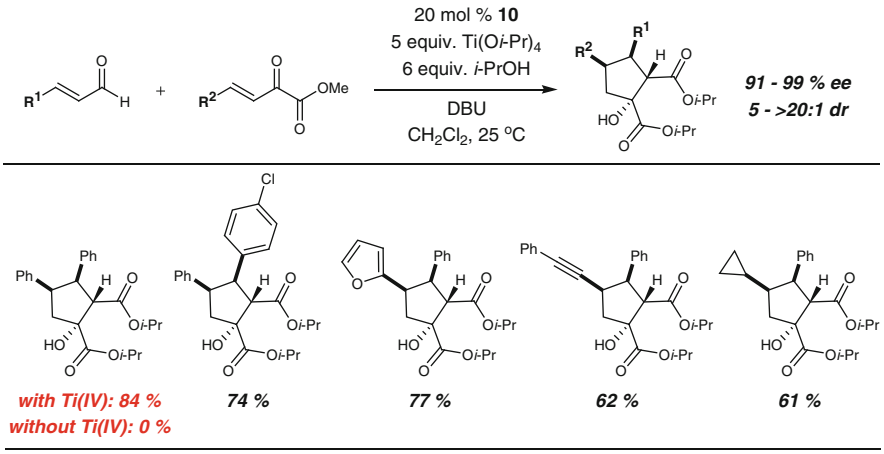

Scheme 26 Substrate scope for the synthesis of tetrasubstituted cyclopentanes

3.5.3 Synthesis of Highly Substituted Cyclopentanes

The successful incorporation of Ti(O*i*-Pr)$_4$ as a Lewis acid in NHC reactions prompted us to explore various electrophiles in formal cycloaddition reactions with enals. Another objective was to develop a system that would allow the synthesis of cyclopentane frameworks that would retain the carbonyl of the initial α,β-unsaturated aldehyde (or prevent the elimination of CO_2), thus providing more opportunities for further manipulation of the functional groups. We anticipated that β,γ-unsaturated α-ketoesters could benefit from Lewis acid activation and be suitable reacting partners (Scheme 26) [156–163]. We found that catalyst **10** could be employed with a large excess of Ti(O*i*-Pr)$_4$ without shutting down the NHC catalysis [164]. The role of Ti(IV) in this reaction is crucial with respect to the reactivity, since *no product is observed when the reaction is performed with only the NHC* (see when R^1 and R^2 = Ph). A wide variety of substrates bearing aryl, alkyl, and alkynyl substituents can undergo this transformation to afford highly substituted cyclopentanes with four contiguous stereogenic centers in excellent enantioselectivity and diastereoselectivity levels.

3.5.4 Enantioselective Synthesis of γ-Butyrolactones with a Chiral Lewis Acid

The discovery that NHC reactions can be performed in the presence of Lewis acids inspired us to explore the possibility of using a chiral Lewis acid as the only component for the control of the enantioselectivity [153]. We selected the dimerization of enals as a platform to test our idea to access γ-butyrolactones since no

efficient NHC-catalyzed method is available for the enantioselective synthesis of these molecules [165, 166]. The use of 20 mol% of (*R*,*R*)-Ti(TADDOL) [167] as a Lewis acid generated the *cis* product as a single diastereoisomer and 60% ee [Eq. (2)]. This result highlights the great potential for the integration of chiral Lewis acids for the development of NHC-catalyzed reactions. Our research group is investigating this new type of cooperative catalysis to enable the invention of new chemical processes.

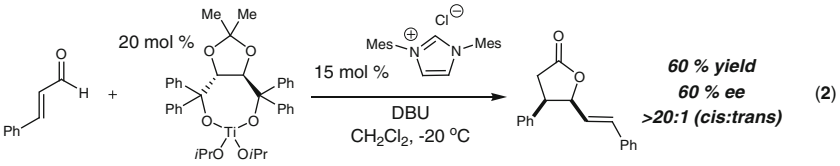

(2)

4 Conclusion and Perspectives

Since the beginning of our involvement with carbene catalysis, we have succeeded in the development of a host of new Lewis base-catalyzed reactions. Inspired by the work of Liebig, Breslow, and Enders, we first explored new variants of the intermolecular Stetter reaction to avoid the formation of benzoin byproducts. Our early work with homoenolate chemistry led to new formal cycloaddition processes to access various heterocycles with high levels of diastereoselectivity and enantioselectivity. This concept of carbene activation was then extended to the generation of enolate equivalents. This class of nucleophiles proved to be very fruitful for the development of new reactions, such as the desymmetrization of 1,3-diketones and the synthesis of dihydrocoumarins using rebound catalysis. More recently, we have demonstrated the compatibility of early metals as Lewis acids with NHCs. This new type of cooperative catalysis can improve the reactivity and impact the selectivity of important chemical processes. The work with chiral Lewis acids establishes significant potential for the improvement and the invention of NHC-catalyzed reactions. Continued fundamental studies from all laboratories involved with NHCs aimed at understanding the structure and reactivity of NHC-bound intermediates will enable new concepts and reactivity trends in this emerging and exciting research field.

Acknowledgments We gratefully acknowledge Northwestern University, the National Institute of General Medical Sciences (R01GM73072), the Sloan Foundation, Abbott Laboratories, Amgen, AstraZeneca, Boehringer-Ingelheim, GlaxoSmithKline, and Novartis for their generous support of our research program. FQRNT (Fonds québécois de la recherche sur la nature et les technologies) is also gratefully acknowledged for a postdoctoral fellowship to B.C.D. Lastly, we thank all current and former Scheidt group members for their heartfelt dedication and lasting contributions.

References

1. Ojima I (ed) (2010) Catalytic asymmetric synthesis. Wiley-VCH, Weinheim
2. Eder U, Sauer G, Wiechert R (1971) Angew Chem 83:492–493; Angew Chem Int Ed 10:496–497
3. Berkessel A, Gröger H (eds) (2005) Asymmetric organocatalysis. Wiley-VCH, Weinheim
4. List B (2007) Chem Rev 107:5413
5. Enders D, Grondal C, Hüttl MRM (2007) Angew Chem 119:1590; Angew Chem Int Ed 46:1570
6. Almasi D, Alonso DA, Nájera C (2007) Tetrahedron: Asymmetry 18:299
7. Erkkilä A, Majander I, Pihko PM (2007) Chem Rev 107:5416
8. Dondoni A, Massi A (2008) Angew Chem Int Ed 47:4638
9. Grondal C, Jeanty M, Enders D (2010) Nat Chem 2:167
10. Doyle AG, Jacobsen EN (2007) Chem Rev 107:5713
11. Taylor MS, Jacobsen EN (2006) Angew Chem Int Ed 45:1520
12. Yu X, Wang W (2008) Chem Asian J 3:516
13. Zhang ZG, Schreiner PR (2009) Chem Soc Rev 38:1187
14. Terada M (2010) Synthesis 1929
15. Biddle MM, Lin M, Scheidt KA (2007) J Am Chem Soc 129:3830
16. Palomo C, Oiarbide M, Lopez R (2009) Chem Soc Rev 38:632
17. Ooi T, Maruoka K (2007) Angew Chem Int Ed 46:4222
18. List B (2001) Synlett 1675
19. List B (2004) Acc Chem Res 37:548
20. Mukherjee S, Yang JW, Hoffmann S, List B (2007) Chem Rev 107:5471
21. Melchiorre P, Marigo M, Carlone A, Bartoli G (2008) Angew Chem Int Ed 47:6138
22. Denmark SE, Beutner GL (2008) Angew Chem Int Ed 47:1560
23. Fu GC (2004) Acc Chem Res 37:542
24. Miller SJ (2004) Acc Chem Res 37:601
25. Enders D, Narine AA (2008) J Org Chem 73:7857
26. Williams RR (1936) J Am Chem Soc 58:1063
27. Mizuhara S, Handler P (1954) J Am Chem Soc 76:571
28. Enders D, Balensiefer T (2004) Acc Chem Res 37:534
29. Nair V, Bindu S, Sreekumar V (2004) Angew Chem 116:5240; Angew Chem Int Ed 43:5130
30. Zeitler K (2005) Angew Chem 117:7674; Angew Chem Int Ed 44:7506
31. Marion N, Diez-Gonzalez S, Nolan SP (2007) Angew Chem 119:3046; Angew Chem Int Ed 46:2988
32. Enders D, Niemeier O, Henseler A (2007) Chem Rev 107:5606
33. Zeitler K (2008) In: Reetz MT, List B, Jaroch S, Weinmann H (eds) Organocatalysis. Springer, Heidelberg, pp 183–206
34. Glorius F, Hirano K (2008) In: Reetz MT, List B, Jaroch S, Weinmann H (eds) Organocatalysis. Springer, Heidelberg, pp 159–181
35. Biju AT, Kuhl N, Glorius (2011) Acc Chem Res 44 (Article ASAP)
36. Wanzlick H-W (1962) Angew Chem Int Ed Engl 1:75
37. Wanzlick H-W, Kleiner H-J (1964) Angew Chem Int Ed Engl 3:65
38. Schönherr H-J, Wanzlick H-W (1970) Chem Ber 103:1037
39. Schönherr H-J, Wanzlick H-W (1970) Justus Liebigs Ann Chem 731:176
40. Walentow R, Wanzlick HWZ (1970) Naturforsch B: Chem Sci 25:1421
41. Marion N, Diez-Gonzalez S, Nolan SP (2007) Angew Chem 119:3046; Angew Chem Int Ed 46:2988
42. Arduengo AJ III (1999) Acc Chem Res 32:913
43. Seebach D (1969) Synthesis 1:17
44. Gröbel BT, Seebach D (1977) Synthesis 357
45. Page PCB, Van Niel MB, Prodger JC (1989) Tetrahedron 45:7643

46. Yus M, Najera C, Foubelo F (2003) Tetrahedron 59:6147
47. Corey EJ, Seebach D (1965) Angew Chem Int Ed Engl 4:1075
48. Seebach D, Corey EJ (1965) Angew Chem Int Ed Engl 4:1077
49. Wöhler F, Liebig J (1832) Ann Pharm 3:249
50. Lapworth A (1903) Transactions 83:995
51. Ugai T, Tanaka S, Dokawa S (1943) J Pharm Soc Jpn (Yakugaku Zasshi) 63:296
52. Breslow R (1958) J Am Chem Soc 80:3719
53. Breslow R, Schmuck C (1996) Tetrahedron Lett 37:8241
54. White MJ, Leeper FJ (2001) J Org Chem 66:5124
55. Phillips EM, Chan A, Scheidt KA (2009) Aldrichim Acta 42:55
56. Sheehan JC, Hunneman DH (1966) J Am Chem Soc 88:3666
57. Bredig G, Fiske PS (1912) Biochem Z 46:7
58. Bredig G, Minaeff M (1932) Biochem Z 249:241
59. Prelog V, Wilhelm M (1954) Helv Chim Acta 37:1634
60. Enders D, Kallfass U (2002) Angew Chem Int Ed 41:1743
61. Stetter H (1976) Angew Chem Int Ed Engl 15:639
62. Harrington PE, Tius MA (1999) Org Lett 1:649
63. Anjaiah S, Chandrasekhar S, Gree R (2004) Adv Syn Cat 346:1329
64. Enders D, Balensiefer T (2004) Acc Chem Res 37:534
65. Kerr MS, de Alaniz JR, Rovis T (2002) J Am Chem Soc 124:10298
66. Kerr MS, Rovis T (2004) J Am Chem Soc 126:8876
67. de Alaniz JR, Rovis T (2005) J Am Chem Soc 127:6284
68. Moore J, Silvestri AP, de Alaniz JR, DiRocco DA, Rovis T (2011) Org Lett 13:1742
69. Liu Q, Rovis T (2009) Org Lett 11:2856
70. DiRocco DA, Oberg KM, Dalton DM, Rovis T (2009) J Am Chem Soc 131:10872
71. DiRocco DA, Rovis T (2011) J Am Chem Soc 133:10402
72. Um JM, DiRocco DA, Noey EL, Rovis T, Houk KN (2011) J Am Chem Soc 133:11249
73. Jousseaume T, Wurz NE, Glorius F (2011) Angew Chem Int Ed 50:1410
74. Page PCB, Klair SS, Rosenthal S (1990) Chem Soc Rev 19:147
75. Cirillo PF, Panek JS (1992) Org Prep Proced Int 24:553
76. Bonini BF, Comes-Franchini M, Fochi M, Mazzanti G, Ricci A (1998) J Organomet Chem 567:181
77. Brook AG (1974) Acc Chem Res 7:77
78. Schinzer D, Heathcock CH (1981) Tetrahedron Lett 22:1881
79. Ricci A, Degl'Innocenti A, Mordini A, Reginato G, Colotta V (1987) Gazz Chim Ital 117:645
80. Mattson AE, Bharadwaj AR, Scheidt KA (2004) J Am Chem Soc 126:2314
81. Xin LH, Johnson JS (2003) Angew Chem Int Ed 42:2534
82. Bharadwaj AR, Scheidt KA (2004) Org Lett 6:2465
83. Mattson AE, Bharadwaj AR, Zuhl AM, Scheidt KA (2006) J Org Chem 71:5715
84. Mattson AE, Scheidt KA (2004) Org Lett 6:4363
85. Stetter H, Lorenz G (1985) Chem Ber 118:1115
86. Hayakawa S, Michiue T, Okamoto M, Hatakeyama S, Ohta S (1988) Heterocycles 27:457
87. Evans DA, Fandrick KR, Song H-J (2005) J Am Chem Soc 127:8942
88. Myers MC, Bharadwaj AR, Milgram BC, Scheidt KA (2005) J Am Chem Soc 127:14675
89. Davies DH, Hall J, Smith EH (1991) J Chem Soc Perkins Trans 1:2691
90. Ji J-X, Chan ASC (2010) In: Ojima I (ed) Catalytic asymmetric synthesis, 3rd edn. Wiley-VCH, Weinheim, pp 439–498
91. Csákÿ AG, de la Herrán GD, Murcia MC (2010) Chem Soc Rev 39:4080
92. Nickhorn A, Lambert JL (1964) J Am Chem Soc 86:4604
93. Freeman JP, Plonka JH (1966) J Am Chem Soc 88:3662
94. Nair V, Vellalath S, Babu BP (2008) Chem Soc Rev 37:2691
95. 2004 Natural Products Gordon Research Conference, Tilton
96. Chan A, Scheidt KA (2005) Org Lett 7:905

97. Burstein C, Glorius F (2004) Angew Chem Int Ed 43:6205
98. Sohn SS, Rosen EL, Bode JW (2004) J Am Chem Soc 126:14370
99. Chan A, Scheidt KA (2006) J Am Chem Soc 128:4558
100. Maki BE, Chan A, Phillips EM, Scheidt KA (2007) Org Lett 9:371
101. Maki BE, Scheidt KA (2008) Org Lett 10:4331
102. Maki BE, Chan A, Phillips EM, Scheidt KA (2009) Tetrahedron 65:3102
103. De Sarkar S, Studer A (2010) Angew Chem Int Ed 49:9266
104. De Sarkar S, Studer A (2010) Org Lett 12:1992
105. De Sarkar S, Grimme S, Studer A (2010) J Am Chem Soc 132:1190
106. De Sarkar S, Biswas A, Song CH, Studer A (2011) Synthesis 1974
107. Padwa A (ed) (1984) 1,3-Dipolar cycloaddition chemistry. Wiley, New York
108. Gothelf KV, Jørgensen KA (1998) Chem Rev 98:863
109. Pearson WH (2002) Pure Appl Chem 74:1339
110. Carruthers W (1990) Cycloaddition reactions in organic synthesis. Pergamon, Elmsford
111. Dorn H, Otto A (1968) Chem Ber 101:3287
112. Shintani R, Fu GC (2003) J Am Chem Soc 125:10778
113. Suárez A, Downey CW, Fu GC (2005) J Am Chem Soc 127:11244
114. Shintani R, Hayashi T (2006) J Am Chem Soc 128:6330
115. Suga H, Funyu A, Kakehi A (2007) Org Lett 9:97
116. Syroeshkina YS, Petukhova VY, Kachala VV, Nelyubina YV, Makhova NN (2010) Russ Chem Bull Int Ed 59:1433
117. Chan A, Scheidt KA (2007) J Am Chem Soc 129:5334
118. He M, Bode JW (2005) Org Lett 7:3131–3134
119. Confalone PN, Huie EM (1988) Org React (NY) 36:1
120. Gothelf KV, Jørgensen KA (2000) Chem Commun 1449
121. Jen WS, Wiener JJM, MacMillan DWC (2000) J Am Chem Soc 122:9874
122. Martin JN, Jones RCF (2002) Synthetic applications of 1,3-dipolar cycloaddition chemistry toward heterocycles and natural products. In: Padwa A, Pearson WH (eds) The chemistry of heterocyclic compounds series, vol. 59. Wiley, Chichester pp 1–81
123. Feuer H, Torssell K (2008) Nitrile oxides, nitrones, and nitronates in organic synthesis: novel strategies in synthesis, 2nd edn. Wiley-Interscience, Hoboken
124. Phillips EM, Reynolds TE, Scheidt KA (2008) J Am Chem Soc 130:2416
125. Bryans JS, Wustrow DJ (1999) Med Res Rev 19:149
126. Tassone DM, Boyce E, Guyer J, Nuzum D (2007) Clin Ther 29:26
127. Cooper JR, Bloom FE, Roth RH (2003) The biochemical basis of neuropharmacology, 8th edn. Oxford University Press, Oxford
128. Sibi MP, Shay JJ, Liu M, Jasperse CP (1998) J Am Chem Soc 120:6615
129. Myers JK, Jacobsen EN (1999) J Am Chem Soc 121:8959
130. Horstmann TE, Guerin DJ, Miller SJ (2000) Angew Chem Int Ed 39:3635
131. Doi H, Sakai T, Iguchi M, Yamada K, Tomioka K (2003) J Am Chem Soc 125:2886
132. Chan A, Scheidt KA (2006) J Am Chem Soc 128:4558
133. He M, Struble JR, Bode JW (2006) J Am Chem Soc 128:8418–8420
134. He M, Uc GJ, Bode JW (2006) J Am Chem Soc 128:15088–15089
135. Phillips EM, Wadamoto M, Chan A, Scheidt KA (2007) Angew Chem Int Ed 46:3107
136. Wadamoto M, Phillips EM, Reynolds TE, Scheidt KA (2007) J Am Chem Soc 129:10098
137. Phillips EM, Wadamoto M, Scheidt KA (2009) Synthesis 687
138. Phillips EM, Roberts JM, Scheidt KA (2010) Org Lett 12:2830
139. Dias LC, Aguilar AM (2008) Chem Soc Rev 37:451
140. Kimball DB, Silks LA III (2006) Curr Org Chem 10:1975
141. Phillips EM, Wadamoto M, Roth HS, Ott AW, Scheidt KA (2009) Org Lett 11:105
142. Kawanaka Y, Phillips EM, Scheidt KA (2009) J Am Chem Soc 131:18028
143. He M, Bode JW (2005) Org Lett 7:3131
144. Raup DEA, Cardinal-David B, Holte D (2010) Nat Chem 2:766

145. Sugiura M, Kobayashi S (2005) Angew Chem Int Ed 44:5176
146. Lee SK, Tambar UK, Perl NR, Leighton JL (2010) Tetrahedron 66:4769
147. Feske MI, Buitrago Santanilla A, Leighton JL (2010) Org Lett 12:688
148. Burgess K, Perry MC (2003) Tetrahedron: Asymmetry 14:951
149. Nolan SP (ed) (2006) *N*-heterocyclic carbenes in synthesis. Wiley-VCH, Weinheim
150. Glorius F (2007) Top Organomet Chem 21:1
151. Hahn FE, Jahnke MC (2008) Angew Chem Int Ed 47:3122
152. Nair V, Vellalath S, Poonoth S, Suresh E (2006) J Am Chem Soc 128:8736
153. Chiang P-C, Kaeobamrung J, Bode JW (2007) J Am Chem Soc 129:3520
154. Cardinal-David B, Raup DEA, Scheidt KA (2010) J Am Chem Soc 132:5345
155. Patel D, Liddle ST, Mungur SA, Rodden M, Blake AJ, Arnold PL (2006) J Chem Soc Chem Commun 1124
156. Evans DA, Johnson JS, Olhava EJ (2000) J Am Chem Soc 122:1635
157. Wada E, Koga H, Kumaran G (2002) Tetrahedron Lett 43:9397
158. Koga H, Wada E (2003) Tetrahedron Lett 44:715
159. Kurosu M, Porter JR, Foley MA (2004) Tetrahedron Lett 45:145
160. Ünaleroglu C, Temelli B, Demir AS (2004) Synthesis 2574
161. Hughes KD, Nguyen T-LN, Dyckman D, Dulay D, Boyko WJ, Giuliano RM (2005) Tetrahedron: Asymmetry 16:273
162. Evans DA, Dunn TB, Kvoernø L, Beauchemin A, Raymer B, Olhava EJ, Mulder JA, Juhl M, Kagechika K, Favor DA (2007) Angew Chem 119:4782; Angew Chem Int Ed 46:4698
163. Kaeobamrung J, Bode JW (2009) Org Lett 11:677–680
164. Cohen DT, Cardinal-David B, Scheidt KA (2011) Angew Chem Int Ed 50:1678
165. Li Y, Zhao Z-A, He H, You S-L (2008) Adv Synth Catal 350:1885
166. Matsuoka Y, Ishida Y, Saigo K (2008) Tetrahedron Lett 49:2985
167. Seebach D, Beck AK, Heckel A (2001) Angew Chem Int Ed 40:92

Top Organomet Chem (2013) 44: 261–280
DOI: 10.1007/3418_2012_48

Published online: 11 August 2012

Asymmetric Autocatalysis of Pyrimidyl Alkanol

Kenso Soai and Tsuneomi Kawasaki

Abstract We have discovered an asymmetric autocatalysis in the enantioselective addition of diisopropylzinc to pyrimidine-5-carbaldehyde, where the product, 5-pyrimidyl alkanol, acts as highly efficient asymmetric autocatalyst. Asymmetric autocatalysis proceeded quantitatively (>99%), affording itself as a near enantiomerically pure (>99.5% ee) product. An extremely low enantiomeric excess (ca. 0.00005% ee) can automultiply during three consecutive asymmetric autocatalysis to >99.5% ee. Circularly polarized light, quartz, chiral organic crystals, and statistical fluctuation of ee in racemate, which are considered a possible candidate for the origin of chirality, act as the chiral source in asymmetric autocatalysis. Asymmetric autocatalysis has the enormous power to recognize the isotope chirality arising from the small difference between carbon (carbon-13/carbon-12) and hydrogen (D/H) isotopes.

Keywords Amplification of ee · Asymmetric autocatalysis · Automultiplication · Chiral discrimination · Circularly polarized light · Quartz · Isotope chirality · Origin of chirality · Pyrimidyl alkanol · Spontaneous absolute asymmetric synthesis

Contents

K. Soai (✉) and T. Kawasaki
Department of Applied Chemistry and Research Institute for Science & Technology, Tokyo University of Science, Kagurazaka, Shinjuku-ku, Tokyo 162-8601, Japan
e-mail: soai@rs.kagu.tus.ac.jp

Abbreviations

BDL	Below the detectable level
Bu	Butyl
CD	Circular dichroism
CPL	Circularly polarized light
DAIB	3-Exo-(dimethylamino) isoborneol
DMNE	*N*,*N*-dimethylnorephedrine
DPMPM	Diphenyl(1-methylpyrrolidin-2-yl)methanol
ee	Enantiomeric excess
Et	Ethyl
i	*Iso*
l	Left-handed
n	Normal
PEAE	2-[(1-phenylethyl)amino]-ethanol
Pr	Propyl
R	Rectus
r	Right-handed
S	Sinister
t	Tertiary

1 Introduction

Asymmetric autocatalysis is a reaction in which chiral product acts as a chiral catalyst for its own production. The process is an automultiplication of chiral compound. Asymmetric autocatalysis has inherent advantages over usual non-autocatalytic reaction: (1) high efficiency because the process involves self-replication and (2) the amount of catalyst increases during the reaction because the product is a catalyst. In ideal cases, catalytic activity does not decrease; (3) separation of product from the catalyst is not necessary because the structures of product and catalyst are the same.

We found asymmetric autocatalysis of pyrimidyl alkanol **1** [1–10]. Pyrimidyl alkanol **1** acts as asymmetric autocatalyst in the enantioselective addition of diisopropylzinc (*i*-Pr_2Zn) to pyrimidine-5-carbaldehyde **2** to produce more of itself with the same absolute configuration [11] of >99.5% enantiomeric excess (ee) in a yield of >99% (Scheme 1) [12]. Thus, pyrimidyl alkanol **1** automultiplies in

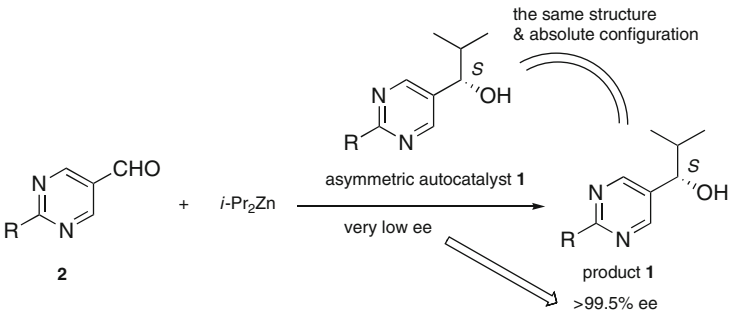

Scheme 1 Asymmetric autocatalysis with amplification of ee

practically perfect manner [13]. Moreover, significant amplification of ee is observed in the reaction. Starting from asymmetric autocatalyst with extremely low ee of ca. 0.00005%, three consecutive asymmetric autocatalysis enhanced the ee to >99.5% and the amount by the multiplication factor of ca. 630,000 times.

Asymmetric autocatalysis with amplification of chirality is a very efficient method of asymmetric catalysis. One of the implications is that the existence of a chemical reaction has been shown in which very slight bias of chirality can be amplified significantly to reach almost enantiopure. The reaction has been employed for the study on the origins of homochirality and on the chiral discrimination. We describe how we find the reaction and the recent aspects of asymmetric autocatalysis.

2 Background

Every researcher has his/her own background, and nearly all research projects have their background, too. Our (K.S.) background starts from when K.S. was a graduate student in Prof. Teruaki Mukaiyama's group at the University of Tokyo. Our project was enantioselective addition of organometallic reagents to aldehydes using chiral ligands. Enantioselective addition of butyllithium and diethylmagnesium to benzaldehyde in the presence of chiral β-aminoalcohol **3** derived from (*S*)-proline afforded 1-phenylpentanol and 1-phenylpropanol with >90% ee, respectively (1979) (Scheme 2) [14]. We also observed that diethylzinc (Et_2Zn) adds to benzaldehyde in the presence of the same chiral ligand. Although the ee of the product was BDL, the result first revealed that β-aminoalcohol activates Et_2Zn to add to aldehyde.

After finishing postdoc with Prof. Ernest L. Eliel at the University of North Carolina at Chapel Hill, K.S. got the position in Tokyo University of Science and became independent in 1981. Then, Oguni reported in 1984 that Et_2Zn adds to benzaldehyde to give 1-phenylpropanol with 48% ee using leucinol, a β-aminoalcohol, as a chiral catalyst [15]. As described, we had been dealing with

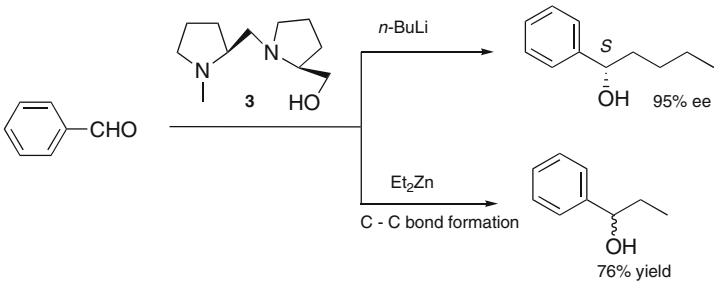

Scheme 2 Enantioselective addition of organometallic reagents to aldehyde using a chiral ligand, β-aminoalcohol derivative

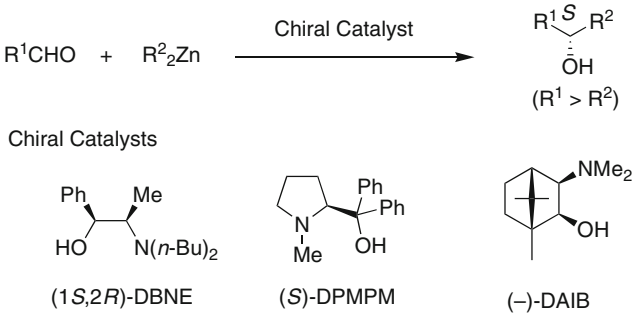

Scheme 3 DPMPM, DBNE as chiral catalysts for the enantioselective addition of dialkylzincs to aldehydes

the enantioselective addition of organometallic reagents to aldehydes; we have devised our own β-aminoalcohol such as DPMPM [16] and DBNE [17] for the highly enantioselective addition of dialkylzincs to aldehydes (Scheme 3). Independent research of Noyori reported that DAIB is a highly enantioselective catalyst for the reaction [18].

When diastereomeric β-aminoalcohols were used in the Et_2Zn addition to benzaldehyde, the absolute configuration of the product is controlled by the chirality of alcohol moiety, and not by the chirality of amine moiety (Scheme 4). Catalysts **4** and **5** have the same stereogenic center of amine moiety but the opposite stereogenic center of alcohol moiety. Catalyst **4** gives (*S*)-alkanol, whereas catalyst **5** gives (*R*)-alkanol. The result shows that the stereogenic center of alcohol moiety has stronger asymmetric power [16, 19].

We got an idea that chiral aminoalcohol-catalyzed addition of dialkylzinc to amino aldehyde should give chiral aminoalcohol and that, in an ideal case, the structure of chiral catalyst and that of the product may become the same!

We have published many papers on the catalytic enantioselective addition of dialkylzincs to aldehydes using DPMPM and DBNE as chiral catalysts [20]. One of

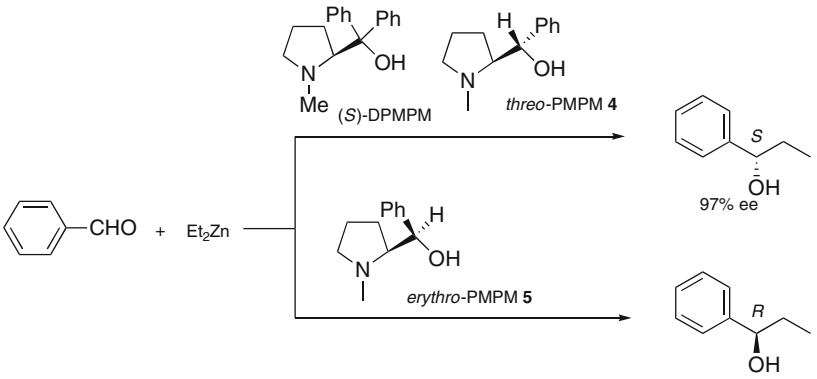

Scheme 4 Diastereomeric β-aminoalcohols

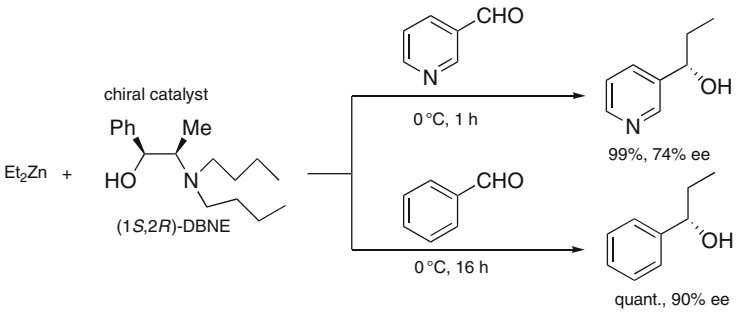

Scheme 5 Faster reaction with pyridine-3-carbaldehyde than benzaldehyde

our projects was the enantioselective alkylation of pyridine-3-carbaldehyde with dialkylzinc using a chiral catalyst. In 1989, we published the enantioselective addition of dialkylzinc to pyridine-3-carbaldehyde using DBNE as a chiral catalyst to afford 3-pyridyl alkanol (Scheme 5) [21]. We noticed that the reaction of Et_2Zn to pyridine-3-carbaldehyde using DBNE at 0°C was complete within 1 h, whereas the same reaction with benzaldehyde required 12 h. This suggests that the alkylzinc alkoxide of 3-pyridyl alkanol formed in situ acts as catalyst for the addition of dialkylzinc to aldehyde.

Meanwhile, we noticed a short review by Wynberg in the same year on asymmetric autocatalysis [22]. He introduced the theoretical paper of Frank [23] on spontaneous asymmetric synthesis. He explained that no experimental realization of asymmetric autocatalysis had ever been achieved. He also described the potential difficulties to realize asymmetric autocatalysis: (1) chiral product should have the catalytic activity for producing itself, (2) asymmetric autocatalyst of certain absolute configuration should induce the same absolute configuration of the product, and (3) enantiomeric excess of the product should not decrease because the repeated

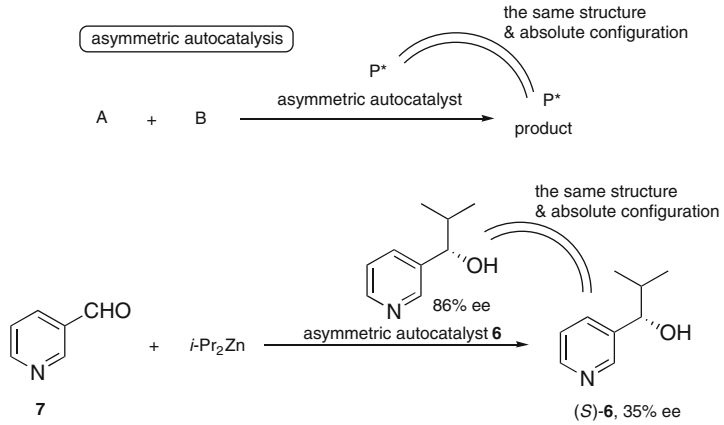

Scheme 6 The first asymmetric autocatalysis of pyridyl alkanol

autocatalytic reaction would lower the ee to racemate. He concluded the experimental realization of asymmetric autocatalysis is not for the chemists who need a stream communication, and he would leave the subject as a challenge for "red-blooded" chemists. Then, our challenge for asymmetric autocatalysis became a clear subject.

As described in the preceding sections, we already had experience on the enantioselective alkylation of aldehydes with dialkylzincs and the enantioselective synthesis of 3-pyridyl alkanol. In 1990, we found the first asymmetric autocatalysis of (*S*)-3-pyridyl alkanol **6** in the enantioselective addition of *i*-Pr_2Zn to pyridine-3-carbaldehyde **7** to produce more of itself of 35% ee with the same *S* configuration (Scheme 6) [24]. Although the ee of product **6** decreased compared to that of the initial catalyst, the newly formed predominant enantiomer of the product is the same with that of asymmetric autocatalyst **6**. We claim that this is the first asymmetric autocatalysis, that is, catalytic replication of chiral compound with the generation of new stereogenic centers.

Then, our effort has begun for finding a truly efficient asymmetric autocatalysis. There were inherent difficulties in making effort to find highly efficient asymmetric autocatalysis: (1) there is no guarantee of the real existence of efficient asymmetric autocatalysis. This aspect is in sharp contrast to the synthesis of natural products. That is, even when the target structure is very complicated in natural product synthesis, the existence of the compounds is guaranteed; (2) when one tries to find efficient non-autocatalytic asymmetric catalysis, one can fix the structure of catalyst and find the efficient matching by screening the structures of substrates. One can also fix the structure of substrate and varies the structures of catalysts to find the best matching.

However, in the research on asymmetric autocatalysis, one cannot fix the structure of asymmetric autocatalysis and survey the various structures of substrates. If the methyl substituent, for example, on the asymmetric autocatalyst is changed to ethyl

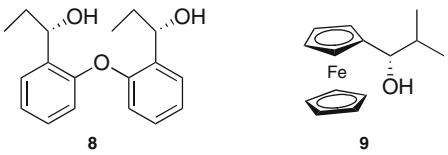

8 9

Scheme 7 Asymmetric autocatalysts of diol and ferrocenyl alkanol

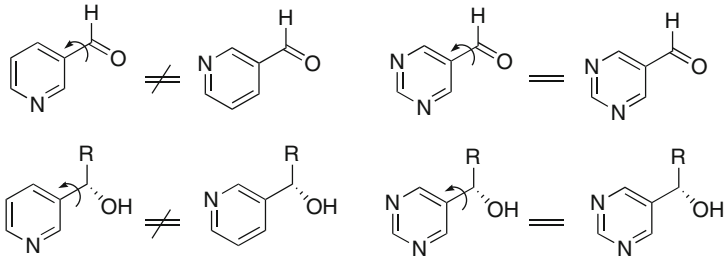

Scheme 8 Rotation of the bonds of pyridine and pyrimidine system

substituent, the same change should be done on the structure of substituent of the substrate. In general, changing the two factors at once is not the common way of a research because one cannot derive the rational conclusion of a factor.

Despite the difficulties as described above in finding efficient asymmetric autocatalysis, we had strong passion to keep doing the research. We modified the structure of original pyridyl alkanol by putting the substituent and also found that a certain chiral diol **8** [25] and ferrocenyl alkanol **9** [26] act as asymmetric autocatalysis (Scheme 7).

One day, we reasoned as follows: in pyridyl alkanol system, rotations of pyridine ring of alkanol and 3-carbaldehyde to 180° generate rotational isomers (Scheme 8). In asymmetric synthesis, the lesser number of (rotational) isomers of reactive species often affords the product with higher ee. Thus, we decided to examine 5-pyrimidyl alkanol as an asymmetric autocatalyst. Rotation of pyrimidine rings of 5-pyrimidyl alkanol and pyrimidine-5-carbaldehyde to 180° along the bond between pyrimidine ring and the formyl group should give the same structure with the original ones.

As we had expected, the first asymmetric autocatalysis of pyrimidyl alkanol in the addition of *i*-Pr_2Zn to pyrimidine-5-carbaldehyde gave a promising result. We refined the reaction conditions and ee became near 90% ee. Moreover, amplification of ee was observed in the reaction. Starting from pyrimidyl alkanol with 2% ee, consecutive asymmetric autocatalysis using the product of one round as asymmetric autocatalyst for the next round afforded alkanol with 88% ee (see Scheme 1). At this stage, we found the first asymmetric autocatalysis with amplification of chirality. These results were published in Nature in 1995 [11].

As described, it took us for 5 years to find pyrimidyl alkanol since the initial asymmetric autocatalysis of pyridyl alkanol of 1990. Soon after pyrimidyl alkanol, we also found efficient systems of asymmetric autocatalysis with 3-quinolyl alkanol [27] and 5-carbamoyl-3-pyridyl alkanol [28].

In the following sections, we describe the state of the art of asymmetric autocatalysis.

3 The Correlation Between the Origin of Chirality and Enantioenriched Compound by Asymmetric Autocatalysis

How and when biomolecules achieved high enantioenrichment is an attractive issue requiring significant research. Several mechanisms have been proposed for elucidating the origins of the chirality of organic compounds [29–33]. Although the initial enantiomeric imbalance can be introduced via these proposed mechanisms, a suitable amplification process is required to reach single-handedness of biological organic compounds. Therefore, asymmetric autocatalysis with amplification of ee gives a strong correlation between the origin of chirality and the homochirality of organic compounds. Then, an experiment on the effect of proposed chiral factors as the origin and trigger of biological homochirality can be performed in conjunction with asymmetric autocatalysis.

3.1 Circularly Polarized Light

Enantioenriched organic compounds such as leucine [34] and hexahelicene [35] with only ca. 2% ee have been induced by the irradiation with CPL. These low enantiomeric enrichments have not been correlated with the homochirality of organic compounds. We performed the direct irradiation of CPL to the asymmetric autocatalyst **1**. (*R*)- and (*S*)-pyrimidyl alkanols **1** exhibit positive and negative Cotton effects in circular dichroism (CD) spectra at 313 nm, respectively [36]. Therefore, the direct irradiation of *rac*-alkanol **1** by CPL would induce the asymmetric photodegradation of pyrimidyl alkanol **1**. Indeed, direct irradiation of *rac*-**1** by *l*-CPL and the subsequent asymmetric autocatalysis produce highly enantioenriched (*S*)-alkanol **1** with >99.5% ee (Scheme 9). On the other hand, irradiation with *r*-CPL instead of *l*-CPL formed (*R*)-**1** with >99.5% ee. This process provides direct correlation of the handedness of CPL with that of the organic compound.

3.2 Chiral Inorganic Crystal of Quartz

Chiral crystals provide an environment for the discrimination of chiral molecules, so their possible roles in the origin of biological homochirality have been discussed

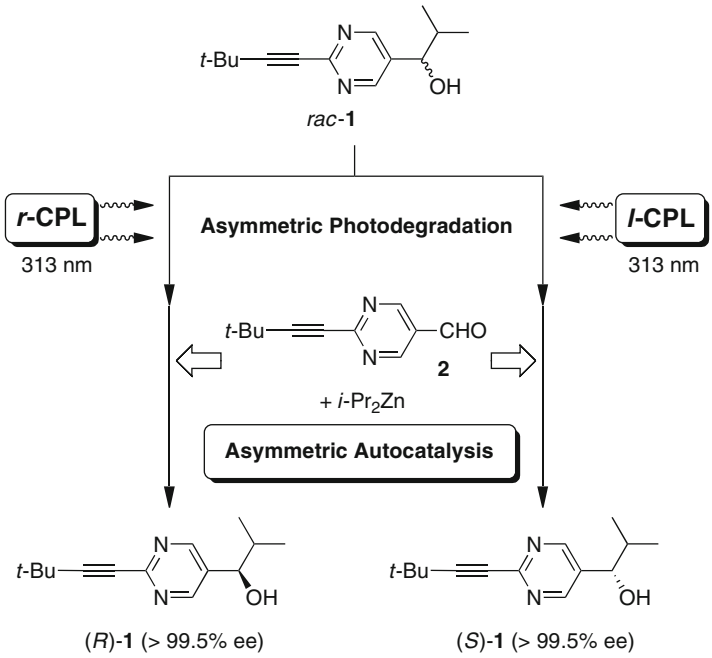

Scheme 9 CPL irradiation of asymmetric autocatalyst and subsequent amplification of ee by asymmetric autocatalysis

for a long time [37]. However, no apparent asymmetric induction using chiral minerals has been observed. So we performed an asymmetric autocatalysis triggered by D- and L-quartz. When pyrimidine-5-carbaldehyde **2** was treated with *i*-Pr_2Zn in the presence of D-quartz powder, (*S*)-pyrimidyl alkanol **1** with 97% ee was obtained in a yield of 95% (Scheme 10) [38]. In contrast, in the presence of L-quartz, (*R*)-**1** with 97% ee was obtained in a yield of 97%. These reproducible results clearly show that the absolute configurations of the pyrimidyl alkanol **1** formed were regulated by the chirality of quartz. A small enantiomeric imbalance of the initially formed pyrimidyl alkanol zinc alkoxide induced by quartz was amplified significantly by the subsequent consecutive asymmetric autocatalysis to produce pyrimidyl alkanol **1** with very high ee.

3.3 Chiral Crystal of Achiral Organic Compound

Some achiral organic compounds form chiral crystals, with each crystal exhibiting one of the two possible enantiomorphs, and the stereospecific reactions using these chiral organic crystals as reaction substrate have been studied [39]. However, to the best of our knowledge, enantioselective reaction using chiral organic crystals as a

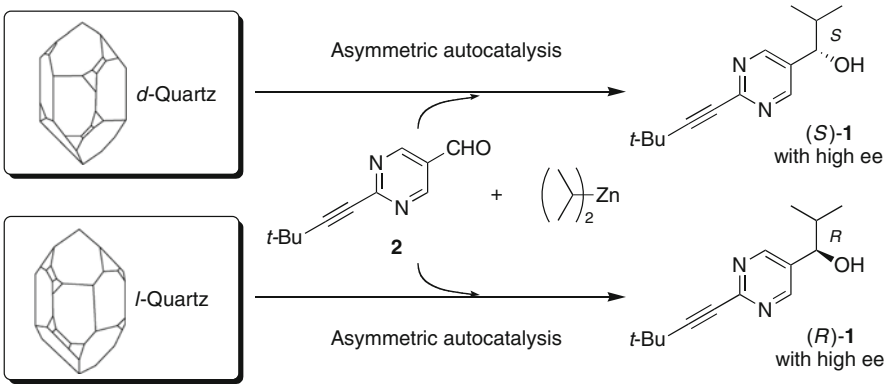

Scheme 10 Asymmetric autocatalysis induced by chiral inorganic crystal of quartz

source of chirality has not been reported. Thus, we have investigated the asymmetric autocatalysis using chiral crystal composed from achiral organic compound [40].

Cytosine is an essentially flat achiral molecule. However, it was found that when crystallization of cytosine was conducted from methanol with stirring without adding any seed crystal, chiral powder-like crystals that exhibit either plus or minus Cotton effect in solid-state CD spectra at ca. 310 nm were formed [41]. The stochastic behavior of the formation of [CD(+)310_{Nujol}]- and [CD(−)310_{Nujol}]-crystal of cytosine was observed. Furthermore, the chiral crystals that are spontaneously formed with stirring are used as chiral triggers for asymmetric autocatalysis (Scheme 11). When pyrimidine-5-carbaldehyde **2** and *i*-Pr_2Zn reacted in the presence of a [CD(+)310_{Nujol}]-crystal of cytosine, enantioenriched (*R*)-pyrimidyl alkanol **1** was obtained after the subsequent autocatalytic amplification of ee. On the other hand, spontaneously obtained [CD(−)310_{Nujol}]-cytosine crystal induced the production of enantioenriched (*S*)-alkanol **1**. These results clearly exhibit the correlation between the chirality of the crystal of cytosine and the absolute configuration of the resulting alkanol **1**.

In addition, the enantiomorphous crystals composed of achiral hippuric acid [42], benzil [43], and tetraphenylethylene [44] have been used successfully as chiral inducers in asymmetric autocatalysis. Chiral crystal of anhydrous cytosine formed from achiral monohydrate by the thermal dehydration [45] can also work as origin of chirality of asymmetric autocatalysis.

3.4 Spontaneous Absolute Asymmetric Synthesis

Spontaneous absolute asymmetric synthesis, that is, the formation of enantioenriched compound without the intervention of any chiral factors, has been proposed as one of the origins of biological homochirality in nature [29, 46, 47]. It has been well

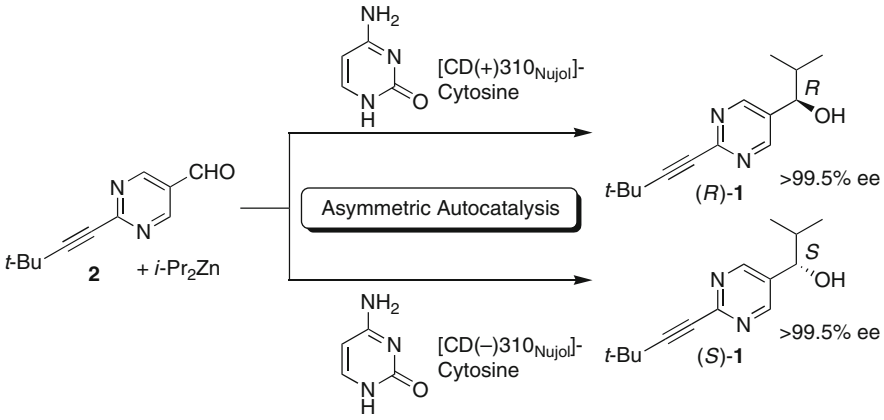

Scheme 11 Highly enantioselective asymmetric autocatalysis using chiral crystal of cytosine

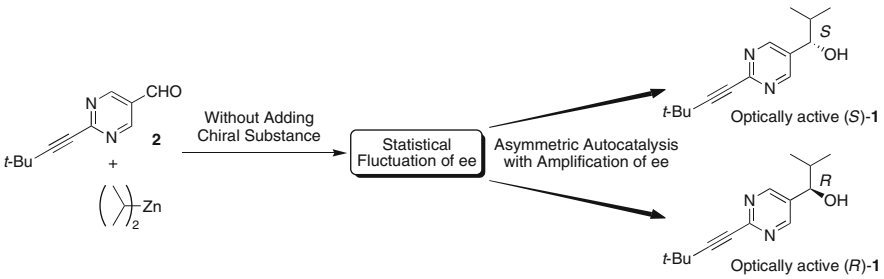

Scheme 12 Spontaneous absolute asymmetric synthesis

accepted that, without the intervention of any chiral factor, the probability of the formation of *R* and *S* product is 50 to 50 (50:50); racemate is formed. However, according to the theory of statistics, the numbers of *R* and *S* enantiomers are not exactly the same, that is, there is almost always the fluctuation in numbers of enantiomers [48]. We thought that, when a reaction system involves asymmetric autocatalysis with amplification of ee, the initial small fluctuation of ee in racemic mixtures that arises from the reaction of achiral reactants can produce an enantiomerically enriched product (Scheme 12).

The reaction of pyrimidine-5-carbaldehyde **2** and 2-methylpyrimidine-5-carbaldehyde with *i*-Pr_2Zn without adding a chiral substance produced enantioenriched (*S*)- or (*R*)-pyrimidyl alkanol **2** and 2-methylpyrimidyl alkanol, respectively [49]. When 2-alkynylpyrimidine-5-carbaldehyde **2** reacted with *i*-Pr_2Zn in a mixed solvent of ether and toluene, the subsequent one-pot asymmetric autocatalysis with amplification of ee gave enantiomerically enriched pyrimidyl alkanol **1** whose ee was well above the detection level [50]. The absolute configurations of the pyrimidyl alkanol **1** exhibit an approximate stochastic distribution of *S* and *R* enantiomers (formation of *S* 19 times and *R* 18 times).

We have demonstrated the stochastic formation of (*S*)- and (*R*)-5-pyrimidyl alkanol **1** from pyrimidine-5-carbaldehyde **2** and *i*-Pr_2Zn without the intervention of a chiral auxiliary. We believe that the approximate stochastic behavior in the formation of alkanol **1** fulfills one of the conditions necessary for chiral symmetry breaking by spontaneous absolute asymmetric synthesis.

4 Chiral Sensing of Small Chirality by Asymmetric Autocatalysis

As mentioned in the preceding section, the significant amplification of enantiomeric purity from a small value can be achieved by asymmetric autocatalysis of pyrimidyl alkanol. Thus, if the enantioenrichment of the initially formed asymmetric autocatalyst could be introduced by a discrete chiral factor, we can expect to obtain pyrimidyl alkanol with a detectable ee by the asymmetric autocatalytic amplification of ee. The sense of the ee should be controlled by the configuration of the originally used external chiral factor. We have examined the discrimination of a tiny chirality by using asymmetric autocatalysis.

4.1 Chiral Amino Acids Arising from Hydrogen-Isotope Substitution

Glycine and α-methylalanine are achiral amino acids; however, deuteration of one of the hydrogens of the methylene group of glycine and one methyl group of α-methylalanine makes these compounds chiral because of the hydrogen-isotope substitution. We used the chiral isotopomer of glycine-α-*d* **10** and α-methyl-d_3-alanine **11** as chiral initiators in the enantioselective addition of *i*-Pr_2Zn to pyrimidine-5-carbaldehyde **2** to afford, in combination with asymmetric autocatalysis, pyrimidyl alkanol **1** with significantly high ee (Scheme 13) [51]. The absolute configuration of the corresponding alkanol **1** was controlled efficiently by the chirality resulting from hydrogen-isotope substitution. When the *i*-Pr_2Zn addition to aldehyde **2** was performed in the presence of (*S*)-**10**, (*S*)-5-pyrimidyl alkanol **1** was obtained in high ee. On the other hand, in the presence of (*R*)-**10** instead of (*S*)-**10**, (*R*)-**1** was formed. In addition, α-methyl-d_3-alanine **11** can also act as origin of chirality in asymmetric autocatalysis with amplification of ee.

This is the first example of a highly enantioselective reaction induced by chirality resulting from deuterium substitution of amino acids. In addition, chirally deuterated primary alcohols [52] and chiral amino acid derivatives with partially deuterated substituent such as monodeuterated methyl group ($-CDH_2$) can induce the chirality in asymmetric autocatalysis [53].

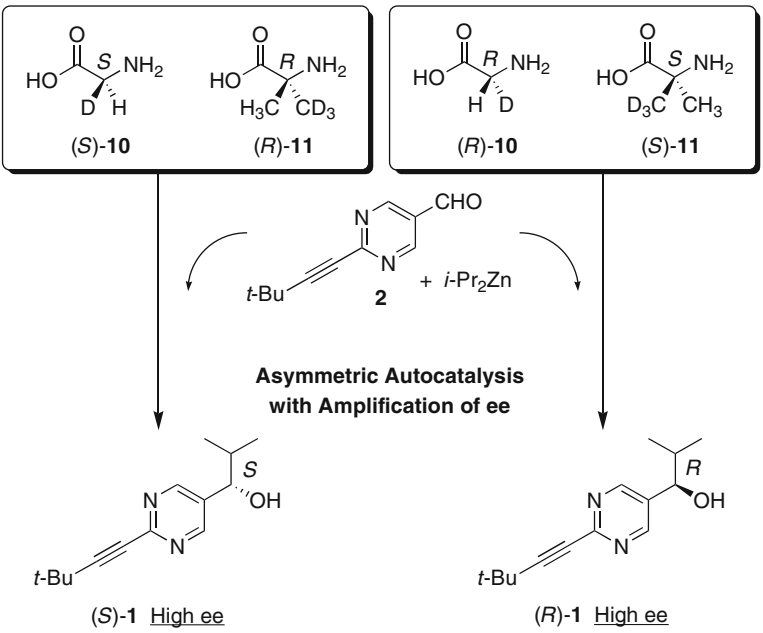

Scheme 13 Enantioselective synthesis induced by chiral hydrogen isotopomers of amino acids in conjunction with asymmetric autocatalysis

4.2 Discrimination of Chiral Compound Arising from Carbon-Isotope Substitution

Carbon-isotope chirality is experimentally difficult to discriminate because the chirality originates from the very small difference between the carbon-12 and carbon-13. Therefore, it has been a question whether isotopically substituted carbon chiral compounds can induce chirality in some enantioselective reactions. To address this problem, we performed asymmetric autocatalysis triggered by a chiral compound arising solely from carbon-isotope substitution.

Chiral carbon isotopomer of diphenylmethanol **12** was used as chiral trigger of asymmetric autocatalysis. When *i*-Pr_2Zn addition to pyrimidine-5-carbaldehyde **2** was performed in the presence of (*S*)-diphenylmethanol **12** arising from ^{13}C substitution of the phenyl group, (*S*)-pyrimidyl alkanol **1** was obtained with high ee (Scheme 14) [54]. In contrast, (*R*)-**12** afforded (*R*)-**1**. In addition to compound **12**, the isotope enantiomer of **13** and **14** can also act as chiral triggers of asymmetric autocatalysis to afford pyrimidyl alkanols **1** with high ee that have the corresponding absolute configurations as those of the isotopically substituted carbon chirality of **13** and **14**.

This is the first example of the chiral effect, that is, asymmetric induction by carbon isotopically chiral compounds. The neglected carbon-isotope chirality of

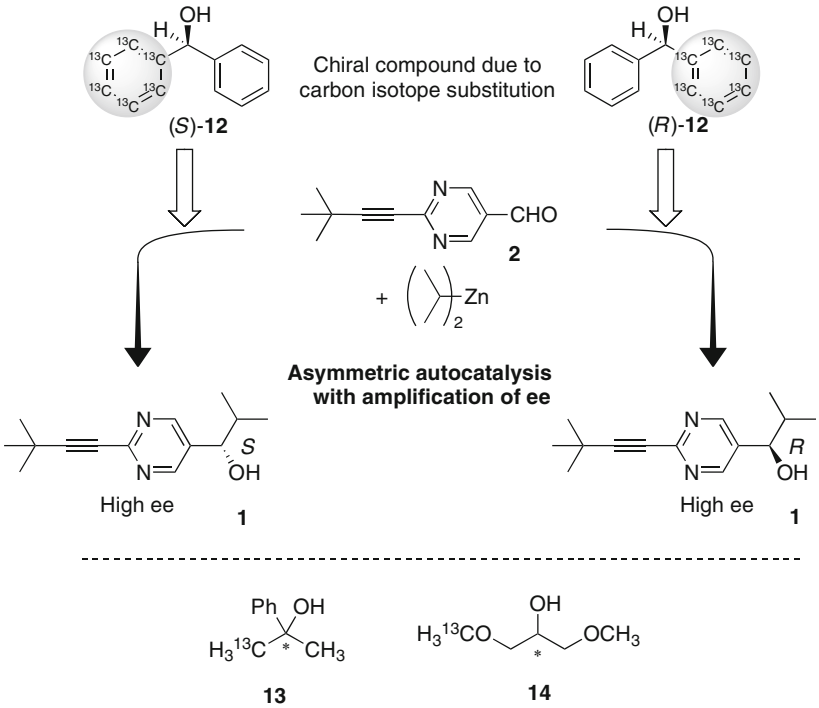

Scheme 14 Asymmetric autocatalysis triggered by carbon isotopically chiral diphenylmethanol

many organic compounds on earth can thus be discriminated by asymmetric autocatalysis, which is a highly sensitive reaction for recognizing and amplifying the extremely small chiral influence between ^{12}C and ^{13}C.

5 Reversal of Enantioselectivity by the Cooperative Operation of Two Chiral Catalysts

Catalytic asymmetric synthesis is a major focus in the field of synthetic organic chemistry. In asymmetric catalyses, achiral additives can enhance the enantioselectivity, and achiral cocatalyst can cooperatively participate in the event of enantioface selection. We have reported on the unusual reversal of enantioface selectivity that the two *R*-affording chiral catalysts cooperate to give the opposite *S* enantiomer. That is, the enantioselective addition of *i*-Pr_2Zn to pyrimidine-5-carbaldehyde **1** was carried out catalyzed by a mixture of two chiral catalysts DMNE and 2-[(1-phenylethyl)amino]-ethanol (PEAE) (Scheme 15) [55]. The reaction using (1*R*,2*S*)-DMNE alone afforded (*R*)-5-pyrimidyl alkanol **1**, and (*R*)-PEAE alone also catalyzed the production of (*R*)-**1** with the same enantioface selectivity.

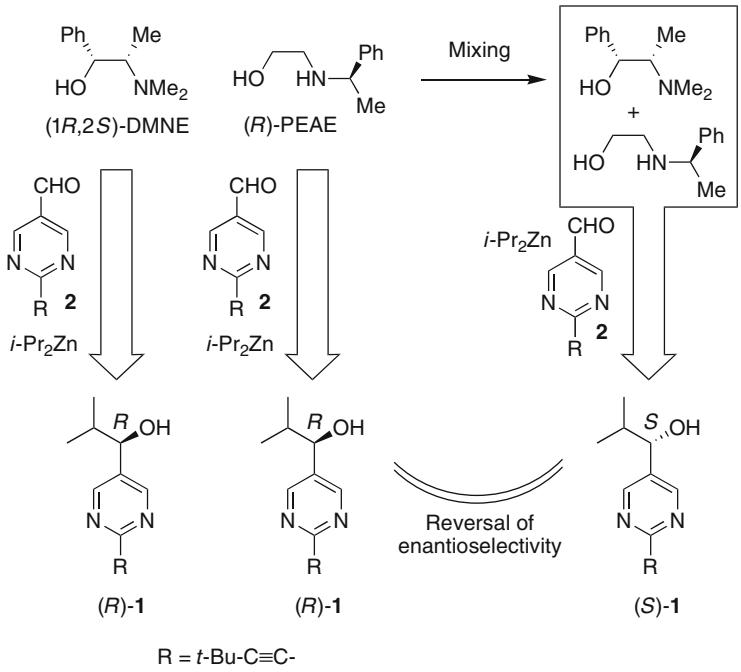

Scheme 15 Reversal of the enantioface selectivity by mixing two chiral β-amino alcohol catalysts

However, we observed a reversal of the enantioselectivity by mixing these two chiral catalysts, that is, (*S*)-**1** was synthesized by using (1*R*,2*S*)-DMNE and (*R*)-PEAE as mixed catalysts.

To the best of our knowledge, this phenomenon is unprecedented in catalytic asymmetric synthesis. In addition to our previous results [56, 57] of the enantioselectivity reversal based on the addition of achiral catalyst, these results should be possibly understood that the heterochiral aggregate acts as the catalytic species in the enantioselective dialkylzinc addition to the aldehydes.

6 Summary

In summary, we have described how we find out the asymmetric autocatalysis with amplification of chirality in the reaction between pyrimidine-5-carbaldehyde and *i*-Pr_2Zn. 2-Alkynyl-5-pyrimidyl alkanol is a highly enantioselective asymmetric autocatalyst with greater than 99.5% enantioselectivity for the addition of *i*-Pr_2Zn to the corresponding pyrimidine-5-carbaldehydes. Furthermore, it was found that enantiomeric excess of asymmetric autocatalyst enhances during the reaction. Thus, (*S*)-pyrimidyl alkanol with as low as ca. 0.00005% ee enhanced its ee to

>99.5% ee after three consecutive asymmetric autocatalyses. Asymmetric autocatalysis with amplification of enantiomeric excess enables a chiral compound with tiny enantiomeric imbalance to become highly enantiomerically enriched without the assistance of any other chiral auxiliary. Thus, the correlation was achieved between the origin of chirality and highly enantioenriched compound mediated by the amplification of ee by asymmetric autocatalysis. The chirality of CPL was directly correlated with the chirality of the pyrimidyl alkanol with high ee by asymmetric autocatalysis. Chiral inorganic crystal of quartz can act as the chiral trigger to afford (*S*)- and (*R*)-5-pyrimidyl alkanol with high ee. Chiral organic crystals composed of achiral compounds such as cytosine act as the initial source of chirality of asymmetric autocatalysis to produce the highly enantiomerically pure product. Asymmetric autocatalysis can amplify the tiny chirality such as spontaneously generated stochastic fluctuation of ee in the racemic compound; therefore, enantioenriched 5-pyrimidyl alkanol can be obtained without intervention of chiral auxiliary. Bimodal distribution in the formation of (*S*)- and (*R*)-alkanol, for the first time, fulfills one of the conditions necessary for chiral symmetry breaking by spontaneous absolute asymmetric synthesis.

We have demonstrated that the asymmetric autocatalysis of pyrimidyl alkanol is an efficient method to discriminate the cryptochirality. Amino acids that are chiral because of hydrogen-isotope substitution such as glycine-α-*d* and α-methyl-d_3-alanine can induce asymmetric autocatalysis with amplification of ee. In addition, carbon-isotope chirality can induce asymmetry in the enantioselective addition of *i*-Pr_2Zn to pyrimidine-5-carbaldehyde to afford enantiomerically enriched pyrimidyl alkanol. Thus, chiral carbon isotopomers can act as chiral triggers of asymmetric autocatalysis, which can recognize and amplify the tiny chirality generated from the difference between carbon-13 and carbon-12. The result is the first example that a chiral compound resulting from carbon-isotope ($^{13}C/^{12}C$) substitution controlled the enantioselectivity of an asymmetric reaction. Reversal of enantioselectivity by using two kinds of chiral catalyst can become one of the approaches to understand the mechanism of asymmetric dialkylzinc addition that the heteroaggregates act as the real catalytic species.

References

1. Soai K, Shibata T, Sato I (2000) Enantioselective automultiplication of chiral molecules by asymmetric autocatalysis. Acc Chem Res 33:382–390. doi:10.1021/ar9900820
2. Soai K, Shibata T, Sato I (2004) Discovery and development of asymmetric autocatalysis. Bull Chem Soc Jpn 77:1063–1073. doi:10.1246/bcsj.77.1063
3. Soai K, Kawasaki T (2006) Discovery of asymmetric autocatalysis with amplification of chirality and its implications in chiral homogeneity of biomolecules. Chirality 18:469–478. doi:10.1002/chir.20289
4. Soai K, Kawasaki T (2008) Asymmetric autocatalysis with amplification of chirality. Top Curr Chem 284:1–33. doi:10.1007/128_2007_138
5. Kawasaki T, Soai K (2010) Amplification of chirality as a pathway to biological homochirality. J Fluor Chem 131:525–534. doi:10.1016/j.jfluchem.2009.12.014

6. Bolm C, Bienewald F, Seger A (1996) Asymmetric autocatalysis with amplification of chirality. Angew Chem Int Ed Engl 35:1657–1659. doi:10.1002/anie.199616571
7. Blackmond DG (2004) Asymmetric autocatalysis and its implications for the origin of homochirality. Proc Natl Acad Sci USA 101:5732–5736
8. Podlech J, Gehring T (2005) New aspects of Soai's asymmetric autocatalysis. Angew Chem Int Ed 44:5776–5777. doi:10.1002/anie.200501742
9. Caglioti L, Zucchi C, Pályi G (2005) Single-molecule chirality. Chim Oggi 23:38–39, 42–43
10. Gehring T, Busch M, Schlageter M, Weingand D (2010) A concise summary of experimental facts about the Soai reaction. Chirality 22(1E):E173–E182. doi:10.1002/chir.20849
11. Soai K, Shibata T, Morioka H, Choji K (1995) Asymmetric autocatalysis and amplification of enantiomeric excess of a chiral molecule. Nature 378:767–768. doi:10.1038/378767a0
12. Sato I, Urabe H, Ishiguro S, Shibata T, Soai K (2003) Amplification of chirality from extremely low to greater than 99.5% ee by asymmetric autocatalysis. Angew Chem Int Ed 42:315–317. doi:10.1002/anie.200390105
13. Shibata T, Yonekubo S, Soai K (1999) Practically perfect asymmetric autocatalysis using 2-alkynyl-5-pyrimidylalkanol. Angew Chem Int Ed 38:659–661. doi:10.1002/(SICI)1521-3773(19990301)38:5%3C659::AID-ANIE659%3E3.0.CO;2-P
14. Mukaiyama T, Soai K, Sato T, Shimizu H, Suzuki K (1979) Enantioface-differentiating (asymmetric) addition of alkyllithium and dialkylmagnesium to aldehydes by using (2S, 2′S)-2-hydroxymethyl-1-[(1-alkylpyrrolidin-2-yl)methyl]pyrrolidines as chiral ligands. J Am Chem Soc 101:1455–1460. doi:10.1021/ja00500a015
15. Oguni N, Omi T (1984) Enantioselective addition of diethylzinc to benzaldehyde catalyzed by a small amount of chiral 2-amino-1-alcohols. Tetrahedron Lett 25:2823–2824. doi:10.1016/S0040-4039(01)81300-9
16. Soai K, Ookawa A, Ogawa K, Kaba T, Ogawa K (1987) Catalytic asymmetric induction. Highly enantioselective addition of dialkylzincs to aldehydes using chiral pyrrolidinyl-methanols and their metal salts. J Am Chem Soc 109:7111–7115. doi:10.1021/ja00257a034
17. Soai K, Yokoyama S, Ebihara K, Hayasaka T (1987) A new chiral catalyst for the highly enantioselective addition of dialkylzinc reagents to aliphatic aldehydes. J Chem Soc Chem Commun 1690–1691. doi:10.1039/c39870001690
18. Kitamura M, Suga S, Kawai K, Noyori R (1986) Catalytic asymmetric induction. Highly enantioselective addition of dialkylzincs to aldehydes. J Am Chem Soc 108:6071–6072. doi:10.1021/ja00279a083
19. Soai K, Ookawa A, Ogawa K, Kaba T (1987) Complementary catalytic asymmetric induction in the enantioselective addition of diethylzinc to aldehydes. J Chem Soc Chem Commun 467–468. doi:10.1039/c39870000467
20. Soai K, Niwa S (1992) Enantioselective addition of organozinc reagents to aldehydes. Chem Rev 92:833–856. doi:10.1021/cr00013a004
21. Soai K, Hori H, Niwa S (1989) Enantioselective addition of dialkylzincs to pyridinecarbaldehyde in the presence of chiral aminoalcohols: asymmetric synthesis of pyridylalkyl alcohols. Heterocycles 29:2065–2067
22. Wynberg H (1989) Asymmetric autocatalysis: facts and fancy. J Macromol Sci Chem A26:1033–1041
23. Frank FC (1953) On spontaneous asymmetric synthesis. Biochim Biophys Acta 11:459–463. doi:10.1016/0006-3002(53)90082-1
24. Soai K, Niwa S, Hori H (1990) Asymmetric self-catalytic reaction. Self-production of chiral 1-(3-pyridyl)alkanols as chiral self-catalysts in the enantioselective addition of dialkylzinc reagents to pyridine-3-carbaldehyde. J Chem Soc Chem Commun 982–983. doi:10.1039/C39900000982
25. Soai K, Hayase T, Shimada C, Isobe K (1994) Catalytic asymmetric synthesis of chiral diol, bis[2-(1-hydroxyalkyl)phenyl]ether, an asymmetric autocatalytic reaction. Tetrahedron Asymmetry 5:789–792

26. Soai K, Hayase T, Takai K (1995) Catalytic chirally self-replicating molecule. Asymmetric autocatalytic reaction of a zinc alkoxide of chiral 1-ferrocenyl-2-methylpropan-1-ol. Tetrahedron Asymmetry 6:637–638
27. Shibata T, Choji K, Morioka H, Hayase T, Soai K (1996) Highly enantioselective synthesis of a chiral 3-quinolyl alkanol by an asymmetric autocatalytic reaction. Chem Commun 751–752. doi:10.1039/CC9960000751
28. Shibata T, Morioka H, Tanji S, Hayase T, Kodaka Y, Soai K (1996) Enantioselective synthesis of chiral 5-carbamoyl-3-pyridyl alcohols by asymmetric autocatalytic reaction. Tetrahedron Lett 37:8783–8786. doi:10.1016/S0040-4039(96)02031-X
29. Mislow K (2003) Absolute asymmetric synthesis: a commentary. Collect Czech Chem Commun 68:849–864. doi:10.1135/cccc20030849
30. Eschenmoser A (1999) Chemical etiology of nucleic acid structure. Science 284:2118–2124. doi:10.1126/science.284.5423.2118
31. Feringa BL, van Delden RA (1999) Absolute asymmetric synthesis: the origin, control, and amplification of chirality. Angew Chem Int Ed 38:3419–3438. doi:10.1002/(SICI)1521-3773(19991203)38:23<3418::AID-ANIE3418>3.0.CO;2-V
32. Weissbuch I, Lahav M (2011) Crystalline architectures as templates of relevance to the origins of homochirality. Chem Rev 111:3236–3267. doi:10.1021/cr1002479
33. Girard C, Kagan HB (1998) Nonlinear effects in asymmetric synthesis and stereoselective reactions: ten years of investigation. Angew Chem Int Ed 37:2923–2959. doi:10.1002/(SICI)1521-3773(19981116)37:21<2922::AID-ANIE2922>3.0.CO;2-1
34. Nishino H, Kosaka A, Hembury GA, Aoki F, Miyauchi K, Shitomi H, Onuki H, Inoue Y (2002) Absolute asymmetric photoreactions of aliphatic amino acids by circularly polarized synchrotron radiation: critically pH-dependent photobehavior. J Am Chem Soc 124:11618–11627. doi:10.1021/ja025959w
35. Kagan H, Moradpour A, Nicoud JF, Balavoine G, Tsoucaris G (1971) Photochemistry with circularly polarized light. Synthesis of optically active hexahelicene. J Am Chem Soc 93:2353–2354. doi:10.1021/ja00738a061
36. Kawasaki T, Sato M, Ishiguro S, Saito T, Morishita Y, Sato I, Nishino H, Inoue Y, Soai K (2005) Enantioselective synthesis of near enantiopure compound by asymmetric autocatalysis triggered by asymmetric photolysis with circularly polarized light. J Am Chem Soc 127:3274–3275. doi:10.1021/ja0422108
37. Hazen R, Sholl M, David S (2003) Chiral selection on inorganic crystalline surfaces. Nat Mater 2:367–374. doi:10.1038/nmat879
38. Soai K, Osanai S, Kadowaki K, Yonekubo S, Shibata T, Sato I (1999) D- and L-quartz-promoted highly enantioselective synthesis of a chiral compound. J Am Chem Soc 121:11235–11236. doi:10.1021/ja993128t
39. Green BS, Lahav M, Rabinovich D (1979) Asymmetric synthesis via reactions in chiral crystals. Acc Chem Res 12:191–197. doi:10.1021/ar50138a001
40. Kawasaki T, Jo K, Igarashi H, Sato I, Nagano M, Koshima H, Soai K (2005) Asymmetric amplification using chiral cocrystals formed from achiral organic molecules by asymmetric autocatalysis. Angew Chem Int Ed 44:2774–2777. doi:10.1002/anie.200462963
41. Kawasaki T, Suzuki K, Hakoda Y, Soai K (2008) Achiral nucleobase cytosine acts as an origin of homochirality of biomolecules in conjunction with asymmetric autocatalysis. Angew Chem Int Ed 47:496–499. doi:10.1002/anie.200703634
42. Kawasaki T, Suzuki K, Hatase K, Otsuka M, Koshima H, Soai K (2006) Enantioselective synthesis mediated by chiral crystal of achiral hippuric acid in conjunction with asymmetric autocatalysis. Chem Commun 1869–1871. doi:10.1039/b602442d
43. Kawasaki T, Harada Y, Suzuki K, Tobita T, Florini N, Palyi G, Soai K (2008) Enantioselective synthesis utilizing enantiomorphous organic crystal of achiral benzils as a source of chirality in asymmetric autocatalysis. Org Lett 10:4085–4088. doi:10.1021/ol801600y

44. Kawasaki T, Nakaoda M, Kaito N, Sasagawa T, Soai K (2010) Asymmetric autocatalysis induced by chiral crystals of achiral tetraphenylethylenes. Orig Life Evol Biosph 40:65–78. doi:10.1007/s11084-009-9183-4
45. Kawasaki T, Hakoda Y, Mineki H, Suzuki K, Soai K (2010) Generation of absolute controlled crystal chirality by the removal of crystal water from achiral crystal of nucleobase cytosine. J Am Chem Soc 132:2874–2875. doi:10.1021/ja1000938
46. Barabas B, Toth J, Palyi G (2010) Stochastic aspects of asymmetric autocatalysis and absolute asymmetric synthesis. J Math Chem 48:457–489. doi:10.1007/s10910-010-9680-8
47. Barabas B, Caglioti L, Micskei K, Palyi G (2009) Data-based stochastic approach to absolute asymmetric synthesis by autocatalysis. Bull Chem Soc Jpn 82:1372–1376. doi:10.1246/bcsj.82.1372
48. Mills WH (1932) Some aspects of stereochemistry. Chem Ind 51:750–759
49. Soai K, Shibata T, Kobata Y (1997) (Japan Kokai Tokkyo Koho) JP 1997 9-268179. Application date: February 1 and April 18, 1996. An abstract of JP9-268179 is readily available from the European Patent Office (http://ep.espacenet.com) and, as JP-09268179 A, from Derwent World Patent Index, update No. 51 of 1997 (accession no. 1997-554699)
50. Soai K, Sato I, Shibata T, Komiya S, Hayashi M, Matsueda Y, Imamura H, Hayase T, Morioka H, Tabira H, Yamamoto J, Kowata Y (2003) Asymmetric synthesis of pyrimidyl alkanol without adding chiral substances by the addition of diisopropylzinc to pyrimidine-5-carbaldehyde in conjunction with asymmetric autocatalysis. Tetrahedron Asymmetry 14:185–188. doi:10.1016/S0957-4166(02)00791-7
51. Kawasaki T, Shimizu M, Nishiyama D, Ito M, Ozawa H, Soai K (2009) Asymmetric autocatalysis induced by meteoritic amino acids with hydrogen isotope chirality. Chem Commun 4396–4398. doi:10.1039/b908754k
52. Sato I, Omiya D, Saito T, Soai K (2000) Highly enantioselective synthesis induced by chiral primary alcohols due to deuterium substitution. J Am Chem Soc 122:11739–11740. doi:10.1021/ja002992e
53. Kawasaki T, Ozawa H, Ito M, Soai K (2011) Enantioselective synthesis induced by compounds with chirality arising from partially deuterated methyl groups in conjunction with asymmetric autocatalysis. Chem Lett 40:320–321. doi:10.1246/cl.2011.320
54. Kawasaki T, Matsumura Y, Tsutsumi T, Suzuki K, Ito M, Soaki K (2009) Asymmetric autocatalysis triggered by carbon isotope ($^{13}C/^{12}C$) chirality. Science 324:492–495. doi:10.1126/science.1170322
55. Kawasaki T, Wakushima Y, Asahina M, Shiozawa K, Kinoshita T, Lutz F, Soai K (2011) Reversal phenomenon of enantioface selectivity by the cooperative operation of two chiral catalysts. Chem Commun 47:5277–5279. doi:10.1039/C1CC10136F
56. Lutz F, Igarashi T, Kawasaki T, Soai K (2005) Small amounts of achiral β-amino alcohols reverse the enantioselectivity of chiral catalysts in cooperative asymmetric autocatalysis. J Am Chem Soc 127:12206–12207. doi:10.1021/ja054323c
57. Lutz F, Igarashi T, Kinoshita T, Asahina M, Tsukiyama K, Kawasaki T, Soai K (2008) Mechanistic insights in the reversal of enantioselectivity of chiral catalysts by achiral catalysts in asymmetric autocatalysis. J Am Chem Soc 130:2956–2958. doi:10.1021/ja077156k

Top Organomet Chem (2013) 44: 281–314
DOI: 10.1007/3418_2012_49

Published online: 18 August 2012

Natural Products as Inspiration for Reaction Development: Catalytic Enantioselective Decarboxylative Reactions of Prochiral Enolate Equivalents

Douglas C. Behenna and Brian M. Stoltz

Abstract This account describes the circumstances leading to our group's innovations in the area of decarboxylative asymmetric allylic alkylation reactions and the initial discovery of palladium phosphinooxazoline complexes as efficient enantioselective catalysts. This chapter also chronicles the growth of the methodology to include several substrate classes, the expansion of the project into several other reaction manifolds, and the use of these reactions in natural product synthesis. Finally, important contributions from other research groups involving related methods or products similar to the α-quaternary products that are the focus of our studies, as well as future directions for asymmetric alkylation reactions, are discussed.

Keywords Allylic alkylation · Asymmetric catalysis · Decarboxylation · Enolate α-alkylation · Palladium catalysis · PHOX ligands · Quaternary stereocenters

Contents

D.C. Behenna and B.M. Stoltz (✉)
Division of Chemistry and Chemical Engineering, The Warren and Katharine Schlinger Laboratory for Chemistry and Chemical Engineering, California Institute of Technology, Pasadena, CA 91125, USA
e-mail: stoltz@caltech.edu

Abbreviations

4ÅMS	4 Ångström molecular sieves
ACN	Acetonitrile
AIBN	2,2′-Azobis(2-methylpropionitrile)
BSA	*O*,*N*-bistrimethylsilyl acetamide
Dba	Dibenzylideneacetone
DME	Dimethoxyethane
DMSO	Dimethylsulfoxide
Dppf	1,1′-Bis(diphenylphosphino)ferrocene
Dr	Diastereomeric ratio
Ee	Enantiomeric excess
KHMDS	Potassium bis(trimethylsilyl)amide
LDA	Lithium diisopropylamide
LHMDS	Lithium bis(trimethylsilyl)amide
PCC	Pyridinium chlorochromate
PHOX	Phosphinooxazoline
Piv	Pivaloyl
Pmdba	Bis(*p*-methoxybenzylidene)acetone
TBAT	Tetrabutylammonium difluorotriphenylsilicate
TBS	*t*-Butyldimethylsilyl
TEA	Triethylamine
THF	Tetrahydrofuran
TMS	Trimethylsilyl
QUINAP	1-(2-Diphenylphosphino-1-naphthyl)isoquinoline

1 Introduction

The use of palladium(II) π-allyl complexes in organic chemistry has a rich history. These complexes were the first examples of a C–M bond to be used as an electrophile [1–3]. At the dawn of the era of asymmetric catalysis, the use of chiral phosphines in palladium-catalyzed allylic alkylation reactions provided key early successes in asymmetric C–C bond formation that were an important validation of the usefulness of the field [4]. No researchers were more important to these innovations than Prof. B.M. Trost and Prof. J. Tsuji [5–10]. While most of the early discoveries in this field provided access to tertiary (3°) stereocenters formed on a prochiral electrophile [Eq. (1)] (Scheme 1), our interest focused on making quaternary (4°) stereocenters on prochiral enolates [Eq. (2)]. Recently, we have described decarboxylative asymmetric allylic alkylation reactions involving prochiral enolates that provide access to enantioenriched α-quaternary carbonyl compounds [11–13]. We found that a range of substrates (e.g., allyl enol carbonates,

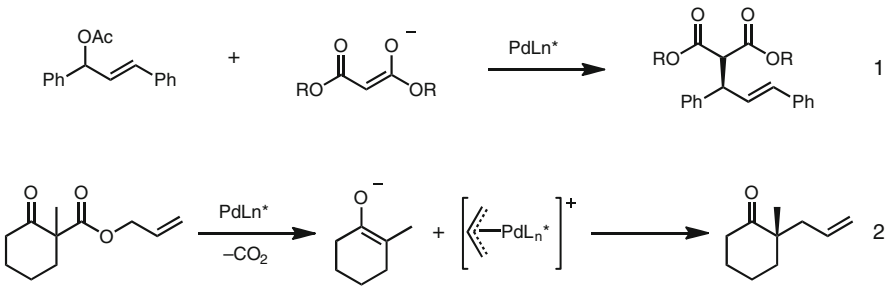

Scheme 1 Representative examples of asymmetric allylic alkylation reactions

silyl enol ethers, β-keto esters, and *N*-protected lactam allyl esters) could undergo allylic alkylation with high degrees of both enantio- and regioselectivity. The enantioenriched α-quaternary carbonyl compounds produced by this method have proven to be valuable building blocks in the synthesis of a wide variety of natural products.

2 Natural Products as Inspiration for Reaction Development

We often target molecules with structures that force us to confront the current limitations of synthetic methods. Elegant syntheses of such molecules require that such deficiencies be overcome. This is certainly true of zoanthenol [14], which has three quaternary stereocenters on its central C ring (Scheme 2). By early 2003 one of us (DCB) had developed a method to construct the ABC rings and two of the three quaternary stereocenters found in this natural product (for a review of other synthetic efforts toward the synthesis of zoanthus alkaloids, see [15]). The installation of the final quaternary stereocenter stood as a daunting challenge. Even installing a single alkyl substituent proved difficult; under numerous conditions, deprotonation occurred at C(11) and not at C(9), as desired [Eq. (3)]. We overcame this by blocking the C(11) position and then methylating C(9) but faced difficulties removing the blocking group and making the final C–C bond of the C(9) quaternary stereocenter [Eq. (4)]. Our initial strategy to make that final bond was to increase the nucleophilicity of the C(9) position and to favor the formation of the quaternary stereocenter using a metallo enamine. However, even under forcing conditions (i.e., refluxing toluene in a Dean–Stark apparatus for several days), very low conversion to the desired enamine was observed with a model ketone [Eq. (5)].

After this setback we scrambled to identify other methods known to preferentially form quaternary stereocenters when the generation of a tertiary stereocenter at a similarly acidic position α to a ketone existed [Scheme 3, Eq. (6)]. With the aid of a Beilstein search, we were reminded of Prof. J. Tsuji's pioneering allylation work [16–19]. In the early 1980s, he had demonstrated that under specific conditions,

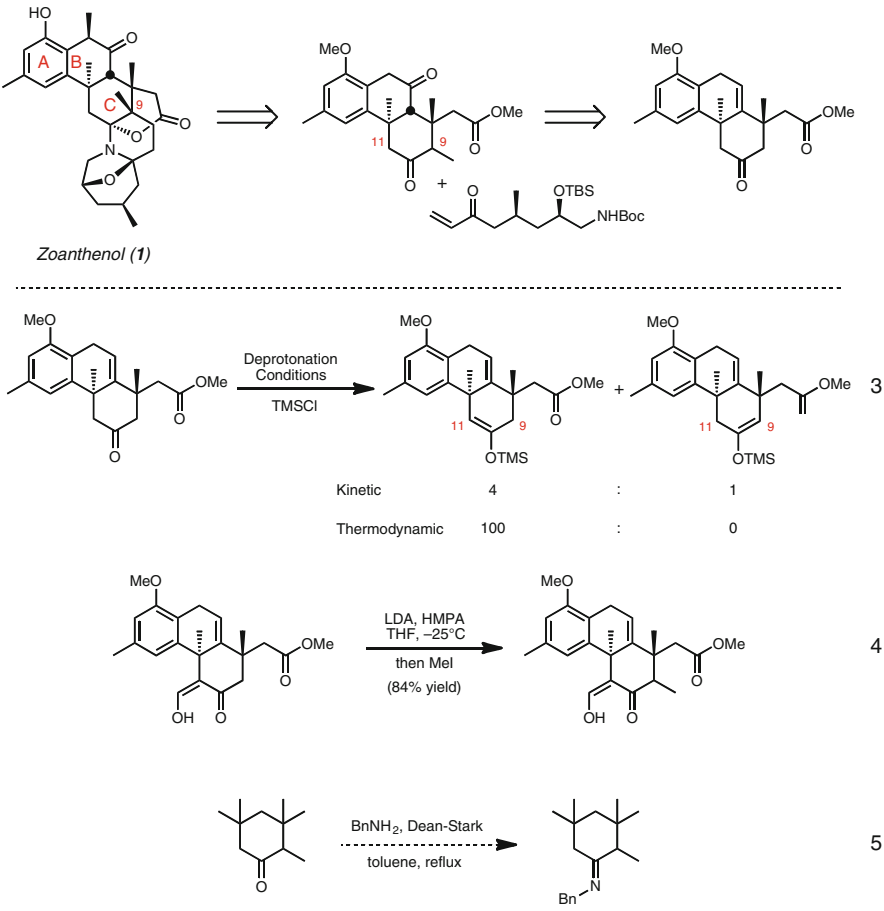

Scheme 2 Retrosynthetic plan and synthetic efforts toward zoanthenol (**1**)

palladium-catalyzed allylation was regioselective and determined by the isomer of the starting material employed.

Our first hurdle was to determine if this selectivity would be maintained in the presence of steric bulk disposed β to the ketone. We synthesized model enol carbonate **4** and were encouraged to find that it selectively produced the desired α-quaternary ketone. Ultimately, difficulties in preparing an appropriate methyl ketone prevented us from executing this strategy, but the selectivity and utility of Tsuji's allylation reaction for making quaternary stereocenters left a lasting impression.

An important aspect to this story was that it occurred at a significant time. DCB had just completed his oral candidacy exam, but the path forward to completing zoanthenol looked daunting. Because DCB was working alone on the synthesis at that time, the amount of work required to move material to the forefront of the

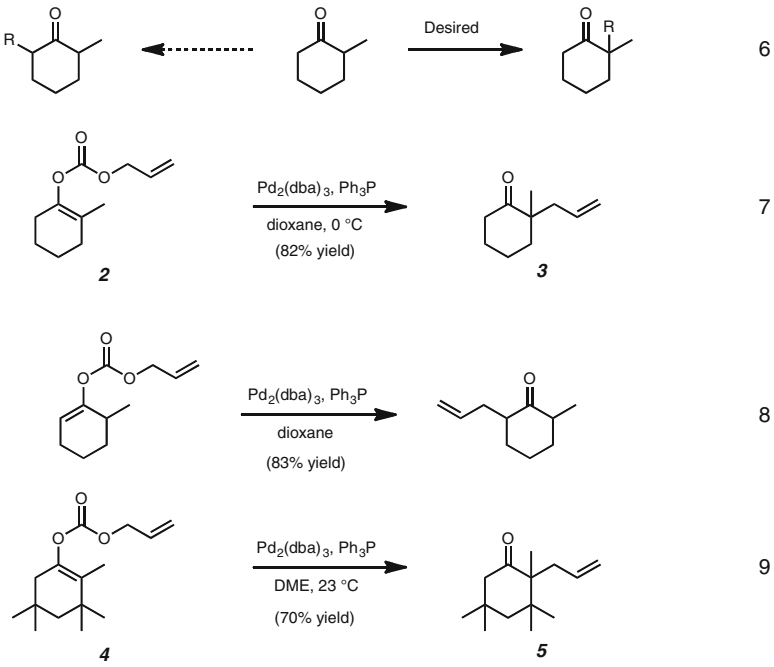

Scheme 3 Tsuji's regioselective allylic alkylation reactions

synthesis was tedious and had slowed progress considerably. DCB wanted to think about a different type of project and mentioned to BMS that an asymmetric version of Prof. Tsuji's allylation reaction, which had the advantage of being able to produce α-quaternary ketones without blocking groups or large differences in the acidity of the α protons, would make an interesting project. DCB was given a couple of weeks to see if he could generate any asymmetry in the reaction.

3 Initial Screening and Optimization

With limited time to show progress on this side project, our approach was straightforward: replace triphenylphosphine with a commonly used chiral phosphine and search for a catalyst that gave useful levels of enantiomeric excess in the product. We selected a simple test system that produced 2-allyl-2-methyl cyclohexanone (**3**), which was not known in enantioenriched form at that time. In the initial screen (Table 1, entries 1–9), we tested several commercially available bisphosphines, monophosphines, and chelating NP ligands. The results were better than we could have hoped. Not only did the reactions proceed exclusively to give α-quaternary ketone **3**, but exciting levels of enantiomeric excess (82%) were observed in the initial screen of ligands! A clear trend from the initial screen was the superiority of

Table 1 Initial screening of chiral ligands in the Tsuji allylic alkylation

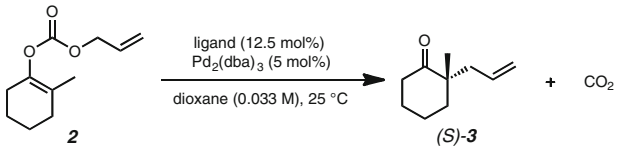

2 *(S)-3*

Entry	Ligand	Time (h)	%Yield[a]	% ee[b]
1	(*R*)-*BINAP*	5	92	5[c]
2	(*R*,*R*)-*Me-DUPHOS*	5	61	0
3	(*R*,*R*)-*DIOP*	2	91	2[c]
4	(*R*)-*MOP*	3	93	18
5	(*R*,*R*)-*Trost ligand* (***6***)	2	97	46[c]
6	(*R*)-*QUINAP* (***7***)	2	98	61
7	(*R*)-*PhPHOX* (***8***)	2	95	62[c]
8	(*S*)-*BnPHOX* (***9***)	3	96	65
9	(*R*)-*i-PrPHOX* (***10***)	3	96	82[c]
10	(*S*)-*t-BuPHOX* (***11***)	2	95	86

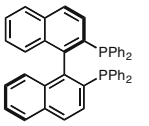

(*R*)-*BINAP*

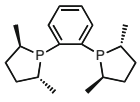

(*R*,*R*)-*Me-DUPHOS*

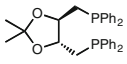

(*R*,*R*)-*DIOP*

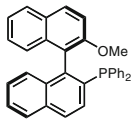

(*R*)-*MOP*

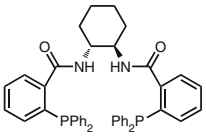

(*R*,*R*)-*Trost ligand* (***6***)

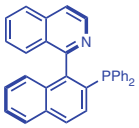

(*R*)-*QUINAP* (***7***)

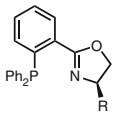

R = *Ph*
(*R*)-*PhPHOX* (***8***)
R = *i-Pr*
(*R*)-*i-PrPHOX* (***10***)

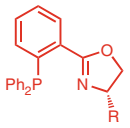

R = *Bn*
(*S*)-*BnPHOX* (***9***)
R = *t-Bu*
(*S*)-*t-BuPHOX* (***11***)

[a]GC yield relative to internal standard (tridecane)
[b]Enantiomeric excess by chiral GC
[c](*R*)-**3** produced as the major product

NP chelating ligands when compared to chelating phosphines. Based on the hypothesis that more steric bulk on the oxazoline of the PHOX ligand was beneficial, the first ligand we synthesized was *t*-BuPHOX. We were pleased to see a significant increase in ee with *t*-BuPHOX. Only a few weeks into the project, it was clear that this project would produce significant and publishable results.

At this point, we could have pursued the optimization of the reaction's enantioselectivity by at least two distinct approaches, optimizing the standard parameters (e.g., concentration, temperature, and solvent) or optimizing the structure of the

Table 2 Non-PHOX ligands synthesized and tested in the asymmetric Tsuji allylation

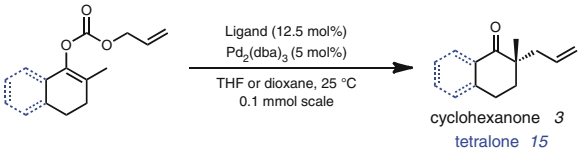

Ligand	% Conversion[a]	% ee[b]	Ligand	% Conversion[a]	% ee[b]
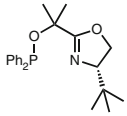	87	56	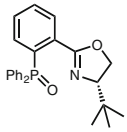	0	ND
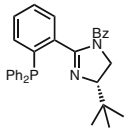	56	79	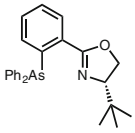	100	52
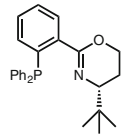	100	45	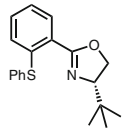	0	ND
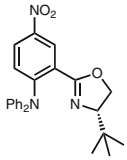	<5	7			

[a]Conversion estimated by TLC analysis or by GC relative to internal standard (tridecane)
[b]Enantiomeric excess measured by chiral HPLC or chiral GC

chiral NP ligand. With *t*-BuPHOX in hand, it seemed likely that changing reaction parameters would get the ee of the reaction consistently above the 90% threshold; thus, we choose to focus on the optimization of typical reaction parameters. We also thought it likely that testing these parameters would take less time than synthesizing additional chiral ligands.

It should be noted that from the beginning of the project, as with the achiral reaction, the chemical yield of the reaction was nearly quantitative. Almost all of the test reactions performed with PHOX ligands were spot-to-spot reactions by

Table 3 Solvent screen of the allylic alkylation reaction using (*S*)-*t*-BuPHOX

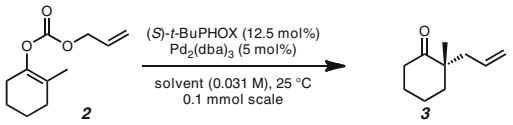

Entry[a,b]	Solvent	Time (h)	% Yield[c]	% ee[d]
1	Dioxane	2	95	86
2	Tetrahydrofuran	2	96	88
3	Diethyl ether	2	98	89
4	*t*-Butyl methyl ether	2	98	89
5	Diisopropyl ether	2	95	89
6	Anisole	3	82	81
7	1,2-Dimethoxyethane	2	72	56
8	Benzene	2	99	88
9	Toluene	2	99	88
10	Ethyl acetate	2	97	86
11	Acetone	3	26	60
12	Triethylamine	2	72	89
13	Fluorobenzene	3	58	51
14	Dichloromethane	3	42	13
15	Chloroform	6	0	NA

[a]Data reported are the average of three trials
[b]All reactions proceeded to complete conversion except entries 13–15
[c]GC yield relative to internal standard (tridecane)
[d]Enantiomeric excess measured by chiral GC

TLC and gave yields greater than 90% when measured by GC or isolated yield. This privileged circumstance simplified the optimization process because we were never forced to make a decision to optimize one valued parameter over another (i.e., we never had to sacrifice yield to get higher ee). However, there were a number of chiral ligands, which had chelate structures that differed significantly from PHOX ligands, that gave low levels of conversion and enantioinduction (Table 2).

The asymmetric allylic alkylation reaction was attempted in numerous solvents with the hope that one would provide higher ee (Table 3). Unfortunately, no solvent produced significantly higher ee, but several interesting trends were apparent. Several of the most common alkyl ether solvents (entries 1–5), as well as aromatic solvents (i.e., benzene and toluene) and ethyl acetate, gave very similar results. Interestingly, using triethylamine as solvent also provided product of high ee (entry 12). Chlorinated solvents (entries 14 and 15) were unusual in that they gave poor chemical yields in the reaction. In general, the solvents that performed well were donating solvents (either σ donating or π donating) and were clustered in a fairly tight range of solvent dielectric constants. These observations suggest that the stabilization of an electron-deficient palladium complex and the association of ion pairs are important properties. For reasons of reproducibility and catalyst solubility, we chose THF as our default solvent, although we would later find that toluene provided better ee in some cases.

Table 4 The effect of water on the allylic alkylation reaction

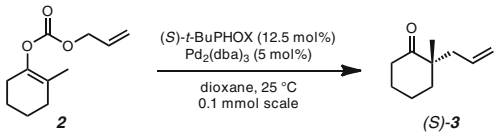

Entry[a]	Concentration (M)	Time (h)	% Yield[b]	% ee[c]
1	0.500	3	81	82
2	0.250	2	90	84
3	0.125	2	94	84
4[d]	0.063	2	99	85
5	0.031	2	95	86

[a]Data reported are the average of three trials
[b]GC yield relative to internal standard (tridecane)
[c]Enantiomeric excess measured by chiral GC
[d]Data reported are the average of two trials

We also examined the sensitivity of the asymmetric alkylation reaction to water and atmosphere. The reaction is quite tolerant to superstoichiometric amounts of water (Table 4). Compared to typical alkali metal enolate-based reactions, this tolerance for water was very surprising. In contrast, the alkylation reaction proved rather sensitive to atmosphere. While the palladium(0) source and (*S*)-*t*-BuPHOX could be weighed without taking any precautions, the complex formed when these two components were solvated was sensitive to atmospheric exposure. Operationally, we found this limited us to reactions no smaller than 0.1 mmol scale if they were to be preformed outside of a glovebox. On smaller scales, reactions would sometimes fail to reach completion likely due to the introduction of very small amounts of oxygen.

Our attempts to increase the ee of the α-quaternary ketone products by lowering the temperature of the reaction also met with limited success. While we did observe a slight increase in ee (89%) at 12°C, further lowering temperatures caused the reaction to stall (Table 5, entry 3). However, higher temperatures did allow for significantly reduced reaction times with only slightly diminished ee in the product (Table 6).

While we generally found the asymmetric allylation reaction to be very robust and reproducible, there was one confounding set of experimental results, which may be instructive to others. Because our initial experiments were carried out in dioxane, we performed a test reaction of each newly synthesized chiral ligand, as well as a calibration reaction using *t*-BuPHOX, in dioxane. However, during the period of about 10 months that we were synthesizing modified PHOX ligands, we noticed that the ee in the control reaction was decreasing. It is very disconcerting to have the control reaction's enantiomeric excess decrease while you are trying to improve enantioinduction in the process! The decrease in ee was pernicious, but significant, and accounted for a few percent ee over the course of the experiments (Scheme 4).

Table 5 Enol carbonate substrates

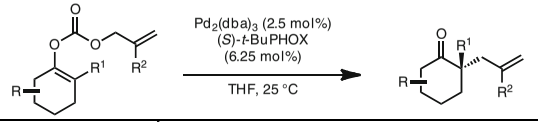

Entry	Product[a]	% Yield[b]	% ee[c]	Entry	Product[a]		% Yield[b]	% ee[c]
1	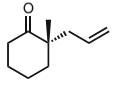	85	87	7	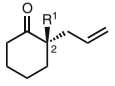	$R^1 = CH_2CH_3$ (***16***)	96	92
2[d]		85	88 (98)[e]	8[f]		$R^1 = t$-Bu	55[g]	82
3[h]		90	89	9		$R^1 = CH_2Ph$	96	85
				10		$R^1 = (CH_2)_3OBn$	87	88
4[f]	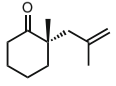	89	91	11	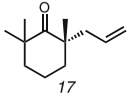		94	92
					17			
5	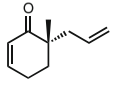	91	89	12[i]	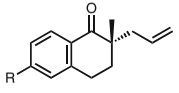	R = H	87	91
				13[i]		R = OCH_3	94	91
6	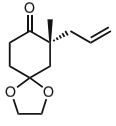	87	86	14	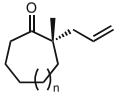	$n = 1$	81	87
				15		$n = 2$	90	79

[a]Reactions were performed using 1.0 mmol of substrate in THF (0.033 M in substrate) at 25°C with 2.5 mol% $Pd_2(dba)_3$ and 6.25 mol% (*S*)-*t*-BuPHOX (**11**), unless otherwise noted. Each reaction was complete in 1–10 h

[b]Isolated yields

[c]Measured by chiral GC or HPLC

[d]Performed on 5.1 mmol scale

[e]In parentheses is the% ee after two recrystallizations of the corresponding semicarbazone

[f]Reaction performed at 12°C (GC yield)

[g]Performed with 5 mol% $Pd_2(dba)_3$ and 12.5 mol% (*S*)-**11**

[h]Isolated yield after conversion to the corresponding diketone via Wacker oxidation

[i]Performed at 10°C

Table 6 The effect of temperature on the allylic alkylation reaction

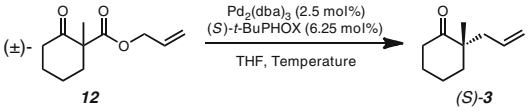

Entry	Temperature (°C)	Time (h)	% Yield[a]	% ee[b]
1	18	48	0	ND
2	25	7.5	85	88
3	30	2.25	82	87
4	35	1.25	85	86
5	40	0.67	86	85
6	60	0.15	82	83

[a]Isolated yield from reaction of 1.0 mmol substrate at 0.033 M
[b]Determined by chiral GC

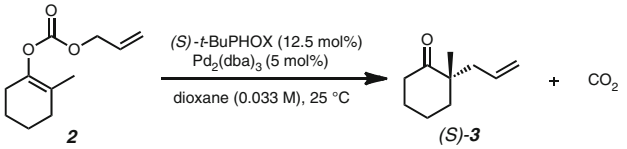

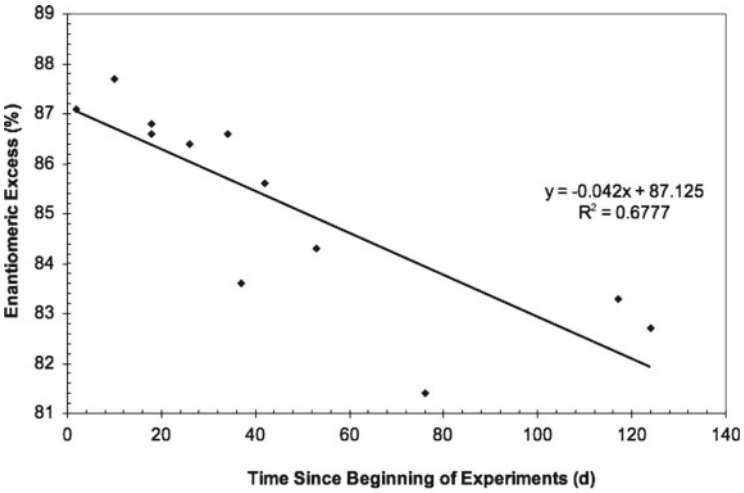

Scheme 4 Plot of enantiomeric excess versus time for the calibration reaction

The fact that the change was roughly proportional to time suggested that some component of the reaction was degrading with storage. There were only five components in the reaction, so we set out to examine each component individually and see what effect it had. New stir bars were purchased. New $Pd_2(dba)_3$ was

purchased and also prepared in the laboratory. New batches of *t*-BuPHOX and the enol carbonate substrate were synthesized. New sodium was added to the dioxane, and it was refluxed for more than 24 h to ensure it was dry. None of these measures resulted in any improvement in the ee of the test reaction. But upon examining the dioxane still, noticeably more solids had formed in the pot, and all of the sodium had been consumed. The dioxane in the still had been previously refluxed with sodium, so it should not have been wet enough to consume all of the new sodium. It dawned on DCB that there was far too much solid in the flask for all of it to be sodium hydroxide. Some of the dioxane had to be reacting. Indeed, most of the solid in the distillation pot was neither soluble in water nor organic solvents. Cleaning out the still pot and redistilling fresh dioxane for a short time restored the lost ee. Our efforts to carefully dry the dioxane were actually contributing to the problem. Ultimately, this episode helped convince us to change our default solvent for these reactions to THF.

4 The Siren Song of Ligand Synthesis

A key advantage of the PHOX ligands, which led us to concentrate on that ligand architecture rather than QUINAP-type ligands, was the availability of straightforward routes to many derivative structures [20–22]. Even a small improvement in the typical ee of the products above the 90% threshold would make the importance of the method self-evident to the synthetic community. Because of our initial success in moving from *i*-PrPHOX to *t*-BuPHOX, we entered this phase of the project convinced that we would quickly find an improved ligand. There was a tremendous feeling of anticipation; we were convinced that every PHOX ligand we made would be the one to break through the 90% ee barrier. In the end, we tested more than 40 PHOX ligands (Table 7). We varied the substituent on the oxazoline, the sterics and electronics of the phosphine donor, the electronics of the nitrogen donor, the identity of the chelating atoms, and the number and type of atoms connecting the donor atoms.

Unfortunately, we were unable to realize a PHOX ligand that significantly increased the ee of the α-quaternary ketone products. However, we did find that tris(*p*-trifluoromethyl) PHOX ligand **14** ($((CF_3)_3$-*t*-BuPHOX) provided a catalyst that was more reactive than the *t*-BuPHOX. In later studies this catalyst was also found to be particularly effective with another class of allylic alkylation substrates. Our work to synthesize a variety of PHOX ligands (particularly those with *para* electron-withdrawing groups on the aromatic rings) also demonstrated that a more universal method for their synthesis was needed and prompted us to investigate a copper-catalyzed method for C–P bond formation [23]. Even with a reliable route for their synthesis, each PHOX ligand required at least three synthetic steps and a few days to synthesize. In the most demanding case, a 14-step synthesis was required to generate adamantyl PHOX ligand **13**. The synthesis of PHOX ligands consumed more time than any other phase of this project. We were transfixed by the

Table 7 PHOX ligands synthesized and tested in the asymmetric Tsuji allylation

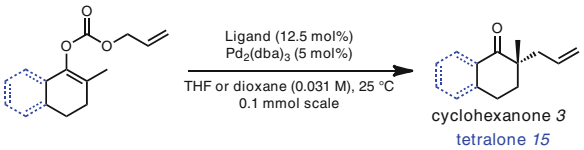

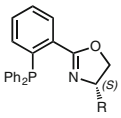	R = *i*-Pr	83% ee (*S*)
	R = *t*-Bu	88% ee (*S*)
	R = $C(Et)_3$	88% ee (*S*)
	R = 1-Ad (***13***)	78% ee (*S*)
	R = Bn	63% ee (*S*)
	R = CH_2-*t*-Bu	59% ee (*S*)
	R = CH_2-1-naphthyl	41% ee (*S*)
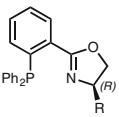	R = *i*-Pr	83% ee (*R*)
	R = Cy	83% ee (*R*)
	R = Ph	65% ee (*R*)
	R = $CHPh_2$	69% ee (*R*)
	R = $C(Me)_2OBn$	85% ee (*R*)
	R = $C(Me)_2OTBS$	85% ee (*R*)
	R = $C(Me)_2OH$	55% ee (*R*)
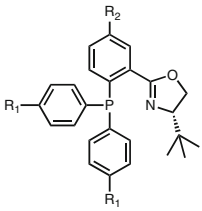	R_1 = Me, R_2 = H	81% ee (*S*)
	R_1 = H, R_2 = OMe	86% ee (*S*)
	R_1 = F, R_2 = H	88% ee (*S*)
	R_1 = H, R_2 = CF_3	89% ee (*S*)
	R_1 = CF_3, R_2 = H	89% ee (*S*)
	R_1 = H, R_2 = NO_2	90% ee (*S*)
	R_1 = CF_3, R_2 = NO_2	87% ee (*S*)
	R_1 = CF_3, R_2 = CF_3 (***14***)	87% ee (*S*)
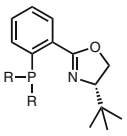	R = Cy	83% ee (*S*)
	R = 2-MePh	79% ee (*S*)
	R = 3,5-CF_3Ph	83% ee (*S*)
	R = C_6F_5	81% ee (*S*)

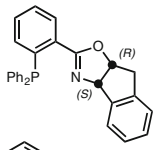	79% ee (*S*)
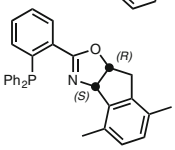	82% ee (*S*)
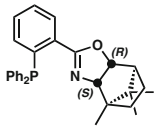	81% ee (*S*)
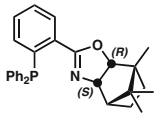	61% ee (*R*)

All reactions proceeded to complete conversion. Enantiomeric excess measured by chiral HPLC or GC

idea that we would be able to find a ligand that would give us a significant improvement in ee over *t*-BuPHOX. In retrospect, it is surprising that we endured in making as many PHOX ligands as we did. Had we accepted that this project was

clearly under the control of "Bercaw's law of initial optimization"[1] earlier, we could have likely completed our initial manuscript 6 months sooner.

5 Broadening the Substrate Scope

With optimized conditions in hand, our next task was to define the substrate scope for the initial manuscript. Overall, this phase of the project went smoothly, but there were a few surprises along the way. The vast majority of the substrates gave α-quaternary ketone products with enantiomeric excesses similar to our model substrate (Table 5). Of particular note, ethyl-substituted ketone **16** was generated in significantly higher ee. Additionally, product ketones with no α-acidic protons (e.g., tetralone, enone, and 6,6-dimethyl substrates) gave slightly higher ee. However, these substrates were less interesting to us because they could be made by Prof. Trost's methods. We chose to focus on substrates with multiple α-acidic sites because we believed this substrate class was an important niche for our reaction. While we were unable to find a catalyst system that consistently produced this class of ketone in significantly greater than 90% ee, we were able to define a reliable recrystallization method that produced α-quaternary ketones of 98% ee [24].

The most difficult task in this part of the project was obtaining the enol carbonate substrates in an isomerically pure form. Standard methods for forming the thermodynamic enolate, which served as a precursor to the fully substituted enol carbonates and ultimately to the α-quaternary ketones we desired, typically resulted in 5–10% of the less substituted enol carbonate isomer. This had no impact on the enantioselectivity of the allylic alkylation reaction, but due to the positional fidelity of the reaction, it did result in yields that were artificially lowered by 5–10% as a result of the formation of the undesired 2,6-disubstituted ketone. Separating the enol carbonate isomers chromatographically was tedious and sometimes untenable. We came upon the idea of trapping the thermodynamically preferred enolates as silyl enol ethers and trying to purify the silyl enol ethers. The silyl enol ether isomers were no easier to separate chromatographically, but we did find that Larock-modified Saegusa–Ito oxidation took place at a significantly faster rate on the less substituted silyl enol ether. The resulting enones were easily separated from the remaining silyl enol ether. With careful reaction monitoring, we could run the oxidations until less than 2% of the undesired (i.e., less substituted enol isomer) remained. When these enriched silyl enol ethers were treated with a nucleophilic base at low temperature and trapped with allyl chloroformate, a similarly isomerically enriched enol carbonate was obtained (Scheme 5). Perhaps the most

[1] This law, which is known to many in Caltech's Chemistry and Chemical Engineering Division, is based on Prof. John E. Bercaw's observation that for a surprisingly large number of reactions, a brief initial optimization often provides results that cannot be surpassed by an exhaustive follow-on optimization effort.

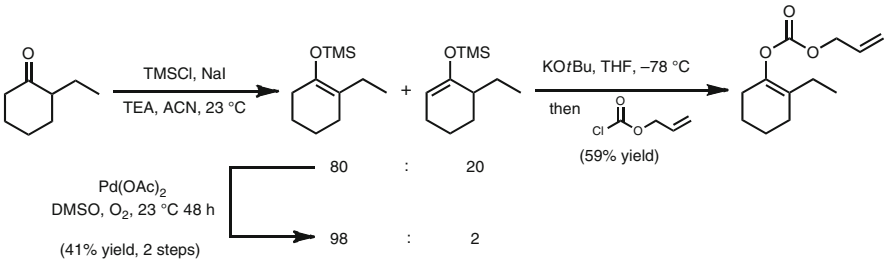

Scheme 5 Synthesis of isomerically pure enol carbonates

important result of trying to obtain isomerically pure allyl enol carbonates was that it gave us access to the corresponding silyl enol ethers.

With a number of silyl enol ethers in hand we considered their use as pronucleophiles in the asymmetric allylic alkylation reaction. We believed that there was significant advantage in their use, namely, that the method would be more widely accepted by the synthetic community if a substrate more familiar than allyl enol carbonates could be used. With regard to catalysis, we reasoned that the alkoxide generated in the initial reaction of diallyl carbonate to form the palladium(II) π-allyl complex **18** might be nucleophilic enough to attack at the silicon atom of the silyl enol ether and generate an enolate. In practice, we found that this small amount of alkoxide was insufficient to promote significant consumption of the silyl enol ether before the reaction was halted by unwanted traces of oxygen or moisture. However, we found that 35 mol% of a dry fluoride source (i.e., TBAT) was able to initiate the reaction. Under the reaction conditions, TBAT cleaves TMS silyl enol ethers almost instantaneously and provides more than sufficient enolate to engage the palladium(II) π-allyl complex. The remaining silyl enol ether is converted to the corresponding enolate by the alkoxide generated from the decomposition of the allyl carbonate. When reactions were performed on a small scale and outside of a glovebox, the use of significantly less than 35 mol% of TBAT often caused reactions to stall before complete conversion of the silyl enol ether was observed.

We were able to envision a reasonable catalytic cycle for the use of silyl enol ethers in the asymmetric alkylation reaction, but there were several complications that could potentially lead to lower enantioinduction in the silyl enol ether reactions (Scheme 6). The generation of the enolate independent of the palladium(II) π-allyl complex and the presence of a tetrabutylammonium counter ion could shift the mechanism of the reaction. We had very little proof at the time, but our working hypothesis was that the C–C bond-forming step occurred in the inner sphere of the palladium atom. We considered the possibility that the conditions used in the silyl enol ether reactions might facilitate an outer sphere pathway resulting in lower ee products. In the event, we found that the ketone products generated from silyl enol ethers did not significantly differ in ee from the equivalent products of allyl enol carbonate reactions (e.g., Table 8 vs. Table 2).

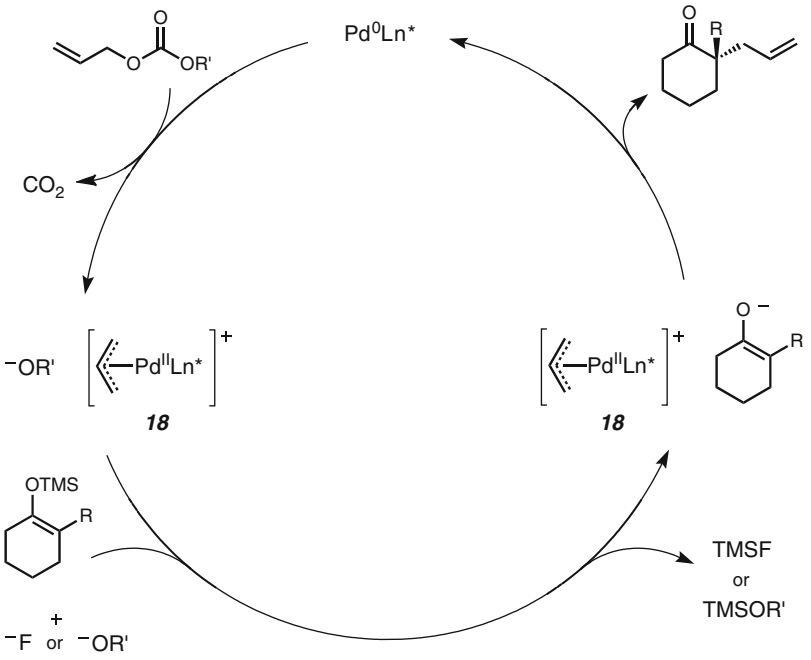

Scheme 6 General catalytic cycle for silyl enol ether alkylation

With two substrate classes in hand and a thorough exploration of catalyst systems completed, we believed the project was mature enough for publication. Gratifyingly, the manuscript was accepted for publication in the *Journal of the American Chemical Society* [24]. It marked a significant milestone in the project, and we were relieved to have it accepted because it was clear that project would expand in numerous directions and become a significant part of the group's research.

6 New Directions for the Asymmetric Reaction

The period following the publication of the first manuscript was the most enjoyable part of the project for us. It was a joy to have many creative coworkers join the project and take it in unexpected directions. It spread much of the burden of substrate and ligand synthesis and of course allowed the group to explore ideas much faster than a single person working on the project could.

First to join the project was a first year graduate student, Justin T. Mohr (a.k.a. JT). His initial aim was to use the reaction as the source of asymmetry in a natural product synthesis. His retrosynthesis required an α–β unsaturated substrate. When DCB had previously made an α–β unsaturated substrate, we found that our methods

Table 8 Silyl enol ether substrates in asymmetric allylic alkylation

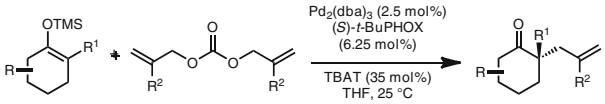

Entry	Product[a]		% Yield[b]	% ee[c]	Entry	Product[a]		% Yield[b]	% ee[c]
1	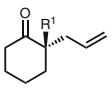	$R^1 = CH_3$	95	87					
2		$R^1 = CH_2CH_3$	96	92	6	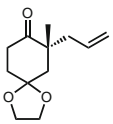		99	81
3		$R^1 = OBn$	83	59					
4[d]	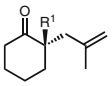	$R^1 = CH_3$	79	91	7	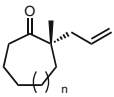	$n = 1$	94	86
5[d]		R^1 = allyl	82	91	8		$n = 2$	96	79

[a]Reactions were performed using 1.0 mmol of substrate in THF (0.033 M in substrate) at 25°C with 2.5 mol% $Pd_2(dba)_3$, 6.25 mol% (*S*)-*t*-BuPHOX (**11**), diallyl carbonate (1.05 equiv), and TBAT (35 mol%) unless otherwise noted. Each reaction was complete in 2–5 h
[b]Isolated yields
[c]Measured by chiral GC or HPLC
[d]Reaction performed with dimethallyl carbonate (1.05 equiv.)

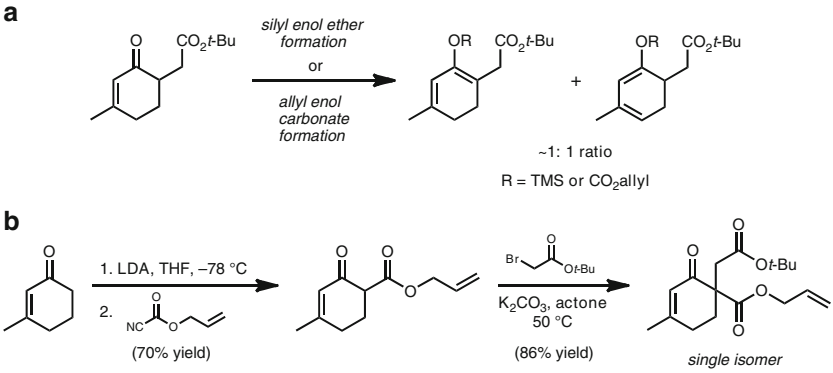

Scheme 7 Selective alkylation of an α–β unsaturated substrate

to make either the enol carbonate or the silyl enol ether resulted in a mixture of products from both α and γ deprotonation. JT found his substrate generated a similar mixture of products (Scheme 7a), but rather than just separating the compounds (and therefore wasting about half of his material, as we had previously done), he decided to fix the problem. Examining this problem of position-selective ketone deprotonation and alkylation, he chose to examine allyl β-ketoesters as substrates. We were confident this classic solution (i.e., the acetoacetic ester synthesis) to selective ketone alkylation would solve the problem of γ deprotonation

(Scheme 7b), but we had stayed away from allyl β-ketoesters as a substrate class because the use of chiral racemic substrates could complicate asymmetric catalysis.

In the 1980s Prof. Tsuji demonstrated that allyl β-ketoesters were good substrates when an achiral catalyst was used [17], but it was unclear that a chiral racemic substrate would interact with a chiral catalyst to give a single product in high ee. A priori, the catalyst could have caused a kinetic resolution of the starting material or had diastereomeric transition states with the two enantiomers of the starting material that provided different levels of enantioselectivity. To his credit, JT was not dissuaded from trying the asymmetric alkylation experiment and found that none of our fears were realized. The asymmetric reaction converted all of the starting material to product without significant kinetic resolution and gave selectivities and yields equivalent to reactions of enol carbonates and silyl enol ethers. This was an important advance for the project. The β-ketoesters substrates are generally easier to make and scale up, more stable, more familiar to synthetic chemists, and can be made in a divergent manner from an advanced intermediate.

As a result of the many advantages of the allyl β-ketoesters, we were able to quickly prepare a large number of substrates and demonstrate that the reaction gave yields and enantioselectivities equivalent to the other classes of substrates (Table 9). Additionally, we were able to access a number of products that we had not been able to access previously, such as enantioenriched tertiary fluorides, vinylogous esters and thioesters, nitrogen heterocycles, and compounds containing multiple quaternary stereocenters. These advances comprised the bulk of our second paper in the field [25].

As the scope of the project began to grow, it became increasingly clear that little more would be gained from further optimization of the current system and that further advances (i.e., reactions generating products with higher ee or new modes of reactivity) would likely require a more precise mechanistic understanding. We were fortunate that Nathaniel Sherden (a.k.a. Nat), who had an undergraduate background in organometallic chemistry, joined the project as a new graduate student. Nat fearlessly took on the challenge of working as an inorganic chemist in an organic group. His most recognized contribution to the project was the identification of the catalyst resting state. The characterization of thermally unstable and previously unknown η^1-allyl Pd(II) carboxylate complexes not only confirmed such a species as the resting state in the reactions of allyl β-ketoesters but also provided strong circumstantial evidence for an inner sphere allylation mechanism (Fig. 1) [26]. It was also an impressive experimental feat. Several batches of crystals, which took months to grow, thermally decomposed before they could be mounted in the diffractometer. These “pop rocks” effervesce and shatter when allowed to sit at temperatures greater than 0°C.

In order to isolate the Pd(II) carboxylate crystals, Nat had to design and synthesize a new Pd(0) source with hydrophobic dibenzylidene ligands that were not prone to cocrystallization and that could be washed away from the Pd (II) complex with hexanes. More generally, Nat’s intellectual curiosity led us to consider many mechanistic possibilities and reaction conditions that would otherwise not have been considered. Sandy Ma and Smaranda Marinescu

Table 9 Allyl β-ketoester substrates in the asymmetric allylic alkylation reaction[a]

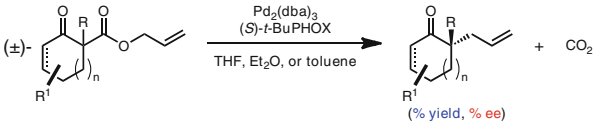

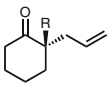	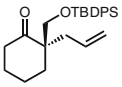	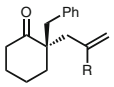	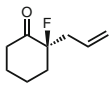
(R = CH_3 85, 88) (R = prenyl 97, 91) (R = $CH_2CH_2CO_2Et$ 96, 90)	(86, 81)	(R = H 99, 85) (R = Ph 96, 94)	(80, 91)
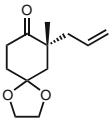	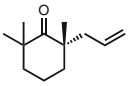	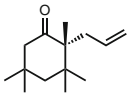	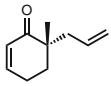
(94, 85)	(89, 90)	(90, 85)	(77, 90)
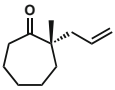	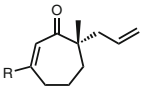	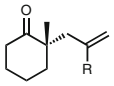	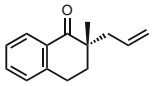
(83, 87)	(R = H 98, 90) (R = O*i*-Bu 92, 85) (R = SPh 86, 89)	(R = CH_3 87, 92) (R = Cl 87, 91)	(97, 92)
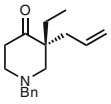	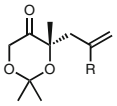	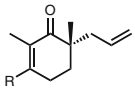	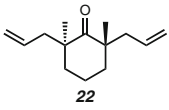
(91, 92)	(R = H 68, 83) (R = Cl 97, 91)	(R = O*i*-Bu 86, 75) (R = SPh 85, 92)	(76, 92)

[a]Yields are reported for 0.5 mmol scale reactions. Enantiomeric excess determined by chiral HPLC or GC

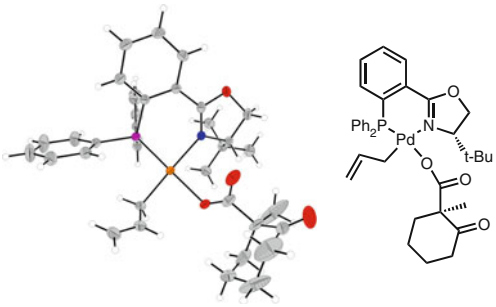

Fig. 1 ORTEP and line drawing views of a rare η^1-allyl Pd(II) carboxylate complex

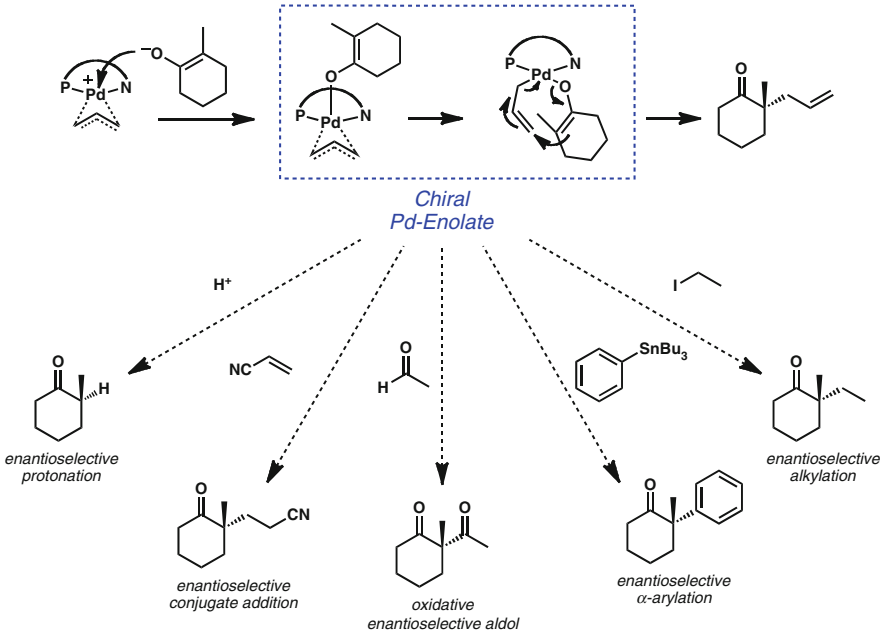

Scheme 8 Catalytic asymmetric enolate transformations

contributed important kinetic data that supported mechanisms involving a single metal center.

The other major influence in our mechanistic thinking was our collaboration with Prof. William Goddard's group and specifically John Keith. Their computational work lends strong support to our initial hypothesis that the reaction proceeds via an inner sphere pathway [27]. Their DFT studies found a low-energy pathway involving an apically coordinated enolate slipping into the square plane of the metal ligand field and undergoing an interesting seven-membered reductive elimination transition state (an intuitive prediction made by us using plastic models years before the DFT results). The collaboration was quite fruitful for both sides. They gave us ideas for several ligands to synthesize, and they became interested in applying the seven-membered reductive elimination transition state in the context of allyl–allyl fragment couplings.

Looking across the three substrate classes (i.e., enol carbonates, silyl enol ethers, and β-ketoesters), we were impressed with the consistency of the enantioselectivity observed in the allylic alkylation reactions. Our working hypothesis for this phenomenon was that all three methods likely converged to a common enolate·Pd(II) π-allyl complex before the enantiodetermining step of the reaction. This idea further led us to wonder if the common enolate·Pd(II) allyl complex could serve as a catalytically generated intermediate in other asymmetric enolate chemistry. Along this line, we envisioned a number of enolate transformations involving a range of electrophiles (Scheme 8).

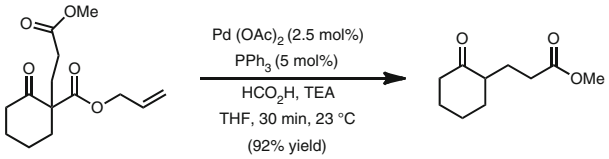

Scheme 9 Catalytic decarboxylation of allyl β-ketoesters

Asymmetric protonation was the first reaction of our chiral enolate we choose to investigate. This project was largely conceived by JT and carried out with help from Dr. Toyoki Nishimata and later Smaranda Marinescu. DCB's main contributions to this project were the synthesis of substrates and suggestions for reaction conditions early in the process of optimizing enantioselectivity in the reaction. Additionally, DCB provided inspiration to JT in the form of a wager. If JT could obtain 80% ee before leaving for the upcoming winter break, DCB would buy him a plane ticket to Hawaii (Scheme 9).

Again we drew from the pioneering work of Prof. Tsuji, who demonstrated that allyl β-ketoesters, when treated with an achiral palladium catalyst and formic acid (presumably acting as both an acid and a reductant), produce a ketone product in excellent yield [28].

Optimization of the chemical yield and ee of the asymmetric protonation reaction proved more challenging than in the case of the alkylation reaction. Key advances were the removal of triethylamine from the original reaction conditions and the use of molecular sieves as an additive. These changes allowed JT to collect on the wager. After a screen of chiral ligands we again found *t*-BuPHOX to be an optimal ligand. A further increase in ee came from thoroughly flame drying the molecular sieves. This protocol allowed us to access a variety of tertiary stereocenters (Table 10) [29].

Unlike the allylic alkylation reactions, which were performed under very similar reaction conditions, each asymmetric protonation substrate required an empirical optimization of the amounts of formic acid and molecular sieves used in the reaction. The importance of the molecular sieves in attaining high ee was unsatisfying because the heterogeneous nature of the reaction complicated any mechanistic studies of the reaction. A homogenous version of the reaction that achieved similar levels of enantioselectivity was later developed [30].

In addition to protonation, a postdoc in the lab, Jan Streuff, explored the use of our catalytically generated enolate in the context of conjugate additions [31]. While the scope of Michael acceptors reactive enough to be intercepted by our chiral enolate complex was limited, we were able to demonstrate a highly diastereo- and enantioselective synthesis of vicinal quaternary and tertiary stereocenters with a number of allyl β-ketoesters. In particular, the most enantio- and diastereoselective reactions of this type were observed with 4-piperidinone-derived pronucleophiles (Scheme 10).

Table 10 Catalytic enantioselective protonation[a]

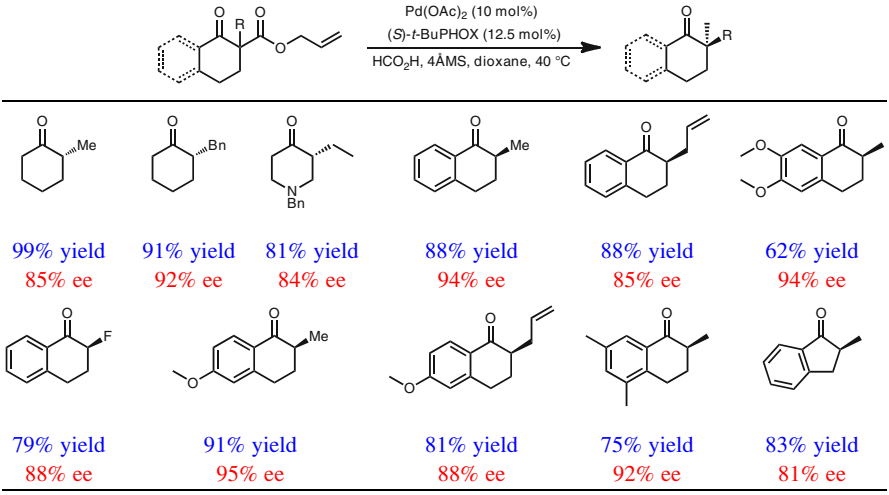

[a]Yields are reported for 0.5 mmol scale reactions. Enantiomeric excess determined by chiral HPLC or GC

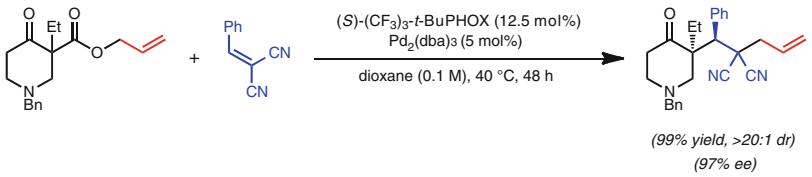

Scheme 10 Catalytic enantioselective Michael addition-allylic alkylation cascade

These methods highlight the promising scope of catalytic enolate generation and the need to develop other catalytic methods for enolate generation that do not use an allyl moiety for initiation. The use of other electrophilic partners in this reaction manifold remains an exciting area of research for the group.

7 Asymmetric Tsuji Alkylation in the Synthesis of Natural Products

As the project has matured, numerous individuals have taken the bold step of carrying out total syntheses that rely on the asymmetric allylic alkylation reaction we developed. By allowing reliable access to enantioenriched quaternary stereocenters, which are difficult to access by other means, the reaction is advantageous in synthetic planning, but in practice it is inherently risky to make a relatively untested synthetic method the cornerstone of one's graduate or postdoctoral studies.

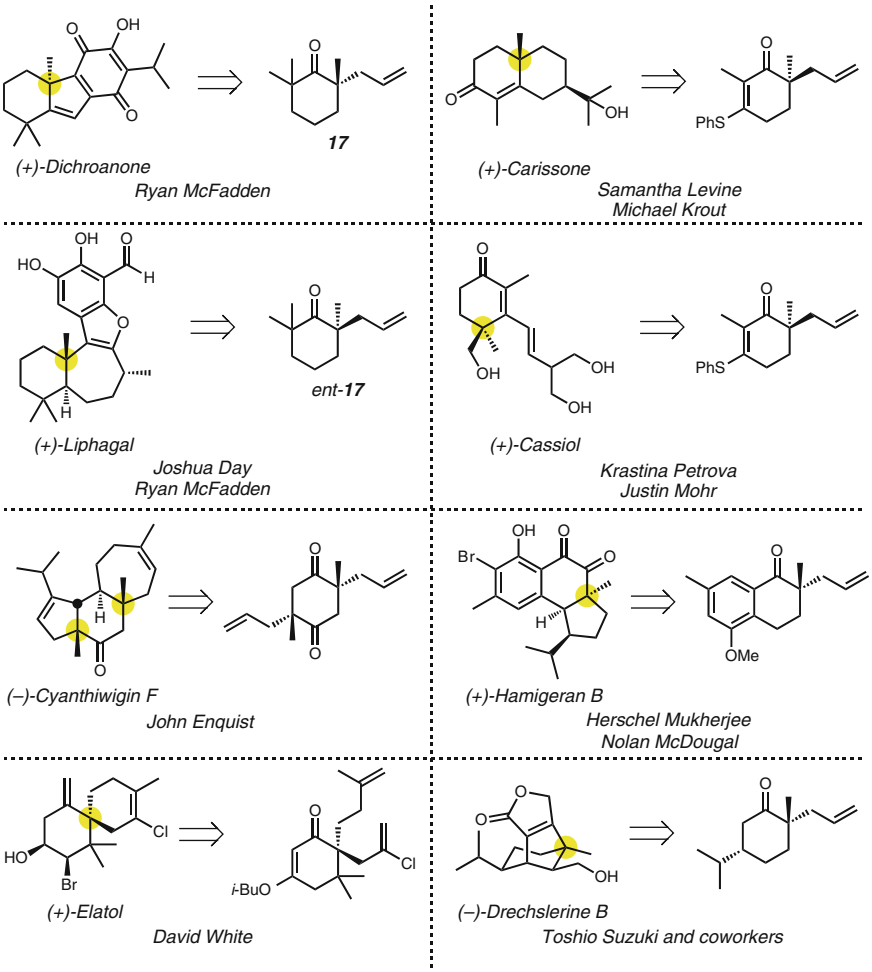

Scheme 11 Natural products synthesized using decarboxylative asymmetric allylic alkylation reactions (with the exception of (−)-drechslerine B, these syntheses were carried out in the Stoltz labs at Caltech)

The utility of a reaction in the synthesis of natural products is often a key measure of a reaction's value. Many more times than not, our method (and the individuals performing the reactions) have proved to be up to the challenge. Watching coworkers find creative ways to apply the reactions we developed has been very gratifying.

In practice, we typically use the asymmetric alkylation reaction early in a synthetic sequence to establish absolute stereochemistry. Strategically, this is beneficial because the quaternary stereocenters that are established are often one of the more challenging features of the target molecule; thus, we achieve a major goal early on, but this strategy also makes it all the more critical that the allylic

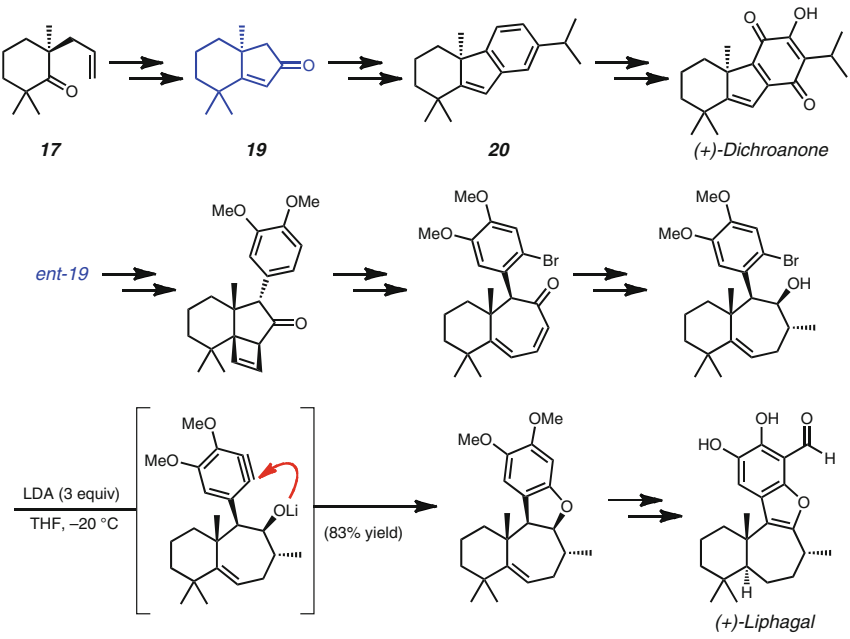

Scheme 12 Synthesis of (+)-dichroanone and (+)-liphagal

alkylation reaction be reliable and scalable. Scheme 11 shows the natural products that have been synthesized using the decarboxylative asymmetric allylic alkylation reaction to date, the individuals primarily responsible for the work, and the α-quaternary ketone that serves as a key intermediate. The structural diversity evident in these natural products (i.e., polycyclic, spirocyclic, and bridged molecules) is a testament to the creativity of the chemists who designed and carried out the syntheses.

Several of the syntheses are of particular note (for descriptions of the syntheses not discussed in detail in text, see [32–35]). Ryan McFadden's synthesis of (+)-dichroanone was the first project in our laboratories to use an enantioenriched α-quaternary ketone product (compound **17**) derived from our method (Scheme 12) [36]. A Wacker–aldol sequence provided enone **19**, which served as the point of divergence for the (+)-liphagal synthesis. Further annulation to arene **20** and an elegant functionalization of the arene nucleus provided (+)-dichroanone. While initial work toward liphagal including the photochemical [2+2] was performed by Ryan, Josh Day was the driving force for the completion of the synthesis [37]. He overcame challenging issues of diastereoselective methylation and hydrogenation and pioneered the late stage use of benzyne chemistry, another focus of research in the lab, to make a critical bond.

The synthesis of (+)-elatol was a collaborative effort between the Stoltz and Grubbs labs at Caltech, specifically David White, who spearheaded the project, and

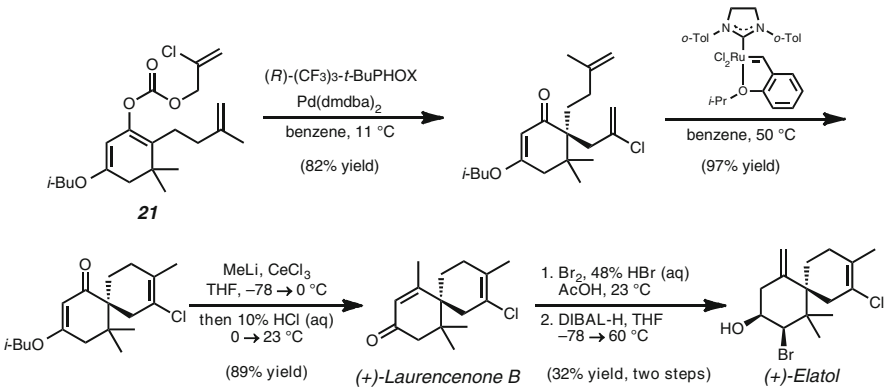

Scheme 13 Synthesis of (+)-elatol

Ian Stewart, a member of the Grubbs laboratory who aided with the key metathesis step [38, 39]. The synthesis highlights the robust nature of the two key steps of the synthesis, asymmetric allylic alkylation and olefin metathesis. The substrate for the asymmetric alkylation reaction is among the most demanding examples investigated. Enol carbonate **21** combines the unusual electronics of a vinylogous ester substrate, the steric hindrance of vicinal geminal dimethyl substitution, a pendant olefin, and a substituted allyl fragment (Scheme 13). Under standard conditions for the allylic alkylation [i.e., (*S*)-*t*-BuPHOX], low yields of the desired ketone were observed. However, reactivity in the alkylation step could be restored by using the more electrophilic PHOX ligand (*R*)-**14**. Ring closing metathesis of the resulting α–ω diene using a highly active catalyst provided the desired tetrasubstituted olefin. After an additional three steps, the synthesis of (+)-elatol was completed in nine steps and 11% overall yield.

The cyanthiwigin natural products are a family of tricyclic molecules featuring two quaternary stereocenters arrayed in a 1,4 relationship on a six-membered ring. A goal of our synthetic plan was to establish both quaternary stereocenters in a single operation. Andy Harned provided a significant precedent when he synthesized C_2-symmetric ketone **22** (Table 9) and demonstrated that two quaternary stereocenters arrayed in a 2,6 relationship could be generated in a single catalytic transformation. John Enquist Jr., who single-handedly completed the project, found that bis(β-ketoester) **23** as a 1:1 mixture of diastereomers, which can be readily assembled from diallyl succinate, undergoes double asymmetric alkylation to give diketone **24** in 99% ee and 4.4:1 dr [40, 41]. The extremely high level of enantiomeric excess observed in the transformation is an example of the Horeau principle at work [42–44], an effect whereby a molecule that would normally be an undesired enantiomer tends to be converted to a diastereomeric product by a second reaction on the same molecule. The formation of the remaining two rings was accomplished in a few elegant steps by means of a metathesis reaction and a radical-based transformation. The resulting tricyclic compound **25** underwent selective enol triflate formation and a

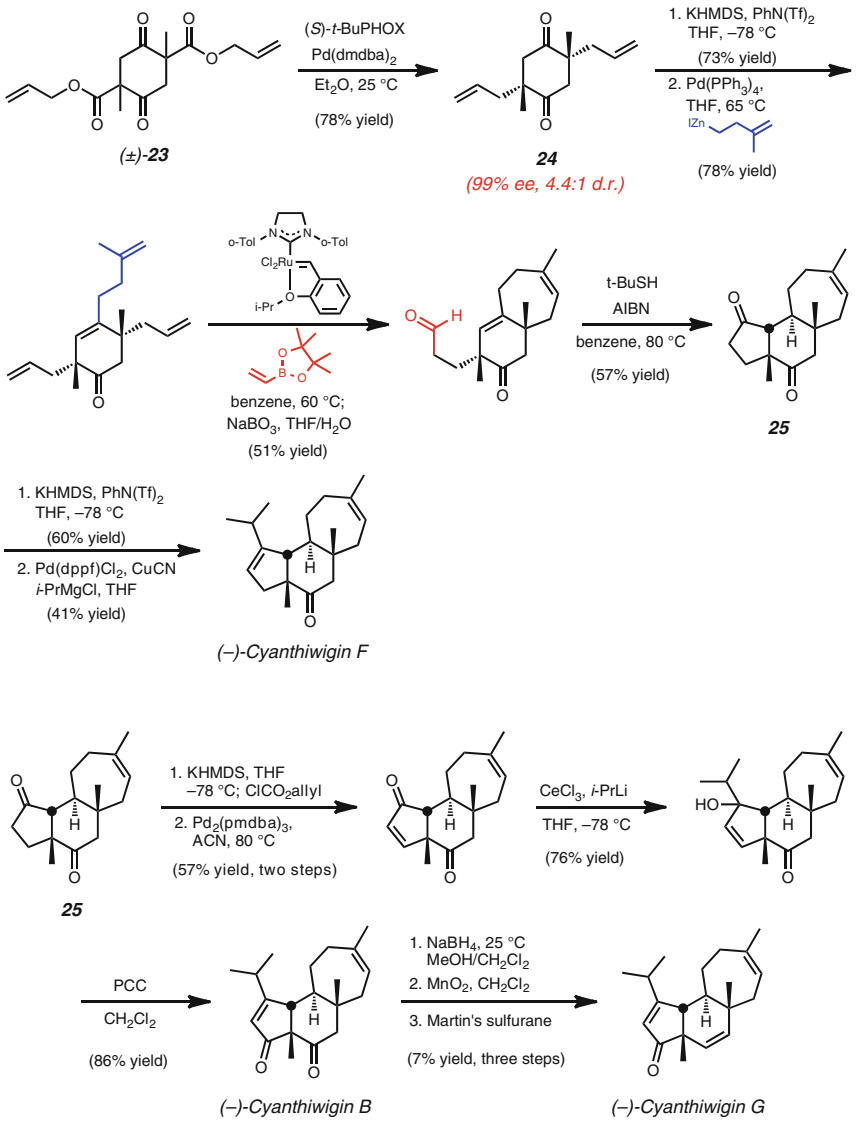

Scheme 14 Synthesis of cyanthiwigins F, G, and B

palladium-catalyzed coupling to afford cyanthiwigin F. Tricycle **25** also served as the branch point for the synthesis of cyanthiwigins B and G. The synthesis of cyanthiwigin F in only nine steps and without the use of protecting groups highlights the utility and efficiency of double enantioselective transformations in the context of stereochemically complex targets (Schemes 14 and 15).

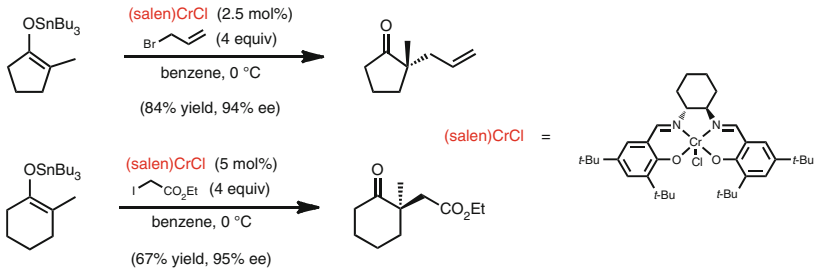

Scheme 15 Asymmetric alkylation of tin enolates

8 Recent Advances and Future Directions in Asymmetric Allylic Alkylation

A comprehensive review of asymmetric allylic alkylation since our initial publication would be beyond the scope of this account. Instead, we will highlight the use of prochiral nucleophiles in asymmetric allylic alkylation reactions. Unlike the majority of asymmetric allylic alkylation reactions, reactions involving prochiral nucleophiles generate a stereocenter on the nucleophile. Major advances have occurred with regard to the classes of prochiral nucleophiles that can be used in these reactions.

Shortly after our initial report, Doyle and Jacobsen disclosed the use of prochiral tin enolates in a salen–chromium complex-catalyzed asymmetric alkylation reaction [45, 46]. It is noteworthy that this reaction was the first example of an asymmetric metal-catalyzed α-alkylation of ketone enolates that utilizes a variety of alkyl halides and is not limited to allylic electrophiles. While this mechanistically interesting reaction does not proceed via a metal π-allyl complex, it is a rare example of a catalytic reaction that provides access to enantioenriched α-quaternary ketones.

Our initial work focused on the use of ketone enolate precursors, especially those derived from cyclic ketones with similarly acidic protons at multiple positions. Previous to our work, Trost et al. focused on the use of in situ generated ketone enolates derived from ketones with a single acidic site or a large difference in acidity between sites and transitioned to stable enolate precursors [47–50]. After our first publication, Trost reported a similar variant of Tsuji's enol carbonate alkylation using ligand **26** [51]. Since then, both groups have targeted the synthesis of quaternary stereocenters and used cyclic systems to simplify issues of enolate geometry. More recently, Trost et al. found that acyclic enol carbonates of defined geometry undergo decarboxylative allylic alkylation to provide ketones with α-tertiary stereocenters. The use of trisubstituted enol carbonates simplifies the synthesis of a specific olefin geometry in the substrate but raises challenges of enolate scrambling and over alkylation of the product. Trost et al. found that reactions catalyzed by a Pd(0) source and anthracene-derived ligand **26** provided

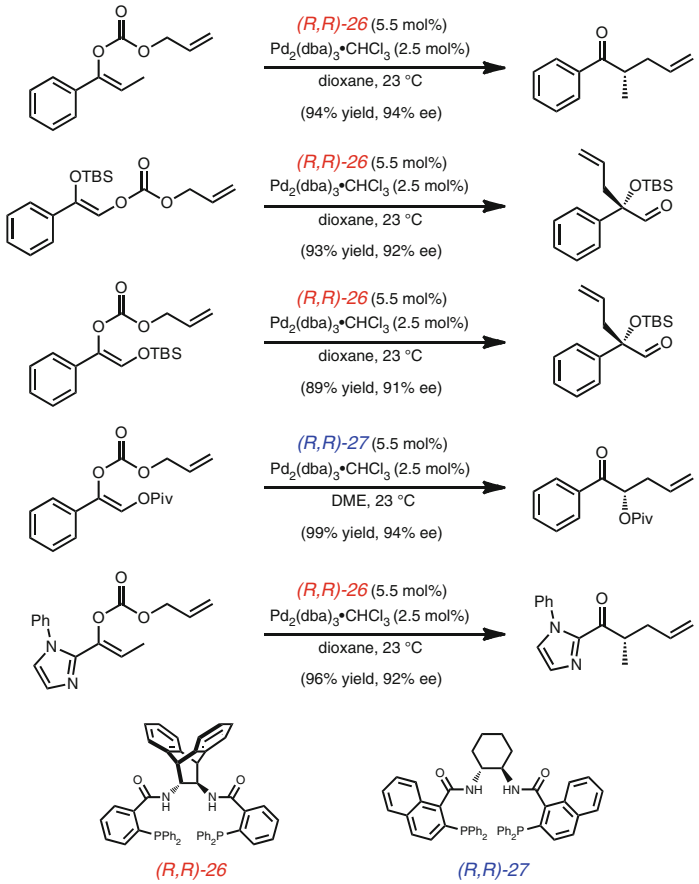

Scheme 16 Enol carbonates derived from acyclic ketones in asymmetric allylic alkylation

both good chemoselectivity for the monoallylated product and excellent enantioselectivity (Scheme 16) [12, 52]. An interesting special class of acyclic enol carbonates produces α-oxygenated ketones [53, 54]. By judicious choice of oxygen protecting group and catalyst system, Trost et al. found that they could alter the relative rates of protecting group migration and allylic alkylation to favor the production of either ketones with secondary oxygenated stereocenters or aldehydes with tertiary oxygenated stereocenters. In another extension of the acyclic methodology, they found that acylimidazole-derived enol carbonates were good substrates for asymmetric allylic alkylation [55]. These products are easily converted to ester derivatives, and thus the acylimidazole-derived enol carbonates can be considered ester enolate equivalents.

Moving away from the use of nucleophilic ketone derivatives, Trost et al. have demonstrated that the conjugate base of 2-substituted pyridine derivatives are

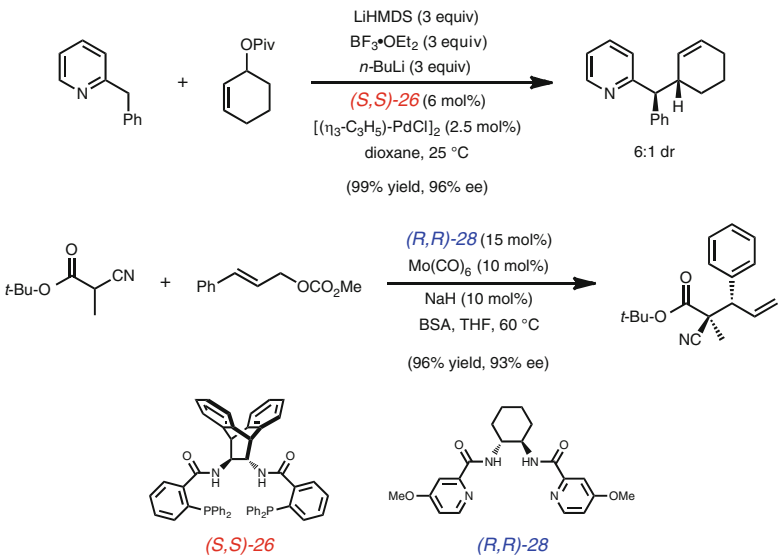

Scheme 17 Non-ketone derived prochiral nucleophiles in asymmetric allylic alkylation

suitable prochiral nucleophiles for asymmetric allylic alkylation in the presence of a Pd(0) source and anthracene-derived ligand **26** (Scheme 17) [56, 57]. This method provides elegant access to challenging doubly benzylic tertiary stereocenters. Very recently, Trost et al. established that malonate-derived cyanoesters can be used as prochiral nucleophiles in asymmetric allylic alkylation reactions to form enantioenriched quaternary stereocenters in the presence of a molybdenum catalyst [58]. This method provides access to a challenging stereochemical motif with excellent positional, diastereo- and enantioselectivity.

Moving away from ketones to other prochiral nucleophiles has also been an important goal in our group. We choose to explore lactam-derived substrates in part because we envisioned that the products formed would be useful intermediates in the synthesis of various alkaloids and because we would be able to modulate the electronics and sterics of the lactam enolate by attaching different groups at nitrogen with the aim of optimizing the enantioselectivity of the allylic alkylation. In the event, we chose to initially test tosyl-protected lactam allyl ester **29** and Boc-protected lactam allyl ester **30** with two Pd·PHOX catalysts in several solvents (Scheme 18).

David White in our lab had tested tosyl lactam **29** several years prior and having determined that the product was of very low ee (less than 5% ee with *t*-BuPHOX in THF) stopped pursuing the substrate class. Our current resolve was buoyed when the Boc-protected derivative produced α-quaternary lactam **32** with significant ee (74% ee). We were also encouraged by the high degree of variability in ee across different solvents and catalysts. These results supported our hypothesis that the nitrogen protecting group would allow us to modulate the properties of the latent

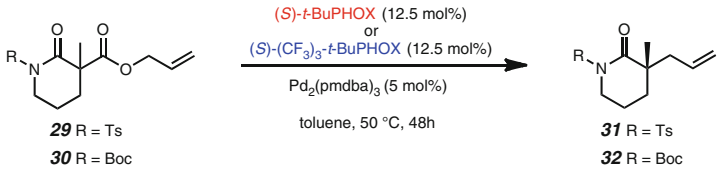

	31		32	
	THF	toluene	THF	toluene
(*S*)-*t*-BuPHOX	4% ee	7% ee	57% ee	74% ee
(*S*)-(CF$_3$)$_3$-*t*-BuPHOX	35% ee	37% ee	70% ee	73% ee

Scheme 18 Initial studies of *N*-protected lactams in asymmetric allylic alkylation

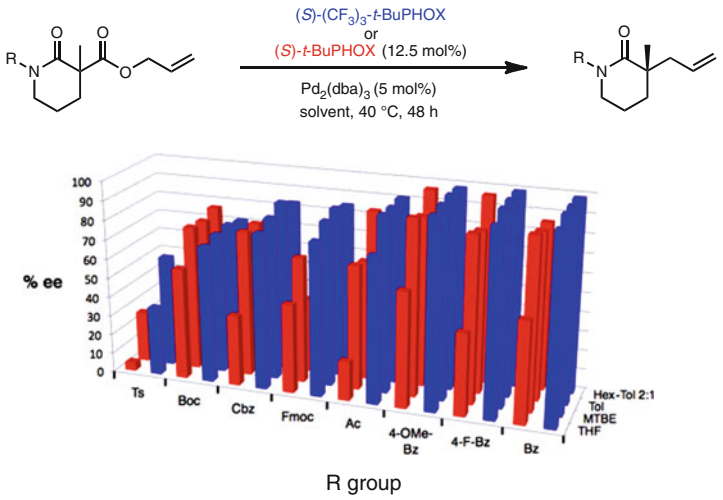

Scheme 19 Screening of reaction conditions in the asymmetric allylic alkylation of lactam allyl esters

amide enolate. A visiting student, Taiga Yurino, synthesized and screened a variety of *N*-protected substrates and discovered that benzoyl type protecting groups provide consistently superior enantioselectivity (greater than 99% ee, Scheme 19). Gratifyingly, Yiyang Liu and DCB were able to demonstrate that the extremely high level of enantioselectivity was general across a range of benzoyl-protected piperidinones and pyrrolidinones (Table 11) [59]. Studies aimed at understanding the origin of the superior enantioselectivity observed with these lactam nucleophiles and the application of the enantioenriched α-quaternary lactams products to alkaloid synthesis are ongoing.

Table 11 Asymmetric allylic alkylation of lactam allyl esters[a]

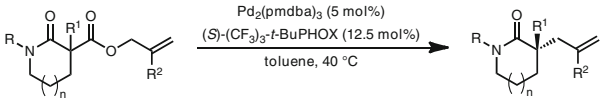

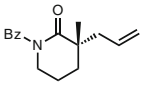	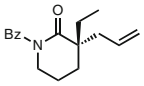	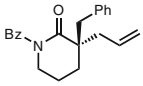	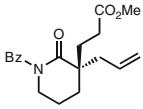	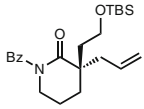
85% yield 99% ee	97% yield 99% ee	85% yield 99% ee	92% yield 99% ee	85% yield 96% ee
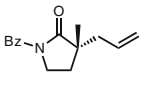	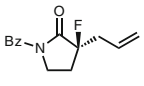	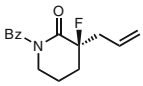	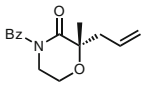	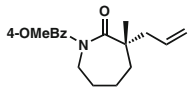
90% yield 98% ee	86% yield 98% ee	89% yield 99% ee	91% yield 99% ee	83% yield 93% ee

[a]Isolated yields are reported for 0.5 mmol scale reactions. Enantiomeric excess determined by chiral HPLC or GC

9 Conclusion and Outlook

Our work in asymmetric decarboxylative allylic alkylation was inspired by the need to construct a challenging quaternary stereocenter within our efforts toward the synthesis of zoanthenol. The methods developed as a result of that initial inquiry have had impact on projects far removed from the initial target. Moreover, the challenges provided by the structures of other natural products have continued to drive the evolution of these methods (e.g., cyanthiwigins – the generation of multiple stereocenters in a single transformation and elatol – the design of more reactive catalyst systems). The other major source of innovation for this project was mechanistic analysis. Our mechanistic thinking was informed by both experimental and computational evidence.

While some aspects of this methodology are likely mature, many areas await further advances. Useful levels of enantioselectivity in the allylic alkylation of cyclic ketone enolate precursors were achieved early in the project, but further work to define a catalyst that routinely provides enantiomeric excesses greater than 95% would be valuable. Additionally, there are still many substrate classes, which should not be considered solved problems, including acyclic substrates, esters, and substrates providing tertiary stereocenters. Other classes of prochiral nucleophiles have yet to be explored. More generally, the ability to catalytically generate an enolate in a chiral environment and react that enolate with a wide range of electrophiles will open up many avenues of research. Broadening our catalyst system for asymmetric *allylic* alkylation into one capable of general asymmetric

alkylation is an ongoing area of research. In order to achieve this goal, new enolate precursors may need to be invented that do not rely on activation of allyl fragments for their release. Asymmetric allylic alkylation has been an active area of research for years and will continue to inspire the invention of new reactions for years to come.

References

1. Smidt J, Hafner W, Jira R, Sieber R, Sedlmeier J, Sabel A (1962) Angew Chem Int Ed 74:93–102
2. Tsuji J, Takahashi H, Morikawa M (1965) Tetrahedron Lett 6:4387–4388
3. Trost BM, Fullerton TJ (1973) J Am Chem Soc 95:292–294
4. Trost BM, Strege PE (1977) J Am Chem Soc 99:1649–1651
5. Trost BM, Lee C (2000) In: Ojima I (ed) Catalytic asymmetric synthesis, 2nd edn. Wiley-VCH, New York, pp 593–649
6. Pfaltz A, Lautens M (1999) In: Jacobsen EN, Pfaltz A, Yamamoto H (eds) Comprehensive asymmetric catalysis, vol 2. Springer, New York, pp 833–884
7. Helmchen GJ (1999) Organomet Chem 576:203–214
8. Trost BM (2002) Chem Pharm Bull 50:1–14
9. Trost BM, Van Vranken DL (1996) Chem Rev 96:395–422
10. Trost BM (1996) Acc Chem Res 29:355–364
11. Behenna DC, Mohr JT, Sherden NH, Marinescu SC, Harned AM, Tani K, Seto M, Ma S, Novák Z, Krout MR, McFadden RM, Roizen JL, Enquist JA, White DE, Levine SR, Petrova KV, Iwashita A, Virgil SC, Stoltz BM (2011) Chem Eur J 17:14199–14223
12. Trost BM, Xu J, Schmidt T (2009) J Am Chem Soc 131:18343–18357
13. Mohr JT, Stoltz BM (2007) Chem Asian J 2:1476–1491
14. Roa CB, Anjaneyula ASR, Sarma NS, Venkatateswarlu Y, Rosser RM, Faulkner DJ, Chen MHM, Clardy J (1984) J Am Chem Soc 106:7983–7984
15. Behenna DC, Stockdill JL, Stoltz BM (2008) Angew Chem Int Ed 47:2365–2386
16. Tsuji J, Minami I, Shimizu I (1983) Tetrahedron Lett 24:1793–1796
17. Shimizu I, Yamada T, Tsuji J (1980) Tetrahedron Lett 21:3199–3202
18. Tsuji J, Minami I, Shimizu I (1983) Tetrahedron Lett 24:4713–4714
19. Tsuji J, Minami I, Shimizu I (1983) Chem Lett 1325–1326
20. Helmchen G, Pfaltz A (2000) Acc Chem Res 33:336–345
21. Williams JMJ (1996) Synlett 705–710, and references therein
22. Peer M, de Jong JC, Kiefer M, Langer T, Rieck H, Schell H, Sennhenn P, Sprinz J, Steinhagen H, Wiese B, Helmchen G (1996) Tetrahedron 52:7547–7583
23. Tani K, Behenna DC, McFadden RM, Stoltz BM (2007) Org Lett 9:2529–2531
24. Behenna DC, Stoltz BM (2004) J Am Chem Soc 126:15044–15045
25. Mohr JT, Behenna DC, Harned AM, Stoltz BM (2005) Angew Chem Int Ed 44:6924–6927
26. Sherden NH, Behenna DC, Virgil SC, Stoltz BM (2009) Angew Chem Int Ed 48:6840–6843
27. Keith JA, Behenna DC, Mohr JT, Ma S, Marinescu SC, Oxgaard J, Stoltz BM, Goddard WA (2007) J Am Chem Soc 129:11876–11877
28. Tsuji J, Nisar M, Shimizu I (1985) J Org Chem 50:3416–3417
29. Mohr JT, Nishimata T, Behenna DC, Stoltz BM (2006) J Am Chem Soc 128:11348–11349
30. Marinescu SC, Nishimata T, Mohr JT, Stoltz BM (2008) Org Lett 10:1039–1042
31. Streuff J, White DE, Virgil SC, Stoltz BM (2010) Nat Chem 2:192–196
32. Levine SR, Krout MR, Stoltz BM (2009) Org Lett 11:289–292
33. Petrova KV, Mohr JT, Stoltz BM (2009) Org Lett 11:293–295
34. Mukherjee H, McDougal NT, Virgil SC, Stoltz BM (2011) Org Lett 13:825–827

35. Hagiwara H, Fukushima M, Kinugawa K, Matsui T, Hoshi T, Suzuki T (2011) Tetrahedron 67:4061–4068
36. McFadden RM, Stoltz BM (2006) J Am Chem Soc 128:7738–7739
37. Day JJ, McFadden RM, Virgil SC, Kolding H, Alleva JL, Stoltz BM (2011) Angew Chem Int Ed 50:6814–6818
38. White DE, Stewart IC, Grubbs RH, Stoltz BM (2008) J Am Chem Soc 130:810–811
39. White DE, Stewart IC, Seashore-Ludlow BA, Grubbs RH, Stoltz BM (2010) Tetrahedron 66:4668–4686
40. Enquist JA, Stoltz BM (2008) Nature 453:1228–1231
41. Enquist JA, Virgil SC, Stoltz BM (2011) Chem Eur J 17:9957–9969
42. Vigneron JP, Dhaenens M, Horeau A (1973) Tetrahedron 29:1055–1059
43. Rautenstrauch V (1994) Bull Soc Chim Fr 131:515–524
44. Baba SE, Sartor K, Poulin J, Kagan H (1994) Bull Soc Chim Fr 131:525–533
45. Doyle AG, Jacobsen EN (2005) J Am Chem Soc 127:62–63
46. Doyle AG, Jacobsen EN (2007) Angew Chem Int Ed 46:3701–3705
47. Trost BM, Schroeder GM (1999) J Am Chem Soc 121:6759–6760
48. Trost BM, Schroeder GM, Kristensen J (2002) Angew Chem Int Ed 41:3492–3495
49. Trost BM, Jäkel C, Plietker B (2003) J Am Chem Soc 125:4438–4439
50. Trost BM, Schroeder GM (2005) Chem Eur J 11:174–184
51. Trost BM, Xu J (2005) J Am Chem Soc 127:2846–2847
52. Trost BM, Xu J (2005) J Am Chem Soc 127:17180–17181
53. Trost BM, Xu J, Reichle M (2007) J Am Chem Soc 129:282–283
54. Trost BM, Xu J, Schmidt T (2008) J Am Chem Soc 130:11852–11853
55. Trost BM, Lehr K, Michaelis DJ, Xu J, Buckl AK (2010) J Am Chem Soc 132:8915–8917
56. Trost BM, Thaisrivongs DA (2009) J Am Chem Soc 131:12056–12057
57. Trost BM, Thaisrivongs DA (2008) J Am Chem Soc 130:14092–14093
58. Trost BM, Miller JR, Hoffman CM (2011) J Am Chem Soc 133:8165–8167
59. Behenna DC, Liu Y, Yurino T, Kim J, White DE, Virgil SC, Stoltz BM (2012) Nat Chem 4:130–133

Top Organomet Chem (2013) 44: 315–334
DOI: 10.1007/3418_2012_51

Published online: 17 August 2012

Acid Catalysis in Organic Synthesis

Hisashi Yamamoto

Abstract New reagents and catalysts have unlimited potential for the future of organic synthesis. We have been interested in Lewis and Brønsted acid catalysis for a number of years. In this chapter, I am going to review on several of these acids and related catalysts from the conceptual aspect of their molecular design and engineering.

Keywords Asymmetric synthesis · Brønsted acid · Cascade reaction · Lewis acid · Super silyl

Contents

After I gave a lecture at Nagoya University more than 30 years ago, the late professor Toshio Goto approached me with his gentle smile and told me, “Hisashi, you are trying to give a molecular shape to an atom of a proton!” I realized this was

H. Yamamoto (✉)
Department of Chemistry, The University of Chicago, 5735 South Ellis Avenue, Chicago, IL 60637, USA
e-mail: yamamoto@uchicago.edu

exactly what I had dreamed of for a number of years and was amazed he had clearly understood my thought and had summarized it with a very brief sentence. Thus, this chapter is simply my scientific adventure to give a molecular shape to a simple proton.

1 Bulky Lewis Acid

I was interested in organoaluminum compounds when I began my scientific career at Kyoto University. An aluminum reagent is generally recognized as making a strong bond with oxygen and nitrogen of the molecule, which gives us a numerous opportunities in the development of new synthetic reactions [1, 2]. Among them, biogenetic cationic transformations were of interest to me since aluminum reagent can behave as an excellent trigger to generate cationic intermediates necessary for a biosynthetic pathway, especially in terpene biosynthesis. For these transformations, a phosphate is an excellent leaving group after complexation with an aluminum reagent. If we used the phosphate of nerol, a smooth cyclization took place and the product was a mixture of limone and terpenolene. We wanted to obtain limone as the sole product and after several trials, finally found that the bulky aluminum aryloxide gave us almost exclusive selective cyclization as shown in Scheme 1 [3].

Presence of the large alkyl substituents at the *ortho* positions of phenoxide appears to be highly favorable for the present selectivity because it provides significant frontal steric hindrance for deprotonation step. After complexation, the oxygen of aryloxide is stereochemically blocked by two tert-butyl groups. This finding turned out to be a general phenomenon for Lewis acid-promoted reactions. We reported several new reactions after this observation, and the following two rearrangement reactions of epoxide [4] and oxirane [5] used the same concept for achieving high selectivity as the Lewis acid–Lewis base cooperative systems (Scheme 2).

Although these bulky Lewis acids offered us great opportunities to develop a number of new reactions based on the Lewis acid–Lewis base cooperative effect, an even more interesting observation is that the sterically bulky aluminum phenoxide was found to be pyrophoric when isolated as a crystalline solid in air. Generally, a simple aluminum phenoxide is not reactive at all. This is understandable since most aluminum compounds in solution exist as dimeric, trimetric, or higher oligomer structures. In contrast, methylaluminum bis(2,6-di-tert-butyl-4-methylphenoxide) (MAD) and aluminum tris(2,6-di-tert-butyl-4-methylphenoxide) (ATPH) are monomeric in organic solvent because of their steric bulkiness [6]. This simple finding led us to start investigations on bulky aluminum reagents utilizing their high oxophilic characters. Thus, these reagents, despite their quite sterical bulkiness, are electrically more reactive than their less bulky analogs. For example, Claisen rearrangements proceed remarkably smoothly even at −78°C in the presence of MABR or MAPH (Scheme 3) [7, 8]. Furthermore, depending on the structural difference of the reagent, we are able to control the transition states of these

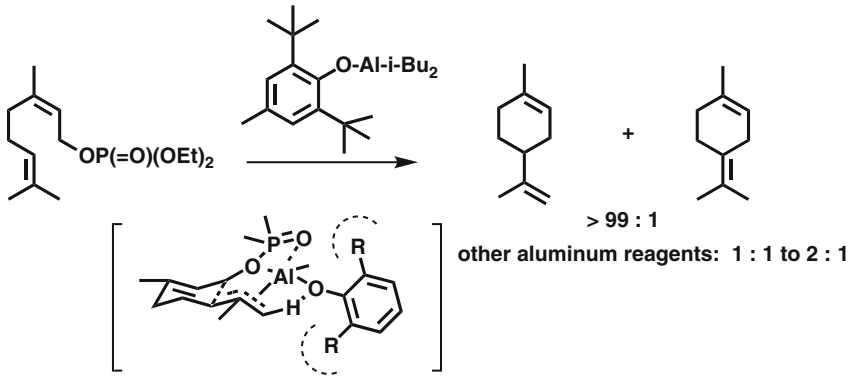

Scheme 1

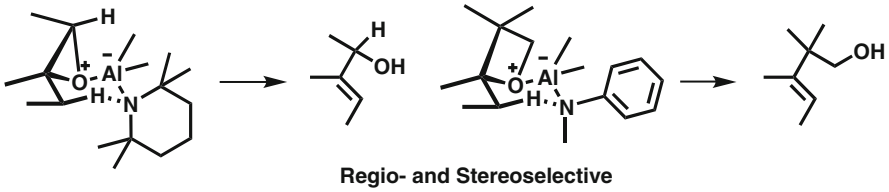

Scheme 2

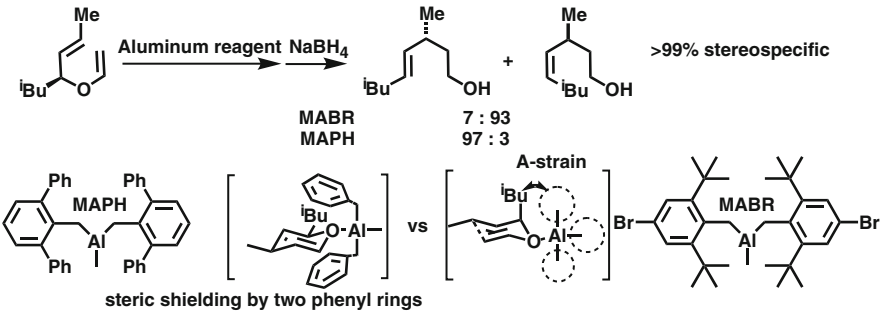

Scheme 3

rearrangements to choose either an E- or Z-selective and stereospecific pathway depends on starting material and the aluminum reagent.

This large frontal steric effect was later used for our almost complete stereo shielding of aromatic carbonyl oxygen from nucleophilic attacks. Thus, aluminum tris(2,6-diphenylphenoxide), ATPH, and aromatic aldehyde form a stable complex from which selective 1,6- addition of aromatic aldehyde was realized using simple alkyllithium nucleophiles [9]. Furthermore, using more reactive acid halides, even simple Grignard reagent attacks at the *para* position of aromatic rings [10].

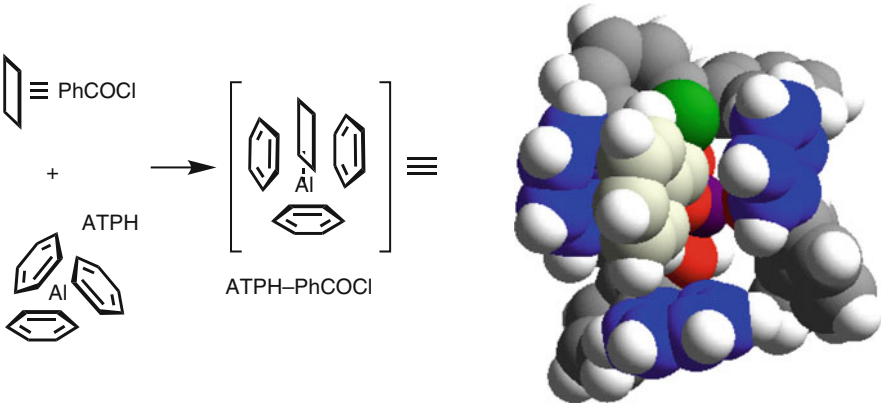

Fig. 1 The induced conformational changes of ATPH for inclusion of PhCOCl

These findings of breaking aromaticity provide a completely new pathway for cyclohexadiene synthesis. The intermediary aromatic carbonyl/ATPH complex based on X-ray crystallographic structures is shown in Fig. 1, displaying the complete stereo-blocking of carbonyl oxygen from the normal carbonyl attack of nucleophiles (Scheme 4).

The extreme bulkiness of these aluminum reagents is able to control the addition reaction of carbonyl compounds by complexation which will or can lead to unexpected stereoselectivity. When MAD was mixed with the carbonyl compound of 4-tert-butylcyclohexanone, a stable 1:1 complex was formed. This complex was treated with methyllithium at low temperature to yield an equatorial alcohol almost exclusively. The observed stereochemical outcome was opposite that of the product from reaction of cyclohexanone with methyllithium. The equatorial selectivity achieved with MAD was found to be almost perfect [11, 12]. Furthermore, if the same reaction conditions are applied to chiral aldehydes, *anti*-Felkin selectivities are observed [12] (Scheme 5).

In coordination with the bulky Lewis acid, the carbonyl group is expected to be partially rehybridized to generate cationic species before the nucleophilic alkylation process. This late transition state of the reaction is very different from the early transition state, which is popular for most of the alkylation of carbonyl compounds. Thus, the stereochemical outcomes of these reactions could be the opposite of what we observed in normal small Lewis acid (Li)/nucleophilic alkylation processes. These observations provide us a critical guideline with which to challenge the carbonyl activation for asymmetric alkylation based on chiral Lewis acid catalysis (Scheme 6).

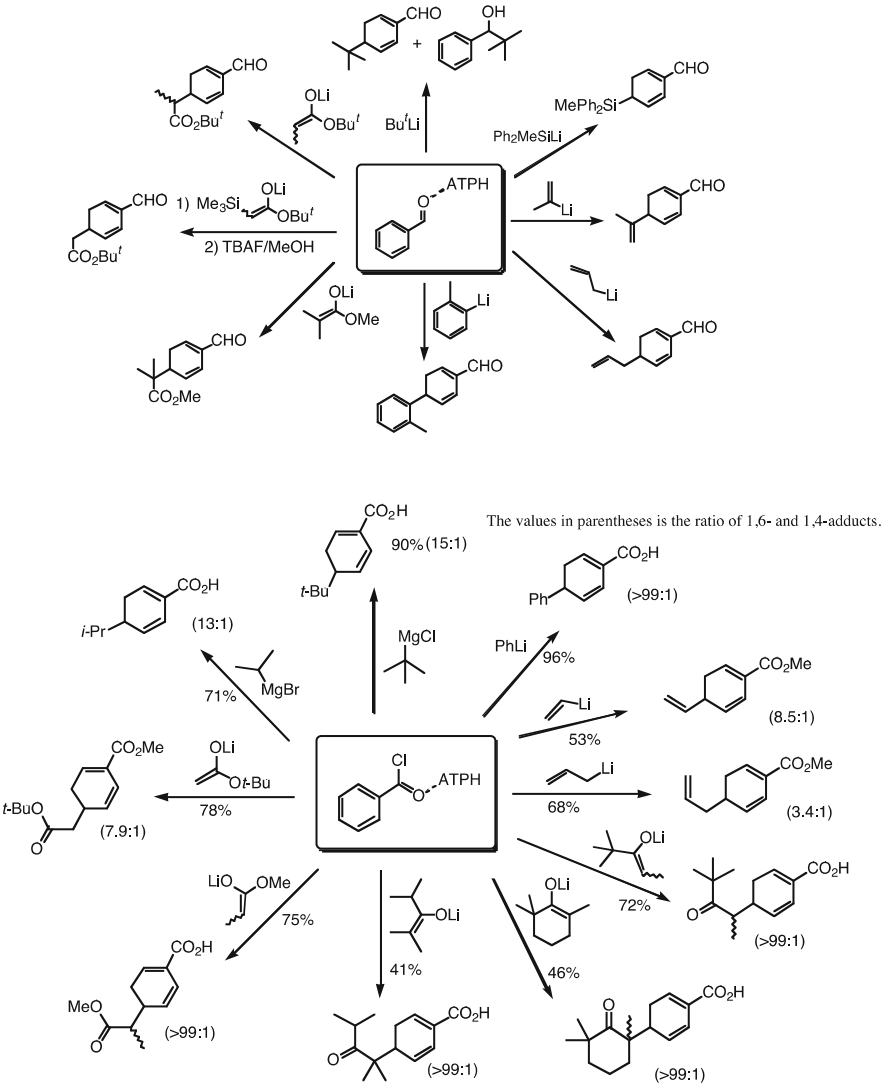

Scheme 4

2 Chiral Lewis Acid Catalysis

In 1988, an ASI workshop on "Selectivities in Lewis acid promoted reactions" was held in Greece, during which I proposed the mechanism of our asymmetric propargylation reaction using chiral allenyl boronic ester [13]. In an enantioface differentiation process, the chiral nucleophile was added to the carbonyl group of aldehydes, thus allowing the preparation of chiral propargylic alcohols [14]. Based

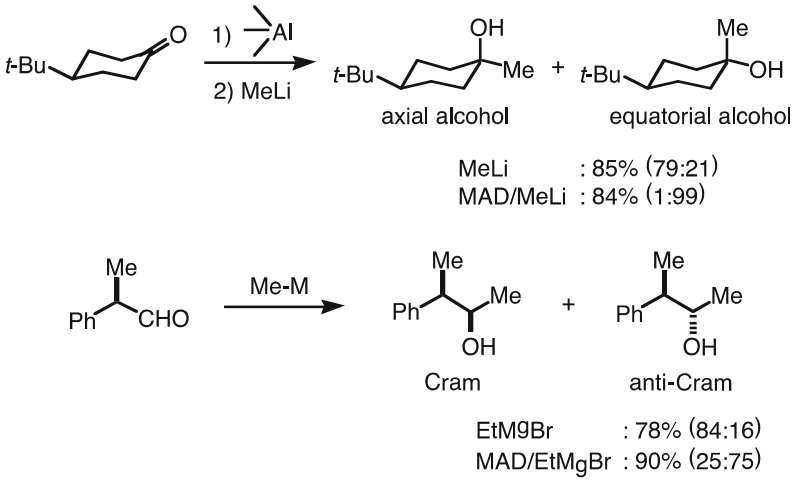

Scheme 5

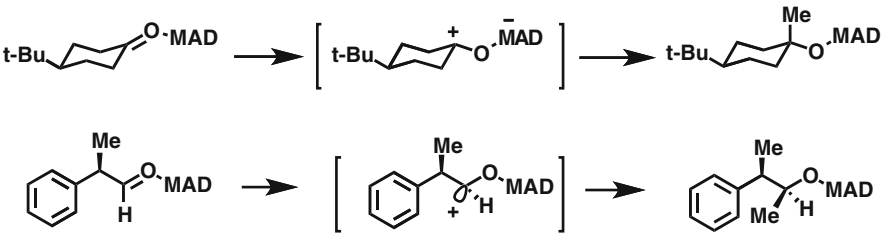

Scheme 6

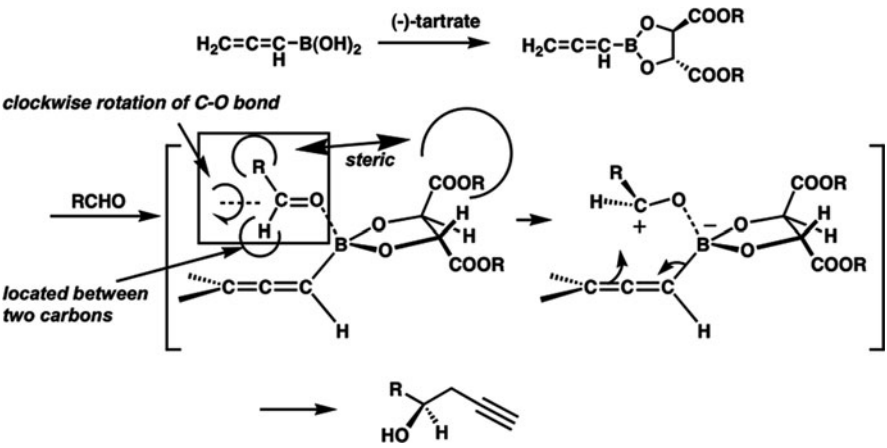

Scheme 7

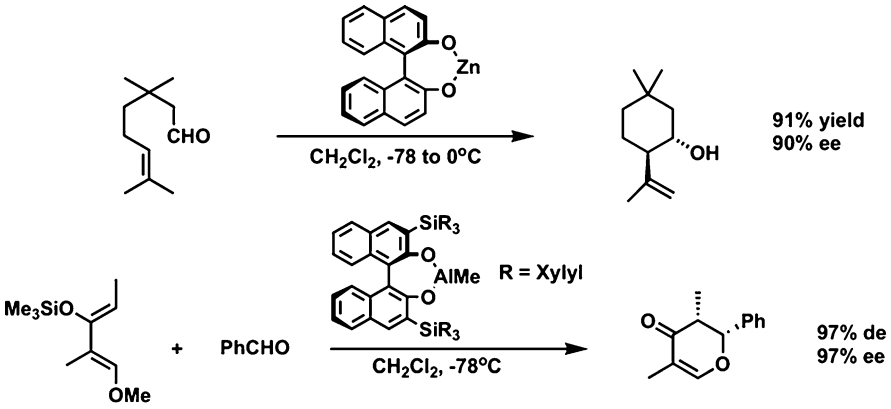

Scheme 8

on the *anti*-coplanar complex structure of carbonyl-boron moieties, we should be able to anticipate the clockwise or counterclockwise rotation of the O–C bond prior to C–C bond formation (Scheme 7). This stereochemical situation may be clear when linear allenyl moiety is attached to the boron atom. In other words, the formyl proton should move either to the back or the front prior to C–C bond formation. It is clear that the direction of the rotation is influenced by the ligand stereochemistry attached to boron metal. Thus, in this particular case, counterclockwise rotation should generate severe steric interaction between R of aldehyde and COOR of the ligand of boron.

The reaction scheme shown above demonstrates that the stereochemistry of the metal ligand does have a significant effect on the direction of the C–O rotation (or rehybridization of the carbonyl group) and thus on the asymmetric induction of the reaction. We therefore initiated new projects to develop a chiral Lewis acid catalyst, which had C-n symmetry elements similar to the tartaric acid ligand of Scheme 7.

For these, several chiral Lewis acid catalysts, which have the C-2 symmetry element, were designed and tested for various asymmetric syntheses, and in 1985 we reported a zinc reagent and in 1988 a bulky aluminum reagent (Scheme 8) [15, 16]. The zinc reagent was used for asymmetric cyclization of unsaturated aldehyde and the aluminum catalyst for asymmetric hetero-Diels–Alder reaction with Danishefsky diene. Both catalysts effectively discriminate the enantioface of aldehydes for reactions.

These reports were the forerunner of a vast amount of present-day research on the binapthol-based asymmetric catalyst. Furthermore, we and other groups have reported various kinds of chiral Lewis acid catalysts which have other C-2-symmetry elements, and all of them have proven quite effective for asymmetric carbon–carbon bond forming processes [17, 18]. Not only the main group of metal catalysts but also transition metal catalysts having the C-2 symmetric structure can be used for asymmetric synthesis via selective activation of carbonyls.

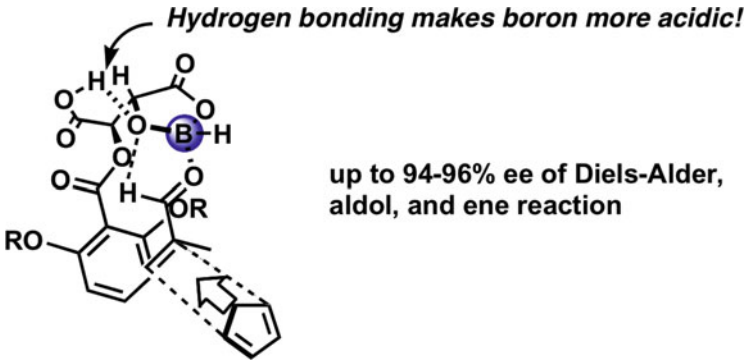

Scheme 9

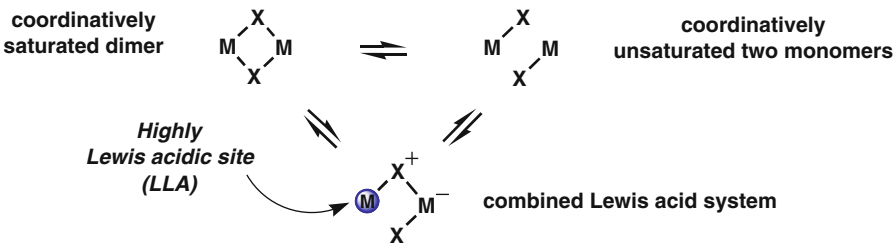

Scheme 10

3 Combined Acid Catalysis

Based on the discussion in the previous section, we screened many C-2 chiral ligands. Among them, we tested various tartaric acid derivatives simply because they are readily availabilities and for their beautiful chiral structures. We reported in 1988 a chiral Lewis acid catalyst of an acyloxyboron with a tartaric acid ligand [19]. This simple catalyst was remarkably effective for aldol, ene, and Diels–Alder reactions in universally high asymmetric inductions. However, the structure of catalyst does not have C-2 symmetry. Interestingly, this catalyst came from as a result of a by-chance discovery. We ordered several tartaric acid derivatives, and one of the compounds purchased from the company was remarkably effective for asymmetric reactions. Surprisingly, however, we found later that the actual structure of the contents of the bottle was a mixture of several derivatives of tartaric acid – most of them differing contents from what was shown on the label! The active component was monoacylated tartaric acid. This unsymmetrical ligand reacts with BH_3 to generate an asymmetric catalyst, which at that time was remarkably reactive and selectively unknown.

After careful investigation of the structure of the catalyst and synthesis of various analogs of the compound, we observed that the high reactivity of the tartaric

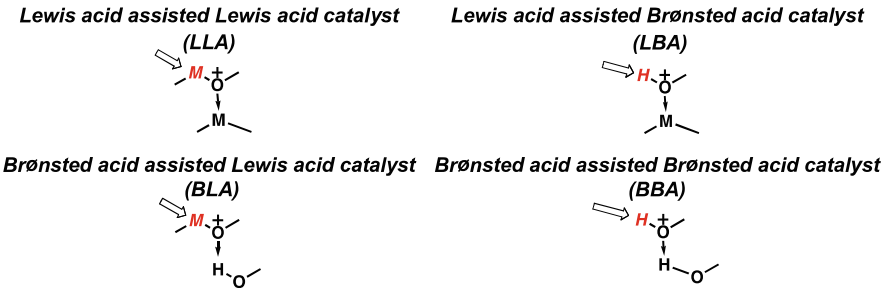

Scheme 11

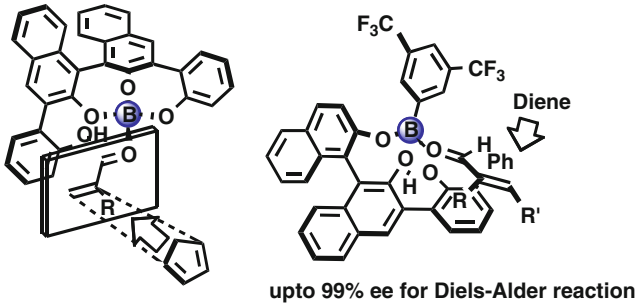

Scheme 12

acid derived catalyst may have originated from intramolecular hydrogen bonding between the terminal carboxylic acid and the alkoxy oxygen attached to boron (Scheme 9).

This was the first unexpected example of the "combined acids system for asymmetric synthesis" (Scheme 10) [20]. It is known that coordinatively unsaturated monomers are far more Lewis acidic than doubly bridged coordinatively saturated dimers [21]. A mono-coordinated complex, however, can be generated in some cases and is even more Lewis acidic than the monomer through the formation of a singly bridged dimer. This species is the combined acid catalyst.

It should be emphasized that we anticipated a more or less intramolecular assembly of such combined systems rather than intermolecular arrangements. Thus, proper design of the catalyst structure is essential for success. The concept of combined acids (Scheme 11), which can be classified into Brønsted acid-assisted Lewis acid (BLA), Lewis acid-assisted Lewis acid (LLA), Lewis acid-assisted Brønsted acid (LBA), and Brønsted acid-assisted Brønsted acid (BBA), can be a useful tool for designing asymmetric catalysis, because combining them can bring out their inherent reactivity by associative interaction, and also provide a more organized structure, both of which allow the securing of an effective asymmetric environment.

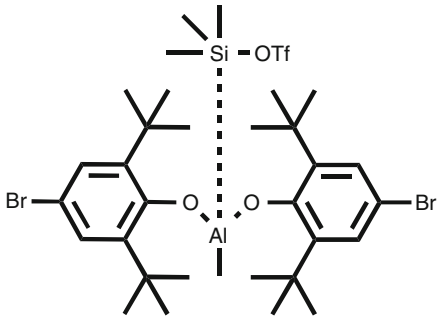

Fig. 2 Possible interaction between the Al atom and the OTf of silyl derivative for generation of reactive silyl catalyst

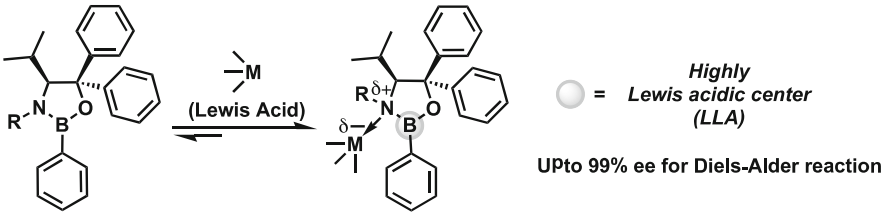

Scheme 13

3.1 BLA

Scheme 12 exemplifies another boron-based BLA which achieves high selectivity through the double effect of intramolecular hydrogen bonding interaction and attractive π−π donor–acceptor interaction in the transition state [22].

3.2 LLA

Remarkable rate enhancement was observed in the trialkylsilyl triflate-catalyzed Mukaiyama aldol reaction of silyl enol ethers aluminum reagent of MABR and TMSOTf combination [23]. Thus, a more strongly Lewis acidic species forms from two different Lewis acids in the presence of an aldehyde (Fig. 2).

Reactive LLA catalysts are relatively well known. Electron-deficient metal compounds can be further activated as electrophiles through hetero- and homodimeric associative interaction. However, full recognition of this synthetically powerful tool does not yet appear to be widespread. It may be further extended to include an asymmetric catalysis design. Scheme 13 is an example of LLA of chiral boron reagent activated by various achiral Lewis acids including SnCl4, AlCl3, FeCl3, and others [24].

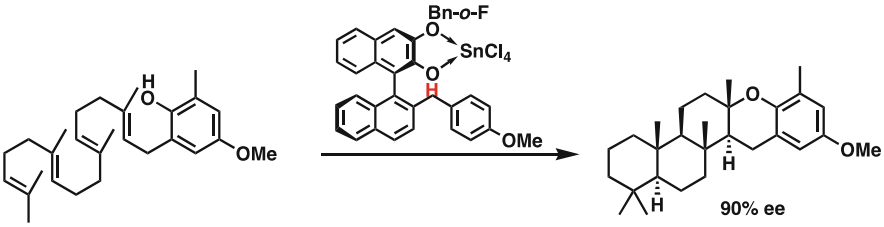

Scheme 14

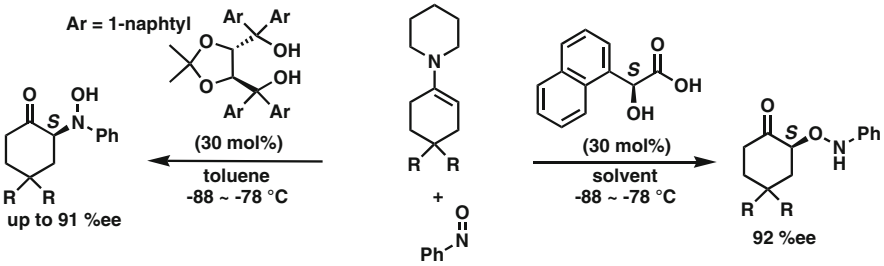

Scheme 15

3.3 LBA

Combining Lewis acids and Brønsted acids to give LBA catalysts can provide an opportunity to design a unique chiral proton. Namely, the coordination of a Lewis acid to the heteroatom of the Brønsted acid can significantly increase its original acidity. An example is shown in Scheme 14 [25]. The reaction generated six stereogenic centers simply from the initial enantioface differentiation of the terminal olefin.

3.4 BBA

Hydrogen bonding can frequently be observed inside enzymes, and such a weak interaction has/plays a crucial role in organizing their three-dimensional structure. Additionally, the hydrogen bonding is often involved in the reaction inside the active site of an enzyme. Such an elegant device could be applicable to asymmetric catalysis. Especially for Brønsted acid catalysis, the design of these catalysts would result not only in formation of a highly organized chiral cavity but also in an increase in the Brønsted acidity of the terminal proton in a much milder way than that of the LBA system (Scheme 15) [26].

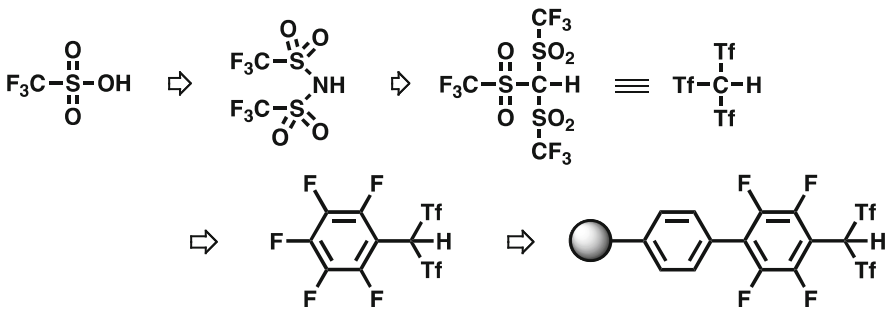

Scheme 16

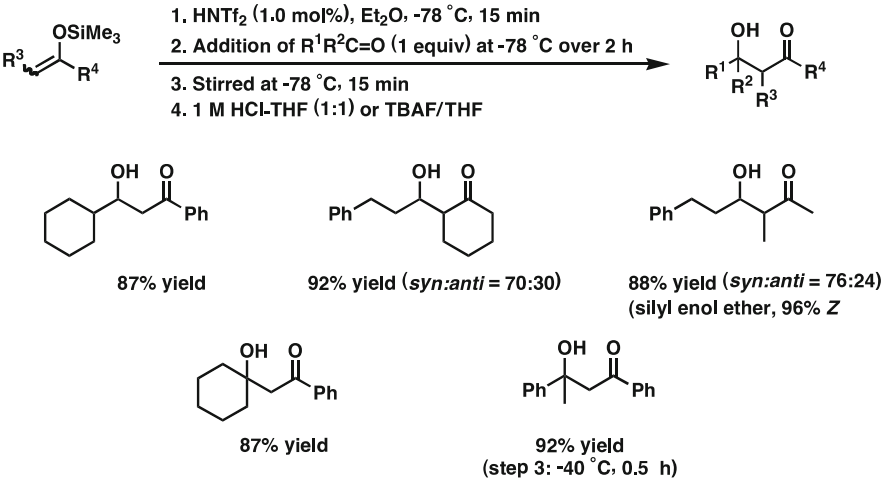

Scheme 17

4 Brønsted Acid Catalysis

Brønsted acid will be an even more important catalyst in future because it is environmentally benign. Generally, Brønsted acid which is stronger than 100% sulfuric acid is called super Brønsted acid by Gillespie [27]. The vast potential of these reagents in the application to lithium batteries and fuel cells is well recognized. Scheme 16 shows a developing trend toward even more environmentally friendly but highly acidic reagents. Furthermore, the sterically larger conjugate base of such a super acid system creates a counter anion which is soluble in organic solvent, an important feature for organic reactions.

Once highly acidic Brønsted acids are in hand, we can also use them as en effective Lewis acid catalysts for various organic transformations. This is simply because the metal attached to such a super conjugate base makes the metal site very

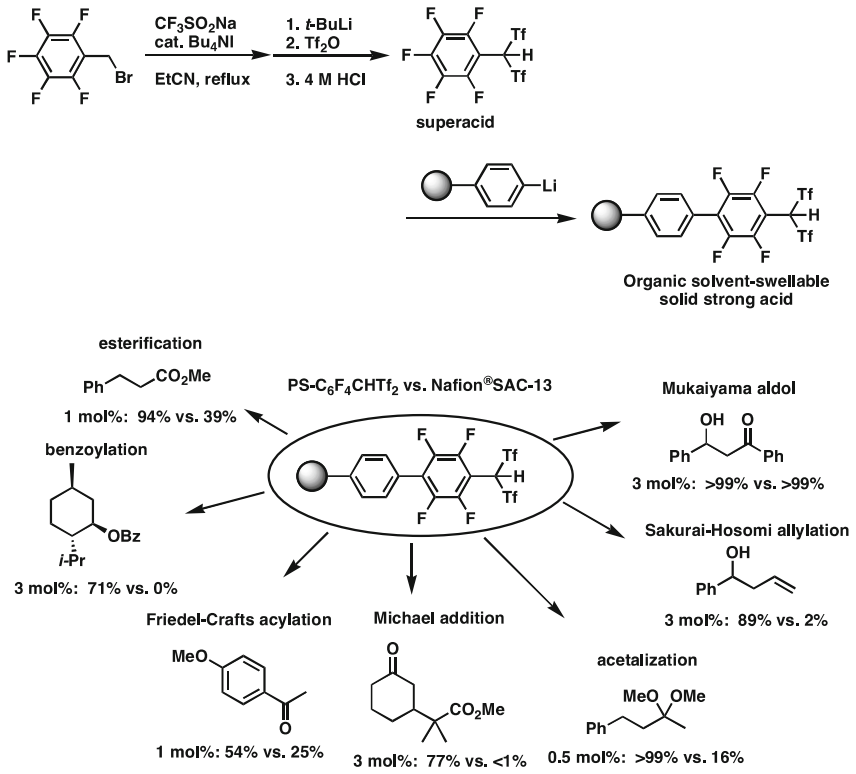

Scheme 18

reactive. The broad utility of these reagents has been demonstrated by simple Mukaiyama aldol reaction as shown in Scheme 22 in which only 1 mol% of catalyst is necessary for the reaction [28] (Scheme 17).

Although the real catalyst in this scheme is not Brønsted acid itself but the Lewis acid of Me_3SiNTf_2, the high reactivity of this Lewis acid catalyst came from the high reactivity of Tf_2NH [29]. The trifluoromethanesulfonyl (triflyl, Tf) group is one of the strongest neutral electron-withdrawing groups. In particular, it greatly increases the acidity of hydrogen atoms at α-positions. The steric and electronic factors of the aromatic ring on arylbis(triflyl)methanes are expected to greatly influence their Brønsted acidity and their catalytic activity and selectivity for organic reactions. We have developed strong carbon Brønsted acids, pentafluorophenylbis(triflyl) methane, and polystyrene-bound tetrafluorophenylbis(triflyl)methane based on this concept (Scheme 18) [30]. The synthesis of the resin-bound Brønsted acid has been accomplished by using the nucleophilic *para*-substitution reaction of lithium pentafluorophenylbis(triflyl)methide with lithiated polystyrenes as a key step. This is the first example of a highly acidic heterogeneous Brønsted acid catalyst that is effectively swollen by nonpolar organic solvents, and, because of its organic solvent

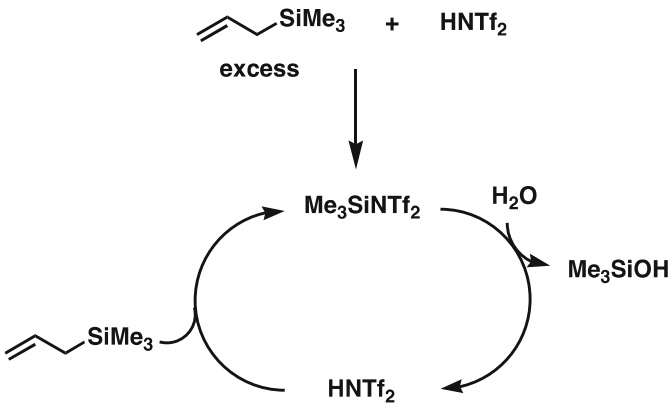

Scheme 19

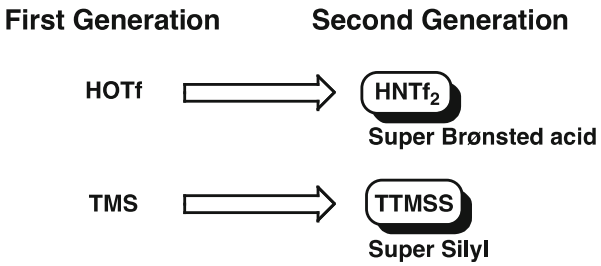

Scheme 20

swellable feature, its catalytic activities are far superior to those of Nafion® SAC-13 [31–33].

As described above, super Brønsted acid catalyst and super silyl catalyst are inextricably linked. This comes from the quick generation of silyl Lewis acid from super Brønsted acid and silyl enol ether (or allylsilane). Since Me_3SiNTf_2 is a moisture sensitive reagent, a small amount of water in the reaction mixture causes its decomposition to give Me_3SiOH and $HNTf_2$. Me_3SiOH will react with Me_3SiNTf_2 and provide inert $Me_3SiOSiMe_3$ and $HNTf_2$. The regenerated $HNTf_2$ will readily react with allyltrimethylsilane and provide Me_3SiNTf_2 again. The repetition of this cycle should produce strictly anhydrous conditions, and thus this catalytic cycle constitutes a self-repair system for Lewis acid catalysis (Scheme 19). The same catalytic repair system can also be effective with silyl enol ether.

The trimethylsilyl (TMS) group is a widely used protecting group and Lewis acid, as well as an important functional group for numerous substrates. For these reasons, we deemed the TMS group to be "generation one." As described earlier (Scheme 20), we have demonstrated that the use of triflimide as a catalyst initiator is very effective for the aldehyde cross-aldol reaction [34, 35]. The success of this reaction proved to be maximal with the use of triflimide as the catalyst as well as the use of tris(trimethylsilyl)silyl (TTMSS) enol ethers (Scheme 20) [36, 37]. The use

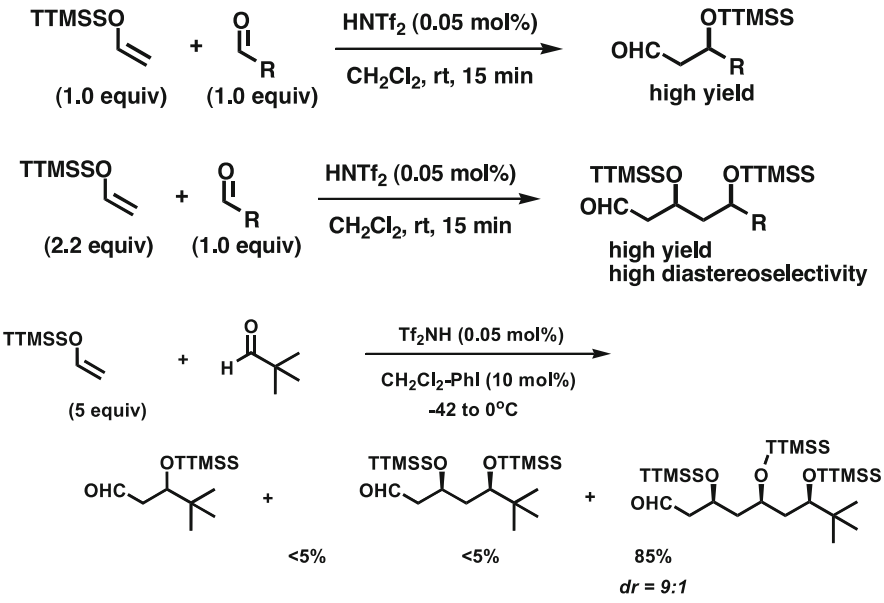

Scheme 21

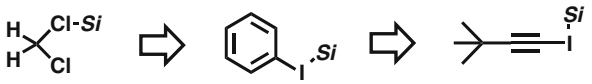

Scheme 22

of the TTMSS group, also referred to as the super silyl group, is one of the keys to this reaction, and its unique reactivity caused us to consider it a second generation silyl group.

The exceptional diastereoselective "control" and high reactivity of the TTMSS (Super silyl) group can be attributed to the two classic arguments of sterics and electronics. The TTMSS group is extraordinarily bulky and has been reported to shield molecular skeletons effectively. After the first addition and silyl transfer, the steric encumbrance of this group is likely to kinetically slow down the addition of a second equivalent of nucleophile to a rate that does not compete with the rate of the first addition. When all of the aldehyde starting material has been consumed, a second addition occurs, giving the products with high diastereoselectivity. After this second addition occurs, the aldehyde has β- and δ-TTMSSoxy groups, and if catalyst coordination takes place, the complex is likely to be too bulky for further additions (Scheme 21).

Finally, the third aldol reaction took place smoothly only in the presence of iodobenzene. This is a remarkable cocatalyst and highly efficient in increasing the reactivity of the aldol reaction. The observation originated from our previous observance that the rate of the reaction increased significantly from toluene to

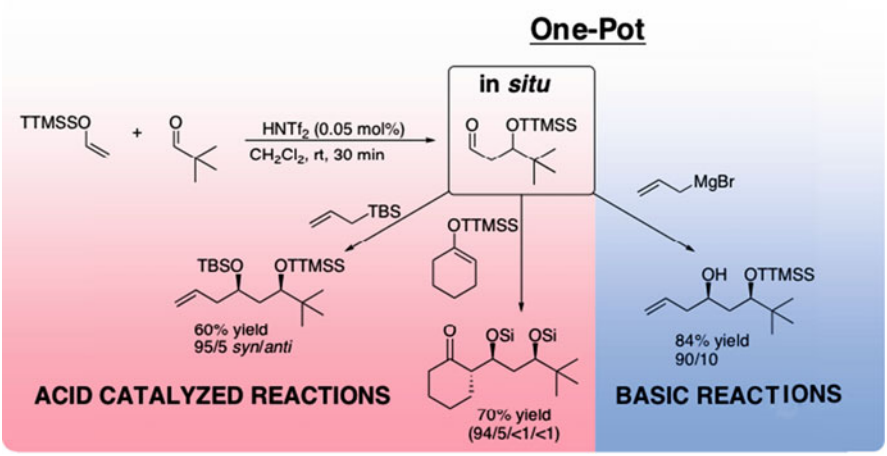

Scheme 23

dichloromethane. We believe this rate enhancement should be attributed to the coordination of halogen atom of dichloromethane, thereby creating the catalyst of partly separated ion pair. Iodobenzene played this role of the activation effectively probably due to the activated catalyst as shown in Scheme 22. Later, we found that the iodoacetylene was even more effective for increasing Lewis acidity of the system.

Intrigued by $TTMSSNTf_2$ catalysis, we used ^{29}Si NMR as an indicator of silicon Lewis acidity and found that the central silicon of $TTMSSNTf_2$ was shifted significantly downfield (>6 ppm) compared to TMS- and $TBSNTf_2$ and only slightly downfield from pentamethyldisilane-NTf_2 (62.2, 55.9, 55.5, and 60.8 ppm, respectively). This trend shows a considerable difference in the cationic nature of silyl groups with only silicon–carbon bonds versus those with silicon–silicon bonds. This high reactivity of silyl enol ether as well as super silyl cation is probably due to the high homo level of the Si–Si and Si–C sigma bond.

With this outstanding one-pot aldol reaction in hand, since the tris (trimethylsilyl)silyl (TTMSS) silyl enol ether undergoes aldehyde cross-aldol reactions with high selectivity and the extremely low catalyst loading (0.05 mol% of $HNTf_2$), we can proceed toward one-pot sequential reactions where acidic or basic nucleophiles can subsequently be added. Various ketone-derived silyl enol ethers, Grignard reagents, and dienes succeeded successfully, generating relatively complex molecular architectures in a single step (Scheme 23). This represents the first case where, in a single pot, highly acidic conditions followed by very basic conditions were tolerated to give products with high diastereoselectivities and good yields [35].

Even more recently, we have shown that the process can be used for enol ether of ketones, which can be generated by carbon centers diastereoselectively in one pot. Scheme 24 shows examples of this reaction as a “four-component one-pot coupling reaction” [38].

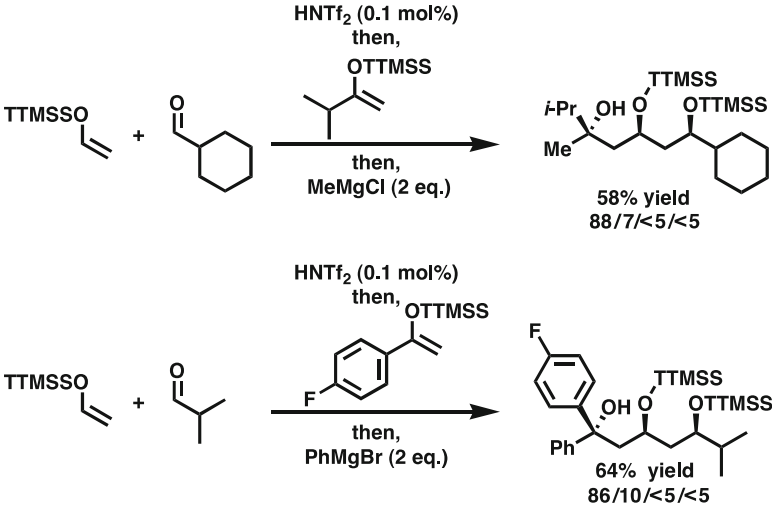

Scheme 24

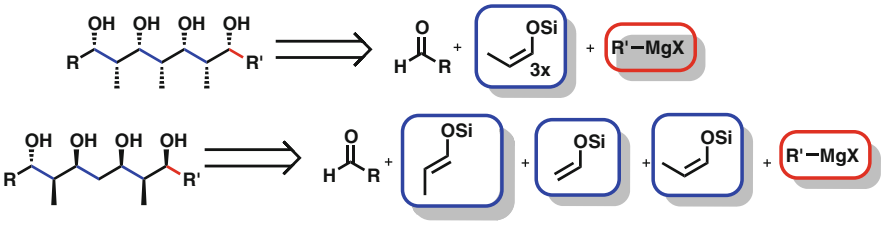

Scheme 25

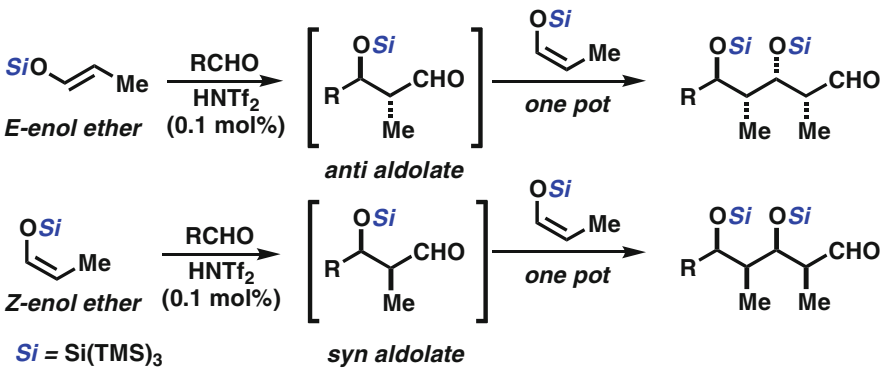

Scheme 26

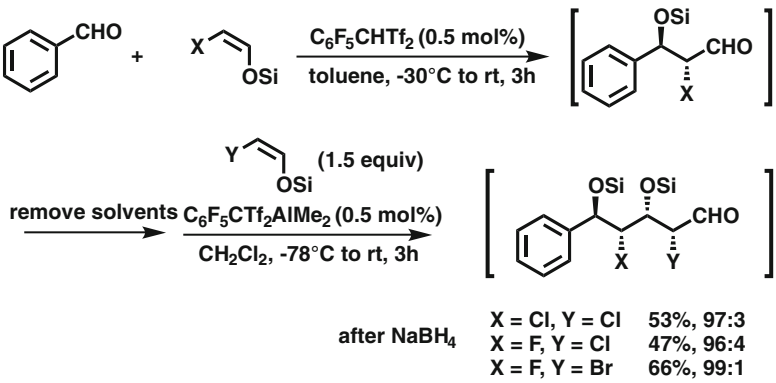

Scheme 27

The process turned out to be a quite flexible cascade reaction, generating complex product in a single operation, and the process could provide numerous stereoselective pathways to generate mono-, di-, and tri-aldol products stereoselectively in a flexible manner (Scheme 25).

This scheme solves the numerous problems of the classical aldol synthesis in building up complex molecules. Since aldehyde aldol did not work very well in the classical procedure, we must have multiple steps including additional protection, reduction, and oxidation. By this multi-step synthesis, even relatively simple di- and tri-aldol molecules required 8–12 steps, respectively. In contrast, the cascade reaction reduces these long steps to a single step to generate the molecules. The following examples of propionate synthesis clearly show the power of the method (Scheme 26).

As shown, not only acetaldehyde and propionaldehyde nucleophiles but alpha-halo acetaldehydes also can be generated without any problems. Thus, the Mukaiyama cross-aldol reaction of α-fluoro-, α-chloro-, and α-bromoacetaldehyde-derived (*Z*)-tris(trimethylsilyl)-silyl enol ethers furnished *anti*-β-siloxy-α-haloaldehydes. Furthermore, a highly diastereoselective, one-pot, sequential double-aldol process, affording novel β,δ-bissiloxy-α,γ-bishaloaldehydes, has been developed. Reactions are catalyzed by $C_6F_5CHTf_2$ and $C_6F_5CTf_2AlMe_2$ (0.5–1.5 mol%) and provide access to halogenated polyketide fragments (Scheme 27).

5 Conclusion

It was a long journey to provide a shape to a simple proton. However, I believe this challenge offered us numerous opportunities to develop new chemistry. Although many of them were far beyond our expectations, they ultimately led us to unexpected solution. We still hope in the future to develop even better and useful acid catalysts for organic synthesis

References

1. Yamamoto H, Nozaki H (1978) Selective reactions with organoaluminum compounds. Angew Chem Int Ed Engl 17:169
2. Matuoka K, Yamamoto H (1985) Selective reactions using organoaluminum reagents. Angew Chem Int Ed Engl 24:668
3. Kitagawa Y, Hashimoto S, Iemura S, Yamamoto H, Nozaki H (1976) Novel nonenzymic heterolysis of an allyl phosphate ester by organoaluminum reagents. J Am Chem Soc 98:5030
4. Yasuda A, Tanaka S, Oshima K, Yamamoto H, Nozaki H (1974) Organoaluminum reagents of type $R^1R^2NA1Et^2$ which allow regiospecific isomerization of epoxides to allylic alcohols. J Am Chem Soc 96:6513–6514
5. Kitagawa Y, Itoh A, Hashimoto S, Yamamoto H, Nozaki H (1977) Total synthesis of humulene. A stereoselective approach. J Am Chem Soc 99:3864
6. Yamamoto H, Yanagisawa A, Ishihara K, Saito S (1998) Designer Lewis acids for selective organic synthesis. Pure Appl Chem 70:1507
7. Maruoka K, Nonoshita K, Banno H, Yamamoto H (1988) Unprecedented stereochemical control in the Claisen rearrangement of allyl vinyl ethers using organoaluminum reagents. J Am Chem Soc 110:7922
8. Nonoshita K, Banno H, Maruoka K, Yamamoto H (1990) Organoaluminum-promoted Claisen rearrangement of allyl vinyl ethers. J Am Chem Soc 112:316
9. Maruoka K, Ito M, Yamamoto H (1995) Unprecedented nucleophilic addition of organolithiums to aromatic aldehydes and ketones by complexation with aluminum tris(2,6-diphenylphenoxide). J Am Chem Soc 117:9091
10. Saito S, Sone T, Murase M, Yamamoto H (2000) Aluminum tris(2,6-diphenylphenoxide)-ArCOCl complex for nucleophilic dearomatic functionalization. J Am Chem Soc 122:10216
11. Maruoka K, Itoh T, Yamamoto H (1985) Methylaluminum bis(2,6-di-tert-butyl-4-alkylphenoxide). A new reagent for obtaining unusual equatorial and anti-Cram selectivity in carbonyl alkylation. J Am Chem Soc 107:4573
12. Maruoka K, Itoh T, Sakurai M, Nonoshita K, Yamamoto H (1988) Amphiphilic reactions by means of exceptionally bulky organoaluminum reagents. Rational approach for obtaining unusual equatorial, anti-Cram, and 1,4 selectivity in carbonyl alkylation. J Am Chem Soc 110:3588
13. Yamamoto H, Maruoka K, Furuta K (1989) In: Schinzer D (ed) Selectivities in Lewis acid promoted reactions. Nato ACI Series, Kluwer Academic Publishers
14. Haruta R, Ishiguro M, Ikeda N, Yamamoto H (1982) Chiral allenylboronic esters: a practical reagent for enantioselective carbon–carbon bond formation. J Am Chem Soc 104:7667–7669
15. Sakane S, Maruoka K, Yamamoto H (1985) Asymmetric cyclization of unsaturated aldehydes catalyzed by a chiral Lewis acid. Tetrahedron Lett 26:5535–5538
16. Maruoka K, Itoh T, Shirasaka T, Yamamoto H (1988) Asymmetric hetero-Diels-Alder reaction catalyzed by chiral organoaluminum reagent. J Am Chem Soc 110:310–312
17. Yamamoto H (1999) Lewis acid reagents: a practical approach. Oxford University Press, Oxford
18. Yamamoto H (2000) Lewis acids in organic synthesis. Wiley-VCH, Weinheim
19. Furuta K, Miwa Y, Iwanaga K, Yamamoto H (1988) Acyloxyborane: an activating device for carboxylic acids. J Am Chem Soc 110:6254–6255
20. Futatsugi K, Yamamoto H (2005) Studies on the mechanism of sesquiterpene biosynthesis. humulene-germacrene rearrangement. Angew Chem Int Ed 44:1924–1942
21. Negishi E (1999) Principle of activation of electrophiles by electrophiles through dimeric association – two are better than one. Chem Eur J 5:411–420
22. Ishihara K, Yamamoto H (1994) Brønsted acid assisted chiral Lewis acid (BLA) catalyst for asymmetric Diels-Alder reaction. J Am Chem Soc 116:1561–1562

23. Oishi M, Aratake S, Yamamoto H (1998) Remarkable enhancement of catalyst activity of trialkylsilyl sulfonates on the Mukaiyama aldol reaction: a new approach using bulky organoaluminum cocatalysts. J Am Chem Soc 120:8271
24. Futatsugi K, Yamamoto H (2005) Oxazaborolidine-derived Lewis acid assisted Lewis acid as a moisture-tolerant catalyst for enantioselective Diels–Alder reactions. Angew Chem Int Ed Engl 44:1484–1487
25. Ishibashi H, Ishihara K, Yamamoto H (2004) A new artificial cyclase for polyprenoids: enantioselective total synthesis of (−)-chromazonarol, (+)-8- epi-puupehedione, and (−)-11´-deoxytaondiol methyl ether. J Am Chem Soc 126:11122–11123
26. Momiyama N, Yamamoto H (2005) Brønsted acid catalysis of achiral enamine for regio- and enantioselective nitroso aldol synthesis. J Am Chem Soc 127:1080–1081
27. Gillespie RJ, Peel TE (1971) Superacid systems. Adv Phys Org Chem 9:1–5
28. Ishihara K, Hiraiwa Y, Yamamoto H (2001) A high yield procedure for the Me_3SiNTf_2-induced carbon-carbon bond forming reactions of silyl nucleophiles with carbonyl compounds: the importance of addition order and solvent effects. Synlett 12:1851–1854
29. Mathieu B, Ghosez L (1997) N-trimethylsilyl-bis(trifluoromethanesulfonyl)imide: a better carbonyl activator than trimethylsilyl triflate. Tetrahedron Lett 38:5497–5500
30. Ishihara K, Hasegawa A, Yamamoto H (2001) Polystyrene-bound Tetrafluorophenylbis (triflyl) – methane as an Organic-Solvent-Swellable and Strong Brønsted acid Catalyst. Angew Chem Int Ed Engl 40:4077–4079
31. Ishihara K, Hasegawa A, Yamamoto H (2002) Single-pass reaction column system with super Brønsted acid-loaded resin. Synlett 8:1296–1298
32. Ishihara K, Hasegawa A, Yamamoto H (2002) A fluorous super Brønsted acid catalyst: application to fluorous catalysis with fluorous solvents. Synlett 8:1299–1301
33. Hasegawa A, Ishikawa T, Ishihara K, Yamamoto H (2005) Facile synthesis of aryl- and alkyl-bis(trifluoromethylsulfonyl)methanes. Bull Chem Soc Jpn 78:1401–1410
34. Boxer MB, Yamamoto H (2006) Tris(trimethylsilyl)silyl-governed aldehyde cross-aldol cascade reaction. J Am Chem Soc 128:48–49
35. Boxer MB, Yamamoto H (2007) “Super Silyl” group for diastereoselective sequential reactions: access to complex chiral architecture in one pot. J Am Chem Soc 129:2762–2763
36. Bock H, Meuret J, Baur R, Ruppert K (1993) 1,4-Di[tris(trimethylsilyl)sily]benzene: synthesis, structural analogy, photoelectron spectrum and ESR/ENDOR characterization of its radical anion. J Organomet Chem 446:113–122
37. Frey J, Schottland E, Rappoport Z, Bravo-Zhivotovskii D, Nakash M, Botoshansky M, Kaftory M, Apeloig Y (1994) The effective ‘size’ of the tris(trimethylsilyl)silyl group in several molecular environments. J Chem Soc, Perkin Trans 2, 2555–2562
38. Boxer M, Yamamoto H (2008) Ketone super silyl enol ethers in sequential reactions: diastereoselective generation of tertiary carbinols in one pot. J Am Chem Soc 130:1580–1582

Index